THE SHANGHAI YANGTZE RIVER TUNNEL

THEORY, DESIGN AND CONSTRUCTION

R. HUANG
EDITOR-IN-CHIEF

Taylor & Francis
Taylor & Francis Group

THE SHANGHAI YANGTZE RIVER TUNNEL
THEORY, DESIGN AND CONSTRUCTION

BALKEMA – Proceedings and Monographs
in Engineering, Water and Earth Sciences

COMPLIMENTARY SPECIAL ISSUE TO THE SIXTH INTERNATIONAL SYMPOSIUM ON GEOTECHNICAL ASPECTS OF UNDERGROUND CONSTRUCTION IN SOFT GROUND – IS-SHANGHAI, SHANGHAI, CHINA, 10–12 APRIL 2008

The Shanghai Yangtze River Tunnel

Theory, Design and Construction

Editor-in-Chief

R. Huang
Commanding Post of Shanghai Tunnel & Bridge Construction, Shanghai, P. R. China

EDITORIAL COMMITTEE

X.J. Dai, Q.W. Liu & Q.Q. Ji
Shanghai Changjiang Tunnel & Bridge Development Co., Ltd., Shanghai, P. R. China

Y.S. Li, Y. Yuan & Z.X. Zhang
Tongji University, Shanghai, P. R. China

Z.Z. Qiao, Z.H. Yang & J.Q. Shen
Shanghai Tunnel Engineering & Rail Transit Design and Research Institute, Shanghai, P. R. China

G.X. Yang, J.X. Lin & H.X. Li
Shanghai Tunnel Engineering Co., Ltd., Shanghai, P. R. China

Taylor & Francis
Taylor & Francis Group
LONDON / LEIDEN / NEW YORK / PHILADELPHIA / SINGAPORE

Front cover photograph (right): Cutter head of slurry shield machine
Front cover photograph (left): Shanghai Yangtze River Tunnel
Back cover photograph: Model test of a single ring

GREAT APPRECIATION TO "THE NATIONAL HIGH TECHNOLOGY RESEARCH AND DEVELOPMENT PROGRAM (863 PROGRAM) OF CHINA (GRANT NO. 2006AA11Z118)" FOR SPONSORING THIS WORK.

Taylor & Francis is an imprint of the Taylor & Francis Group, an informa business

Typeset by Charon Tec Ltd (A Macmillan Company), Chennai, India
Printed and bound in Great Britain by Antony Rowe (A CPI-group Company), Chippenham, Wiltshire.

Published by: Taylor & Francis/Balkema
P.O. Box 447, 2300 AK Leiden, The Netherlands
e-mail: Pub.NL@tandf.co.uk
www.balkema.nl, www.taylorandfrancis.co.uk, www.crcpress.com

ISBN 13: 978-0-415-47161-9 (Hardback and CD-ROM)

The Shanghai Yangtze River Tunnel - Theory, Design and Construction – Huang (ed)
© 2008 Taylor & Francis Group, London, ISBN 978-0-415-47161-9

Table of contents

Preface IX

Keynote lecture

Overview of Shanghai Yangtze River Tunnel Project 3
R. Huang

Special lectures

Fire evacuation and rescue design of Shanghai Yangtze River Tunnel 21
W.Q. Shen, Z.H. Peng & J.L. Zheng

Shanghai Yangtze River Tunnel & Bridge Project management based on lifecycle 27
X.J. Dai

1 Experiment and design

A review of shield tunnel lining design 37
B. Frew, K.F. Wong, C.K. Mok & F. Du

Analysis of the slurry infiltration effect on soil by true triaxial test under the ESEM-scanning 43
X.Y. Hu, Z.X. Zhang, X. Huang & J.Y. Wang

Design and optimization of gasket for segment joint based on experiment and mathematical analysis 53
Z.X. Zhu & M. Lu

Design of hazard prevention system for Shanghai Yangtze River Tunnel 63
X. Wang, Z.Q. Guo & J. Meng

Design of shield work shaft constructed together with cut-and-cover tunnels 69
C.N. He & Z.H. Yang

Experimental study on fire damage to slab of exit flue of shield tunnel 81
Z.G. Yan, H.H. Zhu, T. Liu & Y.G. Fang

Integrated design and study of internal structure of Shanghai Yangtze River Tunnel 85
Y.M. Di, Z.H. Yang & Y. Xu

Preliminary study of temperature rising and cooling measures for long road tunnel 93
W.T. Jiang, J.L. Zheng & H.S. Lao

Research on fireproofing and spalling resistance experiment solution for reinforced concrete structure specimen of tunnel 99
Y.Q. Fan

Study of full-scale horizontal integral ring test for super-large-diameter tunnel lining structure 111
W.H. Cao, Z.J. Chen & Z.H. Yang

The application of single-fluid resisting shear type slurry with synchronized grouting system on large slurry shield machine in Shanghai Yangtze River Tunnel 125
B. Xie

The dielectric constant testing of grouting slurry and soil behind shield tunnel segment in soft soil 131
H. Liu, X.Y. Xie & J.P. Li

2 Construction technology and monitoring

70T hydraulic system truck 141
J.L. Li & Y. Ni

Application of the large-scale integrated equipments in slurry treatment in shield tunneling 145
Y.D. Liu

Attitude surveying of the tunnel shield 155
Y.M. Yu & J.X. Wang

Construction logistics in large diameter and long distance shield tunneling 159
J.G. Yang

Construction technology of shield inspection environment in Shanghai Yangtze River Tunnel 167
G.J. Zhang, F.Q. Yang & F.T. Yue

Deformation monitoring system of circular tunnel cross section 175
J.X. Wang, Y.L. Cao, D.Y. Hou & Y.B. Huang

Driving the slurry TBMs for Shanghai Yangtze River Tunnel 181
G. Ferguson, L. Zhang & Y. Lin

GFRP reinforcement cage erection technology in diaphragm wall 193
K.J. Ye, G.Q. Zhao, D.Y. Zhu & L. Zhang

Importing of shield machine of Shanghai Yangtze River Tunnel and Bridge 199
J. Xu

Key techniques in cross passage construction of Shanghai Yangtze River Tunnel by artificial ground freezing method 205
Z.H. Huang, X.D. Hu, J.Y. Wang, H.B. Lin & R.Z. Yu

TBM options for Shanghai Yangtze River Tunnel Project 211
J. Sun, X.K. Chen & Q.W. Liu

The application of laser tracker in mould/segment measurement 223
D.H. Zhang, N.J. Zhang & Y.P. Lu

3 Theoretical analysis and numerical simulation

A 3D visualized life-cycle information system (3D-VLIS) for shield tunnel 231
X.J. Li, H.H. Zhu, L. Zheng, Q.W. Liu & Q.Q. Ji

Analysis on influence of conicity of extra-large diameter mixed shield machine on surface settlement 237
Q.Q. Ji, Z.H. Huang & X.L. Peng

Numerical study on working ventilation of Shanghai Yangtze River Tunnel 243
J. Ding, T.L. Ge, M. Hu & J.Y. Wang

Optimization design and research of the cross section form and structure for Shanghai Yangtze River Tunnel 247
Y. Xu & W.Q. Ding

Prediction for long-term settlement of Shanghai Yangtze River Tunnel 253
D.M. Zhang, H.L. Bao & H.W. Huang

Simplified analysis for tunnel seismic response in transverse direction 259
A.J. Cao, M.S. Huang & X. Yu

Study on tunnel stability against uplift of super-large diameter shield tunneling 267
J.X. Lin, F.Q. Yang, T.P. Shang & B. Xie

4 Risk assessment and management

Construction risk control of cross passage by freezing method in Shanghai Yangtze River Tunnel 277
X.R. Fan, W. Sun & H.Q. Wu

Crack control measures during segment prefabrication of large diameter bored tunnel 285
B.T. Yan, Z.Q. Ying & K.J. Li

Dynamic risk management practice of construction for the long-distance and largest-diameter tunnel 291
Z.H. Huang, X.L. Peng & W. Fang

Prefabrication supervision of major tunnel lining with high precision 299
H.Y. Gong & X.N. Qiu

Research on vibration monitoring and fault diagnosis for principal bearing in shield machine 305
D.S. Huang, X.Y. Chen, G.J. Zhang & L. Teng

Risk analysis on shield tail seal brush replacing of Shanghai Yangtze River Tunnel 311
Y.R. Yan, H.W. Huang & X.Y. Xie

Shanghai Yangtze River Tunnel split level evacuation provisions 319
B. Frew, Y.F. Cai, K.F. Wong, C.K. Mok & L. Zhang

The construction management informationization practice in Shanghai Yangtze River Tunnel & Bridge Project 325
Z.F. Zhou & H.X Zhang

The structural serviceability of large road tunnel 333
Y. Yuan, T. Liu & X. Liu

Author index 339

The Shanghai Yangtze River Tunnel - Theory, Design and Construction – Huang (ed)
© 2008 Taylor & Francis Group, London, ISBN 978-0-415-47161-9

Preface

A Challenge to the Most Advanced Technology in Today's Tunnel and Bridge Project

December, 2007

Chongming Island, at the mouth of the Yangtze River and embraced by China's East Sea, is China's third largest island. It is also an important strategic area for Shanghai's sustainable development in the 21st century. At present, a 25.5-kilometre long Shanghai Yangtze River Tunnel and Bridge Project is under construction at the mouth of the 10000-li Yangtze River.

Shanghai Yangtze River Tunnel and Bridge Project has been an important strategic decision made by China's Central Party Committee and the State Council. In July 2004, Hu Jintao, CPC Secretary-General, came to Shanghai; he issued important instructions in terms of developing Chongming Island into a modern comprehensive eco-island. On August 15th of the same year, China's State Council approved this project, which began development on December 28th. Currently the largest project in the world combining both bridge and tunnel, it is intended to carry out the national strategic plan: to serve as a transportation artery connecting several areas of China's east coast region; thus a harmonious and integral development of our economic society. Furthermore, it will accelerate the construction of Chongming Eco-Island, and to lay solid foundation for the three-island integration, namely, Chongming, Changxing and Hengsha Islands.

As an essential part of this project, the Shanghai Yangtze River Tunnel is currently one of the largest tunnel projects in the world. With its magnificent scale, stylish design, and creative techniques in construction, it will attract the attention of the international civil engineering world. Its completion will enhance the innovation and development technology in long and large tunnel project design and construction; it will exert a tremendous and far-reaching influence on the tunnel and underground engineering world.

Our scientific and technical workers, faced with the high demands of technology and difficulties of construction, have made positive and significant efforts. They have turned project problems waiting to be solved into theories, used various modern means to conduct scientific experiments, striving to prove such scientific outcomes in practice. Hence, a further elevation of theories, and they ultimately put forward optimized solutions to the problems. Such spirit in working and research methods do not only abide by the scientific view of development, but also effectively promote better and quicker construction.

The Proceedings on Shanghai Yangtze River Tunnel Engineering collects more than forty high quality papers, which cover the investigation, design, construction and operation of the project. It records and summarizes in a way that enables us to see clearly how a series of unprecedented problems in the world history of tunnel construction can be solved. The proceedings reveal the scientific and technological content of the construction of Shanghai Yangtze River Tunnel Project exposes the "pioneering" courage and wisdom of the builders to challenge the world's best. It adds color to the flourishing scientific and technical achievements of China's tunnel and underground engineering. Construction workers and engineers will acquire encouragement and instruction from its reading.

In closing, allow me to express our lofty respect to those builders as well as the scientific and technical workers in the Shanghai Yangtze River Tunnel Project! Congratulations for the publication of *The Proceedings on Shanghai Yangtze River Tunnel Engineering*. And every good wish for the complete success of the 6th International Symposium Geotechnical Aspects of Underground Construction in Soft Ground (IS-Shanghai 2008), as well as a Workshop on the Technique of Shanghai Yangtze River Tunnel.

Xiong Yang

Vice Mayor of Shanghai, Commander in Chief of
Shanghai Yangtze River Tunnel and Bridge Project

Keynote lecture

The Shanghai Yangtze River Tunnel - Theory, Design and Construction – Huang (ed)
© 2008 Taylor & Francis Group, London, ISBN 978-0-415-47161-9

Overview of Shanghai Yangtze River Tunnel Project

R. Huang
Commanding Post of Shanghai Tunnel & Bridge Construction, Shanghai, P. R. China

ABSTRACT: In the paper, an introduction of the construction background and scale of Shanghai Yangtze River Tunnel and Bridge Project and natural conditions of Shanghai Yangtze River Tunnel construction are given. The overall design concept and some critical technical solutions such as segment structure of large diameter bored tunnel, water proofing of segment under high depth and water pressure, long tunnel ventilation system and fire fighting system are described. Characteristics of two mixed TBM with a diameter of 15,430 mm are described. The overall construction methods of tunnel, and critical technical solutions and risk provision measures for large and long river-crossing tunnel such as the front surface stability for bored tunnel construction, floating resistance of large diameter tunnel, long distance construction survey, synchronous construction of internal structure, and cross passage construction of fresh/salty alternating geological/environmental condition are discussed.

1 INTRODUCTION

Shanghai Yangtze River Tunnel and Bridge project is located at the South Channel waterway and North Channel waterway of Yangtze River mouth in the northeast of Shanghai, which is a significant part of national expressway, as shown in Figure 1. It is an extremely major transport infrastructure project at seashore area in China at Yangtze River mouth and also the largest tunnel and bridge combination project worldwide. The completion of the project will further promote the development space for Shanghai, improve the structure and layout of Shanghai traffic system, develop resources on Chongming Island, accelerate economic development in the north of Jiangsu Province, increase the economy capacity of Pudong, accelerate the economy integrity of Yangtze River Delta, boom the economic development of Yangtze River area and even the whole country and upgrade the comprehensive competence of Shanghai in China and even in the global economy.

Shanghai Yangtze River Tunnel and Bridge (Chongming Crossing) alignment solution is the planned western solution which is implemented firstly based on the Shanghai overall urban planning, and comparison between east and west alignment and in combination of various aspects. The western alignment starts from Wuhaogou in Pudong, crossing Yangtze River South Channel waterway to Changxing Island and spanning Yangtze River North Channel waterway to east of Chongming Island.

Figure 1. Site location of Chongming Crossing.

Yangtze River begins to be divided into 3 levels of branches and have 4 mouths flowing into the sea: The South Channel waterway is mixed river trench. The intermediate slow flow area forms Ruifeng shoal which is relatively stable for a long time. The natural water depth makes it as the main navigation channel. However, the North Channel waterway is located in the middle part of river, which is influenced by the south part and branch transition into North Channel waterway. So the trench varies alternatively and the river map is not as stable as South Channel waterway. Therefore, after iterative discussion by several parties,

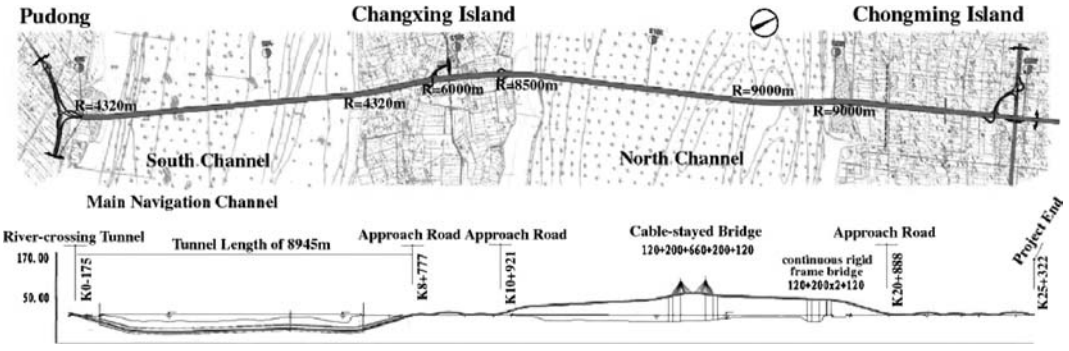

Figure 2. Diagram of Shanghai Yangtze River Tunnel and Bridge.

finally the solution of 'Southern Tunnel & Northern Bridge' is selected. The total project is 25.5 km long, among which 8.95 km is tunnel with a design speed of 80 km/h and 9.97 km is bridge and 6.58 km is land connection with a design speed of 100 km/h, as shown in Figure 2. The total roadway is planned as dual 6 lanes.

2 CONSTRUCTION BACKGROUND AND PLANNING

The planning study of Shanghai Yangtze River Tunnel and Bridge Project (Chongming Crossing) was incepted from 90s of last century. The preliminary preparatory work has lasted 11 years. In May 1993, the National Scientific Committee held the 'Yangtze River mouth crossing significant technical-economical challenges – early stage work meeting'. After one year special investigation, the 'Preliminary study report of significant technical challenges of 'Yangtze River Crossing' was prepared. The pre-feasibility study report was prepared in March 1999. In August 2001, the international concept competition was developed and the 'Southern Tunnel & Northern Bridge' solution was defined. The National Planning Committee approved the project proposal in December 2002. The feasibility study report was approved by the National Development and Reform Committee in November 2004. The preliminary design was approved by the Ministry of Communication in July 2005 and total investment of 12.616 billion RMB was approved for the project.

For the project construction investment, 5 billion was funded by Shanghai Chengtou Corporation (60%) and Shanghai Road Construction Cooperation (40%), and 7.6 billion was financed from Bank Consortium.

Based on the characteristics of the national major project, Commanding Post of Shanghai Tunnel & Bridge Construction was established with approval of Shanghai Municipal Committee. The post is directed by the vice major and composed of staff from Pudong New Area, Chongming County and other committees and bureaus. The main responsibility is to make decision on significant problems and coordinate important items. In order to improve the depth of daily management, office was set up under the commanding post, working together with established 'Shanghai Yangtze River Tunnel and Bridge Construction Development Co., Ltd.' which is mainly in charge of the implementation of the project and daily work of commanding post and performs the investment management on behalf of the client. The specific work is responsible for the financing, investment, construction, operation and transfer of the project. To detail the technical assurance measures, the clients sets up the technical consultant team which provides theoretical support, technical assistance and consultancy service for significant technical challenges during the implementation. Meanwhile, the team is involved in the investigation of significant technical solutions, review of construction method statement and treatment of technical problems to ensure the high quality and safety. International well-known consultancy companies are entrusted for the purpose of application of state-of-art philosophy, most successful experience, optimal concept and most mature management to make the Yangtze River Tunnel and Bridge Project as Century Elite Project.

The project finally initiated on 28th, December 2004 and planned to be open to traffic in July 2010. The main civil structure of the bridge is planned to be closed in June 2008, and tunnel in April 2009.

3 NATURAL CONDITIONS OF TUNNEL PROJECT

3.1 *Environmental conditions*

Shanghai Yangtze Tunnel Project starts from Wuhaogou of Waigaoqiao in Pudong New Area, connected with Shanghai main fast roads such as Middle Ring, Outer Ring and Suburb Ring through Wuzhou Aveneu,

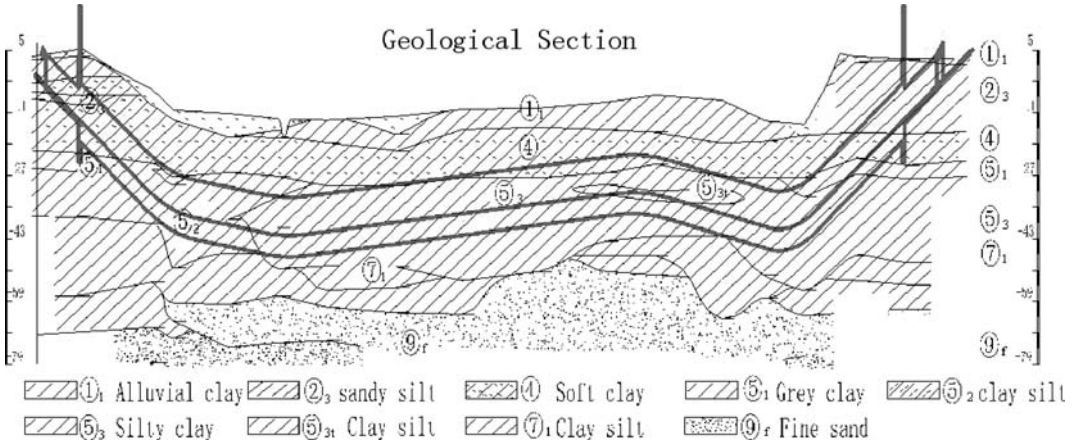

Figure 3. Longitudinal profile of tunnel.

crossing southern water area and lands on Changxing Island 400 m west of Xinkaihe Harbour, connected with Changxing Island road net through Panyuan Interchange. The main building on land is the flood prevention wall on Pudong side and Changxing Island. Others are farm fields. The river-crossing section is mainly the southern water way for navigation which is an important passage for connecting Yangtze Waters with other seashore area in China and oceans worldwide.

There are two sea cables arranged along the bored tunnel axis with a depth of 3 m below natural river bed. One cable is basically located at the west side of the tunnel and goes into the river near Wuhaogou on Pudong side, which is about 1,500 m away from the tunnel. It becomes closer to the tunnel gradually to the north and crosses the tunnel to its east at 240 m from Changxing Island and lands on Changxing Island at 350 m west of Xinkaihe Harbour. The other cable goes into the river near Wuhaogou, 1,300 away from the tunnel. Then it turns to NE first and N at 2,600 m way from Pudong Land Connections, almost identical with the tunnel alignment. And it changes from the west of tunnel to east of tunnel gradually and lands on Changxing Island about 300 m west of Xinkaihe Harbor.

Furthermore, two sunken boats close to Chainage XK2+350 and XK1+500 have been salved before bored tunnel construction. Earth was also filled back at corresponding locations; however, there may be still some remains.

3.2 *River regime and hydrological conditions*

At the mouth of Yangtze River it is tide area with intermediate level. Outside of mouth is regular half day tide and inside is irregular half day shallow tide due to the change of tide wave. Average flood tide time is 5 h and average ebb tide time is 7 h, so total time for ebb and flux is 12 h. The average currency flow is 1.05 m/s for flood tide during flood season and 1.12 m/s for ebb tide. The maximal flow for flood tide is 1.98 m/s and 2.35 m/s for ebb tide.

The underground water type in the shallow stratum at tunnel site is potential water, which has close hydraulic relation with river water. The potential water level is mainly influenced by the Yangtze Rive flux and ebb. The average water level for Waigaoqiao and Changxing Island is 2.8 m and 2.4 m, respectively.

In the stratum ⑦ and ⑨ at site area, the confined water is rich. At most area, the confined water is directly continuous. The confined water level is between −4.15 m and −6.76 m. Furthermore, slight confined water distributes in $⑤_2$, which has certain hydraulic relations with confined water in ⑦.

3.3 *Geological conditions*

The relief of onshore area of the project is 'river mouth, sand mouth, sand island' which is within the major four relief units in Shanghai. The ground surface is even with a normal elevation of 3.5 m (Wusong Elevation). The water area is classified as river bed relief.

The project site has a seismic fortification intensity of 7, classified as IV site. The stratum $②_3$ and $③_2$ sandy silt distributing on Pudong land area is slightly liquefied.

Main geological layers (refers to Figure 3) TBM crosses are: $④_1$ grey muddy clay, $⑤_1$ grey muddy clay, $⑤_2$ grey clayey silt with thin silty clay, $⑤_3$ silty clay, $⑤_3$ tlens, $⑦_{1-1}$ grey clay silt, $⑦_{1-2}$ grey sandy silt, etc. Unfavorable geological conditions are experienced along the axis of the tunnel, such as liquefied soil, quick sand, piping, shallow gas (methane), lens and confined water, etc.

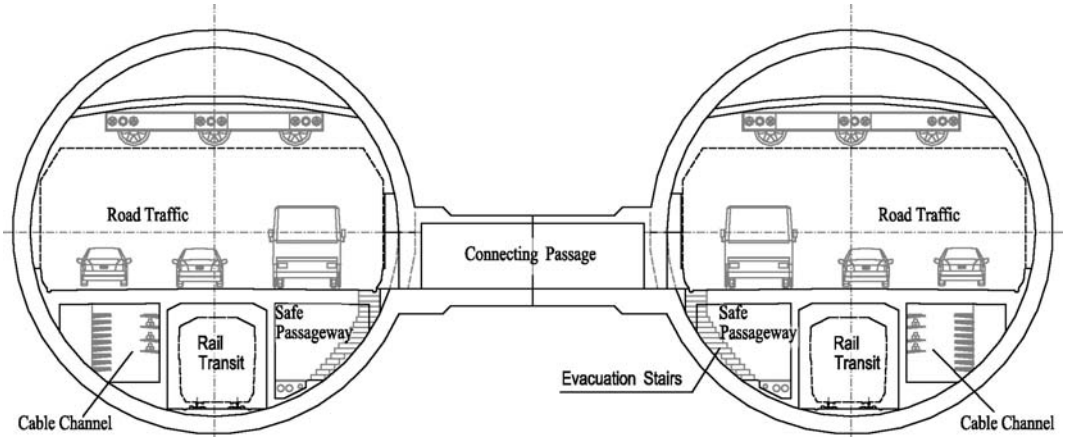

Figure 4. Cross section of bored tunnel.

4 TUNNEL DESIGN SOLUTION

4.1 *Scale*

Shanghai Yangtze River Tunnel is designed as dual 6 lanes expressway, and rail traffic provision is made below the road deck. Seismic fortification level is 7. Design service life is 100 years. The project consists of land connections of Pudong side (657.73 m), river-crossing tunnel (east tube 7,471.654 m and west tube 7,469.363 m) and land connections on Changxing Island (826.93 m). Total length is 8,955.26 m and investment is 6.3 billion RMB. The river-crossing part is twin-tube bored tunnel.

4.2 *Tunnel alignment*

The longitudinal profile of bored tunnel is in a shape of 'W' with a longitudinal slope of 0.3% and 0.87%. The land connections have a longitudinal profile of 2.9%. The minimal curvature radius of horizontal plane is 4,000 m and vertical profile 12,000 m.

4.3 *Building design*

4.3.1 *Cross section of bored tunnel*

Based on structural limit of traffic passage and equipment layout requirement, the internal diameter of lining for bored tunnel is determinated as 13.7 m considering the fitted tolerance of lining at curved section, construction tolerance, differential settlement, and combining the design and construction experience. On the top of tunnel, smoke discharge ducts are arranged for fire accident with an area of 12.4 m^2. Each tunnel has three lanes with a structural clear width of 12.75 m and road lane clear height of 5.2 m. The central part below road deck is for rail traffic provision in future. On the left side, beside the buried transformer arrangement, it also serves as main evacuation stairs. The right side is cable channel, including provision space for 220 kV power cable, as shown in Figure 4.

4.3.2 *Cross-section of land connections*

Working shaft is underground four-floor building: −1 is for ventilation pipe and pump plant for fire fighting; −2 is for road lane with cross over; −3 is for rail traffic provision and power cable gallery and −4 is for waste water pump plant.

The cut-and-cover is designed with a rectangular shape consisting of two tubes and one cable channel. 3 lanes are arranged in each tube. The structural limit is 13.25 m in width and 5.5 m in height, as shown in Figure 5. Upper area with a height of 0.6 m is for equipment provision. The upper part of central gallery is for cable channel, middle part for evacuation and lower part for pipe ditch. Ventilation shaft and building for equipments are arranged above the cut-and-cover tunnel close to the working shaft.

The approach consists of light transition zone and open ramp. The structural limit of cross section is identical with that of cut-and-cover tunnel. Both sides have a slope section with a slope of 1:3 with green planting for protection. The light transition zone is designed as steel arch structure.

4.4 *Structural design*

4.4.1 *Structural design of bored tunnel*

The external diameter of bored tunnel lining is 15,000 mm and internal diameter 13,700 mm, as shown in Figure 6. The ring width is 2,000 mm and thickness is 650 mm. Precast reinforced concrete common tapered segments are assembled with staggered joint. Concrete strength class is C60 and seepage resistance class is S12. The lining ring consists of 10 segments, i.e. 7 standard segments (B), 2 adjacent

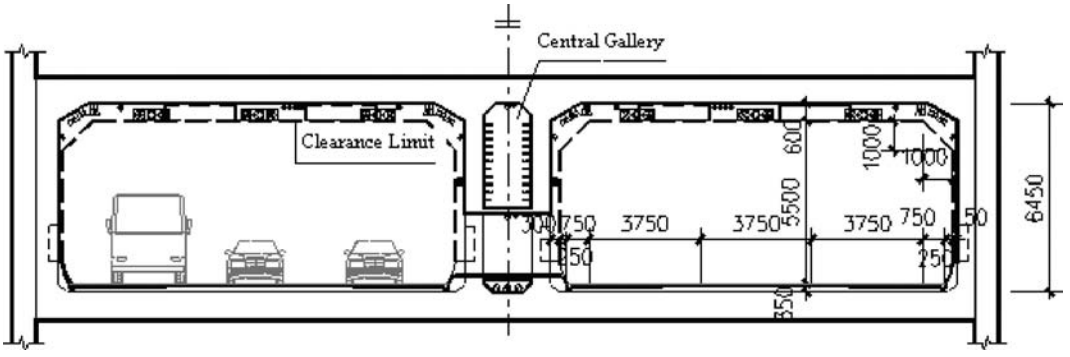

Figure 5. Cross-section of cut-and-cover.

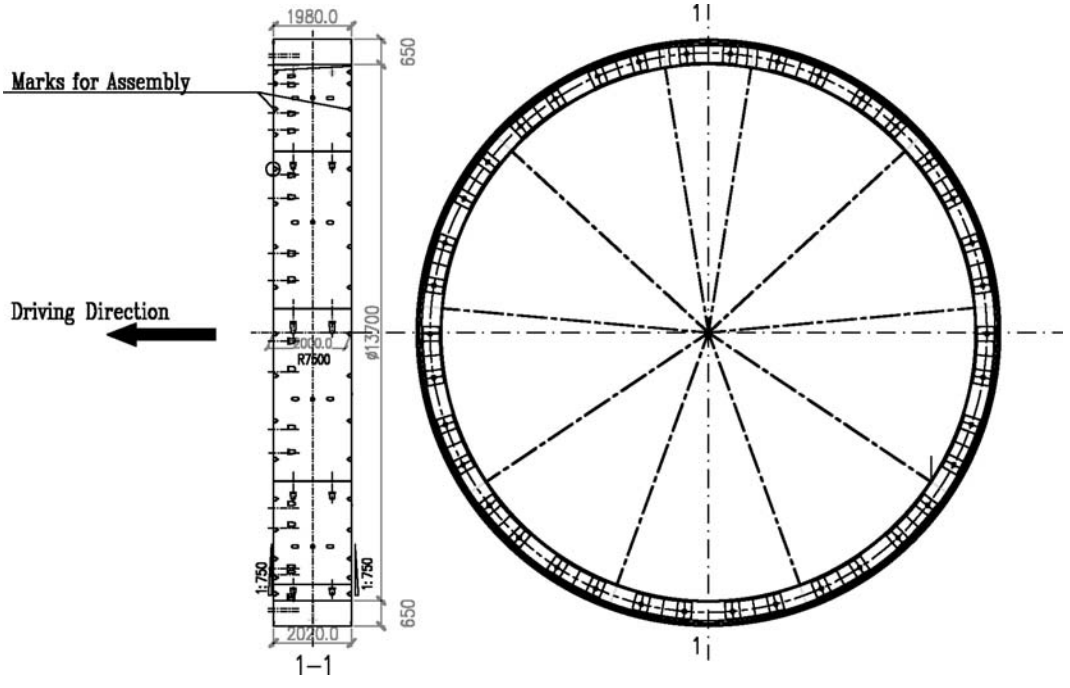

Figure 6. Lining structure.

segments (L), and 1 key segment (F). According to the different depth, segments are classified as shallow segments, middle-deep segments, deep segments and extremely deep segments. Skew bolts are used to connect segments in longitudinal and circumferential direction. 38 × M30 longitudinal bolts are used to connect the rings. 2 × M39 circumferential bolts are used to connect the segments. Shear pins are added between lining rings at shallow cover area, geological condition variation area and cross passage to increase the shear strength between rings at special location and reduce the step between rings.

4.4.2 *Structural design of land connections*

The working shaft and cut & cover tunnel share the same wall. The thickness of diaphragm of working shaft is 1,000 mm, and the inner wall is 500 mm, 1,200 mm, respectively. For the cut-and-cover tunnel, the thickness of diaphragm is 1,000 mm, 800 mm, and 600 mm respectively depending on the excavation depth. The inner structure thickness is 600 mm.

For the open cut ramp, the bottom plate structure thickness is around 500–1,100 mm. Under the bottom plate, bored piles are arranged as up-lifting resistance pile to fulfil the structural floating resistance

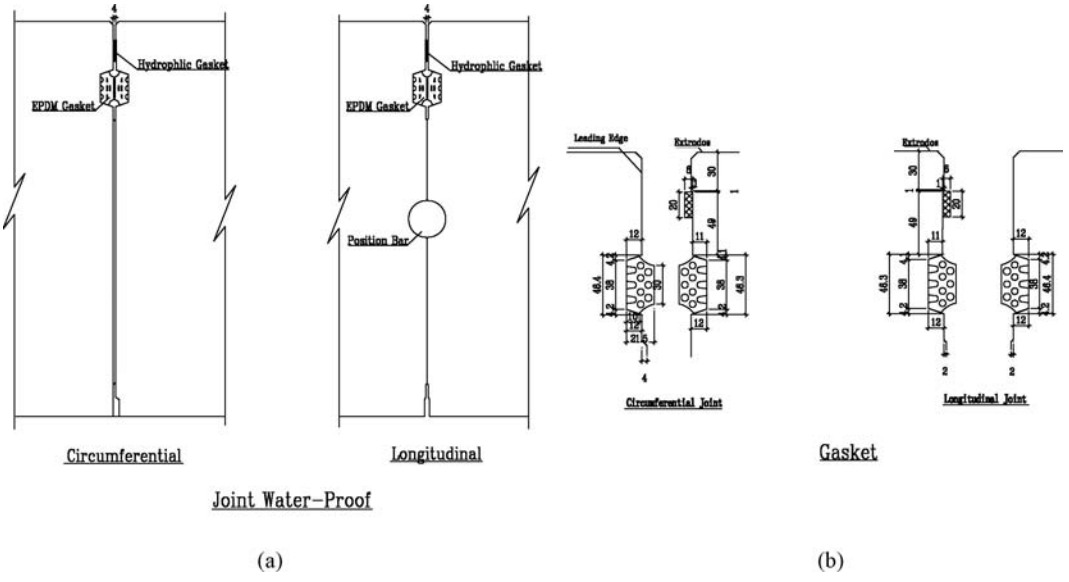

Figure 7. Segment joint water proofing sketch.

requirement. The slope uses in-situ cast reinforced concrete grid and fill earth and green planting in the grid for protection.

4.5 *Structural water-proof and durability design*

4.5.1 *Requirement and standard*

For the bored tunnel and working shaft, the water proof standard of slightly higher than level II is required. For the entire tunnel, the average leakage should be less than 0.05 L/m^2·d. For each random 100 m^2, the leakage should be less than 0.1 L/ m^2·d. The inner surface wet spots should not be more than 4‰ of total inner specific surface area. In each random 100 m^2, the wet spots should not be more than 4 locations. The maximal area of individual wet spot should not be large than 0.15 m^2.

The chloride diffusion coefficient of concrete lining structure of bored tunnel is not more than 12×10^{-13} m^2/s. Concrete seepage resistance class is not less than S12. Furthermore, it is required that under 1 MPa water pressure which is equivalent to 2 times of water pressure for the tunnel with the largest depth, no leakage is occurred when the lining joint opens 7 mm and staggers 10 mm. The safety service life of water proof material is 100 years.

The seepage resistance class of onshore tunnel structure is not less than S10.

4.5.2 *Water proofing design*

The segment joint water proof arrangement consists of EPDM rubber strip with small compressive permanent deformation, small stress relaxation and good aging resistance performance and hydrophilic rubber strip, as shown in Figure 7.

The deformation joint at cut-and-cover tunnel uses embedded water stop gasket, outer paste gasket and inserted sealing glue forming enclosed system. The top plate uses water proof paint as outer water proof layer.

4.6 *Tunnel operation system*

4.6.1 *Ventilation system*

The road tunnel uses jet fan induced longitudinal ventilation combined with smoke ventilation.

The longitudinal ventilation area in tunnel is 82 m^2. Jet fans are suspended above the deck lane and below the smoke discharge duct, supporting induced ventilation in normal operation and congested condition. 78 jet fans with a diameter of 1,000 mm are arranged in each tube from Pudong access to Changxing Island access, every 3 as a group.

Ventilation shafts are arranged on Pudong side and Changxing Island, respectively, housing large ventilation machine and special smoke discharge axial fan. The fans are connected with main tunnel through air inlet and ventilation duct. During normal operation and congested condition, the ventilation machine is turned on to discharge the polluted air in the tunnel. 6 large axial fans with a capacity of 75 m^3/s–150 m^3/s are housed in the working shaft on Changxing Insland and Pudong, respectively.

For normal operation of lower rail traffic, piston ventilation mode is used.

4.6.2 *Water supply and drainage system*

The fire water, washing waste water, and structural leakage are collected by the waste water sump at the lowest point of river. Sump is arranged at upper and lower level, respectively. The lower waste water is drained by the relay of upper sump. The upper sump is arranged on two sides of rail traffic area, housing four pumps which are used alternatively under normal operation and turned on entirely during fire fighting. For lower level, 4 sumps with a dimension of 1,000 × 1,000 × 550 mm are arranged at the lowest point of tunnel where SGI segment is used and above the sump water collection trench with a length of 7 m and a width of 1 m is arranged. One waste water pump is placed in each pit which are used alternatively at normal condition and three are used, one spare during fire fighting.

At each access of tunnel, one rain water sump is arranged to stop water and drain it out of the tunnel. The rain amount is designed based on a return period of 30 years for rainstorm.

4.6.3 *Power supply system*

The electricity load in tunnel is classified as three levels: level I is for ventilation fan, valve, water pump, lighting and monitoring & control system and direct current screen, etc; level II is for tunnel inspection and repair, and ventilation fan in transformer plant; level III is for air conditioning cold water machines.

On Pudong side and Changxing Island, two transformers are arranged. Two independent 35 kV power circuits are introduced respectively and can be used as spare power for the other through two connection cables. Each route ensures the electricity load of level I and II in the tunnel. For the dynamical and lighting load far away from transformers, the power is supplied through 10 kV power supply network in the tunnel and embedded transformers underneath the tunnel to ensure the long distance power supply quality and reduce energy losses. 6 kV power is supplied for the concentrated ventilation fan. Lighting electricity is supplied by independent circuit in power supply system.

4.6.4 *Lighting system*

Light belt is used for lighting in the tunnel. At portal area, natural light transition and artificial light combination is used for lighting. Fluorescence lamp is the main light source in the tunnel. Strengthening lighting uses the high pressure sodium lamp. Taking account of the energy consumption, the application research of LED with high power is being developed. The shift time for emergency lighting in the tunnel should not be larger than 0.1 s and the emergency time is 90 min.

4.6.5 *Monitoring and control system*

The comprehensive monitoring system consists of traffic monitoring system, equipment monitoring system, CCTV monitoring system, communication system, fire automatic alarming system, central computer management system, monitoring and control center. Equipment monitoring system is classified as ventilation subsystem, water supply and drainage subsystem, lighting subsystem, and electrical monitoring subsystem. Monitoring system has access provision for health monitoring system, and expressway net traffic monitoring emergency center, rail traffic monitoring and 220 kV, etc.

The information collected by the tunnel monitoring system, bridge monitoring system, and toll station system is transferred to the monitoring and control center in the tunnel and bridge administration center on Changxing Island. Furthermore, one administration center is arranged at Wuhaogou on Pudong side assisting the daily management and emergency treatment, establishing the three level frame of 'monitoring and control center – administration center – outfield equipment.'

4.7 *Fire-fighting system*

The fire fighting sytem design cosists of balanced and redundant design of safety and function for the entire tunnel structure, building, water supply and drainage and fire fighting, emergency ventilation and smoke discharge, lighting, power supply and other subsystems. The details are as follows:

- Cross passage is arranged every 830 m connecting the upchainage and downchainage tunnel for passenger evacuation with a height of 2.1 m and width of 1.8 m. Three evacuation ladders are arranged between two cross passages connecting the upper and lower level.
- The passive fire proof design uses the German RABT fire accident temperature rising curve. The fire accident temperature is 1,200°C. Fire proof inner lining which ensures the surface temperature of protected concrete segment is not more than 250°C within 120 minutes is selected to protect the arch above smoke duct, smoke duct and crown above the finishing plate. For rectangular tunnel, fire proof material which ensures the structure top plate safety within 90 minutes is selected to protect the top plate and 1.0 m below the top plate. To ensure the passenger evacuation, fire proof bursting resistance fibre is mixed in the concrete bulkhead to achieve no damage of structure when structure is exposed to fire for 30 minutes.
- The ventilation system is designed based on only one fire accident in road tunnel and rail traffic area. The marginal arch area of bored tunnel is used for smoke duct. Special smoke ventilation valve is arranged every 60 m for the smoke ventilation in case of fire accidents on road level. When fire accident occurs in lower level, ventilation fan in the working shaft

is turned on to ventilate the smoke to the side of fire source while passengers evacuate towards the fresh air.

- The emergency lighting is arranged on two sides with the same type. As the basic lighting, inserted into the basic lighting uniformly. Meanwhile, normal lighting and emergency lighting are installed in the cable passage. Evacuation guidance signs are arranged on the two sides of road, cross passage and safety passage. Emergency telephone guidance signs are arranged above the telephones in tunnel.
- Fire water supply at both ends of tunnel is from the DN250 water supply pipe introduced from two different municipal water pipes without fire water pond. One fire fighting pump plant is arranged in working shaft on Pudong side and Changxing Island, respectively. The fire hydrant system is continuous in the longitudinal evacuation passage. Fire hydrant group is arranged every 50 m at one lane side in each tunnel and fire extinguisher group every 25 m. Foam-water spraying system is used in the tunnel which can provided foam liquid continuously for 20 min and arranged every 25 m.
- The communication and linkage of each sub-system of comprehensive monitoring and control system can realize the monitoring, control and test of the whole tunnel such as fan, water pump, electrical and lighting equipment. Fire automatic alarming system can detect the possible hazards such as fire fast, real-time identify and alarm and has the function of passage alarming and tunnel closed. Furthermore, corresponding equipments can be automatically activated to extinguish the fire at early time and organize the hazard prevention to reduce the loss to the minimum extent.

5 Φ 15,430 MM SLURRY MIXED TBM

Two large slurry pressurized mixed shield machines with a diameter of 15.43 m are used for the construction of 7.5 m long bored tunnels.

5.1 *TBM performance and characteristics*

The TBM consists of shield machine and backup system with a total length of 13.4 m and weight of 3,250 t, including cutter head system, shield body, tailskin, main drive, erector, synchronized grouting system, transport system, guidance system and data acquisition system and slurry system.

The TBM has excavation chamber and working chamber. During advancing, the air bubble in the working chamber is adjusted through the control unit to stabilize the slurry level thus balance the water/soil pressure in excavation chamber, as shown in Figure 8.

The thrust system consists of 19 groups thrust cylinders with a total thrust force of 203,066 kN. Cutter

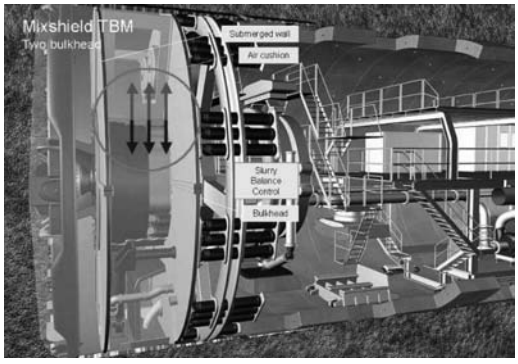

Figure 8. Bulkhead of Mixshield TBM.

head is drived by 15 motors with 250 kW power, so the total power is 3,750 kW. Installation position for two spare motors is also provided. Tailskin seal structure is composed of three rows steel wire brushes and one steel plate brush, forming 3 grease chambers. The erector system is centrally supported with 6 freedom degrees. Vacuum suction plated is used to grasp the segment. 6-point grouting is used for simultaneous grouting.

Backup system consists of 3 gantries: gantry 1 housing the power equipment and control system, gantry 2 housing 3 cranes and bridge section for segment, road element, and other construction material transport, gantry 3 is pipe laying gantry for carrying the extension of the different services such as cable hose, slurry, air and industrial water pipes.

Excavated soil is transported from excavation chamber to the slurry treatment plant (STP) through the slurry pipe in the slurry circulation system. After separation by the treatment equipment, excavated soil with large size is separated and then the recycled slurry is pumped back into excavation chamber and working chamber.

5.2 *Adaptability to the 'large, long and deep' characteristics*

For the TBM construction, firstly the project and crew safety should be ensured. The key for safety of TBM is to protect the cutter head and tailskin, mainly including cutter head design, main bearing seal and tailskin seal assurance. Furthermore, the maintenance and repair of these parts are risk and difficult to access, so the inspection and possibility for maintenance in case of failure must be considered.

5.2.1 *Cutter head and cutting tools*

Cutter head is for soft ground and can be rotated in two directions. The cutter head is pressure resistant steel structure and specific wear protection is arranged

for the periphery area. Special wear protection is also designed for cutting tools.

The closed type cutter head is designed with 6 main arms and 6 auxiliary arms, 12 large material opening and 12 small material opening. The opening ratio is around 29%. 209 cutting tools are arranged on the cutter head, among which 124 fixed scrapers, 12 buckets, 2 copy cutters, 7 replaceable center tools and 64 replaceable tools.

The scrapers are custommade large tools with features of 250 mm width, wear-resistance body and high quality carbide alloy cutting edges whose angle matches the parameter of excavated ground. The scrapers at the edge are used to remove the excavated soil at edge and protect the cutter head edge from direct wear. Copy cutter can automatically extend and retract. The multiple over-cut areas can be setup in the control cabin and corresponding cutting tools position are displayed. The replaceable cutting tools have special seal to prevent the slurry at the front surface enter into the cutter head chamber. During operation, the workers can enter the cutter head chamber to replace the cutting tools under atmospheric condition with high safety, good operation possibility and low risk.

In order to avoid clogging at cutter head center, the opening at center is designed as chute to ease the material flowing. Meanwhile, one bentonite hole is arranged at each opening to ease flushing in case of clogging.

5.2.2 *Main bearing seal*

Two sets seal system are arranged for the main bearing seal design. The outer seal is for the excavation chamber side and inner seal for the shield body with normal pressure. The special seal combination can bear a pressure of 8.5 bar.

Outer seal is to separate the main bearing and excavation chamber. Seal type is axial seal with large diameter, totally 4 lip seals and one pilot labyrinth, thus forming 4 separate areas, as shown in Figure 9.

The inner seal one the gear box side is special axial seal which can carry the pressure of gear chamber.

The seal system has grease lubrication and leakage monitoring system which can monitor the grease amount by pressure and flow monitoring. The seal system has been proved successfully in many projects for several years and become a standard configuration.

5.2.3 *Tailskin*

The tailskin is sealed off by 3 rows steel wire brush and 1 steel plate brush, as shown in Figure 10. Furthermore, 1 emergency seal is arranged between the 3rd row steel wire brush and the steel plate brush. The emergency seal has the function to protect the ring building area from water ingress while changing the

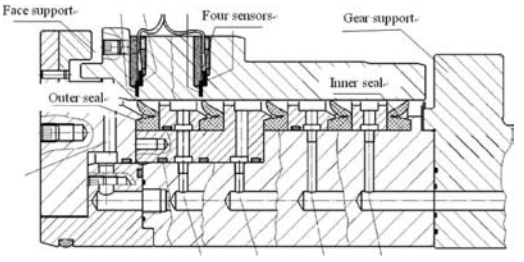

Figure 9. Main bearing seal arrangement.

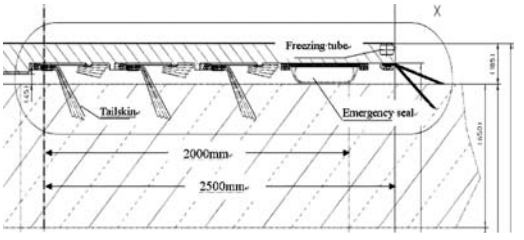

Figure 10. Tailskin structure.

first three steel brush seals. Due to no practical application references of this technology, modeling test has been carried out for the emergency seal installation to confirm the reliability of the emergency seal when the inflatable seal is pressurized to 1 MPa.

Simultaneous grouting lines are arranged at the tail skin, including one standard grout pipeline and one spare pipeline for filling the annulus gap outside the segment after excavation. Furthermore, 19 chemical grout pipes are added for special hardening grout (simultaneous slurry penetrating into cement) or polyurethane for leakage block in emergency condition. 19×3 grease pipes have the function of steel wire brush lubrication and tail skin sealing. The seal system is controlled from the cabinet in automatic and manual modes through time and pressure control.

Furthermore, freezing pipelines are arranged at the tailskin to ease the ground treatment by means of freezing measures in case of leakage and ensure the seal treatment and repair safety.

5.2.4 *Man lock and submerged wall*

During long distance advancing, there is a possibility of operation failure of mixing machine due to large obstacles blocking such as stones, main bearing seal replacement due to wear, submerged wall closed or leakage examination in the air bubble chamber. These maintenance and repair work need workers access the air bubble chamber with a pressure up to 5.5 bar. Therefore, two man locks are arranged to ensure the maintenance and repair workers can access.

The main chamber of manlock can house one 1.8 m stretcher. Under pressure-reducing condition, the medical staff can access the main chamber and organize rescue in case of emergency. Meanwhile, the other man lock can transport the tools, material and equipment from TBM to the air bubble chamber.

The man lock is equipped with poisonous gas detection system which can take the sample of enclosed gas in the man lock. The system information will be displayed at the working position where outside staff is. The man lock also provides the flange connection. Once the rescue and injuries enters into temporary rescue chamber, the temporary chamber can be disassembled fast and transported out of the tunnel, connected with large medical chamber for the convenience of medical work to rescue.

The submerged wall uses hydraulic drive and is equipped with air pressure seal strip. When normal operation in the working chamber is needed, the submerged wall can be closed thus the excavation chamber and working chamber can be separated, and then the valve can be opened for reducing the pressure. At this time, pipe for supplementing slurry which penetrates working chamber can maintain the slurry pressure in the excavation chamber.

6 TUNNEL CONSTRUCTION METHOD

6.1 *Overall arrangement and time schedule*

Based on the overall programming, the construction of working shafts, bored tunnel, synchronous construction of road structure, operation equipment installation and commissioning are the main works and secondary works such as receiving shaft and crosspassage in parallel.

In May 2006, the launching shaft and onshore structures on Pudong side were completed and site assembly of two TBMs started. The east tunnel starts advancing in September 2006, while west tunnel in January 2007. During construction of these two tunnels, the prefabricated road element erection and TBM advancing are synchronous, which on one hand resist the tunnel floating during construction stage and on the other hand provide special truck passage for segments, prefabricated road elements and materials to realize the fast bored tunnel construction. In parallel with bored tunnel construction, the road deck structure construction is also carried out 200–250 m back from segment erection and top smoke duct will start construction in January, 2008, forming gradually working flow in tunnel. After west tube TBM advancing 3 km, the first crosspassage started construction in October, 2007. After the tunnel is through, final connection work of working shaft and road structure is carried out and operation equipment and finishing and pavement work will start.

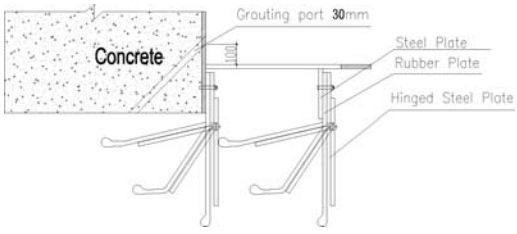

Figure 11. Water stop tank sketch.

6.2 *Main critical technical issues during bored tunnel construction*

6.2.1 *TBM launching and arriving technology*

6.2.1.1 TBM launching

(1) Tunnel eye stabilization

3-axial mixing pile and RJP injection procedure is used surrounding the working shaft to stabilize the ground forming a stabilized area of 15 m in length. 6 dewatering wells for bearing water are supplemented beyond the treated ground area and holes are bored for grouting the annulus to ensure the safety during tunnel gate removal. These three measures application has achieved good performance. During TBM launching, the treated soil is stable.

(2) Tunnel annulus seal

The diameter of tunnel eye is up to 15,800 mm. To prevent the slurry enters into the working shaft from the circular build gap between tunnel eye and shield or segment during launching thus affect the establishment of front face soil and water pressure, good performance seal water stopping facility is arranged. The facility is a box structure with 2 layers water stop rubber strip and chain plate installed, as shown in Figure 11. The outside chain plate is adjustable with 50 mm adjustment allowance. Furthermore, 12 grout holes are arranged uniformly along the outside between two layer water stop on the box for the purpose of sealing in case of leakage at the tunnel eye. The outer end surface of water stop facility shall be vertical to the tunnel axis.

(3) Back support for TBM

The back up shield support includes 7 rings, among which −6 is steel ring composed of 4 large steel segments with high fabrication quality to ensure the circularity and stiffness of the reference ring, as shown in Figure 12. After precise positioning of steel ring, it is supported on the concrete structure of cut and cover tunnel by 19 steel struts with a length of 1.2 m. Other 6 minus closed rings segments are assembled with staggered joint. Inserts are embedded on the inside and outside surface. After each ring building, the circumferential ring and longitudinal ring are connected with steel plate to improve the integrate stiffness and ensure

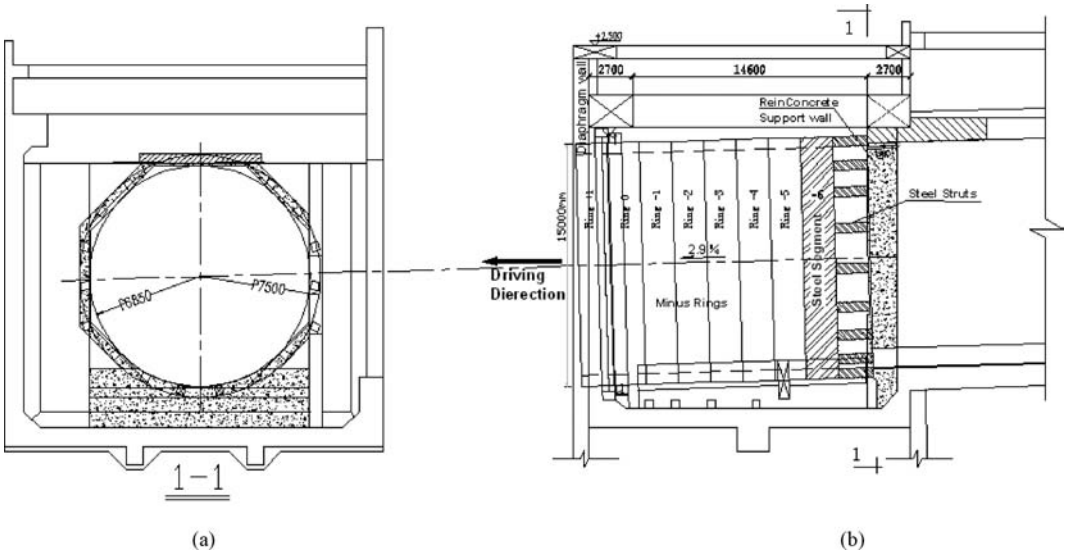

Figure 12. Back supports for TBM.

the circularity and ring plane evenness. Meanwhile, the circumferential plane of each minus ring shall be vertical to the design axis.

6.2.1.2 TBM receiving

(1) Arrangement in receiving shaft

Before TBM receiving, the diaphragm between receiving shaft and cut & cover tunnel and the diaphragm in the receiving shaft between upchainage and downchainage tunnel shall be completed to make the receiving shaft as an enclosed shaft structure. Then MU5 cement mortar is cast in the working shaft with a height of 3 m higher than the TBM bottom. Steel circumferential plate is arranged along the steel tunnel annulus. The inner diameter of steel plate is 5 cm larger then TBM. 18 grout holes are arranged surrounding the tunnel annulus and inflatable bag is installed in the tunnel eye.

(2) TBM arriving

When the cutting surface of TBM is close to the concrete wall of tunnel eye, advancing is stopped. Then pump water in the receiving shaft to the underground water level. Meanwhile, inject double grout into the annulus 30 m back from tailskin through the preset grout hole on the segment to stabilize the asbuilt tunnel and block the water/soil seepage passage between untreated ground and TBM.

After above work, the TBM starts excavation of C30 glass fibre reinforced concrete and accesses the working shaft. The cutting surface accesses into the working shaft and the cutter head will cut the MU5 cement mortar directly and sit on the mortar layer. During accessing into the working shaft, polyurethane is injected through the chemical grouting holes.

(3) Tunnel eye sealing and water pumping

When 2/3 of TBM accesses the receiving shaft, water pumping is started. After pumping the water in the working shaft, continue the TBM advancing and inject the grout timely. When the TBM is in the working shaft, fill air in the inflatable bag in time to make the inflated bag seal the circumferential gap. Meanwhile, grouting is performed through the 18 holes on the tunnel annulus. Grout material is polyurethane. After the gap is fully filled with the grout, the air in inflated bag could be released slowly under close observation. If any water leakage is observed, the polyurethane shall be injected again for sealing.

When the tunnel gate ring is out of the tailskin, the welding work between ring steel plate, seal steel plate and embedded steel plates shall be done immediately to fill the gap between tunnel gate ring and tunnel.

6.2.2 *TBM advancing management*

6.2.2.1 Main construction parameters

During TBM construction, the construction parameters shall be defined and adjusted based on theoretical calculation and actual construction conditions and monitored data to realize dynamical parameter control management.

The advancing speed at beginning and before stop shall not be too fast. The advancing speed shall be increased gradually to prevent too large starting speed. During each ring advancing, the advancing speed shall

be as stable as possible to ensure the stability of cutting surface water pressure and smoothness of slurry supply and discharge pipe. The advancing speed must be dynamically matching with the annulus grout to fill the build gap timely. Under normal boring condition, the advancing speed is set as 2–4 cm/min. If obstacles varying geological conditions are experienced at the front face, the advancing speed shall be reduced approximately according to actual conditions.

Based on the theoretical excavation amount calculated from formula and compared to actual excavated amount which is calculated according to the soil density, slurry discharge flow, slurry discharge density, slurry supply density and flow, and excavation time, if the excavation amount is observed too large, the slurry density, viscosity and cutting face water pressure shall be checked to ensure the front surface stability.

In order to control the excavated soil amount, the flow meter and density meter on the slurry circuit shall be checked periodically. The slurry control parameters are: density $\rho = 1.15$–$1.2\ \mathrm{g/cm^3}$, viscosity $= 18$–25 s, bleeding ratio $<5\%$.

Single type grout is used to inject at 6 locations, which is controlled by both pressure and grout amount. The grout pressure is defined as 0.45–0.6 Mpa. Actual grout amount is around 110% of theoretical build gap. 20 h-shear strength of grout shall not be less than 800 Pa and 28 day strength shall be above the original soil strength.

6.2.2.2 Shallow cover construction

At the launching section, the minimum cover depth is 6.898 m, i.e.0.447D, which is extremely shallow. To ensure the smooth advancing, 1–2 m soil is placed above the top. Meanwhile, in order to prevent slurry blow-out, leakage-blocking agent is mixed in the slurry and surface condition is closely monitored.

6.2.2.3 Crossing the bank of Yangtze River

Before the TBM crossing, the terrain and land feature in the construction surrounding area are collected, measured and photographed for filing. 155 monitoring points are arranged along the bank in 7 monitoring sections. During TBM crossing, the pressure is set according to the water pressure at excavation surface calculated for each ring. The slurry parameter is also adjusted timely based on the surface monitoring information. Grease injection at tail skin is performed well to avoid leakage and synchronous grout amount and quality are strictly controlled.

6.2.2.4 Adverse geological condition

(1) Shallow gas

When the TBM is crossing the deposit on Pudong side, methane gas may be experienced in the shallow area. At this time, the ventilation in the tunnel shall be increased to ensure good ventilation conditions of TBM. The concentration test of methane and combustible gas are carried out.

(2) Lens

Prior to the construction, geological investigation is carried out to learn the general location of prism. During construction, the TBM is set with suitable speed to cross the stratum as fast as safely possible.

(3) Bored hole

Due to the tunnel alignment adjustment, 9 geological bored holes will be experienced along the TBM advancing. During crossing, slurry with large density is used and polyurethane is injected surrounding the tunnel after crossing.

6.2.3 *Quality assurance technical measures for large tunnel*

6.2.3.1 Segment prefabrication

Nine sets steel formwork with high preciseness are used for segment prefabrication to fulfill the technical requirement to segment such as allowable width tolerance ± 0.40 mm, thickness tolerance $+3/-1$ mm, arc length ± 1.0 mm, circular surface and end surface plainness ± 0.5 mm. In order to control prefabrication preciseness strictly and ensure the production quality, special laser survey system is introduced to conduct accurate measurement of segment profile dimension beside traditional survey measurement tools and segment trial assembly.

Fly ash and slag are mixed in the concrete for segment prefabrication. Strictly concrete casting, vibrating and curing procedures are used to control cracks and achieve the water proofing and durability requirement.

6.2.3.2 Segment assembly

The segment assembly shall satisfy the fitted tunnel design axis requirement by segment selection (rotation angle) and meanwhile make the longitudinal joint not on the same line. During the whole assembly process, for straight line, the principle is to erect on left and right at intervals. For curved section, the suitable segment rotation angle shall be selected based on TBM attitude, and segment lipping data.

Secondly, the relative dimension between segment and shield shall be checked to correct the positioning of each ring segment.

Then, each segment building shall be closely contacted. The ring plane and 'T' joint shall be even.

Finally, strictly control the lipping of ring. When the segment lipping exceeds the control value, the rotational angle of segment shall be adjusted timely to ensure the verticality between segment and tunnel axis.

6.2.3.3 Floating-resistance of tunnel

Due to the tunnel diameter up to 15 m, the floating resistance and deformation control during

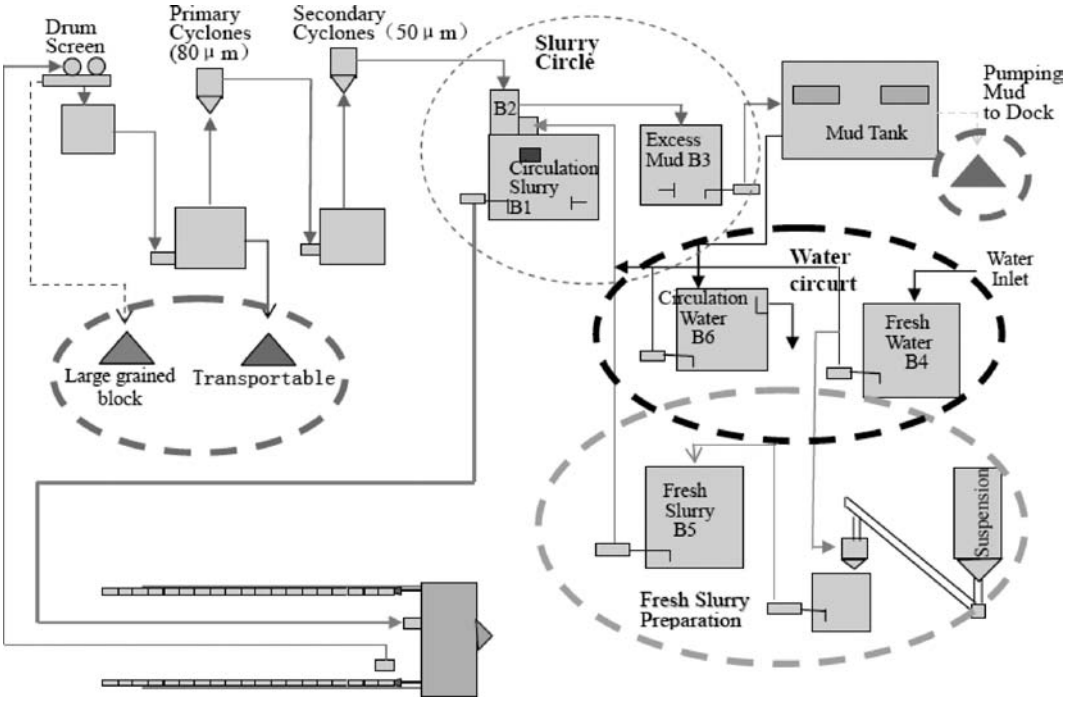

Figure 13. STP system flow chart.

construction for large diameter tunnel are very challenging. The technical measure is mainly to improve the synchronous grouting management. Mortar type grouting material with cementation property is injected at multi-points. Furthermore, grout package with certain strength shall be formed surrounding the tunnel timely to resist the tunnel upfloating. Meanwhile, the tunnel axis shall be strictly controlled during construction and the tight connect between segments shall be improved to achieve the tunnel-floating resistance.

6.2.3.4 Ground deformation control

The ground settlement during TBM construction is mainly contributed by the front surface slurry pressure setup, annulus grouting and shield body tamper. Therefore, the ground settlement variation can directly reflect the TBM construction parameters setup. The crew can correct the construction parameter based on settlement monitoring to increase the deformation.

6.2.4 *Back-up technology for long distance TBM construction*

6.2.4.1 Slurry treatment and transport

The slurry separation system consists of subsystems of treatment, conditioning, new slurry generation, slurry discharge and water supply; with a capacity of 3,000 m^3/h to fulfill the advancing requirement of 45 mm/min, as shown in Figure 13. Based on the geological conditions along the tunnel alignment, the treatment system selects 2 level treatment methods. The initial treatment uses two rolling shieve to separate soil with a size of larger than 7 mm. For secondary treatment, firstly grain with a size of large than 75 is separated by $4 \times \phi$ 750 mm cyclones and then grain with a size of large than 40 μm is separated by $12 \times \phi$ 300 mm cyclones. The slurry spilled at the top of cyclone is transported to conditioning tank for reuse. After adjustment, the density of supplied slurry is 1.05–1.35 g/cm^3. The maintained optimal value is between 1.20 and 1.30 and d50 is between 40 and 50 μm. The STP system circulation efficiency is up to 70%. Discharged slurry and waste is transported to the bardge at riverside by pipes and trucks. The slurry supply pipe has a diameter of 600 mm and discharge pipe 500 mm. To ensure the long distance slurry supply velocity of 2.5 m/s and discharge velocity of 4.2 m/s to avoid slurry settlement in pipe and maintain not too high pressure in the pipe, one relay pump is arranged every 1 km. The pressure at pump outlet is controlled within 10 bar.

6.2.4.2 Axis control and construction survey guidance

Static measurement with GPS control net is used for surface control survey. For elevation control, GPS elevation fit method is used for elevation transfer. Part of basic traverse mark every 500 m is selected as main

traverse. In the tunnel, level II subtraverse is used for the plane control, i.e. construction traverse and control parallel traverse. The control mark has a spacing of 600–900 m. The elevation control survey in tunnel uses level II. The fixed level mark is arranged with a spacing of 80 m.

6.2.4.3 Construction ventilation and fire protection

Due to the large diameter, long distance and 'W' longitudinal slope, especially when the TBM is advancing with a upgrading slope, the heat and humidity generated at the working face can not be discharged naturally thus concentrate at the working face in a shape of fog. Meanwhile, heavy trucks for construction material transport also cause a large amount of waste air in the tunnel. Bad environment will have unfavorable influence on TBM equipment and crew, and also affect the smooth progressing of survey activity.

During construction stage, 2 special axial fans (SDF-No18) are arranged on the surface to provide fresh air to the space below road deck in the tunnel, then the relay fan and ventilation system equipped on the gantry will transport the fresh air to working surface. Meanwhile, other ventilation equipment on the gantry provides fresh air to main secondary equipments of TBM such as transformer, hydraulic equipment and electrical installations.

Adequate fire extinguishers are arranged in the shield and gantry and also oxygen, poisonous gas protection mask are equipped. Fire extinguisher is equipped on each transport truck. Safety staff is equipped with portable gas analysis device for check the air quality in tunnel every day.

6.2.4.4 Material transport

Segment, grout and prefabricated elements, etc are transported to the working area by special trucks from ramp area, through cut & cover tunnel and road deck which is constructed synchronously. Truck transport can avoid the derailing problems during traditional electrical truck transport. Furthermore, the truck has two locos, so the transport efficiency is high.

Prefabricated road element is transported to the gantry 2 by trucks and then lifted and erected by the crane on the bridge beam. Segments are transported to gantry 2 and then transferred to the segment feeder by the crane on the bridge beam and then transported to erection area.

6.2.5 *Critical equipment examination and replacement technology*

6.2.5.1 Main bearing sealing

Four supersonic sensors are installed in the seal arrangement for monitoring the main seal wear condition. Once the abrasion reaches certain value or grease leakage is monitored in the tank, it indicates the main seal needs to be rotated to another oritentation.

Once the seal wear is observed beyond preset value, the surface could be moved to ensure the replacement of main bearing seal. During replacing, the slurry in the chamber must be drained and provide effective support to excavation face. The operation staff shall go to the slurry camber to replace the seal under certain pressure.

6.2.5.2 Abrasion measurement and replacement of cutting tools

The system will be installed on 8 selected scraper positions as well as on two bucket positions. It will be connected to a plug at the rear of the cutting wheel to allow for simple condition diagnosis from a readout device. Conductor loop is embedded in the device. The wear condition of cutting tools can be indicated by checking the closed/open status of loops.

The worker accesses the cutting wheel arms from the center of the main drive. The worker installs the lowering/ lifting frame (with bolts) and screws it to the fixing plate of the tool. The fixing plate is then unscrewed. The worker will then lower the tool using the frame (with bolts). The pressure-tight gate will be closed down. The worn out tool shall be then exchanged with a new one. The tool will be lifted to position behind the gate. The gate will be opened. Then the tool will be put in its final position. The fixing plate is then screwed to the tool support. The frame is transferred to the next tool.

6.2.5.3 Tail seal and steel wire brush replacement

When the leakage is experienced at tail skin, and steel brush is defined to be replaced necessarily, open the emergency sealing and erect special segments. Strengthen the surrounding soil at tail skin with freezing method and then replace first 2 or 3 rows steel brush.

6.3 *Synchronous construction of road deck*

The synchronous construction of road structure includes erection of road element, segment roughening and drilling for inserting rebar, prefabrication of two side ballast, insitu cast corbel and road deck on two sides. According the variation and trend of asbuilt ring deformation and settlement, and the construction progress of 12 m (6rings) per day and based on the requirement of deformation joint arrangement every 30 m, the construction is organized and arranged as flowing operation every 15 m. As shown in Figure 14, the basic construction procedure is as follows:

- Road element installation, 25 rings later than segment erection
- Segment roughening includes the junction surface between ballast and segment and segment inner surface at corbel. The insert bar placing includes the Φ16 bar at ballast and Φ20 bar at corbel. The

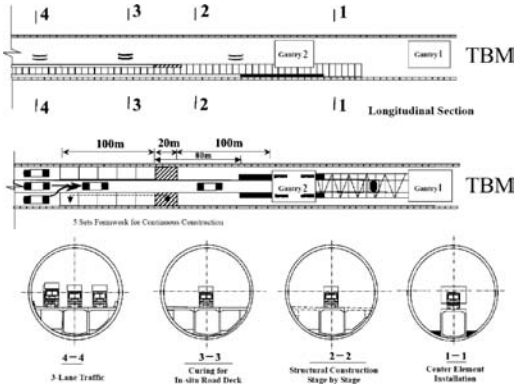

Figure 14. Synchronous construction flow chart.

roughening works at ballast position is carried out at gantry 2, and the roughening operation platform at corbel is fixed to gantry 2. Insert bar placing is following gantry 3. The roughing machine is equipped with dust suction facility which can eliminate the dust to maximum extent.

- Reinforcement placing, formwork erection and concrete casting for ballast is carried out at 15 m behind the gantry 3 and 15 m more behind for corbel, and then another 15 m for road deck. Road deck concrete casting works are located at 250 m–300 m from the segment erection area. After casting, the curing with frame lasts 3 days and formwork is removed on the 4th day. After 28 days curing, the road deck can be open to traffic. During curing, the road deck area is separated. Concrete mixing truck is used for concrete casting.

6.4 *Cross passage construction*

The cross passage which connects the two main tunnels has a length of around 15 m and diameter of 5 m. The construction will be by freezing method for soil strengthening and mining method for excavation.

The freezing holes are arranged as inside and outside rows which are drilled from two sides. The freezing is done from one side or both sides. Inside row holes are drilled from upchainage tunnel, 22 in total and outside row holes are drilled from downchainge tunnel, 18 in total.

Mining method will be used for excavation by area division. Firstly, pilot with a horn opening is excavated, and then the cross passage is excavated to design dimension. The fullsection excavation is done with a step of 0.6 m or 0.8 m.

When the main structure concrete strength reaches 75%, enforced thawing will be carried out. The hot brine for thawing circulates in the freezing pipe and the frozen soil is thawed by section. Based on the informational monitoring system, the soil temperature

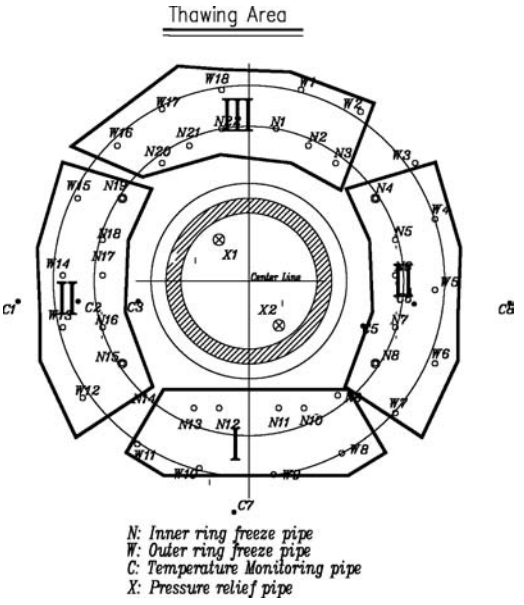

Figure 15. Divided thawing area of cross passage.

and settlement variation is monitored. Grouting pipe is arranged at shallow and deeper area for dense grouting. The overall principle for thawing is to thaw the bottom part, then middle part, and lastly the top part, as shown in Figure 15. When thawing by section is done in sequence, one section is being thawed and subsequent sections maintain the freezing for the purpose of maintaining the cross passage structure and main tunnel as an integrated part thus settlement avoidance before the section grouted.

6.5 *Land connections construction*

The profile dimension of working shaft is 22.4×49 m, with a depth of 25 m. 1.0 m thick diaphragm with a depth of 45 m is used for retaining structure. Open cut is used for excavation. The support system consists of 5 layers reinforced concrete and 1 layer steel support. Inside the pit, 3 m below the bottom, injection is done interval to make the strength not lower than 1.2 MPa. 13.5–16.0 m outside the working shaft is treated. For diaphragm at the TBM accessing into the receiving shaft, GFPR is used instead of normal reinforcement so that the TBM can cut the retaining wall directly and thus avoid the reinforcement cutting and tunnel eye concrete removal, which simplifies the construction procedure, accelerates construction progress and reduces the construction risk.

The excavation depth of pit for Pudong cut-and-cover is 23.1–9.9 m, and Changxing cut-and-cover 17.2 m–8.4 m. According to the excavation depth, diaphragm with thickness of 1.0 m, 0.8 m and 0.6 m is

selected respectively. The support system is composed of reinforced concrete support and steel support. 3 m underneath the pit bottom is strengthened by rotating injection and also the junction between working shaft and cut-and-cut outside the pit to ensure the pit excavation stability.

The ramp is open cut with a slope of 1:3. The slope is protected through green planting in the reinforced concrete grid which is anchored in soil by anchors to prevent from sliding. In order to avoid slope sliding, the slope is strengthened by cement mixed piles with a diameter of 700 mm.

7 CONCLUSION

During the process from planning to implementation, Shanghai Yangtze River Tunnel has experienced various challenges. Technical support of tunnel construction from China and abroad is provided. With independently developed and owned IPR and featured TBM tunnel construction theory and core technology is established, forming the core technology of large and long river-crossing TBM tunnel in China. Special technical issues such as lining structure design of extremely large tunnel, long distance TBM construction and hazard prevention system for long and large tunnel achieve to be internally state-of-art. Relevant standards, codes, guidance, specification and patent technology are developed to improve the technical system of tunnel construction in China and upgrade the internal competence of tunnel engineering.

REFERENCES

Cao, W.X. et al. 2006. Shanghai Yangtze River Tunnel Project design. *Shanghai Construction Science and Technology* 5: 2–6.

Chen, X.K. & Huang, Z.H. 2007. Shanghai Yangtze River Tunnel TBM cutting tools wear detection and replacement technology. *The 3rd Shanghai International Tunneling Symposium Proceedings: Underground project construction and risk provision technology*: 152–157. Tongji University Publication Company.

He, R. & Wang, J.Y. Shanghai Yangtze River Tunnel synchronous construction method statement. *The 3rd Shanghai International Tunneling Symposium Proceedings: Underground project construction and risk provision technology:* 168–177. Tongji University Publication Company.

Sun, J. & Chen, X.K. 2007. Discussion of TBM selection for Shanghai Yangtze River Tunnel. *The 3rd Shanghai International Tunneling Symposium Proceedings: Underground project construction and risk provision technology*: 91–98. Tongji University Publication Company.

Yu, Y.M & Tang, Z.H. 2007. Shanghai Yangtze River Tunnel construction survey technology. *The 3rd Shanghai International Tunneling Symposium Proceedings: Underground project construction and risk provision technology*: 158–167. Tongji University Publication Company.

Zhang, J.J. et al. 2007. Shanghai Yangtze River Tunnel TBM launching construction technology. *The 3rd Shanghai International Tunneling Symposium Proceedings: Underground project construction and risk provision technology:* 144–151. Tongji University Publication Company.

Special lectures

The Shanghai Yangtze River Tunnel - Theory, Design and Construction – Huang (ed)
© 2008 Taylor & Francis Group, London, ISBN 978-0-415-47161-9

Fire evacuation and rescue design of Shanghai Yangtze River Tunnel

W.Q. Shen, Z.H. Peng & J.L. Zheng
Shanghai Tunnel Engineering & Rail Transit Design and Research Institute, Shanghai, P. R. China

ABSTRACT: This article focuses on the tunnel fire, which has been a world concerning problem, especially in large and long road tunnels. Analysis and research are made from three aspects such as planning of fire evacuation and rescue organization, equipment preparation & layout, and flow organization of people and vehicle under fire condition. A feasible evacuation and rescue design is worked out on the basis of the features of Shanghai Yangtze River Tunnel.

1 INTRODUCTION

Shanghai Yangtze River Tunnel runs from the Pudong Wuhaogou in the south, crossing the south channel of the Yangtze River Estuary, and ends on Changxing Island. Its total length is 8,955 m. The tunnel is constructed by shield machine. The tunnel outside diameter is up to Φ 15.0 m. This tunnel engineering scale ranks top in the world. In the shield tunneling section, its upper level is a highway tunnel while its lower level is reserved for rail transit. Shanghai Yangtze River Tunnel, compared to the previous medium and small tunnels, has a more severe conflict in ventilation and fire control because of its long distance and large diameter. Any fire in a tunnel will paralyze transportation of the whole tunnel, lead socioeconomic losses and also bring serious negative effects to the society. To relieve fire hazards, the firefighting design of Shanghai Yangtze River Tunnel follows the "human-based" philosophy and puts emphasis on practicability. The design is briefly introduced hereinafter.

2 FIRE EVACUATION AND RESCUE DESIGN

The fire evacuation and rescue design of a long and large tunnel mainly contains planning of fire rescue organization, linkage of water supply, ventilation and exhaust equipments under a fire condition and organization of people and vehicle evacuation under fire condition. Therefore, in the design of Shanghai Yangtze River Tunnel, feasible rescue organization and implementation flow, safe and reliable fire-extinguishing system, reasonable ventilation and exhaust mode and quick evacuation route from fire site are worked out according to its functional characteristics.

3 PLANNING OF FIRE EVACUATION AND RESCUE ORGANIZATION

Prior to the fire evacuation and rescue design, a preliminary planning of evacuation and rescue organization shall be made. The planning consists of evacuation of passengers from fire site and entry of rescuers into the tunnel.

Based on the overseas experience in tunnel design and the psychological bearing ability of passengers in evacuation from fire site, the evacuation should be optimally controlled within 25 minutes, that is, in 25 minutes, all passengers have evacuated to a safe space isolated from fire. The shield tunnelling section of Shanghai Yangtze River Tunnel is approximately as long as 7.5 km. Cross passageways (8 in total) for evacuation and rescue are set up every 830 m. Due to such large intervals, auxiliary evacuation facilities are provided to work with the cross passages. Smoke exhaust and water firefighting facilities are provided to ensure that passengers can safely evacuate from fire site.

Besides the "evacuation time", the factor that has a great effect on hazard level of a fire in a tunnel is "rescue time". Rescuers of the Shanghai Yangtze River Tunnel are arranged in 3 formations. Initial firefighting is generally conducted by passengers in the car on fire (the 1st formation), tunnel operators and policemen (the 2nd formation), and fire brigade (the 3rd formation). The initial firefighting is especially important. In addition to the firefighting systems in the tunnel, a dedicated firefighting station should be set up at one of tunnel entrances. In light of tunnel fire cases and tunnel fire test, the professional rescue team shall arrive at fire site as soon as possible, generally within 15 minutes. Otherwise, it will get much harder for rescue and fire extinguishing.

4 DESIGN OF FIREFIGHTING EVACUATION AND RESCUE FACILITIES

Based on the above planning of evacuation and rescue organization, separate exhaust duct is designed in the tunnel so that smoke can be exhausted from the nearest duly-opened damper in the case of a fire, which prevents a great deal of smoke from longitudinal propagation along the tunnel, reduces smoke concentration in driveway and save time for evacuation and rescue of passengers. In addition to the 8 cross passages (the primary escape facility that makes the twin tunnels back up each other), longitudinal emergency passage is set up under the road slab of each tunnel and escape stairs are set up to connect the highway and the lower rail transit space. The above design composes a cross and longitudinal evacuation and rescue system for the tunnel (Fig. 1).

At present, for the newly-built tunnels crossing Shanghai Huangpu River (shield method), cross passages are built at about 500 m intervals in general (such as East Fuxing Road Tunnel, Dalian Road Tunnel and Xiangyin Road Tunnel). The intervals of cross passages in foreign existing highway and road tunnels are shown in Table 1.

Since Shanghai Yangtze River Tunnel is located at the estuary of the Yangtze River, engineering construction conditions is complex. There are many risks in construction of cross passage. The design achieves an integrative balance between construction risk and operation risk (including fire accident risk). The interval of cross passages is defined to be about 830 m in consideration of automatic firefighting systems and concentrated smoke exhaust systems in the tunnel. Based on such intervals, the whole shield tunnelling section is equipped with 8 cross passages. The

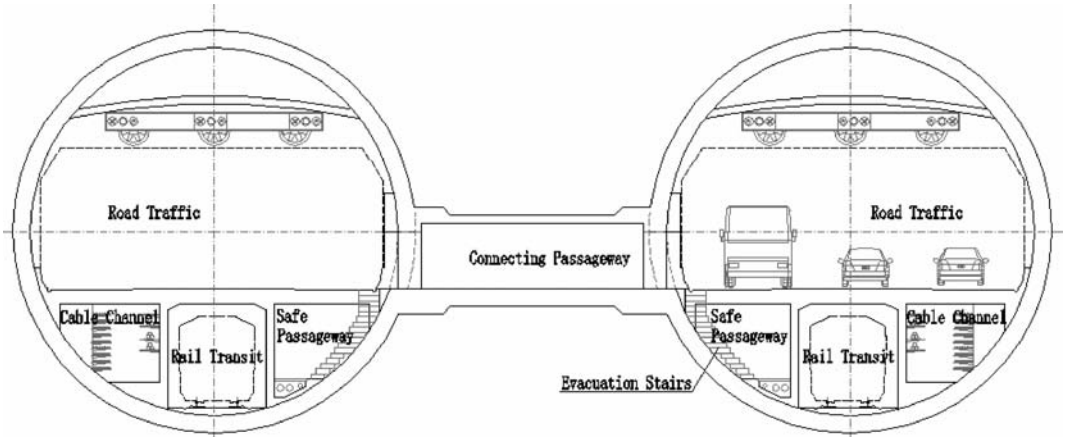

Figure 1. Standard cross section of Shanghai Yangtze River Tunnel.

Table 1. Intervals of cross passage in foreign existing highway and road tunnels.

Tunnel name	Tunnel length	Country	Time	Interval of cross passage	Notes
Kingsway Tunnel	2.20 km	UK	1971	Approx. 335 m	
Tokyo Bay Tunnel	9.5 km	Japan	1997	None	Downward escape exits and escape slides are set up every 300 m under the driveway slab, and longitudinal rescue passageways (evacuation passageways) are set up under the driveway slab.
H-3 Tunnels	/	USA	1997	500 ft	
Westerschelde Tunnel	6.60 km	Netherlands	2002	250 m	
The Fourth Elbe Tunnel	4.40 km	Germany	2003	1.0 km	
Strenger Tunnel	5.75 km	Austria	2004	500 m	
Weser Tunnel	1.60 km	Germany	2004	327 m	
Herren Tunnel	1.06 km	Germany	2005	2 connecting passageway	

passageways are wide enough to accommodate three people or two equipped firefighters. The clearance of the passage is 1.8 m wide and 2.1 m high. The highway level and rail transit level are interlinked by escape stairs. The interval of the escape stairs is about 280 m, and 3 staircases are set up between two cross passages. Once the highway level catches fire, passengers can go to the other tunnel via the cross passages or evacuate to the lower emergency passage via the stairs. Once the rail transit level gets on fire, passengers in the train can go to the upper highway tunnel via the escape stairs and then go to the other tunnel via the cross passages to wait for rescue.

In the evacuation and rescue design of Shanghai Yangtze River Tunnel, the access hatch and cover plates of the escape stairs are key structures. The design of the hatch dimension considers the capacity in escape and the influence on driveways. The deadweight of the cover plates is also crucial in the design because flexible opening and closing of the plates may improve the efficiency in escape. Based on a lot of design scheme comparisons and fabricated 1:1 on-site model test, the width of escape stairs is designed to be 0.7 m, which is enough for one people to pass. The hatch consists of 1 m wide hole and 0.8 m wide hole, and their wide-opened parts are designed to closely integrate with the plane curves of escape stairs. On the principle of no head-touching, the hatch is designed as long as 2.8 m. The cover plates are made of a cast iron with good corrosion resistance and high strength. A booster is set up under cover plate to ensure easy turn-up. Visible emergency evacuation marks are attached to upper side and lower side of cover plate and cross passage, and a yellow forbidden line is marked on road deck at each cover plate to indicate that no vehicle is allowed to be parked at the site of each hatch in any case (Fig. 2).

5 EQUIPMENT OF HAZARD PREVENTION AND RELIEF

The firefighting system for highway tunnel consists of fire hydrant, fire extinguisher and foam-water spray linkage system. Every 25 m is considered as a protection unit. The foam-water spray linkage system exterminates an initial fire and cools major structures of the tunnel for protection and creates conditions for firefighter's extinguishment.

The upper highway tunnel adopts longitudinal ventilation by jet fan and concentrated smoke exhaust system. In a normal or clogged condition, longitudinal ventilation is activated. In the case of fire, arched exhaust duct on the top of the round tunnel will be used for exhausting smoke. Jet fans are hung on the exhaust duct over each driveway to assist inductive ventilation in the case of normal and clogged transport.

According to *Subway Tunnel Design Regulation*, the lower space of rail transit is equipped with one fire hydrant every 50 m. And the space is longitudinally ventilated.

Monitoring system consists of automatic fire alarm subsystems and communication subsystem.

Firefighting equipments, passive fire prevention of major tunnel structure and emergency lighting systems have a good effect on hazard prevention and mitigation.

6 PEOPLE AND VEHICLE FLOW ORGANIZATION UNDER VARIOUS FIRE CONDITIONS

Evacuation direction in fire is another important part of design. On-fire points in Shanghai Yangtze River Tunnel would either on the highway tunnel level or on

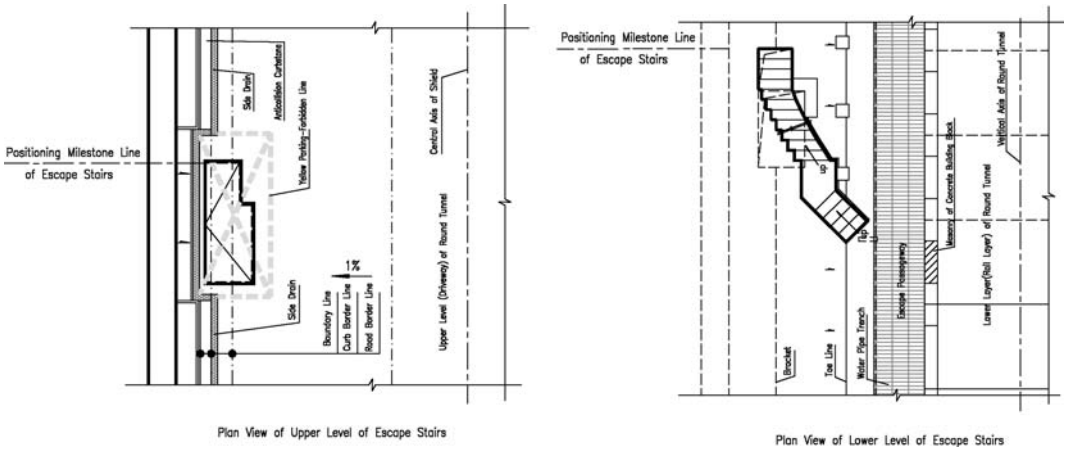

Figure 2. Escape stairs and safe exits.

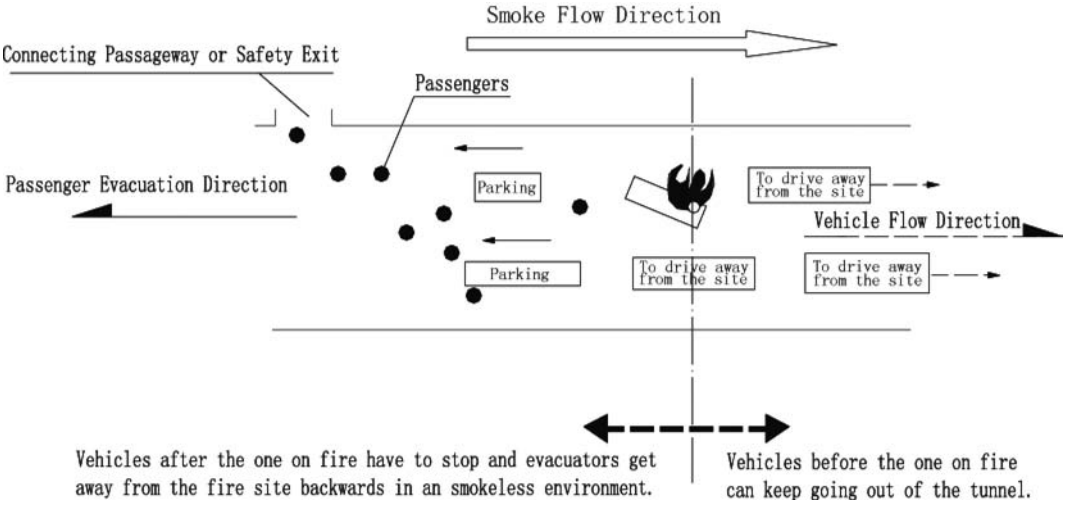

Figure 3. Passenger evacuation in a normal operation condition.

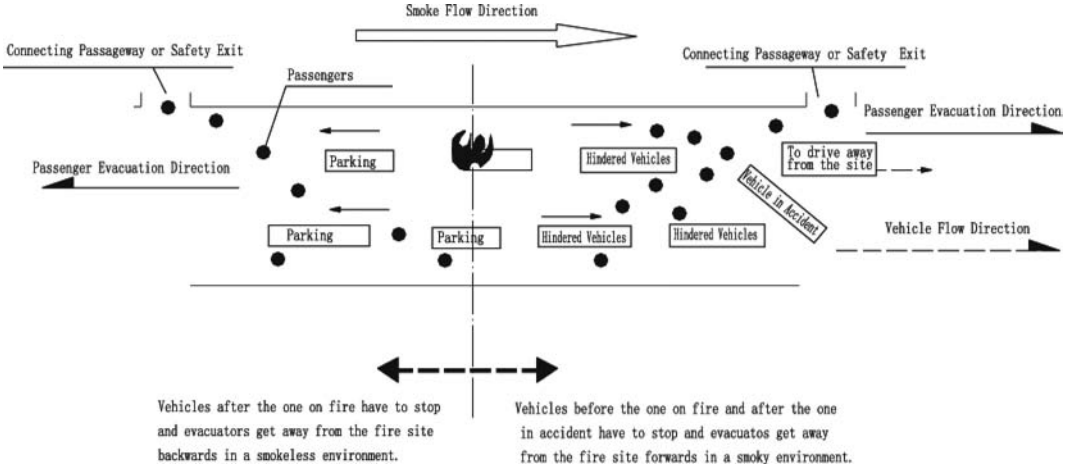

Figure 4. Passenger evacuation in a clogged operation condition.

the rail transit level. In design, only one fire is considered. The fires happening in the highway tunnel can be divided into fire in a normal operation condition and fire in a clogged operation condition.

Case 1: fire breaks out in normal traffic operation. In such a case, vehicles before the one on fire can keep moving while those after the one on fire have to stop by the blocked way forward but not allowed to park within the yellow forbidden line of each hatch (Fig. 3). After identifying the position on fire, central control room will activate a hazard relief program. In the program, the exhaust system is activated; jet fans necessary are switched on to prevent smoke from spreading to the rear area of the fire source. The optimal evacuation route guided by variable information board and public radio will help passengers to evacuate the site quickly and arrive at a smokeless environment. In such a case, the nearest cross passage is the best evacuation route. If there's no cross passages around, passengers can first go to the lower level via the nearest escape stair, and then go to the upper level again via another escape stairs away from fire, and finally go to the other tube by cross passage. Meanwhile, fire brigade can quickly reach the fire site via longitudinal emergency passage and cross passage. Therefore, in a normal operation condition, a fire will not have a great adverse effect on passengers in the tunnel.

Case 2: fire breaks out in jam resulting from a traffic accident. Passengers between the vehicle in accident and the vehicle on fire have to evacuate in a smoky

environment. See Figure 4. Owing to the equipped exhaust system, smoke can be controlled 2.0 m above the road. Passengers in a smoky environment shall be led to a forward cross passage or to longitudinal emergency passage via escape stairs as soon as possible. For a smokeless area, evacuation route shall be based on a principle of proximity, same as that in a normal operation condition.

Case 3: rail transit train catches fire in the tunnel. Vehicles running on the upper highway tunnel should be evacuated at time and vehicles should be forbidden entering the tunnel. The highway tunnel will be used as a passage for evacuation and rescue. Fans in shaft should be switched on to discharge smoke. Passengers in train shall evacuate to the upper highway level against fresh air through emergency passage and escape stair. Meanwhile, ventilation system of the highway tunnel should stop running so that rescuers can go to the lower level to deal with the emergency.

7 CONCLUSION

In the fire design of Shanghai Yangtze River Tunnel, the highway level and the rail transit level are back up mutually; and a series of reliable safety systems is designed in the tunnel, including the fire monitoring system, emergency evacuation system and firefighting system. When a fire occurs in the tunnel, the fire location should be identified firstly, and then a proper ventilation mode, optimal routes for vehicle driving, passenger evacuation, and fire brigade rescue should be implemented to minimize the fire hazard.

REFERENCES

Ove arup & Partners Hong Kong Limtied. 2003. *Special Report XIV of Risk Analysis and Research of Chongming River-crossing Passage Project: Tunnel Fire Risk Analysis.*

Shanghai Tunnel Engineering & Rail Transit Design and Research Institute. 2006. *Study on Design Technology and Hazard Prevention System of Long and Large Shield Tunnel.*

The Shanghai Yangtze River Tunnel - Theory, Design and Construction – Huang (ed)
© 2008 Taylor & Francis Group, London, ISBN 978-0-415-47161-9

Shanghai Yangtze River Tunnel & Bridge Project management based on lifecycle

X.J. Dai
Shanghai Changjiang Tunnel & Bridge Development Co., Ltd., Shanghai, P. R. China

ABSTRACT: Complex project system requires integrated management based on project lifecycle. By the application of integrated organization and project information system, Shanghai Yangtze River Tunnel & Bridge Project realizes the project lifecycle targets. With effective safety management and quality control system, the project construction is guaranteed. And the establishment of project regulation and culture promote the project progress. This paper makes in-depth analysis and discussion of the main components of Shanghai Yangtze River Tunnel & Bridge Project.

1 PROJECT BRIEF INTRODUCTION

As a large-scale transportation infrastructure project in Yangtze River delta of China, Shanghai Yangtze River Tunnel & Bridge Project is one key national high-way project to link up Shanghai land-based areas with Changxing and Chongming Islands. This project adopts the scheme of "South Tunnel and North Bridge" in total length of 25.5 km. Yangtze River Tunnel links the Wuhaogou in Pudong District and Changxing Island, and measures 8.95 km including 7.5 km across the water area. And Yangtze River Bridge crosses Yangtze River North Channel waterway to reach Chenjia Town in Chongming Island, and measures 16.55 km including 9.97 km across the river. In addition, the rail transportation space has been considered to remain in this project planning to utilize limited resources effectively and save construction investment.

1.1 *Project technical specialties*

Shanghai Yangtze River Tunnel & Bridge Project is the largest project combined with tunnel and bridge currently under construction in China, and plenty of construction technique is applied for the first time in the world. Firstly, Yangtze River Tunnel & Bridge Project is a complicated system in technology.

- The specialties such as long pushing distance, big diameter and deep embedded position, have brought extremely high requirements for equipment reliability, construction planning and safety management of tunnel shield engineering.
- Bridge engineering faces complex climate factors such as hydrological & topography conditions, strong wind and tide, and complicated natural surroundings like corrosion alternated with salt and fresh water, which have brought unprecedented technical difficulties on bridge structure design, large bridge construction and project maintenance management.
- As the rail transportation space is remained in this project, the technical difficulties such as foundation settlement, beam structural deformation and beam end corner must be controlled strictly and additive force on foundation produced by continuous welded rail track should be considered during project construction, which demands for greater construction precision.

1.2 *Project management specialties*

As the project having great social influence in Shanghai following the above-mentioned specialties, Shanghai Yangtze River Tunnel and Bridge Project faces great difficulties in project management.

- This is a quite unusual project of "Double Hundred" in Shanghai, i.e. total investment is over thou-sand million Yuan and design service life is over a hundred years.
- As a "three highs" engineering with high technology content, high construction processing requirements and high construction risks, this project demands long science & research preparation period and plenty of research management tasks.

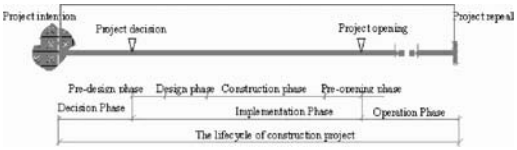

Figure 1. The lifecycle of a construction project.

- This project has complex operation control system, and the systems of operation and maintenance of tunnel and bridge is integrated.
- International construction and consulting teams have participated in this project, and there exist remarkable difference in domestic and foreign project management philosophy.
- The construction above the river and underground tunnel shield driving has to be implemented in the meantime. Therefore, this project faces complicated safety management tasks and plenty of management responsibilities.

2 PROJECT CONSTRUCTION BASED-ON LIFECYCLE INTEGRATION

The above-mentioned specialties determine Shanghai Yangtze River Tunnel & Bridge Project Management to be based on a complex system. According to the theory and practice, it is proved that the means of objective management must be adopted for the project management based on a complex system from the angle of project lifecycle. The project lifecycle means the period from the commencement of project till its repeal including the three stages of project decision, project implementation and project operation generally (Fig. 1). As a complete process, mutual influence, action and restrictions of project lifecycle merged into one must be considered fully.

From the beginning of project decision stage, for Shanghai Yangtze River Tunnel & Bridge Project, the convenience of project construction and operation has been taken fully into account and the needs of economic balanced development in the Yangtze River Delta been demonstrated. At the stage of project design, comparative analysis on construction organizational scheme and project operation capabilities of energy-saving & environmental protection has been carried out for many times, and the project lifecycle quality target & project lifecycle investment objective been considered fully.

Similarly, integrated management must be considered fully for project management based on a complex system. And integrated management is the act and process to integrate two or more management units (elements) into an integrated body (integration). The integrated body (integration) is not simple superposition, but restructure and recombination according to a certain integration mode aimed at improving the integrated function at great degree. For traditional project management mode, Development Management (DM) at the stage of project decision, Project Management on behalf of the Owner (OPM) at the stage of project implementation and Facility Management (FM) at the stage of project operation are separated relatively and led to quite a few abuses as follows (He Q.H. 2005):

- The targets of project investment, project progress and project quality are divorced from the goals of operation costs, project acceptance and project functions, and the needs of final users are departed from the stage of project decision.
- The knowledge and experience possessed by varied project participants cannot be serviced well for the realization of project lifecycle targets, the tasks at different stages cannot be linked up well, and the interfaces between different tasks are difficult to be organized and managed effectively.
- The information produced at different stages of project lifecycle cannot be shared.

For Shanghai Yangtze River Tunnel & Bridge Project, Development Management (DM) at the stage of project decision, Project Management on behalf of the Owner (OPM) at the stage of project implementation and Facility Management (FM) at the stage of project operation are integrated organically in the aspects of management targets, management tasks, management organizations and management measures by the application of integrated management thought, and project management information system based on internet is established to realize the targets of project lifecycle.

2.1 *Lifecycle organization integration*

2.1.1 *Development management (DM), owner's project management (OPM) and facility management (FM)*

(1) As the project development management (DM), Commanding Post of Shanghai Tunnel & Bridge Construction (CPSTB) is founded by Shanghai government and local functional departments with the following main responsibilities:

- To study and determine important problems
- To make overall plan and assort with important items
- To supervise and guarantee the targets of key points

Main members of CPSTB come from local city & county governments, the concerned government departments such as Shanghai Planning Bureau, Mari-time Affairs Bureau, Water Authority and several energy supply enterprises like power companies. Project construction office is responsible for the organization of routine works.

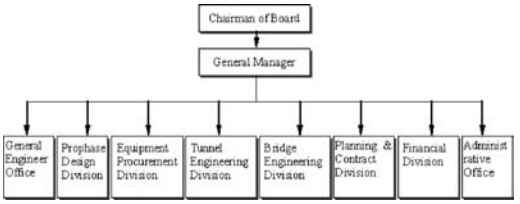

Figure 2. The organization structure of OPM.

CPSTB is only the project decision-making body not to participate in project construction directly, which is different from the operational modes of other key project construction headquarters in China. As absorbing the concerned government departments, good association among the members is not to disturb the project construction during the affairs coordination. From the project practice over these two years, project construction headquarters has played an increasingly important role on special decision, necessary works at early period, difficulty coordination and efficiency increase.

(2) As the project legal person, Shanghai Yangtze River Tunnel & Bridge Development Co., Ltd is the gathering of market mechanism and market elements. The project management company serves owner's management, which is not only the party of owner's project management (OPM), but also the party of facility management (FM) after project completion. The main duties in construction period include fund raising, scheme optimization, project implementation, and those in operation period include repaying loans for the banks, facilities maintenance and proper operation assurance. Presently, as the project is in construction period, the organizational breakdown structure is shown as Figure 2.

- The engineering divisions of tunnel and bridge are functional departments of tunnel and bridge project site management, which are involved in project construction at the early period, site coordination and management works such as progress, quality, safety, civilized construction, project acceptance and measurement.
- The prophase design division is responsible for the design management at earlier stage according to current national & regional technical standards and specifications.
- Chief engineering office is responsible for project quality management, technology, research and file management, dealing with and coordinating the design & construction technical problems.

As the command institutions on site, the engineering divisions of tunnel and bridge establish project management divisions and strengthen special management based on the arrangement of project bidding sections. The engineering divisions of tunnel and bridge directly face all project participants such as construction contractors and suppliers. The organizational breakdown structure of tunnel project is shown as Figure 3.

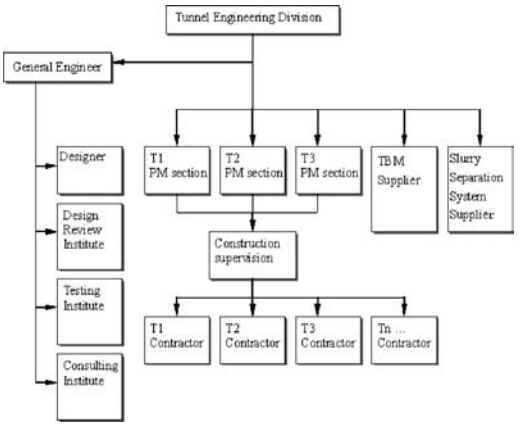

Figure 3. Tunnel project organization structure.

2.1.2 *The integration of DM, OPM and FM*

Based on lifecycle integration, Shanghai Yangtze River Tunnel & Bridge Project has realized the organizational integration, i.e. Shanghai Yangtze River Tunnel & Bridge Development Co., Ltd. and CPSTB construction Office form the combined administration mechanism. In project construction period, CPSTB acts as the party of project decision and general co-ordination, and construction office as its permanent institution and Shanghai Yangtze River Tunnel & Bridge Development Co., Ltd. as project legal person carry on the combined administration. Both parties has formed organic integration on the aspects of management targets, management tasks, management organization and management tools to improve the working efficiency, realize the superposition effect after management resources combination and optimization, and establish the platform combined with governmental development functions and project management, the carrier combined with project construction and investment benefits as well as the mechanism combined with social interests and enterprise efficiency. This is as shown as Figure 4.

2.1.3 *Lifecycle organizational creation*

Lifecycle Organizational Integration covers the organizational creation at different stages. The emphasis of organizational creation is to resolve the selection of project management organization under the lifecycle aim optimization and realize the identity of management target, the connection of management tasks and the complementation of management organizations at varied stages and different project management organizations.

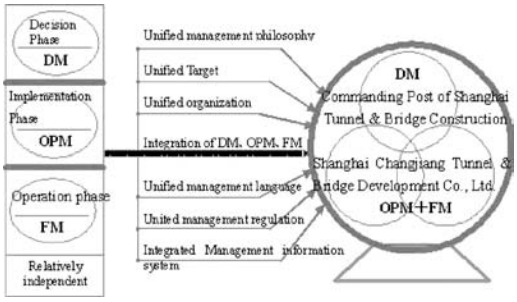

Figure 4. The integration of DM, OPM and FM.

(1) Organizational creation of owner project management

As the management institution during the project construction, Shanghai Yangtze River Tunnel & Bridge Development Co., Ltd. has made the periodic adjustments on organizational structure, for example: Presently, project design and equipment & materials purchasing is completed basically, design division and equipment procurement division have completed their functions. The company has made the adjustments on functional departments according to the features of tunnel & bridge projects, i.e. prophase design division and general engineer office have been merged into new general engineer office, equipment procurement division and planning & contract division have been merged into new planning & contract division, and quality & safety division has been established to be responsible for special management on quality and safety of tunnel & bridge projects.

After the project is completed and put into operation, the company organization is to transfer the organizational mode to realize the transfer and integration of OPM and FM.

(2) Effective combination between construction and technical consultation companies during project construction

For technical consultation, the owner has signed the contracts with several international consulting companies in high reputation such as Maunsell Consultants Asia Limited and Denmark COWI. For the allocation of important engineering equipment, the owner has purchased world-class tunnel shield equipment from German Herrenknecht. For construction technique, the owner has brought about the strength cooperation between Shanghai Tunnel Engineering Co. Ltd. to solely master similar technique of "Tunnel Shield Driving in Long Distance and Large Diameter" in China and French Bouyues with high reputation in the field of international tunnel driving and successful experience of long distance large diameter ($D = 14.87$ m) driving especially in Green Heart Tunnel Project in Holland. As international construction partners with strength cooperation and mutual support of relative advantages participate in Shanghai Yangtze River Tunnel & Bridge Project, all these are no doubt conducive to carry out the construction smoothly and reduce the construction risks.

(3) The establishment of expert advice group to participate in technological decision

The owner has invited thirteen famous experts in bridge and tunnel to form the expert advice group for Shanghai Yangtze River Tunnel and Bridge Project. This group is responsible for theory support, technique instruction and consulting service on vital technique problems occurred in project construction. Meanwhile, it is ready to participate in the demonstration of vital technique schemes, review important construction schemes and deal with key technique problems to ensure the high quality and safety of this project.

2.2 *Project management information system*

The relevant information in the whole project course from project planning, design, construction and operation till project repeal is the working basis of project lifecycle management. Plenty of information is produced and requested by varied organizations during project construction. In the whole period of project lifecycle management, a data-processing information system must be established to assist project lifecycle management. Shanghai Yangtze River Tunnel & Bridge Project management information system has been established based on internet, at the core of owner's project management and with the collaboration of all participants to become an integrated information system to meet the needs of entire-course and all-directional project management. The following main users are included:

- The relevant government departments
- Project developer
- Project owner
- Design institutes
- Project construction supervision units
- Project suppliers
- Project contractors
- Project consulting units

The data of main business modules such as schedule control, quality control, construction management, contract management, equipment management etc. should keep up with project construction simultaneously and reflect dynamic project information to improve the efficiency and transparency of information exchange and provide the data for project operation and maintenance. The function structure of information system is shown as Figure 5.

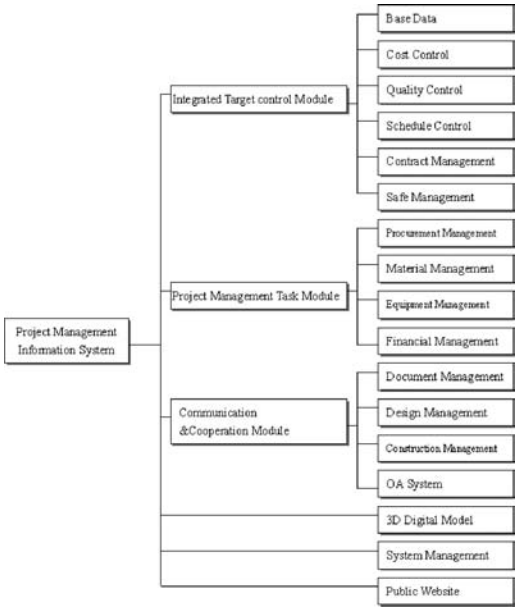

Figure 5. Function structure of management information system.

2.3 *Realization of the targets of lifecycle cost and lifecycle quality*

The integration of Shanghai Yangtze River Tunnel & Bridge Project lifecycle organization makes it possible to realize the targets of Lifecycle Cost and Lifecycle Quality. It is proved based on theory and practice that the stages of project decision and design at the early period should be placed considerable emphasis on to ensure the realization of LCC & LCQ target optimization. Once the project design is completed, Lifecycle Cost has remained the influence in the degree of 15% (Harold Kerzner 1998). For Shanghai Yangtze River Tunnel & Bridge Project, the optimization & comparison of design path, the demonstration of design plan and the analysis of organizational construction scheme have been carried out at the stages of project decision and design at the early period.

- At the stage of project feasibility study, the scheme of "South Tunnel and North Bridge" has been determined. Following the tunnel design analysis on the methods of sunken tube and tunnel shielding based on Lifecycle Cost, the design of tunnel shielding has been recommended.
- Before project preliminary design, the owner has organized the social force to implement the "mountain climbing" program of Shanghai Science & Technology Committee for technical difficulties and key control points during engineering construction and project management, and carry out the tackling of key technique and risks to supply the basis for project preliminary design.
- At the stage of project preliminary design, the tunnel line position has been deflected in the west compared with that in the feasibility study report to keep away from the interference of sunk ships and optical cable lines and ensure the construction quality and safety, the tunnel vertical section determined by the thickness of covered earth to shorten the tunnel length effectively, and the deployment of No. 2 ventilation shaft cancelled to optimize the scheme of ventilation design.
- At the stage of project working drawing design, the rail transportation space has been determined to remain, the design of tunnel & bridge section adjusted, and the new design with minor modification and smallest investment adopted through the design comparison and demonstration.
- After the project commencement, project owner has actively listed "Shanghai Yangtze River Tunnel & Bridge Project in special topic research of '863 Program'" (National High Technology Research and Development Program) in order to construct Yangtze River Tunnel more steadily and much better, standardize the construction technology of large underwater shielding tunnel and supply the construction experience for large tunnel across river and sea in China in future. The research subject is "The Key Technique Study of Shield Tunnel with Long Distance and Large Diameter". With the target background of Shanghai Yangtze River Tunnel & Bridge Project with largest diameter and in combination of highway and rail, this research is focused on the key technique of large tunnel across river and sea such as structure design, construction methods, disaster prevention, formulate core technology group and the relevant technical standards so that the construction level of large tunnel across river and sea in China reaches not only the realistic capability but also the competence in international competition especially in several techniques with advanced world levels.

Through the analysis and demonstration on Lifecycle Cost and Lifecycle Quality at all stages, project owner has brought forward the integration of realized targets.

3 THE ESTABLISHMENT AND IMPLEMENTATION OF PROJECT MANAGEMENT REGULATIONS

Except that the foundation of project management pattern is an outstanding feature of Shanghai Yangtze River Tunnel & Bridge Project based on lifecycle integration, the establishment of sound project

Table 1. The framework of project management regulations.

PM tasks	Main contents	Regulations
Safety Management		Regulation for Safety Management …
Quality Control		Regulation for Quality Control …
Contract Management	Tendering & Contract	Regulation for Contract Coding …
	Equipment & Material	Process of supply of equipment and material …
	Design Revise	Process of design revise …
Information Management	Documentation	Regulation for documentation …
	Science Research	Regulation for Science Research …
Organization coordination	Coordination	Construction measurement Process …
	Performance Evaluation	Process of award and punishment …

management regulation has standard, regular and technological process functions on project process management. The owner has established 36 project construction regulations and clarified the project management into quality management, safety management, contract management, information management etc. The framework of project management regulations is shown as Table 1 in details.

The establishment of project management regulations makes all project participants organize the project construction according to the owner's requirements & regulations and realizes explicit function on safety, quality, progress and investment objectives.

4 SAFETY MANAGEMENT & QUALITY CONTROL

Safety management and quality control are main tasks in the scope of international project management especially for large communications facilities with big construction risk.

(1) To establish safety & quality management system and manage in different levels and definite functions

Sound safety & quality management system is the basis to realize safe construction and quality control. The owner has compiled the safety & quality regulations, specified the quality target and safety regulations, established the system and network of safety & quality management led by construction unit to cover all construction levels, and improved the system constantly.

The function of quality supervision has been strengthened in the course of project construction. The owner has drawn up "Management Rules of Shanghai Yangtze River Tunnel and Bridge Project Construction Supervision" to clarify the relationship among contractors, supervisor and owner, emphasize construction contractors should accept the inspection & management from supervision unit to create the supervision conditions. Meanwhile, the owner has explicitly explained the rights and obligation of supervision unit to all participants to facilitate its works, and put the supervision works into the range of owner's management effectively to regard the supervision as practical extensions of owner's management. In "Quality Inspection and Assessment Rules of Shanghai Yangtze River Tunnel and Bridge Project", the owner has explicitly stated the supervision unit should strengthen standing supervision management in quality control and explicitly explained the relevant key process and concealing works to eliminate potential quality problems.

(2) To optimize the technical solution in construction and focus on the introduction of advanced technology

In principle of Technical Scheme in Advance, the owner has paid attention to the compiling of technical scheme before the project commencement first and then the construction plan. In addition, the owner has entrusted the science & technology committee of Shanghai Urban Municipal Bureau to organize the review and appraisal from the experts on special construction plans so that the construction contractors could revise and supplement the construction plans according to the experts' advice. Following the review and appraisal from the experts, the construction plans have been optimized with more pertinence to reduce the risks of project construction.

(3) To detail the examination of key process and focus on the course acceptance

For some key process, on the basis of self check of construction unit and recheck of supervision unit, the owner has entrusted the third party to carry out independent recheck, for instance: Shanghai Surveying and Mapping Institute is entrusted to resurvey two bearing platform centers of main navigation hole bridge and tunnel underground controlling network, and Marine Survey Group to monitor during the tunnel

driving. As a result, the project construction is under the control. The owner has introduced advanced survey instruments of VMT to test the duct pieces & moulds and entity quality. Compared with traditional survey data, this system has considered the influence of meteorological conditions including temperature, pressure and humidity etc. In addition, this system is not only with high precision but also more objective especially that varied goods produced in different seasons have various dimensions. According to varied geometric information on steel moulds and duct pieces, the owner can make objective and comprehensive appraisal on project quality to master the links in production to be paid attention.

In order to enhance the process control of project quality, the owner has consulted with Shanghai Highway Quality Supervision Station to run project delivery & completion acceptance through project construction, discover the weak links during construction and eliminate hidden troubles the course of project construction. Over a year, plenty of sampling tests have been carried out on the thickness of reinforcement cover, concrete strength, the deflection of pile foundation, the quality of partial raw materials etc. and better effects have been achieved.

(4) To improve the site supervision and strengthen dynamic management

In order to enhance the site supervision of project, the owner has established Shanghai Yangtze River Tunnel & Bridge Project Supervision Group on Site Safety, Quality and Civilized Construction together with construction & transportation department and highway safety & quality supervision station of Shanghai Urban Municipal Bureau. The supervision group not only inspects all construction process irregularly according to "Rules of Comprehensive Assessment on Shanghai Yangtze River Tunnel and Bridge Project", but also carries out overall or special check based on different bidding section and construction contents monthly so as to enhance the establishment of safety & quality management system.

5 THE ESTABISHMENT OF PROJECT CULTURE

Project culture is a kind of organization culture formed in the organizations involved in the project construction. It consists of ideology and substantial configuration such as culture concept, ethics, values and behavior principles, which is accepted mutually by all organization members participated in project construction. In contrast to enterprise culture produced in one organization, project culture is formed mutually by many organizations (i.e. interorganization culture). The establishment of project culture is the expansion of owner's enterprise culture intension and surpasses enterprise cultures of all units involved in the project construction. And the performance of project culture has invisible good influence on the completion of project target (Ding S.Z. 2004).

The core of Shanghai Yangtze River Tunnel & Bridge Project means that as an integrated whole, the spirit of cooperation based on equality and respect is advocated between owner and all participants to manage harmoniously and accomplish this harmony engineering concerned only with people. The establishment of the project culture is one main task of owner's project management, and owner is the major motivator to form this project culture. During the construction of Shanghai Yangtze River Tunnel & Bridge Project, as the project owner, Shanghai Yangtze River Tunnel & Bridge Development Co., Ltd. fully respects the cooperative parties following the contract performance and pays the fees regularly and effectively, which has set an example to drive forward the project culture core of equality, respect and cooperation. The establishment of the project culture has completed.

6 CONCLUSIONS

Confronted complex technique environment and construction environment, Shanghai Yangtze River Tunnel & Bridge Project integrated project organization and targets based on project lifecycle. The establishment of project information system provides an information communication platform for project participants. By the long science & research preparation, project safety management and quality control are implemented effectively. And the establishment of project regulations and culture promote the project progress on the side. The project management experience of Shanghai Yangtze River Tunnel & Bridge Project will be a good reference for another largescale facility construction project in China.

REFERENCES

Ding, S.Z. 2004. Towards the development of an integrated Management procedure lifecycle management system for construction project. *Construction Economics* 5: 21–25.

Harold, Kerzner. 1998. *Project management: a system approach to planning, scheduling and controlling*. International Thomson Publishing Inc.,

He, Q.H. 2005. *The research of lifecycle integrated management for construction project*. Tongji University PhD dissertation.

1 Experiment and design

The Shanghai Yangtze River Tunnel - Theory, Design and Construction – Huang (ed)
© 2008 Taylor & Francis Group, London, ISBN 978-0-415-47161-9

A review of shield tunnel lining design

B. Frew, K.F. Wong & C.K. Mok
Maunsell Geotechnical Services Ltd., Maunsell Aecom Group, P. R. China

F. Du
Maunsell AECOM Shanghai, P. R. China

ABSTRACT: According to guidelines for the design of shield tunnel lining issued by International Tunnelling Association (ITA, 2000), the member forces of tunnel lining could be computed by (1) Bedded frame model method; (2) Elastic equation method; and (3) Muir Wood model. In this paper, these methods are reviewed and compared, taking Chongming Tunnel Project as example. Based on the analysis results, the limitation of each design method is discussed. The suitability of design methods for soft ground tunnel is also evaluated.

1 INTRODUCTION

Since 1980s, urban developments in many cities in China have been experiencing continuous growth and expansion. Therefore, it is necessary for the developing cities to have efficient and economic urban civil infrastructure systems to accommodate the traffic demand with rapid growth. Because of shortage of land resources, subway system is an obvious solution to meet the traffic demand and to minimize the impact on the existing traffic during construction. Shield tunneling is one of the most popular tunneling methods for the construction of subway tunnels in soft soil ground. During construction of shield tunnel in soft ground, ground deformation will be induced and the surrounding soils will act on the shield lining segments. Therefore, tunnel lining plays very important role to support the excavated space and engineers have to carry out tunnel lining design very carefully with consideration of using appropriate models and design methods.

2 CROSS-RIVER TUNNEL PROJECT AT CHONGMING IN SHANGHAI

Chongming South Channel Tunnel in Shanghai is 9 km long. The method of shield construction will be adopted to build the tunnel and it will be the world's biggest bored tunnel underneath water. This tunnel is part of the 25 km long, 12.3 billion yuan Shanghai–Chongming expressway, linking the Changxing and Chongming islands to the city. After the completion of this project, it will take less than 30 minutes to drive from Wuhaogou in Pudong to Chenjiazhen in Chongming.

3 TUNNEL LINING DESIGN METHODS

In this section, three commonly-used tunnel lining design methods are reviewed as the followings:

3.1 *Bedded frame model method*

The bedded frame model method is a method to compute member forces of tunnel lining with a matrix method using a computer because this model is multiple statically indeterminate. This method can evaluate the following conditions (ITA, 2000):

- Nonuniformly varying load due to change of soil condition;
- Eccentric loads;
- Hydrostatic pressure;
- Spring force to simulate subgrade reaction; and
- Effect of joint by simulating joints as hinges or rotation springs.

In this study, a structural engineering software called Microstran is used to model the shield tunnel lining as a bedded frame model. The typical loading model for bedded frame method is shown in Figure 1.

3.2 *Elastic equation method*

The elastic equation method which is commonly used in China and Japan is a simple method for calculating member forces without a computer. However, it

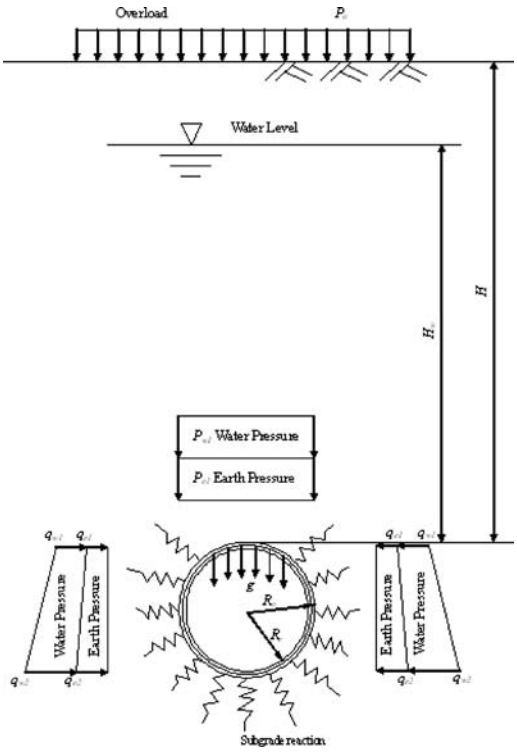

Figure 1. Typical loadings for bedded frame model.

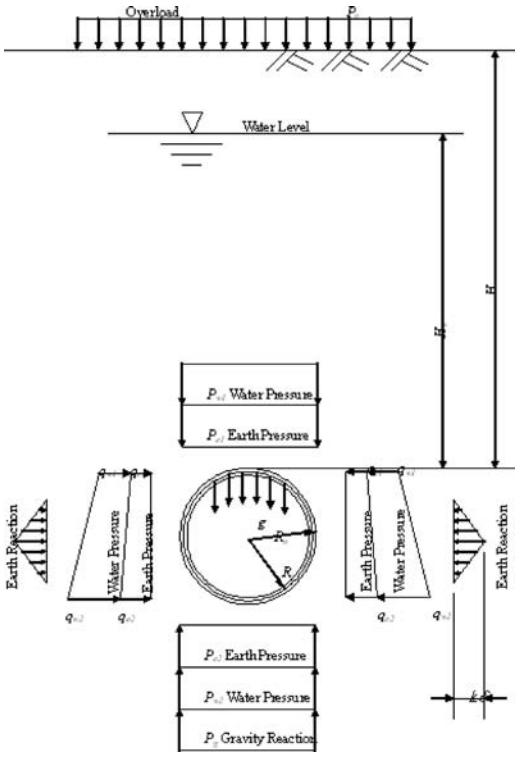

Figure 2. Loads acting on the shield based on elastic equation method.

cannot evaluate the above-mentioned conditions 1) to 5). In this method, water pressure is evaluated as the combination of vertical uniform load and horizontally uniformly varying load. The horizontal subgrade reaction is simplified as a triangularly varying load. The load condition of elastic equation method is shown in Figure 2. The formulae for the internal forces caused by the different loads based on elastic equation method are shown in Table 1.

3.3 *Muir wood model*

Muir Wood (1975) gave a corrected version of Morgan's more intuitive approach, again assuming an elliptical deformation mode (Fig. 3). The tangential ground stresses are included, but that part of the radial deformation which is due to the tangential stresses is omitted. Making allowances for some pre-decompression of the ground around the opening before the lining is placed. Muir Wood proposed to take only 50% of the initial ground stresses into consideration. The moments may be reduced even more by reducing the lining stiffness by an amount equivalent to the effect of less rigid hinges. However, Curtis (1976) supplemented Muir Wood's formulae by the inclusion of radial deformation due to tangential stress. Based on Muir Wood model, the formulae for the internal forces are shown as the following:

$$N_{Hoop} = ((P_{VMax}+P_{HMax}) / (2(1+RC))) R_0 \quad (1)$$

$$RC = R_0 E_{Soil} (1-\nu_l^2) / \eta t E_{Conc} (1+\nu) \quad (2)$$

$$I_e = I_j + I_s (4 / n_S) \quad (3)$$

$$N_{Max} = N_{Hoop} + M_{Max} / R0 \quad (4)$$

$$N_{Min} = N_{Hoop} - M_{Max} / R0 \quad (5)$$

$$M_{Max} = (P_{Vmax}-P_{HMax})(\eta R_0)2 / [6 + 2\{(\eta R_0)3E_{Soil} / [E_{Conc} I_e (1-\nu)(5-6\nu)]\}] \quad (6)$$

Where,

N_{Hoop} = Circumferential hoop thrust per unit length of tunnel

N_{Max} = Maximum axial force in lining per unit length of tunnel

N_{Min} = Minimum axial force in lining per unit length of tunnel

M_{Max} = Maximum bending moment in lining per unit length of tunnel

Table 1. Formulae for the internal forces caused by the different loads based on elastic equation method (Ding et al., 2004).

Loads	Beam bending moment	Lining ring hoop force
Vertical earth pressure and water pressure $P_{e1}+P_{w1}$	$M=\frac{1}{4}(1-2\sin^2\theta)\times(P_{e1}+P_{w1})R_c^2$	$N=(P_{e1}+P_{w1})R_c\sin^2\theta$
Later earth pressure and water pressure (rectangle part): $q_{e1}+q_{w1}$	$M=\frac{1}{4}(1-2\cos^2\theta)\times(q_{e1}+q_{w1})R_c^2$	$N=(q_{e1}+q_{w1})R_c\cos^2\theta$
Later earth pressure and water pressure (triangle part): $q_{e2}+q_{w2}-q_{e1}-q_{w1}$	$M=\frac{1}{48}(6+3\cos\theta-12\cos^2\theta-4\cos^3\theta)\times(q_{e2}+q_{w2}-q_{e1}-q_{w1})R_c^2$	$N=\frac{1}{16}(-\cos\theta+8\cos^2\theta+4\cos^3\theta)(q_{e2}+q_{w2}-q_{e1}-q_{w1})R_c$
Horizontal earth resistance: $q_k=k\delta$	For $0\le\theta\le\frac{\pi}{4}$, $M=(0.2346-0.3536\cos\theta)k\cdot\delta\cdot R_c^2$ For $\frac{\pi}{4}\le\theta\le\frac{\pi}{2}$, $M=(-0.3487+0.5\sin^2\theta)+0.2357\cos^3\theta)\cdot k\cdot\delta\cdot R_c^2$	For $0\le\theta\le\frac{\pi}{4}$, $N=0.3536\cos\theta\cdot k\cdot\delta\cdot R_c$ For $\frac{\pi}{4}\le\theta\le\frac{\pi}{2}$, $N=(-0.7071\cos\theta+\cos^2\theta+0.7071\sin^2\theta\cos\theta)k\cdot\delta\cdot R_c$
Lining unit weight: g	For $0\le\theta\le\frac{\pi}{2}$, $M=(-\frac{1}{8}\pi+\theta\sin\theta+\frac{5}{6}\cos\theta-\frac{1}{2}\pi\sin^2\theta)\cdot g\cdot R_c^2$ For $\frac{\pi}{2}\le\theta\le\pi$, $M=(\frac{3}{8}\pi-(\pi-\theta)\sin\theta+\frac{5}{6}\cos\theta)g\cdot R_c^2$	For $0\le\theta\le\frac{\pi}{2}$, $N=(-\pi\sin\theta+(\pi-\theta)\sin\theta+\pi\sin^2\theta+\frac{1}{6}\cos\theta)g\cdot R_c$ For $\frac{\pi}{2}\le\theta\le\pi$, $N=((\pi-\theta)\sin\theta+\frac{1}{6}\cos\theta)g\cdot R_c^2$

Note: The values beyond the expressed range can be easily obtained as the loads and lining are symmetric.

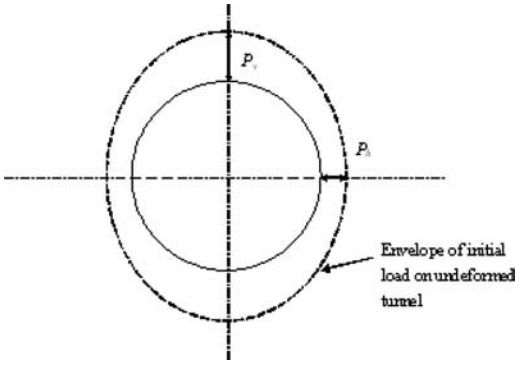

Figure 3. Initial loading on tunnel prior to deformation.

P_{VMax} = Maximum vertical loading acting on tunnel crown
P_{HMax} = Maximum horizontal loading acting on horizontal axis of tunnel
R_0 = Radius to extrados of tunnel lining
ν_l = Poisson's ratio for lining
ν = Poisson's ratio for ground
E_{Soil} = Young's modulus for ground
E_{Conc} = Young's modulus for lining
T = Segment thickness
η = Ratio of radius of lining centroid to that of extrados
n_S = Number of segments per ring
I_s = Second moment of area of lining per unit length of tunnel
I_j = Second moment of area of joint
I_e = Effective value of second moment of area for a jointed lining

Muir Wood method is recommended on structural design of tunnels in United Kingdom.

4 COMPARISON BETWEEN TUNNEL LINING DESIGN METHODS

The above-mentioned tunnel lining design methods are used to compute bending moment and axial force of tunnel lining. However, the member forces calculated by different methods are not consistent, varying with design assumptions. Taking Chongming Tunnel Project as example, a number of loading cases which are shown in Table 2 are used to calculate the member forces with different methods in order to compare these methods and investigate their differences. Based on the analysis results, the limitations and suitability of these design methods are then evaluated.

4.1 *Bending moment*

The maximum bending moment computed by different design methods for each loading case is shown in Figure 4. Comparing with different design methods,

Table 2. Loading cases of tunnel lining design for Chongming Tunnel Project.

Cases	Soil cover (m)	Cohesion (kPa)	Friction angle (Degree)	Unit weight (kN/m^3)	Soil type	Es (Mpa)	Water level (mPD)	Water height above crown (m)	Surcharge (kPa)
Case 1	9.125	4.5	27.5	17.64	Clay	6.59	3.27	7.27	20
Case 2	18.725	7.8	28.4	18.04	Mixed	16.83	3.27	26.77	No
Case 3	18.525	10.0	27.5	17.64	Clay	12.00	3.27	34.77	No
Case 4	12.135	7.9	27.5	17.97	Mixed	10.40	3.27	24.02	No
Case 5	17.725	10.0	27.5	17.83	Clay	12.00	3.27	30.27	No
Case 6	9.365	5.0	27.15	17.39	Clay	5.12	3.27	10.77	No
Case 7	12.375	7.7	25.9	17.19	Clay	10.30	3.27	11.27	20
Case 8	8.915	6.5	26.4	17.18	Clay	8.06	3.27	8.77	No

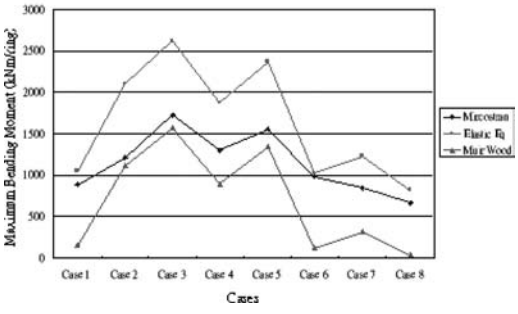

Figure 4. The maximum bending moment computed by different design methods for each loading cases.

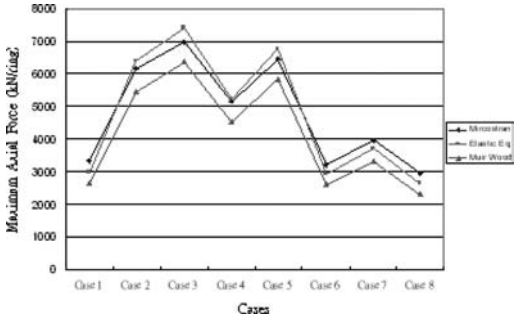

Figure 5. The maximum axial force computed by different design methods for each loading cases.

for all loading cases, the highest and lowest maximum bending moment were obtained by using elastic equation method and Muir Wood model respectively. Therefore, the bending moment computed by elastic equation is comparatively conservative whereas Muir Wood is comparatively aggressive. High construction cost will be induced by overestimated bending moment but high risk of tunnel instability will be induced by underestimated bending moment.

From the results of cases 2, 3 and 5, the higher the soil cover and water depth above tunnel crown, the higher will be the maximum bending moment. It is also seen from the results of cases 1, 6 and 8 that the maximum bending moment decreases significantly with decreasing soil and water depths. For cases 1, 6 and 8, the ratio of vertical loading to horizontal loading (P_v/P_h) tends to unity, as a result, the bending moments obtained by Muir Wood model are very small for those cases, compared to other methods.

4.2 *Axial force*

The maximum and minimum axial forces computed by different design methods for each loading cases are shown in Figure 5 and Figure 6 respectively. For all cases, the difference of axial force obtained by different methods is not significant. From the results of

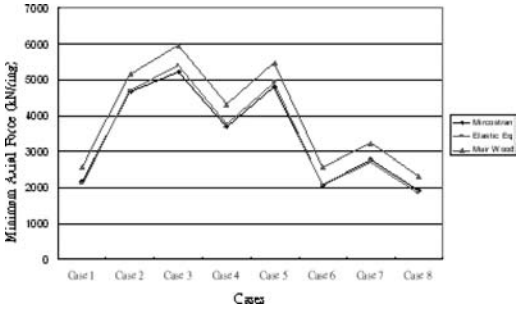

Figure 6. The minimum axial force computed by different design methods for each loading cases.

cases 2, 3 and 5, the higher the soil cover and water depth above tunnel crown, the higher will be the axial force. Contrarily, the lower the soil and water depths, the lower will be the axial force, as seen from the results of cases 1, 6 and 8.

4.3 *Limitations and suitability of design methods*

According to the assumptions of Muir Wood and elastic equation methods, the tunnel shape is limited to be circular only. However, bedded frame model can be

applied to compute member forces not only for circular tunnel, but also non-circular tunnel cross-sections.

The location and magnitude of subgrade reaction vary with the deformation of tunnel lining which depends on loading conditions, soil properties and lining stiffness. Muir Wood model obtains a solution by considering a circular lining deformed into the elliptical mode in elastic ground whereas elastic equation method assumes the combination of vertical uniform load and horizontally uniformly varying load acting on the lining. These greatly simplify the solution. However, in reality, the loading condition is complicated and non-uniform. Also, the subgrade reaction is not as simple as horizontally triangularly varying load as assumed by elastic equation method. Therefore, Muir Wood model and elastic equation method are not accurate enough to be used in detailed design of tunnel lining with complicated loading conditions, but they are good approaches to estimate member forces for preliminary design (simple tunnel lining design) problem. Bedded frame model can be adopted to provide a better simulation of the interaction between the lining and soil and complicated loading conditions as spring force to simulate subgrade reaction and no-uniformly varying load due to change of soil condition can be applied in the model of tunnel underneath water.

The number and orientation of joints have significant influence on the maximum bending moment induced in the jointed lining, for a given range of ground condition, tunnel depth and lining flexibility (Hefny and Chua, 2006). If the segments are staggered, the moment at the joint is smaller than the moment of the adjacent segment. To simplify the model, the circumferential joint is usually assumed to have the same rigidity as that of the segment. As a result, the moment for the design of joint is overestimated and that occurring at the segment is not calculated correctly. This problem can be solved by applying rotational springs at the circumferential joints in bedded frame model. As for elastic equation method, flexural rigidity at joint and distribution of bending moment near the circumferential joints are also taken into consideration, using the effective ratio of the bending rigidity, η, and bending distribution factor, ζ, respectively. The values of the bending moments used for the segment and the joint are assumed to be $\mathrm{Mo}(1+\zeta)$ and $\mathrm{Mo}(1-\zeta)$ respectively. However, such a condition physically has no basis so that it is then impossible to calculate actual distribution of the bending moment by using this assumption (Koyama, 2003).

All in all, bedded frame model is better than Muir Wood and elastic equation methods, in terms of simulation of tunnel shape, lining and ground interaction, loading conditions and joint behavior. However, it is time-consuming to establish a bedded frame model.

5 CONCLUSIONS

Taking Chongming Tunnel Project as example, three tunnel lining design methods (bedded frame model method, elastic equation method and Muir Wood model) were reviewed and compared. The analysis results showed that the highest and lowest maximum bending moment was obtained by using elastic equation method and Muir Wood model respectively. The bending moments obtained by Muir Wood model are very small while the ratio of vertical loading to horizontal loading (P_v/P_h) tends to unity. The results also showed that the higher soil cover and water depth above tunnel crown would obtain higher maximum bending moment and axial force.

According to the analysis results, it is concluded that elastic equation method is a comparatively conservative estimate for computing the bending moment of tunnel lining whereas Muir wood method is a comparatively aggressive. High construction cost will be induced by overestimated bending moment but high risk of tunnel instability will be induced by underestimated bending moment. Besides, in terms of simulation of tunnel shape, lining and ground interaction, loading conditions and joint behavior, bedded frame model is a more appropriate method to design tunnel lining, compared to Muir Wood model and elastic equation method. Therefore, bedded frame model is highly recommended to be used for tunnel lining design for Chongming Tunnel Project – the world's biggest bored tunnel underneath water.

REFERENCES

Curtis, D.J. 1976. Discussions on "The circular tunnel in elastic ground". *Geotechnique* 26:231–237.

Ding, W.Q., Yue, Z.Q., Tham, L.G. et al. 2004. Analysis of shield tunnel. *International Journal for Numerical and Analytical Methods in Geomechanics* 28:57–91.

Duddeck, H. & Erdmann, J. 1982. Structural design models for tunnels. *Proc. 3rd Int. Symp on Tunnelling*:83–91.

Hefny, A.M. & Chua, H.C. 2006. An investigation into the behavior of jointed tunnel lining. *Tunnelling and Underground Space Technology* 21 (3–4):428–433.

I.T. A. Working Group on general approaches to the design of tunnels. 1988. *Guildelines for the design of tunnels. Tunnelling and Underground Space Technology* 3(3):237–249.

I.T. A. Working Group No. 2. 2000. Guidelines for the design of shield tunnel lining. *Tunnelling and Underground Space Technology* 15(3):303–331.

Koyama, Y. 2003. Present status and technology of shield tunneling method in Japan. *Tunnelling and Underground Space Technology* 18:145–159.

Muir Wood, A.M. 1975. The circular tunnel in elastic ground. *Geotechnique* 25(1):115–127.

The Shanghai Yangtze River Tunnel - Theory, Design and Construction – Huang (ed)
© 2008 Taylor & Francis Group, London, ISBN 978-0-415-47161-9

Analysis of the slurry infiltration effect on soil by true triaxial test under the ESEM-scanning

X.Y. Hu, Z.X. Zhang & X. Huang
Key Laboratory of Geotechnical & Underground Engineering, Ministry of Education, Tongji University, Shanghai, P. R. China
Department of Geotechnical Engineering, School of Civil Engineering, Tongji University, Shanghai, P. R. China

J.Y. Wang
Shanghai Tunnel Engineering Co., Ltd., Shanghai, P. R. China

ABSTRACT: Slurry shield method is a wide-used tunnelling method in saturated soft soil, especially for cross-river cases under the high water pressure and complex geological condition. However, in extremely unfavorable geological conditions, face instabilities may occur. In order to better understand the mechanism of face stability, this paper presents a series of tests: slurry infiltration testing, strength testing by a true triaxial apparatus and the filter cake microstructure behavior scanning by an ESEM apparatus. The results of the tests will be a help to explain the following problems: shield tunnelling in heterogeneous soils, the matched slurry additives for corresponding soil layers, the effects of the slurry penetration and gelling on the strength of soil under different conditions and different microstructures of the filter cake upon the infiltration of the slurry.

1 INTRODUCTION

Slurry shield tunnelling has been successfully applied worldwide in recent years due to its virtues such as excellent construction quality, high efficiency and reliable used in the unfavorable geological conditions, e.g. saturated soft or coarse, highly permeable soil. In a slurry shield, the support of the face which balances the front water and earth pressures is provided by a pressurized mixture of clay and water. However, under extremely unfavorable geological conditions, face instabilities may occur. G. Anagnostou and K. Kovári (1994, 1997) researched the mechanics of face failure and discussed the time-dependent effects associated with the infiltration of slurry into the ground ahead of the face. Li and Zhang (2006) mentioned that the support effectiveness of the slurry will decrease due to the constant infiltration into the soil, especially in the sandy soil with high permeability and proposed an infiltration model to quantify the influence of the decreasing of the face stability. With respect to the excavation in sandy soil and based on the results of a model test, Cheng et al. (2001) studied the mechanical mechanism of the face stability maintained by the pressured slurry during slurry shield tunnelling, the stress variation law of the soil ahead the cutting face, as well as combined with the mechanics that the slurry pressure exerted on the front soil and the formed filter cake configuration, they also proposed a formula for critical slurry pressure in the medium coarse sand ground condition. The aforementioned researches are based on the phenomenon that the slurry will permeate into the cutting face to some extent, and such permeation may increase the pore water pressure which results in a drop of effective slurry pressure. Concerning these kinds of questions, A. Mori and K. Kurihara (1995) elucidated the mechanism of increase in pore water pressure during tunnel driving and showed that the amount of such increase in pore water pressure varies depending on the seepage velocity of the slurry into the cutting face. As the slurry gradually infiltrated into the soil, a layer of filter cake is expected to form clinging on to the cutting face which is used for transferring the support pressure onto the soil. However, in coarse, highly permeable soils, the suspension penetrates the ground and the required support pressure cannot be reached, (P. Fritz, 2003). And he studied the effects of the additives polymer, sand, vermiculite and proposed that a suspension containing the three additives in well defined proportions enables the formation of a tight filter cake even in highly permeable soils. Based on the Tunnel project of Fuxing East Road crossed the Huangpu River in Shanghai, China, Deng (2005)

presented a new Polymer-MMH slurry, it has certain good characters and stability, such as control the clay decentralization and the sand decentralization flow, ameliorate the mechanical composition of the slurry, shorten the filter cake forming interval and improve the compactness of the filter cake.

The aforementioned research works related to the supporting effect of slurry in shield tunnelling play a fundamental and tremendous role in tunnel design and construction; however, in this paper we will only focus on the following problems which may need further consideration and research:

- Current researches have been carried out only for a homogeneous soil at the tunnel face, therefore, the influence of heterogeneity of the soil, especially the location of horizontal layer boundaries on the formed filter cake quality and the supporting ability are researched;
- The slurry used and the mechanics of face stability for clay or sandy soil are different, thus, criteria for filter cake formation under the corresponding soil are presented, along with the optimal matched slurry;
- Plastering of slurry on the cutting face produces a layer of filter cake that helps to stabilize individual soil grains, but the filter cake itself may not strong enough to produce a structural support effect that would make any significant contribution to the globe stability, thus, the support effect is measured quantitatively which combines both overburden pressure and the lateral supporting pressure from the slurry together; with respect to the overburden pressure, it takes the three kinds of tunnel embedded depths into consideration, namely, shallow buried, normal buried and deep buried, and for each buried condition, the corresponding lateral pressure is calculated with the methods of active earth pressure and earth pressure at rest, respectively.
- The effects of the slurry penetration and gelling on the strength of soil are studied, whether it increases or reduces the soil strength are discussed in terms of quantitative index which include strength index from macroscopic aspect and structural variation index from microscopic aspect.

In this paper, a test program is proposed with expect to clarify the aforementioned problems. And a series of true triaxial tests with three distinct principal stresses will be performed to investigate the response of a certain soil to the slurry gradual infiltration under various stress paths and to clarify the occurrence of shear localization and possible failure mode. Furthermore, Environmental Scanning Electron Microscope (ESEM) studies are going to be conducted to help understand the microstructure behavior and the changes in the microstructure of the filter cake upon the infiltration of the slurry, it will be also used to examine the physical bonding and gelling effects between the soil and the corresponding slurry. Finally, based on the strength tests which can be also used for measuring the infiltration volume and ESEM studies, we can establish the relationship between micro-structural parameters and soil strength in quantitative terms.

2 CASE STUDY OF SHANGHAI YANGTZE RIVER TUNNEL

2.1 *Background*

Shanghai Yangtze River Tunnel is composed of the approach on Pudong side (657.73 m long), river-crossing section (7,471.654 m for East chainage and 7,469.363 m for West chainage) and the approach on Changxing Island (826.93 m), totally 8,955.26 m. The investment is 6.3 billion RMB. The river cross section is two tube bored tunnel. The tunnel main parameters and effect chart are shown in Figure 1.

The longitudinal profile of river-crossing section is in W-shape. And the longitudinal slope for river-crossing area is 0.3% and 0.87%, and 2.9% for the approach. The ground is a mixture of sand, clay, broken rock and groundwater. The shield mainly crosses over ②$_3$, ④, ⑤ layers, and partly tunnelling in ③$_1$, ③$_2$, ⑦$_{1\text{-}1}$ and ⑦$_{1\text{-}2}$ layers. Table 1 shows the types of strata and corresponding soil parameters.

The first Herrenknecht S-317 Mixshield is currently the world's largest tunnel boring machine (TBM), with a diameter of 15.43 m. This giant TBM will construct these three-lane road tunnels, at depths of up to 65 m beneath the Yangtze River in Shanghai-Pudong. The picture of this largest diameter is shown in Figure 2.

2.2 *Load calculation and analysis section*

The slurry supporting pressure (P_s) is calculated by the following equation:

$$P_s = P_w + P_0 + P_{soil} \tag{1}$$

Where: P_w is the groundwater pressure which also can be regarded as interstitial hydraulic pressure. Generally, the groundwater pressure is incorporated with the soil pressure calculation in the clay ground condition, attentively, for a cross-river tunnel, the pressure induced by the gravity of the water above the river bed should be considered; P_0 is the set-up pressure estimated by experiences which takes considerations of slurry pressure variation in the feeding and discharging pipelines or other value setting deviations, the value always sets between 20–30 kN/m^2; P_{soil} is the horizontal soil pressure acts on the cutting face, shown in Figure 3. The basic calculated method can be referred to the following methods in Table 2.

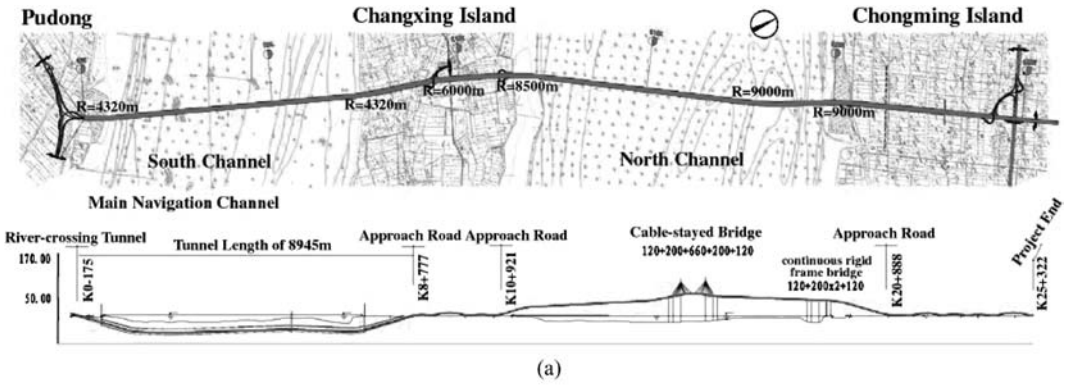

(a)

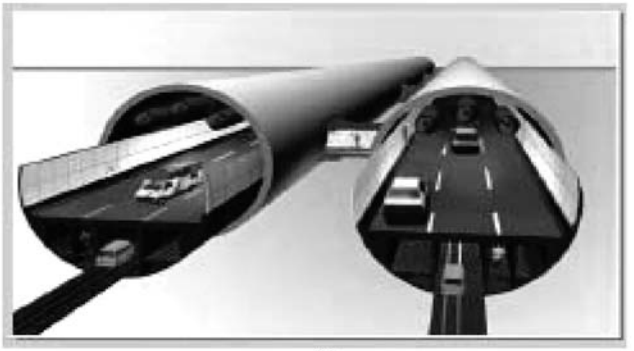

(b)

Figure 1. Tunnel scope and tunnel transverse section. (Shanghai Yangtze River Tunnel & Bridge Construction Co., Ltd., 2005).

Table 1. Types of strata and corresponding soil parameters.

Strata	Water content w %	Void ratio e –	Unit weight γ kN/m^3	K_0 –	c kPa	φ °	Permeability (20°, cm/s) K_v	K_h	Compression coefficient a_v MPa^{-1}
①$_2$Mud	44.1	1.23	17.3		12	14.5	1.81E−7	8.16E−7	0.77
①$_3$Brown sandy silt	29.9	0.85	18.6	0.34	6	31.5	9.11E−4	1.51E−3	0.22
②$_3$Grey sandy silt	31.3	0.89	18.4	0.37	10	28.0	1.12E−4	1.79E−4	0.27
③$_1$ Grey muddy silty clay	40.1	1.11	17.7	0.60	13	16.0	2.09E−6	3.57E−6	0.55
③$_2$Grey sandy silt	31.1	0.88	18.5	0.33	9	28.5	1.0E−4	2.0E−4	0.25
④$_1$Grey muddy clay	50.0	1.40	16.8	0.66	11	11.0	3.05E−7	5.42E−7	1.08
⑤$_1$Grey clay	37.5	1.07	17.8	0.51	16	17.5	2.15E−7	3.77E−7	0.60
⑤$_2$Grey clay silt	33.3	0.94	18.1	0.40	11	25.0	8.55E−5	1.55E−4	0.32
⑤$_3$Grey silty clay	35.1	1.01	18.0	0.48	17	18.5	1.99E−6	3.21E−6	0.48
⑤$_{3t}$Grey clay silt	32.9	0.94	18.2	0.41	11	26.5	3.55E−6	7.13E−6	0.33
⑦$_{1\text{-}1}$Grey clay silt	30.1	0.85	18.6	0.37	9	28.5	7.90E−4	1.19E−3	0.20
⑦$_{1\text{-}2}$Grey sandy silt	29.2	0.84	18.6	0.38	8	30.5	2.60E−4	4.59E−4	0.19
⑦$_2$Grey silty sand	23.2	0.70	19.1	0.33	4	33.5	2.11E−3	3.20E−3	0.11

The parameters in Table 2 are defined as follows: γ is the unit weight of the soil (kN/m^3), is the soil cohesive strength (kPa), φ, φ' are soil internal friction angle and effective internal friction angle, respectively, H, h is the tunnel embedded depth from the axial line to the ground surface and the cover depth between the crown of tunnel and ground surface respectively, K_a is the coefficient of active earth pressure, K is the

coefficient of the lateral pressure, $2B$ is the loosening range, W_0 is the surcharge on the ground surface.

With respect to analysis section, three different cross-sections will be taken as follows:

Case 1:

The cross-section almost corresponds to the shallowest soil cover above the tunnel, the river bed here lies in −12.30 m, as illustrated in Figure 4, the tunnel diameter is 15.43 m, thus the cover above the tunnel crown can be figured out.

Case 2:

The cross-section almost corresponds to the deepest soil cover above the tunnel, the river bed here located in 0.00 m, as illustrated in Figure 5.

Case 3: cross over ⑦$_{1\text{-}1}$ layer

Based on the geological condition in Shanghai Yangtze River tunnel, the shield mainly crosses over ④, ⑤ layers as shown in Figures 5 and 6 and the case of tunnelling over ⑦$_{1\text{-}1}$ layer is rare, thus, it is necessary to take the case into account. The river bed here located in −10.87 m, the axial line of the tunnel locates in −37.60 m, then the ratio of cover above the tunnel crown C to the tunnel diameter D is 1.2. The diagram of the case is shown in Figure 6.

According to the cases aforementioned, we can calculated the corresponding vertical overburden pressure σ_v and the slurry supporting pressure P_s

Figure 2. Shield machine used in Shanghai Yangtze River Tunnel.

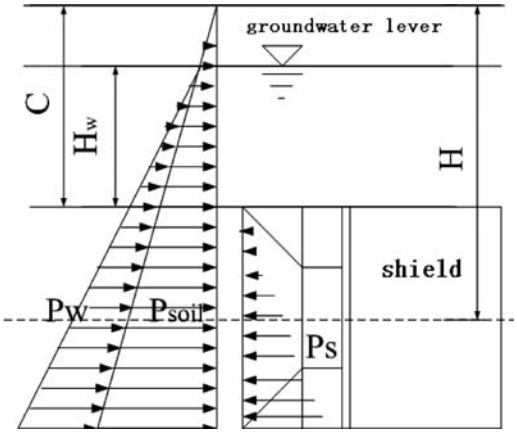

Figure 3. Diagram of the pressures act on the cutting face.

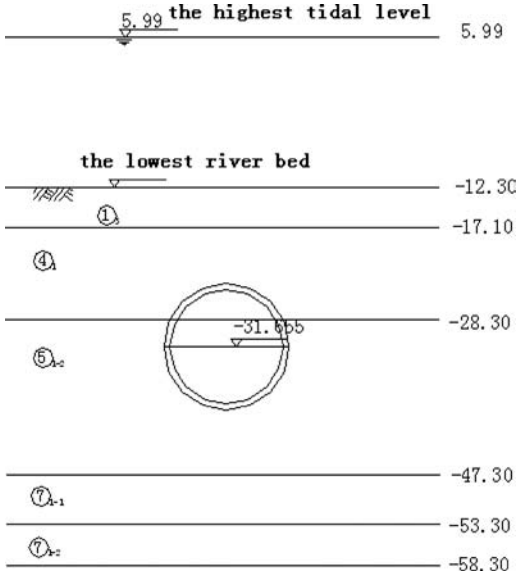

Figure 4. Cross-section of case 1.

Table 2. Calculation methods of horizontal soil pressure.

Vertical overburden soil pressure	The types of soil pressure	Equation	The applied soil type
$\gamma \cdot H$	Active earth pressure	$\gamma \cdot H \cdot \tan^2(45° - \varphi/2) - 2c \cdot \tan(45° - \varphi/2)$	Clay soil
		$\gamma \cdot H \cdot \tan^2(45° - \varphi/2)$	Sandy soil
	Earth pressure at rest	$\gamma \cdot H \cdot (1 - \sin\varphi')$	Clay soil
Based on Terzaghi loosening pressure	loosening pressure	$\frac{K_a B(\gamma - c/B)}{K \tan\varphi} \cdot (1 - e^{-K \tan\varphi \cdot h/B}) + K_a W_0 \cdot e^{-K \tan\varphi \cdot h/B}$	Sandy soil, hard clay soil

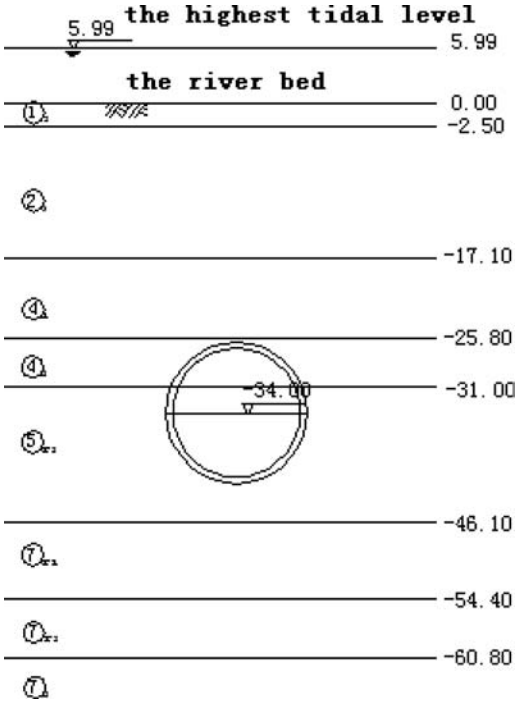

Figure 5. Cross-section of case 2.

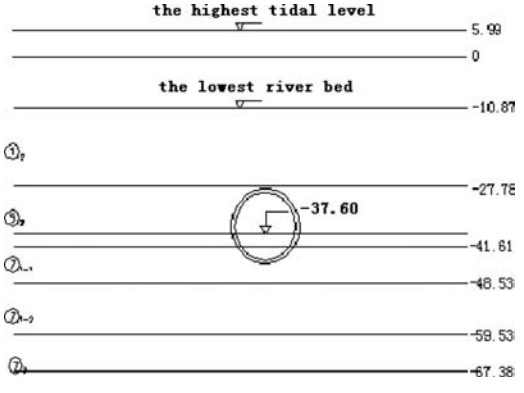

Figure 6. Cross-section of case 3.

in terms of total stress and effective stress methods, shown in Table 3.

In Table 3, the parameters σ_v, P_{su} and P_{sl} denote vertical overburden pressure, slurry supporting pressure calculated by earth pressure at rest and slurry supporting pressure calculated by active earth pressure, respectively.

3 TEST SET-UP

3.1 *True triaxial test apparatus*

In order to simulate the actual stress condition in the process of the shield tunnelling at laboratory scale, the true triaxial test apparatus is adopted in our test. The apparatus not only can consider the confining pressure (the minor principal stress) and the axial pressure (major principal stress) just as the normal triaxial test apparatus does, but also can be used for intermediate principal stress simulation which significant affects the failure mode and the apparent peak strength. (Huang, W.X. et al. 2007).

Figure 7(a), (b) shows the true triaxial test apparatus used in this test. The apparatus is equipped with hydraulic load rams equipped with linear variable displacement transducers for the axial and radial strain, external measurement of the axial strain, pressure transducers for the cell pressure and the pore pressure as well as a volume variation indicator. Each one of the horizontal loading rams has an internal load cell and there is only one load cell with the top vertical ram. Pressure-volume controllers that have been used to measure pressure/volume are also integrated with the true triaxial system; it uses hydraulic digital servo-control for maintaining the necessary test conditions.

The apparatus is designed for a brick-shaped sample which is encased in a rubber membrane in the process of test. The vertical and lateral stresses are applied using rigid jack and fluid circulation pressure and regarded as major and intermediate principal stresses; the minor principal stress is applied by air pressure in the chamber. The main technical indexes of the true triaxial test apparatus are exhibited in Table 4.

Table 3. Pressures calculated by two methods under the three cases.

	Pressures (kPa)					
	Effective stress method			Total stress method		
Cases	σ'_v	P'_{su}	P'_{sl}	σ_v	P_{su}	P_{sl}
$C = 0.7D$	144.28	90.7	68.85	520.73	385.15	339.69
$C = 1.7D$	259.16	147	128.4	659.06	389.36	314.39
Cross over ⑦$_{1\text{-}1}$ layer	200	118.15	98	636.21	490.44	407.12

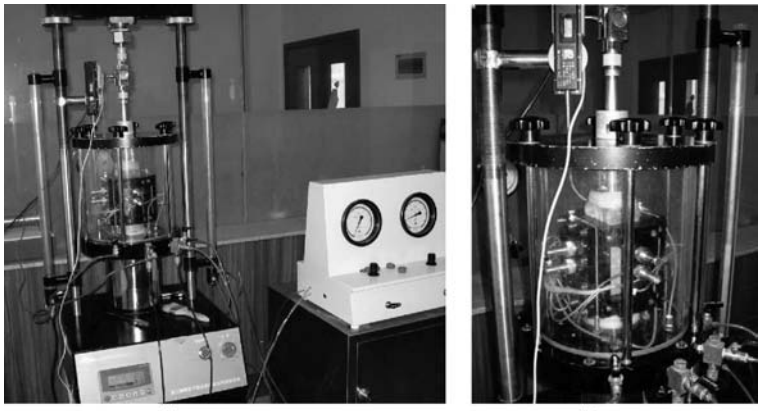

Figure 7. Set-up of true triaxial testing system.

Table 4. Main technical indexes of the true triaxial test apparatus.

Items		Technical indexes
Sample dimension (mm)		$70 \times 70 \times 120$
Major principal stress (MPa)		0–4
Intermediate principal stress (MPa)		0–1.5
Minor principal stress (MPa)		0–1
Pore pressure (MPa)		0–1
Volume variation (ml)		0–100
Displacement (mm)	Direction of major principal stress	0–30
	Direction of intermediate principal stress	0–7
	Direction of minor principal stress	0–7
Accuracy of transducers (‰)		<3–5

Data from the experiments are logged electronically. All the transducers in the set-up are connected to a controller through the computer interface unit for data acquisition and control. The controller itself is also connected to the computer. Computer-aided testing system software automated various phases of testing such as consolidation, and application of stresses for applying a predetermined stress path or stain path.

3.2 *ESEM apparatus*

The Field-Emission Environmental Scanning Electron Microscope (ESEM-FEG) with Energy-Dispersive Spectroscopy (EDS) used in our test is produced by Philips NV, in Holland with the type of XL30 ESEM-FEG (shown in Figure 8(a), (b)), it has a versatile microscope with 2 nm ultimate resolution. ESEM is chosen over a conventional Scanning Electron Microscope (SEM) because materials samples examined by ESEM do not need to be desiccated, coated with gold palladium or high vacuum and thus their original characteristics can be preserved for further testing or manipulation.

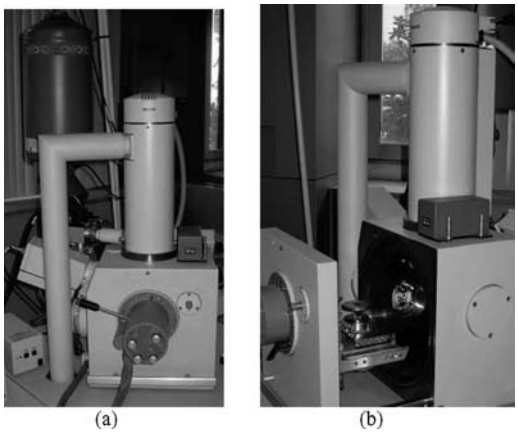

Figure 8. Set-up of ESEM apparatus.

3.3 *Test program*

3.3.1 *True triaxial test processing*

A total of three types of soils (homogeneous clay soil ④$_1$, sandy soil ⑦$_{1\text{-}1}$ as well as heterogeneous soil ⑤$_2$

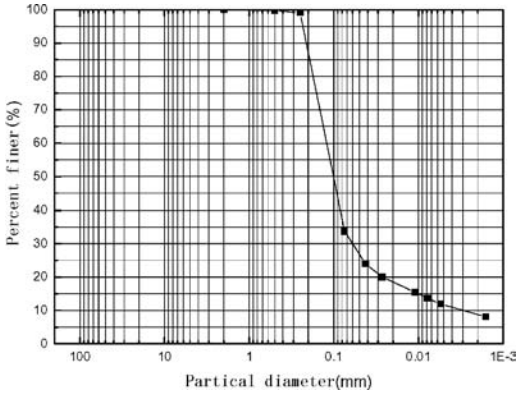

Figure 9. Particle size distribution for soil used.

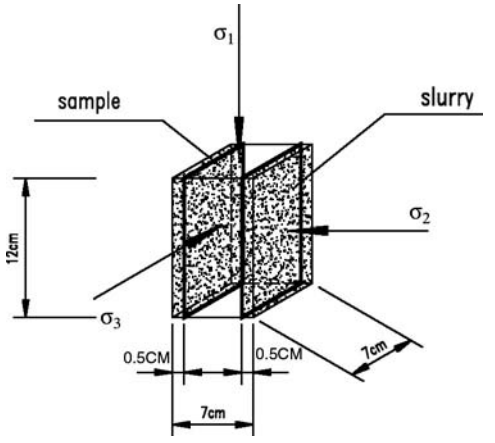

Figure 10. Sample dimension and notation for principal stress.

and ⑦$_{1\text{-}1}$) encountered in Shanghai Yangtze River Tunnel project will be used in the test program. The test program will consist of the sieve analysis, true triaxial test, and the ESEM study. Figure 9 shows the particle size distribution of the soil used (layer ⑦$_{1\text{-}1}$).

For each soil type, a serial of true triaxial tests will be conduced firstly using brick-shaped samples (70 mm × 60 mm × 120 mm), with 120 mm in height, 70 mm × 60 mm of the horizontal section and 5 mm at each sides in σ_2 direction is reserved for slurry injection, as illustrated in Figure 10. For future reference, the vertical stress is denoted σ_1, and the horizontal stressed are denoted σ_2 and σ_3 (Fig. 10), they are the principal stresses which are set according to the calculation results in Table 3. σ_1 and σ_2 correspond to the vertical overburden pressure and slurry supporting pressure, respectively. Under the "undrain" condition, the results of the total stress method will be used, while for "drain" condition, the data from the effective stress method will be applied.

To simulate the process of the slurry gradual infiltration into the soil, "drain" condition will be considered, moreover, the "drain" phase is also reproduced with the intent to study the time dependent response, when the excavation is completed (the face of the tunnel is far away from the section under study) or during a standstill for segments assembling, etc. While, it is of interest to point out the different trends of behavior exhibited by the samples, depending on the excess pore pressure values, and to simulate the stress conditions at laboratory scale in the near vicinity of the tunnel, during face advancement, therefore, the "undrain" condition will also be carried out in the test.

The objective of the tests performed under the true triaxial state of stresses is to determine the respective stress-strain curves and to measure the stresses at material fracture for described loading program which should be based on the actual condition during shield tunnelling. Various combinations of the stress tensor compononts and at least two different loading paths are necessary to obtain information of the sample state at failure under the slurry gradual infiltration and the shape of the limit failure surface subjected to triaxial state of stresses. The loading paths shown in Figure 11 for the true triaxial states of stresses consist of two stages. The stage 1 is a phase of a monotonic increase of hydrostatic stress up to prescribed value σ_3, in the stage 2 the triaxial state of stresses is a combination of hydraulic stress σ_3 and different biaxial compression pressures σ_1 and σ_2. In the program of the true triaxial test apparatus, the coefficient of intermediate principal stress $b = (\sigma_2 - \sigma_3)/(\sigma_1 - \sigma_3)$ is introduced and used to characterize the role of intermediate principal stress variation on stress state through the different b values. Thus, in the stage 2, the vertical normal stress σ_1 is gradually increased, and simultaneously, the intermediate principal stress σ_2 corresponds to change according to a certain b value. The two values σ_1 and σ_2 are increased up to 15%–20% of the total axial strain which can be regarded as the material failure that occurs for $\sigma_{1f} = \sigma_3 + \Delta\sigma_1$, $\sigma_{2f} = \sigma_3 + \Delta\sigma_2$ respectively. The loading paths illustrated in Figure 11.

To obtain several combinations of the stress tensor components, the various levels of the hydraulic stress σ_3 and b values will be considered under the "drain" or "undrain" conditions in our test program, shown in Table 5.

As shown in Figure 11, the samples are initially consolidated at the appropriate confining cell pressure corresponding to values in Table 5 under "drain" or "undrain" conditions. This is followed by controlled stress path loading, in which the axial stress is imposed at a rate of 0.36 mm/min for "drain" condition and 6 mm/min for "undrain" condition in the major principal direction. The test is terminated when σ_1 and σ_2

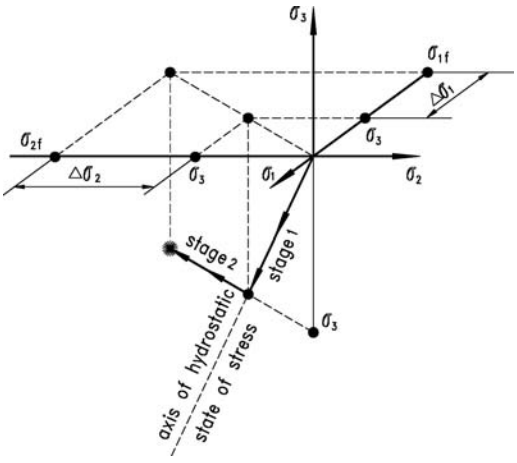

Figure 11. Loading path for Stage 1 and Stage 2 of true triaxial loading (*point corresponding to material failure).

Table 5. Serials of true triaxial tests in program.

	Drain condition		Undrain condition	
Serials	σ_3(kPa)	b	σ_3(kPa)	b
1	75	0.2, 0.4	225	0.2, 0.4
2	100	0.2, 0.4	250	0.2, 0.4
3	125	0.2, 0.4	275	0.2, 0.4
4	150	0.2, 0.4	300	0.2, 0.4

reach certain values which result in 15%–20% of the total axial strain and cannot be reached any further.

Noticeably, accordingly to the three geological conditions illustrated in Figure 4–6, we only calculated the relative vertical overburden pressure σ_v and the slurry supporting pressure P_s which corresponding to the major principal stress σ_1 and the intermediate principal stress σ_2, respectively. Thus, the initial confining pressures σ_3 in Table 5 are decided by the different K_0 values which mean coefficient of earth pressure at rest. So, we can deduce the following equation:

$$\begin{cases} K_0 = \sigma_3/\sigma_1 \rightarrow \sigma_3 = K_0 \cdot \sigma_1 \\ b = (\sigma_2 - \sigma_3)/(\sigma_1 - \sigma_3) \rightarrow \sigma_2 = \sigma_1[b(1-K_0)+K_0] = B \cdot \sigma_1 \end{cases} \quad (2)$$

According to σ_{1f} and σ_{2f} values acquired at the end the shearing phase, we can back-calculate the corresponding K_0 and B values and establish their relationships.

3.3.2 *ESEM image processing*

We wonder whether the infiltration of the slurry would increase the inherent strength of filter cake and what effects would the different types of the slurries have on the compactness of the filter cake. Additionally, image processing of photographs taken by the ESEM can be used to relate the macrostructure of the sample strength to the microstructure of the filter cake. We are specifically interested in analyzing the variation characteristics of the pore size, pore form and the grain form as well as the contact relationships between each grain, and the grains arrange orientability, their orientation towards the vertical axial line of the sample. we can express above features by the following microscopic parameters: void ratio e, numbers of pores n_p, numbers of grains n_g, pore average diameter d_p, grain average diameter d_g, pore average area a_p, grain average area a_g, pore abundance C_p, grain abundance C_g, pore oriented frequency $F_P(\alpha)$, grain oriented frequency $F_g(\alpha)$, pore distribution dimension D_{pd}, grain distribution dimension D_{gd}.

The ESEM specimens are chosen at the filter cake surface and the shear band surface. Small specimen (about 10 mm diameter and 5 mm height) is carefully removed along the crosssection and scanned along its thickness in its original state.

4 CONCLUSION

This study has presented a program of true triaxial tests to investigate the mechanics of the face stability at different levels of confining pressures, overburden pressures and the slurry supporting pressures. The test has two functions, one for slurry infiltration testing in terms of the water discharge volume verse time under the different pressures, which can be used to test the quality of the formed filter-cake; the other for the strength testing which can be used to analysis the strength variation of the sample as the slurry gradual infiltration. In order to test the macroscopic phenomena and parameters from the true triaxial tests, a serial of ESEM studies are added into our program with expect to understand microstructure behavior and the changes in the microstructure of the filter cake upon the infiltration of the slurry and establish the relationship between microstructural parameters and strength coefficients in quantitative terms.

ACKNOWLEDGMENT

The authors wish to thank Prof. YANG Yi-zhang from Tongji University for his great help in true triaxial test and engineer XU Jian-bo from Shanghai Tunnel Engineering Co., Ltd. for his help in test material provision.

REFERENCES

Anagnostou, G. & Kovári, K. 1994. The face stability of slurry-shield-driven tunnels. *Tunnelling and Underground Sapce Technology* 9:165–174.

Cheng, Z.L. & Wu, Z.M. 2001. Experimental research of the face stability during a slurry shield tunneling in sand soil condition. *Journal of Yangtze river scientific research institute* 18:53–55.

Deng, Z.Y. 2005. *Research on the Face Stability of Slurry-Shield-driven Tunnels*. M.D. thesis. Tongji University, Shanghai, China.

Fritz, P. 2003. Slurry shield tunneling in highly permeable ground. *12th Panamerican Conference on Soil Mechanics and Geotechnical Engineering, 39th U.S. Rock Mechanics Symposium.*

Huang, W.X. et al. 2007. Analysis of the failure mode and softening behaviour of sands in true triaxial tests. *International Journal of Soils and Structures* 44:1423–1437.

Li, Y. & Zhang, Z.X. 2006. Analysis of the effect of slurry penetration on the face stability during a slurry shield tunneling. *Rock and Soil Mechanics* 27:464–468.

Mori, A. & Kurihara, K. 1995. A study on face stability during slurry-type shield tunneling. *Underground Construction in Soft Ground*: 261–264.

The Shanghai Yangtze River Tunnel - Theory, Design and Construction – Huang (ed)
© 2008 Taylor & Francis Group, London, ISBN 978-0-415-47161-9

Design and optimization of gasket for segment joint based on experiment and mathematical analysis

Z.X. Zhu & M. Lu
Shanghai Tunnel Engineering & Rail Transit Design and Research Institute, Shanghai, P.R. China

ABSTRACT: This article introduces the waterproof design method for segment joint of extra-large, extra-long, and deep subaqueous shield tunnel. The joint sealing gasket has experienced a complete watertight test including compression deformation, horizontal joint and cross-shaped joint tests, and durability test including thermal ageing, mass change ratio, stress relaxation and creep deformation. The mechanical model, calculation, mathematical analysis and results on the basis of the above tests are systematically introduced. And it demonstrates the significance to optimization and improvement of gasket design.

1 INTRODUCTION

Shanghai Yangtze River Tunnel of Chongming River-crossing Passage starts from Wuhaogou Pudong, passes through South Harbor of Yangtze River, and ends at Changxing Island to connect with Yangtze River Bridge. It is totally 8,893.33 m long. Pudong offshore section is 657.83 m long, and Changxing Island offshore section is 829.93 m long. The river-crossing section consists of 2 shield tunnels. The upward and downward lines are respectively 7,471.65 m and 7,469.36 m long. There are 8 cross passages every approx. 830 m. The upper level of tunnel section is used for highway, and the lower level includes the reserved rail transport space, equipment pipe gallery, the wastewater pump station and etc. The reinforced concrete segment of tunnel lining is assembled in staggered jointing. The outer diameter of lining is 15 m, the thickness of segment is 650 mm, the width of ring is 2,000 mm and the strength of concrete is C60.

Due to large depth of embedment, the river-crossing road tunnel with ultra-large diameter has to bear very large hydraulic pressure. Therefore, requirement on the waterproof design (mainly including self-water resistance, joint water resistance and cross passage's water resistance for prefabricated concrete segment structure and cast-in-situ concrete structure) for the tunnel is very high. For waterproof design characteristics of world-famous long and large submarine tunnel, see Table 1.

2 WATERPROOF DESIGN PRINCIPLE OF TUNNEL LINING

Depending on the engineering characteristics of ultra-large diameter shield tunnel, we firstly ascertained the design principle of "based on self-water resistance of concrete structure, focusing on joint water resistance and providing multiple protective measures to ensure the long waterproof performance under high hydraulic pressure and opening of joint".

3 WATERPROOF GRADE OF TUNNEL LINING

Generally, water resistance for road tunnel up to Grade 2 is enough. However, in consideration of being a large and importance road tunnel, the offshore section, mid-river shield tunnel section and cross passage for this tunnel shall be provided with water resistance above Grade 2. See Table 2. In order to reach this waterproof grade, the waterproof performance of joint gasket is the key point technically.

4 DESIGN AND OPTIMIZATION OF GASKET FOR JOINT

Water resistance of joint for the lining structure is especially important in the waterproof measure for shield tunnel. This article focuses on the design and optimization of the flexible rubber gasket which is the main protection measure for joint waterproof in Depending on research and contrast of different joint water resistance designs for many domestic and foreign subaqueous shield tunnels (see Tables 1 and 2), and on the basis of the structural characteristics of segments of the shield tunnel, we mainly considered.:

(1) Use single or double waterproof gaskets

Most of the shield tunnels are only provided with single flexible gasket. Only the No. 4 Tunnel of Elbtunnel in

Table 1. Characteristics of waterproof design for five world-famous long and large subaqueous shield tunnels.

	Hamburg, Germany No. 4 Tunnel of Elbtunnel	Japan Tokyo Bay Road Tunnel	Denmark Store Baelt Channel Tunnel	Holland Green Heart Road Tunnel
Basic structure parameters	D (OD): 13.75 m δ (segment thickness): 0.70 m B (segment width): 2 m H (embedment depth): 50 m	D (OD): 13.90 m δ (segment thickness): 0.65 m (inner lining thickness 0.35 m) B (segment width): 1.5 m H (embedment depth): 60 m	D (OD): 8.5 m δ (segment thickness):.0.40 m B (segment width) 1.65 m: H (embedment depth): 75 m	D (OD): 14.5 m δ (segment thickness):.0.60 m B (segment width): 2 m H (embedment depth): 40 m
Allowable leakage in design	The entire tunnel: $\leq$0.1$\sim$0.175 L/m^2·d	No leakage after lining casting	The entire tunnel: $\leq$0.1 L/m^2·d any 100 m^2 $\leq$0.1$\sim$0.175 L/m^2·d	
Waterproof technology or measure	Max. designed hydraulic pressure 1 MPa P (max. test hydraulic pressure) 1.2 MPa, t (opening of joint) = 6 mm, d (staggered joint displacement) = 15 mm: no leakage. P = 0.9 MPa, t = 9 mm, d = 15 mm: no leakage.	P (max. test hydraulic pressure) 0.6 MPa, t (opening of joint) = 5 mm: no leakage. P = 1 MPa, t = 3 mm: no leakage (the test is carried out depending on double depth of actual embedment)	=0.1 l/m.d (within any 10 m) <=0.3l/m.d	
Gasket	The joint uses two pieces of EPDM flexible rubber packing (PhoenixM385.65)	One water-swelling flexible gasket, expansion ratio 200$\sim$300%, cross section dimension: 30 mm $\times$ 10 mm; a buffer plate for circumferential and longitudinal faces of inner joint	A CR flexible rubber gasket	The joint uses EPDM flexible rubber gasket (Phoenix M style); water-stop strips are set outside joint edge of some segments.
Waterproof characteristics	Double gaskets are provided so that the circumferential face is stable and the water-leaking position can be determined easily. However, the cost is high and work procedure is complicated.	Water leakage is small after initial lining and is less after providing waterproof layer and inner lining. Durability of expansion gasket material is verified through test.	Focusing on water resistance and anti-corrosion of backfill injecting material of segment, acting as secondary measure of joint waterproofing	Water-stop strip can stop the mud, backfill injecting mortar, and improve the waterproofing.

Table 2. Water resistance and durability design parameter for three large domestic subaqueous road shield tunnels.

No.	Tunnel	Basic structure parameter	Allowable leakage in design	Watertight grade of segment and single leakage inspection	Technical requirement on joint water resistance test	Joint gasket	Waterproof characteristics
1	Shanghai East Yan'an Road River-cross Tunnel	Tunnel outer diameter of 11 m, internal diameter of 9.9 m, maximum embedment of 36 m	Leakage of the entire tunnel $\leq 0.1\ L/m^2 \cdot d$ Leakage within any 100 m^2 $\leq 0.2\ L/m^2 \cdot d$ (actual leakage $< 0.06\ L/m^2 \cdot d$)	$\geq$S8 0.8 Mpa, 6 h: permeation height $\leq$10 cm	0.8 Mpa hydraulic pressure, displacement by 10 mm, longitudinal joint opening 8 mm, circumferential joint opening 5 mm: no leakage	CR gasket, asymmetrical groove, a gasket (different circumferential faces with respect to two gasket cross sections)	Gaskets with different cross sections are designed based on circumferential free of tongue-and-groove and large relative step of segment.
2	Dalian Road River-cross Tunnel	Tunnel outer diameter of 11 m, internal diameter of 10.04 m, maximum embedment of 35 m	Leakage of the entire tunnel $\leq 0.08\ L/m^2 \cdot d$ Leakage within any 100 m^2 $\leq 0.16\ L/m^2 \cdot$ d	$\geq$S10 0.8 Mpa, 3 h: permeation height $\leq$5 cm	0.8 Mpa, displacement by 10 mm, circumferential and longitudinal joint open 8 mm: no leakage	A perforated EPDM rubber and water-swelling rubber compound gasket (a buffer plate in addition)	Matching structure characteristics and alternate joint; buffer plate
3	Shanghai Yangtze River Tunnel	Tunnel outer diameter of 15 m, internal diameter of 13.7 m, maximum embedment of 46 m	1. Leakage of the entire tunnel $\leq 0.05\ L/m^2 \cdot$ d, leakage within any 100 m^2 $\leq 0.1\ L/m^2 \cdot d$; 2. Wet spot of inner surface $\leq$4‰ of total surface area, wetted imprints within any 100 m^2 $\leq$4 points, max. area of single wetted imprint $\leq 0.15\ m^2$.	$\geq$S12 0.8 Mpa, 3 h: permeation height $\leq$5 cm	1 Mpa, displacement by 10 mm, circumferential and longitudinal joints open 7 mm: no leakage	Perforated EPDM rubber gasket; polyurethane expansion strip in the gap between circumferential and longitudinal joints along the outside of its groove	The structure and style of gasket is analyzed with finite-element mathematical model. Durability index tex and service life calculation make it more reliable. Sealing strip will enhance waterproof function of joint and solve the problem that the backfill injecting liquid or leaking water permeates to the assembly face along the outside of gasket groove.

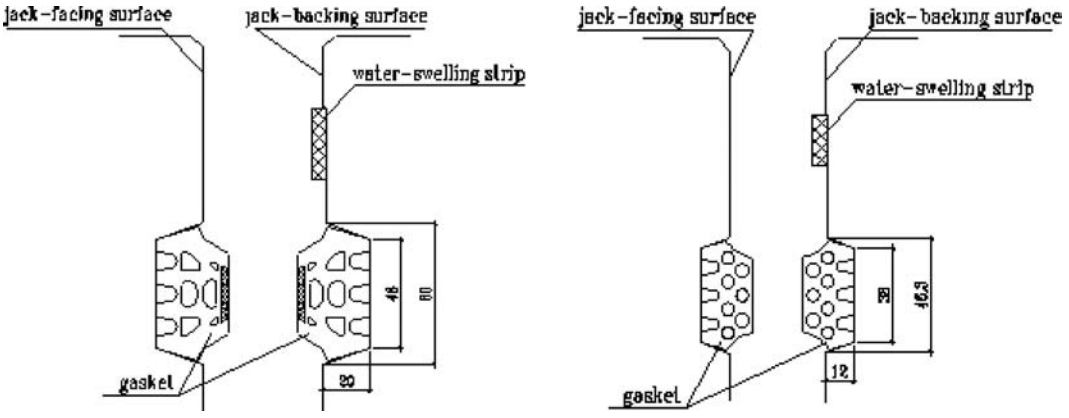

Figure 1. Water resistance of flexible rubber gasket and joint between double protection lines of sealing strip: (a) Initially de-signed gasket cross-section and groove dimension; (b) Optimized gasket cross-section and groove dimension.

Hamburg, Germany (Table 1), the approx. 14 m large-diameter shield tunnel, is provided with double sealing gaskets. In despite of under high hydraulic pressure, Tokyo Bay Tunnel is only provided with one gasket and the inside of another one is only made of buffer material. Usually, Japan uses double perforated flexible rubber gaskets in gravity current sewage shield tunnels to satisfy large deformation as well as avoid impact of sewage medium on expansion rubber, and uses double water-swelling rubbers in gravity current shield-driven water tunnels. The successful examples in China include Shangzhong Road Shield Tunnel, of which the segment structure is similar to that of Shanghai Yangtze River Tunnel and the joint between segments is only provided with single gasket. Through contrast of these two options, we decided to use single flexible rubber gasket for Shanghai Yangtze River Tunnel. The single gasket, together with the sealing strip, forming double protection, is proposed as the joint waterproof design in initial (Fig. 1).

(2) Structure, water resistance and durability of gasket

For the gasket, research on water resistance and durability shall be emphasized. In addition to common measures, we had done following things: (1) test of stress relaxation for perforated special cross-section flexible gasket, improve the style and distribution of holes and grooves, and perform finite-element analysis to determine the optimal cross section structure; (2) For hydro swelling gasket, test of wetting and drying cycle impact and expansion resin precipitation for water-swelling rubber. The former depends on period and times of cycle, and the latter depends on control of interference of other filling materials in the educt on test result.

4.1 *Material and performance of gasket and sealing strip*

4.1.1 *Determine gasket material and performance*

The flexible rubber gasket is made of EPDM rubber or the compound of EPDM rubber and water-swelling expansion rubber. For performance of each material, see Tables 3 and 4.

4.1.2 *Determine material and performance index of sealing strip*

Water-swelling strip was mounted to the outside of the flexible rubber gasket. The sealing strip will prevent the backfill injection liquid and shield tail grease from flowing into the joint and improve the durability of gasket.

The sealing strip was made of water-swelling rubber and polyurethane elastomer. For performance index of polyurethane elastomer, see Table 5.

The polyurethane elastomer was the new waterproof material imported from Japan. The significant advantage of polyurethane is small ratio of mass change and increased tensile strength of material after expansion. Its disadvantage is high unit price.

4.1.3 *Determine durability of rubber gasket's rubber and sealing strip's material*

Due to long-term compression and shearing, impact of environment and temperature, and corrosion of chemical pollutant, the rubber of flexible rubber gasket will suffer from ageing problems such as creep deformation and stress relaxation etc. Its durability can be verified through following tests.

(1) Durability control for flexible rubber

Forecast the service life of EPDM rubber on the basis of the ratio of tensile strength and elongation under 70° in 72 h and permanent

Table 3. Performance index of EPDM rubber.

Item	Rigidity (°)	Tensile strength/MPa	Tensile yield (%)	Anti-mildew grade	Ageing resistance (ratio of change) (70°C, 96 h)		
					Ratio of tensile strength change (%)	Ratio of tensile yield change (%)	Rigidity change (°)
Index	62° ± 5°	≥10.5	≥350	≥Grade 1	≥−15	≥−30	≤+6°

Table 4. Performance index of water-swelling expansion rubber.

Item	Rigidity (°)	Tensile strength (MPa)	Tensile yield (%)	Ratio of mass change (%)	Ratio of volume increase (%)	Repeated immersion test		
				180d		Tensile strength (MPa)	Tensile yield (%)	Ratio of volume increase (%)
Index	45° ± 7°	≥3	≥400	≤2%	≥400	≥2	≥250	≥300

Note: The water-swelling performance indices of water-swelling rubber and sealing strip used in flexible rubber gasket are the same.

Table 5. Performance index of polyurethane elastomer.

Item	Rigidity (°)	Tensile strength (MPa)	Tensile yield (%)	Ratio of volume increase (%)	Ratio of mass change (%)
					Heating and accelerating
Index	43° ± 7°	≥0.4	≥800	≥360	≤2.5

compression deformation through hot-air accelerated ageing and one-hundred-year stress relaxation through Arrhenius equation (stress relaxation ≤25%, on the basis of the special equation between compression stress characteristic change and ageing time and temperature).

(2) Durability control for water-swelling rubber

Determine the durability of water-swelling rubber and polyurethane expansion strip on the basis of resin precipitation rate (180 days ≤2%) after long-term immersion as well as the change ratio (100 times) of tensile strength, elongation rate and expansion rate under repeated wetting and drying. There is a polyurethane expansion strip on the outer face of flexible rubber gasket. It is used as the first protection line so that the durability of flexible rubber gasket is enhanced.

4.2 *Structure design for gasket cross-section*

4.2.1 *Initial determination of gasket groove and structure*

4.2.1.1 Determination of basic dimension

Step 1: Determine the dimension of segment groove. According to domestic and foreign engineering experiences, and depending on the compression stress control of compressing the entire flexible rubber gasket into the groove, determine the proper dimension of groove. Step 2: Determine the size of flexible rubber gasket. After deciding the groove dimension, determine the height and width of flexible rubber gasket on the basis of the maximum opening and the pressure for compressing it into the groove. The above calculation shall be based on equation (1)–(3).

(1) A: Cross-section of groove, A0: Cross-section of flexible rubber gasket

Adjust the openings of gasket, number and dimension of grooves, and the joint opening to be borne by the gasket. Satisfy with the requirement of the equation:

$$A=1\text{-}1.15A0 \tag{1}$$

(2) The maximum compression ratio of flexible rubber gasket

$$\alpha=\frac{T-A}{T} \qquad \alpha'=\frac{T-A-B}{T} \tag{2}$$

Where, α the minimum compression ratio of flexible rubber gasket; B 1/2 of allowable design opening of joint; A depth of gasket groove; T height of flexible rubber gasket.

(3) Allowable opening of gasket

For short-term water resistance, the stress of contact face occurring due to compression of sealing material

shall exceed the designed hydraulic pressure. For long-term water resistance, the contact face stress shall be no less than the actual hydraulic pressure. The allowable opening of gasket under designed hydraulic pressure shall satisfy with the equation below:

$$\delta \le BD/(\rho_{\min} - 0.5D) + \delta_0 + \delta_s \quad (3)$$

Where, δ allowable joint opening value (mm) of flexible rubber gasket in circumferential joint and under the designed hydraulic pressure; $\rho_{\min}$ the minimum curvature radius of longitudinal deflection of tunnel (mm); D outer diameter of lining (mm); B width of segment (mm); δ_0 circumferential clearance possibly occurring in production and construction (mm); δ_s joint deformation gain occurring due to anaphase deformation of tunnel (mm).

4.2.1.2 Initial determination of detailed structure of gasket

Three cross-sections of flexible rubber gasket were considered on the basis of above equations (1)–(3).

Step 3: Reasonably decide the holes (position and shape) within flexible rubber gasket. Optimize the design of holes within flexible rubber gasket on the basis of step 1 and step 2.

Main issues in consideration:

- Coordinated deformation of hole;
- Pressure for compressing the entire flexible rubber gasket into groove, i.e. the closed compression (KN/m);
- Value and distribution of contact stress of segment under the maximum opening;
- Shape of compression deformation curve. For further optimization, impact of stress concentration caused by different holes, long-term stress relaxation and creep deformation on long-term waterproof performance shall be considered.

Finally, we determined the optimal gasket cross-section through modification to the cross-sections of these three new gaskets given in Figure 2.

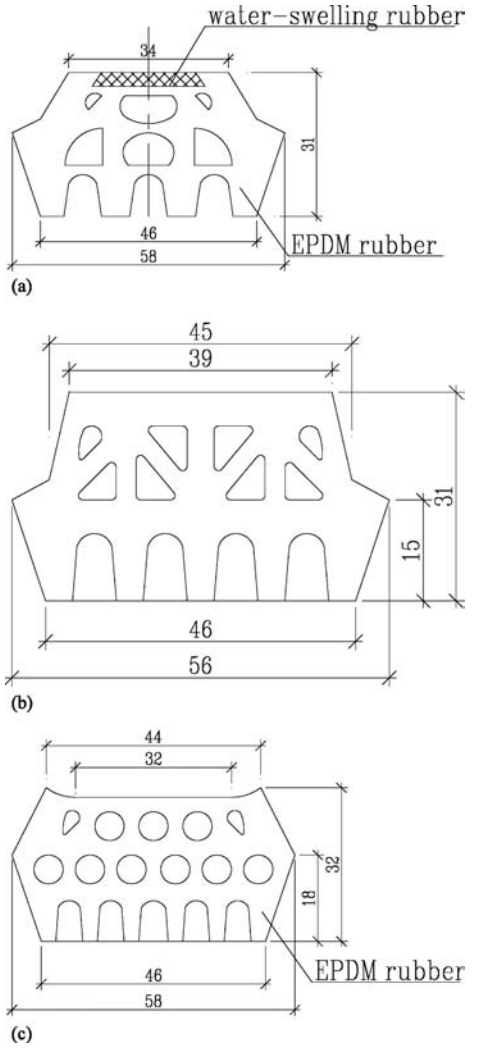

Figure 2. Cross-sections of three flexible rubber gaskets.

4.3 *Research on gasket and strip optimization*

In order to comprehensively understand and verify the short-term and long-term waterproof performance of water-swelling strip, polyurethane flexible strip and EPDM rubber gasket, we established the test methods on the basis of the characteristics of each cross-section.

4.3.1 *Watertight test for gasket and strip*

- Compression deformation test for gasket: ① compression deformation test of bar sample (Fig. 3); ② compression deformation test of frame sample.
- Impact of expansion force of polyurethane flexible strip and water-swelling rubber strip on concrete segment.
- Watertight test (Table 6, Table 7) of flexible rubber gasket and strip (including post-ageing):① Watertight test of horizontal joint (Fig. 4); ② Watertight test of T-shaped joint (Fig. 5).

4.3.2 *Durability test of gasket and strip*

- Compression creep test of flexible rubber gasket (Fig. 6).
- Stress relaxation test of flexible rubber gasket (Fig. 7).
- Durability test of flexible rubber gasket and strip: ① mass change rate after soaking ② repeated wetting and drying test; ③ watertight test of flexible rubber gasket and strip after ageing.

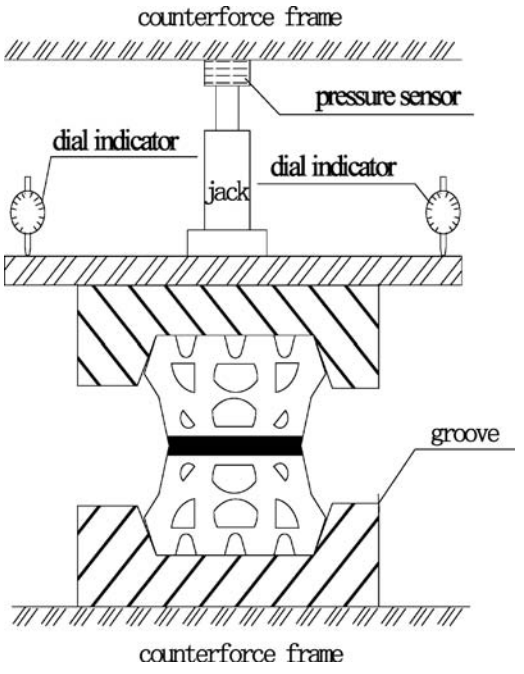

Figure 3. Compression deformation test of bar sample.

Table 6. Watertight test of horizontal joint.

Test item	Material	Work condition
Watertight test of horizontal joint	Water-swelling rubber strip	No staggered joint
	Polyurethane flexible strip	No staggered joint
	Flexible rubber gasket	No staggered joint Staggered joint
	Combined action of polyurethane flexible strip and flexible rubber gasket	No staggered joint Staggered joint
	Combined action of polyurethane flexible strip and flexible rubber gasket after being immersed in chlorine salt	No staggered joint Staggered joint

4.3.3 *Mathematical analysis on gasket cross-section*

(1) Step 1

After compression deformation test, water resistance tests of horizontal joint and T-shaped joint of the original flexible rubber gasket, and elaborated analysis, it was thought that the gasket was capable of reaching certain waterproof standard, but its closed

Table 7. Watertight test of T-shaped joint.

Test item	Material	Work condition
Watertight test of T-shaped joint	Polyurethane flexible strip	No staggered joint
	Combined action of polyurethane flexible strip and flexible rubber gasket	No staggered joint Staggered joint

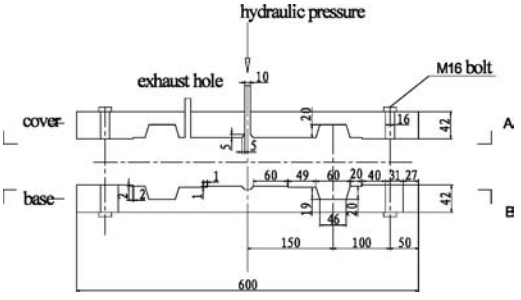

Figure 4. Watertight test device for horizontal joint.

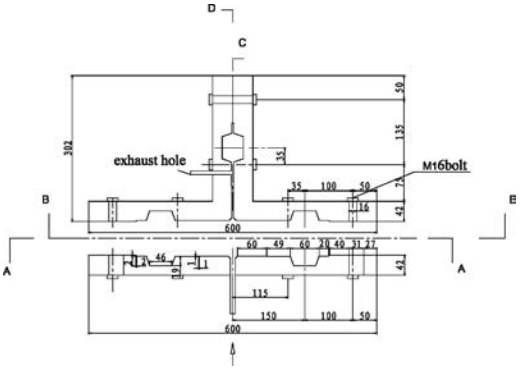

Figure 5. Watertight test device fort-shaped joint.

compression force was high (62 kN/m), which would bring negative impact on segment assembly. Meanwhile, in order to decrease the cost of work, on the premise of maintaining the good hydraulic pressure resistance performance, the small sized groove and flexible rubber gasket was chosen. See Figures 1–2.

(2) Step 2

On the basis of groove dimension (Fig. 1), three flexible rubber gaskets for optimizing cross-sections were designed (Fig. 8). After that, a mathematical model was built. The calculation and analysis was made by finite-element method. We screened out one gasket which was broken after deformation. Then, watertight test, compression deformation test, creep test and stress

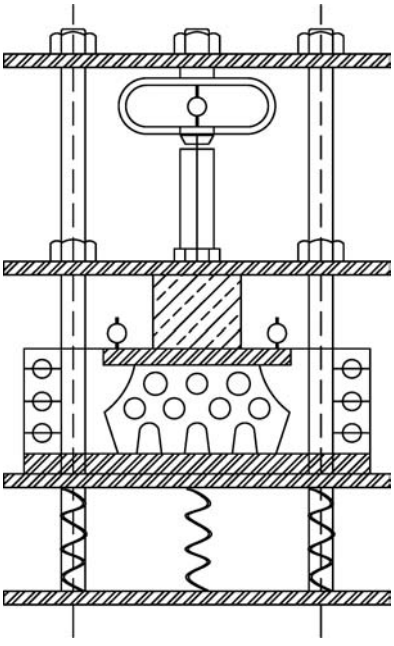

Figure 6. Device for compression creep deformation test.

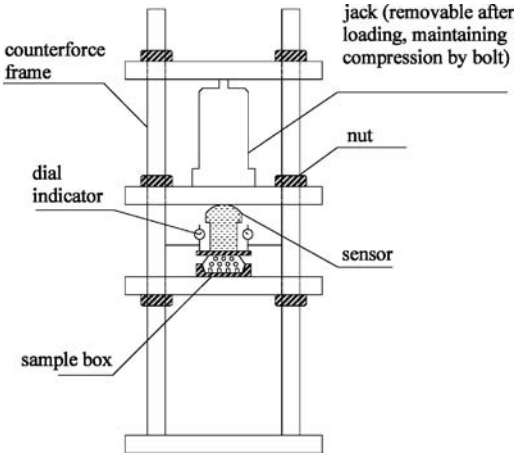

Figure 7. Device for stress relaxation test.

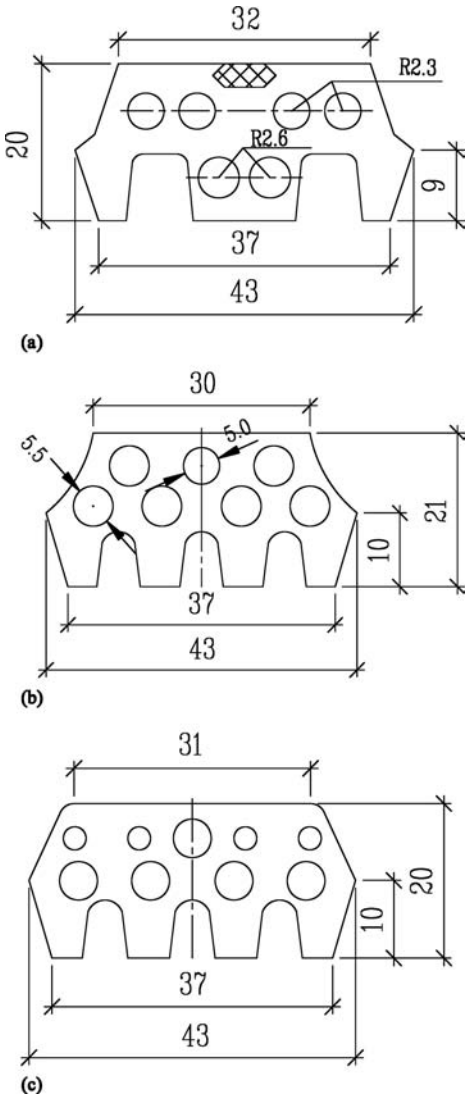

Figure 8. Three gaskets for cross section optimization.

relaxation test were made for the other two gaskets (Fig. 9) to verify which style was optimal for cross section.

Next, the height of gasket was optimized. And the relative watertight tests were made. The results were ideal. Therefore, the gasket cross-section to be used in engineering was finally determined. This flexible rubber gasket could meet the requirements of 7 mm of joint opening, 6 mm of staggered joint and 1.04 Mpa of hydraulic pressure resistance. Its compression stress was 43 kN/m, and the stress relaxation was 25% (stable after 36d) which meet the waterproof requirement of this project.

(3) Step 3

In order to further improve the safety coefficient of flexible rubber gasket, we proposed the fourth cross-section style. We first selected the gasket structure with smaller round-hole diameter and rubber rigidity as the preferential cross-section. The watertight test and compression deformation test were conducted. Next, creep test and stress relaxation test were made for this cross-section. Based on the results of above tests, the cross-section was optimized, the safety co-efficient of

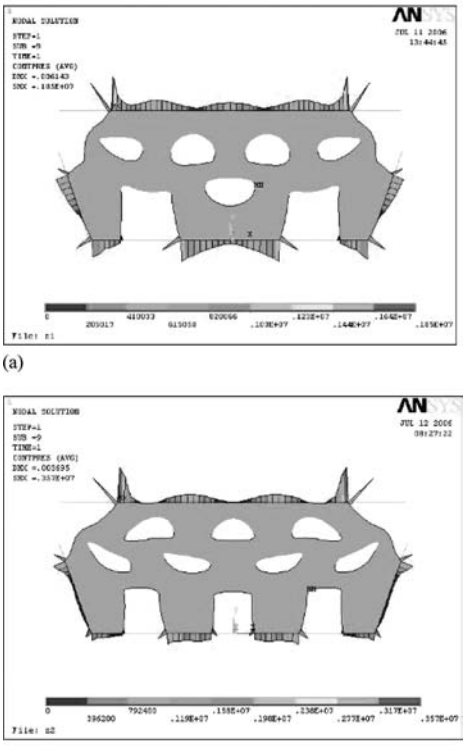

(a)

(b)

Figure 9. Contact stress of two gaskets when joint opening by 7 mm.

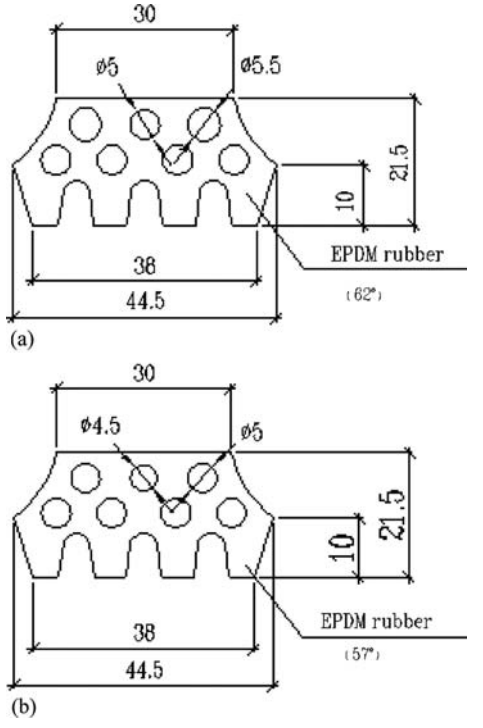

Figure 10. Gasket cross sections used in the project.

which was further improved (Fig. 10). New flexible rubber gasket could reach the requirement: 8 mm of joint opening, 6 mm of staggered joint and 1.04 Mpa of hydraulic pressure resistance. Its compression stress was 55 kN/m, and stress relaxation was 20% (stable after 58d). The stress relaxation performance of new gasket was better than that of the gasket used in the project.

4.3.4 *Results of gasket cross section study*

Different from the common use of the same gasket for various depths of tunnel embedment, the optimal gaskets were chosen based on the test results of the above three-step-test. Since the gasket of style 2 is better than that of style 1 in water tightness performance, we shall apply the style 2 into the joints between linings for ultra-deep, deep and mid-depth tunnel; applying the style 1 into the joints between linings for shallow tunnel. (Fig. 10) Thus, only change the size and arrangement of hole (the rubber rigidity could be adjusted properly) could the perforated gasket made with extrusion microwave sulfuration technology satisfy with the watertight and closed compression force requirement for different water depth conditions while no changes to the appearance and dimension (gasket groove and processing mould remained) are necessary.

Depending on calculation by finite-element method, the section compression-deformation, compression contact stress and vertical stress distribution are gotten. The gasket compression-deformation curve is calculated. Then stress-relaxation curves reflecting the constant displacement under various deformations are calculated. By polynomial fit algorithm, the function is come up with reflecting the relationship between stress and time of the gasket cross-section used in project. The function is $\sigma = e^{-0.313-3.05\times10^{-7}t}$. When $t = 100$ years, the contact surface stress of two flexible rubber gaskets under specified joint opening after 100 years are respectively 0.56 Mpa and 0.71 Mpa. This shows that the gasket can meet the water-proof requirement of 100 years service. See Table 8.

4.3.5 *Results of water-swelling strip study*

For the strip, a series of tests were made such as watertight test, impact test on the concrete segment, mass change ratio test and repeated wetting and drying test etc. The conclusions are:

- The water-swelling strip can bear certain hydraulic pressure only in case of small joint opening.

Table 8. Contact stress relaxation.

	Initial contact stress (MPa)	Fitting Function	Residual stress after 100 years (MPa)	Attenuation rate	Safety coefficient
Cross section applicable in the project	1.05	$\sigma = e^{-0.313-3.05\times10^{-7}t}$	0.56	47%	$0.56/0.52 = 1.08$
The improved cross section	1.18	$\sigma = e^{-0.254-2.01\times10^{-7}t}$	0.71	40%	$0.71/0.52 = 1.37$

Therefore, it functions as auxiliary water resistance in case of small opening of joint.

- The expansion force of water immersed strip is much less than the compression strength of segment concrete and will have no impact on segment.
- Under the same test condition, mass change ratio of polyurethane elastomer and water-swelling rubber is 1.75% and 2.84% respectively. The mass change ratio of polyurethane elastomer is obviously less than that of water-swelling rubber. This means that the expansion durability of polyurethane elastomer is better than that of water-swelling rubber.
- According to the repeated wetting and drying test, for the expansible performance, the impact of chlorine salt in underground water on water-swelling rubber is larger than that on polyurethane elastomer. The design expansible ratio of both materials can satisfy with the design requirement. But expansible ratio of water-swelling rubber is higher than that of polyurethane elastomer, while the expansible stability of polyurethane elastomer is better.

Based on the above test results and considering engineering cost, polyurethane elastomer strip is selected to apply into the joint between linings at tunnel consolidation area and water-swelling rubber strip is used in the joint between linings at non-consolidation area. Meanwhile, the strips are mounted into the longitudinal joints between segments and the circumferential joints backside of the jack (L-shaped). This ensures that the strip will not be exposed during segment assembly, and the negative impact of strip due to pre-expansion is reduced.

5 CONCLUSIONS

The following points shall be taken as the keys of optimization in future gasket design and research.

- In this watertight test, most of the water leakage happened, not between gaskets, on the contact surface between gasket and concrete groove. Therefore, the bottom and both sided of gasket contacting with the groove should be strengthened, so as to be capable of resisting the test hydraulic pressure.
- The water-swelling rubber strip would leave the surface of compound gasket, because the molded vulcanized water-swelling rubber and the EPDM rubber gasket are not integrated with each other after embedding the former into the latter by manual work. At present many manufacturers have developed one-process formation technology of EPDM rubber and water-swelling rubber. This technology ensuring the integrity of water-swelling rubber and EPDM rubber should be widely applied.
- During the segment assembly, the gasket in longitudinal joint cannot be compressed completely because it is within the shield shell. And the high closed compression force of gasket will not easy for joint compacting. Thus, it's difficult to insert the key segment. The adoption of technology of coating organic silicon film-forming material on the surface of rubber will significantly reduce the resistance of insertion. It overcomes the disadvantages of traditional antifriction measures, and ensures a stable waterproof performance.
- Finite-element calculation method shall be taken as an important auxiliary way to determine the cross-section prior to indoor test. Carrying out test on the basis of the calculation result is an effective way to reasonably decide the final cross-section. Further test and mathematical analysis are of expansible stress change of expansion material under different compression conditions and of impact on durability of compound gasket.

ACKNOWLEDGEMENTS

We hereby appreciate Dr. Zhengyu Lei who is mainly in charge of the above finite-element analysis and research work.

REFERENCES

Lu, M., Cao, W. B & Zhu, Z.X. 2007. Waterproof technology of extra-large diameter shield tunnel. *Underground Engineering and Tunnel.* Supplementary.

Zhu, Z.X & Modern. 2002. Waterproof technology of shield tunnel. *Underground Engineering and Tunnel.*

Zhu, Z.X. Innovative technologies of tunnel waterproofing and some thoughts. *China Architecture Waterproofing.*

The Shanghai Yangtze River Tunnel - Theory, Design and Construction – Huang (ed)
© 2008 Taylor & Francis Group, London, ISBN 978-0-415-47161-9

Design of hazard prevention system for Shanghai Yangtze River Tunnel

X. Wang, Z.Q. Guo & J. Meng
Shanghai Tunnel Engineering & Rail Transit Design and Research Institute, Shanghai, P. R. China

ABSTRACT: The fire prevention system of Shanghai Yangtze River with long distance and large diameter was detailed presented from the point view of composition, design method and application prospect.

1 INTRODUCTION

Fire controlling has become the most important consideration for the tunnels with the increase of long and large tunnel projects. In recent years, fire accidents occur frequently all over the world in the tunnel, which is a very important clue to draw more consideration on the fire control of the tunnel. The tunnel and passengers objectively face great risk if only depends on few escape passages once a fire happened in the tunnel. The fire accidents of long tunnel with large diameter will be more serious. Consequently, the investigation on tunnel ventilation, fatigue and rescue as well as hazard prevention, reduction and precaution technologies became more important especially for the long and large tunnel in their operation stage.

Shanghai Yangtze River Tunnel is a River-crossing Passage and runs from Pudong Wuhaogou to Changxing Island. The total length of the tunnel is 8.1 km. The shield method is employed for the tunnel excavation. The external diameter of the tunnel is up to 15.0 m, which is the largest one in the world up to the present. The tunnel was designed as 6-lane bi-direction expressway with a space below reserved for rail transport. As a result, the hazard prevention is comparably more complicated for Shanghai Yangtze River tunnel.

2 FIRE PREVENTION SYSTEM

2.1 *Overall design concept*

Shanghai Yangtze River Tunnel (from the entrance to the exit) is as long as 8.1 km. The large volume of transport and proportion of freightage result in more risk of fire accident. The fires occur in long and large tunnels in recent years have some significant features, for example, the fire arising from a freight vehicle is hard to extinguish; the firefighting measures could not be made full use in a complicated environment once a fire breaks out; fire equipment could not used correctly in a fire; drivers and passengers were too scared to find the escape way and had very little knowledge on how to properly use escape facilities. Therefore, it is not enough for firefighting only depends on the fire equipment. As a result, a full fire prevention system should be equipped in long and large tunnel.

Fire prevention system of Yangtze River Tunnel is designed based on a "safety-chain" philosophy. The safety chain composed of hazard prevention, hazard reduction and hazard relief. Hazard prevention is to guarantee running safety and reduce the accidence frequency. Hazard reduction is intended to decrease the negative effect on permanent structures and personal safety. Hazard relief is to remove the hazard quickly and effectively.

2.2 *System structure*

The fire prevention system is designed based on the "people-oriented" principle. The fire system could be implemented by the combination of ventilation, fire control, illumination, evacuation, rescue and monitoring. Anyway, the safety of the tunnel is always the precondition for the operation of the fire prevention system. The fire prevention system could yield its function through the coordination and redundancies of water supply & drain, monitoring, ventilation, power supply & illumination, structure fire resistance and structure safety. The fire prevention system structure is shown in Figure 1.

3 DESIGN OF HAZARD PREVENTION SYSTEM

3.1 *"Hazard prevention" design*

The main purpose of "hazard prevention" design is to guarantee the safety of driving safety, equipment

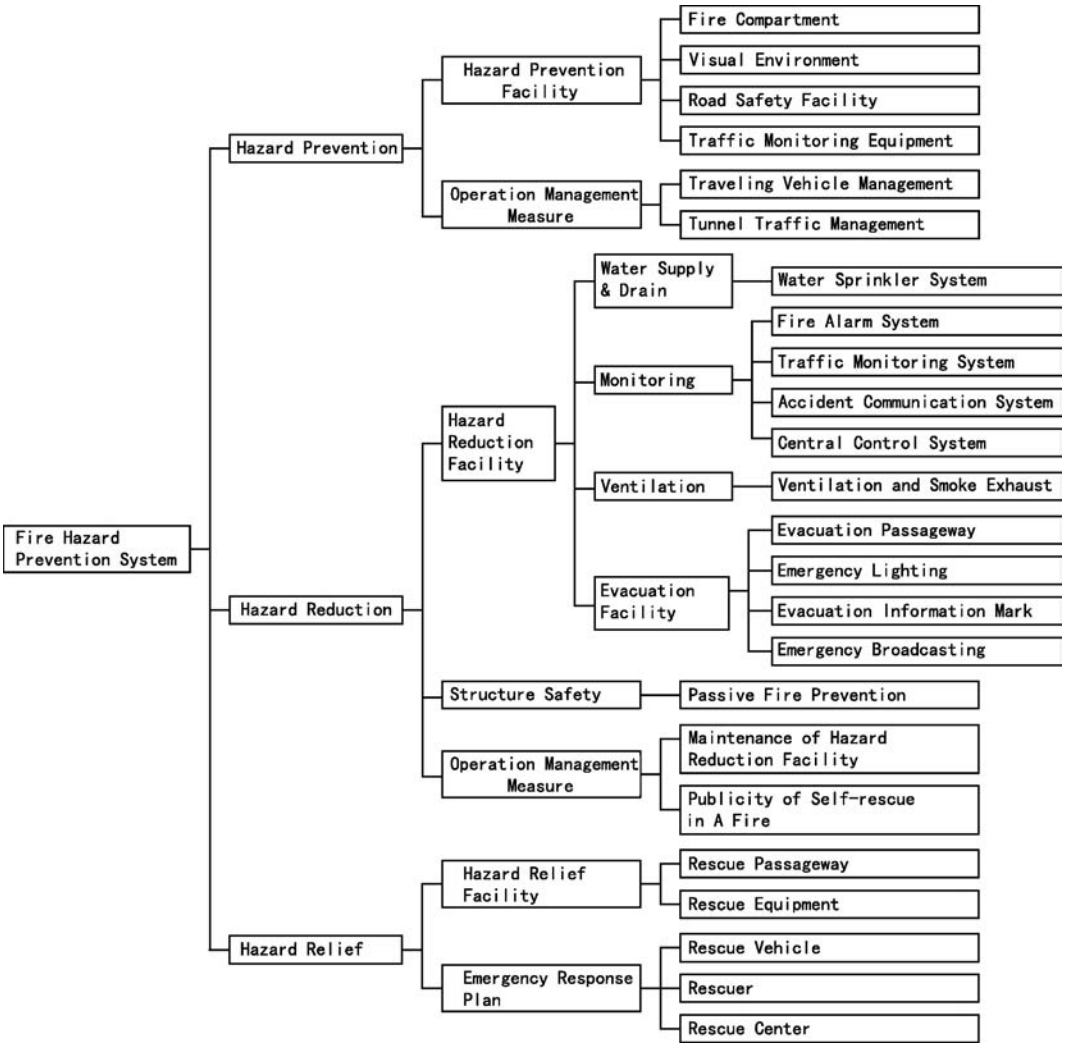

Figure 1. Structure of fire prevention system.

operation and structure as well. Besides the ordinary measures, some special measures were adopted in the design to prevent the hazard for the long and large tunnel. These measures were presented in the following.

3.1.1 *Fire compartment*

It has been accepted that the fire frequency is much higher for bi-directional driving than unidirectional driving in a single tube. So, Shanghai Yangtze River Tunnel was designed with bi-directional lanes in two tubes to reduce the fire risk. The set-up of the fire compartment was carried out in response to the zone functions of the tunnel. The zone functions could be divided as driving and non-driving, traffic and equipment, traffic and safe evacuation. The fire compartments were separated completely because their fire resistance capacities were different. For Yangtze River Tunnel, it was divided into 2 fire compartments of upper level and lower level. The upper level was used for highway traffic; while the lower level used as cable channel, reserved rail transit and safety passageway. The location of each functional zone depended on their function. The safety passageway connects both the road traffic space and the rail transport space to accommodate evacuation from both of them; and the cable channel serves for both the road traffic space and the rail transport space.

3.1.2 *Road safety*
The safety of driving was the key factor that should be considered in the design of the tunnel alignment and longitudinal slope. Some special measures have been applied for such key points as junctions and precipitous slopes along the tunnel alignment. Anti-collision curbstone and sidewall protection structure are used to improve shock resistance of the tunnel and to reduce vehicle's kinetic energy caused by impacting and then to lower the fire probability arising from collision in case of a traffic accident.

3.1.3 *Visual environment*
Each tunnel entrance was equipped with a light transition section to decrease the adverse influence of Black Hole Effect. Visual environment is provided with anti-dazzle light as well. Visual environment of long and large tunnel should be properly changed to relieve visual fatigue. Various traffic and evacuation marks should be legible and identifiable.

3.1.4 *Equipment system*
The Yangtze River Tunnel was provided with ventilation and cooling measures to avoid self-ignition resulting from an overheat environment. In addition, the tunnel was also equipped with monitoring, information release and communication systems to improve the tunnel's capacity on traffic control.

3.1.5 *Management measures*
A traffic control plan was implemented to monitor the dynamic state of the traffic volume at each entrance, exit and inside of the tunnel. The monitoring system could be linked with the whole road network to control the traffic volume and reduce the unfavorable conditions of traffic jam for firefighting. The vehicle types going through the tunnel should be up to the provision of the tunnel. Vehicles with dangerous goods were forbidden.

3.2 *"Hazard reduction" design*

There were two concepts used in the Hazard reduction design. One is the active operating of the combined firefighting equipments in case of a fire. The other is people evacuation after a fire.

The first concept involves fire detection, water sprinkling, ventilation and exhaust smoke systems. Regardless of the technologies or measures used for hazard reduction, reliability of equipments and compatibility between systems were the precondition to reduce the hazard.

3.2.1 *Fire detection & alarm system*
Early detection on a tunnel fire was favorable for controlling fire development. The fire detecting system was composed of fire detection, monitoring, alarm and information handling. The ordinary fire detection technologies used for a tunnel were two-wavelength fire detection, optical fiber & grating and fiber optic Raman reflection. The two-wavelength detection system was used to directly detect the flame wavelength. It was accurate but easily resulted in a blind zone because of a barrier. Besides, the sensitivity could be deteriorated due to the polluted air. The optical fiber system works by detecting the temperature. The blind zone could be avoided with dense measuring points. But the smoke floating caused by ventilation resulted in the detection errors. Considering the scale of Shanghai Yangtze River tunnel, the optical fiber & grating detection system was used because it was interfered by the environment minimally. Under a normal operation condition, the system could work as a temperature detection system to avoid overheating in the tunnel. Additionally, the system was equipped with alarm button, alarm phone and monitoring camera.

3.2.2 *Water sprinkler system*
There were many different ways to extinguish the fire, such as fire cock and fire extinguisher, water-spray system, foam-water sprinkling linkage system, high-pressure fog water mist and A-type foam extinguishing system. The foam-water spray system was used in Yangtze River Tunnel.

3.2.3 *Ventilation & exhaust system*
Considering the length of Yangtze River tunnel, the highway tunnel was designed with longitudinal ventilation by jet fan and smoke exhausting. Smoke exhausting duct was set on the roof of the tunnel. Longitudinal ventilation was used under normal condition. In case of a fire, smoke could be discharged via the exhausting duct. The measure of smoke exhausting not only could reduce the smoke density around the fire site but also could prolong the safe time to some extent for escape and rescue.

3.2.4 *Communication system*
When a fire happened, communication system in the tunnel was a favorable safeguard for evacuation and rescue. Communication could be made by emergency phones set in the tunnel and the personal mobile phone. Dedicated leakage cables were set up for tunnel management, public security and fire control.

3.2.5 *Central control system*
Central control system was the core of all linked systems to deal with the detected information and to carry out the mission of hazard prevention. The system could enable all the linkage equipments after receiving hazard alert. The communication system could be made use to contact with outside of the tunnel.

Safe evacuation and rescue system were another important means of hazard prevention and reduction, which included civil engineering facilities for

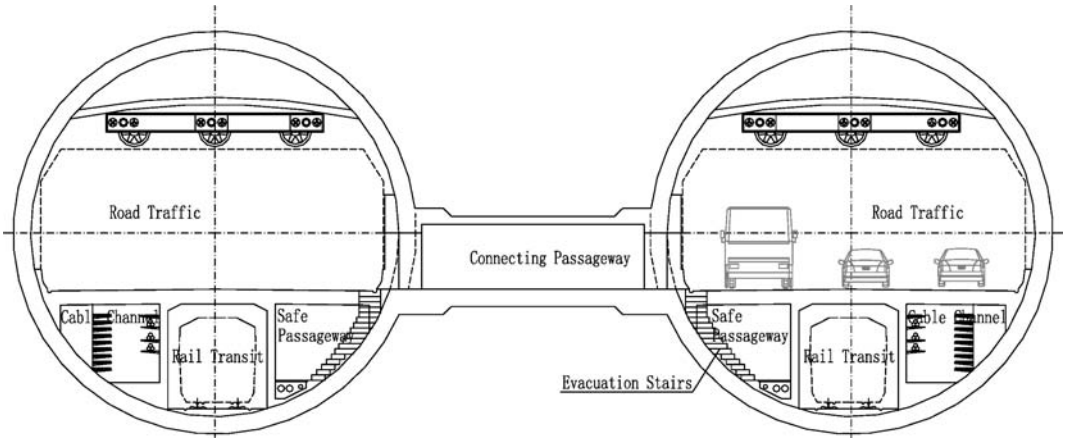

Figure 2. Cross section of Yangtze River Tunnel.

safe evacuation, emergency lightings and evacuation indications.

3.2.6 *Safe evacuation*

Yangtze River Tunnel was designed for both highway traffic and rail transport. Therefore, the design of safe evacuation should meet the two different evacuation requirements. The evacuation design should be based on construction risks and testing of site manipulation.

The Yangtze River Tunnel has 8 connecting passageways between upper and lower levels spaced about 860 m intervals. Evacuation stairs were set up between upper level and lower level at about 270 m intervals to connect safety passageways. The evacuation of upper level depended on the connecting passageways and downward evacuation to rail transit level. The lower level was provided with longitudinal evacuation along safety passageways and upward evacuation via escape stairs (Fig. 2). Shafts at both ends of the tunnel connected with each level and were equipped with escape stairs to the ground.

3.2.7 *Emergency lighting & evacuation indicators*

Each function zone of Yangtze River Tunnel was equipped with emergency lighting. In addition to the illumination requirement, the high temperature resistance requirement should be met for the lighting so that the lighting could be still used after a fire breaks out.

Evacuation indicator system of Yangtze River Tunnel consists of self-luminescent indication sign, variable information board, emergency broadcasting and indication sign of evacuation exit. Evacuation indicators should display uniform information and give as simply and clearly information as possible of the fire site and escape route.

3.2.8 *Structure fire protection*

Fire protection measures were taken for the crown, structural slab of the tunnel and exhaust duct slab to ensure both the safety of evacuators and rescuers within the first 30 minutes in a fire and the safety of tunnel crown structure within 2 hours in the fire.

3.2.9 *Facilities maintenance and management*

In daily operation, tunnel management and maintenance department should periodically maintain the facilities and equipments. The ordinary maintenance could be keeping the downward exit cover, the exhaust air valve, firefighting pump, fire cock and other firefighting equipments in a normal state.

For operation management of such a long and large tunnel, publicity was necessary to acquaint tunnel passengers with potential dangers, instructions of firefighting facilities in the tunnel and escape methods.

4 DESIGN OF HAZARD RELIEF SYSTEM

4.1 *"Hazard relief" system*

Hazard relief system was designed for professional persons of fire-fighting, first-aid and emergency rescuing. The system included rescue passage, rescue equipment and rescue program.

4.2 *Rescue facility*

The rescue passage should be designed considering the capacities of evacuation facilities and cover all the tunnel involves both the road and rail level of tunnel. Firefighting entrance from ground and emergency connecting lane between bi-directional lanes in shaft were built for rescuers quickly access enter the

tunnel. Cross passage and evacuation stairs were set up to shorten the rescue distance between two tunnels. Passage dimensions should be large enough for firefighting persons and equipments.

The fire cock joints were reserved respectively in road and rail level of the tunnel and the ground. A dedicated communication channel was planned to keep contact between the tunnel and the central control room at any time.

4.3 *Operation management*

The special firefighting station, where the emergency equipment storage, emergency center and emergency personnel were stand-to for action, was set up near both entrances of the Yangtze River Tunnel. When a fire occurs, reparation, rescue and fire control actions will be quickly taken according to the emergency plan.

5 CONCLUSION

The fire prevention system of Shanghai Yangtze River tunnel was designed considering function of the tunnel and the ground condition as well as construction technology of the tunnel. The design principle of hazard prevention may be basically identical for different tunnels. However the detailed technical solutions of hazard prevention were probably different. The primary system of hazard prevention for Shanghai Yangtze Tunnel was introduced. More further and detailed research on the system was still in process.

REFERENCES

China Public Security Department. 2005. *Overview of Worldwide Tunnel Fire and Firefighting Technology of Surban Tunnel and Subway Fire Safety Report.*

Directive 2004/54/EC of the European Parliament and the Council. 2004. *On Minimum Safety Requirements of Tunnels in the Trans-European Road Network.*

Shanghai Tunnel Engineering & Rail Transit Design and Research Institute. 2006. *Study on Design of Large and Long Shield Tunnel Structures and Hazard Prevention System.*

The Shanghai Yangtze River Tunnel - Theory, Design and Construction – Huang (ed)
© 2008 Taylor & Francis Group, London, ISBN 978-0-415-47161-9

Design of shield work shaft constructed together with cut-and-cover tunnels

C.N. He & Z.H. Yang
Shanghai Tunnel Engineering & Rail Transit Design and Research Institute, Shanghai, P. R. China

ABSTRACT: In this paper, optimal design of retaining and bracing structure system is conducted with regards to the special circumstance in construction of the Shanghai Yangtze River Tunnel. In the project, two shield work shafts in Pudong and Changxing Island are constructed together with the cut-and-cover tunnels. Elevation of tunnel floors and plan layouts are changed, combining with a serial of requirements on shield launching etc. The optimal design fully embodies advanced technology, saving project investment and shortened time of implementation etc., which provides instructive references for future analogous projects.

1 DESCRIPTION AND CHARACTERISTICS OF THE PROBLEM

In the construction of long and large shield tunnels, the shield work shaft is usually constructed together with the cut-and-cover tunnels to speed up the construction. Enough space should be provided for the installation and disassembly of the shield and the tunnel at one time. This kind of work shafts is actually not the ordinary fully enclosed framed structure. For example, the shield machine used for the Shanghai Yangtze River Tunnel is a large slurry shield. Considering the synchronizing construction, three frames are required behind the shield head. The linkage steel beam should be set between the frames to transport the segments, slurry silos, pre-cast components and other materials. A work shaft and four cut-and-cover tunnels are required to be constructed synchronously due to the requirements of the shield installation in the shaft and its launching. The total length of this structure is 110 m. In addition, holes should be reserved at the head of the work shaft for the shield to launch and receive. The earth foundation outside the tunnel should be reinforced. The back should be connected with the cut-and-cover tunnel. Difference of elevations presents in tunnel floors. All of these put new demands for designing.

2 FUNCTIONS AND DIMENSIONS OF WORK SHAFT

2.1 *Requirements for shield launching and receiving during construction stage*

The clear sizes inside the work shaft, including the plan layout and the elevation of the bottom slab, should be determined comprehensively according to many factors, such as the shield diameter, the tunnel line spacing, technical requirements for shield launching or arriving the shaft, installation of water-proof auxiliary devices at tunnel face, tunnel center heights, installation of back segment, lift and assemble of the shield and installation of the back up system, the construction space needed inside the shaft and so on.

2.2 *Configuration requirements for tunnel operation, equipment room layout, and evacuation and rescue routes during normal operation stage*

There are two shield work shafts in the Shanghai Yangtze River Tunnel, of which the Pudong work shaft size is 48 m × 22 m. The depth of the bottom slab is 23.663 m. During the construction stage the work shaft acts as a launch shaft; during the operation stage is a ventilation room on the 1st underground floor and vehicle lanes on the 2nd underground floor. Emergency evacuation routes are set between the vehicle lanes. When accidents occur inside the tunnel, the vehicles may be evacuated immediately. Emergency passages, fire and rescue spaces, electrical cable trench, ventilation rooms and drain water pumping room are on the third underground floor. The layer of cable and pipe lines is set on the fourth underground floor.

The dimension of Changxing Island work shaft is 22.4 m × 49 m, the depth of the bottom slab is 24.4 m. During the construction stage it acts as the shield reception shaft. Besides, delivery and exhaust airway, which connects with the ground ventilation room, are also set during the operation stage. The 1st underground floor of the work shaft is of equipment rooms.

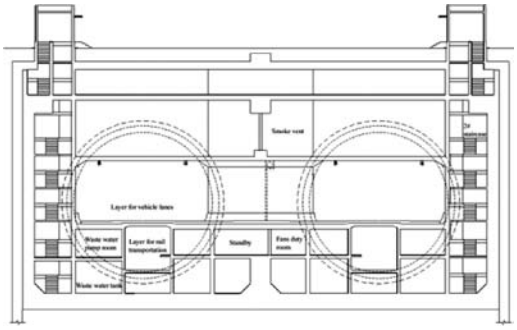

Figure 1. Section layout of Changxing Island work shaft.

The 2nd underground floor is of vehicle lanes, emergency evacuation routes being set between the vehicle lanes as well. Emergency passage with round tunnel sections, fire and rescue space and electrical cable trench are set on the third underground floor. Two escape stairs are available inside the work shaft for the evacuation in emergency and for the structure maintenance (Fig. 1).

2.3 *Brief description of inner structure design of work shaft*

The dimension of the work shaft in longitudinal and transverse directions should be determined according to the shield line spacing and the spaces for shield launching and receiving. Compared with the other forms of single or double circular planes, the rectangular work shaft has several advantages of the smaller ground area, the larger inner space, the reasonable and flexible layout, high efficiency of space usage, and good cooperation with construction technologies etc. As the work shaft size is rather large, its length-to-width ratio is nearly 2:1. Two holes for shield break-in and break-out reach 16 m diameter. In addition to construction requirements inside the work shaft for the shield launching and arriving, the function requirements of work shaft operation are also considered. Considering the work shaft bracing system, two horizontal frames and one vertical frame are built along the depth and longitudinal direction of the work shaft to decrease the horizontal span of the side wall and upgrade the special performance of the work shaft. In the shield construction stage, the main structural members and components inside the shaft, such as two horizontal frames, one vertical frame, side walls, and bottom slabs, form a stable box-shaped special system. The diaphragm wall may be used as part of the main structure, forming a lamination wall together with the inner wall, and undertakes the structure force endurance. During the operation stage the vehicle lane level slab, safety route level slab, equipment level slab, structure top slab, partition wall, and stairs and elevator shaft etc are set inside the work shaft to meet the operation requirements.

3 DESIGN OF SHIELD WORK SHAFT

3.1 *Project construction conditions*

3.1.1 *Geology conditions*

The Pudong shaft is at the northern side of the Wuhaogou Dam. The site of the work shaft is mostly consisted of farmer lands and fish pools. The soil layers from top to lower are: Layer ①$_1$ is artificial filled earth, 1.5 m thick; Layer ②$_3$ is grey sandy silt, about 5.3 m thick; Layer ③$_1$ is grey silty clay, about 4.7 m thick; Layer ③$_2$ is grey sandy silt, about 2.4 m thick; Layer ④ is grey silty clay, about 12.2 m thick; Layer ⑤$_1$ is grey clay, about 4.8 m thick; Layer ⑤$_2$ is grey clay silt, 11.5 m; Layer ⑦$_2$ is grey sandy silt, about 20 m thick; Layer ⑧ is grey fine sand. The slab elevation of the work shaft is −21.163 m, located at the joint of Layer ④ and Layer ⑤$_1$.

The Changxing Island work shaft is at the Dam along the southern bank of the Changxing Island. The soil layers from top to lower are: Layer ①$_1$ is manual backfilled soil, about 0.5 m thick; Layer ②$_3$ is grey sandy silt, about 18.5 m thick; Layer ④$_1$ is grey silty clay, about 8.0 m thick; Layer ⑤$_1$ is grey clay, about 3.5 m thick; Layer ⑤$_2$ is grey clay silt, 21 m; Layer ⑦$_{1\text{-}1}$ is grey sandy silt. The slab elevation of work shaft is −21.7m, located in Layer ④$_1$.

The depth of ground water at the work shaft position is 0.5–0.8 m. Layer ⑦ is the first artesian aquifer layer with water head depth of 6.10 m (elevation is −3.36 m). The underground water of the planned construction site has no corrosive effect on concrete and steel bars, but has lightly corrosive effect on the steel structure. The layer ②$_3$ in the site area is silt soil with strong penetrability. It is easy to cause shifting sand and piping. Light liquefaction is likely to occur under the seismic condition of Magnitude 7. Layer ④$_1$ is grey silt, which is soft and easy to deform.

3.1.2 *Project environment condition*

Most part was farmer lands and fish pools along the work shaft route. According to the surrounding environment of the work shaft and the excavated depth, the safety degree of the foundation pit is specified as Grade II (The comments of the *Code for design of building foundations* DGJ08-11-1999). It means the maximum settlement of the ground outside the pit must be less than 2‰H_0; the maximum horizontal displacement of the retaining wall must be less than 3‰H_0; the maximum settlement of the land surface outside the pit must less than 2‰H_0 (H_0 is the excavating depth of the foundation pit).

Figure 2. Dalian Road Tunnel – Shield launching.

Figure 3. Fuxing (E) Tunnel – Foundation pit excavation.

3.2 *Comparing and selection of design schemes*

3.2.1 *Comparison between caisson method and the cut-and-cover method with diaphragm wall*

The maximum depth of the two work shafts is 24.4 m. The diaphragm wall scheme or caisson scheme might be used for deep foundation pit projects in Shanghai. Both construction methods have been maturely experienced in the design and construction in Shanghai area. As a whole, the diaphragm wall technology has the following advantages: less influence on the environment during construction; rigid and well integrated so small deformation of foundation and structure will be produced; suitable for retaining structures for super deep foundation pits; applicable to forming a superposed wall together with the inner wall; good durability and anti-penetrability. Therefore many shield work shafts of the cross-river tunnel in Shanghai have successfully constructed by the cut-and-cover method with diaphragm wall as retaining system and reinforced concrete structures as excavation supporting system. See details in Figure 2 to Figure 5.

The caisson method is one of the main construction methods adopted in underground projects. It has the advantages of occupying small areas, excavating little earth, and has small effect on surrounding buildings. It is widely used in underground constructions,

Figure 4. Xiangyin Road Tunnel – inner structure construction.

Figure 5. Changjiang Tunnel – Enclosure structure construction.

especially under limited land use and confined environment conditions or with large embedded depth. It is commonly used in bridge pier foundations, pump stations, shield or pipe-jacking work shaft projects of municipal engineering.

Both methods have mature experiences in Shanghai. However, the cut-and-cover method with diaphragm wall system is suggested to be the design scheme of the work shaft considering few buildings around, low requirements for environment control, and open work shaft structure being capable of being constructed together with the cut-and-cover tunnels to ensure the construction schedule. A comprehensive comparison is shown in Table 2.

3.2.2 *Design of retaining and supporting system*

The work shaft is considered to be constructed together with the cut-and-cover tunnels. The supporting system adopts five reinforced concrete supporting braces and one steel supporting brace (of which the 1st and 2nd waling be integrated with the upper frame and middle frame in the shaft). In the design, 23 diaphragm walls

Table 1. Examples of the cut-and-cover method with diaphragm wall in work shaft excavation in Shanghai area.

Project	Dalian Road Cross-river tunnel		Fuxing (E) Road Cross-river tunnel		Xiangyin Road Cross-river tunnel		The Yangtze Rive tunnel	Shangzhong Road Cross-river tunnel
	Puxi Shaft	Pudong Shaft	Puxi Shaft	Pudong Shaft	Puxi Shaft	Pudong Shaft	Pudong Shaft	Pudong Shaft
Sizes (m)	36.4 × 21.0	36.2 × 20.6	35.9 × 20.6	36.2 × 21.2	38.0 × 22.5		48.0 × 22.0	46.0 × 22.0
Depth (m)	20.177	23.834	23.652	20.858	21.15	22.70	23.963	26.20
Retaining structure	1 m wall							1.2 m diaphragm wall
Supporting system	4 concrete supporting braces +1 steel supporting brace		5 concrete supporting braces +1 steel supporting brace		4 concrete supporting braces +1 steel supporting brace		5 concrete supporting braces +1 steel supporting brace	5 concrete supporting braces

Table 2. Comparison of construction schemes for work shafts.

Implementation scheme Project	Diaphragm wall as retaining wall in excavation	Caisson method
Structure reasonability	Adopts 1 m thick underground continuous wall, the supporting system adopts 5 steel concrete supports + 1 steel support. The maximum displacement of the wall body is 52–54 mm, the enclosure may be also used as the horizontal frame of the work shaft, the underground wall and the inner wall form a superposed structure and commonly bear the forces. The structure is well integrated and reasonably designed.	Along the sinking well depth there set the bottom frame, middle frame, and top frame, horizontally set the vertical frame. These may perfect the structure force bearing system. The structure has good integrity and the concrete quality is easily guaranteed.
Connect with the adjacent tunnel sections	The connection with the round tunnel and cut & cover sections are cast-in-place in the enclosure structure. The construction accuracy may be guaranteed.	The connection accuracy is controlled by the well sinking accuracy. Temporary steel door sealing shall the be set at the connection with round tunnel and cut & cover sections. As the sinking well will influence the surround earth body, the enclosure structure of cut & cover sections is prone to cause collapse when shaping the grooves, and make the construction of the adjacent cut & cover sections more difficult.
Implementation feasibility	Take the underground continuous wall as the work shaft enclosure, construct with excavating method, the quality may be guaranteed by rich experiences. May be synchronously constructed with adjacent cut & cover sections to ensure the construction time schedule.	The construction occupies small land sizes. But as the sinking well section is a rectangular of nearly 1:2, and the sinking speed reaches 26 m, there is rather difficulties in the making, sinking rectifying, bottom sealing in water, plane location and elevation accuracy of the sinking well. Only after completing the well sinking may the excavating of the adjacent cut & coversection start, this will influence the construction schedule.
Requirement for environment protection	When construction, there shall be little vibration and noise; when pit excavating, the wall body shall has little distortion, the surround land surface shall has little sinking and little influence to the surround buildings, in order to guarantee the safety of the surround environment.	The sinking well will cause damage to the surround earth body when sinking, and cause disturbance, cracks and sink to the surround earth body.

of 1 m thickness and 45 m depth are adopted as retaining structures. The wall toe is at the layer⑤$_3$ of grey silt clay. Locking pipe connections are adopted in the joint of diaphragm walls as shown in Figure 6.

Because the work shaft slab is deep, locating in Layers ④$_1$ and ⑤ of soft and silt soil, rotary concrete-jetting strips are adopted to improve the foundations over 3 m below the bottom of excavation in order to control deformation and prevent the uplift. The unconfined compressive strength of soil after reinforcement $\geq$1.2 MPa. In order to increase the compressive strength of the soil on rear of the work shaft and prevent the diaphragm wall on the corner from getting too much distorted, the outside of the foundation pit on connection place of the work shaft and the cut & cover sections will be fixed by the rotary concrete-jetting method. The reinforcement range is from the ground surface to 3 m below the bottom of the work shaft pit. The unconfined compressive strength of soil after reinforcement is $\geq$1.0 MPa. Considering that the difference of the slab elevation of the work shaft and the adjacent cut-and-cover tunnel is about 2.8 m, the soil within the range of 3 m from the entrance of a cut-and-cover tunnel will be improved to increase the earth stability of the excavation. The reinforcement depth is from the bottom of the cut-and-cover tunnel to 3 m below the bottom of the work shaft pit.

3.2.2.1 Design loads

Permanent loads: include dead load, load of earth covering, lateral water and earth pressure. Of these, the lateral earth pressure is calculated by the active Rankine pressure formulation. The total stress method is used for the clay soil while the effective stress method is used for the sandy soil during the construction stage. During the operation stage the effective stress method is used.

Live loads: Ground overload, generally being set as 20 kN/m^2; Construction load, equipment load, considered according to the actual conditions; Accidental load: seismic load.

3.2.2.2 Design parameters

1. Lateral earth pressure outside the wall is calculated by the active Rankine pressure formulation. The total stress method is used for the clay soil while the effective stress method is used for the sandy soil. In analysis, C and ϕ are taken as peak values.

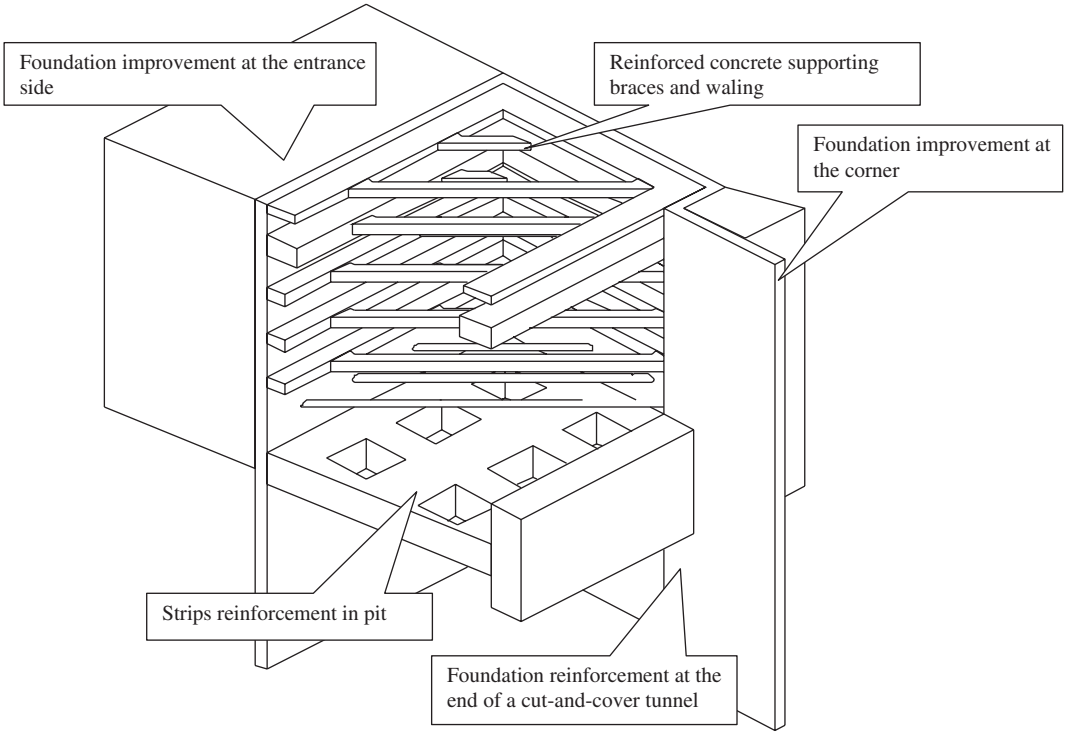

Figure 6. Layout of the underground retaining structures.

2. Passive earth pressure inside the wall is simulated by a serial of horizontal springs with horizontal foundation stiffness, KH:
   Layer ① to Layer ⑤$_1$: 10,000 kN/m^3
   Layer ⑤$_3$: 15,000 kN/m^3
   Layer ⑦: 30,000 kN/m^3
   Soil improvement at the pit bottom: 20,000 kN/m^3

The above values take account of the linear variation in 3 to 4 m under the excavating surface, and 2 m under excavating surface for the reinforced earth.

Material: The concrete strength grades of diaphragm walls, supporting braces, waling are subaqueous C30. Impermeability grade is S8. The steel bar is HRB335. Steel supporting brace is ϕ 609(t = 16) with steel grade of Q235B.

3.2.2.3 Layout of supporting system

According to the work shaft plane and the character of nearly 1:2 length-width ratio, four knee braces are set in each supporting plan in the work shaft, as shown in Figure 7, to facilitate the excavation.

3.2.2.4 Calculation model for the retaining structure

During construction stage a diaphragm wall is generally analyze as a vertical elastic foundation beam according to the excavation condition. The structure analysis is carried out on the principle of "distort first, then support". Based on the construction condition of the foundation pit, the calculating process is divided into eight steps, including excavating, gradually supporting, bottom slab casting, and brace demolishing. These factors must be correctly simulated during the calculation procedures.

The calculation of excavation stage is shown in Figure 8. Calculated results are shown in Figure 9.

4 DESIGN CHARACTERISTICS AND TECHNICAL INNOVATIONS

4.1 *Mixing pile technology adopted in foundation reinforcement at the entrance for shield launching and receiving*

In order to guarantee the safety for shield launching, the earth body surrounding the tunnel entrance should be improved prior to the shield launching in most cases. Several methods are available for reinforcing the earth. Of these, the ground freezing method is formerly used. But this method cannot effectively control the swelling and thaw collapse caused by freezing technology. In this project, a shield hole with the 16 m diameter should be reserved in the inner wall of the work shaft since the diameter of the round tunnel is up to 15 m. As a result, the head surface of diaphragm walls has to bear the high water and earth pressure at

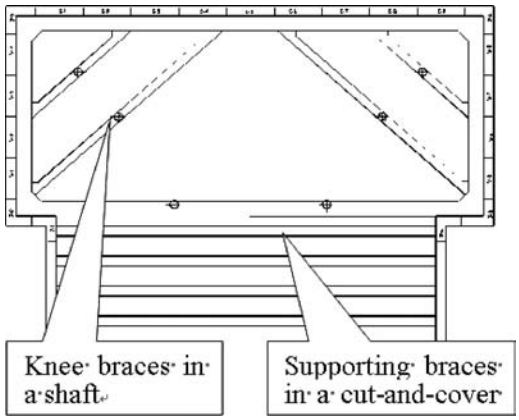

Figure 7. Layout of supporting system in work shaft.

the entrance side (the head surface of the work shaft) of a single wall. According to the earth stability during the shield launching and receiving, the entrance of the work shaft should be reinforced by deep mixing piles to improve the force bearing of the head surface of diaphragm walls. The range of improved foundations is over 16 m along the tunnel longitudinal direction and 25 m along the depth. The reinforcement depth shall be 25 m. The strength index, qu $\geq$1.0 MPa. The mixing pile at the work shaft end is constructed before the excavation of the work shaft, considering after the foundation is reinforced. Consequently C and Φ of the earth body will be increased and the lateral pressure will be decreased (Fig. 10). The comprehensive distortion of diaphragm walls at both sides will then cause the relocation of inner forces in diaphragm walls. Therefore the total stability of diaphragm walls at both sides is evaluated by the incremental method in design, as shown in Figures 11 and 12, and the work shaft foundation pit excavation is simulated with integral model to calculate the space. During the former experiences, there were disagreements about the configure forms of the enclosure in the work shaft, and whether the enclosure shall be cut through at cut & cover section mouths. In this calculation these problems are also calculated. See details in Figure 12 and Table 3.

Seeing from the calculation result in Figures 9, 10, and 11, considering the C and Φ value improvement of foundation reinforcement earth body and the decreasing of the single side pressure, general distortion at two sides of diaphragm walls is balanced under the support action, and causes the force relocation in the diaphragm wall. The effect of end reinforcement is very distinctive because the integral distortion trends to occur at the reinforcing side. The horizontal distortion in the pit of non-reinforced end and the positive bending moment at the inner side of the diaphragm wall is lightly increased. The negative bending moment at the outer side of the diaphragm wall just above the

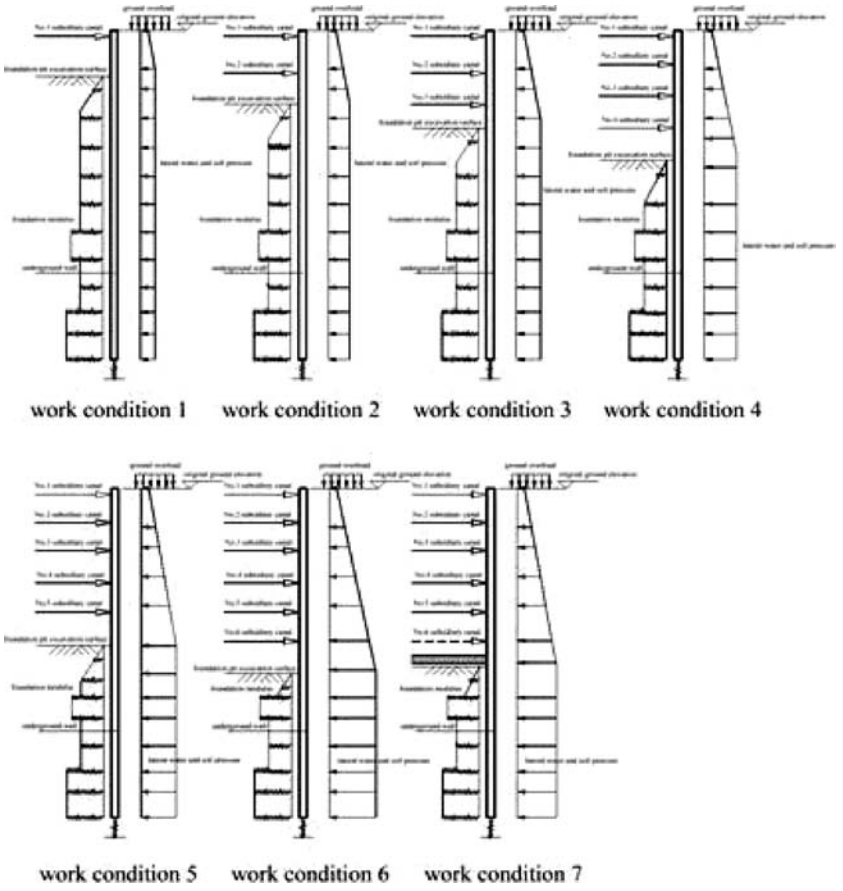

Figure 8. Calculation sketch of diaphragm walls in excavation stage.

foundation pit excavating surface is lightly decreased while it is lightly increased below the excavating surface. As to the reinforced end which is under the mutual support action, the integral distortion and inner side positive bending moment of diaphragm wall is decreased largely due to the extrusion of the non-reinforced section. In addition, the negative bending moment of diaphragm wall at the outer side above the excavating surface is increased largely. In view of above, full attention must be paid in practical design.

Seeing from Table 3, whether the waling is cut-through at the cut-and-cover tunnel entrance or not has little influence on the distortion control in excavating stage because a supporting system is usually set in cut-and-cover tunnels at the connection places of the work shaft and cut-and-cover tunnels. However the selection of the waling rigidity may have certain influence on the distortion at the joint of the work shaft and cut-and-cover tunnels. Whether the waling is cut-through or not at the entrance of cut-and-cover tunnels, the inner stresses in diaphragm walls vary only 5% and about 10% in each waling. It can be concluded that the cut-through state of the waling has less influence on inner force in the whole work shaft. For safety and convenience, one to two cut-through may merely be selected in foundation pit construction.

The maximum bending moment of diaphragm walls in non-reinforced area is 2201 kN.m, where the steel contained is about 190 kg/m^3. The maximum bending moment of diaphragm walls in reinforced area is 911 kN.m, where the steel contained is about 154 kg/m^3. So after the work shaft end is reinforced by mixing piles, the work shaft force bearing conditions are improved, the comprehensive costs of the retaining structures as well as the inner structure is obviously decreased.

4.2 *Use of glass fiber-reinforced polymer (GFRP) concrete that may be cut by shield directly*

The scheme of shield launching in water is adopted in the Changxing Island work shaft in order to ensure the

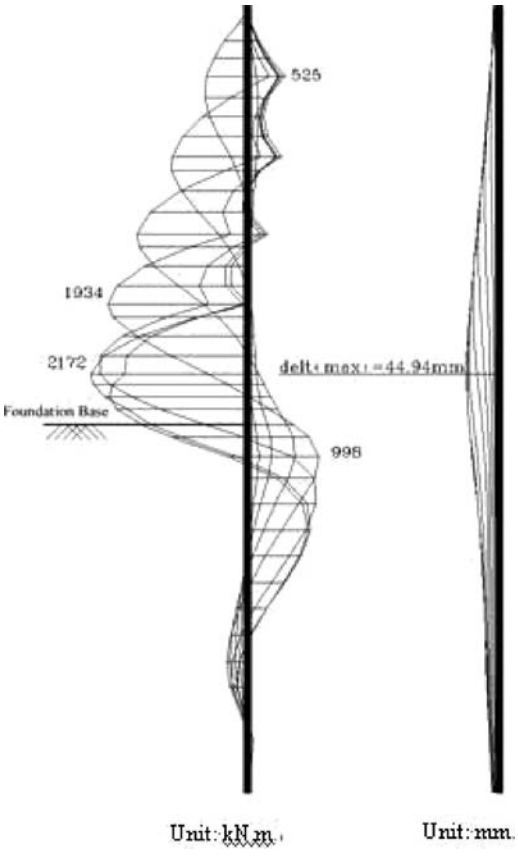

Figure 9. Envelops of bending moment and displacement for diaphragm walls.

successful demolition after the shield launching and to facilitate the consequent works. The shield will be used to cut the diaphragm wall directly for shield launching. For this purpose, eight pieces of diaphragm walls are designed specially at the entrance side, as shown in Figure 14.

According to construction conditions, the most unsafe state of the inner structure is at the completion of bottom slabs and inner walls in the work shaft.

At that time the force bearing system of the work shaft consists of bottom slabs, inner walls, two horizontal frames, and a vertical frame. Of these the diaphragm wall in the work shaft and inner wall forms the superposed wall to bear the forces.

The end surface of the diaphragm wall is a single wall structure. Its horizontal support locates at the middle frame and bottom slabs. The calculated span is up to 19.4 m as shown in Figure 15. Referring to the relative product document, the tensile limit of glass fiber reinforcement bar is 480 MPa. Elastic modulus is 40.8 GP.

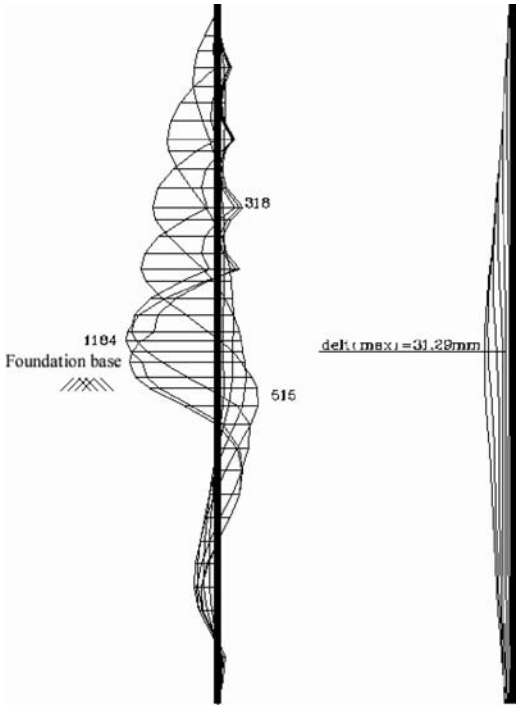

Figure 10. Considering the single side pressure is decreased.

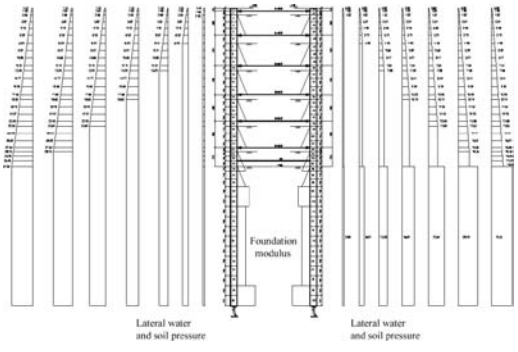

Figure 11. Simple calculation of integral underground wall of two sides in excavation stage.

Concrete strength grade is subaqueous C30. Calculations of GFRP strength, crack width, flexibility, creep fatigue, and cutting performance are carried out referring to the "Guide for the Design and Construction of Concrete Reinforced with FRP Bars" (reported by ACI Committee 440).

Within the calculation span, no banding is allowable in the configured GFRP bars. The longitude HRB335 main bars of the diaphragm wall within the

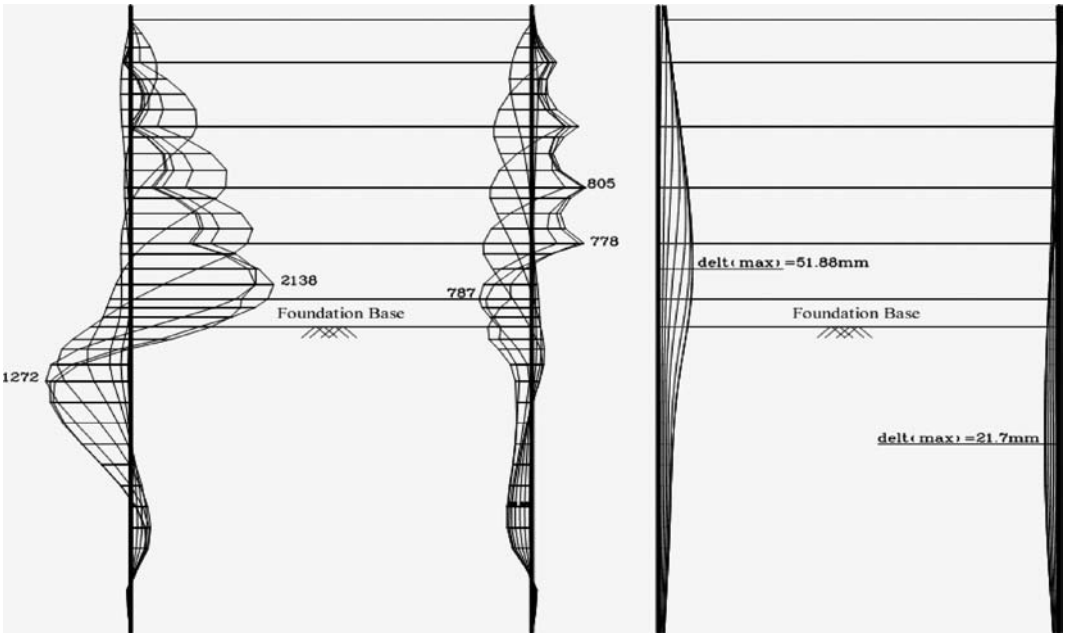

Figure 12. Envelop of bending moment of two sides integral underground wall (kN.m) and envelop of displacement (mm).

Table 3. Calculation comparing of enclosure forms.

		Enclosure cut-through	Enclosure not cut-through
Diaphragm wall distortion		Eastern and western side of diaphragm wall (37 mm) Southern side of diaphragm wall (35 mm)	Eastern and western side of diaphragm wall (36 mm) Southern side of diaphragm wall (36 mm)
Diaphragm wall inner force		Eastern and western side of diaphragm wall M+ = 2,201 kN.m Southern side of diaphragm wall M− = 911 kN.m	Eastern and western side of diaphragm wall M+ = 2,090 kN.m Southern side of diaphragm wall M− = 864 kN.m
Inner force of each supporting brace	No. 1	M + = 4,380 kN.m, M− = 24,300 kN.m	M+ = 4,860kN.m, M− = 28,800 kN.m
	No. 2	M+ = 24,900 kN.m, M− = 120,000 kN.m	M+ = 24,600 kN.m, M− = 138,000 kN.m
	No. 3	M+ = 5,960 kN.m, M− = 22,600 kN.m	M+ = 5,930 kN.m, M− = 23,600 kN.m
	No. 4	M+ = 7,370 kN.m, M− = 26,700 kN.m	M+ = 6,910 kN.m, M− = 26,800 kN.m
	No. 5	M+ = 13,100 kN.m, M− = 46,500 kN.m	M+ = 11,800 kN.m, M− = 45,300 kN.m
	No. 6	M+ = 2,430 kN.m, M− = 7,310 kN.m	M+ = 1,780 kN.m, M− = 7,010 kN.m

pre-embedded steel ring are all extended to the pre-embedded steel ring and then break down. The GFRP bars and HRB335 main bars are overlapped in the middle frame and bottom slabs in Figures 15 and 16. According to the existing projects, the overlap length of glass fiber reinforcement bars and ordinary steel bars should not be less than 50d. The horizontal truss of the underground wall within the pre-embedded steel ring adopts Φ22@200 GFRP bars. Additional Φ22@200 (both in horizontal and vertical directions) GFRP anti-cut bars should be configured within this range.

4.3 *Construction together with the consequent cut-and-cover tunnels*

Construction together with the consequent cut-and-cover tunnels is benefit to save the materials and time, to decrease construction budgets and speed up construction schedules.

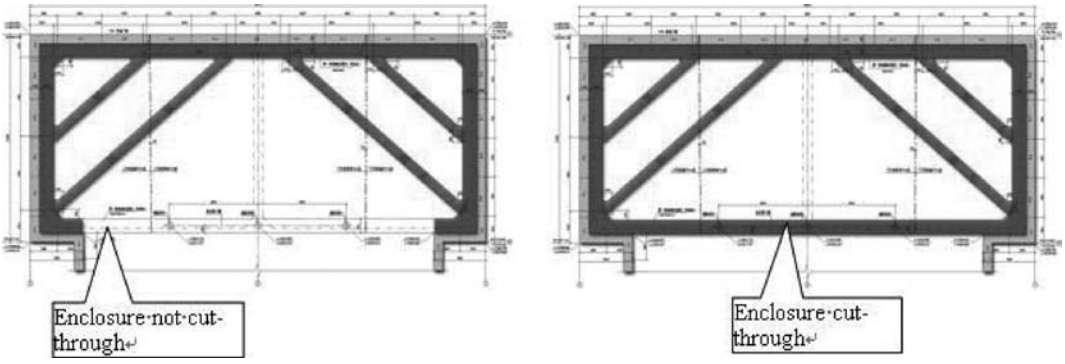

Figure 13. Calculation illustration of enclosure forms.

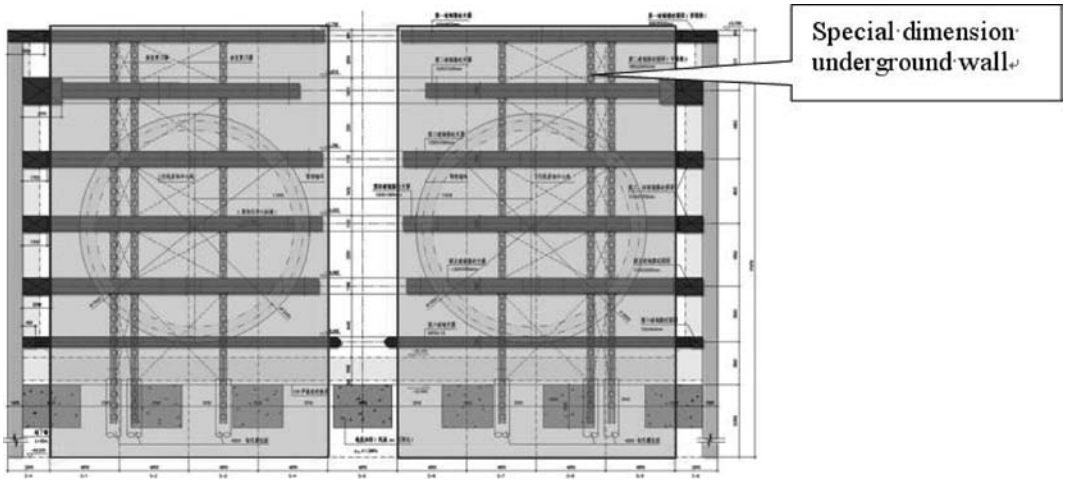

Figure 14. Distribution range of diaphragm walls with special dimension.

5 COMPARISON BETWEEN DESIGN ANALYSIS AND FIELD MEASUREMENTS

5.1 *Layout of test points in work shaft*

The test points in the work shaft foundation pit is emphasized on the horizontal distortion of the diaphragm wall and inner force of the wall body. Assistant data of relative earth pressure, pore water pressure, and ground settlement may be measured as well. At the end surface, it is mainly to configure stress test points on the steel bars of middle diaphragm wall of ordinary dimension. The burial depth of the test points is 5 m, 13 m and 22 m below the ground. Same as it, steel bar stress test points shall be configured on the corner of work shaft and the cut-and-cover tunnels. The wall body distortion is mainly measured in the middle of the work shaft end span (ordinary dimension diaphragm wall), special dimension diaphragm wall and two side spans.

5.2 *Test data comparing and analyzing*

Based on the field measurements, the integral inner force of work shaft diaphragm wall is basically similar to the calculation results as shown in Table 4. Taking the test data obtained from work shaft end (reinforcement side) (Fig. 17), the diaphragm wall distortion and stress of the work shaft end experienced a complex changing process. During the excavation of foundation pit, the steel bars in the outer side pressure area of diaphragm wall and within 10 m of inner and outer side are affected very slightly. With the increase of the

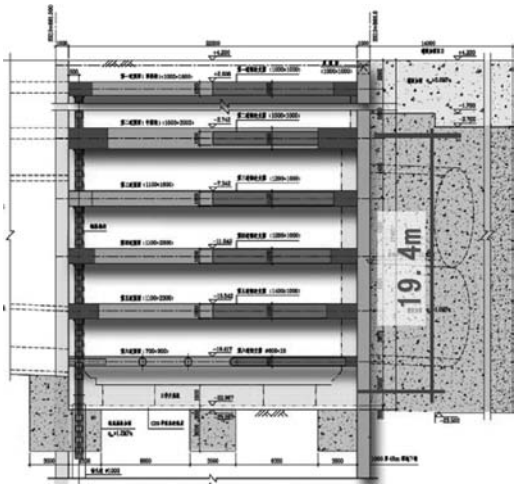

Figure 15. Calculation of diaphragm wall span with special dimension.

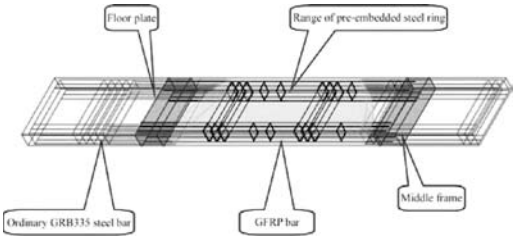

Figure 16. GFRP bars configuration illustration.

excavation depth, the steel bar stress of the diaphragm wall inner side near the excavation ground in the tensile area is gradually increased. The actual excavation condition during the construction influences the diaphragm wall distortion and inner stress largely. During the excavation of the Changxing Island work shaft, the climate factor (met rainstorm) makes it impossible to transmit the construction materials, and the 4th and 5th waling is not provided in time, which causes mutation of steel bar stress in diaphragm walls within the depth of 14 to 18 m. The maximum stress was up to 112 MPa. After the support is completed, the relative steel bar stress is gradually stable and fade out.

According to the field measurements, the integral distortion and analysis result has large difference. As the foundation pit is rather regular, the length-width ratio is close to 1:2, in addition, the inside of the shaft adopt four knee bracing, that makes the whole foundation pit very spacious. In excavating near to bottom slabs of the foundation pit, the maximum distortion of Pudong work shaft diaphragm wall is 51 mm, closing to the theoretical calculation results. Because the

Figure 17. GFRP bars binding site.

Table 4. Calculation and actual test comparing of the work shaft southern side underground wall stress.

	Plane supposed model	Dimensional calculation model	Actual test data
Steel bar stress in diaphragm walls	southern side diaphragm wall 143 MPa	southern side diaphragm wall 121 MPa	southern side diaphragm wall 112 MPa

Changxing Island work shaft is not excavated with wedge cut method, the excavation surface of the work shaft is exposed to the air for too long time. Although the work shaft end is reinforced with mixing piles, the long edge effect of the end and the climate factor make the horizontal displacement of the longer edge is distinctly larger than the shorter edge. Further more, as the horizontal displacement increasing of the longer edge side gives a strong constrain on the shorter edge, the foundation pit integral distortion above the −20m excavation surface trends to the two shorter edges. This phenomenon has some difference compared with the integral calculation results.

6 CONCLUSIONS

- Different design scheme were presented for the work shaft constructed together with the cut-and-cover tunnels. Analysis of the supporting structure in Pudong and Changxing Island work shaft was carried out. The analysis results were compared to the field measurements to facilitate the systematically understanding and grasping the actual force bearing condition and distortion characteristic of non-closed plane work shaft foundation pit. It is also helpful to

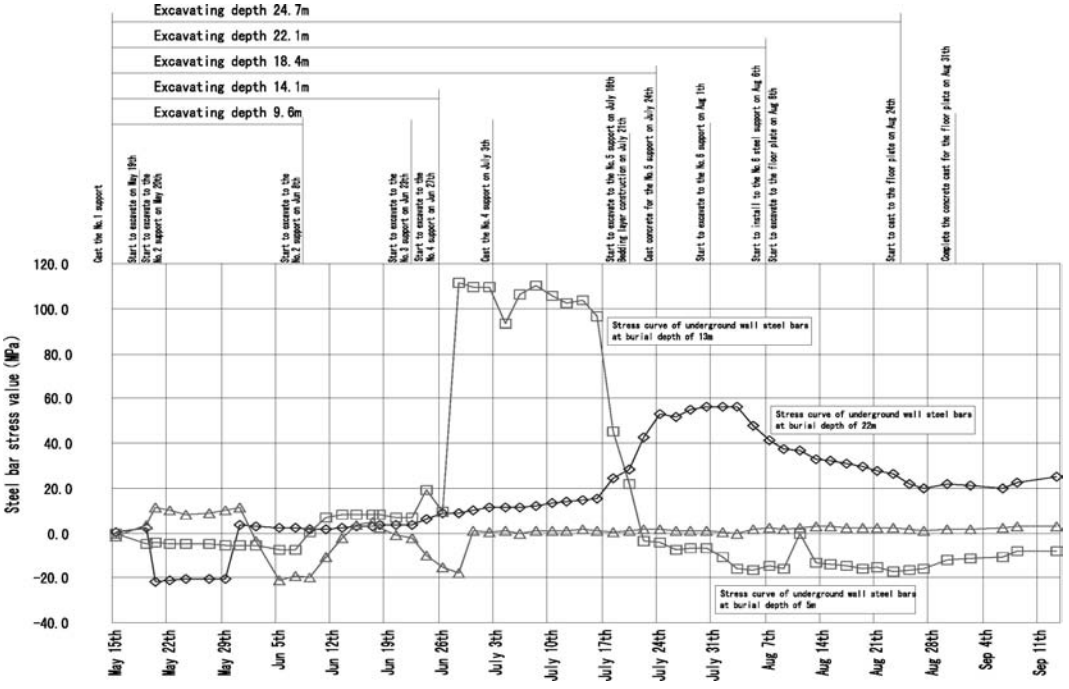

Figure 18. Steel bar stress-time curve.

timely adopt relative measurement and improve the utility effects of the supporting design.

- Combining with the shield launching, the work shaft end is reinforced with mixing piles. The supporting structures (including inner structures) design takes full consideration of the advantageous factors to improve force bearing conditions of the diaphragm wall.
- The foundation pit supporting design should consider the dynamic influence of earth excavation and excavation method or sequences to the horizontal supporting structure systematic distortion and force bearing condition, to enforce the project dynamic monitoring and timely analyzing of the results, and to study and embody it in actual construction design. Through observing and accumulating data documents, scientific bases are provided for scientific study and structure design.

REFERENCES

Fan, W.C. & Wan, Y.P. 1992. *The Model and Computation of Flow and Combustion*. Hefei: University of Science and Technology of China Press.

Qiao, J.S., Tao, L.G. & Mi, S.Y. 2004. Simulation study on deformation characteristics of ground surface in horizontal freezing construction of metro tunnel. *Chinese Journal Of Rock Mechanics And Engineering* 23(5):2643–2646.

Wang, W.S., Wang, J.P., Jing, X.W., et al. 2004. Experimental study of temperature field in course of artificial freezing. *Journal of China University of Mining & Technology* 33(4):388–391.

NFPA 130. 2003. *Standard for Fixed Guideway Transit and Passenger Rail Systems.*

The Shanghai Yangtze River Tunnel - Theory, Design and Construction – Huang (ed)
© 2008 Taylor & Francis Group, London, ISBN 978-0-415-47161-9

Experimental study on fire damage to slab of exit flue of shield tunnel

Z.G. Yan, H.H. Zhu, T. Liu & Y.G. Fang
Key Laboratory of Geotechnical & Underground Engineering, Ministry of Education, Tongji University, Shanghai, P. R. China
Department of Geotechnical Engineering, School of Civil Engineering, Tongji University, Shanghai, P. R. China

ABSTRACT: To understand fire damages to slab of exit flue of shield tunnel under fire scenarios and find proper method to prevent slab concrete from spalling, fire experiment is carried out. Approximate RABT curve with 1.5 h or 2 h duration was employed in the experiment. Eight concrete slab specimens, five of which is mixed with polypropylene fiber were tested in the experiment. The experiment results indicate that mixing polypropylene fiber into concrete is effective to avoid concrete spalling and to weaken damage to the exit flue slab under high temperature.

1 INSTRUCTION

There is a great deal of fire accidents, which has high peak temperature, rapid heating speed and long duration in traffic tunnels. For example, Mont Blanc Tunnel fire in 1999 and St. Gotthard Tunnel fire in 2001. And most of these fire accidents result in heavy damage to tunnel lining and operation facility besides traffic breakdown and people death, as shown in Figure 1 and Figure 2.

Exit flue is designed to exhaust hot smoke efficiently in fire accidents in some of shield tunnels. Exit flue is constructed near the roof of tunnel lining through installing reinforced concrete slab with exhaust port. Generally, the thickness of the exit flue slab is 15–25 cm, varying with shield tunnel diameter. Considering the function of slab of the exit flue, maintaining its integrality (no spalling) and high safety level is very important.

This paper present the results of experiment on fire damage to the slab of the exit flue and anti-spalling performance of the slab concrete mixed with polypropylene fiber.

2 EXPERIMENT ARRANGEMENT

Component and mixing proportion of the concrete of the slab used in the experiment is shown in Table 1. And the mixing proportion of the concrete used in the experiment is the same as ones used in the real shield tunnel project of the Yangtze River Tunnel in Shanghai. Property of polypropylene fiber used in this experiment is also shown in the Table 1.

Figure 1. Fire damage to tunnel segments in Channel Tunnel fire (Kirkland 2002).

Figure 2. Fire damage to tunnel lining in Shanghai Metro tunnel fire.

Table 1. Property of concrete and polypropylene fiber.

Concrete mixing ratio /kg/m^3					
Cement (52.5)	Water	Medium sand	Broken stone (5–40 mm)	Breeze (S95)	Water reducing agent (SP406)
288	168	760	1,124	72	5.6
Polypropylene fiber MP-I fiber Diameter = 31 μm, Length = 6 mm,18 mm, Tensile strength = 475 MPa, Elastic modulus = 4.5 GPa, Extension rate at break = 30%, Blend capacity = 2.5 kg/m^3					

Figure 3. Photo of experiment setup.

According to the experiment set-up, dimension of the specimens are 500 mm in length, 350 mm in width and 250 mm in thickness. Eight concrete slab specimens, five of which is mixed with polypropylene fiber were tested in the experiments.

As shown in Figure 3, Testing System for Tunnel Lining Under High Temperature (200610030454.9), which include heating sub-system, thermal insulation sub-system, mechanical-thermal boundary condition sub-system, loading sub-system and data acquiring sub-system is employed in this experiment.

According to the features of traffic tunnel fire, which is high peak temperature, rapid heating speed and long duration, approximate RABT curve with duration longer than 30 minutes is used in the experiment.

Furthermore, testing series are shown in Table 2.

3 RESULTS AND DISCUSSIONS

3.1 *Temperature distribution within the slabs*

Figure 4 to Figure 6 show the temperature distribution within the specimens in different testing series.

Table 2. Testing series.

No.	Concrete age/d	Blend capacity of polypropylene fiber/kg/m^3	Fire scenarios
FT1	108	2.5	Approximate RABT curve, 1.5 h
FT2	108	2.5	
FT3	110	No fiber	
FT4	108	2.5	
FT5	110	No fiber	
FT6	106	2.5	
FT7	110	No fiber	Approximate RABT curve, 2.0 h
FT8	106	2.5	

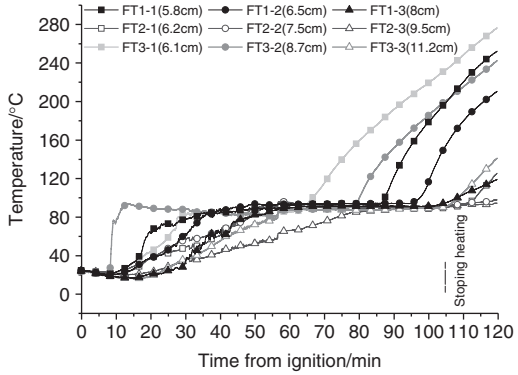

Figure 4. Temperature-time curves of the specimens of FT1, FT2 and FT3.

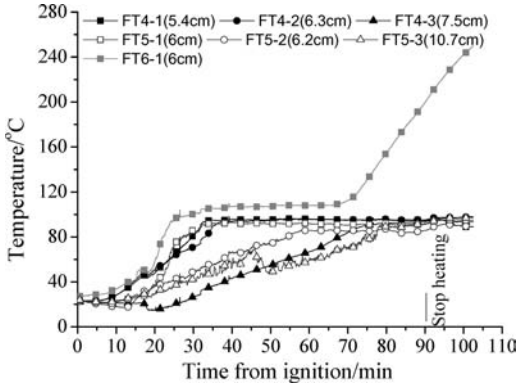

Figure 5. Temperature-time curves of the specimens of FT4, FT5 and FT6.

Because of high thermal capacity and low coefficient of heat conductivity of concrete, heat conduction is slow in the concrete slabs, and both temperature and its increasing speed are less than the temperature within the furnace.

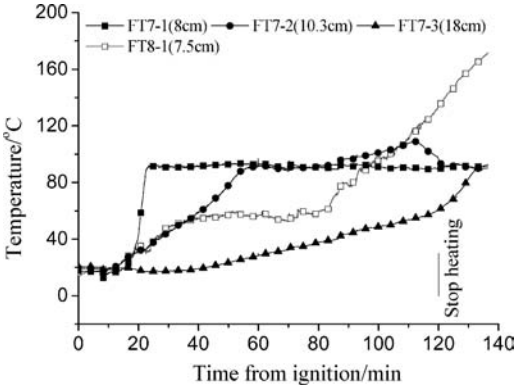

Figure 6. Temperature-time curves of the specimens of FT7 and FT8.

Furthermore, a "temperature platform", which means temperature stop increasing, occurs in the temperature-time curves when temperature within the specimens reaches near 100°C. The "temperature platform" of concrete near the heating face of the slabs occurs early than concrete far from the heating face of the slabs. However, the length of "temperature platform" of the latter is longer than the former. The reason why "temperature platform" occurs is that water in the slab concrete begins vaporizing when temperature increase to 100°C. Water vaporizing, which is a heat-absorbing procedure results in the temperature of the slab concrete stop increasing and maintain the value of approximate 100°C for a period between 50 to 90 minutes until vaporizing procedure is finished. "Temperature platform" is good to the slab concrete and reinforcement bar because "temperature platform" delay the fast increasing of temperature and the failure time of concrete slab, when temperature increases to the limit-temperature of concrete of slab under fire scenarios.

3.2 *Concrete spalling under high temperature*

Concrete spalling under high temperature is major damage to tunnel structure besides mechanical characteristic deterioration, large displacement due to heat and durability deterioration. So how to prevent tunnel structure from spalling is a very important issue in its design and construction.

As shown in Figure 7, high temperature may cause heavy damage to the slab specimens without polypropylene fiber in terms of large surface cracks and little spalling.

However, the experiment reuslts indicate that the specimens mixed with 2.5 kg/m^3 polypropylene fiber present good integrity and no spalling is found in the fire scenarios of approximate RABT curve, 1.5–2 h duration. Furthermore, no obvious cracks occur in the surface of the specimens mixed with polypropylene fiber, as shown in Figure 8.

Figure 7. Spalling and cracks of the specimen without polypropylene fiber.

Figure 8. Spalling and cracks of the specimen mixed with polypropylene fiber.

The reason why polypropylene fiber can prevent or weaken concrete from spalling is that pores initially occupied by polypropylene fiber will form a pore-net after the polypropylene melting under its melting-point (160°C); these pore-net increases significantly the permeability of concrete and relieve the accumulation of vapor pressure, which result in concrete spalling (Andrew, 2004).

4 CONCLUSIONS

Experimental study is conducted in this paper on fire damage to the slab of the exit flue and anti-spalling performance of the slab concrete mixed with polypropylene fiber. Considering high temperature

will present a heavy damage to the slab of the exit flue, it is very important to find proper method to protect it. Based on the experiment results, mixing polypropylene fiber into concrete is an effective method to avoid concrete spalling and to weaken damage to the exit flue slab under high temperature.

ACKNOWLEDGEMENT

The authors would like to thank the financial support of National 863 Project: Study on key construction technologies of super large-section and long shield tunnel (2006AA11Z118).

REFERENCES

Andrew, K. 2004. Improving concrete performance in fires. *Concrete* 38(8):40–41.

Kirkland, C.J. 2002. The fire in the channel tunnel. *Tunnelling and Underground Space Technology* 17(2):129–132.

The Shanghai Yangtze River Tunnel - Theory, Design and Construction – Huang (ed)
© 2008 Taylor & Francis Group, London, ISBN 978-0-415-47161-9

Integrated design and study of internal structure of Shanghai Yangtze River Tunnel

Y.M. Di, Z.H. Yang & Y. Xu
Shanghai Tunnel Engineering & Rail Transit Design and Research Institute, Shanghai, P. R. China

ABSTRACT: With regards to the tunnel clearance, space arrangement of Shanghai Yangtze River Tunnel, and comprehensively considering of the requirements of construction method and schedule to the internal structure, the road deck slab, smoke duct slab, drainage pump house and cross passages are designed integrally, which achieves good technical and economic benefits.

1 INTRODUCTION

Shanghai, a city known as the "Oriental Pearl", is one of the economic and cultural centers in China. It is also the original place in which river-crossing tunnel are developed in China. With the implementation of construction Shanghai as the "economic center, financial center, trade center and navigation center", urban river-crossing road tunnel has been developed rapidly. These aqueous tunnels such as Dapu Road Tunnel, south line and north line of East Yan'an Road Tunnel, Dalian Road Tunnel, East Fuxing Road Tunnel and Xiangyin Road Tunnel witness the city's development and prosperity. The accomplishment of these tunnels has boosted the urban sustainable development in Shanghai. As the continuing development of design and construction technology of modern tunnel, the diameter of shield tunnel has increased from 11 m, 13.36 m to 14.5 m and even 15.0 m; the tunnel scale has developed from one tube with two lanes to one tube with three lanes on double-deck, one tube with four lanes on double-deck, and one tube with three lanes on single deck; the length of shield tunnel has increased from 1.2 km, 1.5 km to 7.47 km. At present, accompanied by the larger tunnel diameter, the longer distance of single driving length, the faster driving speed of mechanized shield, the shorter construction period, the design and construction of tunnel lining segment and internal structure are required to meet the demand of workshop pre-fabrication, site assembling, fast construction. Particularly, in design of internal structure, the construction procedure of TBM driving, lining assembling and transportation of vehicles during construction must be considered comprehensively.

2 PROJECT BRIEF INTRODUCTION

2.1 *Overview of project*

Shanghai Chongming River-Crossing Passage is composed of Yangtze River Tunnel and Yangtze River Bridge. The project, located in an estuary of Yangtze River, starts from Wuhaogou, Pudong District, Shanghai in the south and crosses the South Harbor of Yangtze River to Changxing Island, then crossed the North Harbor of Yangtze River to Chongming Island. Shanghai Yangtze River Tunnel, crossing the South Harbor, includes the offshore section in Pudong (experimental section), middle section in the river and the offshore section on Changxing Island.

Shanghai Yangtze River Tunnel is designed in bi-directional six-lane highway standard (Road Class I standard). The design speed is 80 km/h. The rail transit space is preserved under the road deck. The total length of the tunnel is 8,954.0 m, of which 7,472.11 m is shield tunnel constructed by slurry pressure shield with diameter of 15.43 m. The tunnel lining adopts the universal trapezoidal segment assembling in staggered joint. The external diameter of the lining is 15.0 m, the internal diameter is 13.7 m and the ring width is 2.0 m. Eight cross passages are set between two tubes at the road deck level. Four pump houses are set at every two lowest points. No matter for its length or diameter, Shanghai Yangtze River Tunnel Project lists the No. 1 shield tunnel in China, even in the world.

2.2 *Tunnel internal space layout*

Shanghai Yangtze River Tunnel has two tubes. Each tube has three lanes. The width of the lane is 3.75 m^3;

the lateral clear width is 0.75 m × 2. The construction clear width is 12.75 m, and the clear height is 5.2 m. The smoke duct, smoke outlet and jet fan are set above the lane. The variable information plate, lighting appliance, emergency broadcast, vidicon, water spray nozzle and etc. are arranged above the lane in accordance with the requirements. The cable channel (220 kV cable channel is preserved), preserved rail transit space, longitudinal safety passage are under the road deck. Safety exit is open on the road deck; and the longitudinal safety passage and road deck are connected by escaping stair. Eight cross passages are arranged between upper and lower levels for escaping and rescuing in the event of accident. According to the requirements of construction layout and clearance (Fig. 1), the design contents of internal structure of tunnel are mainly road deck, road surface paving, evacuation stairs between up and down levels, top smoke duct slab and etc. This paper is focused on the design of road deck and road surface paving structure.

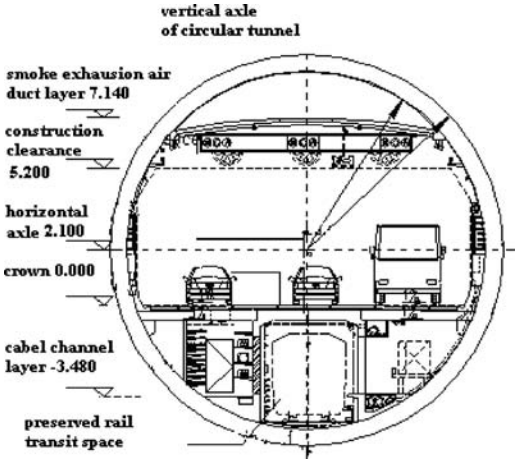

Figure 1. Cross section layout of circular tunnel.

2.3 *Requirements of synchronized construction process*

According to previous tunnel construction experience, in view of the segment transportation, construction operation face during shield excavation and slope adjustment of road, internal structure is cast in-situ when settlement and deformation is stabilized after tunnel driving through by shield machine. But this Yangtze River Tunnel is a super-large and super-long tunnel, the traditional process construction will experience considerable longer construction period and increased construction risk. In order to meet the requirements of overall construction schedule, the segment transportation and road structure construction during the process of shield excavation are considered in together. According to the successful experience of existing project, and using the successful experience of Green Heart Tunnel of Netherlands, the synchronized construction process is adopted in this project. According to shield mechanical process and pipelining of backup system layout (As is shown in Figure 2), the implementation of road structure of the tunnel is divided into two phases: Phase I in which the prefabricated components of road deck are installed while shield driving (segment assembling); and the special lifting devices of the prefabricated components are laid on No. 2 backup system; Phase II in which the lower part of tunnel lining and other structures of road deck is cast in situ when there is a certain distance from the excavation face. The road surface layer and curbstone are constructed after the settlement of the tunnel is

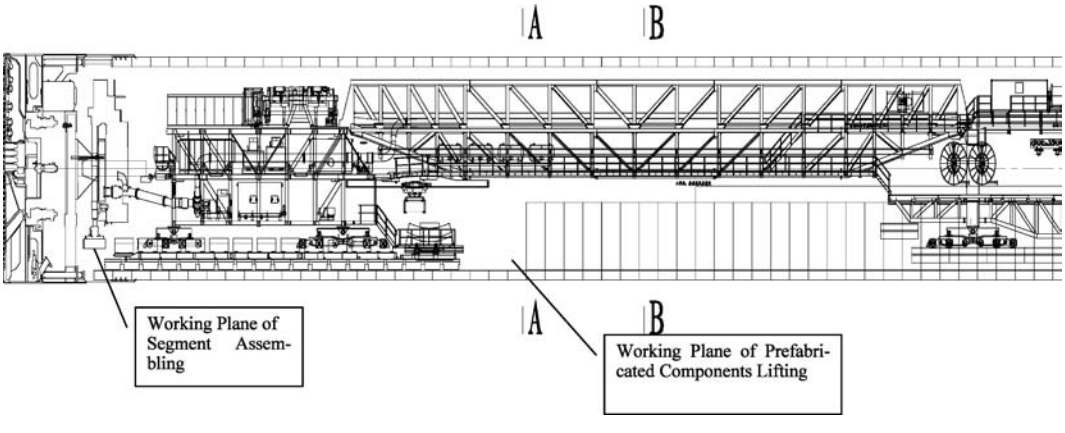

Figure 2. Shield machinery and backup system layout.
* The left of A is segment-lifting area, A is working plane of prefabricated components (Phase I), the right of B is working plane of cast-in-situ section structure (Phase II)

stabilized. From the design perspective, the process is divided the original integral cast-in-situ structure into prefabricated components and cast-in-situ structure. The prefabricated components match with shield for synchronized construction. In addition, the cast-in-situ structures are implemented on the base of meeting the transportation of segment and grouting material. The process has great advantages:

- The prefabricated components can be paved instantly during the driving of shield, achieving instant synchronized construction process with high efficiency;
- The backup system and material transportation vehicle can run on the installed prefabricated components, which optimizes construction process (avoiding previous turning over of railroad tie of backup system, the truck transports the materials to the working surface directly instead of electric locomotive) and provides advantageous conditions for accelerating project process;
- Due to large diameter (Φ15 m) and large thickness change of covering soil (minimum thickness of covering soil is only 6.3 m), thus the volume of annular space between shield and tunnel is large. While the synchronized construction is adopted, the load of prefabricated components can increase the anti-floating capacity of the circular tunnel during construction;
- Synchronizing with the shield excavation, the cast-in-situ structures such as road deck are only about 200 m behind backup system. The left and right segmental and subdivision construction is implemented, ensuring the accessibility of transportation line. The overall construction period can be shortened by 12 months comparing with previous construction solution.

2.4 *Study of design problems caused by synchronized construction*

According to the requirements of synchronized construction, the design of internal structure of the tunnel, especially the design of deck slab, shall be considered according to actual construction, and the following problems shall be noticed:

- Because the prefabricated structure of deck slab which is lifted at early stage is used as the temporary road for flatbed transporting segment during construction, the structural design and internal force calculation shall take both construction phase and operation phase into account.
- The connection style of the fabrication of the cast-in-situ road deck structure with prefabricated structure and tunnel lining structure.
- The selection of general calculation model of road deck and internal force combination.
- Study and design of tunnel road surface pavement because there exit difficulties resulting from synchronized construction such as high probability of subgrade surface (prefabricated structure) displacement.
- The other structures inside of tunnel such as the upper smoke duct slab, cross passage, pump houses corresponding to construction process shall be designed and studied.

3 MAIN DESIGNS OF INTERNAL STRUCTURE OF SHANGHAI YANGTZE RIVER TUNNEL

3.1 *Design of road deck structure*

3.1.1 *Design solution of road deck structure*

According to the requirements of synchronized construction and taking the construction requirements of rail transit into consideration, the structure of road deck is divided into three parts of square type prefabricated components, steel reinforcement planting bracket and cast-in-situ road deck. It is implemented in two phases. Phase I: the prefabricated square type prefabricated components are installed while shield driving (Fig. 3), meeting the transportation requirement of shield segments. Phase II: the steel reinforcement of bracket is planted on tunnel segment at both sides; the bracket is cast; and the ballast at the bottom of the tunnel is constructed; then the road deck on both sides of square type prefabricated components are cast in place; finally, the road surface layer and curbstone are cast in place (Fig. 4).

During the clearance design of internal structure, the shield driving errors (±135 mm in vertical and ±150 mm in horizontal) are taken into account. In

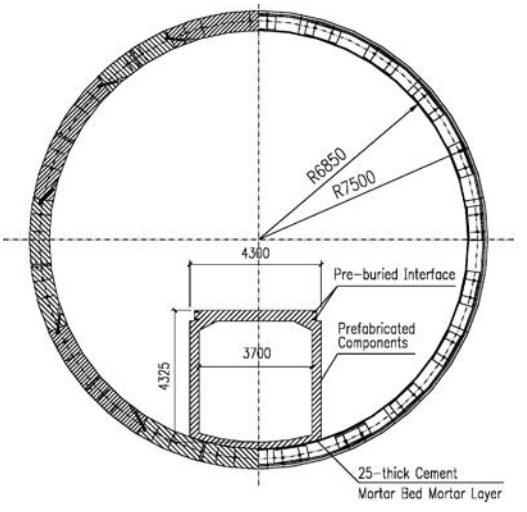

Figure 3. Cross section of road structure, phase I.

order to meet the requirement of line fitting, 12 cm-thick concrete leveling layer is set on the top layer of road deck (1% of transverse slope is considered, the minimum thickness is 8 cm). The steel mesh reinforcement is set internally.

In order to make road deck free to expand longitudinally under the influence of temperature changes, the deformation joint is set at regular length (about 30 m) longitudinally. The deformation joint is the same as the circular seam of square type frame.

3.1.2 *Design of square type structure*

According to construction space requirement of rail transit under the road deck and taking the segment transportation into account, the prefabricated square type components of road deck are adopted in this project. The outside dimension of prefabricated components is 4.5 m × 4.3 m (As is shown in Figure 5). After lift and positioned, it is firstly used as the temporary road of flatbed transporting segment during construction. During construction period, the main loads which shall be considered in the calculation of square type structure are:

- Permanent load: Self-weight of the structure
- Construction load (load of transporting vehicle and etc.)

The structural characteristics of prefabricated square type frame are as follows:

- According to the requirement of curve radius of the line, the prefabricated square type frame is fabricated in accordance with standard block of 2 m for each section.
- Groove is set at both sides of prefabricated square type frame, connecting to cast-in-situ road deck. The steel reinforcement connector is preserved, ensuring prefabricated square type frame and cast-in-situ road deck to form three-span continuous slab which is stably stressed.
- Three M24 inclined bolts are used to connect the sections of prefabricated square type frame, for the convenience of construction and position. The longitudinal deformation and coordination capacity of prefabricated square type frame is also increased.
- Each prefabricated square type frame acts on segment in the form of four points. 25 mm thick of bed mortar is paved firstly at the position of installing square type frame.
- Types of square type frames: According to the requirements of building, ventilation, equipment and road traverse trench, different types of square type frames are prefabricated. In addition, the

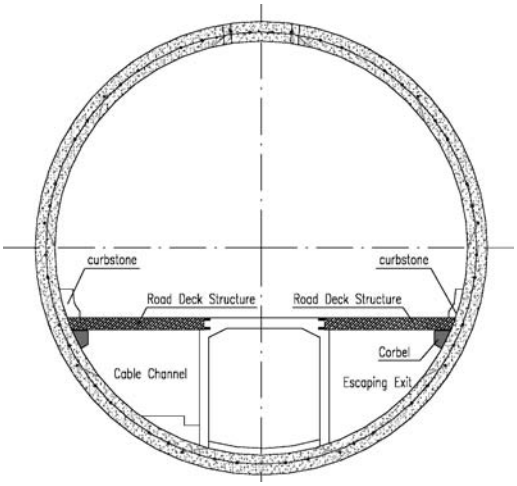

Figure 4. Cross section of road structure, phase II.

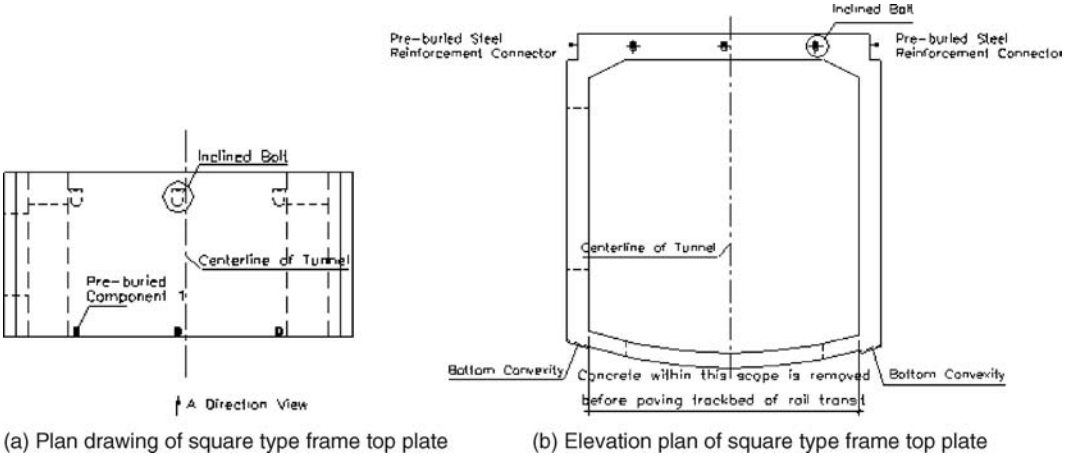

Figure 5. Structural drawing of prefabricated square type frame.

equipment pipes are embedded in prefabricated square type frame.
- Layout of prefabricated square type frames.

The layout of prefabricated square type frames is similar to that of tunnel segments. The principles are as follows:

- The prefabricated square type frame shall be laid along the horizontal and longitudinal curves of the road line. The centerline of the road and the elevation of crown shall be taken as the standard. The allowable deviation shall be no more than 110 mm.
- In order to meet the requirements of horizontal curve fitting and vertical curve fitting, the low pressure asbestos rubber board can be stuck on the top and side surfaces of prefabricated square type frame according to stepped appearance while constructing.
- The deformation joint is set at regular length (about 30 m). The position of deformation joint shall avoid safety exit and equipment manhole.
- The allowable deviation of positioning of prefabricated square type frame of shall be no more than 2 m.

3.1.3 *Bracket design*

The road deck on the segment of tunnel is supported by bracket and the neoprene plate is underlaid. The road deck can slide horizontally. The steel reinforcement planting is used to connect bracket and segment. The intrados of the segment at the position of steel reinforcement planting shall be chiseled. According to the layout of shield backup system, this work can be implemented on No. 2 backup system on which the lifting of square type components has been finished (Fig. 6).

3.1.4 *Cast-in-situ road deck on both sides*

The total width of the carriageway is 12.25 m. It is divided into 3 lanes. In design, the analysis and calculation are separately implemented for construction phase and operation phase. During construction period, analysis is focused on fabricated square type frame.

During operation period, the construction of road deck connecting with prefabricated square type frame has been finished. The road deck is calculated according to three-span continuous slab (the disadvantageous working condition that the bottom purlin of prefabricated square type frame is removed is considered).

The loads considered while calculating are:

- Permanent load
  a. Self-weight of the structure;
  b. Secondary dead load (self-weight of pavement and fixed equipments).
- Basic variable load (Road -Class I)
- Internal force combination of components

The structural internal force envelope diagram is drawn according to the most disadvantageous load combination during construction period and operation period. The structural strength, rigidity and crack width are calculated according to internal force envelope diagram.

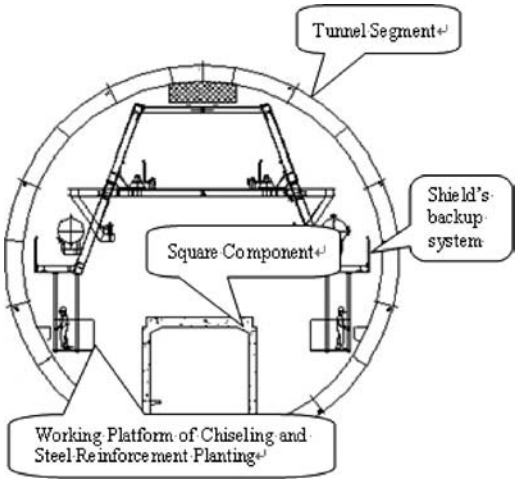

Figure 6. Working platform of chiseling and steel reinforcement planting.

3.2 *Study of road structure solution*

In order to ensure the good condition of road pavement performance, the following design principles of road pavement in the tunnel shall be met:

(1) Adapting internal environment characteristics of tunnel

As a relatively closed operating system, the internal environment of the tunnel is characterized as loud noise and bad ventilation. Therefore, the surface structure of the road shall be capable of suppressing and reducing the noise of vehicle running, and the dust as

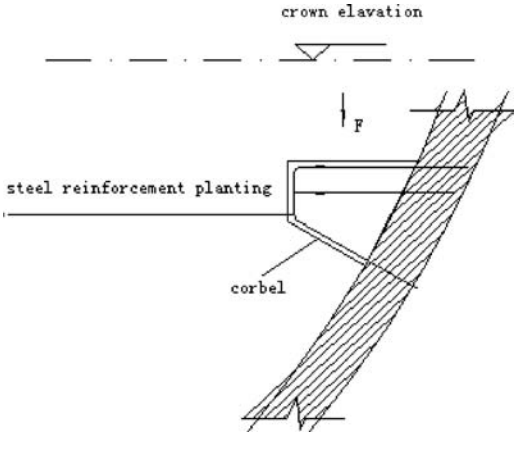

Figure 7. Calculation diagram of road deck bracket.

Figure 8. Real pictures of synchronized construction.
* 1. Lifting of square components;
2. Cast-in-situ ballast;
3. Carbeling and steel reinforcement planting of segment in Position of bracket;
4. Cast-in-situ lane plate steel reinforcement;
5. Double-head truck used for transporting segments;
6. Transportation passage of square type components.

much as possible. The materials used for road pavement shall have good flame-retardant performance. In addition, the less influence to construction environment shall be taken into account while selecting materials, such as selecting the materials which can be used at lower temperature and reduce the emission of harmful gas.

(2) Ensuring the stress characteristics of the road structure

Actually, the asphalt pavement and cement concrete subgrade surface form the compound road structure. This structure is characterized by comfortable traveling of flexible road surface. At the same time, due to the mutation of the materials in the joint of asphalt pavement and cement concrete subgrade surface, the stress status of asphalt structural layer at this position is disadvantageous. The damages such as interlayer slide are easy to occur. Therefore, not only good interlayer joint of road pavement structure, but also good joint between road pavement and subgrade surface (reinforced concrete prefabricated component top surface) is demanded. The interface processing of subgrade surface and selecting proper transition road structure materials are significant.

(3) Ensuring working characteristics of subgrade surface

The subgrade surface is assembled by square type prefabricated components of 2 m long sections. Under the action of vehicle load, the vertical relative displacement between sections may cause damage of asphalt pavement. Two ways of solving the problems deserved to study are eliminating or reducing relative vertical displacement between sections of subgrade surface and improving the load resisting performance of asphalt pavement.

(4) Ensuring the internal accessing space of tunnel

Due to limited internal space of the tunnel, in order to improve the vehicle running conditions, the space is reserved as much as possible. The space coverage of structures shall be reduced. Meanwhile, the pavement structure shall meet the performance requirement of the road.

(5) Good durability

Due to narrow internal space of the tunnel, road maintenance not only causes large interference to traffic but also has large potential safety hazard. Therefore, the performance reduction of road surface inside the tunnel shall be lower. It is appropriate to select durable pavement materials.

Through the mechanism analysis and calculation of the internal structure and pavement, it is concluded preliminarily that there exist two special positions while asphalt road structure is paved on top surface of prefabricated square type reinforced concrete components. One is the transverse joint between sections of prefabricated components, another is transverse deformation joint every 20–30 m longitudinally. The road pavement structure in these two positions may be damaged due to the downwarping of prefabricated component top surface. Through the vertical displacement calculation of the prefabricated square type reinforced concrete frame, mechanical analysis such as stress analysis of road pavement structure and stress evaluation of road, as well as comparisons of performance, cost and construction influence, 8–15 thick C30 concrete (with bi-directional $\phi 8$ @200 steel mesh reinforcement) is used for road pavement to solve axles controlling difficulty and uncertainty at the same time of shield excavation and used as sticking transition material for subgrade surface bond. The surface layer adopts 4 cm AC-20 + 4 cm fire resistant modified asphalt SMA13 + 6 cm AC-20 medium particle asphalt concrete. At the position of structural deformation joint, the cement concrete is paved for setting real joint. The width of the joint is the same as that of structural deformation joint. At the deformation joint,

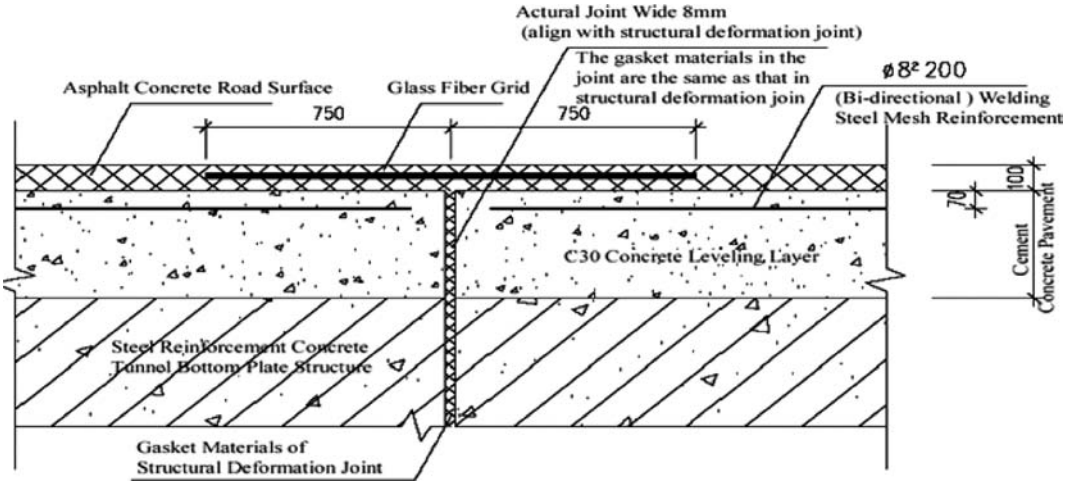

Figure 9. Structure of road pavement layer in deformation joint.

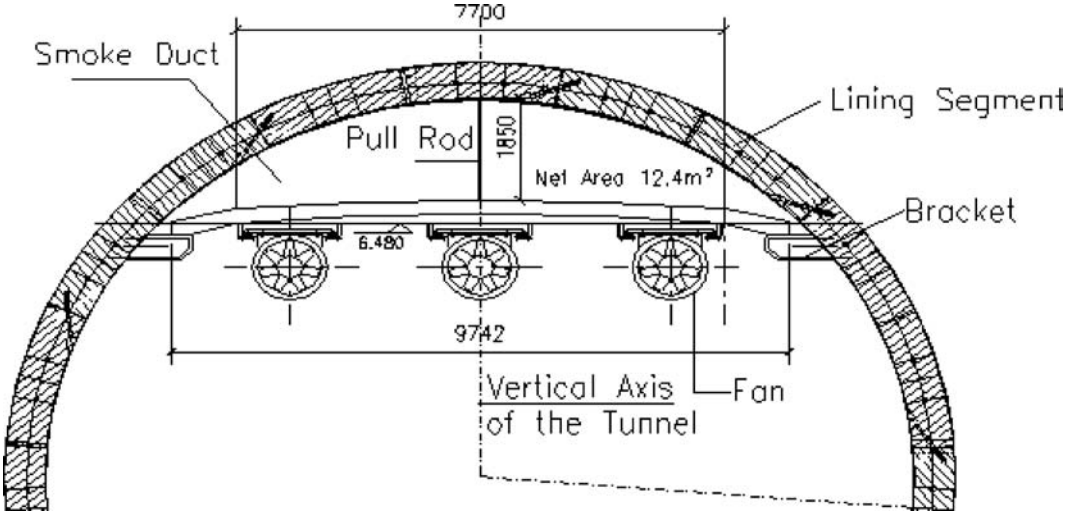

Figure 10. Structure of smoke duct slab.

the glass fiber grid is set between two pavement layers of asphalt concrete. The details are shown in Figure 9.

3.3 *Structural design of smoke duct slab*

The longitudinal ventilation and concentrated smoke exhaustion are used in Shanghai Yangtze River Tunnel. In view of synchronized construction process, the construction of smoke duct slab cannot influence the transportation of lining segment. The steel reinforcement planted bracket is set on segment. The smoke duct and vehicle running space are separated by light beam plate structure placed on bracket. The area of smoke duct is about 12.4 m^2. See Figure 10. During the construction, the bracket can be steel reinforcement planted and cast firstly. Then the smoke duct slab is installed after deformation of the tunnel is stabilized.

The standard smoke duct slab combines 250 mm-thick reinforced concrete cast-in-situ smoke duct slab and prefabricated smoke duct slab. The cast-in-situ reinforced concrete beam is set at the position of smoke outlet. The box shape steel beam is set at the position of the fan. Both ends of beam and plate are placed at the cast-in-situ reinforced concrete bracket. The bracket is fixed on tunnel segment structure through steel reinforcement planting. The construction is carried out after the deformation of the tunnel is stabilized. Firstly, the bracket is steel reinforcement planted and cast,

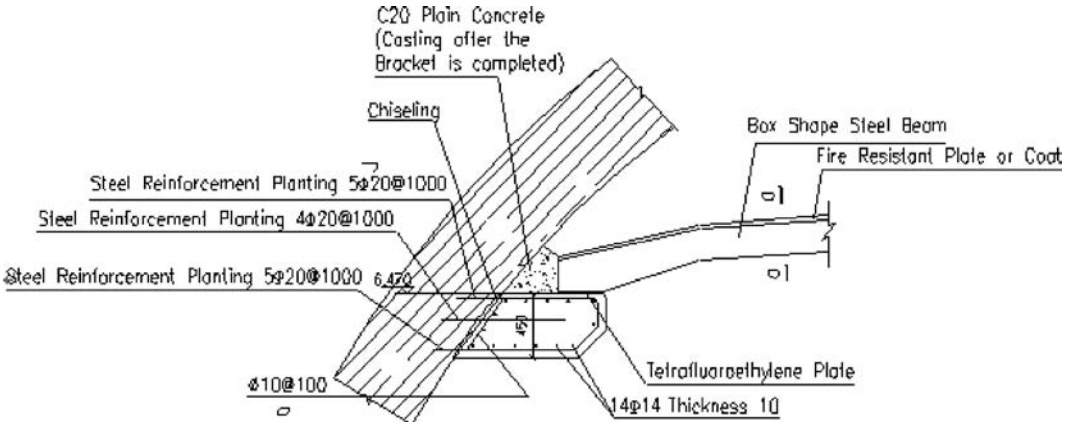

Figure 11. Structure of smoke duct slab bracket.

then, the prefabricated beam plate is installed. In view of fire resistant and anti-spalling of the smoke duct slab, the dispersing monofilament polypropylene fiber shall be mixed into concrete slab. The mixing amount is 2.5 kg/m^3; the surface of the steel beam is covered by light fire resistant thick plate (or fire resistant coat). The steel beam shall be rust removed before covering and the anti-rust paint shall be painted.

The key element of smoke duct slab construction is bracket design. (Fig. 11) The bracket design shall be considered the two conditions. One is that the bracket structure is positioned in the standard section of smoke duct (without fan). The other is that the bracket structure is located at fan position. Due to the bracket on which the smoke duct placed is anchored on tunnel segment by planting steel reinforcement, the tunnel lining structure is still required to meet the strength and deformation. In addition, the working area of bracket construction is relatively small. Thus, more lane plate space can be saved to meet the requirement of synchronized construction.

4 CONCLUSIONS

The synchronized construction of internal road structure in this project is achieved through the combination of prefabricated square type frame and cast-in-situ road structure. The structural design is feasible, in accordance with the standard of road Class I. Comparing with the section of former integral reinforced structure, the section area of this structure is small, thus the materials are saved; under the condition of normal materials transportation, the road deck is completed at the same time. The construction progress speeds up largely.

The road slab is supported on tunnel segment by bracket. The steel reinforcement planting for bracket and segment is feasible.

According to mechanical analysis to road pavement structure, it is demanded that road slab is processed integrally. In view of feasibility of construction, the main measures are: prefabricated square type frames are connected by three M24 inclined bolts longitudinally. The longitudinal steel reinforcement of cast-in-situ slab correspondingly in both sides are laid continuously; the steel reinforcement connector is embedded in horizontal sides of prefabricated square type frame, ensuring the reliable connection of cast-in-situ concrete in both sides. The concrete structure at the deformation joints every 20–30 m (including prefabricated square type frame and cast-in-situ reinforced concrete) are completely separated.

After Yangtze River Tunnel Project introduces machineries and processes of synchronized construction, through the integrated design to internal structures such as tunnel road deck, upper smoke duct slab, drainage pump house and cross passage, the structures not only meet building space requirements, but also exert no effect on the transportation while constructing, which makes synchronized construction process successful.

Synchronized construction process reduces the construction period effectively and creates obvious economic benefits. It creates the conditions for using the tunnel in advance correspondingly and generates active social benefits. Especially at the background of rapid economic development and infrastructure construction, this kind of effective construction design concept is promising in the future.

REFERENCES

Bickel, J.O. & Kuesel, T.R. 1982. *Tunnel Engineering Handbook*.

Hygienic Standards for the Design of Industrial Enterprises. *GBZ1-2002*.

The Shanghai Yangtze River Tunnel - Theory, Design and Construction – Huang (ed)
© 2008 Taylor & Francis Group, London, ISBN 978-0-415-47161-9

Preliminary study of temperature rising and cooling measures for long road tunnel

W.T. Jiang, J.L. Zheng & H.S. Lao
Shanghai Tunnel Engineering & Rail Transit Design and Research Institute, Shanghai, P. R. China

ABSTRACT: The ventilation of road tunnel is to control the pollutant concentration and visibility in tunnel effectively. Take Yangtze River Tunnel as an example, the article addresses that the temperature rising in long road tunnel must be concerned. In addition, the reason causing air temperature rising in road tunnel, the calculation of temperature rising and temperature reducing measures are preliminarily discussed.

1 ADDRESSING OF THE PROBLEM

For a long time, as a kind of safe, comfortable and environment-friendly protection measure, road tunnel ventilation plays an important role in tunnel operation and management. Generally speaking, the ventilation system of road tunnel must have the following functions:

- Under normal and congested traffic conditions, the pollutant concentration can be diluted to meet the hygienic standard and visibility standard and to meet the requirement of diluting bad odor. In addition, the air quality and noise near tunnel portal and surrounding environment shall be controlled.
- In the event of fire, the ventilation system shall be capable of exhausting smoke and controlling the diffusion of smoke and heat. At the same time, certain fresh air can be provided to create conditions for safe evacuation of drivers and passengers and rescuing of firefighters.

Generally, for small and medium tunnel with low-density traffic flow or shorter length, if the tunnel ventilation ensures air quality (i.e. CO concentration and visibility) to meet a certain standard, the air temperature in tunnel will be in a reasonable range, which will not influence safety operation of the vehicles. Therefore, in general, the influence of temperature was not considered in previous ventilation design of urban road tunnel.

Actually, when the vehicle runs in the tunnel, the burning of gasoline or diesel oil not only exhausts burned gas but also exhausts a lot of waste heat. Generally, the temperature of gas exhausted by domestic-made cars is about 550°C. The exhaust gas temperature of imported cars is about 500°C. The heat emission amount is considerable, which would raise the temperature in tunnel. For short tunnel, the problem of temperature rising is not severe. However, for long tunnel with high-density of traffic flow in hot summer, especially under the condition of soil and tunnel structure with bad heat dissipation, the control of tunnel temperature cannot be ignored.

When we carried out the ventilation design of Yangtze River Tunnel, we found that the influence of temperature rising of this tunnel could not be neglected. So far, there are no standards on road tunnel temperature, calculation method of heat dissipation amount and cooling measures applicable to road tunnel. Now, according to the ventilation design of Yangtze River Tunnel, the air temperature rising inside of long road tunnel is preliminarily discussed.

2 TEMPERATURE STANDARD OF ROAD TUNNEL

The temperature standard of the tunnel shall ensure the comfort of passengers under normal and congested operation conditions and an appropriate working environment for maintenance staff in tunnel. In addition, project investment and operation cost are the factors which shall be taken into consideration.

Firstly, the passengers' need shall be considered. When there is air conditioning in vehicle, the higher temperature in tunnel can be adopted. Theoretically, the temperature which can ensure the normal operation of vehicle air conditioning is acceptable. Thus, as long as the temperature in tunnel is not more than 45°C and the vehicle air conditioning can operate normally, the passengers will have a good environment in vehicle.

Table 1. Air temperature standard of road tunnel.

Air temperature inside tunnel (°C)	Allowable staying time (min)
<40	Long time
40–42	<5
42–45	≤1
>45	Forbidden

Table 2. Vehicle fuel consumption.

Vehicle type	Fuel	Fuel consumption (L/100 km)
Minibus	Gasoline	5–8
Microbus	Gasoline	8–13
Motor Coach	Diesel Oil	23–30
Small Truck	Diesel Oil	11–12
Medium Truck	Diesel Oil	17–19
Truck	Diesel Oil	20–36

Under bad vehicle conditions (no air conditioning in the vehicle), the temperature standard in tunnel shall be lower than the former. At the same time, the ride time of passengers shall be taken into account while deciding temperature standard. The temperature shall not be too high for longer ride time. The temperature can be appropriately increased if the ride time is short.

To sum up, according to Hygienic Standards for the Design of Industrial Enterprises (GBZ 1-2002) and other standards of temperature design for high air temperature places, the temperature inside of road tunnel can be decided referring to following values and in accordance to the tolerance of human body.

In addition, if the work of maintenance staff in tunnel is considered, the air temperature in tunnel shall not be more than 40°C.

Similar to the standard of pollutant concentration in tunnel, the design value of air temperature inside of tunnel and distribution curve of temperature are relevant to the ventilation mode of the tunnel. When longitudinal ventilation is adopted, the distribution curve of temperature in tunnel is a slash, which increases gradually from entrance to exit. The temperature near exit is the highest. The passengers bear the higher temperature only in the latter part of the tunnel for a short time. The relatively higher temperature in tunnel can be adopted.

When transverse ventilation is adopted, basically, the distribution curve of temperature in tunnel is a straight line. The passengers bear the same level of temperature in the tunnel for a long time. It is appropriate to adopt the temperature of less than 40°C.

In a word, concerning tunnel temperature standard, the designer shall take account of the ventilation mode, and the bearing time of passengers. And then adopt an appropriate value according to Table 1.

3 CALCULATION OF HEAT LOAD AND TEMPERATURE INSIDE OF ROAD TUNNEL

3.1 *Calculation of heat load*

The main heat source inside road tunnel is the heat emitted from vehicle fuel.

According to relevant statistical data, the existing vehicle fuel consumption of our country is shown in Table 2.

The heat emission amount of vehicle is calculated according to fuel consumption per hundred kilometers. The fuel consumption of above table is that under economic speed. The oil consumption is much higher in actual running. The calculation shall take this factor into consideration. According to traffic volume and vehicle running time in tunnel, the total fuel consumption in tunnel can be calculated. The quantity of combustion for gasoline is 46.2×106 J/kg. The quantity of combustion for diesel oil is 42.8×106 J/kg. The quantity of heat production in tunnel can be calculated.

The air temperature in tunnel lies on outside air temperature, ventilation quantity of the tunnel and heat transferring of tunnel wall.

This article will not discuss the adoption and calculation of outside air temperature and tunnel ventilation quantity.

The heat transferring quantity of tunnel wall is closely related to tunnel envelop structure, type of soil around the tunnel and soil moisture content, etc. The design of tunnel cross section largely influences heat transferring quantity. For example, for many shield tunnel, there is pipeline corridor or air duct at the bottom of road deck. A lot of cables are set in pipeline corridor. The cables themselves generate certain quantity of heat. In addition, generally, the space outside the vehicle passing clearance is equipped with equipment cabinets, air ducts or attached with fireproof panel, which weaken the heat transferring from the tunnel wall to the surrounding soil.

The heat transferring quantity of soil lies on soil type, moisture content and permeability coefficient (i.e. migration speed of water). Generally speaking, cohesive soil is waterproof layer in soil layer with bad heat conductivity. However, silt and sand are permeable layers with good heat conductivity. Only when the permeability coefficient of soil is more than 10^{-4}cm/s, can have larger influence on heat conductivity of soil.

See Table 3 for heat performance of common soil and envelop structures.

According to above-mentioned parameters, the temperature in tunnel can be predicted by computer simulation.

Table 3. Heat performance of common soil and envelop structures.

Type	Moisture content (%)	Thermal conductivity (Btu/hr-Fo-ft)	Thermal diffusivity (ft^2/hr)
Sand	0.2	0.16	0.01
	30	0.95	0.03
Crushed feldspar	4	0.63	0.03
Crushed granite	4	0.63	0.03
Crushed dark rock	4	0.50	0.03
Sility loam	4	0.54	0.02
	10	0.83	0.025
Fine sandy loam	0.3	0.19	0.01
	27	1.33	0.03
Loamy sand	0	0.11	0.01
	5	0.29	0.015
Sandy clay loam	0	0.09	0.01
	0	0.09	0.01
Arenaceous clay	13	0.14	0.02
	25	0.24	0.025
Sility loam	10	0.75	0.025
	20	0.83	0.03
Sility clay loam	10	0.75	0.025
	20	0.79	0.03
Clay	1.4	0.14	0.01
	67	0.87	0.04
Humus soil	4	0.08	0.01
	67	0.21	0.04
Concrete sandstone	0	0.54	0.019
	10	0.70	0.025

4 REAL MEASUREMENT OF TEMPERATURE IN TUNNEL

In 2005, Shanghai Tunnel Engineering and Rail Traffic Design and Research Institute, assisted by relevant agencies, implemented real measurements of temperature in Shanghai East Yan'an Road Tunnel in winter and summer. The tunnel has four lanes in bi-direction. The total length is 2,260 m, of which approximate 1,788 m is buried section. The traffic volume was about 2,500 vehicles/h while measuring, mainly minibus (about 80%). The average speed was about 50 km/h.

In January 2005, the winter measurement, the air temperature at entrance was 6°C–7°C; the air temperature at exit was 17°C–18°C. The average temperature rising was 11°C.

In August 2005, the summer measurement, the air temperature at entrance was 32°C–33°C, the relative humidity is 68%; the air temperature at exit was 42°C–43°C, the relative humidity is 38%. The average temperature rising was 10°C. The relative humidity decreased by about 30%.

From the real measurements in winter and summer, we can see that the temperature rising of tunnel is quite obvious.

5 EXAMPLE OF TEMPERATURE RISING CALCULATION FOR LONG TUNNEL

Yangtze River Tunnel is part of Shanghai Chongming River-Crossing Passage, which starts from Wuhaogou, Pudong and ends at Changxing Island. The tunnel is composed of double tubes, each of which has three lanes. The traffic runs in a single direction in each tube. The total length of buried section is 8,100 m. The calculated speed in tunnel section is 80 km/h. The predicted traffic volume during peak-hour in future is 3,263 pcu/h. The length of shield tunnel in the river section is 7,500 m.

The top part of the tunnel is equipped with air duct and the bottom part is equipped with cable channel and pipeline corridor. The heat conductivity effect of over 60% of areas which can conduct the heat is bad. However, most of other wall surfaces are covered by fireproof panels and decorative boards.

According to soil layer conditions shown in geological section map, the tunnel is basically buried in gray silty clay, gray silty clay and gray clay silt. The moisture content is between 33.3%–50.2%. The permeability coefficient in vertical direction is 3.23×10^{-7}cm/s–6.23×10^{-6}cm/s and the permeability coefficient in horizontal direction is 5.31×10^{-7}cm/s–9.15×10^{-6}cm/s.

According to calculation, the heat quantity will be 19,600 kw/tube in future. The ventilation quantity to dilute pollutant concentration is far from meeting the temperature-reducing requirement. SES4.1 computer program is used to simulate the temperature and ventilation quantity in tunnel. Under normal speed, the ventilation quantity is about 704.7 m^3/s. The highest temperature in tunnel is about 55°C. Therefore, the cooling measures must be considered.

Figure 1 is the curve of predicted temperature in tunnel. The figure is shown that the air temperature in tunnel has exceeded 45°C when the vehicle driving into the tunnel for 4,500 m.

6 TUNNEL COOLING SYSTEM

According to the above-mentioned contents, the vehicle running generates a lot of waste heat, which will raise the tunnel temperature obviously. Especially for long tunnel, the temperature shall be checked and calculated. In order to ensure the comfort of passing people, safe driving and safe operation of equipments inside of the tunnel, the cooling measures must be adopted when the tunnel temperature is too high.

The common cooling measures are:

(1) Concentrated Cold Supply for Temperature Reduction

The concentrated refrigeration plant can be adopted. The Channel Tunnel adopts this kind of method. It is

based on a closed circuit chilled water, and includes 2 cooling plants, total 40 MW, located at Sangatte and Shakespeare Cliff, supplying cold water (4°C, 220 l/s) through 200 km of pipes of diameters 400 and 320 mm.

According to the scale of Yangtze River Tunnel, the cold quantity of each refrigeration plant is about 12 MW. If the cooling system adopts the type of that of Channel Tunnel, 600 m^2 refrigeration room shall be provided in each air shaft. The installed capacity of tunnel increases about 4,200 kW, namely, the total installed capacity of tunnel ventilation increases by 50%.

If using this method, the cost and operation cost is very high. The cooling method of Channel Tunnel is the most expensive cooling system in the world.

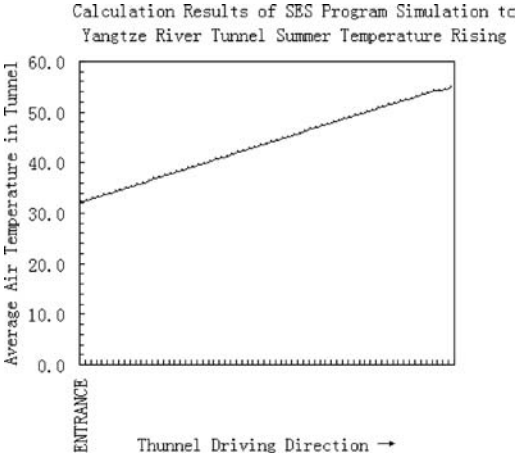

Figure 1. Curve of predicted temperature in tunnel.

In addition, the cooling method at the end of the tunnel is worth further discussing. Therefore, the cooling system of using concentrated refrigeration plant is technically feasible. But from the aspect of economy, it shall be carefully considered.

(2) Water Spraying for Cooling

The heat generation of vehicles, lighting lamps in tunnel is largely sensible heat. The humidity diffusion is low. According to the real measurement of the tunnel, the relative humidity at the entrance is about 70%, while the relative humidity at the exit is only 35%–40%. There is good condition to realize cooling by evaporation. Generally speaking, the latent heat of vaporization of water is 2.40 kJ/g (related to temperature). The heat is equal to more than five times of heat required to heat up the water from 1°C to 100°C. This means that if little water is sprayed in tunnel, the heat absorption is considerable if the water can be evaporated within a certain period of time. The cooling effect is obvious.

The calculation indicates that if the water spraying quantity of 4.7 kg/s (i.e. 16.9 T/h) for single tube is fully evaporated, the temperature at the exit of Yangtze River Tunnel can be controlled within 40°C. The relative humidity is about 51.4%.

Generally, the air handling units are used for water spray cooling system. But in tunnel, the feasibility shall be further studied.

The simplest method is to spray the water on road surface directly. Through water evaporation, a lot of latent heat of vaporization is absorbed from surrounding air to achieve temperature reduction. If this method is adopted, the influence of water spraying on vehicle running and evaporation efficiency shall

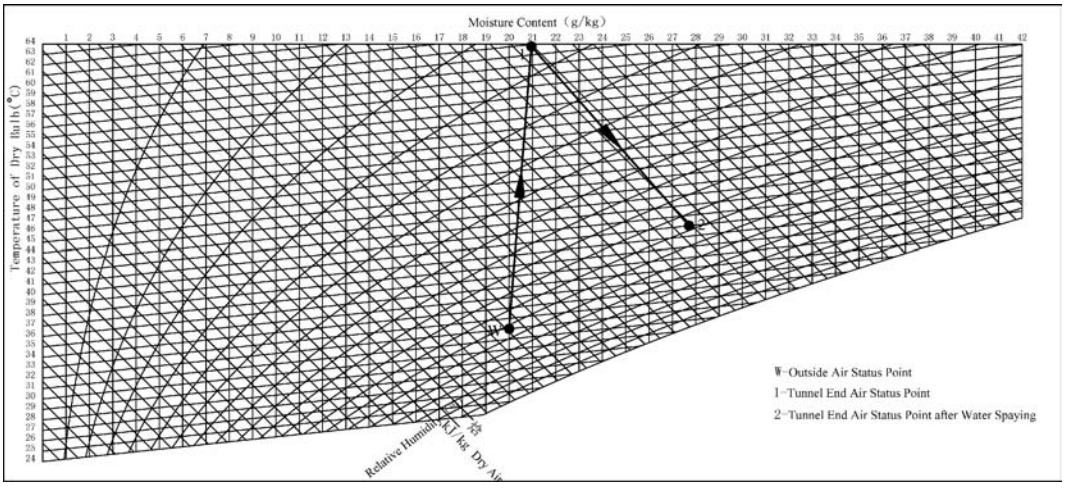

Figure 2. Air enthalpy moisture graph of road tunnel temperature reduction.

be considered. At present, the cooling measures of Yangtze River Tunnel are still studied.

Figure 2 is enthalpy moisture graph of tunnel cooling.

(3) Comprehensive Measures for Tunnel Temperature Control

In addition to adopt effective cooling measures, the countermeasures in management shall be strengthened. For example: in Yangtze River Tunnel, the temperature and humidity monitoring points shall be set; if necessary, in addition to start up cooling measures, the vehicle volume entering into the tunnel shall be appropriately controlled in high temperature season.

7 CONCLUSIONS

The above analysis combined with project example illustrates that in design of long tunnel shall be considered the temperature, besides pollutant concentration meeting hygienic requirement. The air temperature standard in tunnel and cooling measures shall combine with actual project for further discussion. Of course, the water spraying for cooling can yet be regarded as a kind of convenient and economic controlling measure.

REFERENCES

Code for Ventilation and Illumination of Road Tunnel JTJ026.1-1999.

Code for Design of Road Tunnel JTG D70-2004.

Code for Design of Heating Ventilation and Air Conditioning GB50019-2003.

Hygienic Standards for the Design of Industrial Enterprises GBZ1-2002.

National Fire Protection Association 502-2001.

NFPA 130 Standard for Fixed Guideway Transit and Passenger Rail Systems 2003.

Relevant Data of Meetings for Permanent International Association of Road Congresses (PIARC-1999, 2003).

The Shanghai Yangtze River Tunnel - Theory, Design and Construction – Huang (ed)
© 2008 Taylor & Francis Group, London, ISBN 978-0-415-47161-9

Research on fireproofing and spalling resistance experiment solution for reinforced concrete structure specimen of tunnel

Y.Q. Fan
Shanghai Tunnel Engineering & Rail Transit Design and Research Institute, Shanghai, P. R. China

ABSTRACT: In the design of Chongming River-crossing Passage of Yangtze River Tunnel of Shanghai, the upper space of the round tunnel is taken as the smoke exhaust duct. As this duct is designed to exhaust the smoke after a fire, the smoke duct board will sustain bi-directional high temperature. In addition, the top of tunnel will affect by smoke temperature. The traditional fire protection measures do not work well in this project. Therefore, to verify the fireproofing performance of the structure, fireproofing tests are performed on (1) reinforced concrete board containing PP fibres and steel fibres of different brands and different contents and (2) the reinforced concrete board with fireproofing plate and fireproofing coating on the outside. The test results provide valuable suggestions on the economic and efficient fireproofing design for engineering and lining structure.

1 INTRODUCTION

Shanghai Yangtze River Tunnel is designed according to the standard of Bi-directional Six-Lane Express Highway (Grade I Highway). The designed vehicle speed in the tunnel is 80 km/h. Space under the lane board is reserved for rail transport. The total length of the tunnel is 8,954.0 m, including 7,472.11 m shield-constructed round tunnel. The outside diameter, inside diameter and ring width of linings are 15.0 m, 13.7 m and 2.0 m respectively. Staggered joint assembling method is used for general wedged lining structure. Smoke exhaust ducts formed through separating smoke duct plates are on the arch crown of the tunnel (Fig. 1).

In this experiment, we simulated the fireproofing properties, including the stress-strain relationship of reinforced bar, concrete stress-strain relationship and crack condition of high-performance concrete duct piece and cast-in-situ smoke channel plate structure, of the structure of Shanghai Yangtze River Tunnel, which was in the deepest location of earth covering. These properties vary with the change of temperature and time.

In addition, we conduct fireproofing experiment to reinforced concrete board containing PP fibres and steel fibres of different brands and in different contents and the reinforced concrete board with fireproofing plate and fireproofing coating on the outside. The purpose is to verify the fireproofing performance of the structure to provide valuable reference for economic, efficient and easy-to-construct fireproofing design for engineering and lining structure.

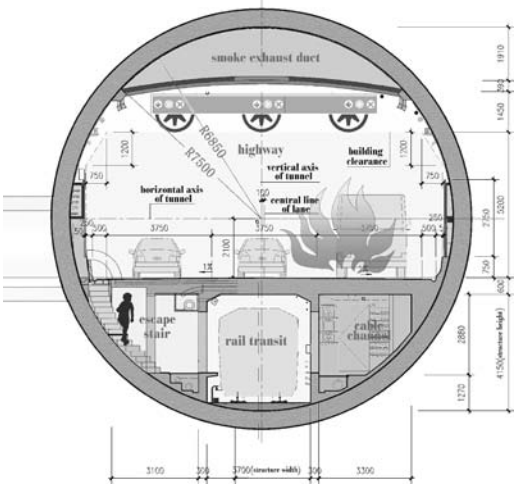

Figure 1. Structure of round shield tunnel.

2 CHOOSING TEMPERATURE RISE CURVE

Figure 2 shows the tunnel temperature rise curve frequently used in tunnel works of western counties. RABT temperature rise curve is suitable to city transport tunnel. Considering the test condition that the temperature rise limit of existing test furnace in Shanghai is 1,100°C, we decided to use Hydrocarbon Curve. The burning time is 120 minutes.

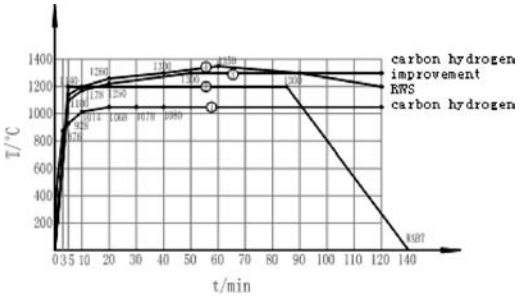

Figure 2. Curve of temperature rise in fire (carbon hydrogen improvement carbon hydrogen).

3 CHOOSING FIREPROOFING MATERIAL FOR SPECIMEN

Typically, the concrete grade is between C50 and C60 for the lining structure of large shield tunnels and between C30 and C40 for the inside structure (e.g. smoke duct plate) of shield tunnel and the structure of immersed tunnels. Taking these into consideration, we tested the following three fire-proofing & spalling-resisting measures for the specimen respectively:

- Filling fibre into the structure concrete; Fibre includes Asota's AFC fibre, GRACE's PP fibre, Changjian's PP fibre and Harex steel ingot milling fibre.
- Attaching fireproofing plate to the inside of structure; Plates include Promat's fireproofing plate, Kanghuoba fireproofing plate and Xinlong's fireproofing plate.
- Coating fireproofing paint onto the inside of structure.
- Coating includes Fulong 106-2 fireproofing coating, M-cera fireproofing coating and GRACE z-146 fireproofing coating.

4 DESIGN REQUIREMENT OF TESTS

(1) Specimen dimension:

Considering that tunnel structure will sustain the impact of fire most severely and may have concrete spalling, the reinforced bar strength will decrease obviously within 100–200 mm in the fire, and the dimension of test furnace is limited, the dimension of the specimen is determined as: $0.65 \times 3.045 \times 0.250$ m;

(2) Joint Seam Processing

During the test, the impact of joint seam on duct pieces and waterproof sealing material should be simulated.

The cross-shaped seam should be preformed on the fireproofing plate to examine the fireproofing effect of the seam.

(3) Test Load

During the test, the actual loading condition of the structure should be simulated.

5 SPECIMEN FABRICATION

5.1 *Type and quantity of specimens*

Fill the PP fibre and steel fibre into C60 and C30 concrete and the content ratio is given in Table 1. Make 12 groups of fibre concrete specimens and small blocks.

Introduction of specimens:

(1) Reinforced concrete vs. specimen with fireproofing fibre

Take then reinforced concrete specimen as the comparison specimen to concrete specimen with fire-proofing fibre. Each group includes two specimens, with a dimension of $0.65\,\text{m} \times 3.045\,\text{m} \times 0.25\,\text{m}$ ($\text{L} \times \text{W} \times \text{H}$). Apply load to these specimen in the high temperature tests to simulate the internal stresses in reality.

(2) Concrete with a fireproofing plate on the surface

Take the plain concrete with a fireproofing plate on the surface as the test specimen. Each group includes two specimens, each of which is $0.65\,\text{m} \times 3.045\,\text{m} \times 0.25\,\text{m}$ ($\text{L} \times \text{W} \times \text{H}$) to simulate the internal stresses in reality. The cross-shaped seam, of which the width equals to the one used in the field, should be provided for fireproofing plate attachment.

(3) Concrete with fireproofing paint coated on the surface

Take the plain concrete with fireproofing paint coated on the surface as the test specimen. Each group includes two specimens, each of which is $0.65\,\text{m} \times 3.045\,\text{m} \times 0.25\,\text{m}$ ($\text{L} \times \text{W} \times \text{H}$). Load is applied according to the condition in the field.

5.2 *Reinforcement design for specimens*

(1) Stressed Condition of engineering structure

The cross section dimension and the concrete model of Shanghai Yangtze River Tunnel duct piece are respectively $2.0\,\text{m} \times 0.65\,\text{m}$ ($\text{W} \times \text{T}$) and C60. The standard inner force of the cross section of duct piece going deepest into the earth covering is: $\text{M} = 1{,}403$ Kn m/ring, and $\text{N} = 6{,}600$ kN/ring. The concrete protection layer thickness is 50 mm, the HRB335 steel is $18\phi 28$ (ratio of reinforcement $= 0.95\%$), and reinforced bar stress $\text{s} = 237$ Mpa.

(2) Component and load design

Figure 3 shows the loading device used in this test. The load is determined according to the stresses of the main bar in the actual tunnel and the width of cracks.

Table 1. Type and quantity of specimens.

No.	Specimen Dim.	Material				Load-bearing state	Coring Qty.	Note
		RC	Filling amount of steel fibre	Filling amount of PP fibre	Fireproof plate / coat			
1-1	0.6 ×	C60	–	–	–	UP	2	Asota fibre
1-2	3.125 ×	C60	–	2.0 kg/m^3	–	UP	2	Harex fibre (the
1-3	0.25 m	C60	30 kg/m^3	1.0 kg/m^3	–	UP	2	same below)
1-4		C60	40 kg/m^3	0.6 kg/m^3	–	UP	2	
1-5		C60	–	2.0 kg/m^3	–	UP	2	
1-6		C60	30 kg/m^3	1.0 kg/m^3	–	UP	2	
1-7		C60	40 kg/m^3	0.6 kg/m^3	–	UP	2	
1-8		C60	30 kg/m^3	1.0 kg/m^3	–	UP	2	GRACE
1-9		C60	–	2.0 kg/m^3	–	UP	2	
1-10		C60	–	2.4 kg/m^3	–	UP	2	Changjian
1-11		C60	–	–	PROMAT	UP	2	
1-12		C60	–	–	PROMAT	UT	2	
1-13		C60	–	–	Xinlong	UP	2	
1-14		C60	–	–	Xinlong	UP	2	
1-15		C60	–	–		–	2	
1-16		C60	–	–		UT	2	
1-17		C50	–	–	–	UP	2	
1-18		C30	–	–	–	UP	2	
1-19		C40	30 kg/m^3	1.0 kg/m^3	–	–	2	Asota fibre
1-20		C40	–	2.0 kg/m^3	–	–	2	Asota fibre
1-21		C60	–	–	M-cera-1(coat)	UP	2	M-cera (hi-aluminum cement)
1-22		C60	–	–	M-cera-2(fireproof coat)	UP	2	M-cera (hi-aluminum cement)
1-23		C60	–	–	106-2 fireproof coat	UP	2	Fulong
1-24		C60	–	–	Fireproof mosaic	UP	2	GRACE

*UP = unbalanced pressure, UT = unbalanced tension.

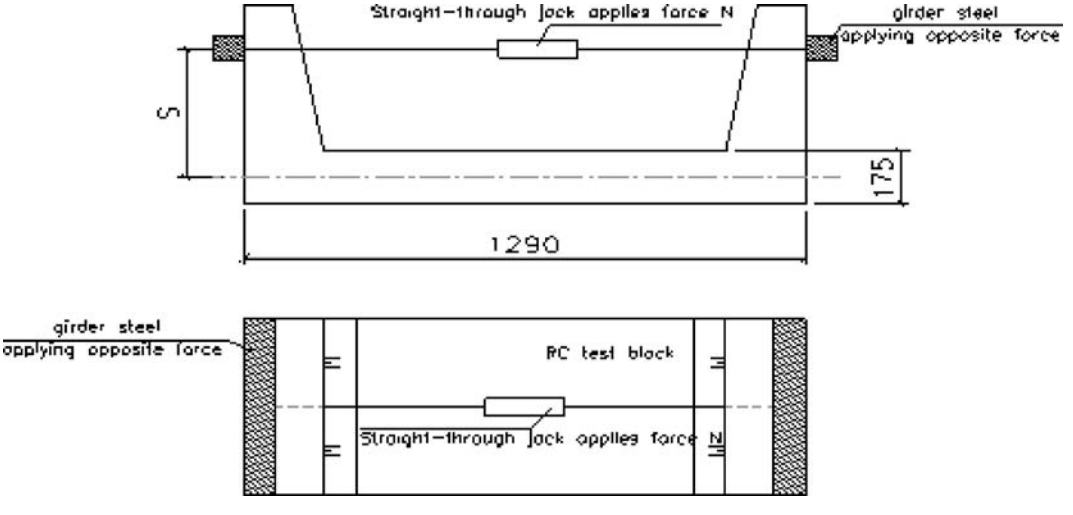

Figure 3. Specimen loading.

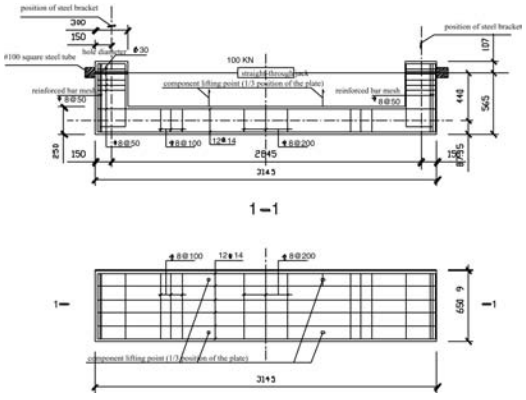

Figure 4. Concrete specimen reinforcement.

Figure 5. Standing / horizontal fireproof test furnace (1.15 m × 1.15 m).

Take 0.65 m × 3.145 m × 0.250 m RC flat plate as the specimen. The model of RC is still C60. In order to reflect the fireproofing characteristics of duct piece, the calculation is conducted on the basis of equivalent reinforced bar stress under loads and the crack width of duct piece going deepest into the earth.

From the analysis, the outer load is 95 kN (actually 100 kN). Here, the crack width $w_{max} = 0.2$ mm, $\sigma_s = 220$ Mpa and $A_s = 947\,mm^2$. Reinforcement is 12Φ14, HRB335. Hoop reinforcement along the width is Φ8@100, HRB335. Figure 4 shows the test reinforcement. From the calculation, the specimen flexibility occurring due to its dead weight under fire-free condition is 1.89 mm.

6 TEST DEVICES

We chose Far East Fire Testing Center for our tests because the devices are advanced, the test organization is authorized. A small horizontal chamber furnace was used in the test as seen Figure 5 to 7.

Because the fireproof test furnace is incapable of bearing the designed specimen pressure, a floor steel bracket is designed to support the concrete specimen. Figure 6 shows the sketch of the setup of the fireproof test furnace, concrete specimens and steel bracket.

7 MEASUREMENTS OF TEST

7.1 *Temperature measurement*

We ignite the burning chamber from the front face with gas burner. During the burning test, the

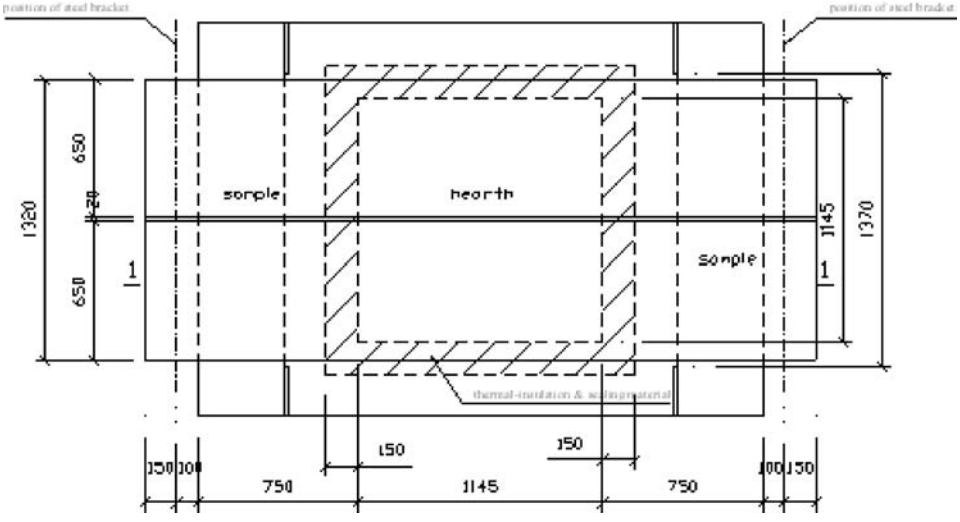

Figure 6. Plane view.

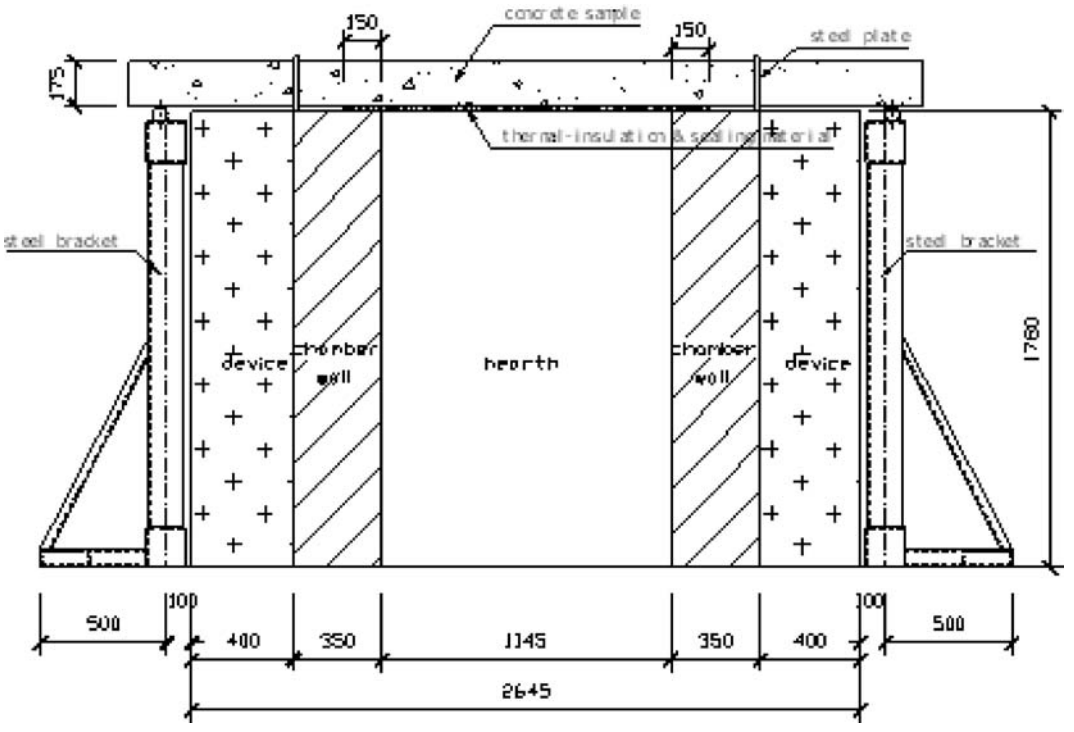

Figure 7. Setup of fireproof test furnace, concrete specimen and steel bracket.

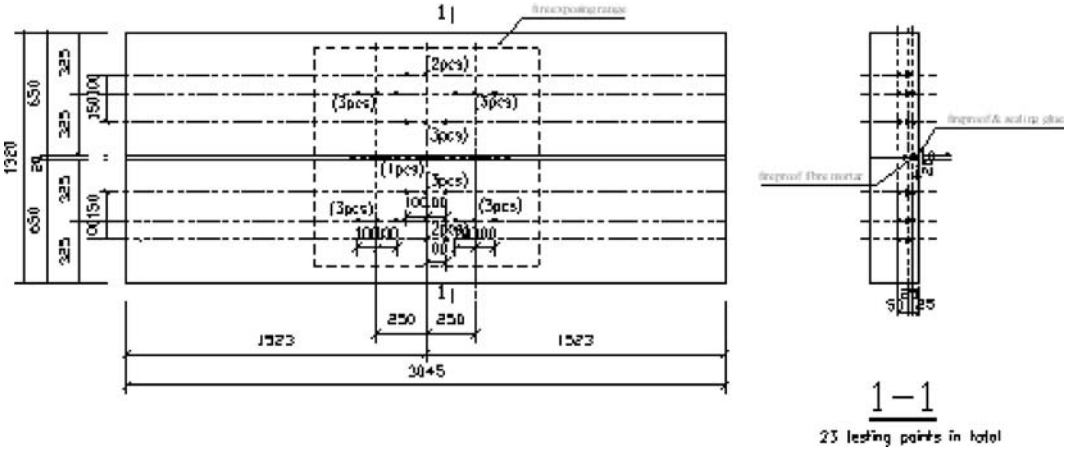

Figure 8. Arrangement of testing points.

temperature within the burning chamber is operated and controlled, and NiCr-Ni shell thermocouple is connected to remote control & record system. During all the tests, use a thermocouple to measure the temperature rise in RC specimens. Figure 8 shows the arrangement of testing points.

7.2 *Measure of compression strength, elastic module, and moisture content*

- Compression strength and elastic ratio measurement prior to temperature rise:

Three cubic blocks ($15 \times 15 \times 15$ cm) are made for each specimen group. Strength and elastic ratio tests

for concrete are conduct. Then the specimens are put into the furnace.

- Measuring compression strength and elastic module after temperature rise test:

Solid strength test is conducted on the core area of the specimen after burning. Three groups are chosen. Each group includes 3 specimens from left, middle and right. Elastic module of the entire model after burning can be tested by applying load to the specimen.

- Moisture -content measurement:

A cubic block ($15 \times 15 \times 15$ cm) is put into the furnace under 105°C until it becomes stable. Then it is dried on the day of burning test. Calculate the water content based of the loss of the mass.

8 ANALYSIS ON PARTIAL TEST RESULT

Fireproofing & spalling-resisting tests have been conducted on four types of specimens (24 groups), of which the concrete contains fireproof fibre, fireproof coating and fireproof plate. During the test, we simulated the eccentric compression conditions under the most dangerous working condition in the use of structures. The fire-facing surface is the tensioned surface. After 120 min temperature rise (max. 1,100°C), the protection structure of each specimen maintains almost intact with no concrete spalling and surface-layer peeling off. Whereas, the fireproof test result varies depending on the protection methods. Details can be seen in Table 2.

9 CONCLUSIONS

9.1 *Conclusion from model tests for the same fireproof measure*

(1) Fireproof fibre concrete

In this test, ASOTA, GRACE and CHANGJIAN fireproof fibre and Harex steel fibre were used. Burning analog tests are also conducted on the basis of the filling content given by each provider. According to the test results, the melting fibre leaves holes for escaping of vapor. When the concrete is heated, it increases heat permeability, reduces the inner-hole pressure, and avoids spallinging of concrete in the fire. When the structure is in its highest deflection, the ratio of deflection and span is much less than 1/30 (the highest deflection of 26 cm: ratio of deflection and span 1/120), the temperature of reinforced bar 50 mm to it rises to 449°C, the strength of reinforced bar falls to 50%. At this time, the structure still not collapses yet.

The cost of PP fibre is very low. It can be mixed with the concrete mixture directly during pouring. PP fibre can prevent from over-pressure of holes in concrete as well as avoid spallinging. Whereas, it cannot prevent from the rise of concrete temperature. Therefore, it can be used in the top and inner structures which are easy to be fixed. For the stressed structures and components which play an important and major role in ensuring the safety of the main structure, thermal insulation measures such as fireproof plate should be taken.

(2) Fireproof Plate of Tunnel

We also used Promat, Kanghuoba, Xinlong and M-cera fireproof plates in the test. They were constructed and mounted by individual providers. According to the test results, each of them can avoid the transfer of temperature and reach the requirement of protection when there is a fire. Whereas, Xinlong fireproof plate had damages and fallings in the fire.

Comparison of fireproof performance of different plates (a) Except for Promat plate, the highest temperature of specimen 50 mm to the fire-facing surface can be controlled under 150°C. It can protect the concrete layer effectively, avoid spallinging and ensure the structure and component's bearing capacity in fire due to low temperature rise of the reinforced bar. (b) The fasteners, which may most probably transfer heat when the entire fireproof structure contacts the specimen, occupy 5.5% of the total area of the specimen. The heat transferred by them will not have impact on the specimen, which means the possibility of transferring heat directly to the reinforced bar within the specimen is low. Therefore, the safety is relatively high.

(3) Fireproof Coating of Tunnel

We used Fulong 106-2, GRACE Z-146 and M-cera fireproof coatings in this test. They were constructed and mounted by individual providers. The test results show that each of them plays a certain role in avoiding the transfer of temperature in fire.

With respect to fireproof performance:

- Except for GRACE Z-146, temperature 50 mm to the fire-facing surface in the specimen can be controlled under 100°C. It can protect the concrete layer effectively and solve the problem in relation to fireproof and spalling resistance of concrete. Meanwhile, neither reinforced bar strength nor the bearing capacity will decrease. Whereas, the service life is only 10–15 years, which means in-time repair and replacement are required.
- The fireproof measure can prevent heat from being transferred into the specimen effectively.
- M-cera, the special thermal-insulating and fireproofing material for road and tunnel, is made of high-quality ceramic aggregated with organic and inorganic compound method. It is provided with fine thermal shock resistance and endurance. In the quick

Table 2. Comparison of fire protection measures and test conditions for tunnel.

Type of measure	No.	Basic condition of specimen						Result of fireproof test	Result of mechanics test	Damage Evaluation	Difficulty of implementation		
		Material	Fireproof measure	Elastic Module ($\times 10^4$N/mm^2)	Concrete strength ratio(%)	Water content (%)	Water absorption				requirement on space	Impact on schedule	requirement on maintenance
Plain concrete	1-1	C60			121	1.46	1.22	The highest temperatures of specimens in the depth of 25 mm, 50 mm and 100 mm are respectively 713°C, 533°C and 216°C. The average temperatures are respectively 654°C, 487°C and 215°C. Temperature in the edge joint is 337°C. The concrete after burning is grayish white and has several irregular cracks on the burning face. There are transverse cracks on the side of specimens. The damage depth of specimen is 6–10 cm, the loosening depth is 4–7 cm, and the specimen deflection is 18.0 mm.	The remaining percentage of the compression strength of the concrete tested with rebound method is 57.2%, and that of the compression strength of the concreted tested with coring method is 38.5%. The ratio of ultrasonic velocity is 0.9.	Moderate damage	–	–	–
	1-17	C50			112	2.91	2.49	The highest temperatures of specimens in the depth of 25 mm, 50 mm and 100 mm are respectively 484°C, 402°C and 111°C. The average temperatures are respectively 454°C, 295°C and 108°C. Temperature in the edge joint is 101°C. After the burning test, the concrete is in grayish white. There are many irregular cracks on the burning face and transverse cracks on the side of the specimens. The damage depth of specimen is 7–11 cm, the loosening depth is 4–8 cm, and specimen deflection is 13.95 mm. The peeling off on the surface of concrete is serious.	The remaining percentage of the compression strength of the concrete tested with rebound method is 65.9%, and that of the compression strength of the concreted tested with coring method is 39.8%. The ratio of ultrasonic velocity is 0.5.	Serious damage	–	–	–
	1-18	C30			130	3.42	2.84	The highest temperatures of specimens in the depth of 25 mm, 50 mm and 100 mm are respectively 666°C, 447°C and 100°C. The average temperatures are respectively 611°C, 315°C and 100°C. Temperature in the edge joint is 101°. After the burning test, the concrete is in grayish white. There are many irregular	The remaining percentage of the compression strength of the concrete tested with rebound method is 45.8%, and that of the compression strength of the concreted tested with coring method is 34.1%. The ratio of ultrasonic velocity is 0.5.	Serious damage	–	–	–

(Continued)

Table 2. Comparison of fire protection measures and test conditions for tunnel.

Type of measure	No.	Basic condition of specimen						Result of fireproof test	Result of mechanics test	Damage Evaluation	Difficulty of implementation		
		Material	Fireproof measure	Elastic Module ($\times 10^4$N/mm^2)	Concrete strength ratio(%)	Water content (%)	Water absorption				requirement on space	Impact on schedule	requirement on maintenance
								cracks on the burning face and transverse cracks on the side of the specimens. The damage depth of specimen is 7–11 cm, the loosening depth is 4–8 cm, and specimen deflection is 12.37 mm. The peeling off on the surface of concrete is serious. After the test, both two specimens have rupture and peeling off on their fire-facing surfaces. The entire specimen group has undamaged structure, and the reinforced bar protection layer is basically undamaged.					
Filling fireproof fibre	1-2	C60	2.0 kg/m^3 PP	5.12	125	1.61	1.61	The highest temperatures of specimens in the depth of 25 mm, 50 mm and 100 mm are respectively 629°C, 465°C and 161°C. The average temperatures are respectively 611°C, 461°C and 156°C. Temperature in the edge joint is 337°C. The concrete after burning is grayish white and has several irregular cracks on the burning face. There are transverse cracks on the side of specimens. The damage depth of specimen is 7–10 cm, the loosening depth is 4–7 cm, and the specimen deflection is 26.0 mm.	The remaining percentage of the compression strength of the concrete tested with rebound method is 38.1%, and that of the compression strength of the concreted tested with coring method is 47.2%. The ratio of ultrasonic velocity is 0.9.	Moderate damage	No	No	No
	1-3	C60	30 kg/m^3 steel fibre, 1.0 kg/m^3 PP		114	1.45	1.24	The highest temperatures of specimens in the depth of 25 mm, 50 mm and 100 mm are respectively 598°C, 538°C and 190°C. The average temperatures are respectively 587°C, 414°C and 144°C. Temperature in the edge joint is 192°C. The concrete after burning is grayish white and has several irregular cracks on the burning face. There are transverse cracks on the side of specimens. The damage depth of specimen is 6–9 cm, and the loosening depth is 4–8 cm.	The remaining percentage of the compression strength of the concrete tested with rebound method is 42.8%, and that of the compression strength of the concreted tested with coring method is 40.8%. The ratio of ultrasonic velocity is 0.8.	Moderate damage	No	No	No

1-4	C60	40 kg/ m^3steel fibre, 0.6 kg/ m^3PP	125	1.30	1.30	The highest temperatures of specimens in the depth of 25 mm, 50 mm and 100 mm are respectively 547°C, 402°C and 192°C. The average temperatures are respectively 482°C, 390°C and 178°C. Temperature in the edge joint is 192°C. The concrete after burning is grayish white and has several irregular cracks on the burning face. There are transverse cracks on the side of specimens. The damage depth of specimen is 7–10 cm, and the loosening depth is 4–7 cm.	The remaining percentage of the compression strength of the concrete tested with rebound method is 40.4%, and that of the compression strength of the concreted tested with coring method is 38.6%. The ratio of ultrasonic velocity is 0.8.	Moderate damage	No	No	No
1-10	C60	2.4 kg/ m3PP	4.89	119	1.22	1.07	The highest temperatures of specimens in the depth of 25 mm, 50 mm and 100 mm are respectively 562°C, 394°C and 150°C. The average temperatures are respectively 509°C, 367°C and 129°C. Temperature in the edge joint is 393°C. The concrete after burning is grayish white and has several irregular cracks on the burning face. There are transverse cracks on the side of specimens. The damage depth of specimen is 7–10 cm, the loosening depth is 4–7 cm, and specimen deflection is 13.95 mm.	The remaining percentage of the compression strength of the concrete tested with rebound method is 53.3%. The ratio of ultrasonic velocity is 0.8.	Moderate damage	No	No	No
Fireproof plate	1-11	C60	PRO-MAT plate		1.71	1.34	The highest temperatures of #1–11 specimens in the depth of 25 mm, 50 mm and 100 mm are respectively 245°C, 131°C and 76°C. The average temperatures are respectively 195°C, 99°C and 54°C. The concrete after burning is in its primary color and has no crack on the burning face. There are a few transverse cracks on the side of specimens. The damage depth of specimen is 4–7 cm, the loosening depth is 2–5 cm, and specimen deflection is 4.37 mm.	The remaining percentage of the compression strength of the concrete tested with rebound method is 78.9%, and that of the compression strength of the concreted tested with coring method is 60.5%. The ratio of ultrasonic velocity is 1.0.	Light damage	Small	Large; mounting sequence is required	High; keep ventilated and dry
Xinlong Plate	1-13	C60			1.85	1.67	The highest temperatures of #1–13 specimens in the depth of 25 mm, 50 mm and 100 mm are respectively 109°C, 104°C and 65°C. The average temperatures are respectively 104°C, 98°C and 50°C. The concrete after first burning is in its primary color and has no		Light damage	Small	Large; mounting sequence is required	High; keep ventilated, dry, anti-scumming

(Continued)

Table 2. Comparison of fire protection measures and test conditions for tunnel.

Type of measure	No.	Basic condition of specimen						Result of fireproof test	Result of mechanics test	Damage Evaluation	Difficulty of implementation		
		Material	Fireproof measure	Elastic Module ($\times 10^4$N/mm^2)	Concrete strength ratio(%)	Water content (%)	Water absorption				requirement on space	Impact on schedule	requirement on maintenance
								crack on the burning face. There are a few transverse cracks on the side of specimens. The damage depth of specimen is 3–6 cm, the loosening depth is 2–4 cm, and specimen deflection is 2.71 mm. The specimens are lightly damaged. After the test, it is obvious that the two inorganic fireproof plates on the fire-facing faces of the specimen have peeled off, the bottom face and the remaining fireproof mud condensate expose, and the protection layer of reinforced bar is undamaged.					
	1-24	C60	M–cera plate					The highest temperatures of specimens in the depth of 25 mm, 50 mm and 100 mm are respectively 161°C, 152°C and 89°C. The average temperatures are respectively 131°C, 104°C and 76°C. The concrete after burning is in its primary color and has several irregular cracks on the burning face. There are transverse cracks on the side of specimens. The damage depth of specimen is 5–7 cm, the loosening depth is 2–3 cm, and specimen deflection is 9.60 mm.	The remaining percentage of the compression strength of the concrete tested with rebound method is 80.8%. The ratio of ultrasonic velocity is 0.7. There is partial peeling off on the fireproofing plate.	Light damage	Small	Large; mounting sequence is required	High; keep ventilated and dry
	1-25	C60	KHB multi function plate					The highest temperatures of #1–25 specimens in the depth of 25 mm, 50 mm and 100 mm are respectively 57°C, 43°C and 23°C. The average temperatures are respectively 51°C, 37°C and 50°C. The concrete after first burning is in its primary color and has no crack on the burning face. There is no transverse crack on the side of specimens. There is partial burning loss on the surface of fireproof plate of thermal insulation layer of #1–25 specimens.		Light damage (estimated)	Small	Large; mounting sequence is required	High; keep ventilated, dry, anti- scumming

1-21	C60 (concrete protection layer, 25 mm; with PP steel fibre)	Fulong 106-2 paint	The highest temperatures of specimens in the depth of 25 mm, 50 mm and 100 mm are respectively 98°C, 98°C and 97°C. The average temperatures are respectively 97°C, 88°C and 64°C. The concrete after burning is grayish white and has several irregular cracks on the burning face. There are transverse cracks on the side of specimens. The damage depth of specimen is 6–9 cm, the loosening depth is 4–6 cm, a little concrete peels off and specimen deflection is 6.12 mm.	The remaining percentage of the compression strength of the concrete tested with rebound method is 61.5%. The ratio of ultrasonic velocity is 0.8.	Moderate damage	Large; coating is required	High; keep ventilated and dry	High
1-23	C60 (concrete protection layer, 25 mm)	M-cera paint	The highest temperatures of specimens in the depth of 25 mm, 50 mm and 100 mm are respectively 101°C, 101°C and 68°C. The average temperatures are respectively 100°C, 99°C and 58°C. The concrete after burning is its primary color and has several irregular cracks on the burning face. There are transverse cracks on the side of specimens. The damage depth of specimen is 5–7 cm, the loosening depth is 2–3 cm, and specimen deflection is 7.66 mm.	The remaining percentage of the compression strength of the concrete tested with rebound method is 78.2%. The ratio of ultrasonic velocity is 0.9. There is partial peeling off on the fireproofing plate.	Light damage	Large, coating is required	High; keep ventilated and dry	Small

temperature rise stage, it can prevent structure from damages. It also avoids toxic gas producing in a fire. Meanwhile, it is provided with favorable applicability to suit for construction of curved face of inner wall of each tunnel.

- Fulong 106-2 fireproof coating for tunnel, made with organic and inorganic compound method, is provided with fine thermal shock resistance and endurance and applicable to quick temperature rise. It produces no toxic gas in fire. It also has fine applicability.
- Grace Z-146 fireproof coat for tunnel can embed the fireproof sheets into the concrete protection layer on the surface of structure in the prefabrication stage of concrete structure so that the sheets incorporate into the concrete structure. It allows certain amount of heat being transferred inwards through the partition of fireproof coating. As the concrete in the partition will produce transverse cracks after being heated, the further spread of crack can be stopped and the transfer of heat can be reduced. It is provided with fine thermal shock resistance, endurance and applicability to construction of curved face of inner wall of each kind of tunnel. However, there is no example of engineering application for it yet.

9.2 *High-performance waterproof concrete structure is provided with certain fireproof and spalling performance*

Generally, although high-grade HPC has higher strengths than ordinary concrete, it suffers from spalling more easily than ordinary concrete. The reason is that when heated, HPC with a higher density tends to produce higher pressures within the hole. The pressure close to the surface of concrete is highest. Therefore, HPC will have sheet-shaped concrete peeling off successively in the fire.

However, C60 concrete used in this test did not show spalling. The main factors having impact on the spalling of concrete include temperature rise rate (especially more than 3°C/min), impermeability of material, water-content saturation degree of hole, reinforcement and load, among which the impact of water-content saturation degree of hole is the most important factor. According to the test, the average water content of the specimens is 1.22%, and the water content rate does not exceed 2–3% of the weight of concrete. Therefore, it cannot produce higher in-hole pressure within the concrete, and therefore no sheet-shaped concrete peeling off occurs in the fire.

In high-temperature burning, the deflections (12.5 mm–29.0 mm) of specimens with different fibre filling amount have small differences. However, all of them are higher than the deflection of specimen used in fireproof plate (deflection: 2.64 mm–4.37 mm). In the burning process, deflection spread of specimens occurs mainly within the first 30 min, in which the deflection occupies above 50% of the total deflection.

After being burned, concrete strength of fireproof specimens without thermal insulation decreases obviously. For instance, the remaining percentages of concrete strength of two C40 specimen groups were only 54.8% (#1-20, 2.0 kg/m^3 PP fibre filled) and 66.8% (#1-19, 3.0 kg/m^3 steel fibre and 1.0 kg/m^{3}PP fibre filled) of the designed strength respectively; the remaining percentage of the concrete of C50 specimens (#1-18, any measure taken) was only 34.1%; however, that of the specimens with fireproof plate and coat reached 73.8%–97.0% of the designed strength.

After burning, the concrete on fire-facing surface became loose and had many fine cracks, which directly influenced the impermeability of concrete. The impermeability after sampling was only P2/P3.

For specimens without thermal-insulating protection, the damage of high-temperature burning to concrete is direct. The ultrasonic velocity of concrete in burning area of structural specimen was significantly larger than that of concrete in non-burning area. Therefore concrete will become loose after burning. According to measurement on the specimens, there was boundary of damaged layer approximately 5 cm to the burning surface. This was much better for specimens with protection by fireproof plate or coating.

After burning, we tested the mechanical properties of the reinforced bar. The bar was directly picked among the specimens after burning. The test result shows that high-temperature burning basically does not have an obvious impact on the mechanical properties of reinforced bar. Except for one in #1-19 specimens, the yield strength of reinforced bar of other specimens is similar to that in the standard. The tensile strength and elongation of reinforced bar were up to the requirement of HRB335 steel.

REFERENCES

Gabrid Alexande Khoury. 2000. Effect of fire on concrete and concrete structures. *Prog. Struct Engng* 2:429–447.

Huo, R., Hu, Y. & Li, Y.Z. 1999. *Introduction for Architectural Fire Safety Engineering*. Hefei: Press of USTC.

Wu, Z.P. & Li, S.T. 1996. *Architectural Material's Fire Characteristics and Fire Protection*. Beijing: China Building Material Industry Press.

The Shanghai Yangtze River Tunnel - Theory, Design and Construction – Huang (ed)
© 2008 Taylor & Francis Group, London, ISBN 978-0-415-47161-9

Study of full-scale horizontal integral ring test for super-large-diameter tunnel lining structure

W.H. Cao, Z.J. Chen & Z.H. Yang
Shanghai Tunnel Engineering & Rail Transit Design and Research Institute, Shanghai, P. R. China

ABSTRACT: The article introduces a full scale horizontal integral ring test of lining structure of Shanghai Yangtze River Tunnel which is the largest diameter tunnel in the world (ϕ 15 m). In the test, one ring with a full width of 2 m was placed between two rings with a half width of 1 m. The rings are erected with staggered joints. 44 sets of horizontal action jacks and 44 sets of vertical action jacks are used to simulate the load response of the tunnel lining under different embedded depths, different lateral pressures and inter-ring pressing forces. Through analysis of the experimental data, the actual structural safety of lining ring is evaluated. For the first time we discover that the axial force is transferred as well as bending moment between rings with staggered joints. These results provide the reliable basis for structure design optimization.

1 INTRODUCTION

Shanghai Yangtze River Tunnel is designed in accordance with bi-directional six-lane highway design standard. It starts from Wuhaogou of Pudong and crosses over South Harbor of Yangtze River and finally ends at Changxing Island. The total length is 8.955 km, of which 7.471 km is shield tunnel. The outer diameter is the lining is 15.0 m, and the inner diameter is 13.7 m. The width of ring is 2.0 m. The assembling method of universal wedge lining structure with staggered joints is adopted.

The design of lining considers the structural safety, the construction quality, and the project investment of the tunnel. Therefore, many newly built large tunnel projects in the world implement full-scale (or a proper scale ratio) test to validate the reasonability, feasibility of structural design and requirement of construction quality control. Thus, the suggestions could be proposed for design optimization to achieve better technical and economic benefits.

2 TEST DESIGN

The test design mainly includes the designs of load, test ring and loading system and testing point arrangement.

2.1 *Load design*

The maximum embedment depth of Shanghai Yangtze River Tunnel is about 29.4 m. In order to simulate the real conditions of the project and make the test be able to use as a reference for the later projects, this test chose the embedded depths of 15 m and 29.4 m. Thus, six cases are designed as follows:

- Cases I–III: equivalent loads are applied according to the conditions with an embedded depth of 15 m and lateral pressure coefficients of 0.68, 0.70 and 0.72. The purpose is to observe the stress distribution, deformation and crack development of lining structure and the load condition of longitudinal bolts between rings.
- Cases IV–VI: equivalent loads are applied according to the conditions with an embedment of 29.4 m and lateral pressure coefficients of 0.68, 0.70 and 0.72. The purpose is to observe the stress distribution, deformation and crack development of lining structure and the effect of staggered joint on stress distribution of the lining structure.

2.1.1 *Principles of load design*

The inner diameter of lining ring of Shanghai Yangtze River Tunnel is 13.7 m. The segment thickness is 65 cm. The whole ring is divided into 10 segments, among which No. 1 is the key segment, No. 2s are adjacent segments and others are standard segments (Fig. 1).

According to the calculation, the maximum bending moment of lining ring is at 0° section. The maximum axial force is near 90° and 270° sections. The calculated deformation of diameter is 34 mm. Thus, load design is based on both simulating actual loads of the structure and internal forces of important sections. Here 0° section was chosen as important

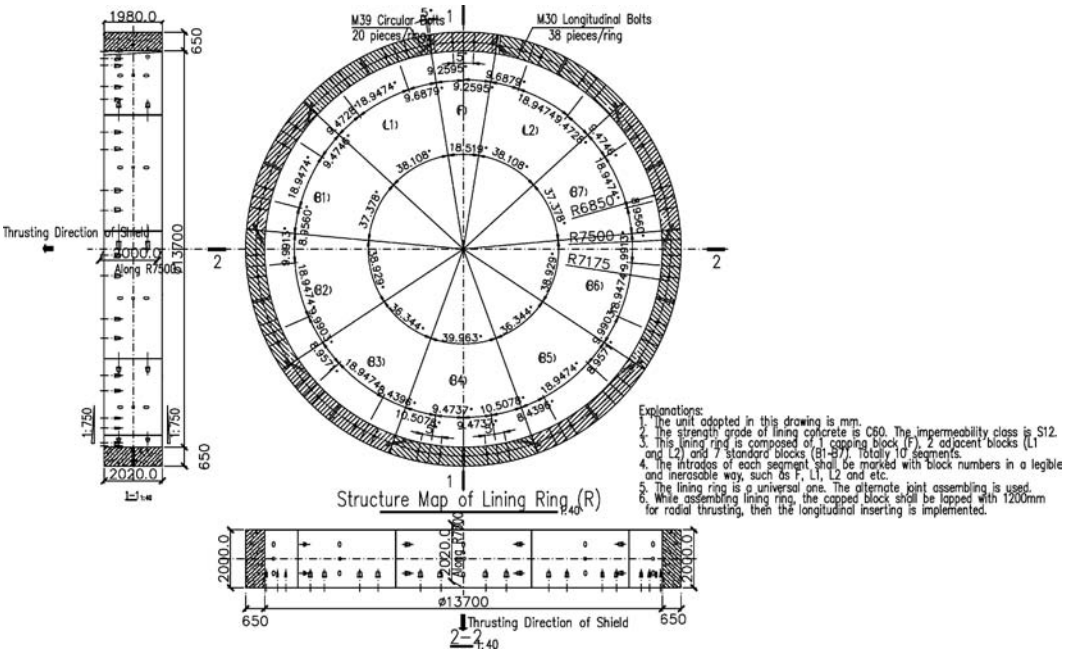

Figure 1. Structure of lining ring of shanghai Yangtze river tunnel.

section. Considering the stability of the system during test, the equivalent load acting on lining ring was symmetrically arranged according to 1/4 circle.

(1) Principle of internal force simulation
The test examines the stress distribution of key sections under six design conditions. The goal is to study bearing capacity of the important sections and to seek the possibility of reinforcement optimization.

(2) Horizontal equivalent loads
In order to simulate the water and earth pressures exerted on lining ring, 44 sets of jacks are set up on the outside of lining ring. The thrust force of jack should not exceed 1,500 kN/ring/set. According to the thrust force of each jack, these 44 sets of jacks are further divided into four groups of P1, P2, P3 and P4 as shown in Figure 2. The load is applied in 10 levels until it reaches the target value. Data are collected after the load is stabilized. The same procedures are followed for unloading.

(3) Vertical equivalent load
In order to simulate the thrust action of the shield jack, 44 sets of vertical action jacks are setup for the full ring (Fig. 2). The thrust forces of vertical jacks are 1,500 kN/point and 3,000 kN/point, respectively.

2.1.2 *Calculation of test design*
The routine method is modified for this calculation. The single ring is considered to be homogeneous circular. Because the existence of longitudinal joint will lower the bending rigidity of the ring, the bending rigidity is taken as ηEI (η is effective coefficient of flexural rigidity (<1)). After the displacement y in horizontal diameter of circular ring is calculated, It is substituted into equation $PP = k \cdot y$ to calculate the resisting force on both sides (Fig. 3). Then, the bending moment is redistributed considering the integral reinforcement effect after the segment was erected with staggered joints.

Internal force of joint:

$$M_{ji} = (1-\xi)M_i, N_{ji} = N_i \quad (1)$$

Internal force of segment:

$$M_{si} = (1+\xi)M_i, N_{si} = N_i \quad (2)$$

where, ξ adjusting coefficient (here, $\xi = 0.3$);
M_i, N_i: calculated bending moment and axial force of homogenous circular ring model respectively;
M_{ji}, N_{ji}: the adjusted joint bending moment and axial force;
M_{si}, N_{si}: the adjusted bending moment and axial force of segments.

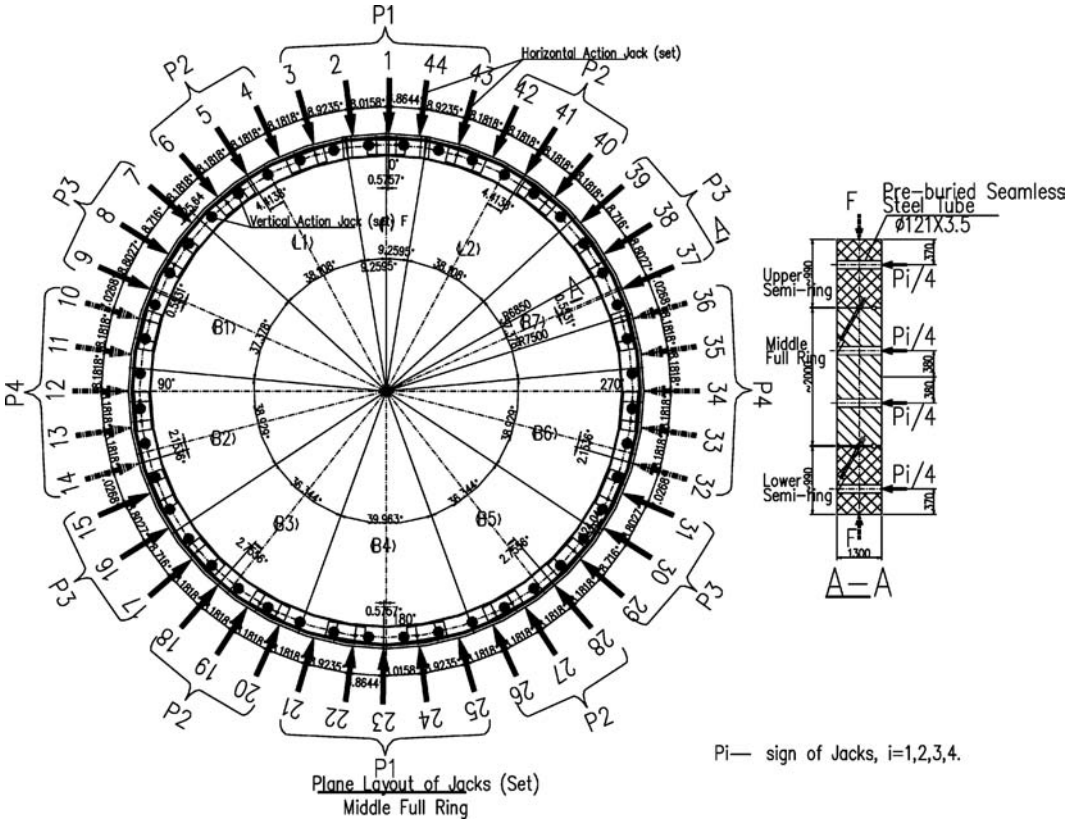

Figure 2. Equivalent load layout of testing lining ring.

2.1.3 *Equivalent load calculation*

The assumption of the calculation of equivalent load was similar to that of the modified routine method. Assuming that lining ring is a homogeneous circle and the force of jack is exerted on lining ring in form of a concentrated force at the position shown in Figure 3. Through numerous tests, the thrust forces of jacks (set) are obtained, which are listed in Table 1. The internal force deviation at the corresponding position of the important section (0° position) is controlled within 1.5%.

2.2 *Testing ring, testing site and loading system*

2.2.1 *Design of test ring*

The test is conducted one full ring with a width of 2 m in the middle, one upper ring and one lower ring with a width of 1 m. The test is focused on the middle ring. The rings were assembled with staggered joints in horizontal direction. The rotating angle between rings is 94.7368°. There still 3 straight joints existed (Fig. 4).

The 44 horizontal equivalent loads are divided into four groups of P1–P4 to apply on the test ring. At the same time, there are 44 vertical equivalent loads applied on test ring. To facilitate the passing of steel drawbars in the loading system, 176 (44×4) steel sleeves with a diameter of 121 mm are set on the segment of test ring (positioning error is less than 10 mm). The reinforcement of test ring segment is designed according to the calculation results of Case V.

2.2.2 *Testing site*

The testing site is located in the manufacturing workshop of segment production base of Shanghai Yangtze River Tunnel in Wuhaogou of Pudong. The span of the workshop is 24 m. The bottom elevation of the crane beam is 7.0 m, which can meet the height requirement of a full-scale test of 2 full segment rings (1 full ring and 2 semi-rings). The picture of the site is shown in Figure 4.

2.2.3 *Design of loading system*

(1) Horizontal loading and reaction system

There are total 44 loading points for horizontal loading (Fig. 5). The load of each loading point is transferred to the central steel ring through the reacting beam, the steel drawbar and the distribution beam.

All these components form a self-balanced loading system (Fig. 6). All horizontal loads are divided into four groups. Different combination of the load groups are adopted according to equivalent loads of different design cases. The maximum thrust force of jack during test is 224 tons/point.

(2) Vertical loading and reaction system
There are total 44 loading points for vertical loading. Each loading point forms a self-balanced loading system, consisting of jack, upper and lower steel beams and four steel drawbars (Fig. 7). The maximum load of each loading point during test is 300t.

(3) Antifriction setup between test rings and ground of testing site
The thin steel sheet is put on the ground for leveling. To ensure the free deformation of the lower part of the test ring, 44 roller supports are set below the test ring. There are 10 steel balls (ϕ100 mm) inside each support (Fig. 8). The lubrication is painted on steel balls to eliminate the friction between the bottom surface of test ring and the ground.

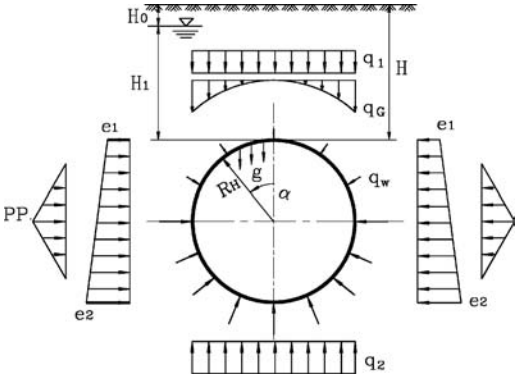

Figure 3. Calculation diagram of modified routine method. *In the figure, H0-Depth of underground water (m); H1-Height of hydrostatic head; H- Embedment depth (m); q1-Top vertical earth pressure (kPa); q2-Vercial reaction of bottom foundation (kPa); qG -Earth pressure of extrados (kPa); qW-Hydrostatic pressure (kPa); e1-Top horizontal earth pressure (kPa); e2-Bottom horizontal earth pressure (kPa); PP-Earth pressure of lateral triangle (kPa); RH-Calculated radius (m);g-Self-weight of lining (kPa); α-Angel between calculated section and vertical axle (°), counterclockwise direction is considered as positive.

(4) Loading, unloading and time control of pressure stabilization
The loading and unloading processes are executed with steps in the test. The stabilization time for each loading step is controlled within 30 minutes. The data is collected at the 5th, 15th, 30th minute after the load is applied. For unloading, the stabilization time for each step is controlled within 15 minutes. The data collection time is at the 15th minute after each step of unloading.

2.3 *Measurement contents, measurement methods and testing point arrangement*

2.3.1 *Principles of testing points arrangement*

- The testing points were arranged according to testing contents. The test focuses on the middle full ring and considers the upper and lower semi-ring as supplementary.
- According to the pre-calculation, the testing points are mainly set up at the points with large calculated internal forces and deformations and typical points.
- According to results of the calculation, proper testing components and instruments are selected to meet the testing precision requirement.

2.3.2 *Measuring contents and measurement methods*

(1) Measurement of stress in major rebar
B × 3AA-120 Type foil strain gauge is used for measurement of stress in major rebar. The area in which strain gauge will be attached is sanded with a grinder first and then polished with fine sand paper. After the area is cleaned, the foil strain gauge is attached to the major reinforcement with 502 glue. After the wire is welded, the gauges are labeled with numbers. After the gauges pass the insulation inspection, they will be sealed with 703 glue. After 1–2 hour (s), a layer of waterproof and high performance epoxy resin is applied to protect strain gauges from damage during segment casting and curing.

For the convenience of comparison, the vibrating string gauge is used to measure the stress of major rebar.

Table 1. Equivalent jack (Set) thrust force values for each ring.

Embedment depth	Cases	Lateral pressure coefficient	P1 (kN)	P2 (kN)	P3 (kN)	P4 (kN)
15 m	I	0.72	6.30	578	537	574
	II	0.70	6.30	570	530	558
	III	0.68	6.30	562	522	542
29.4 m	IV	0.72	1,120	985	923	990
	V	0.70	1,120	980	923	970
	VI	0.68	1,120	970	903	946

(2) Stress measurement of circumferential and longitudinal bolts

The foil strain gauge is used as the measurement sensor for circular and longitudinal bolt stress. The sticking and sealing procedures are similar to that of measurement of major reinforcement bar.

(3) Measurement of circumferential concrete strain

DX50AA-120 type long gauge-length (planned gauge-length: 50 mm) foil strain gauge is used for the measurement of circumferential concrete strain. It is sealed and protected from moisture and damage.

(4) Measurement of radial deformation and tangential deformation of the integral ring

The measurement sensors for radial deformation and tangential deformation of integral ring are set in pairs. The electronic displacement sensors with appropriate range and precision are selected. They were fixed on fixed objects with universal magnetic brackets for measurement.

(5) Measurement of radial, tangential horizontal dislocation of circular joints, measurement of radial horizontal displacement for longitudinal joint

The sensor used here is the same as that for measuring radial and tangential deformation of the integral ring.

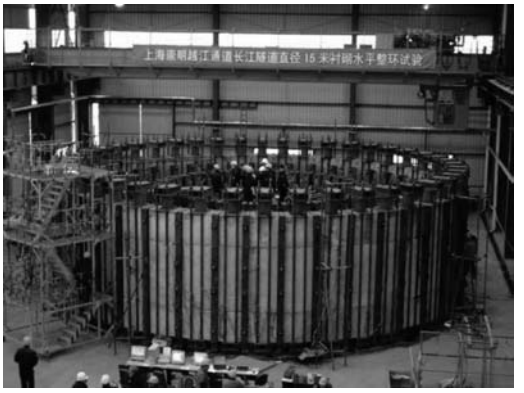

Figure 5. Field picture of testing site.

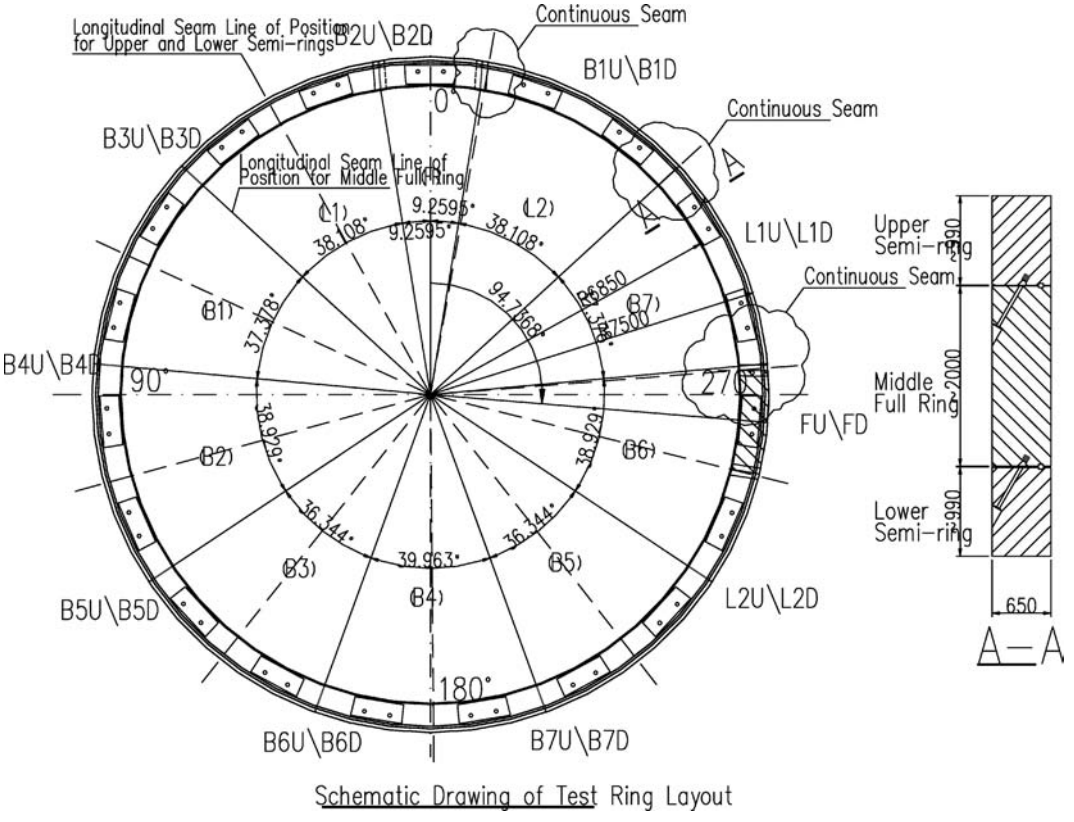

Figure 4. Schematic drawing of test ring layout.

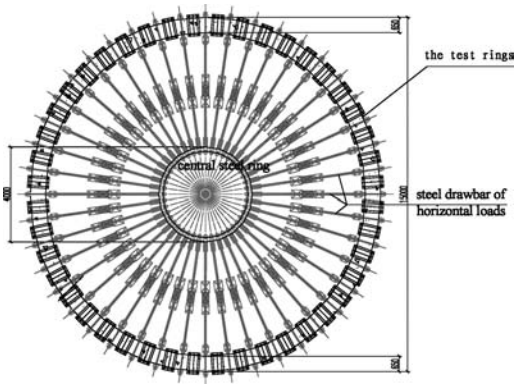

Figure 6. Top view of loading system.

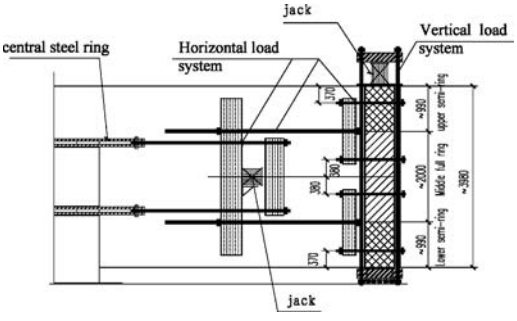

Figure 7. Side view of loading system.

(6) Measurement sensor of joint angular aperture
The measurement of joint angular aperture is to measure the relative displacement (i.e. gap changes) between segments on both sides of joint. Therefore, the electronic displacement sensor is used.

(7) Crack observation
The vertical and horizontal lines were drawn with colors inside and outside of testing segments to form rectangular node. The width of crack is measured with comparing paper and steel ruler. The crack development is traced after the each load step.

(8) Measuring instruments
Except for crack observation, both stress and deformation measurement use non-coulometric method. The complete set of testing instrument is composed of multi-point junction box, DH3816 Static Data Collector, microcomputer and supporting components (Fig. 9). The strain measuring range of the testing instruments is $-2 \times 104 - 2 \times 104\,\mu\epsilon$. And the resolution is $1\,\mu\epsilon$. The zero drift shall be no more than $4\,\mu\epsilon$/h. The uncertainty of the system shall be less than 0.5%. The instrument is characterized by correctness, reliability and rapidity (440 testing points are collected within 10 s).

Figure 8. 2 Picture of roller support.

(9) Summary of testing points arrangement
The range of numeric values, precision and quantities of above-mentioned testing points are summarized as follows (Table 2).

2.4 *Design of supplementary test*

According to preliminary analysis on testing results of design cases, the necessary relevant tests were supplemented to meet the requirements of structural bearing capability and sensitivity analysis. The supplementary tests mainly include tension test of drawbar and the test on influence of circular and longitudinal bosses on internal force.

2.4.1 *Tension test of drawbar*

(1) Testing method
On the same section of 80 steel drawbars (ϕ80), a strain gauge is attached to the top and bottom positions respectively (Fig. 10). The tensile stress of drawbar is taken as the average measurements of two gauges. The corresponding relations between the oil pressure of jack and the tension of drawbar can be established.

(2) Testing requirement
The corresponding relationship between jack thrust force and tension of drawbar and deviation proportion at each load are provided.

2.4.2 *Test on influence of circumferential and longitudinal bosses on internal force*

(1) Testing method
Six to eight concrete strain gauges are attached on the internal and external surfaces below circular surface boss of 0°, 90°, 180° and 270° of middle full ring. They are 100 mm away from circular surface. They are used to measure the concrete stress variation under the same level of load.

Six to eight concrete strain gauges are attached with equal space at the internal and external surfaces below

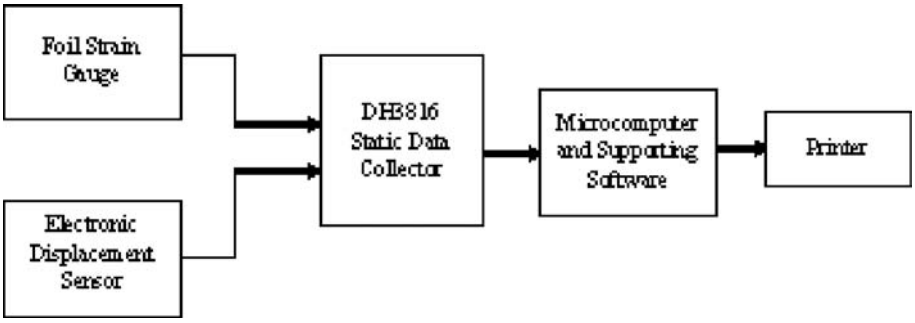

Figure 9. Flow chart of testing data collecting and analyzing system.

Table 2. Summary of testing points arrangement.

Name of testing points	Range of testing values	Precision	No.
Reinforcement stress	−335–335 MPa	0.1 MPa	316
Radial displacement for integral ring	−150–150 mm	0.1 mm	16
Tangential displacement for integral ring	−150–150 mm	0.1 mm	16
Radial displacement for longitudinal joint	−20–20 mm	0.01 mm	10
Radial displacement for circular joint	−20–20 mm	0.01 mm	15
Tangential displacement for circular joint	−20–20 mm	0.01 mm	15
Circular concrete stress	−40–3 MPa	0.1 MPa	20
Circular bolt stress	0–480 MPa	0.1 MPa	18
Bolt stress	0–400 MPa	0.1 MPa	8
Longitudinal joint angular aperture	−20–100 mm	0.1 mm	40
Crack observation	–	0.01 mm	–
Total			474

longitudinal seam boss of 90°, 160°, 270° and 310° of middle full ring, about 300 mm away from longitudinal joint to measure concrete stress variation under same level of load.

(2) Testing requirement
According to the stress distribution, the influence of circumferential and longitudinal bosses on circular and longitudinal driven forces is deducted. The reasonable positions of testing points arrangement under normal testing conditions is known, and the basis for accepting or rejecting and modifying existing data is obtained.

2.5 *Design of failure test*

2.5.1 *Testing method*
Firstly, the thrust force of four sets of jacks (P1–P4) was applied to design condition VI gradually;

Figure 10. 80 steel drawbars.

secondly, keep the thrust force of jack P1 constant and decrease the thrust force of jacks (P2–P4) gradually; when the diameter deformation of test lining ring reached 8‰ D (D refers to the outer diameter of test lining ring) or 0.3 mm crack occurred on the surface of the concrete, it was regarded that the test lining ring had been damaged. Then, according to the corresponding bias pressure no less than that while damaging, P1–P4 was gradually unloaded according to proportion until to zero.

2.5.2 *Testing requirement*
The data collecting time for each step of the load should be strictly controlled. Only after one step of the load is stabilized should the next step of load be applied. The main controlling parameters of test lining ring for each step of the load should be analyzed in time, especially the deformation and the crack development condition of the test lining ring, to ensure the smooth completion of the test.

Table 3. Diametral deformation and internal force at case of failure.

Load case		10′-5	10′-6	10′-7
0°–180° diametral deformation (mm)	Theoretical value Δ1	31.6	35.6	39.6
	Testing data Δ1′	33.0	38.1	45.4
	Δ1′/Δ1	1.04	1.07	1.15
90°–270° diametral deformation (mm)	Theoretical value Δ2	24.4	28.4	32.6
	Testing data Δ2′	22.9	27.3	33.6
	Δ2′/Δ2	0.94	0.96	1.03
Bending moment of section 180° (kNm/ring)	Theoretical value M	1,429.0	1,584.0	1,753.0
	Testing data M′	2,197.0	2,406.0	2,688.0
	M′/M	1.54	1.52	1.53
Axial force of section 180° (kN/ring)	Theoretical value N	−6,800.0	6,718.0	−6,618.0
	Testing data N′	−11,372.0	10,887.5	−10,391.0
	N′/N	1.67	1.62	1.57
Crack aperture(mm)	Theoretical value W	0.13	0.18	0.25
	Testing data W′	0.15	0.20	0.25
	W′/W	1.15	1.11	1.0

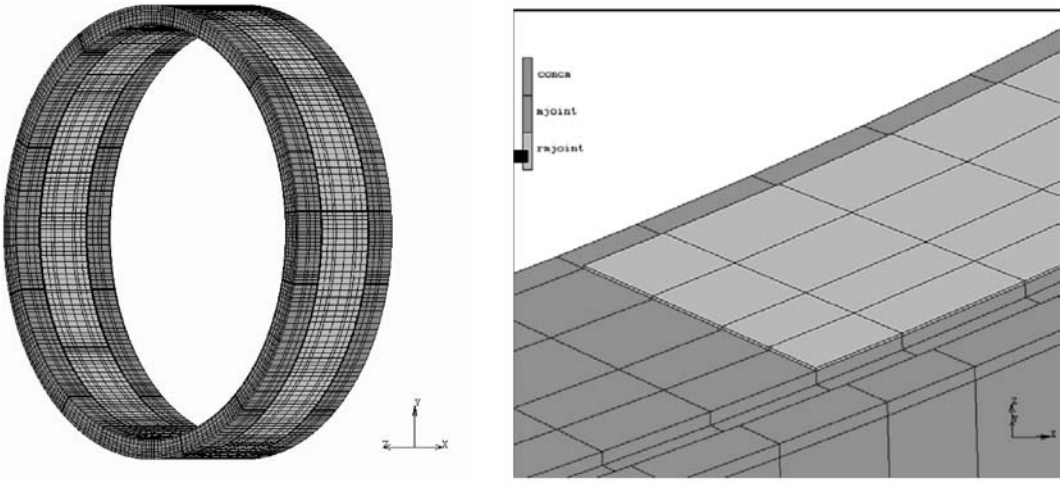

(a) 3-D Finite element model. (b) Element mesh of circular structure.

Figure 11. 3-D Finite element method model and the overview of the mesh.

2.6 *Order of test condition arrangement*

According to the thrust force of jacks exerted for each case and the layout of the testing equipments, the testing sequence is designed as follows: case I→ case II→ case III→ case IV→ case V→ case VI→ supplementary test→ case of failure.

3 TESTING DATA ANALYSIS

The collected testing data includes integral ring radial/tangential displacement, stress in major rebar, circumferential/longitudinal bolt stress, horizontal dislocation of the joint, stress in concrete, joint angular aperture and concrete crack propagation.

4 COMPARISION BETWEEN THEORETICAL CALCULATION AND TESTING DATA

The comparison between the theoretical calculation and testing data mainly focuses on the middle full ring. The symmetry of structure and the equivalent load are considered. The 0° and 180° sections of testing ring are considered to be the important sections.

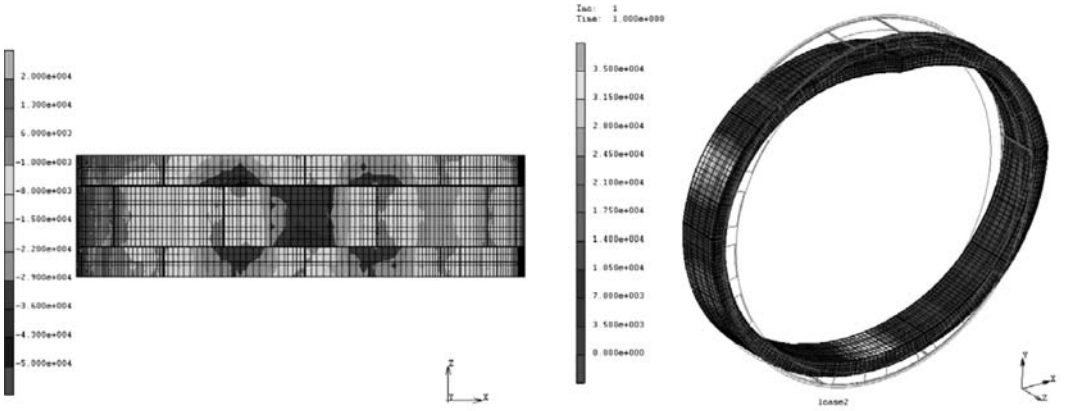

(a) Circumferential stress contour near 1800.

(b) Maximum principle stress contour of middle full ring.

Figure 12. Contour map of stress for case VI.

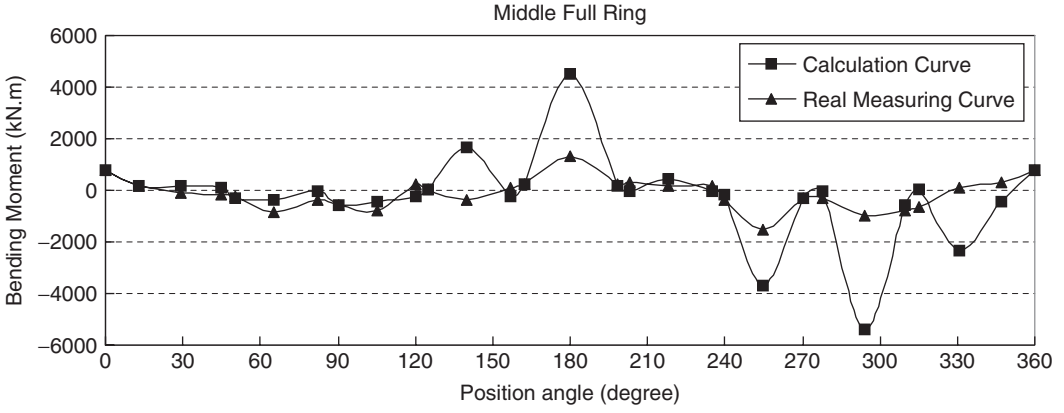

Figure 13. Comparisons of calculated value and testing results of bending moment for middle full ring.

4.1 *Comparison between theoretical calculation and testing data for homogeneous circular ring method*

See Table 3 for values of diametral deformation and internal forces under damage condition.

4.2 *Comparison of numerical simulation results and testing data*

The case VI is simulated with 3-D finite element model (Fig. 11) and the results are compared with the testing data.

4.2.1 *Internal force comparison*

Figure 12 shows the stress contour for case VI. The comparison of bending moment and axial force deducted from stress calculated results of middle full ring and testing results are shown in Figures 12–14.

4.2.2 *Deformation comparison*

The displacement vector graph of case VI for middle full ring and the comparison with testing results are as shown in Figure 15.

5 CONCLUSIONS AND SUGGESTIONS

5.1 *Bearing capability evaluation of lining ring*

From the testing conditions of case at failure, the following suggestions could be obtained:

- The maximum crack aperture of the lining ring at failure is 0.3 mm. The maximum diametral deformation reaches 3.61‰. All of these exceeded the limit for a normal operation of lining ring (crack aperture $\leq$0.2 mm, diametral deformation $\leq$3‰). However, while the maximum crack aperture

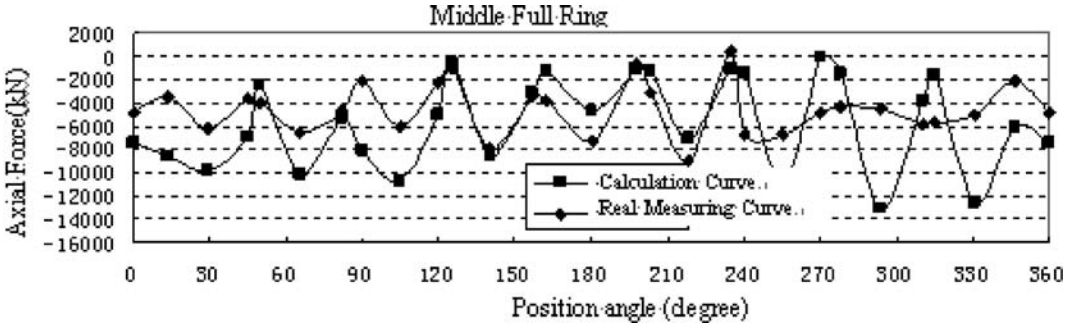

Figure 14. Comparisons of numerical calculation and testing results of axial force for middle full ring.

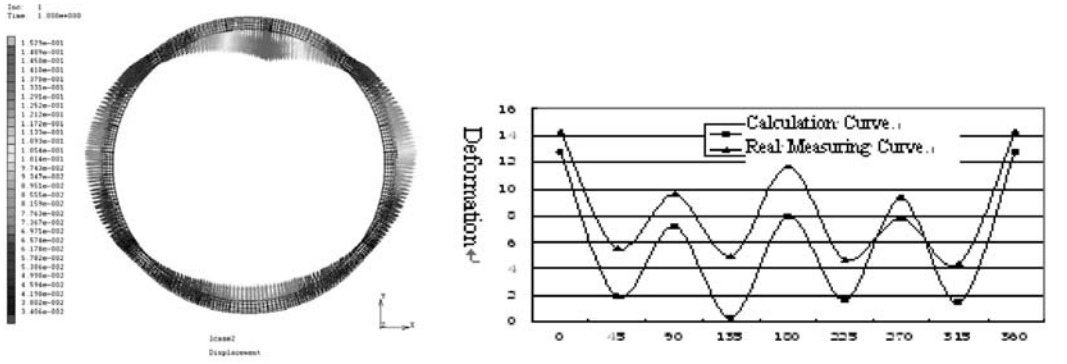

(a) Displacement vector graph

(b) Comparison of numerical calculation and testing results of deformation.

Figure 15. Displacement vector graph of middle full ring under design condition VI and comparison with testing results.

reaches 0.2 mm, the maximum diameter deformation is 2.54‰, which still below the limit for normal operation of lining ring.

- The measured stress in rebar ranges from −234.0 to 196.5 MPa, which does not exceed the design strength f_y (300 MPa) of steel reinforcement.
- The testing data demonstrates that the internal force at the position of 180° is remarkably larger than that in the position of 0°. The analysis demonstrated that there are 7 staggered joints within the scope of 0°–270° and there are 3 straight joints within the scope of 270°–360° (0°). There are joints left or right side of key segment (within 1 m), and the right joints are almost straight joints. Therefore, the internal force in the position of 180° shows obvious staggered joint transmission effect. The internal force is dramatically large.
- The maximum value of concrete tensile stress is 7.9 MPa, which occurs on the outer surface of the arc in the position of 270°. But the crack is not observed.
- The stresses of longitudinal and circumferential bolts do not exceed the yield strength of bolts.
- The maximum aperture of longitudinal joint is 3.82 mm, which meets the waterproof requirement of less than 6 mm of aperture for longitudinal joint. The maximum displacement amount of longitudinal joint is 1.03 m. The maximum radial displacement of circumferential joint is 0.86 mm. The tangential displacement amount is close to radial value.

5.2 *Load effect of cases I–VI*

1. With the decreasing of lateral pressure coefficient, the change of bending moment is more regular comparing with the change of the axial force. The change is more dramatic. At the embedment depth of 15 m, the bending moment increases from 92.88 kNf.m to 707.06 kN.m with the decreasing of lateral pressure coefficient. At the embedment depth of 29 m, the bending moment increases from 831.30 kN.m to 1,298.10 kN.m with the decreasing of lateral pressure coefficient. At the embedment depth of 15 m, the axial force increases from 3,118.23 kN to 4,349.37 kN with the decreasing of lateral pressure coefficient. At the embedment

depth of 29.4 m, the axial force changes from 8,192.51 kN to 7,204.80 kN with the decreasing of lateral pressure coefficient. The change ratio of bending moment ranges from 1.56 times to 3.66 times. The change ratio of axial force is between 0.88 times and 1.39 times.

2. The deformation is more sensitive to the changes of the lateral pressure coefficient. The radial deformation rate of the lining ring increases as the lateral pressure coefficient decreases almost linearly. The maximum increase is 0.2‰ at the embedment depth of 15 m and 0.65‰ at the embedment depth of 29.4 m.
3. With the changes of lateral pressure coefficient, the stress of the connecting bolt and angular aperture of joint varies without regular patterns. However the stress does not exceed the yield strength of the bolt. In addition, both longitudinal bolts and circular bolts are under pressure. The analysis shows that the measured stress of the connecting bolts is actually the stress increment, not including the pre-stress generated during bolt fastening. When the pressure is exerted on the joint, the bolt is released gradually. This induces negative changes of the stress.

5.3 *Analysis of equivalent flexural rigidity and bending moment transfer coefficient of lining ring*

For the structure-load model, the key parameters for the calculation of the internal force and the deformation of lining ring using the modified routine method are equivalent flexural rigidity and bending moment transfer coefficient for the staggered joint assembling.

5.3.1 *Equivalent flexural rigidity u*

The reduction parameter η (effective coefficient of flexural rigidity) is introduced because of the reduction of whole rigidity resulting from joints between segments. Hence, the equivalent rigidity of lining ring is ηEI ($0 < \eta \leq 1$).

The equivalent rigidity can be achieved by comparing the measured deformation and theoretical calculation by giving different values of η.

According to the testing condition of case at failure, $\eta = 0.7$–0.8 can be deducted comparing the measured deformation and the theoretical calculation.

5.3.2 *Bending moment transfer coefficient for staggered joint assembling*

For staggered joint assembling method, according to the results of testing data, there not only bending moment, but also the axial force transferred longitudinally between adjacent rings. In order to consider the bending moment and axial force transferring between adjacent lining rings, the bending moment transfer coefficient ξ (transfer coefficient of axial force ξ') is introduced. The ratio of bending moment (axial force) calculated by bending moment (axial force) transferred from adjacent longitudinal joint to the bending moment (axial force) calculated according to homogeneous circular ring method is $\xi(\xi')$.

According to the bending moment and the axial force from test, the transfer coefficient of bending moment and axial force can be calculated. In the test the following formula is used:

$$\xi = [\text{Mm-(Mu+Md)}]/[\text{Mm+(Mu+Md)}] \tag{3}$$

$$\xi' = [\text{Nm-(Nu+Nd)}]/[\text{Nm+(Nu+Nd)}] \tag{4}$$

$$k_\theta = \frac{M}{\theta} \tag{5}$$

where, Mm, Nm, bending moment, axial force of alternate joint position of middle ring from test;

Mu, Nu: bending moment, axial force of joint position corresponding to upper semi-ring, the average value of bending moments and axial forces at both sides of joint is used;

Md, Nd: bending moment, axial force of joint position corresponding to lower semi-ring, the average value of bending moments and axial forces at both sides of joint is used.

From the data in position of 180° of important sections, the value of ξ is 0.40–0.66 and the value of ξ' is 0.42–0.53.

5.4 *Discussion about rigidity of longitudinal and circumferential joints*

Beam-Spring Model is taken as the calculation model of shield tunnel structure in this study. The rigidity parameters of joint should be determined while calculating.

5.4.1 *Rotational rigidity k_θ of longitudinal joint*

The rotational rigidity k_θ of longitudinal joint considers the whole rigidity of segment. Thus, it will influence the internal force response. To determine rotational rigidity k_θ of longitudinal joint, the joint test is carried out. If the test is not able to conduct, the existing data from the literature can be used. Or theoretical calculation can be combined with the empirical values. Generally, the theoretical value of k_θ is under-estimated. Thus, the theoretical value should be appropriately modified.

The test analysis is carried out according to linear relation:

$$k_\theta = \frac{M}{\theta} \tag{5}$$

where, M: bending moment of joint (kN·m); θ: relative angular aperture of joint (rad).

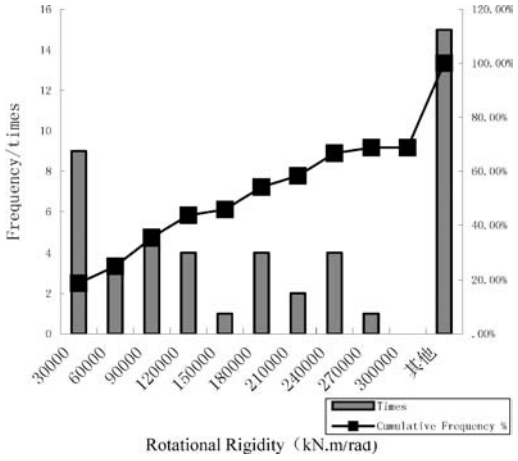

Figure 16. Histogram of rigidity distribution.

The influence of the axial force and the pre-stress of bolt are not considered in formula (5). The measured bending moment corresponds with a certain axial force (eccentricity). The calculation of the rigidities is shown in Figure 16. The cumulative frequency (less than 90,000 kNm/rad) is 35.4%. The cumulative frequency (less than 240,000 kN·m/rad) is 66.7%.

5.4.2 *Circumferential joint*

The values of axial rigidity k_n and tangential rigidity k_s for the circumferential joint can be set according to the axial rigidity and tangential rigidity of the connecting bolt. k_s includes radial shearing rigidity k_{sr} and circumferential shearing rigidity k_{st}. If the test does not involve in the contents of this aspect, the theoretical calculation can be used. It is determined with radial and longitudinal shearing rigidities. From the testing results, the radial and tangential displacement amount of this test ring is within 1 mm. The radial and tangential displacement amounts are almost the same.

5.5 *Suggestions and optimization of lining structure design*

The reinforcement of this test ring is designed according to design condition V (corresponding to super-deep embedment section). According to the comparison analysis, the measurement of crack aperture and steel reinforcement stress are almost the same as theoretical calculations. In addition, according to the parameters during test, the lining structures of deep buried and shallow buried sections are back analyzed. Thus, the reinforcement is appropriately optimized. Good economic effects are achieved.

Under the applied vertical load, cracks occur near the loading plate of jacks. Considering the larger thrust force of shield jack under construction (especially under deviation correction condition) of large diameter of the lining ring, the material strength may be not enough at some localized areas. Therefore, the steel mesh reinforcement is designed in the position where jacks act.

The difference of internal force distribution for integral ring between joint and central area of segment is large (the bending moment of end position is only about 1/4 of that of central position for same segment). The reinforcement at the end position can be reduced appropriately, especially near staggered joint areas.

The distribution of straight joint and staggered joint between rings has a complex influence on structural internal forces and deformations. The force transfer between rings is also not regular. Therefore, the numbers of straight joints between adjacent rings should be reduced during construction.

Around staggered joint areas, the transfer effect of longitudinal forces between lining rings is efficient (for example, at the position of 180°). And the bending moment and the axial force are all transferred longitudinally. The transfer coefficient of bending moment is 0.40∼0.66. The transfer coefficient of axial force is 0.42∼0.53. Namely, during staggered joint assembling, the axial force increases with the increase of section bending moment at the joint position. Therefore, the reinforcement design is reasonable in this project. More economic profits are yielded. On the other hand, only two M39 circular bolts are set within the ring width of 2 m. The flexural rigidity k_θ of joint is relatively small. Therefore the longitudinal transfer coefficient ξ is greater than 0.3.

The result of the supplementary tests demonstrates that there is no stress concentration appeared in joint boss.

The stresses of circumferential and longitudinal bolts are small. However, they provide necessary safety conservation for assembling construction and special unfavorable conditions.

In design of lining structure, it is appropriate to adopt a single segment assembling method: all non-staggered joints or all staggered joints. If the conditions of lining ring are complicated, it is possible to be affected by detrimental factors of both.

5.6 *Others thoughts*

The test studies the mechanical behavior of a large-diameter lining structure with a staggered joint assembling (partially straight joint) method. For tests in the future, the following aspects can be considered:

- Testing method: There is a big difference between the position of segment ring (horizontal) in the test and that in real working conditions. Further study can be done on how to eliminate its influence.

- For the test of the large-scale structure, better monitoring system of loading efficiency is needed to facilitate a better data analysis.
- It is suggested that the segment joint test is added to understand more about the performance of this kind of joints so as to provide accurate parameters for design.

REFERENCES

International Tunneling Association, Tunneling and Underground Space Technology, 2000. *Guidelines for the Design of Shield Tunnel Lining.*

Liu, J.H. & Hou, X.Y. 1991. *TBM Tunnel.*

Shanghai Tunnel Engineering & Rail Transit Design and Research Institute. 2000. *Optimized design and Application of Circular Tunnel Lining of Subway.*

Shanghai Tunnel Engineering & Rail Transit Design and Research Institute. 2007. *Study on technical issues of Large and long tunnel structures – Results analysis of lab experiments and field tests of horizontal full-ring lining segments.*

Shanghai Tunnel Engineering & Rail Transit Design and Research Institute. 2003. *Full-scale Full Ring Tests with Staggered Joints of Shield Tunnel Lining of Double-O Tunnel (DOT).*

Zhu, W. 2001. *Tunnel Standard Code (TBM).*

The Shanghai Yangtze River Tunnel - Theory, Design and Construction – Huang (ed)
© 2008 Taylor & Francis Group, London, ISBN 978-0-415-47161-9

The application of single-fluid resisting shear type slurry with synchronized grouting system on large slurry shield machine in Shanghai Yangtze River Tunnel

B. Xie
Shanghai Tunnel Engineering Co., Ltd., Shanghai, P. R. China

ABSTRACT: The single-fluid slurry with synchronized grouting system was used in the super-large slurry shield machine of Shanghai Yangtze River Tunnel. It is one of the achievements in our company' scientific research projects in 2005. The slurry system with a national patent has the high qualities such as fluidity, lower grouting rate and insusceptible to the dilution or permeation induced by underground water and supporting slurry at the tunnel face. In addition, the slurry has certain shear strength, it not only meets the void-filling requirement, but also controls shield pose and decreases the extent of segment dislocation through shell-grouting construction mode, which effectively protects the rear part of a shield machine and the tunnel from uplifting. The application of this patent slurry and the relevant data analysis results with respect to Shanghai Yangtze River tunnel are introduced in detail in this paper.

1 INTRODUCTION

The synchronized grouting system used in the process of shield-driven tunneling has the following advantages:

- To control the soil displacement and settlement around the tunnel effectively;
- To improve the lining early stage stability and resist the buoyancy and the tunnel force;
- Forming a protective layer around the lining, it effectively enhances impermeability of a tunnel.

However, the aforementioned advantages cannot be completely achieved. The large slurry shield machines with synchronized grouting double-liquid slurry were widely adopted in the cross-river projects in Shanghai, i.e., Yan'an Road cross-river tunnel, Dalian Road cross-river tunnel, as well as Xiangyin Road cross-river tunnel. The injected slurry is made up of two components: Component A contains cement, bentonite, stabilizing fluid and water; Component B contains only sodium silicate (water-glass). The two components have been mixed by equipment before injected into the segments back gap, then the mixed slurry coagulates as soon as being pressured into the gap and the compressive strength of the coagulated slurry structure will gradually increase with time. Whereas, according to the analyzed data from the process of construction, the double-liquid synchronized grouting method used in the slurry shield-driven tunneling has the following shortcomings:

- The mixed slurry by two components must keep enough fluidity to avoid slurry coagulation in mixer and guarantee the slurry properly filled, but it is difficult to control the slurry coagulation;
- The mixed slurry is susceptible to the dilution or permeation induced by underground water and supporting slurry at the tunnel face, but it is difficult to control the slurry coagulation rate and coagulated slurry strength;
- The pressured slurry is apt to split into the excavated soil and fill the soil beyond the gap which results in the actual grouting volume far exceeding the theoretical value (about 180–250% of the calculated value), moreover, these impose some extent disturbance on the soil mass and lead to grouting cost increasing;
- The strength of the coagulated slurry structure is not evenly distributed and the vertical displacement of the tunnel in the process of the tunneling will influence the resisting leakage effect of the lining;
- Complicated equipments for mixing and grouting slurry system and high demand to the frequency and quality of the pipeline cleaning;
- The method tends to induce ground surface settlement, so the supplemental grouting is generally needed.

Table 1. The basic properties of the single-fluid slurry.

Items	Standard
Permeability	5×10^{-5} cm/s
Density	$>1.80\,g/cm^3$
Slump (fresh mixed slurry)	12–18 cm
Slump (10–30 H)	$\geq$5 cm
Yield strength (10–30 H)	800 kPa
Water loss under pressure (7′30″, 1bar)	$<$15 ml
Expelling volume	$<$5 ml
Durable time	10–30 H
Compressive strength	90d, $>$1.0 MPa
Slurry grouting rate	100–120%

The super-large slurry shield machines with the diameter of 14.87 m and 15.43 m which wedge in the world's largest diameter range were successfully applied to the projects of Shangzhong Road cross-river tunnel and Shanghai Yangtze River tunnel, respectively. With the increase of the excavated face, the buoyancy force acted on the segment is larger than its self weight; this will tend to make the segment float upward when it separates from the frame. Therefore, synchronized grouting slurry with high quality which used to fill the gap between the segments and the excavated face plays a critical role on the tunnel stability. It is necessary to make a synchronized grouting single-fluid slurry for the large slurry shield-driven tunnel.

2 THE PROPERTY REQUIREMENTS TO THE SYNCHRONIZED GROUTING SINGLE-FLUID SLURRY AND THE COMPONENT MATERIALS IN THE LARGE SLURRY SHIELD-DRIVEN TUNNEL

2.1 *The property requirements to the synchronized grouting single-fluid slurry in the large slurry shield-driven tunnel*

According to the field geological condition, the standard for the slurry properties are regulated as follows Table 1.

2.1.1 *Slurry density*

In order to guarantee the tunnel stability at the early and later stages, the slurry density should exceed the density of the natural soil mass, besides, the similarity of the slurry properties compared with natural soil mass and the interaction between the segments and the high quality slurry will play an important role to the stability of the tunnel. The slurry density required in the research is larger than 1.85.

2.1.2 *Slump value*

The increased excavated face of the large slurry shield-driven tunnel results in some special problems, such as slurry flowing distance increment and higher tunnel buoyancy, etc. Therefore, the synchronized grouting slurry used in a super-large tunnel should have favorable fluidity and filling ability. Based on the performance of the grouting pump, the initial slump value of the designing slurry is 12–14 cm.

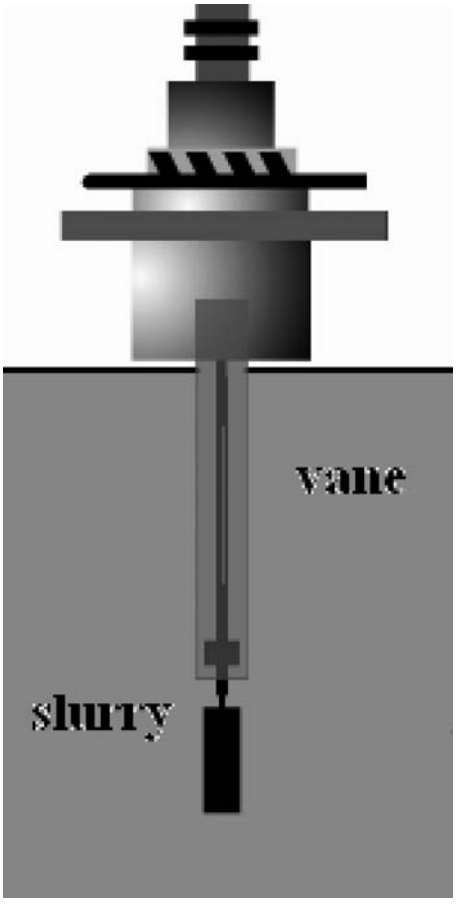

Figure 1. Yield strength testing instrument.

2.1.3 *Yield strength*

The slurry remains flowing state when the tunnel frame gradually separated from the segments. Thus, the internal friction force and the yield strength are two key slurry parameters which can be used to resist tunnel floating upward.

Figure 1 shows the yield strength testing instrument for fresh mixed slurry; it can be used to measure the value of the slurry yield strength.

It will take about 20 hours from the slurry preparation, slurry grouting, to the tunnel fame have just separated from the segments. If the calculated slurry

yield strength is larger than or equal to 0.8 kPa after 20 hours, the problem of tunnel floating upward can be controlled.

2.1.4 *Expelled volume*

The method for expelling volume measurement is as follows: fill 2,000 ml measuring tank with 2,000 ml fresh mixed slurry, close the tank in case of water volatilization and measure the expelling volume from slurry surface after standing 2 hours. Due to the different density of slurry components, the workability may be poor after mixed them together: the material with high density and low density will sink and float, respectively. In addition, the slurry layering degree and the expelling volume will increase.

2.1.5 *Durable time*

Durable time denotes the interval from the slump value of the fresh mixed slurry to the dropped value 5 cm. As for the large diameter and long distance shield driven, in order to guarantee the safety of tunneling, the lump value of the slurry should be maintained as long as possible, this will also reduce some unnecessary problems such as high pump pressure, pipeline blocking and cleaning which caused by the decrease of the slurry lump value. According to the geological condition and construction condition, the lump value of any standard slurry is required to exceed or equal to 5 cm in 20 hours so as to guarantee the pump work smoothly.

2.1.6 *The strength of the coagulated slurry structure*

According to the mix proportion, two test blocks with different dimensions (Φ 3.81 × 8.0 mm and 70 × 70 × 70 mm) are made and maintained under the environment of 20 ± 3°C and relative humidity ≥95%. To test the strength of the coagulated slurry block at the early stage (1d, 3d, 5d, 7d, 14d), the small dimension block is used; while testing the compressive strength at 28d, 60d, 90d, the bigger dimension block is used. The slurry compressive strength at 28d and 90d are required to exceed 0.5 MPa and 1.0 MPa, respectively.

2.1.7 *Slurry grouting rate*

Slurry grouting rate denotes the ratio of the actual gap volume the slurry filled to the actual gap volume. Considering the slurry shrinkage and permeability effects, the slurry grouting volume must slightly larger than the gap volume. At present, the range of the slurry grouting rate in a tunnel construction is 180%–250%, approximately. Moreover, the lining back-filled grouting forms a protective cover with certain strength outside the tunnel, this cover will increase the tunnel waterproof ability. Therefore, the slurry grouting rate is regulated less than or equal to 120% in this research.

2.2 *The property requirements to the component materials of the synchronized grouting single-fluid slurry in the large slurry shield driven tunnel*

Table 2. The property of the component materials of single-fluid slurry.

Material name	Requirement
Hydrated lime	Calcium hydroxide content ≥95% and the remains of 320 mesh sieve ≤0.5%
Fly ash	Refer to Shanghai ash standard
Fine sand	The remains of 8 sieve pore = 0, 50 pm fine composition ≤20%
Bentonite	The remains of 200 mesh sieve≤5%, expansion ratio:18–20 ml/g
Water	Live use water
Additive	Specific weight:1.06 ± 0.01 (20°C), water reducing ratio: 20–30%, hydration control ability >20 H, hydrolysis degree <30%

Table 3. Statistical value for test point step of lining 1–100 in Yangtze River Tunnel.

	Total test points	Step value (mm)			
		0	0–6	6–8	8–10
Number	496	19	461	14	2
Percentage (%)		3.83	92.94	2.82	0.4

3 ENGINEERING APPLICATION

Based on the successfully applied of the synchronized grouting single-fluid slurry to the Shangzhong Road cross-river tunnel, the same slurry system is also used for the large slurry shield machine in Shanghai Yangtze River tunnel. And the research results from this project which include construction parameters and segment step values are compared to the correspond indexes got from double-liquid synchronized Grouting in earlier slurry shield-driven tunnel.

3.1 *Test results*

3.1.1 *Ring-step value*

Summarizing the measurement data from every test point between ring 1 to 10 in Yangtze River tunnel, the average ring-step value reduces by 30%–40% compared to the value measured form the double-liquid synchronized grouting method. Therefore, the type of slurry plays a critical role in tunnel stability controlling. Table 3 is the statistical data and Figure 2 shows the step changing trend of test points 1#–4# in each ring.

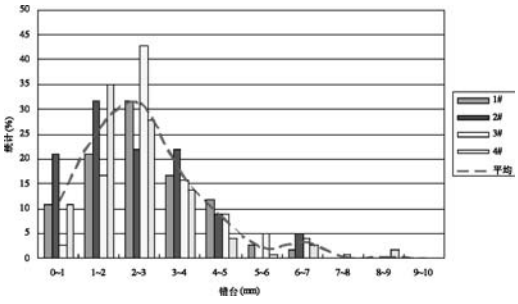

Figure 2. Step changing trend of test points 1#– 4#.

3.1.2 *Comparison between single-fluid slurry and double-fluid slurry*

Table 4 shows the comparison of technology and effectiveness between single-fluid slurry and double-fluid slurry.

3.1.3 *Comparison between single-fluid slurry and double-fluid slurry on economic terms*

Based on the successfully applied of the first single-fluid slurry with synchronized grouting method in the Shangzhong Road cross-river tunnel, the same slurry technology is also used for the large slurry shield machine in the Shanghai Yangtze River tunnel. Compared to the earlier double-liquid synchronized grouting technology, the new single-fluid grouting technology has its distinct advantages in tunnel stability, construction efficiency and innovation. Thus, the successfully development of this new slurry has great social benefits and economic benefits.

The economic comparisons between double-liquid slurry and single-fluid slurry used in Shanghai Yangtze River tunnel are shown in Table 5.

4 CONCLUSION

Our research achievements have been successfully employed in the whole line of Shangzhong Road cross-river tunnel and Shanghai Yangtze River tunnel. At present, the south line of the former project has completed, while the tunnel of the later has driven more than 2,000 rings. Shown by a series of construction data, the synchronized grouting single-fluid slurry used in the two tunnels has the following advantages:

- The slurry component materials are cheap and pollution-free, besides, they have abundant resources;
- Compared to the synchronized grouting used in earlier tunneling, the new slurry has great pumping and filling effects, as well as lower grouting rate and grouting cost;
- If the slurry yield strength is larger than 0.8 kPa within 20 hours, the slurry has its own ability to

Table 4. The comparison of technology and effectiveness between single-fluid slurry and double-fluid slurry.

Comparison items	Double-fluid slurry	Single-fluid slurry
Slurry components	(a) Cement, bentonite, stabilizing fluid , water; (b) Sodium silicate	Hydrated lime, fly ash, sand, bentonite, additives, and water.
Indexes of fresh mixed slurry	Specific weight: 1.21, initial setting time: about 10 s, fluidity:10 ± 7 s	Specific weight >1.85, initial setting time >30 h, slump value: 12–14 cm
Slurry mixer	Ordinary automatic mixer	Automatic supply system
Slurry conveying pipe	(a)Φ3 inch; (b)Φ2 inch	Slurry transportation vehicle, grouting pipe: Φ 5 inch
Grouting pump	Extrusion pump	Double bar piston pump
Grouting points	$\geq$2 points 2 pumps control 1 point	6 points 1 pump controls 2 points
Face slurry	Unpreventable	Preventable
Shield tail slurry	Thin, easy leaking	Thick, no leaking
Strength of the coagulated slurry structure	$R_1 = 0.1$ MPa, $R_1 = 2.0$ MPa, $R_{28} = 4.0$ MPa	$R_{28} \geq 0.5$ MPa, $R_{90} \geq 1.0$ MPa
Grouting rate	$>180\%$	$\leq 120\%$
Ring-step value under construction	>1 cm	0–6 mm(generally)
Supplemental grouting	yes	no
Cleaning frequency for equipment and pipeline	Every lining	3–7days

Table 5. The economic comparison between double-liquid slurry and single-fluid slurry.

	Double-liquid slurry	Single-fluid slurry
Backwall gap (m^3/ring)	20	20
Grouting rate (%)	180	120
Material cost (Yuan/m^3)	210	200
Material cost (Yuan/ring)	7,560	4,800
Reducing rate (%)	36.51	
Supplemental grouting cost	*	
Total cost (Yuan/ring)	$36.51 + ^*$	4,800

resist tunnel floating upward and the ring-step value can be controlled in the range 0–6 mm, which less than the value of double-liquid slurry;

- In synchronized grouting, bentonite and other additives are mixed together, the method not only reduces the slurry water demand, but also produces the slurry with good slump holding capacity and great pump ability in 20 hours;
- The slurry effectively prevents the tunnel floating upward, ground settlement, and also helps to control shield posture and tunnel axial line. Besides, there is not blocking phenomena in the pipeline even if the slurry long staying in the pipe;
- The slurry checks the mud water back-running without putting any influence on shield tail devices, and it avoids being diluted or dispersed by underground water;
- Compared with the double-liquid slurry, the cost of the new slurry reduces by 30% or more;
- The slurry has the ability of anti-vibration fluidization.

REFERENCES

Duddeck, H. & Erdmann, J. 1982. Structural design models for tunnels. Proc. 3rd Int. *Symp on Tunnelling*: 83–91.

Hefny, A.M. & Chua, H.C. 2006. An investigation into the behaviour of jointed tunnel lining. *Tunnelling and Underground Space Technology* 21 (3–4):428–433.

Jiang, J.C. & Guo, Z.L. 2004. *Safety System Engineering*. Beijing: Chemical Industry Press.

I.T.A. Working Group on general approaches to the design of tunnels. 1988. Guildelines for the design of tunnels. *Tunnelling and Underground Space Technology* 3(3):237–249.

Richard, E., Barlow, Jerry B., et al. 1975. *Reliability and Fault Tree Analysis*. Philadelphia: Society for Industrial and Applied Mathematics.

Shanghai Tunnel Engineering Co. Ltd. 2007. Shield-driven technique for tunnel with super large diameter and long distance. *Technical Report*.

The Shanghai Yangtze River Tunnel - Theory, Design and Construction – Huang (ed)
© 2008 Taylor & Francis Group, London, ISBN 978-0-415-47161-9

The dielectric constant testing of grouting slurry and soil behind shield tunnel segment in soft soil

H. Liu & X.Y. Xie
Key Laboratory of Geotechnical & Underground Engineering, Ministry of Education, Tongji University, Shanghai, P. R. China
Department of Geotechnical Engineering, School of Civil Engineering, Tongji University, Shanghai, P. R. China

J.P. Li
Shanghai Metro Operation Co., Ltd., Shanghai, P.R. China

ABSTRACT: Grouting behind segments is a key process in constructing a shield tunnel, which is very important to the shield tunnel's final longitudinal settlement. So we use GPR (Ground Penetrating Radar) to take nondestructive detection on the distribution of grouting behind segments. Determination of the velocity of the electromagnetic wave in the medium is a key technique for assuring the detecting precision and figures identification. In this paper, the coaxial probe method with a network analytic instrument was firstly introduced to detect the dielectric constants of the grouting slurries and soils behind shield tunnel segment, which have a large effect on the measurement result of GPR. Some comparison and direction deduce analyses on obtained graph were done, and all these provide a basis for the GPR detection on the distribution of grouting behind segments.

1 INTRODUCTION

Ground Penetrating Radar (GPR) method is a kind of the broad-spectrum electromagnetism technique to assure distribute of underground medium. Ground Penetrating Radar adopts time area impulse radar and emits broad-high frequency electromagnetism impulse into underground medium. When the electromagnetism wave is spreading in the underground medium, some attribute, such as the spread velocity and cycle of the electromagnetism wave are changing, moreover there are reflections and refractions of electromagnetism wave at the medium interface where some electromagnetism attributes have changed. Received antenna can receive the reflectance signal. We can attain to probe into the underground target through analyzing that signal. GPR is untouchable, fleetness, lossless and intuitionistic method to explore some underground targets. So that is one of important methods in physical geography exploration engineering field. Especially, GPR technique has been gradually implicated in grouting exploration field behind shield tunnel segment in soft soil.

Some causes at home and abroad indicate that shield tunnel construction induced a lot of deforming factors. The plenitudinous simultaneous synchronized grouting method is effective to reduce ground settlement. Whether grouting is plenitudinous or not, whether slurry is running off, disturbs around soil and shrinks itself during slurry concreting, which are main factors to induce additive deformation, based on settlement observation to control grouting, it is blindness to choose reference points, because it is very difficult to exactly know where asymmetry parts of grouting are.

It is very urgent to study grouting exploration field behind shield tunnel segment in soft soil. during applying GPR to explore the effect of grouting behind shield tunnel segment in soft soil, one key is to get the velocity of the electromagnetism which is determined by the dielectric constant of the soil and grouting material behind shield tunnel segment. So using GPR to explore the effect of grouting behind shield tunnel segment in soft soil will depend on making sure the dielectric constant of soil and grouting material.

When GPR explores the quality of the tunnel structure and grouting material behind shield tunnel segment in soft soils, the section planes of GPR become complicated, because of the interfere of the grouting material distributing and other outside factors. Reflect wave simulations are processed, when the dielectric constant, the electric conductivity, the thickness and radar wavelet. But the dielectric characters of the tunnel structure and radar wavelet are unknown and changing following time, frequency and sites, if the dielectric conductivity is assumed to be

invariable, it falls short of the fact. The dielectric constant is complicated and mutable.

- The category and material component are different, especially water cement ratio, which are changing along with time. Furthermore, soil granulometric composition and moisture content are varying. All these affect the dielectric constant is complicated and mutable.
- There are high humidity and different temperature inside of tunnel, which have relations with the dielectric constant.
- Because both grouting material and soil are heterogeneous material, which communicate with the dielectric constant.
- The dielectric constant depends on the frequency of electromagnetism wave.

If we can use the timely dielectric constant and radar wavelet to simulate the reflect wave, the result of GPR exploring will accord with the fact very well and exact estimate the status of the grouting behind segment at the tail. Accordingly, the GPR exploring mages are exact distinguished.

In this paper, a lab coaxial probe method was firstly proposed for measuring the dielectric constant of grouting materials and the clay soil in the stratum layer where shield tunnel was constructed. Then the velocities of electromagnetic wave in these materials were achieved through their dielectric constant, which is basis for the GPR explosion.

2 THE THEORY AND METHOD OF COAXIAL PROBE METHOD

2.1 *The microwave test theory*

The coaxial probe method is a method that the termination-open circuit coaxial probe clings to the measured material to get complex dielectric constant of material by measuring the reflection coefficient from termination probe. The coaxial probe is shown on Figure 1.

The diameter of outer and inner conductor is 3.00 mm and 0.66 mm. The diameter of ring flange is 19.00 mm. The relatively complex dielectric constants and relatively complex permeability of filling medium in probe are ε_i and μ_i respectively. The relatively complex dielectric constants and relatively complex magnetic conductivity are ε_s and μ_s. If it is supposed that only TEM dominant mode can be outputted from the coaxial probe and devisor $e_j\omega_i$ can be omitted, resultant electric and magnetic field of forward wave and backward wave can be described by Eqn. (1) and (2).

$$E_{ri} = \frac{A}{r}\left[\exp\left(-jk_i z\right) + \Gamma\exp(jk_i z)\right] \tag{1}$$

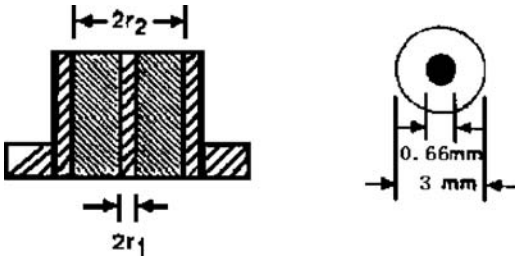

Figure 1. The sketch map of the coaxial probe.

$$H_{ri} = \frac{A}{\eta_i r}\left[\exp\left(-jk_i z\right) - \Gamma\exp(jk_i z)\right] \tag{2}$$

where,

$$k_i = w\times\sqrt{\mu_0\varepsilon_0\mu_i\varepsilon_i}\ , \quad \eta_i = \sqrt{\mu_0\mu_i/\left(\varepsilon_0\varepsilon_i\right)}$$

Γ is the coefficient of reflection, A is the amplitude of forward wave electric field head face of the probe. The electromagnetic field can be expressed as integral accumulation Eqn. (3) and (4) which includes all the plane waves, such as higher modes plane wave.

$$H_{rs} = \int_0^\infty B\left(k_c\right)Y(k_c)\left[\exp(-rz) - \Gamma_b\left(k_c\right)\exp(rz)\right]J_1\left(k_c r\right)k_c dk_c \tag{3}$$

$$E_{rs} = \int_0^\infty B\left(k_c\right)\left[\exp(-rz) + \Gamma_b\left(k_c\right)\exp(rz)\right]J_1\left(k_c r\right)k_c dk_c \tag{4}$$

Based on the transverse component continuity boundary condition, we can get Eqn. (5).

$$\int_0^\infty B\left(k_c\right)\left[1+\Gamma_b\left(k_c\right)\right]J_1\left(k_c r\right)k_c dk_c = \begin{cases}\dfrac{A(1+\Gamma)}{r} & a\le r\le b\\ 0 & r\le a, r\le b\end{cases} \tag{5}$$

The coefficient of reflection Γ can be determined by Eqn. (5) and Bessel function orthogonal.

$$B\left(k_c'\right)\left[1+\Gamma_b\left(k_c'\right)\right]k_c' = A(1+\Gamma)\left[J_0\left(k_0' a\right) - J_0\left(k_c' b\right)\right] \tag{6}$$

Eqn. (6) is from Eqn. (5) by integral operation, and substituted into Eqn. (5), we get the coefficient of reflection expression, which is Eqn. (7).

$$\frac{1-\Gamma}{1+\Gamma} = \frac{\eta_i}{In(b/a)}\int_0^\infty Y\left(k_c\right)\frac{1-\Gamma_b\left(k_c\right)\left[J_0\left(k_c a\right) - J_0\left(k_c b\right)\right]^2}{\left[1+\Gamma_b\left(k_c\right)\right]k_c} \tag{7}$$

2.2 *The coaxial probe test method*

The sketch map of the coaxial probe holder is shown on Figure 2. The coaxial probe is composed of flange coaxial transmission lines which terminal is open circuit.

The coaxial probe is connected with network analyzer HP8753E (Fig. 3) by a coaxial cable which diameter is 3 mm. we use the coaxial probe holder to

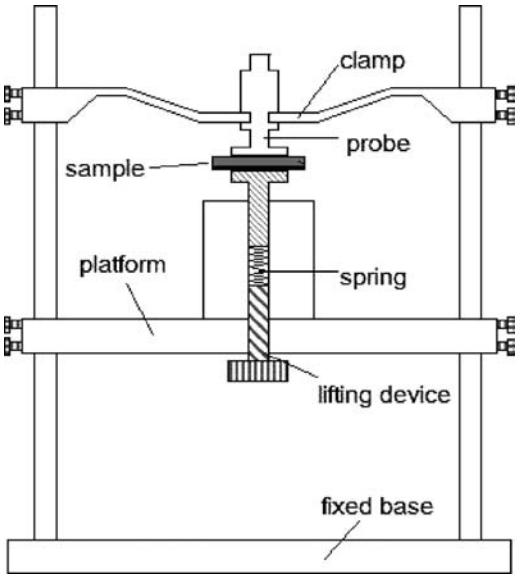

Figure 2. The sketch map of the coaxial probe holder.

Figure 3. The picture of network analyzer HP8753E.

fix the coaxial probe and eliminate the air gap between sample and probe.

Before we use the network analyzer HP8753E to measure the dielectric constant of sample, we have to revise the analyzer with air, short circuit block and de-ionized water at which is 25 degree Centigrade in order to calculate the system error.

The frequency range of network analyzer HP8753E is 30 kHz–6 GHz, which can be divided into at most 401sections. By HP85070 computing software we can easily get the dielectric constant of sample at each frequency section.

3 THE DIELECTRIC CONSTANT TESTING OF GROUTING SLURRY USED IN SHIELD TUNNELS

The main aim of this test is to obtain the dielectric constant of different kinds of grouting slurry used in shield tunnels at different ages (3hours, 3days and 28days)under different testing frequency (20 MHz–2 GHz).

3.1 *The material liquid ratios and characteristics of the grouting slurry used in the test*

There are mainly three kinds of grouting slurry used in shield tunnels, which are the inertia slurry, the common cement slurry and cement-sodium silicate double slurry. The proportions of different kinds of slurry are various. We often choose different grouting slurry basing on different soil layers, different geological conditions, different constructions and different construction purpose. Furthermore before the construction we have to do some grout mix test to determine the grout mix design.

In this dielectric constant test, we get three kinds of grouting slurry which are often used in shanghai shield tunnel from different sites.

Slurry A is a kind of common cement slurry and its material liquid ratio is listed in Table 1. Its main component is cement slurry, so it has good fluidity but need a long time to get consolidated. Slurry B is a kind of inertia slurry and its material liquid ratio is listed in Table 2. It has a high early strength and a bad fluidity. Slurry C is a kind of cement-sodium silicate double slurry which is prepared in library according to its proportion. Its material liquid ratio is listed in Table 3. It is mixed by cement slurry and sodium silicate and it can consolidate in only several seconds.

3.2 *The dielectric constant testing of grouting slurry samples*

After we fetched the grouting slurry from the site, we made 3 samples whose size are 70 mm × 70 mm × 70 mm with each slurry, and these samples were put into the standard constant temperature and humidity cement maintenance box in order to simulate the maintenance condition of construction in tunnels. Because of the especial request of the coaxial probe and the measured sample surface in intimate contact, we must politure these samples with fine emery cloth before the dielectric constant test. And we test these samples' dielectric constant at different gout ages (Fig. 4).

3.3 *The dielectric constant testing results of grouting slurry samples*

The dielectric constant testing results of the grouting slurry samples at different ages under the testing frequency range of from 20 MHz to 2 GHz are shown in Figure 5, Figure 6 and Figure 7.

Table 1. The material liquid ratio of grouting slurry A (cement slurry).

Component	Cement (kg)	Fly ash (kg)	Sand (kg)	Bentonite (kg)	SY-1adjust agent (kg)	ND-105water reducer (kg)	Water (kg)
Content	1,000	1,818	1,200	200	6.5	2.6	800

Table 2. The material liquid ratio of grouting slurry B (common cement slurry).

Component	Fine sand (kg)	Fly ash (kg)	Water (kg)	Argil (kg)
Content	600	310	500	90

Table 3. The material liquid ratio of grouting slurry C (cement-sodium silicate double slurry).

Component	Cement (kg)	Fly ash (kg)	Bentonite (kg)	Water (kg)	Sodium silicate(35°C) (kg)
Content	100	66	5	100	30–50

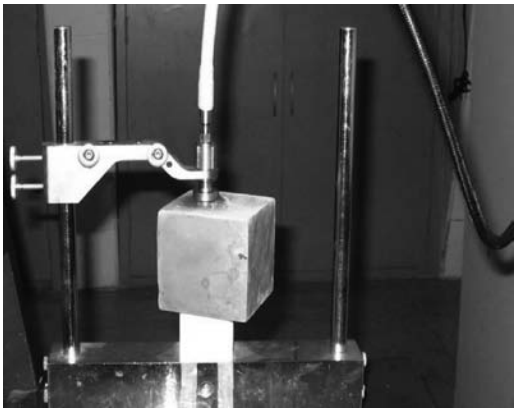

Figure 4. The sketch map of dielectric constant testing of the grouting slurry sample.

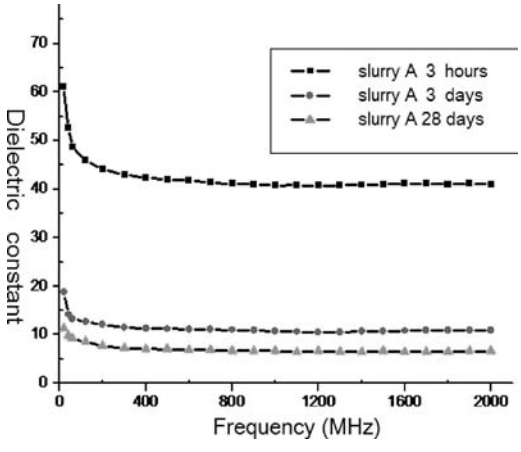

Figure 5. The curve of dielectric constant of the grouting slurry sample A at the age of 3 hours, 3 days and 28 days changing in frequency.

3.4 *The result analysis of dielectric constant of grouting slurry samples*

From the testing results in Figure 5, Figure 6 and Figure 7, we know that the curves of dielectric constant changing in frequency are almost in the same shape. The dielectric constant reduces sharply as the testing frequency increases to 200 MHz but almost keeps invariable as the testing frequency is larger than 200 MHz.

From the contrast of the dielectric constant of the slurry at different ages, we can divide the change of dielectric constant along with age into three stages. Firstly, in the initial setting period of the grouting slurry, this is about in three days, the dielectric constant of the grouting slurry decreases obviously in time as its water content reduces largely, from 43 to 12 at the frequency of 500 MHz in Figure 5. Then, the change rate becomes very slow in the stage of the slurry' consolidation, which is about from the third day to the twenty-eighth day, from 12 to 9 at the frequency of 500 MHz in Figure 5. After the slurry has completely consolidated, its dielectric constant will keep invariable.

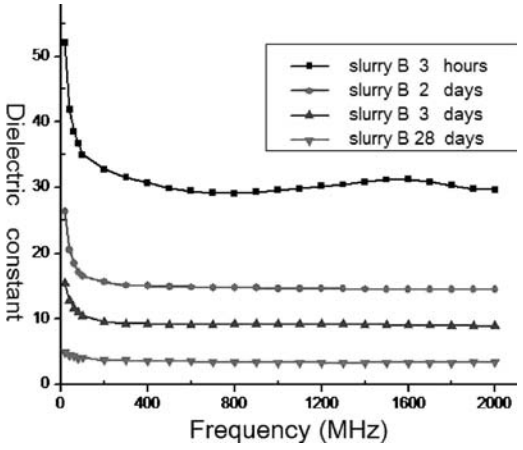

Figure 6. The curve of dielectric constant of the grouting slurry sample B at the age of 3 hours, 2 days, 3 days and 28 days changing in frequency.

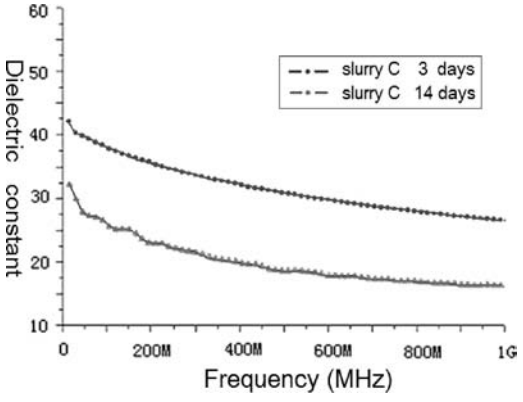

Figure 7. The curve of dielectric constant of the grouting slurry sample B at the age of 3 days and 14 days changing in frequency.

4 THE DIELECTRIC CONSTANT TESTING OF SOIL SAMPLES

In this test, we got the dielectric constant of the samples in the soil layers where all shield tunnels are constructed in shanghai, and did some analysis on the results.

4.1 *The characteristics of the soil samples*

Because the depth in which the shield tunnels in shanghai are buried almost all from the third stratum to the seventh stratum. So we get three undisturbed soil samples (Fig. 8) in each stratum (from the third stratum to the seventh stratum) by drilling. These samples are reserved in a cylinder with a diameter of 7.5 cm and a height of 30 cm and sealed with waxes to prevent the water loss and the original structure failure. The serial numbers and prosperities of these samples are listed in Table 4.

Figure 8. The picture of the undisturbed soils.

Table 4. The serial numbers, strata, buried depths and water contents of thse soil samples.

Serial number	Stratum	Buried depth (m)	Water content (%)
3-1	Gray mud-siltly clay	−6	52.7
3-2	Gray mud-siltly clay	−7	52.0
4-1	Gray muddy clay	−10	59.3
4-2	Gray muddy clay	−11	64.4
5-1	Gray clay ground	−15	37.0
5-2	Gray silty clay	−18	38.3
5-3	Gray silty clay	−19	39.7
6-1	Sap green silty clay	−20	25.3
6-2	Sap green silty clay	−22	26.4
6-3	Olive drab silty clay	−23	27.1
7-1	Olive drab sandy silt	−25	31.4
7-2	Olive drab sandy silt	−28	30.1
7-3	Olive drab silty sand	−30	28.9

4.2 *The dielectric constant testing of the soil samples*

Before the dielectric constant test, we take out the soil sample from the cylinder and cut it into three small samples with a thickness of about 5 cm, then test the dielectric constant of each small sample with the method of the coaxial probe method (Fig. 9). We get the dielectric constant of each undisturbed soil sample on an average of the testing result of the three small samples.

4.3 *The dielectric constant testing results of soil samples*

The dielectric constant testing results of the undisturbed soil samples in different soil layer in Shanghai

under the testing frequency range of from 20 MHz to 2 GHz are shown in Figure 10, Figure 11, Figure 12, Figure 13, and Figure 14.

4.4 *The result analysis of dielectric constant of undisturbed soil samples*

From the testing results of soil samples, we know that the curves of dielectric constant changing in frequency are almost the same with the grout. The dielectric constant reduces sharply as the testing frequency increases to 500 MHz but almost keeps invariable as the testing frequency is larger than 500 MHz.

Because the common GPR antenna' frequencies are 250 MHz, 500 MHz and 1.0 GHz, so we list the water content and dielectric constant at the testing frequency of 250 MHz, 500 MHz and 1.0 GHz of the undisturbed soil samples in different soil layers in shanghai in Table 5. From the contrast of the dielectric constant and water content of different soil samples, we discovered

Figure 9. The dielectric constant testing of soil.

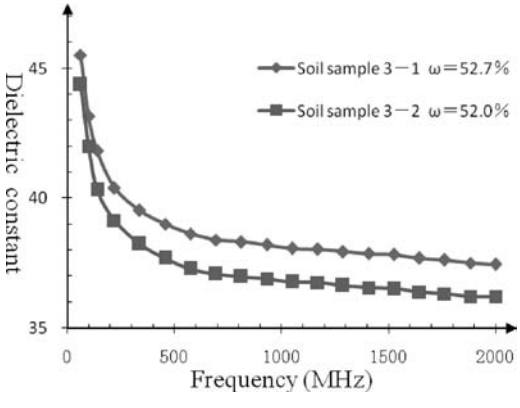

Figure 10. The curve of dielectric constant of the soil samples in the third soil layer (3-1, 3-2) changing in frequency.

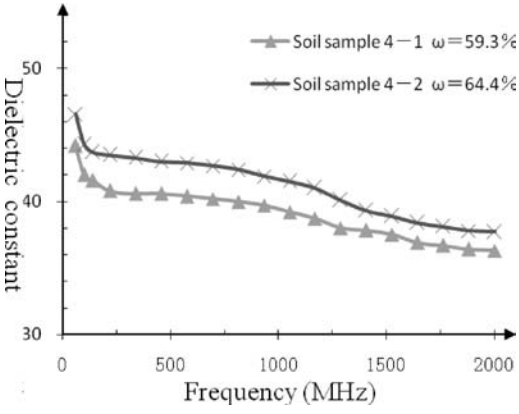

Figure 11. The curve of dielectric constant of the soil samples in the fourth soil layer (4-1, 4-2) changing in frequency.

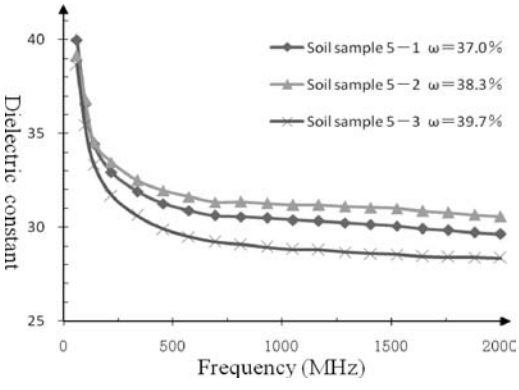

Figure 12. The curve of dielectric constant of the soil samples in the fifth soil layer (5-1, 5-2, 5-3) changing in frequency.

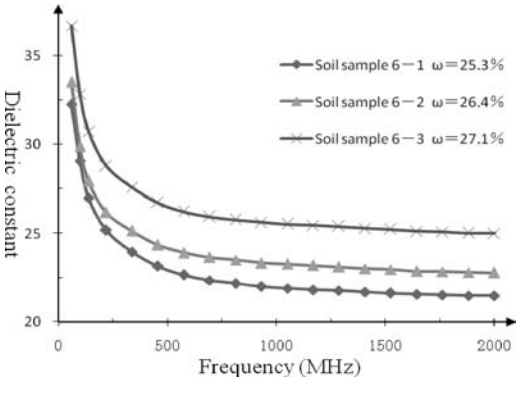

Figure 13. The curve of dielectric constant of the soil samples in the sixth soil layer (6-1, 6-2, 6-3) changing in frequency.

that the dielectric constant of the soil is directly proportional with its water content. It means that water content of the soil is the most important influence factor of its dielectric content.

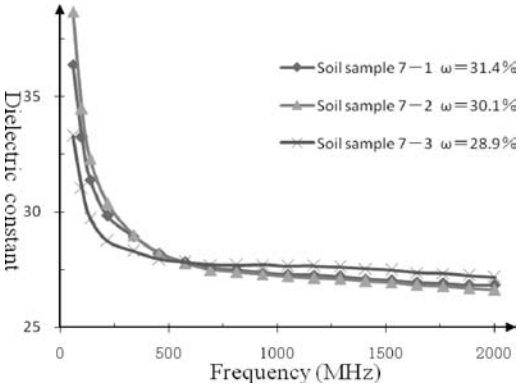

Figure 14. The curve of dielectric constant of the soil samples in the seventh soil layer (7-1, 7-2, 7-3) changing in frequency.

Owing to the diversity of dielectric constants of the different soil samples in the same soil layer is little, we could take the average of the dielectric constants of the different soil samples in the same soil layer as the dielectric constant of the soil in this soil layer. Table 6 gives the dielectric constant of the soil in the layers where shield tunnels are constructed in Shanghai under different frequency, which are the same as the frequency of the common GPR antenna. So we could refer to this table to get the dielectric constant of the soil behind the segment of shield tunnel before the GPR detecting the distribution of grouting in Shanghai.

From the dielectric constants of the soil in different layers and grouting slurry A at the different ages under the testing frequency of 250 MHz, 500 MHz and 1.0 GHz listed in Table 6, we discovered that the dielectric constant of grouting slurry at the age of 3 hours ranges from 40 to 43, which is close to the ones of the clay soil. So it is unbefitting to detect the distribution of the grouting behind the segment of shield tunnel using GPR shortly after the slurry has been grouted into the gap of the shield tail. But at the slurry age of three days, the dielectric constant of the grouting

Table 5. Water content and dielectric constant of the soil of different soil layers under different frequency.

Soil sample	Soil layer	Water content par (%)	Frequency (250 MHz)	Frequency (500 MHz)	Frequency (1.0 GHz)	Frequency (1.5 GHz)
3-1	Gray mud-siltly clay ground	52.7	39.9	38.9	38.0	37.8
3-2	Gray mud-siltly clay ground	52.0	38.6	37.6	36.9	36.5
4-2	Gray muddy clay ground	59.3	40.8	40.6	39.8	37.5
4-3	Gray muddy clay ground	64.4	43.0	43.0	42.6	38.9
5-1	Gray clay ground	37.0	32.3	31.1	30.5	30.1
5-2	Gray silty clay ground	38.3	32.7	31.7	31.1	31.0
5-3	Gray silty clay ground	39.7	31.1	29.6	28.8	28.5
6-1	Sap green silty clay ground	25.3	24.5	22.8	21.9	21.6
6-2	Sap green silty clay ground	26.4	25.5	24.0	23.2	23.0
6-3	Olive drab silty clay ground	27.1	28.1	26.4	25.6	25.2
7-1	Olive drab sandy silt ground	31.4	29.4	28.0	27.5	27.0
7-2	Olive drab sandy silt ground	30.1	29.5	27.8	27.2	26.9
7-3	Olive drab silty sand ground	28.9	28.3	27.7	27.7	27.5

Table 6. Dielectric constant of slurry A of different age and soil of different soil layers in Shanghai under the frequency of 250 MHz, 500 MHz and 1.0 GHz.

	Frequency (250 MHz)		Frequency (250 MHz)		Frequency (250 MHz)	
	Dielectric constant	velocity (m/ns)	Dielectric constant	velocity (m/ns)	Dielectric constant	velocity (m/ns)
Mud-siltly clay ground	39.3	0.48	38.3	0.48	37.5	0.49
Muddy clay ground	42.9	0.46	41.8	0.46	41.2	0.47
Clay ground	32.0	0.53	30.8	0.54	30.1	0.55
Silty clay ground	26.0	0.59	24.4	0.61	23.6	0.62
Sandy silt ground	29.1	0.56	27.8	0.57	27.5	0.57
Slurry A (3hours)	43.8	0.45	42.0	0.46	40.8	0.47
Slurry A (3hours)	11.6	0.88	11.2	0.90	10.7	0.92
Slurry A (3hours)	7.5	1.09	7.0	1.13	6.7	1.16

slurry is about 10, which is about 25 percent of the one of the mucky clay soil; 30 percent of the clay and 45 percent of the silty clay, so the electromagnetic wave will be reflected largely and we will get very good effect when we using GPR to detect the distribution of grouting behind segment at this time. Then second time compensatory grouting could be carried on basing on the results of GPR detecting to assure that the gap of the shield tail is fully filled.

5 CONCLUSION

After the research and analysis of the dielectric constant of the filling grouting slurry behind shield tunnel segment and undisturbed soil sample of different soil layers in shanghai, we discovered that the dielectric constant is different along with the frequency, water content, and material composition and so on. So it is very necessary to test the dielectric constant of the grouting slurry and the soil behind the segment of shield tunnel to improve the GPR detecting precision before using GPR to detect the distribution of grouting behind the segment.

At the slurry age of three days, the dielectric constant of the grouting slurry is much smaller than that of the soil, and we will get very good effect when we using GPR to detect the distribution of grouting behind segment at this time. And table 6 has listed the dielectric constant of soil in the layers where the shield tunnels are constructed in Shanghai.

REFERENCES

Huang, H.W., Liu, Y.Y. & Xie, X.Y. 2003. The application of GPR to grouting distribution behind segment in shield tunnel. *Rock and Soil Mechanics* 24:353–356.

Huang, H.W. & Zhang, D.M. 2001. The ground surface settlement induced by construction of tunnel and monitor on site. *Journal of Rock Mechanics & Rock engineering* 20: 1814–1820.

Li, D.X. 1994. The method and application of GPR. *Geology Publishing Company*.

Liu, Y.Y. 2003. *Non-damaged test research on back-grouting of shield tunnel in soft soils*. Dissertation of Master.

Du, J., Huang, H.W. & Xie, X.Y. Applications of dielectric permittivity of grouting material to GPR image identification. *Rock and Soil Mechanics* 27:1219–1223.

2 Construction technology and monitoring

The Shanghai Yangtze River Tunnel - Theory, Design and Construction – Huang (ed)
© 2008 Taylor & Francis Group, London, ISBN 978-0-415-47161-9

70T hydraulic system truck

J.L. Li & Y. Ni
Bouygues Shanghai Engineering Co., Ltd. Shanghai, P.R. China

ABSTRACT: The TLC 70C1 type hydraulic system truck is been designed for Shanghai Changjiang River Tunnel project. The purpose to manufacture it is this type of truck can be used to take special parts which be too weight to be load on the normal truck, such as road elements, segments, motor tank. The loads for the truck can reach 70 ton. The arrangement for its loads is: two road elements which can reach 40 ton, four segments which can reach 64 ton, a motor tank with two segments which can reach 66 ton. The truck is driven by hydraulic oil, the loads support by hydraulic oil jacks, and the direction of tires controlled by hydraulic oil jacks, off course the height of the truck can adjusted by the hydraulic oil jack. In electronic aspect, the truck is controlled by PLC system.

1 INTRODUCTION

The assembly construction of TLC 70C1 truck can be separated to nine parts: loads frame suspending jack system, hydraulic driving system, following system, direction turning system, driver's cabair system, other hydraulic system, and electronic system. The hydraulic system is used to drive the truck running, to adjust the direction of each tire and to adjust the height of the truck. First the truck's engine make the hydraulic pump work, then the hydraulic oil be absorbed out from the oil tank and sent to each oil circuit, at last the high pressure oil be sent to hydraulic motor and drive the motor revolving. Off course the high pressure oil can be sent to other circuit such as turning jack and suspending jack to drive the truck to finish the turning action and height adjust action.

2 MAIN PROBLEMS EXIST IN WORKING

When first four trucks arrived to our jobsite, the problems happen mainly on hydraulic system. Usually the hydraulic oil leaks after the trucks be used. Especially when the trucks are running, hydraulic oil be pressed out from the oil circuit. We also can find hydraulic oil be sprayed on the ground. If we don't solve the problems immediately, the most of the hydraulic oil will be loss and some hydraulic parts will be damaged.

3 ANALYSIS FOR THE PROBLEMS

Recently, the hydraulic oil problems usually happened on TCL 70T type trucks. According to the comparison

Figure 1. TLC 70C1 type hydraulic system truck.

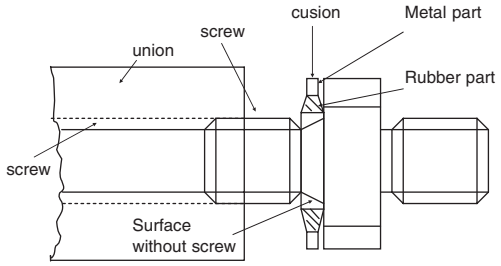

Figure 2. Union assembly to union cross.

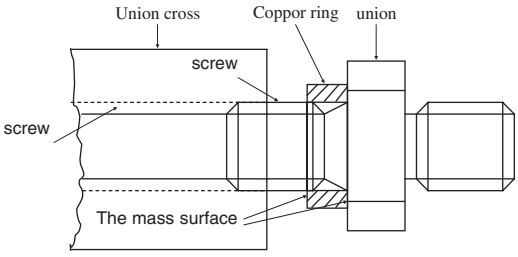

Figure 3. Union assembly to union cross.

by each truck, the hydraulic oil leakage problem often happened on some special parts.

First, most of the hydraulic oil leaking problem happened on running circuit which special be used to sent the hydraulic oil from hydraulic oil tank to the hydraulic motors. When the trucks are running, the oil pressure becomes higher than usual. So the sealing parts are easier to be damaged than usual. In this case, if the sealing parts aren't be used suitably, all the sealing parts will be destroyed faster than normal. In other case, all the hydraulic oil hoses are connected to the unions, then the unions are connected to union crosses. And the sealing parts between the unions and the union crosses are the cushions. But the hole diameter of cushions is bigger than the threads and axis what you can see in Figure 2. So when we fix a new cushion onto union to seal, the center lines for the cushion and the union aren't the same. Then some rubber which be used to manufacturing the cushion be pressed by metals, and the sealing parts may have already be destroyed. If this time the hydraulic oil pressure increases to a higher value, the leakage problem will happen.

How to solve this problem? That means we must change all the cushions which be used in this constructions. We machined some new type of cushions which without any rubber and all the parts be manufactured by copper. It's look like a copper ring, two parallel plate with a hole inside. But we need to pay more attention to the diameter of the hole and the width dimension of the ring. The hole diameter should be suitable to the thread and the axis. In other aspect, the width dimension of the ring should be larger than the one of the space between the thread and the nut. We measured the space's dimension; I suggest the width of copper ring should be 3 to 5 centimeter. Because the plasticity of the copper material, the assembly can be sealed by the new type of cushion like Figure 3 when you tightening union to union cross and the oil leaking problem will never happen again like before.

Second, the hydraulic problem caused by the wrong type of the connection between the union and the hydraulic oil hose. As what we know about the hydraulic system joint connection type, there are two types for the connection, one is plate to plate which

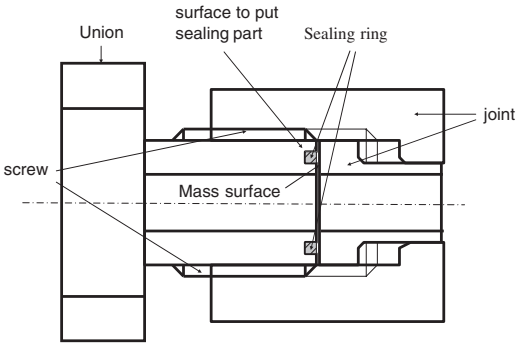

Figure 4. Plate surface mass type.

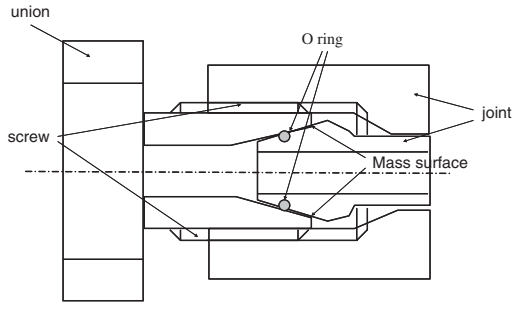

Figure 5. Mass surface with 24 degree gradient.

looks like Figure 4, the other is reducers extenders to reducers extenders which looks like Figure 4. According to the working principle of plate to plate connection type, the sealing ring be put into oil groove which be machining on one connector's plate and the plate of the sealing ring is about 2 to 3 monometer higher than that of connector. When the union be connected to the hydraulic oil hose, just the oil leaved during the space can touch the sealing ring. That means low oil pressure is exerted on the sealing ring. So the sealing ring can be used for a long time in this joint connection type. As Figure 5 description, one match surface is inside, one is outside. But both of them are cone. When the reducer extenders are connected at the beginning, the

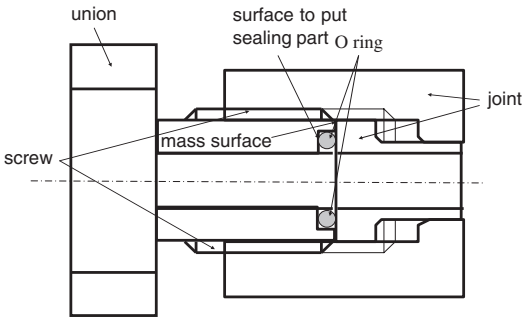

Figure 6. Plate surface mass type with problem.

space is big and more oil which during the space can touch the sealing ring. At the same time, the oil pressure on the sealing ring is large. When the hydraulic oil system running, the oil pressure increases to a high point, the space between two cone surfaces decrease and oil become less. Of course the oil pressure on the sealing ring decrease to a low point and the parts can be used for more time than plate to plate type.

According to the explanation for these two type connection, all the sealing parts can be used for a long time, but why the sealing parts are destroyed so frequently on all the TLC 70T type trucks? When the sealing parts be damaged and we change the new one for the connections, we found the connection have some wrong construction like Figure 6. Because of this, the oil pressure on the sealing parts is higher than normal. Off course the pressure is higher than usual when the hydraulic oil system running.

From the image No.5, we can see two plates before the thread, and the sealing ring be put on the second plate. Because of this construction problem, most surface of the sealing ring touch the O ring surface. At the same time, the pressure applied on the sealing parts is higher than both two type connection. Even if the hydraulic system is working in a normal condition, the life of sealing parts is shorter than what they should be. When the hydraulic system running to a high point pressure condition, everyone during sealing parts which be used in these construction can be damaged soon. What we can do is to modify the hydraulic connection joint construction. One method is to modify the wrong construction to type one connection like picture 3 described and to use the ED sealing ring. The other method is to change the construction to type two connection like picture 4 and to use O type sealing ring.

4 CONCLUSIONS

As the description, the TCL 70C1 type truck be manufactured according an abnormal standards, the designer should pay more attention to the truck's working environment the capability of each parts the choice for each parts. During the working period, if we want to solve the hydraulic oil leaking problem, we need to modify the construction for some connection such as the hydraulic hose joint. Specially the hydraulic oil leaking problems happened while the trucks running, the truck should be stopped at once and asked the technical to repair. Of course, we should pay more attention to the daily check weekly check and monthly check work, the oil leaking problems will happen less during the using period.

REFERENCES

Chen, Y., Pan, G.Q. 1990. *Shield Construction Technology.* Shanghai: Shanghai Science and Technology Literature Press.

Haggag, Salem, Rosa, Aristoteles, Huang, Kevin, et al. 2007. Fault tolerant real time control system for steer-by-wire electro-hydraulic systems. *Mechatronics* 17(2–3): 129–142.

The Shanghai Yangtze River Tunnel - Theory, Design and Construction – Huang (ed)
© 2008 Taylor & Francis Group, London, ISBN 978-0-415-47161-9

Application of the large-scale integrated equipments in slurry treatment in shield tunneling

Y.D. Liu
Shanghai Tunnel Engineering Co., Ltd., Shanghai, P. R. China

ABSTRACT: The development of integrated modules in Slurry Treatment at home and abroad was presented. The compositions and functions of the modules were introduced. The application of integrated modules in Slurry Treatment system, which called MS from France, in Shanghai Yangtze River tunnel were described. It could be a reference for the choice of slurry treatments during slurry shield construction.

1 INTRODUCTION

1.1 *The development of integrated modules in slurry treatment system*

The matching slurry separation treatment system and equipments have appeared since the slurry balance shield came out. Slurry treatment is one of the important factors for the shield normal advancing, which directly influences construction progress, cost and environmental protection. Smaller occupied area and higher effect of slurry treatment equipments became more and more important with the tunnel construction gradually developing from urban fringe to city center and the restriction of construction site. Therefore, the high-efficiency integrated slurry treatment equipments have been the first choice for the owners and construction units.

1.2 *Development status abroad*

In the short recent more than ten years, the forms of slurry treatment varied greatly which had experienced multiple modification and improvement. It has been developed into the direction of integrated modules with the increasing of environmental protection consciousness and requirements in city. Nowadays the prevalent integrated modules consist of vibrating screen, dewatering screen, and cyclone, which are mostly developed by Japan, Germany and France, such as “Aocun”, “Shabao” and “MS”. They nearly monopolize international market of slurry treatment engineering which is being applied in Shanghai Yangtze River Tunnel, Cross-River Tunnel in Xinjian and Renmin Road of Shanghai.

1.3 *Development status at home*

At the end of last century, in China several companies of slurry treatment equipments including “Black Cyclone” in Yichang and “Boyuan” in Taiwan could manufacture various integrated modules in Slurry Treatment equipments, which was the most famous for “black cyclone”. In 1992 last century, the separation system equipments were originally used for separating heavy metals from oil sand for the domestic oilfields. After the application of the slurry shield in China, especially in 1994 when slurry shield was first introduced in the South line of Yan’an East Road tunnel, “Black Cyclone” company had aimed at the market of slurry separation treatment technology. It began to manufacture different series and scales of integrated module equipments in Slurry Treatment in 2004, of which the maximum processing capacity could reach 500 m^3/h. Several years later, it nearly seized half of the market of slurry treatment equipments in tunnel engineering in China. Now “Black Cyclone” is almost leaving its footprint on any different scales of tunnel construction which are contracted by the companies related to “China Railway” or “China Tunnel” in Guangzhou, Nanjing, Wuhan, Beijing, Henan and other cities.

Recently, all the slurry equipments of some other companies including “Boyuan” have reached the professional perfection in Taiwan. Besides its extension in local Taiwan, it has also been applied in tunnel engineering of subway in Tianning Temple in Beijing, and

Table 1. The adaptive geological conditions of integrated modules in slurry treatment.

Name of particle group			Rang of article size/mm
Large particle goup	Boulder (block stone) particle		>200
	Cobble (gravel) particle		200–60
Coarse particle group	Gravel	Coarse gravel particle	60–20
		Fine gravel particle	20–2
	Sand	Coarse sand particle	2–0.5
		Medium sand particle	0.5–0.25
		Fine sand particle	0.25–0.075
Fine particle group	Silt particle		0.075–0.005
	Clay particle		0.005–0.002
	Colloidal particle		<0.002

will spread to other subway tunnel engineering which is being planned in Shenyang and Wuhan. It is reported that the separation treatment capacity of "Boyuan" is higher than that of "Black Cyclone".

2 THE ADAPTIVE GEOLOGICAL CONDITIONS OF INTEGRATED MODULES IN SLURRY TREATMENT

The adaptive geological conditions of integrated modules in slurry treatment are given in the following Table 1.

When the shield is driven in the stratum with large particles, the vibrating screen module needs to add the pre-separating screen. The pre-separating screen, which is one kind of vibrating screen like a bar, can eliminate the large particles so that the impact force to the next vibrating screen module can be alleviated.

3 THE COMPOSITION AND FUNCTION OF INTEGRATED MODULES IN SLURRY TREATMENT

The integrated modules are constituted by five modules, including vibrating screen, sand remover, dewatering screen, soil remover and transitional groove.

3.1 *The vibrating screen module*

The vibrating screen module is the first procedure of separation system. Its main function is to preliminarily isolate the large coarse particles from the slurry which is discarded by the shield. It utilizes the amplitude of the vibrating screen and eliminates the residual soil through the parabolic movement path so as to prepare for the next procedure of sand remover. The vibrating screen module consists of screen, vibrator, feeding device and other devices. The screen structure form, vibrator frequency and amplitude that determine the treatment capacity and separation size of the vibrating screen are required by the feeding particle size of the next sand remover module.

3.2 *Sand remover and soil remover module*

Sand remover and soil remover module are composed by cyclone, stent, working pump, valve and so on. Because of no powered cyclone, fluid need depend on other device to enter the cyclone in the tangent direction under the certain pressure and rotate at high speed inside. In the center of the cyclone, the negative pressure was produced, and the micro particles which have light proportion will flow out from upper hole while the larger particles which have heavy proportion will be discharged from bottom hole. Due to various dimension of the cyclone, the produced negative pressure is different and the separated particle size varies.

3.3 *Dewatering screen module*

The main function of the dewatering screen is to dewater the slurry drained from the bottom hole of the sand remover, decrease the moisture content of residual soil, recycle the separation of useful coarse particles from slurry, and reduce the amount of the discarded slurry and transportation cost of residual soil. The structure of dewatering screen is similar to that of the vibrating screen, and the screen structure form, vibrator frequency and amplitude that determine the treatment capacity and the separation size of the dewatering screen are required by the feeding particle size for the next soil remover module.

3.4 *Transitional groove module*

The main functions of the transitional groove module is to temporarily store and buffer the slurry from the vibrating screen, dewatering screen and sand remover modules. There is one diaphragm in the inner-cavity structure of groove. The slurry can be deposited, filtered, and overflowed in the diaphragm.

4 APPLICATION OF INTEGRATED MODULES IN SLURRY TREATMENT

4.1 *Overseas application*

4.1.1 *Germany "Shabao" integrated modules in slurry treatment*

Germany "Shabao" integrated modules in slurry treatment are given in following Figure 1.

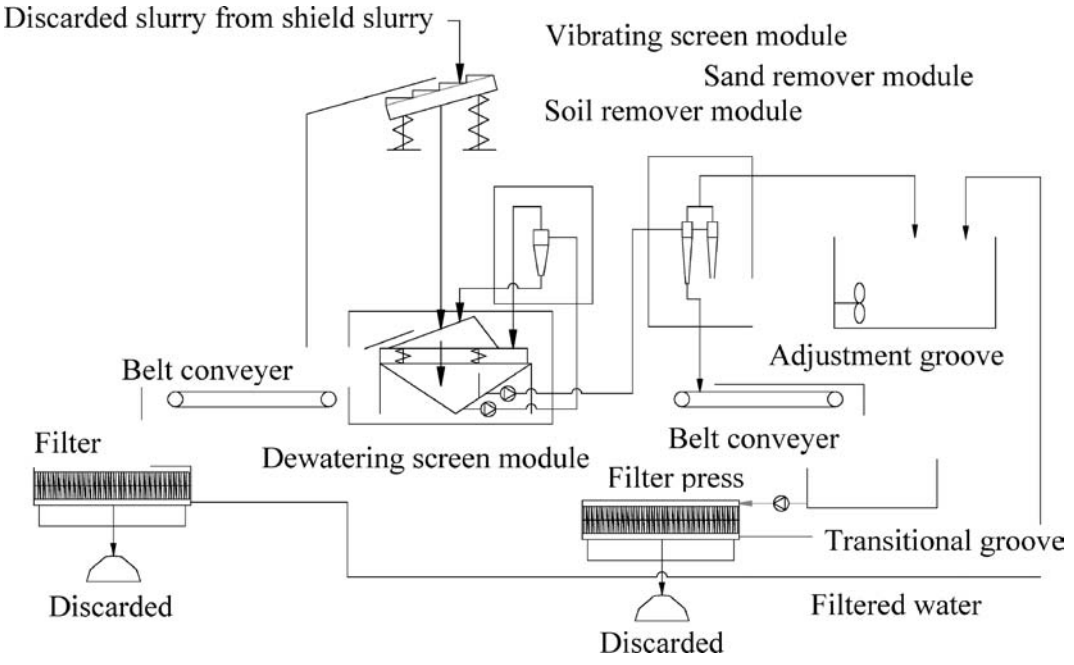

Figure 1. Germany "Shabao" integrated modules in slurry treatment.

The "SALALA" drainage engineering is located at center zone of urban in Singapore. The ground condition is medium or coarse sand and gravel stratum. The water content of the soils is about 37%. The slurry balanced pipe jacking with diameter of 3 meters can excavate 12 meters a day. The length of pipe segment was 1.2 meters. According to geological condition and construction capacity in Singapore, the Germany "SALALA" integrated modules equipment in slurry treatment and the system module had two-level separation treatment system was adopted. The total system treatment capacity was 100 m^3/h. The fist-level system was managed by vibrating screen which could separate medium or coarse sand and gravel larger than 4 mm. The second-level system was managed by sand remover module, which was composed by ten 15 cm-diameter cyclones and working pumps. It could separate slurry particles which were larger than 40–60 μm into adjustment groove. Then the separated slurry particles together with the added bentonite and additive were made into working slurry again and sent into the shield. The residue was delivered into the pool, and then removed away by digging machine, so the construction site was very clean. The whole set of module system just took the area for 4 m^2, which seemed to have great effect.

The Luomazhhou subway tunnel starts from Jiulong airport in Hong Kong to Victoria Bay. The geological condition is mainly limestone (the strength is 80 MPa), and part of stratum is soft soil. Slurry balanced and mixed Cutterhead shield was employed. The diameter of the shield was 8.8 m. Two-level vibrating screen module, sand remover module, dewatering screen module, soil remover and transitional groove module were chosen for the slurry treatment with a capacity of 600 m^3/h.

The first-level of the two-level vibrating screen was the bar-shaped pre-separating screen. It could separate gravel, block and coarse sand larger than 30 mm. The second-level was the plate-shaped vibrating screen. It could separate medium and coarse sand larger than 4 mm from the slurry.

Sand remover module could treat the particles which were larger than 74μm, eliminate the particles between 30 and 74 μm. Sand remover recycled the separation of the more coarse particles from the slurry which came from the bottom hole after dewatering. Finally, soil remover separated the particles which were larger than 0.04 mm from the remained slurry.

Particles between 20 and 40 μm could be dealt with by soil remover. The smaller particles would be delivered into adjustment adequate. The system was additionally equipped with one slurry separation device which had frame cushion filter press. The system main function was to press the sand and gravel of the discarded slurry into mud cake so that the transportation cost could be alleviated and the clean water extruded from the discarded could be recycled into

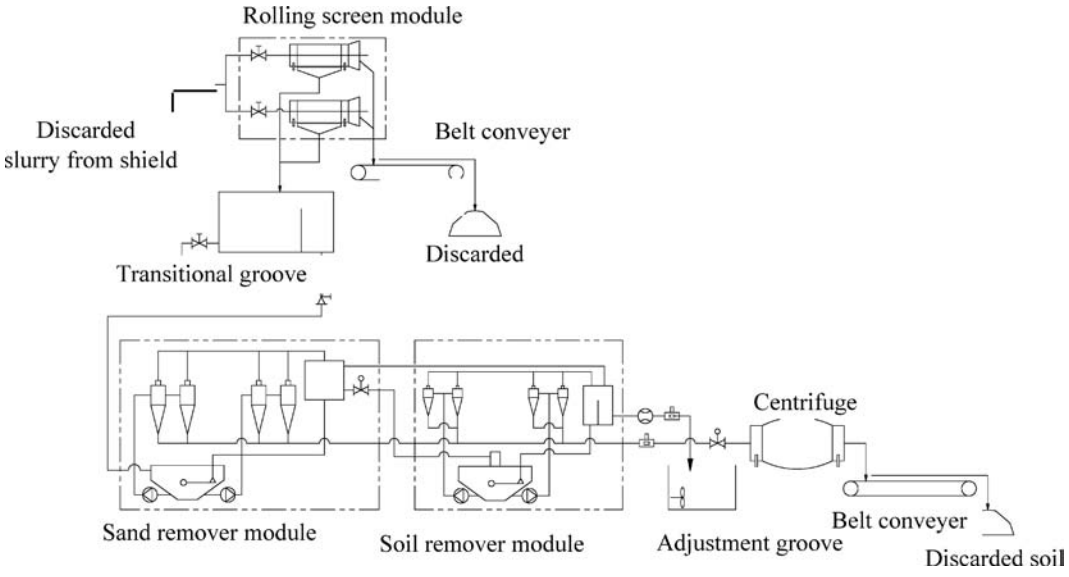

Figure 2. France MS integrated modules in slurry treatment.

groove. The whole set of module system just took the area for 6 m^2, which had great effect.

4.1.2 *France MS integrated modules in slurry treatment*

The slurry shield was employed in two tunnels construction in Kuala Lumpur. The excavation distances were 600 and 800 meters respectively. The first layer of the ground soil was white limestone (the strength is 110 MPa), the beneath layer was soft soil. France MS integrated modules was composed by the rolling screen substituted for vibrating screen module, sand remover module, soil remover module, transitional groove module and centrifuge instead of dewatering screen module. The system capacity was 1600 m^3/h.

The rolling screen could separate gravel, block and coarse sand which were larger than 7 mm from slurry. The other particles would get into the sand remover module. The sand remover module could filter the particles which were larger than 0.075 μm out from the bottom hole. The particles which were smaller than 0.075 μm would be flowed out from the upper hole. Then the soil remover would separate the rest particles which were larger than 0.02 mm, and the particles larger than 20 μm would be dewatered by the centrifuge. The working principle of the soil remover was similar to that of the sand remover. All the discarded slurry of coarse particles was sent to storage truck by belt machine. The system treatment process can be seen in Figure 2.

4.2 *Domestic application*

4.2.1 *Germany "Shabao" integrated modules in slurry treatment*

Shangzhong Road Tunnel in Shanghai has two lines of South line and North line. South line is 1,270 m long while North line is 1,274 m long. The slurry and air pressure balanced shield was employed with the external diameter of 14.87 m. The tunnel mainly crossed the soils of clay, silty clay and clay with sand. Germany "Shabao" integrated modules in slurry treatment were used. The slurry was treated and separated in sequence by the vibrating screen, sand remover, dewatering screen, soil remover and groove module.

The treatment capacity of the whole module system was 500 m^3/h. "Shabao" system could effectively decrease the slurry specific gravity and sand content. The quality of soil membrane could be improved, and then the slurry consumption could be greatly reduced. Good economic benefit could be yielded. The module system now is being applied in tunnel projects of Longhua and Xinjian Road in Shanghai.

4.2.2 *France MS integrated modules in slurry treatment*

Shanghai Yangtze River Tunnel in Shanghai also has two lines of East line and West line. East line is 7,471.65 m long while West line is 7,469.36 m long. The external diameter of the shield is 15 m and the internal is 13.7 m. The shield mainly crossed the soils of grey muddy clay, grey clay, grey muddy and silty clay layer, grey clayed silt with thin silty clay, grey

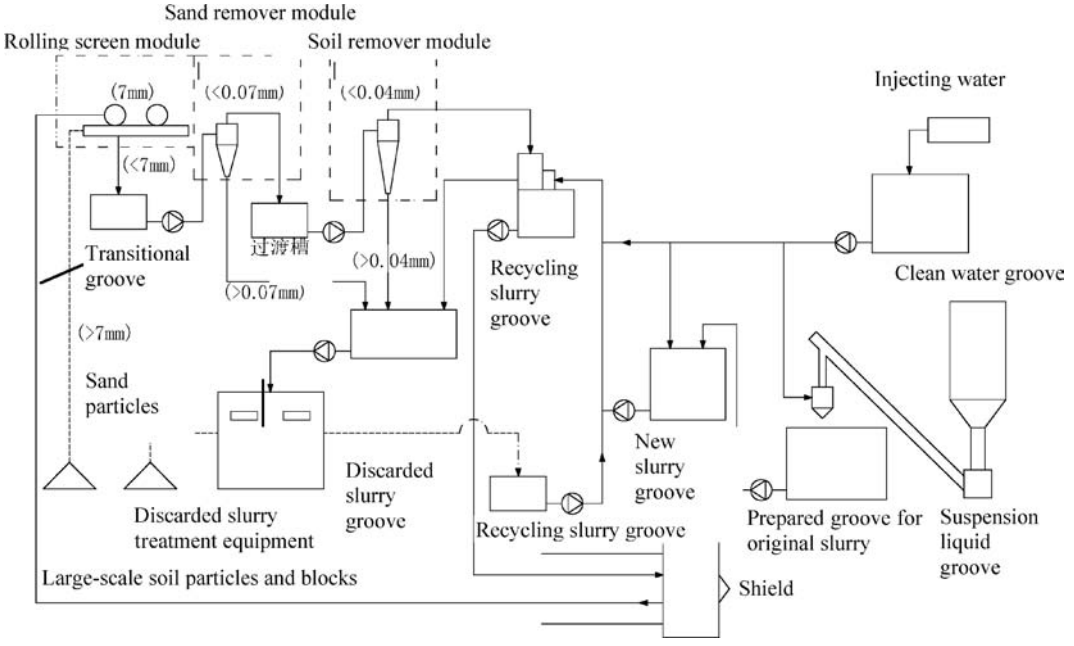

Figure 3. The integrated modules system in slurry treatment in Yangtse River Tunnel.

muddy and silty clay and grey sandy silt. France MS integrated module equipments was adopted, which were composed by the rolling screen, sand remover, soil remover (cleaner) and other slurry recycle utilization modules. The system was shown in Figure 3.

The rolling screen module could deal with the particles which were larger than 7 mm. The residue left on the screen could be sent out to soil collection pits and the residue under the screen was directly transported to the sand remover module for secondary separation through the distribution box (transitional groove). Then the particles smaller than 75 μm were delivered to the soil remover module for the third-level separation so that the particles which were larger than 40 μm would be removed to the discarded slurry groove. The particles which were smaller than 40 μm would be sent to the recycling slurry groove for recycle utilization.

4.2.2.1 The parameters of "MS" slurry treatment system

The parameters of "MS" slurry treatment system were designed according to the excavation rate of 27 m per day, the speed of 45 mm per minute and the amount of slurry output of 2,000–3,000 m^3/h from one shield.

The density of feeding slurry into the shield was between 1.05 and 1.35 g/cm^3, and the optimal value was maintained between 1.20 and 1.30 g/cm^3. Each shield owned two rolling screens between which the spacing was 7–8. The sand remover ensured the separation for the diameter between 70 and 80 μm, while the soil remover made sure that the particles size were between 40 and 50 μm was separated.

4.2.2.2 Application effect and test analysis of the slurry treatment system in typical soil layers

From January to March in 2007, the separation and treatment process of "MS" in the typical soil layers such as grey sandy silt and grey sandy silt layer was tested. The change of slurry density is shown in Figure 4 to Figure 9.

The curves of feeding and discharged slurry density and their difference in the upline of the Shanghai Yangtze River Tunnel were given in Figure 4 and Figure 5. The densities of the feeding and discharged slurry were similar (the difference was about 0.11 t/m^3) and the feeding density ranged from 1.25 t/m^3 to 1.30 t/m^3 which was designed under the index of 1.05–1.30 t/m^3. It was testified that the effect of "MS" slurry treatment equipments to separate coarse particles could almost satisfy the index between the tunnel rings from 358 to 626.

According to the Figure 6, there was no obvious difference between the density of slurry feed into rolling screen and coming out from the upper hole of sand remover, which was only amount to 0.01 t/m^3.

From the Figure 7 and Figure 8, it could be found there was also no significant difference between the density of slurry coming out from the upper hole of sand remover and soil remover, which was only amount to 0.03 t/m^3.

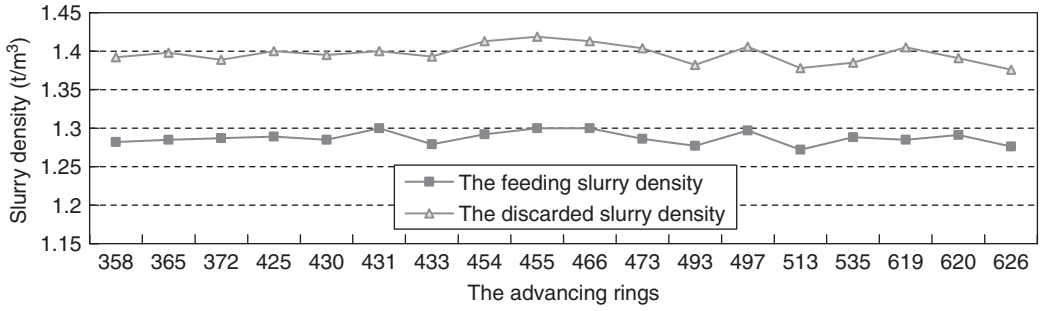

Figure 4. The development of the feeding and discharged slurry density of the shield employed in the upline of Shanghai Yangtze River Tunnel.

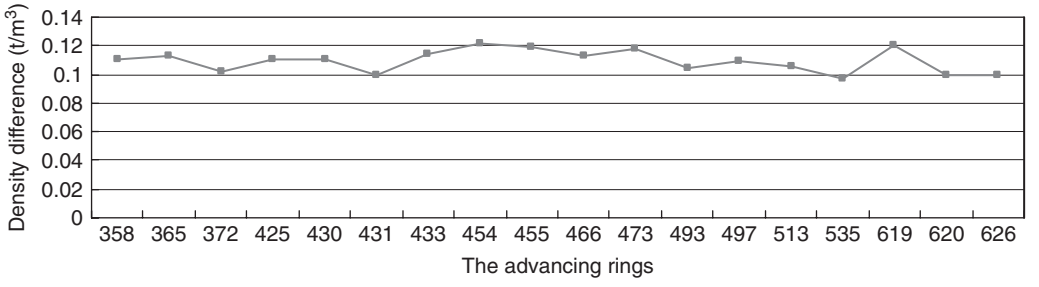

Figure 5. The trend of the feeding and discharged slurry density difference of the shield employed in the upline of Shanghai Yangtze River Tunnel.

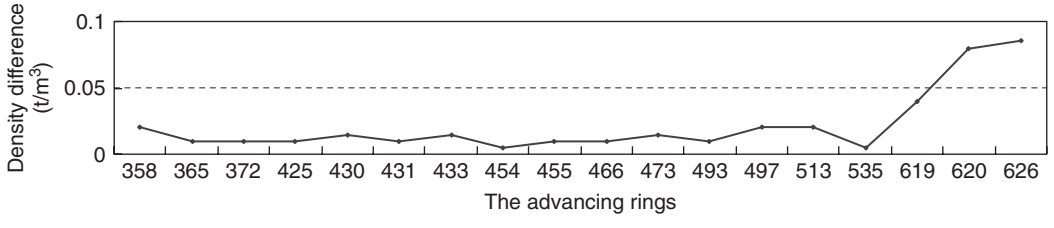

Figure 6. The trend of the density difference of slurry feeding into rolling screen and coming out from the upper hole of sand remover in the upline.

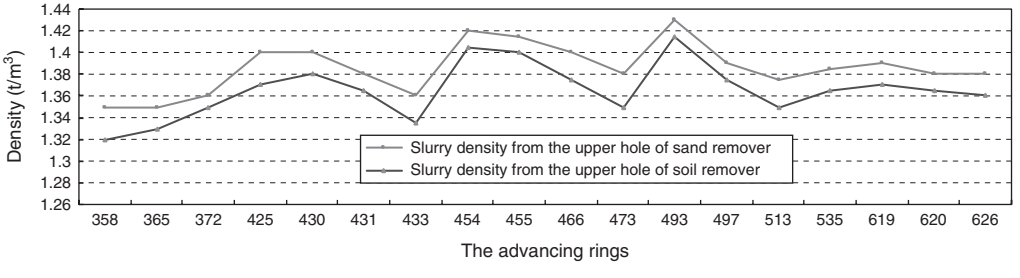

Figure 7. The trend of the density slurry coming out from the upper hole of sand remover and soil remover in the upline.

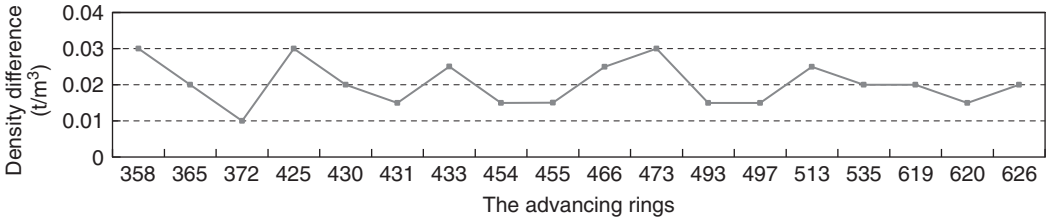

Figure 8. The trend of the density difference of slurry coming out from the upper hole of sand remover and soil remover in the upline.

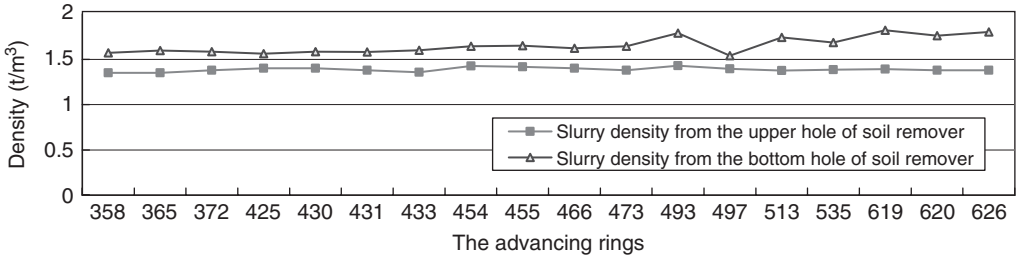

Figure 9. The trend of the slurry density coming out from the upper and bottom holes of sand remover in the upline.

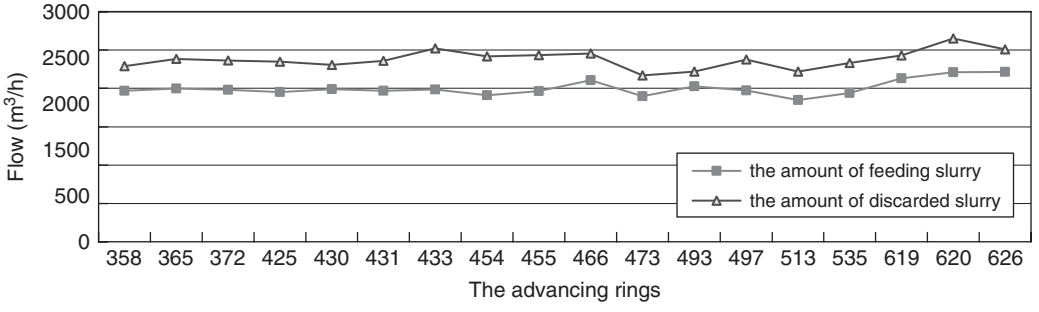

Figure 10. The trend of the amount of feeding and discarded slurry in the upline of the Yangze tunnel in Shanghai.

As was shown in Figure 9, the change of the slurry density coming out from upper and bottom hole of the sand remover was the same. When the density of slurry coming out from the upper hole of the sand remover was large, and so was that of the slurry from bottom hole of the sand remover. On the contrary, when the density of slurry coming out from the upper hole of the sand remover was small, and so was that of the slurry from bottom hole of the sand remover. Besides, the density difference between them was about 0.3 t/m^3.

Figure 10 described the trend of the amount of feeding and discarded slurry. As was depicted in Figure 10, the amount of feeding slurry was about 2000 m^3/h, and the discarded slurry was 2500 m^3/h. The difference between them reached 500 m^3/h around. The shield was driven at the speed of 45 mm/min. About 500 m^3/h of residual soil was discarded as much as slurry flow difference under the condition of normal shield advancing. Therefore, the slurry treatment system could basically guarantee the shield normal working.

Figures 11 and 12 described the density curve of feeding slurry in different soil layers. From the Figure 11, when the shield in the upline was driving through clayed silt layer, the average relative density of slurry which needed treatment was about 1.30 g/cm^3, and after treatment, the density turned to be 1.24 g/cm^3–1.33 g/cm^3.From Figure 12, it could be found when the shield in the upline was driving through sandy silt layer, the average relative density of slurry which required treatment was about 1.29 g/cm^3, and after treatment, the density turned to be 1.27 g/cm^3–1.31 g/cm^3. According to the relative

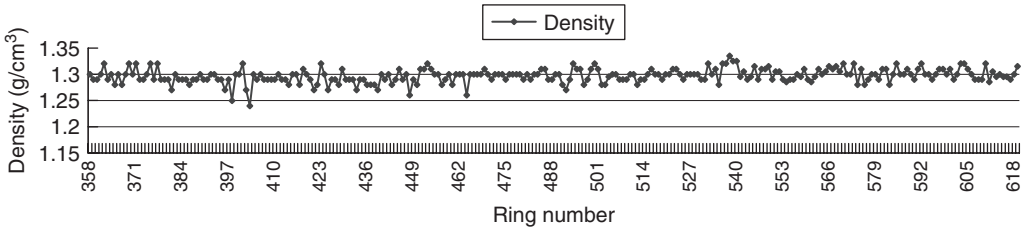

Figure 11. The density curve of feeding slurry in ⑤$_2$ clayed silt layer in the upline of Yangze Tunnel in Shanghai.

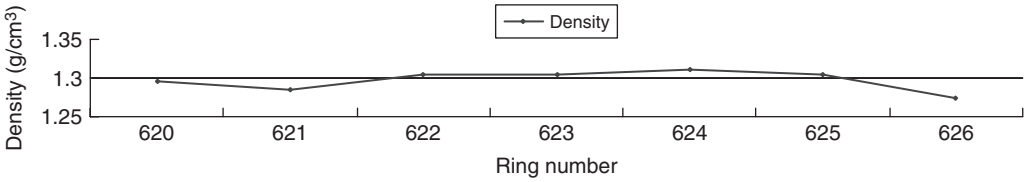

Figure 12. The density curve of feeding slurry in ⑦$_{1\text{-}1}$sandy silt layer in the upline shield of Yangze Tunnel in Shanghai.

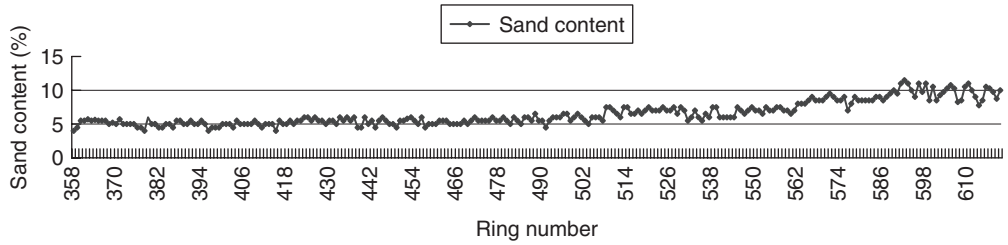

Figure 13. The sand content curve of feeding slurry in ⑤$_2$ clayed silt in the upline shield in Shanghai Yangze Tunnel.

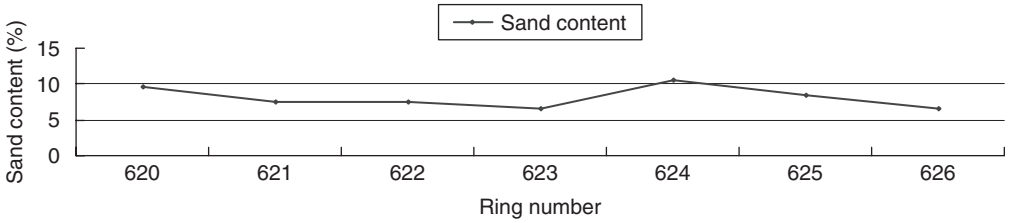

Figure 14. The sand content curve of feeding slurry in ⑦$_{1\text{-}1}$sandy silt in the upline shield in Shanghai Yangze Tunnel.

density index of treated slurry, it was shown that the MS system applied in sandy silt layer was more effective than that in clayed silt.

Figures 13 and 14 showed the sand content curve of feeding slurry in different soil layers. It was found that in Figure 13, after treatment during the upline shield driven in the clayed silt, the sand content index of feeding slurry was between 4% and 11%. From the Figure 14, after the MS treatment during the upline shield driven in sandy silt, the sand content index of feeding slurry was between 6.5% and 10%. So the MS system applied in removing sand in sandy silt functioned better than in clayed silt, and decreased the sand content in slurry more effectively.

Figure 15 and 16 showed the viscosity curve of feeding slurry in different soil layers. It could be reflected in Figure 15 that after the MS treatment during the upline shield driven in clayed silt, the viscosity index of feeding slurry was between 17 and 20 s. From the Figure 16, during the upline shield driven in sandy silt, after the MS treatment, the viscosity index of feeding slurry was between 17 and 18 s.

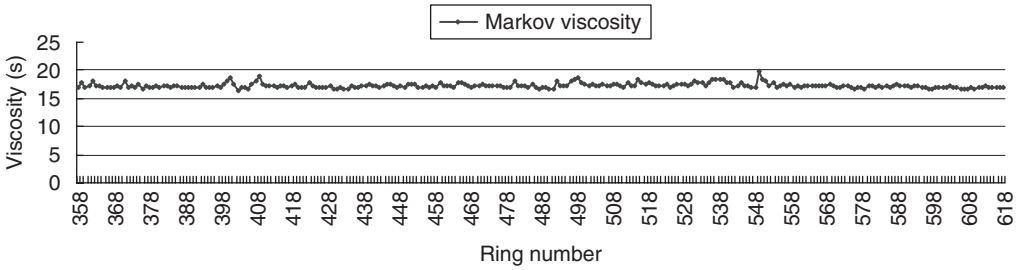

Figure 15. The viscosity curve of feeding slurry in the upline shield in ⑤$_2$ clayed silt in Shanghai Yangze Tunnel.

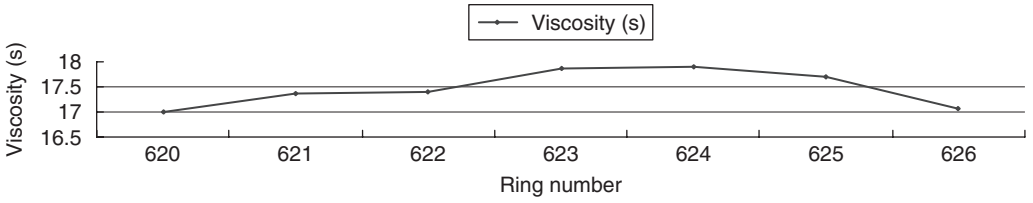

Figure 16. The viscosity curve of feeding slurry in the upline shield in ⑦$_{1\text{-}1}$ sandy silt in Shanghai Yangze Tunnel.

4.2.2.3 Application results

Nearly two months later, the maximum difference of cohesion index between two kinds of stratum treated by MS slurry treatment system was two seconds. After the treatment, the slurry density approximately satisfied the design standard of 1.05–1.35 t/cm^3. The treatment capacity of system could basically ensure normal driving of the shield.

5 CONCLUSIONS

By the absorption and digestion of the integrated modules in slurry treatment in Shanghai Yangtze River Tunnel, it is showed that the integrated and modular separation system in slurry treatment takes small area, controls the density of slurry well, and the slurry equipment is highly automatic and reliable, which ensures the equipment normal operation and management. When turning to another project, the first three modules can be centralized as one processing unit. The integrated modules system in slurry treatment behaves greatly flexible, and it not only adapts to slurry separation and treatment in soft clayed in Shanghai, but also is applied in soils which has large amount of sand and gravel. The cellular modules in the integrated modules system can be organically and freely allocated according to the diameter of shield, excavation speed, geological condition and treatment capacity.

REFERENCES

Chen, K. 2004. Mud treatment of construction technique with shield machine for across Yangtze River Tunnel of Chongqing city. *Underground Construction*: 34–37.

Chen, Y. & Pan, G. Q. 1990. *Shield Construction Technology. In Shanghai*, Shanghai Science and Technology Literature Press.

Gu, G. M. & Tang, J. F. 2007. Application of slurry disposal system of tunnel shield machine for building subaqueous tunnel across Huangpu River. *Construction Mechanization*: 46–50.

Liu, Y. D. & Wang, H. X. 2007. Slurry treatment and separation for a slurry shield. *Modem Tunneling Technology* 44(2): 56–60.

The Shanghai Yangtze River Tunnel - Theory, Design and Construction – Huang (ed)
© 2008 Taylor & Francis Group, London, ISBN 978-0-415-47161-9

Attitude surveying of the tunnel shield

Y.M. Yu
Shanghai Tunnel Engineering Co., Ltd., Shanghai, P. R. China

J.X. Wang
Dept. of Surveying and Geo-Informatics, Tongji University, Shanghai, P. R. China

ABSTRACT: The paper presents an attitude determination method for the tunnel shield in the tunnel construction. Before the construction, the relation between the characteristic points of the tunnel shield and the reflectors is determined by the initial surveying. The corresponding parameters are taken as the initial conditions. During the construction, the transformation between the real-time locations and the initial conditions of the reflectors is determined by measuring the coordinates of the reflectors in the project coordinate system. Therefore, the real-time positions of the characteristic points of the tunnel shield can be derived. Compared to the designed axis, the deviation of the tunnel shield is calculated, which will be employed to control the direction of the tunnel driving. The numerical results show that the presented method is feasible and efficient in the real tunnel construction application.

1 INTRODUCTION

Tunnel shield is one of the major techniques employed in tunnel constructions. One of the most critical issues is to determine the real-time attitude of the shield by surveying in order to control the driving along the designed axis. In the method presented in this paper, three or more reflectors are installed at the rear of the tunnel shield before the construction. In a temporary but arbitrary coordinate system, the corresponding coordinates of the reflectors and the characteristic points on the tunnel shield are determined by the initial surveying. Since the reflectors are fixed on the shield, their internal relation does not change during the driving procedure. Therefore, by measuring the real-time coordinates of the reflectors, the coordinates of the characteristic points of the tunnel shield can be easily calculated in real time through the coordinate transformations. Compared to the designed values of these characteristic points, the deviation can be computed and used to control the construction procedure.

2 INITIAL SURVEYING

Before driving the tunnel, the initial surveying has to be carried out. The procedure can be done as follows. Several reflectors, which can be measured by total station, are installed at the rear of the tunnel shield. Since the dimensional attitude can be determined by at least three points, at least three reflectors are required. Theoretically, these points can be distributed arbitrarily. However, the distances among the reflectors should be as far as possible and in a good geometry for a better accuracy. The attitude of the tunnel shield is determined by three characteristic points. Considering the computational effort, three points are generally chosen as the center of the front (FO), the center of the rear (O), and the point of the right rear margin (R). The relation among these reflectors (points 1, 2, and 3) and three characteristic points (FO, O, and R) are demonstrated in Figure 1. Note that

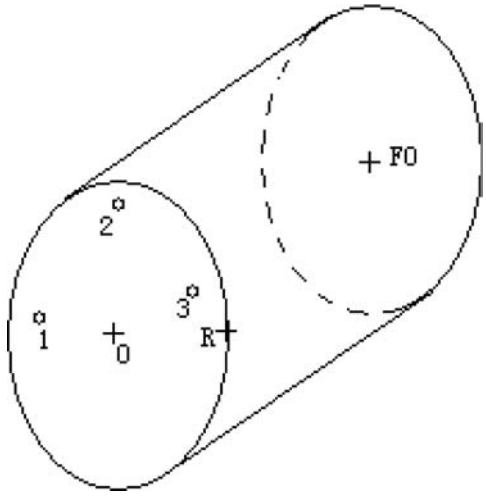

Figure 1. Reflectors and characteristic points on the tunnel shield.

before the rotation of the shield, point R and point O are the same height.

A small control network is designed around the tunnel shield. Therefore, the coordinates of the reflectors can be determined by total station in the same coordinate system. If the characteristic points cannot be measured directly, they can be derived indirectly by fitting the circular center through other points on the circular plane. The coordinates of the reflectors and the characteristic points are saved as the initial conditions in the coordinate system.

3 REAL-TIME ATTITUDE SURVEYING OF THE TUNNEL SHIELD

During the tunnel construction, the coordinates of the reflectors in the project coordinate system can be measured by total station. Therefore, the reflectors are expressed in both the initial system $(xx_i \ yy_i \ hh_i)^T$ and the project system $(x_i \ y_i \ h_i)^T$, and the relation is formulated as follows:

$$\begin{pmatrix} xx \\ yy \\ hh \end{pmatrix} = \begin{pmatrix} x_0 \\ y_0 \\ h_0 \end{pmatrix} + R_1(\alpha)R_2(\beta)R_3(\gamma)\begin{pmatrix} x \\ y \\ h \end{pmatrix} \tag{1}$$

where $(x_0 \ y_0 \ h_0)^T$ is the shift parameter vector; α, β, γ are the rotation angles, and the corresponding rotation matrices are:

$$R_1(\alpha) = \begin{pmatrix} 1 & 0 & 0 \\ 0 & \cos(\alpha) & -\sin(\alpha) \\ 0 & \sin(\alpha) & \cos(\alpha) \end{pmatrix}$$

$$R_2(\beta) = \begin{pmatrix} \cos(\beta) & 0 & -\sin(\beta) \\ 0 & 1 & 0 \\ \sin(\beta) & 0 & \cos(\beta) \end{pmatrix}$$

$$R_3(\gamma) = \begin{pmatrix} \cos(\gamma) & -\sin(\gamma) & 0 \\ \sin(\gamma) & \cos(\gamma) & 0 \\ 0 & 0 & 1 \end{pmatrix}$$

For these reflectors, the error equation of the measurements is formulated as follows:

$$\begin{pmatrix} v_{xi} \\ v_{yi} \\ v_{hi} \end{pmatrix} = \begin{pmatrix} x_0 \\ y_0 \\ h_0 \end{pmatrix} + R_1(\alpha)R_2(\beta)R_3(\gamma)\begin{pmatrix} x_i \\ y_i \\ h_i \end{pmatrix} - \begin{pmatrix} xx_i \\ yy_i \\ hh_i \end{pmatrix} \tag{2}$$

with $(v_x \ v_y \ v_h)^T$ the transformation residues.

The approximate values of the unknown parameters are $x_0^0, y_0^0, h_0^0, \alpha^0, \beta^0$, and γ^0. Taking the partial derivatives of the unknown parameters, the above equation can be linearized as follows:

$$\begin{pmatrix} v_{xi} \\ v_{yi} \\ v_{hi} \end{pmatrix} = \frac{\partial v_i}{\partial (x_0 \quad y_0 \quad h_0)^T}\begin{pmatrix} \delta x_0 \\ \delta y_0 \\ \delta h_0 \end{pmatrix} + \begin{pmatrix} \frac{\partial v_i}{\partial \alpha} & \frac{\partial v_i}{\partial \beta} & \frac{\partial v_i}{\partial \gamma} \end{pmatrix}\begin{pmatrix} \delta\alpha \\ \delta\beta \\ \delta\gamma \end{pmatrix} - l_i \tag{3}$$

where the partial derivatives and the measurement corrections are:

$$\frac{\partial v_i}{\partial (x_0 \quad y_0 \quad h_0)^T} = I$$

$$\frac{\partial v_i}{\partial \alpha} = \frac{\partial R_1(\alpha)}{\partial \alpha}R_2(\beta)R_3(\gamma)\begin{pmatrix} x_i \\ y_i \\ h_i \end{pmatrix}$$

$$\frac{\partial R_1(\alpha)}{\partial \alpha} = \begin{pmatrix} 0 & 0 & 0 \\ 0 & -\sin(\alpha^0) & -\cos(\alpha^0) \\ 0 & \cos(\alpha^0) & -\sin(\alpha^0) \end{pmatrix}$$

$$\frac{\partial v_i}{\partial \beta} = R_1(\alpha)\frac{\partial R_2(\beta)}{\partial \beta}R_3(\gamma)\begin{pmatrix} x_i \\ y_i \\ h_i \end{pmatrix}$$

$$\frac{\partial R_2(\beta)}{\partial \beta} = \begin{pmatrix} -\sin(\beta^0) & 0 & -\cos(\beta^0) \\ 0 & 0 & 0 \\ \cos(\beta^0) & 0 & -\sin(\beta^0) \end{pmatrix}$$

$$\frac{\partial v_i}{\partial \gamma} = R_1(\alpha)R_2(\beta)\frac{\partial R_3(\gamma)}{\partial \gamma}\begin{pmatrix} x_i \\ y_i \\ h_i \end{pmatrix}$$

$$\frac{\partial R_3(\gamma)}{\partial \gamma} = \begin{pmatrix} -\sin(\gamma^0) & -\cos(\gamma^0) & 0 \\ \cos(\gamma^0) & -\sin(\gamma^0) & 0 \\ 0 & 0 & 0 \end{pmatrix}$$

$$l_i = -\begin{pmatrix} x_0^0 \\ y_0^0 \\ h_0^0 \end{pmatrix} - R_1(\alpha^0)R_2(\beta^0)R_3(\gamma^0)\begin{pmatrix} x_i \\ y_i \\ h_i \end{pmatrix} + \begin{pmatrix} xx_i \\ yy_i \\ hh_i \end{pmatrix}$$

With these partial derivatives and the measurement corrections of the reflectors, a normal matrix can be formulated and solved to get the unknown parameters. The calculating procedure is done by iteration till convergence.

With the solved shift and rotation parameters, the coordinates of the characteristic points in the project coordinate system $(x_i \ y_i \ h_i)^T$ can be determined from the initial coordinates $(xx_i \, yy_i \, hh_i)^T$, using the inversion of equation (1):

$$\begin{pmatrix} x \\ y \\ h \end{pmatrix} = R_3^T(\gamma) R_2^T(\beta) R_1^T(\alpha) \begin{pmatrix} xx - x_0 \\ yy - y_0 \\ hh - h_0 \end{pmatrix} \quad (4)$$

The calculated coordinates of points O and FO in the project system can be projected onto the designed axis. Compared to the designed coordinates, the deviation with respect to the design axis is calculated. In addition, the rotation angle of the current status of the tunnel shield is derived by the coordinates of points O and R.

4 NUMERICAL EXAMPLE

Table 1 shows the coordinates of the reflectors and characteristic points in the initial coordinate system. The real-time surveying coordinates of the reflectors at one epoch are listed in Table 2.

Based on the method described above, the shift and rotation parameters are solved as follows:

$$\begin{pmatrix} x_0 \\ y_0 \\ h_0 \end{pmatrix} = \begin{pmatrix} -453.726039740553 \\ 15{,}158.9584651243 \\ -16{,}199.6079580212 \end{pmatrix}$$

$$\begin{pmatrix} \alpha \\ \beta \\ \gamma \end{pmatrix} = \begin{pmatrix} 0^0 00'01''545884 \\ 358^0 20'22''86915 \\ 293^0 23'33''019594 \end{pmatrix}$$

Using equation (4), the coordinates of the characteristic points are determined in Table 3.

The coordinates of points O and FO in Table 3 can be projected onto the designed axis. Compared to the designed coordinates, the deviation of the tunnel with respect to the designed axis is therefore determined, which will control the digging procedure.

5 CONCLUSIONS

Attitude surveying of the tunnel driving is one of the most important techniques employed in tunnel constructions. The method presented in the current paper makes use of the initial surveying to determine the relation between the fixed reflectors and the characteristic points of the tunnel shield before the tunnel construction. Since this relation is rigid, it can be treated as the initial condition. In addition, it does not change when the shield attitude changes. During the construction, the coordinates of the reflectors in the project coordinate system are measured by total station. The corresponding coordinates of the characteristic points of the tunnel shield can be derived by the shift and rotation transformation parameters and the initial conditions. By projecting the coordinates onto the designed axis, the deviation values of the current tunnel shield are determined, which will control the procedure of driving tunnels. Theoretically, the mathematical model involved in the computation is rigorous. The practical example shows the strong feasibility in the real tunnel construction application.

Table 1. Coordinates in initial coordinates system.

Point	xx	yy	hh
O	0.0000	0.0000	0.0000
FO	100.0000	0.0000	0.0000
R	0.0000	25.0000	0.0000
1	0.0000	−20.0000	1.0000
2	0.0000	0.0000	20.0000
3	0.0000	20.0000	1.0000

Table 2. Surveying coordinates in the project coordinate system.

Reflectors	x	y	h
1	20,365.572	8,847.492	−14.717
2	20,347.434	8,855.938	4.275
3	20,328.860	8,863.372	−14.717

Table 3. Coordinates of the characteristic points of the shield in the project coordinate system.

Point	x	y	h
O	2,0347.2044	8,855.4060	−15.7166
FO	2,0386.9063	8,947.1848	−18.6151
R	2,0324.2592	8,865.3316	−15.7168

REFERENCES

Guo, L.G. & Fan, G.Y. 1984. *Least Square Method and Survey Adjustment. Shanghai*: Tongji University Press.

Surveying Research Group of Wuhan Surveying Technical University & Geodesy Research Group of Tongji University. 1983. *Control Survey*. Surveying Press.

Wang, J.X., Xu, C. & Lu, C.P. 2002. Real-time surveying of immersed tube. *Acta Geodaetica Etet Cartographica Sinica* 31.

The Shanghai Yangtze River Tunnel - Theory, Design and Construction – Huang (ed)
© 2008 Taylor & Francis Group, London, ISBN 978-0-415-47161-9

Construction logistics in large diameter and long distance shield tunneling

J.G. Yang
Shanghai Tunnel Engineering Co., Ltd., Shanghai, P. R. China

ABSTRACT: In the period of shield tunnelling, transportation is a fairly critical junction which affects directly the work schedule. On the site of Shanghai Yangtze river tunnel project, its transportation mode has been replaced with one ever used before, i.e. let a tandem cockpit truck run the horizontal transportation, together with an optimization of transportation route. The new transportation mode enhances greatly the advance rate.

1 INTRODUCTION

Shanghai Yangtze river tunnel Project is the one that links Shanghai to Changxing island. In other words, a mega infrastructure project configured with bi-directional with 6 lanes for coastal traffic at the estuary of Yangtze River.

As a circular tunnel with inner diameter 13.7 m and outer diameter 15 m, and about 7.5 km long for a single excavation. There are 8 cross passages between two tunnels and 4 mid-river pump-stations along the alignment. Two mega dimension slurry shields, each is 15.43 m in diameter, have been launched from the shafts in WuHaoGou, from Pudong to Changxing island. Tunnel's total length is 7,471.65 m and 7,469.36 m. 6,872.37 m and 6,854.91 m are under the river for the east and west parts, respectively. The tunnel max gradient is 2.9%, and the min radius of curvature is 4,000 m. RC segment with 2 m width and 65 cm thickness are used as a full ring lining of staggered joints. A conventional tapered segmental ring which composed of 10 segments, in detail, 7 typical segments and 2 adjacent segments and one key block respectively. As shown in Figure 1.

Road decking is done either in pre-fabricated and in-situ manners for carriageway within tunnel, Figure 2 shows the details.

The shield machine is made by Herrenknecht in Germany. Its diameter is 15.43 m and the total length is 134 m. In detail, Gantry No. 1 is 30 m long in 4 levels, enclosing major equipment for the shield; gantry No. 3 is 33 m long for a simultaneous extension of pipe intended for shield thrust and gantry No. 2 is about 65 m long between gantries No. 1 and No. 3, which includes the lifting and hauling devices of segment and other pre-fabricated elements.

2 CONSTRUCTION LOGISTICS

Construction logistic is conducted from surface to shield rear in a horizontal transportation manner. Various materials for shield tunnelling are segments (10 segments for each ring and 16.3 t for the heaviest one), grouting materials (2 tanks per ring and 12 m^3/tank), pipes for pumping, bolts, tail grease, hydraulic oil, and pipe rack or miscellaneous.

Material for road building is mainly composed of hollow square component and RC, of which segment, slurry tank, hollow square component and pipes should be transported by tandem cockpit truck and other miscellaneous materials are by forklift. Road pavement material is transported directly by lorry and ready-mix truck to the excavation face.

3 TRANSPORTATION SYSTEM WITHIN SHIELD MACHINE

Segment conveyor could be loaded at one time and placed under gantry No. 1, as shown in Figure 4. Gantry No. 2 is a framework structure (Fig. 5) with two levels. The upper level is a 50 t crane supplying segment and slurry tank, the lower level is a 20 t crane at its fore end. In order to turn over segment and invert block, a 30 t crane at its rear end is used to lift the hollow square component.

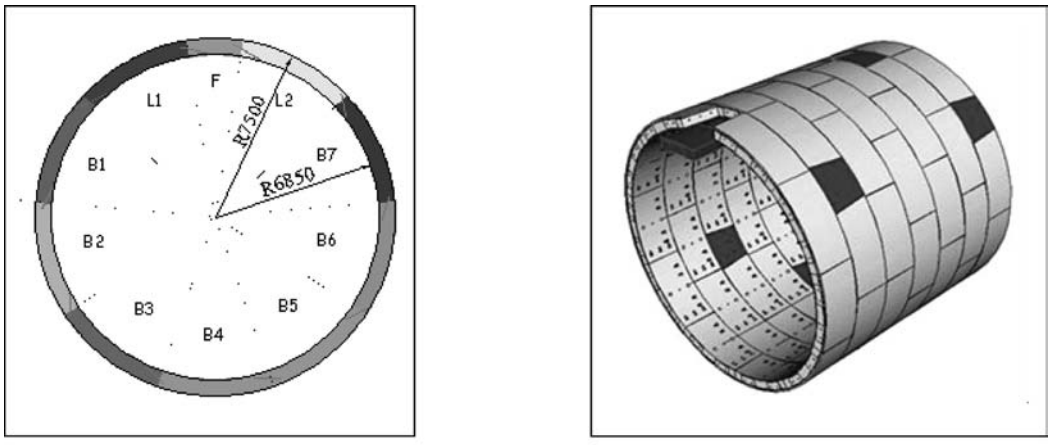

Figure 1. Segment cross-section.

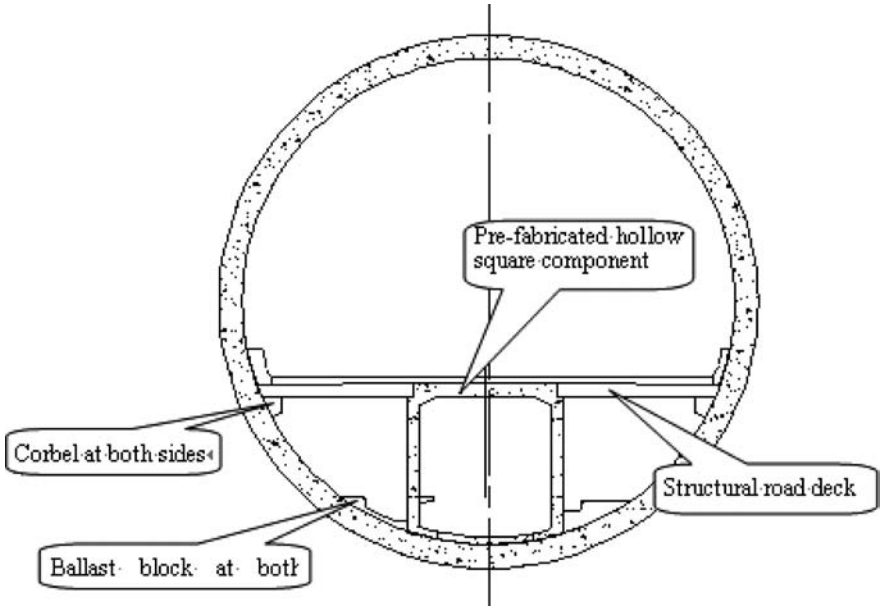

Figure 2. Carriageway structure within tunnel.

Simultaneous construction was even considered during TBM design stage, as for guide tracks to be laid at both sides of hollow square component, a part of engineering materials for convenient layby, and transportation during shield tunnelling.

4 TRANSPORTATION IN TUNNEL

Ten segments, two slurry tanks and one hollow square component are needed for each ring erection. In addition, one set of pipe is needed for every 5 ring erection and 21 sorties are required for a tandem cockpit truck fully loaded.

4.1 *Selection of transportation*

4.1.1 *Technical requirement for a tandem cockpit truck*

It is quite reasonable to select a tandem cockpit truck as transportation means after comparison in terms of

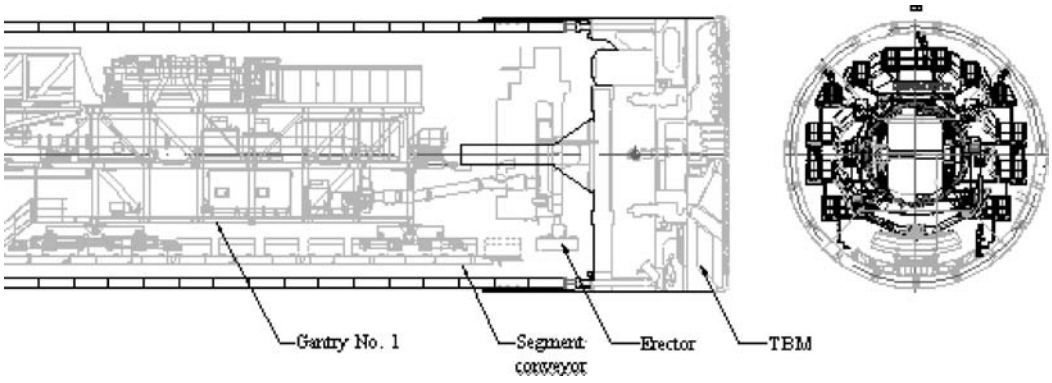

Figure 3. Segment conveyor within TBM.

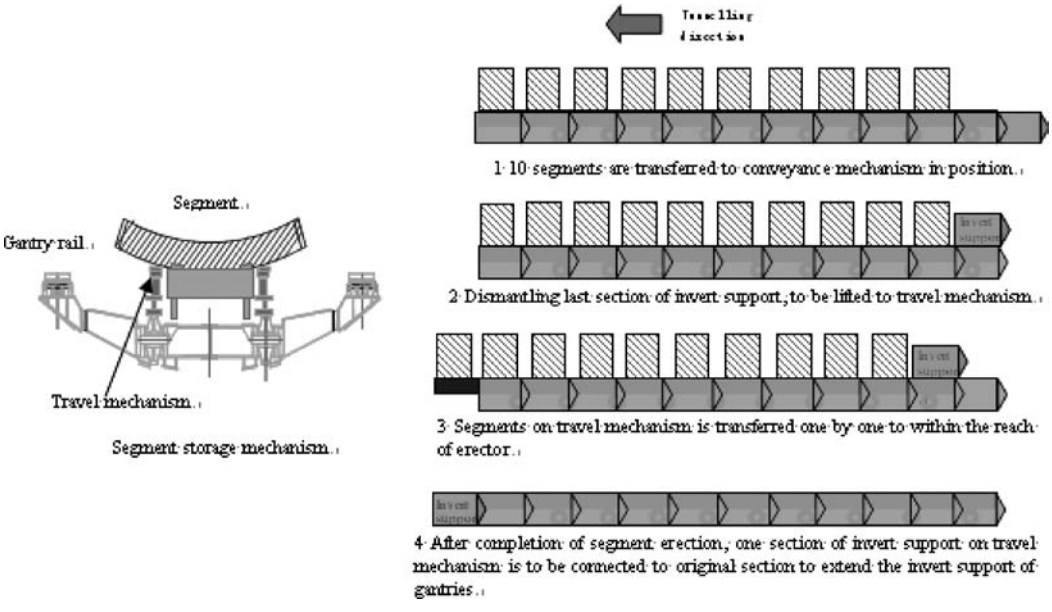

Figure 4. Flow chart of segment conveyor.

single haulage distance and shipment material, such as pump, pipes, and hollow square.

Design criteria for truck dimension:

- Length: to be able to contain both segment and tank at the same time on the trailer, the final truck length is 12.60 m.
- Height: Trailer top deck should be less than 1,600 mm to pavement, as 30 t crane is raised to its max height with its lower structure 1,600 mm to the pavement. Otherwise, hollow square could not be lifted. Body height during driving is 1,400 mm and adjustable during idling in a range of 1,250 mm–1,600 mm.
- Width: hollow square is 4,300 mm in width and the truck should be less than 4,300 mm and lift invert by dedicated lifting device on 30 t crane. In addition, the width of truck should be 2.5 m to meet the requirement of segment or tank.
- Loading capacity: no more than 2 segments (about 32 t), 1 fully filled slurry tank (34 t for the fully filled 12 m^3 tank) could be loaded onboard the vehicle (Fig. 6).

4.1.2 *Support vehicle*

Top deck of the vehicle is covered by a layer of steel plate which is unbearable to be loaded, except the two

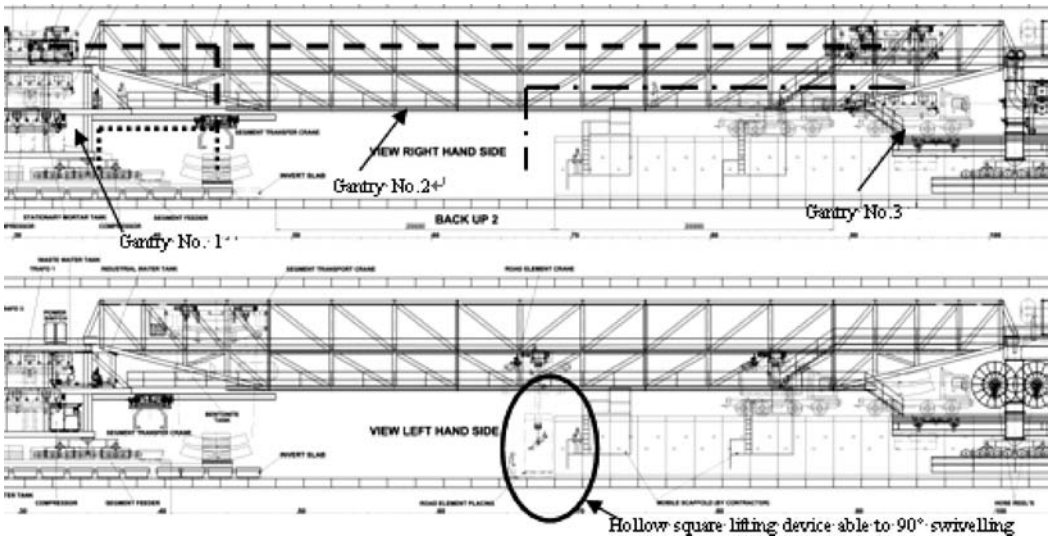

Figure 5. Schematic view of Gantry No. 2.
*Dotted line as route traveled by 50 t crane for segment and slurry tank transportation.
Square line as route traveled by 20 t crane on gantry No. 1, feeding conveyors with segments.
Dot hyphen line as route traveled by 30 t crane to haul hollow square component.

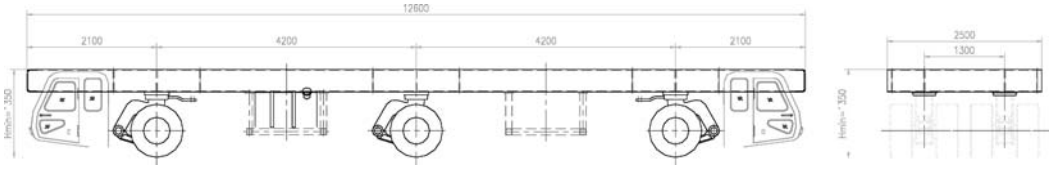

Figure 6. Tandem cockpit truck.

#18H steels. Therefore, it is necessary to design corresponding supports for a load of segment and slurry tank.

4.1.2.1 Combination onboard vehicle

As aforementioned logistics: onboard the vehicle, the 6 shipment combinations include: ① tank + tank ② segment + segment ③ hollow square + hollow square ④ tank + segment ⑤ tank + hollow square ⑥ segment + hollow square. As shown in Figure 7.

Now for a new logistics scheme, there are only three combinations: ① tank + segment ② segment + segment and ③ segment + hollow square. In Figure 7, the first truck load with 1 tank and 2 segments in place, shield tunnelling could then start off. Because a multiple trucks are set to run transportation and travel time is almost the same for each truckload. The new logistics does not affect work schedule and it is safer for hauling.

4.1.2.2 Design of support

As affected by travel clearance within the gantry and lift-off height, the height of support (Fig. 8) is also constrained.

As supports themselves have to bear 2 segments (about 33.5 t), their safety coefficient is to be enhanced by setting at both side's additional channel steels to resist the integral bending moment.

Segment lifting device on surface is different from that in tunnel in terms of its lifting manner, it is therefore necessary to select a reasonable spacing to avoid the support from being interfered by lifting device.

The larger the spacing between supports, the more its height will be. After comparative study, the eventual spacing between supports would be within 1,600 mm to 1,800 mm. The sleeper log should be inserted to a certain height to clear off the range from both lifting devices on surface and within shaft. Furthermore, rubber pads are provided for rest-on of a hollow square, at the outer side of two supports located at the fore end of tandem cockpit truck.

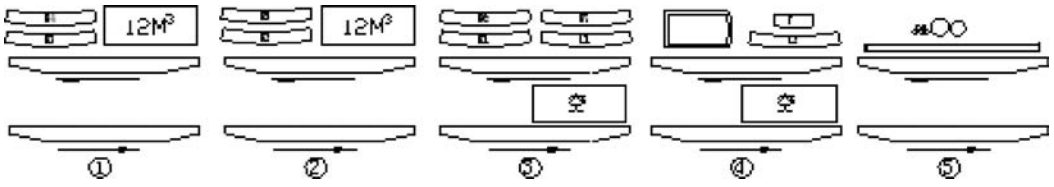

Figure 7. Hauling sequence diagram.

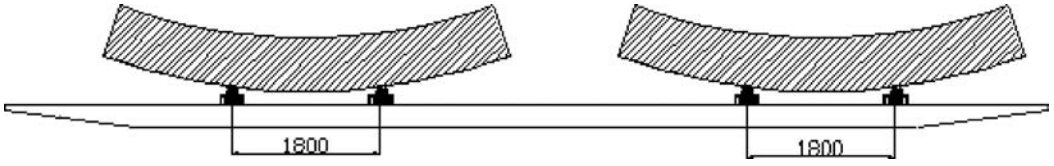

Figure 8. Support design scheme.

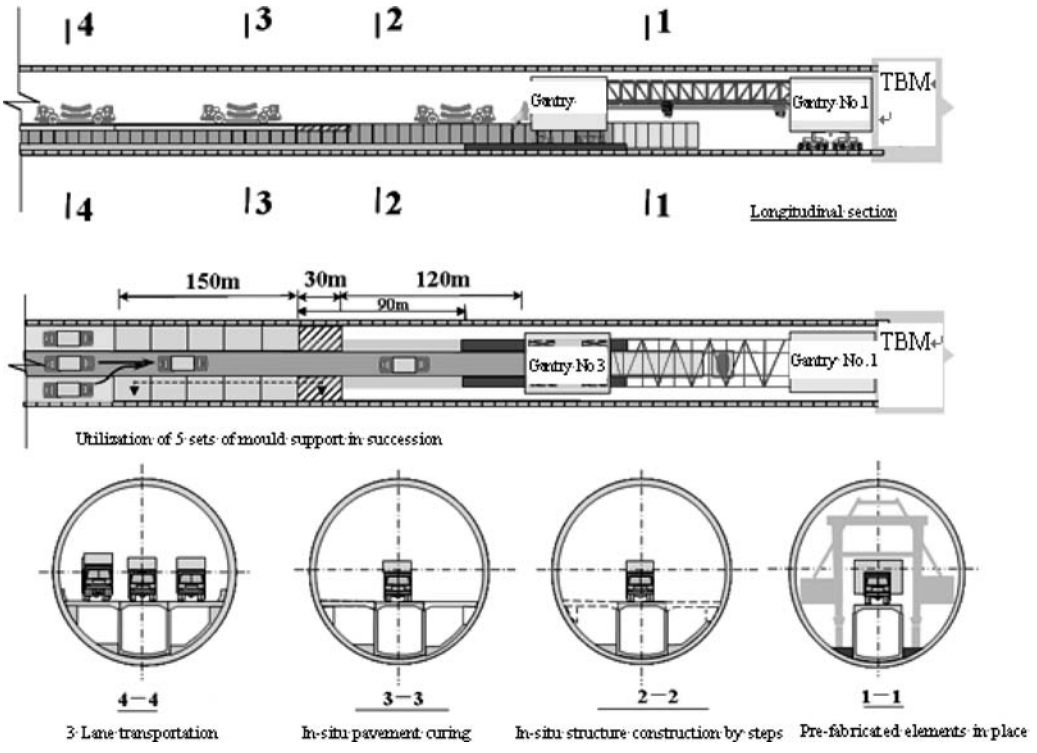

Figure 9. Schematic transportation route.

4.2 *Requirement criteria for hauling vehicles within tunnel*

4.2.1 *Route*

From the starting point of transportation, there is a bend followed by a straight section including open cut part, cut & cover part and a 300 m single lane behind gantry No. 3 (Fig. 9).

- On surface, operation time for a lift of 2 segments is 3 minute, one truck-load of 4 segments lasts for 6 min, respectively. While a lift

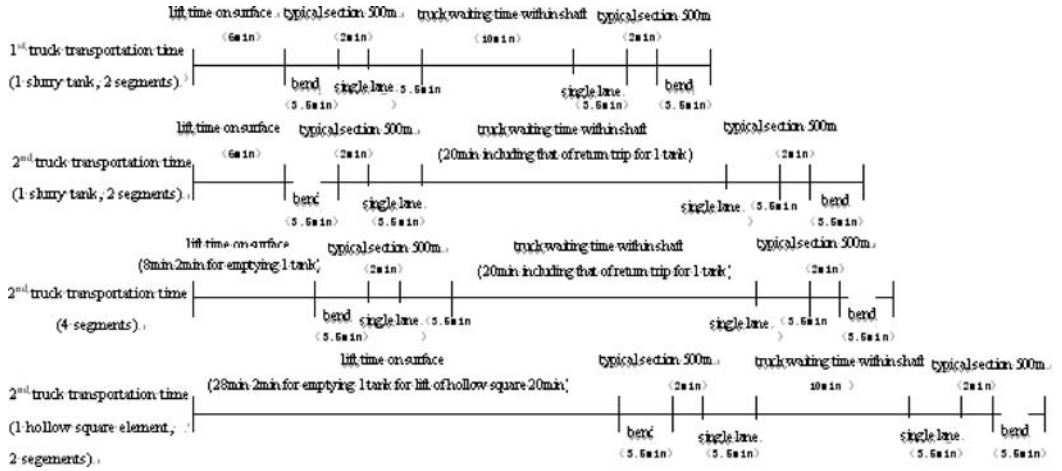

Figure 10. Comparision diagram of logistic scenarios.

of slurry tank requires the same time as that of segment.

- Drive time from start-off to the bend is 3.5 min.
- Drive time for single trip along 300 m single lane is 3.5 min.
- Driving speed along conventional section is 15 km/h.
- Dperation time for a lift of a hollow square is 20 min.
- Dperation time for a lift of pump pipe is 3 min.
- Waiting time within shaft is averaged at 10–20 min (4 truckloads are needed for erection of one ring, of which 2 truckloads of emptied tank in return trip are necessary during which period of time and there are 20 min of idling).

4.2.2 *Logistic scenario of one single vehicle*

When shield tunnelling reaches 300 m location, a comparison is made between logistic scenarios of 1 vehicle and 2 vehicles (Fig. 10).

From Figure 10, it can be seen that under operation of 1 fully loaded truck, erection of one ring could be achieved within 180 min with relevant engineering material transportation, i.e. theoretically, 8 rings/day erection could be met.

4.2.3 *Logistic scenario of 2 vehicles*

From Figure 11, it can be easily seen that in terms of one ring erection, total time T for material supply is divided into three portions:

Portion 1 is the time needed for truck No. 1 from start-off point to pass-off point (t1).

Portion 2 is the time needed for truck No. 2 from pass-off point returning to the surface (t2).

Portion 3 is the sortie time needed for truck No. 4 (t3).

$$T = t1 + t2 + t3 \quad (1)$$

Truck No. 1, right after finishing 3 sorties, is to prepare for the start of next ring erection. Therefore, in a sense of continuous job, the transportation time for Ring 1 is from the beginning of truck No. 1 to the end of truck No. 3, and T1 = 88 min.

Therefore, in normal construction process, time needed for each ring erection should be theoretically between T and T1, or nearer to T1.

4.2.4 *Logistic scenario of total transportation process within tunnel*

With respect to the integral length of tunnel, it is 7.5 km long. In all 4 trucks employed, take 5 rings as a cycle and based on the calculation results, 626 minutes are able to meet the work schedule requirement.

5 SLURRY CONVEYANCE SYSTEM

5.1 *System set-up*

Slurry conveyance in the project is composed of Pump on the surface, P2.1 within TBM and P2.X is slurry discharge pump. Its conveyance and discharge lay-out are shown in Figure 12.

Conveyance pipework is composed of 10 m single length of ϕ600 (590 mm bore) and ϕ500 (488 mm bore) slurry discharge pipes.

5.2 *Arrangement of relay pumps*

As slurry pipework is composed of several sections of pipe conduit, such as bend, control valve, various connective fittings connected in series, which can cause pressure dropped within pipework. Therefore, its total pressure loss is equal to the loss along the chainage of pipework.

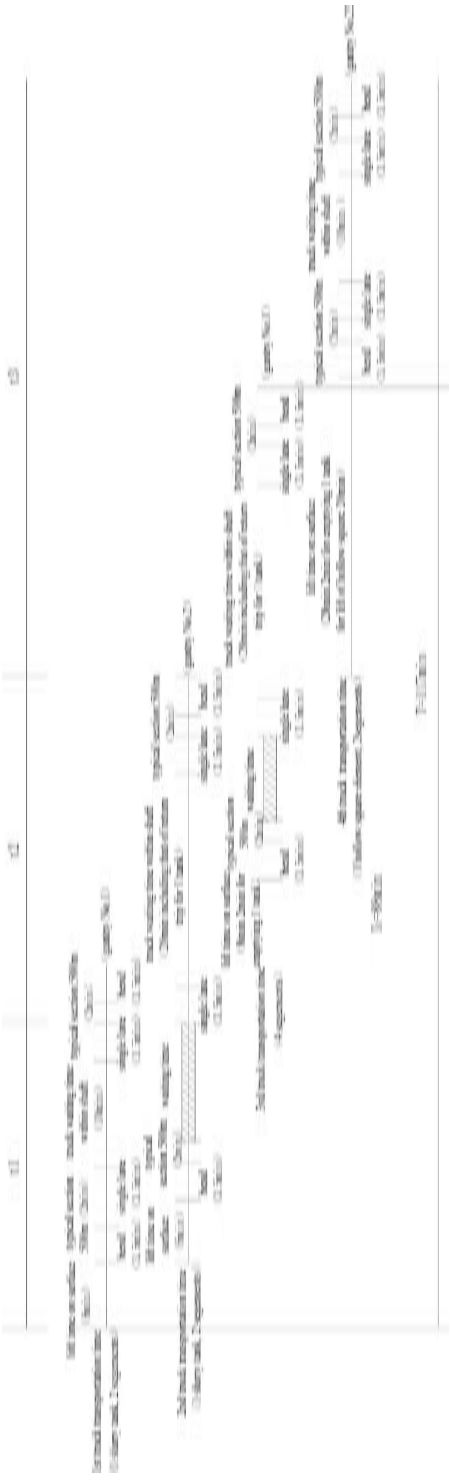

Figure 11. Schematic scenario of 2 vehicle transportation.

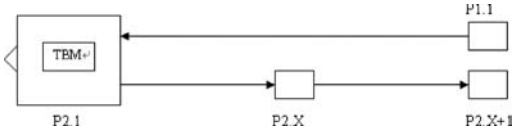

Figure 12. Schematic slurry conveyance and discharge pumps layout within tunnel.

Table 1. Conveyance equipment.

Equipment	Power/kW	Lift/m	Max flow/ m^3h^{-1}
P1.1	750	68	2,000
P2.X	1,100	52	3,000

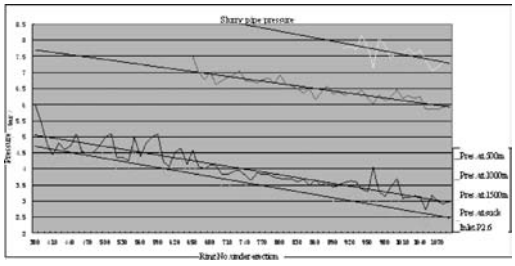

Figure 13. Pressure variation in slurry pipework between Ring #380 and Ring #1090 during shield tunelling.

Δp_λ and Δp_ζ total of local pressure drops:

$$\Delta p = \sum \Delta p_\lambda + \sum \Delta p_\zeta = \sum \lambda \frac{l}{d} \frac{\rho v^2}{2} + \sum \zeta \frac{\rho v^2}{2} \quad (2)$$

Where λ is pressure drop coefficient of straight pipe; ζ is the pressure drop coefficient of bend; l is the pipe length; d is the pipe diameter; ρ is the pressure within the pipe; v is the slurry flow rate.

Since calculation by formula can not give pressure loss along pipework due to numerous pipe sections and pipe fittings, let alone helically welded pipes. Then it is appropriate to deduce approximately pressure loss within pipework for per unit pipe length. For the slurry pipework within the tunnel, there is a slurry pressure sensor at interval of 500 m. By monitoring slurry pressure variation via these pressure sensors located at 500 m, 1,000 m, 1,500 m and pump P2.6 (at 350 m), the following curve (Fig. 13) is obtained after data analysis.

From Figure 13, the stepwise extension of tunnel, the slurry pressure drop along locations of the pipework tends to be the same as those at suction port of discharge pumps. Pressure loss along the pipework can be approximately analyzed under normal recycling of slurry conveyance (Fig. 14).

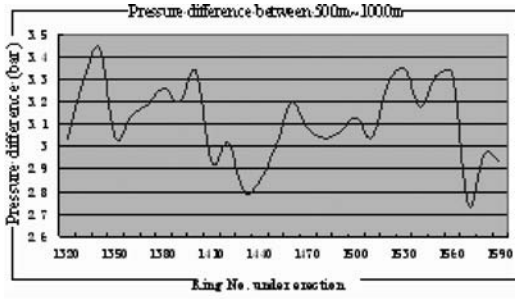

(a)

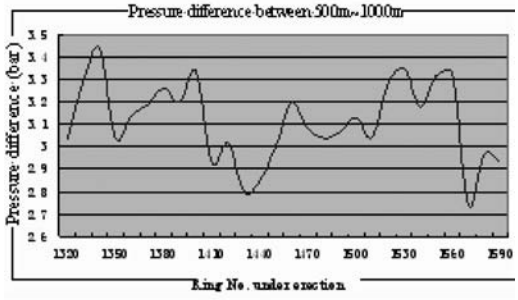

(b)

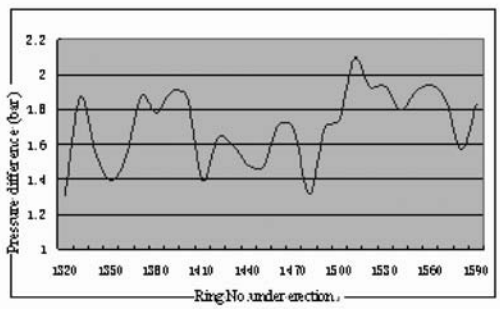

(c)

Figure 14. Pressure difference at 500 m intervals along slurry discharge pipework during shield tunnelling between Ring #1,320 and Ring #1,590.

The value of pressure difference between various locations shown in the table 2 is taken from the monitoring data of Ring #1,320 and Ring #1,590, while elevation difference is calculated from designed tunnel axial line. Under the conditions of 1.4 g/cm^3 density, the pipe friction loss is from 0.47 bar/100 rings to 0.66 bar/100 rings; pressure variation at pump is 9 in average. Since 30 days are required for installation of relay pump within tunnel, it is generally believed that relay pump is to be installed at erection of Ring #300 for pump P2.1 before its maximal value is reached. If no gradient is assumed, 9.2 bar is basically required for

Table 2. Average pressure difference at different intervals.

	500–1,000 m	1,000–1,500 m	1,500–2,000 m
Pressure difference (bar)	3.1	1.6	1.7
Elevation difference (m)	10.39	3	1.7
Potential difference (bar)	1.45	0.42	0.24
Pipe friction loss (bar)	1.65	1.18	1.46
pipe friction loss at 200 m intervals (bar)	0.66	0.47	0.58

Table 3. Relay pump lay-out for slurry discharge within tunnel.

Relay pump within tunnel	P2.6	P2.5	P2.4	P2.3
Installed location	Ring #175	Ring #960	Ring #2,250	Ring #3,200

relay pump within tunnel. Table 3 shows Relay pump layout for slurry discharge within tunnel.

6 CONCLUSION

After reasonable research of construction logistics, i.e. by saving cost and enhancing construction efficiency, a stronger logistics system has been provided for shield tunnelling in Shanghai Yangtze River tunnel. In addition, the research result can benefit other tunnels in design and construction stages.

REFERENCES

Hong, S.W., Bae, G.J., Kim C.Y., et al. 2003. Virtual reality (VR) – based intelligent tunneling information system. *Proceedings of 29th ITA World Tunnelling Congress: (Re) Clamming the underground space*.

Huang, Z.X., Liao, S.M., Liu, G.B., et al. 2000. Optimization of segment joint position of shield tunnel in soft ground. *Underground spac.* (12): 268–275.

Liu, Y.J., Gao, G.F. & Feng, W.X. 2004. Study on optimization design of cross section of the large-span highway tunnel. *Liao Ning communication science and techlonogy* (2): 48–50.

Ruwanpura, J.Y. & Ariaratnam, S.T. 2007. Simulation modeling techniques for underground infrastructure construction process. *Tunnelling and Underground Space Technology* 22(5–6):553–567.

Tsutsui, M., Chikahisa, H., Kobayashi, K., et al. 2004. Stereo vision-based mixed reality system and its application to construction sites. *ISRM International Symposium/3rd Asian Rock Mechanics Symposium (ARMS): Contribution of Rock Mechanics to the New Century*: 223–228, Kyoto, Japan.

The Shanghai Yangtze River Tunnel - Theory, Design and Construction – Huang (ed)
© 2008 Taylor & Francis Group, London, ISBN 978-0-415-47161-9

Construction technology of shield inspection environment in Shanghai Yangtze River Tunnel

G.J. Zhang & F.Q. Yang
Shanghai Tunnel Engineering Co., Ltd., Shanghai, P. R. China

F.T. Yue
China University of Mining & Technology, Xuzhou, P. R. China

ABSTRACT: During the construction of large diameter and long-distance shield tunnel, it is necessary to inspect or replace the shield equipment under the ground or even in the bed of deep water, due to the hydrogeologic conditions, unknown underground obstacles, failures and service life of construction equipment. Theoretical design and construction technology were performed according to the working environment where shield tunnel equipment should be maintained or replaced in the Yangtze River Tunnel Project. Furthermore, correlative technical measures and emergency plans were prepared.

1 INTRODUCTION

Since the 20th century, tunnel construction technology has been greatly improved all over the world. Many projects have been constructed successfully, such as the English Channel Tunnel, Denmark Storebelt Super Large Channel Tunnel, Tokyo Bay Highway Bridge and Tunnel in Japan, Chesapeake Bay Bridge and Tunnel in the United States, the fourth tunnel of the Elbe River in Hamburg of Germany, the "Green Heart" Tunnel and the second Westershede Highway Tunnel in Netherlands.

It is necessary to inspect and replace the equipments (the cutters, the shaft bearings, the tail sealing, the propulsion jack, etc.) below the ground as well as in the river bed, lake bed or sea bed for any type of shield machines due to different hydrogeologic conditions in different areas, unknown underground obstacles, failures and service life of construction equipments.

In Tokyo Bay Tunnel Project, multi-shield machines were used, which avoided the failures and replacement of the equipment.

With the use of multi-shield machines, a service tunnel was constructed together with two main tunnels in the English Channel Tunnel Project. If necessary, the main tunnels can be reinforced by grouting or freezing from the service tunnel. In addition, maintenance and replacement of shield equipments could be implemented in the main tunnels.

In the Netherlands "Green Heart" Tunnel Project, sternal pores used for freezing or grouting were reserved in the head of shield machine and freezing loop-tubes were set in the shell plates at the shield tail, while good preparations were made for the working environment of equipment maintenance and replacement. The shield machine used in the second Westershede Highway Tunnel Project in Netherlands had the function of changing cutters in the shield.

In Germany Elbe River Tunnel Project, workers can enter five main wheel ribs of a cutter head to change cutters under normal atmosphere condition. However, when repairing the steel members or scraping soil cutters of secondary wheel spokes, workers must enter the pressure driving bin to change cutters under pressurization condition.

The shield machines used in Shanghai Yangtze River Tunnel Project were analogous to those used in the Germany Elbe River Tunnel, which is called "Trude" shield machine. Workers could also enter six main wheel spokes of the cutter head to replace cutters under atmospheric pressure condition freely. But only when the safe inspection environment was formed at the head of the shield to change cutters under pressurization condition as repairing steel members or scraping soil cutters of secondary wheel spokes before entering pressure driving bin.

2 SHANGHAI YANGTZE RIVER TUNNEL AND INSPECTION ENVIRONMENT

2.1 *Shanghai Yangtze River Tunnel*

The Shanghai Yangtze River Tunnel crosses the Yangtze River from Pudong Wuhaogou to the

Table 1. The main technical parameters of shield equipments which may be inspected or replaced.

	Items	Technical parameters	Remarks
Shield tail	Diameter	15,370 mm	
	Sealing system	Four steel brushes	Three steel wire brushes, a steel plate
	Emergency sealing system	1	inflatable emergency sealing system
	Preformed freezing loop-tubes	1 (44 mm × 84 mm)	outside the shield tail
Cutter head	Diameter	15,430 mm	
	Structure	Six-star layout spokes	
	Cutters	Soil cutters (some could be replaced)	Cutters replaced in the arm of cutter head under normal atmosphere
	Abrasion monitoring system	Eight scrapers, two blades	
Cutter head drive	Main drive	Center rotary	Fixed
	Main shaft bearing	Three roller bearings	
	Maximum sealing working pressure	0.75 MPa	
	Motor driver	15 motors	Power of 250 kW

Changxing Island. Two shield tunnel construction schemes are adopted in this project. The external diameter of the shield machine is 15 m. A twin slurry-balanced shield machines were used boring 7.5 m per step with an excavation diameter of 15.43 m. The maximum thickness of the soil layer is about 27 m above the two tunnels. The maximum depth of water is about 33 m above the soil. The largest water pressure at the bottom of the tunnel is about 0.55 MPa.

The shield machine mainly crosses through silt, clay, clay silt, muddy silty clay mingled with sandy silt, sandy silt mingled with silty sand, muddy clay, sandy silt mingled with silty sand. The cutters or shield tail brushes are easy to be abrased by sandy soil.

2.2 *Inspection and replacement of shield equipment*

Table 1 lists main technical parameters and equipment components, which should be inspected or replaced.

According to geological, hydrological and project conditions near the entrance of the Shanghai Yangtze River Tunnel, both shield machines were equipped with emergency inflatable sealing systems at the shield tail to meet the requirements during driving the total length of 7.5 km tunneling. Cutter replacement technology is used in the arm of cutter head under normal atmosphere (1/3 of the cutters may be replaced) and tail reserved freezing pipes (Fig. 1) if equipment inspection and replacement are possible.

2.3 *Inspection environment and auxiliary technologies*

In addition to conventional technical measures, some auxiliary technologies are ready to special situations of equipment inspection and replacement in the Shanghai Yangtze River Tunnel. They includes overhauling or replacing steel wire brushes when tail sealing system is failed, overhauling and changing

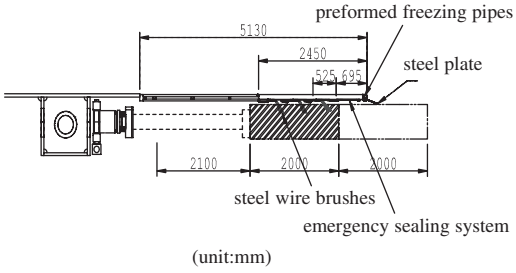

Figure 1. Inflatable sealing system at shield tail.

more cutters, and removing obstacles at the excavation face. Equipment inspection and replacement construction environment should be created quickly in the river bed under high water pressure, outside of cutter head, in the shield machine, or in the completed tunnel.

Traditional supplementary technologies include pneumatic process, chemical reinforcement, freezing method and precipitation method, or multiple measures including the above methods. Experiences and engineering cases show that pneumatic process, freezing method, chemical reinforcement such as slurry method and horizontal rotary spouting method are more appropriate for inspection environment construction in shield machine or in the tunnel under the deep water.

3 DESIGN AND CONSTRUCTION OF SHIELD INSPECTION ENVIRONMENT

3.1 *Inspection environment design and construction scheme of shield head or tail*

3.1.1 *Soil freezing reinforcement of the excavation face in front of shield machine*

The right position for setting freezing pipes and reinforcement construction whether from the ground

(water) surface or from inside of the shield machine is first selected according to the position of shield, project conditions, and construction conditions. Then the main parameters of soil are determined for reinforcement, such as the thickness, the scope, the temperature, and the intensity, respectively.

3.1.2 *Design of shield tail shed, value and zone of reinforced thickness*

After design of inspection environment, the construction technologies should also be further studied, such as prediction technique for equipment (components) inspection and replacement, inspection and changing technique of cutters, cutter head and steel wire brushes, technique of removing obstacles on the excavation face, researches on emergency plans of inspection environment construction, effects of detection technique of maintenance environment construction.

3.2 *Parameters determination of inspection environmental design and construction before the head of shield*

A maintenance environment should be created in front of the cutter head if the head of the shield needs inspection outside of the cutter head and the shield is driven under the river. A frozen reinforced soil plate was formed before the shield resists water pressure. A frozen curtain was formed around the cutter head to seal water pressure and soil pressure through freezing method.

3.2.1 *Related calculating parameters and design loads*

Figure 2 shows the force diagram of the frozen reinforced soil. Table 2 lists the parameters of water pressure, soil pressure and the loads.

3.2.2 *Calculation dimension of frozen soil*

Thickness of reinforced frozen soil which resists the water and earth pressure ahead of the shield is determined based on the theory commonly used in Japan.

The formula to calculate the thickness is:

$$h = [(\beta \times P(D/2)^2 / \sigma)K]^{1/2} \quad (1)$$

where: h – soil reinforced thickness, m;
σ – flexural-tensile strength at an average temperature of $-10°C = 2.1$ MPa.

Finite element method is used to check the flexural-tensile strength and shear strength of the whole frozen soil at a temperature of $-10°$C under water pressure and soil pressure by general software ANSYS. In the numerical simulation, Young's modulus and Poisson ratio is 150 MPa and 0.35, respectively.

The simulation results show that the maximum tensile stress is 1.1 MPa at the edge of frozen soil, which is

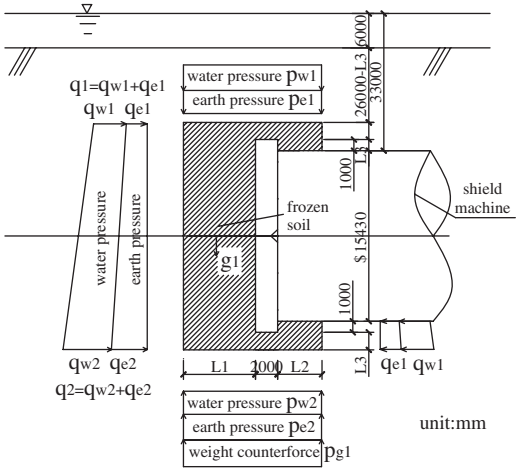

Figure 2. Force diagram of the frozen reinforced body.

less than the flexural-tensile strength limit of 2.1 MPa if the temperature is below $-10°$C. The safety factor nearly reaches 2. The maximum compressive stress is 3.1 MPa at the edge of frozen soil, which is less than the uniaxial compressive strength of 3.4 MPa at a temperature below $-10°$C. The safety factor is about 1.1. The maximum shear stress is 0.8 MPa at the lower bound of frozen soil, which is less than the shear strength of 1.68 MPa if the temperature is below $-10°$C. The safety factor is 2.1.

3.2.3 *Dimension of frozen reinforced zone*

The thickness of the frozen soil in front of the cutter head is taken as 6.03 m, which is enough to resist the earth and water pressure in front of the excavation face. For the sake of safety, the thickness should be 8.5 m taking into account of the space for replacement of the cutter head. The thickness of the frozen soil behind the cutter head is computed as 5 m for resisting water pressure and earth pressure, the dimension should be 5.5 m considering the safety. The calculated frozen arched shell dimension is 8 m, and 8.5 m is employed. The dimension of the reinforced zone is shown in Figure 4.

3.2.4 *Layout of freezing holes*

According to the design of the frozen curtain and the shield structure, the freezing holes are set upward (almost in horizontal direction) and downward in front of the shield machine. In doing so, a frozen soil plate is formed to resist the water pressure and earth pressure ahead. Moreover, a set of freezing holes are arranged around the shield head to enhance the freezing effects. Thus, two independent frozen zones in front of the head and around the shield machine are formed to seal the head of the shield. There are 444 freezing holes in total, while 152 holes are in front of the face along the rows from A to G and 292 holes are around the shield along

Table 2. Parameters in finite element simulation (27 m deep soil).

Items	Symbols	Value	Units	Items	Symbols	Value	Units
Soil depth	H	19.0	m	Upper loads	Pw_1	250.0	kN/m
Maximum water level of Yangtze River	H_w	25.0	m		Pe_1	152.0	kN/m
Water Depth	H_s	6.0	m	Horizontal Loads (soil and water load seperated)	qw_1	250.0	kN/m
Outer diameter of frozen soil	D	29.4	m		qe_1	106.4	kN/m
Unit weight of water	γ_w	10.0	kN/m^3		qw_2	544.3	kN/m
Saturated unit weight of soil	γ_s	18.0	kN/m^3		qe_2	271.2	kN/m
Submerged unit weight of soil	γ_s'	8.0	kN/m^3	Total horizontal loads (Soil load plus water load)	Q_1	281.4	kN/m
Horizontal soil pressure coefficient	K_0	0.7			Q_2	652.2	kN/m

Table 3. Results of frozen reinforced thickness.

Average temperature of frozen soil/°C	Flexural-tensile strength of frozen soil, σ/MPa (−10°C)	Soil and water pressure, P/MPa	Excavation diameter of frozen soil, D/m	Coefficient	Safety factor	Thickness of frozen soil, h/m
−10	2.1	0.57	15.43	1.5	1.5	6.03

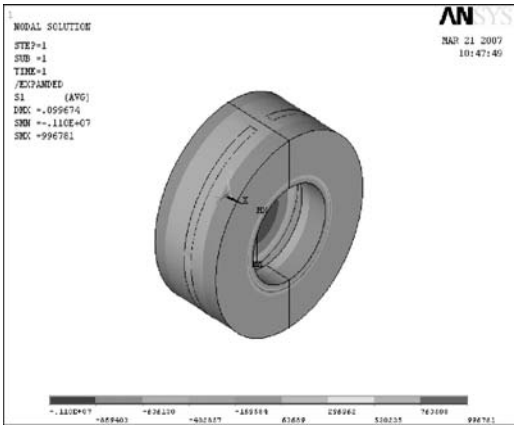

Figure 3. Distribution of the first principal stress.

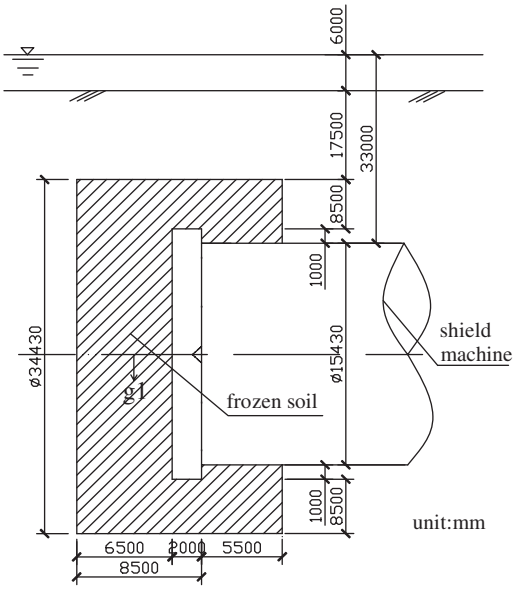

Figure 4. Frozen soil zone.

the rows from O to T. As shown in Figures 5 and 6, appropriate rearrangements of freezing holes are necessary before the construction of the freezing holes in order to avoid the pipeline inside and the important components of the shield machine.

3.2.5 *Determination of freezing parameters*

Designed brine temperature is between −28°C and −30°C. The flux of single freezing hole should be greater than 5 m^3/h. Final freezing hole spacing L_{max} should be not larger than 2,500 mm. The developing velocity of the frozen soil is 30 mm/d. The time for the frozen curtain formation may be 45 days, the design thickness should be formed in 60 days. There are 13 temperature measuring holes. Φ89 × 6 mm in dimension, 20# low-carbon seamless steel pipes with hoop steel inside for lining are chosen for freezing pipes. Temperature measuring pipes is 20# low-carbon seamless steel pipes with Φ32 × 3 mm in dimension. The

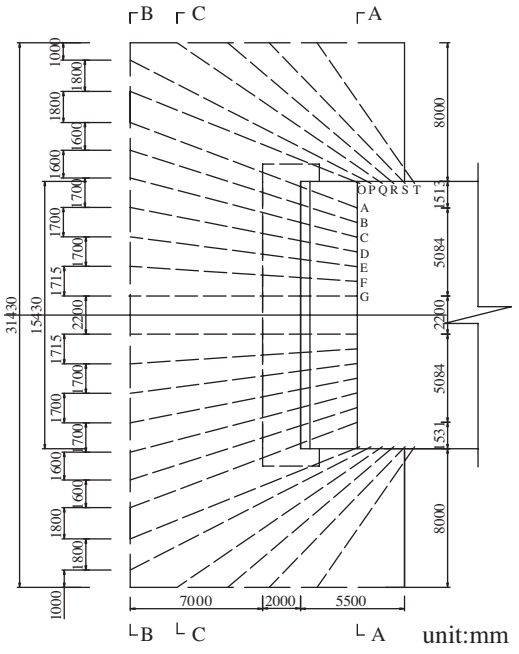

Figure 5. Design of the frozen zone.

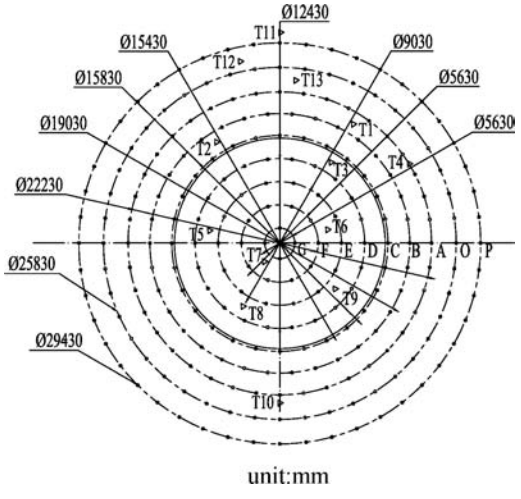

Figure 6. A-A cross section of the frozen zone.

liquid feed pipe is Φ38 mm welded steel pipes. The brine water dry tubes and fluid distribution rings are Φ168 × 5 mm seamless steel pipe.

3.2.6 *Frozen construction research*

1. The freezing holes construction procedure is: localization, opening of the hole and installation of the pipes in the porthole, installation of the device into the porthole, drilling holes, measuring, sealing the bottom of the hole, and then carrying out bulge test. The deviation of the drilling should be controlled less than 1%. The spacing of the two finished holes should be less than 2.5 m to ensure the thickness of the frozen curtain. Otherwise supplementary holes are required.
2. The installation of the freezing station includes freezing station layout, equipment installations, pipeline connections and insulation work, dissolving calcium chloride, and filling the units with fluorine and oil.
3. Positive freezing: it is necessary to carry out the debugging and test running after the installation of the equipment. When test run is carried on, then, adjusting the pressure, the temperature or other state variables if necessary, in order to make sure that the units are running under the requirements of related technological codes and equipment request. During the freezing process, it is necessary to carry out timing examination of the temperature and flux of the brine, the expansion situation of the frozen curtain, and then readjust the system parameters. After the system runs normally, positive freezing could be carried on.
4. Excavation and support construction: when frozen results meet the design requirements, partition excavation could be carried out after well preparation of construction and confirmed exploration. Excavation should follow the NATM principles, on which short spacing of driving and masonry technology should be employed. In every cross-section, two smaller cross sections were applied and the excavation distance is 600–800 mm per step. The ordinary pickaxe is inapplicable due to the high intensity and good ductility of the frozen soil. So air pick is needed.
5. Excavation should follow the procedure: the upper part first and then the lower part, the outer part first and then the center part.
6. The temporary supports consist of circular struts made of 20# I-shaped beams. In order to enhance the stability of the supports, each support is stiffened by five horizontal struts and five vertical struts. The spacing of the arch support is similar to the tunnel excavation depth, which is about 0.6–0.9 m. The braces along the longitudinal direction are set to strengthen the integral stability. All the steel supports should be covered with planks to control the deformation of frozen wall and to reduce the energy loss of frozen wall. The planks are adjacent to the frozen wall, attempting to reduce the gaps of supports. Moreover, the gaps should be filled with fine yellow sand. If the gaps become large, thick planks or wood wedge is preferable.
7. Tube drawing scheme uses defreezing method with manual compulsion. Hot brine is used to circulate

in the frozen tubes after the frozen soil around the tubes was thawed. Two jacks are fixed in both sides of the frozen tubes using the forces of 6 tons to draw out them. When the drawing length of the tubes is about 0.5 m, the hot brine circulation can be stopped and the brine can be discharged through pressure ventilator. At the same time, the tubes can be drawn out quickly by manual calabash. During drawing, the frozen tube and the hook must be in a line and the tubes should also be rotated frequently. If they cannot be drawn out, the frozen soil should be thawed again until the tubes are easy to be pulled out.

3.3 *Design and construction of shield tail brushes inspection environment*

3.3.1 *Freezing Design*

Pressure distributions of reinforced body near the shield tail are shown in Figure 7, which is due to the geological information.

3.3.1.1 The dimension calculation of reinforced zone

Up to now, no theory and formula are available to calculate the frozen reinforced soil under this operating mode like the Shanghai Yangtze River Tunnel. Numerical simulation is used to determine the dimension of reinforced zone through pilot calculation. Thickness of the frozen soil is 0.3 m along radial direction. The length is 0.2 m along axial direction. The numerical results show that for the frozen reinforced soil the maximum tensile strength is 1.4 MPa, which is less than the flexural-tensile strength of 2.1 MPa at a temperature below −10°C. The safety factor is 1.5. The maximum compressive stress is 1.4 MPa, which is less than the uniaxial compressive strength of 3.4 MPa if the temperature is below −10°C. The safety factor is 2.4. The maximum shear stress is 0.46 MPa at the lower bound of frozen soil, which is less than the shear strength of 1.68 MPa below −10°C. The safety factor is 3.6.

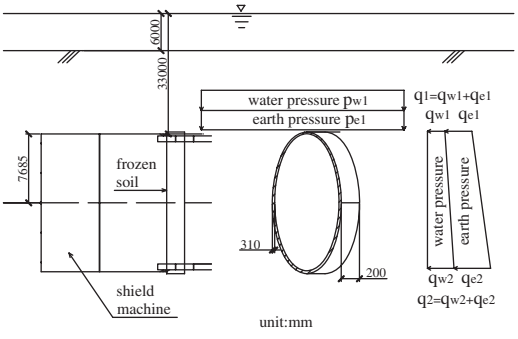

Figure 7. Pressure distributions of frozen soil near shield tail.

The thickness of the frozen soil along radial direction is calculated as 0.3 m. The actual thickness is taken as 0.35 m. Moreover, the length is 0.2 m along axial direction and the selected thickness is 0.5 m, as shown in Figure 8.

3.3.1.2 Conceptual design of frozen soil

Tilted frozen holes are drilled around the rings from inside of the tunnel to reinforce the stratum near shield tail. This measure will freeze the zone of steel wire brushes and the outer soil. Frozen curtain with high strength, which is well sealed, is then formed. The subsequent step is to remove the rings and to replace the steel wire brushes according to the frozen situation.

To ensure enough space for replacing the brushes of shield tail, the needed dimension of the frozen curtain is 500 mm × 350 mm behind the shield tail through freezing method, which will resist exterior water pressure and soil pressure.

3.3.1.3 Freezing holes layout and refrigerating output design

According to the frozen curtain design and the tunnel structure, tilted frozen holes are drilled around the concrete rings from inside of the tunnel. The separation angle of declining holes and the perpendicular line is 30°. Layout of the freezing pipes in the shield tail is shown in Figure 9.

Designed brine temperature is between −28°C and −30°C. The flux of single freezing hole should be greater than 5 m^3/h. Final freezing holes spacing L_{max} should be smaller or equal to 1,200 mm. The development velocity of the frozen soil should be 25 mm/d.

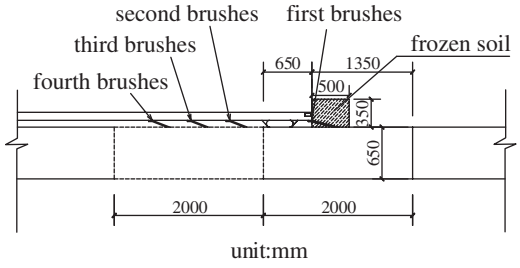

Figure 8. Schematic plan of frozen reinforced zone.

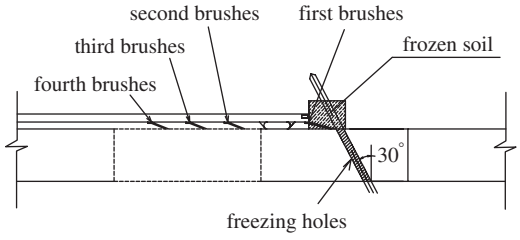

Figure 9. Arrangement of freezing holes.

The time for the frozen curtain formation should be 24 days whereas the design thickness should be formed in 48 days.

The total length of the freezing pipes is 67.8 m. The length of thorough freezing pipes is 33 m. The other 34.8 m pipes are frozen partially. Energy loss of partial frozen is 50% in computation. Then the total energy needed is 2,708.22 J.

3.3.2 *Freezing reinforcement*

The process of freezing reinforcement is as follows: cleaning up the shield and construction site above the ground to ensure good quality; laying down two pipelines of Φ50 mm in the shield construction location. The pipelines are used to provide water for drilling freezing pipes, discharging pollution water, and supplying and discharging water in freezing. A row of freezing holes is arranged in the frozen zone. There are 44 holes within the total length of 67.8 m. In order to save energy and weaken effects of low temperature, partial freezing technique is used in the freezing pipes inside of the rings. $\Phi 89 \times 6$ mm in dimension, 20# low-carbon seamless steel pipes are chosen for freezing. The freezing holes are arranged according to the construction datum mark and the frozen holes construction documents. The deviation of the hole dimension should be controlled within 30 mm. The depth of the drilling holes must be greater than the limits specified in codes. The construction procedures for freezing holes are as follows: location, porthole drilling and installation of pipes, equipment installation at the porthole, drilling, measuring, and sealing.

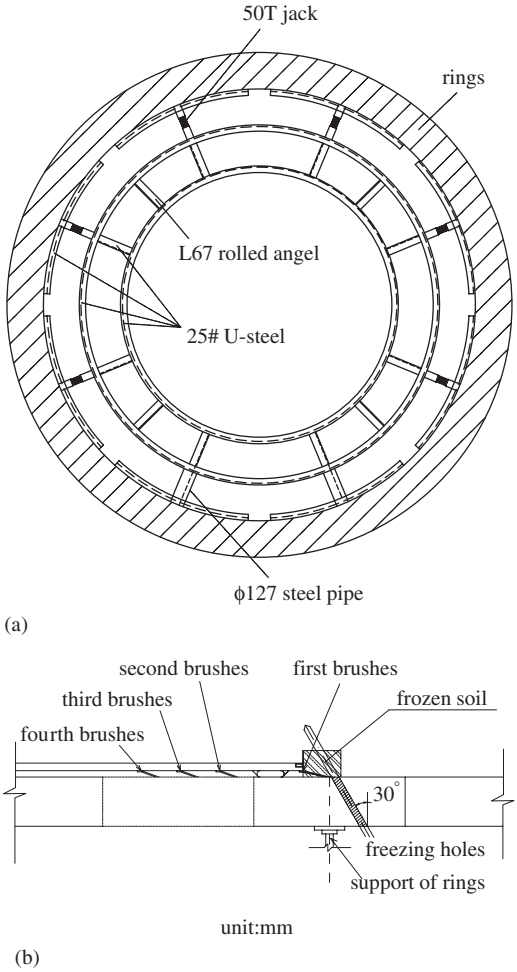

Figure 10. Steel support structures of rings with opened holes.

As far as the hole position is determined, the ring to be drilled needs reinforcement, such as setting steel bracket at the inner ring. Support sites should avoid the drilling part as shown in Figure 10.

Because the distance is large between the jack and the third ring, the steel supports are used to lengthen the jack to reach the third ring. The procedure of installing steel supports are to set a part of steel support after the removal of a piece of ring, and then, to remove the next ring after the force of the jack is applied and the structure is stable. More details are shown in Figure 11. Both sides of the steel supports are connected to the jack and the rings by bolts or welding, which ensure adjacent steel supports not to move or even fall off as installation of other steel supports.

There are 16 holes for temperature measurement, which are distributed uniformly around the rings and at the middle of two group freezing pipes for the purpose of measuring the development of frozen curtain. Temperature measurement holes are embedded directly in the rings through drilling holes as shown in Figure 12.

3.4 *Construction monitoring*

Precise mercury thermometer and the digital temperature sensor were installed on the brine loop pipes. The survey frequency is 2 times per day. Flux gauges were installed on the brine loop tubes and the measurement

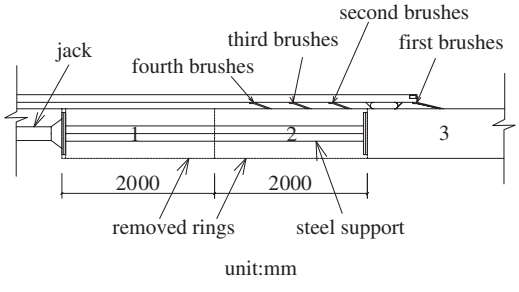

Figure 11. Support mode of shield after removal of rings.

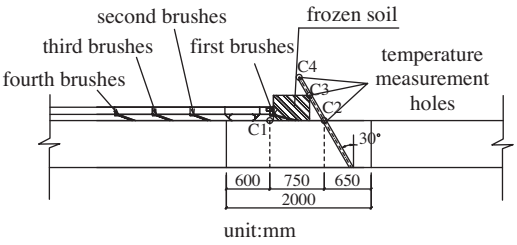

Figure 12. Arrangements of vertical temperature measurement holes.

frequency is 2 times per day as well. Thermo junction was installed on the head of each freezing instrument to measure the temperature, and the frequency is 2 times per day. Liquid level monitoring and warning devices were installed in the brine case. Furthermore, the water pressure of loop tubes, water pressure for freezing and temperature are also should be measured for 2 times a day.

3.5 *Construction emergency plans*

A spare freezing unit is prepared in site. When the working freezing unit breaks down, the spare freezing unit takes effect. Maintenance is carried out for the fault unit immediately. That is to say, there is always a spare freezing unit for emergency. Double circuit is used in the work location. Two-way-high-voltage inlet wire is ready for each substation and distribution station. When one circuit is out of work, the other circuit can be switched on for power transmission. This plan ensures trouble-free operation during the freezing construction. Some items should be well prepared such as freezing of liquid nitrogen, fast freezing ponding equipment of polyurethane foam, quick-drying cement, and double slurry grouting. Moreover, technicists are arranged to check and watch on duty. Report and treatment should be taken as soon as possible if there is something wrong.

4 CONCLUSIONS

Through study of reinforcement design and construction technology of the shield inspection environment, conclusions can be drawn as follows:

- The method that environment reinforcement of shield inspection by using freezing method is feasible. During the construction, freezing method can display its technical advantages including the good adaptability and small impact on environment, and so on.
- After the shield is driven into the soil at one side of the river, two schemes of freezing method are available if the inspection environment is needed. One scheme is to drill tilted holes from inside of the shield, another is to slot V-shaped hole from the ground surface. The former is better because the length of freezing holes is short. The deviation of drilling holes can be easily controlled. As a result, the freezing effect is better. However, its fault is that aperture should be opened in the shield.
- After the shield is driven into the soil under the deep water, three kinds of arrangements for freezing holes could be carried out, such as uptilt direction, nearly horizontal or downhill direction from inside of the shield.
- If the second, third, or fourth tail sealing brushes are needed to be replaced, the freezing holes are drilled around the rings from inside of the shield. The soil around the tail and the steel plate is frozen to form a well sealed curtain with high strength. Then the tail brushes inspection environment is formed after the removal of the rings.
- Further study is needed to save construction cost and ensure construction safety in various construction situations.

REFERENCES

Cui, H.T. 2004. A Research over environmental impact parameter of manual horizontal ground freezing in a metro tunnel. *RAILWAY STANDARD DESIGN* (1):61–63.

Lin, Z. & Yang J.J. 2003. Analysis on temperature field of freezing shaft wall with three rows of freezing tubes. *MINE CONSTRUCTION TECHNOLOGY* 24(3):21–24.

Qiao, J.S., TAO, L.G. & Mi, S.Y. 2004. Simulation study on deformation characteristics of ground surface in horizontal freezing construction of metro tunnel. *CHINESE JOURNAL OF ROCK MECHANICS AND ENGINEERING* 23(5):2643–2646.

Wang, W.S., Wang, J.P., Jing, X.W., et al. 2004. Experimental study of temperature field in course of artificial freezing. *JOURNAL OF CHINA UNIVERSITY OF MINING & TECHNOLOGY* 33(4):388–391.

Wu, X.Z., Li, D.Y. & Jin, M. 2004. Construction technology analysis of the horizontal freezing method adopted in construction of side channels of the test section of nanjing subway, *CONSTRUCTION TECHNOLOGY* 31(1):40–42.

Wu, X.Z., Zhang, Q.H., Li, D.Y., et al. 2003. Waterproofing technology and leaking analysis for shield -driven tunnel of the nanjing subway, *CHINA BUILDING WATERPROOFIN* (4):15–17.

Zhou, W.B. 2004. Construction technology and applications of shield tunnel. *CHINA ARCHITECTURE & BUILDING PRESS*.

The Shanghai Yangtze River Tunnel - Theory, Design and Construction – Huang (ed)
© 2008 Taylor & Francis Group, London, ISBN 978-0-415-47161-9

Deformation monitoring system of circular tunnel cross section

J.X. Wang & Y.L. Cao
Department of Surveying and Geo-informatics, Tongji University, Shanghai, P. R. China
Key Laboratory of Advanced Engineering Survey of SBSM, Shanghai, P. R. China

D.Y. Hou
Leica Geosystems (Shanghai) Co., Ltd., Shanghai, P. R. China

Y.B. Huang
Shanghai Tunnel Engineering Co., Ltd., Shanghai, P. R. China

ABSTRACT: Three-dimensional coordinates of a series of points on the tunnel cross section are collected by the major station. Firstly, a two-dimensional plane is fitted according to these points. After eliminating very scattered points, the coordinates are projected onto a fitted plane. Secondly, the coordinates of the center of an optimal circle and its radius are derived from the projected tunnel cross points. Finally, the corresponding coordinates of the circle center in the tunnel coordinate system are determined by coordinate transformation from the projected coordinates. Compared to the designed values, the transformed coordinates are employed to monitor and analyze the deformation of the tunnel cross section.

1 INTRODUCTION

The urban railway traffic system is developing fast in cities with their rapid growth nowadays. Subway is accepted as the main transportation tool by more and more people as a result of its convenience. Therefore, the safety requirement about the subway tunnel is correspondingly much higher. The major task for railway traffic administration department is to ensure a safety operation of the subway. The deformation of the subway tunnel is inevitable as the long-playing use as well as the pile upon the subway tunnel. Therefore, it is very important to monitor the deformation and make sure that is on the safe side.

The paper talks about a data processing method that can be used in the deformation monitoring of the tunnel cross section. A set of discrete points on the border of the tunnel cross section are measured by major stations and a two-dimensional plane is fitted according to their 3D coordinates. These points are projected onto the fitted plane and transformed to a plane coordinate system after translation and rotation. On the fitted plane, these projected points are used to fit a plane circle, and the coordinates of the center of the circle and the radius are obtained. Some points with large observations errors are eliminated in these processes. Then the coordinates of the center of the circle are transformed back to the tunnel coordinate system. Compared with the radius and the coordinates of the centre with the design value, the deformation monitoring of the tunnel is fulfilled.

2 THE SURVEYING OF THE TUNNEL CROSS SECTION

In order to monitor, firstly, it should ensure the accuracy of the position of the cross section so that it can be compared with its designed section. Then one has to make sure that the cross section is in the normal direction of the mileage point. The longitudinal section should be considered too. If the surveying section is not in the vertical plane, it is needed to be adjusted according to the grade of the mileage point. The raw observation data are treated with the Leica TPS1200 tunnel section surveying software carried by a major station. The elements of plane curve and vertical curve may be treated as the input of the software. After setting out the central pile of the surveying tunnel section and centering the major station on the central pile point, the machine will rotate to the tunnel cross section automatically. The machine has a function of surveying without cooperative target. It can survey automatically according to the preset values. The data collected from the surveying cross section are stored in the memorizer of the instrumental compact flash card in form of text

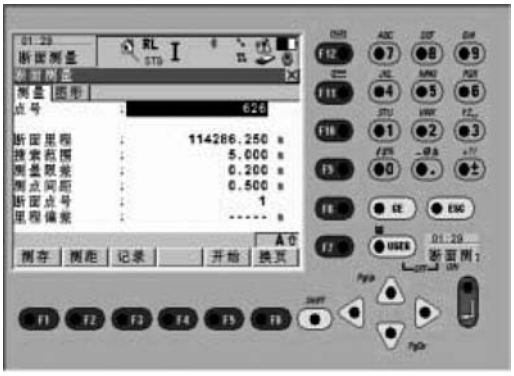

(a)

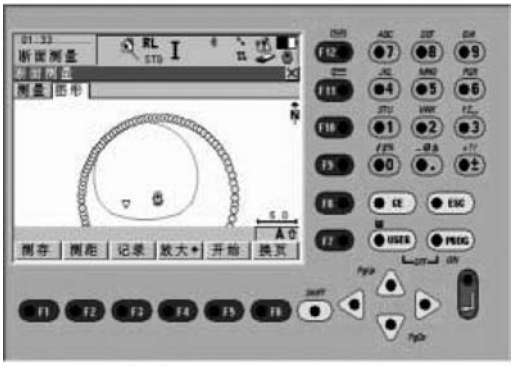

(b)

Figure 1. The software carried by the tunnel section surveying machine.

files. To analyze the data, data have to be extract from the CF card.

3 FITTING THE DIMENSIONAL PLANE

Theoretically, the points measured from the tunnel cross section are in the same plane. Practically, it is impossible due to measuring errors. The way to optimize this situation is to eliminate unreasonable measurements with the least-square method and find out the best fitting dimensional plane.

The coordinates of the observation data are expressed as $(x_i \;\; y_i \;\; h_i)^{\mathrm{T}}\; i = 1, 2, \ldots, n)$. Thus we have the equation of the fitting plane of tunnel section as follows:

$$ax + by + ch + d = 0 \tag{1}$$

where $(a \;\; b \;\; c)^{\mathrm{T}}$is the unit vector of the normal direction of the plane. We could make $a > 0$ in order to fix the unit vector uniquely. If $a = 0$, then $b > 0$. If $a = 0$ and $b = 0$, then $c > 0$. It is impossible that a, b, c are zeros at the same time.

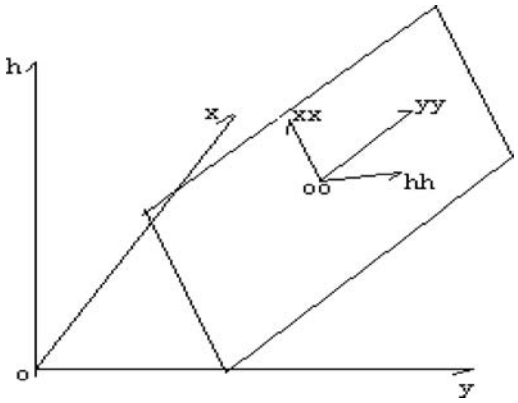

Figure 2. The sketch map of the relationship between the surveying coordinate system and the plane coordinate system.

The distance between observation point and fitting plane is shown in equation (2):

$$v_i = -ax_i - by_i - ch_i - d \tag{2}$$

In order to fit a plane which is closest to the observations, we sum the square of the distance between observation points and plane least. According to the principle of least squares, i.e., $V^T PV = \min$, equation (2) follows the parameters of the plane function a, b, c, d. Using the conditional expression $a^2 + b^2 + c^2 = 1$, we can adjust the parameters a, b, c to the unit value.

We have thus obtained the equation (1). The residual of the equation (1) expressing with v_i is the distance between the point *i*and plane. The projection coordinates of point *i*on the plane is $(xp_i \;\; yp_i \;\; hp_i^{\mathrm{T}})$. We can get:

$$\begin{cases} xp_i = x_i + av_i \\ yp_i = y_i + bv_i \\ hp_i = h_i + cv_i \end{cases} \tag{3}$$

4 TRANSFORMATION BETWEEN THE SURVEYING COORDINATE SYSTEM AND THE PLANE COORDINATE SYSTEM

We shall first set up a plane coordinate system $(oo - xxyyhh)$, in which two main axes *xx* and *yy* are in the plane and the third axis *hh* has the same direction with the normal line of the plane. In the plane coordinate system, the height is zero for all projection points $(hh = 0)$, which is shown in Figure 2 below.

The origin of plane coordinate system is *oo*and its coordinates defined in the surveying coordinate system are:

$$oo\begin{cases} x_{oo}=\dfrac{\sum_1^n xp_i}{n} \\ y_{oo}=\dfrac{\sum_1^n yp_i}{n} \\ h_{oo}=\dfrac{\sum_1^n hp_i}{n} \end{cases} \tag{4}$$

The direction of *xx* axis in the surveying coordinate system $o-xyh$ is from *oo* to a point in the plane that cannot be *oo* point. It is suggested to choose the first surveying point (xp_1 yp_1 hp_1) and the direction from *oo* to the first survey point is the direction of *xx* axis $(e_{xx1}\ \ e_{xx2}\ \ e_{xx3})^{\mathrm{T}}$.

$$\begin{cases} e_{xx1}=\dfrac{xp_1-x_{oo}}{d} \\ e_{xx2}=\dfrac{yp_1-y_{oo}}{d} \\ e_{xx3}=\dfrac{hp_1-h_{oo}}{d} \end{cases},$$

$$d=\sqrt{(xp_1-x_{oo})^2+(yp_1-y_{oo})^2+(hp_1-h_{oo})^2} \tag{5}$$

The direction of *hh* axis in the survey coordinate system is just the direction of the normal line:

$$(e_{hh1}\quad e_{hh2}\quad e_{hh3})^{\mathrm{T}}=(a\quad b\quad c)^{\mathrm{T}} \tag{6}$$

The *yy* axis is perpendicular to both *xx* axis and *hh* axis and its direction in the surveying coordinate system is the cross-multiplying term of *xx* axis and *hh* axis.

$$(e'_{yy1}\quad e'_{yy2}\quad e'_{yy3})^{\mathrm{T}}=(e_{xx1}\quad e_{xx2}\quad e_{xx3})^{\mathrm{T}}\times(e_{hh1}\quad e_{hh2}\quad e_{hh3})^{\mathrm{T}} \tag{7}$$

The coordinates of a point in the surveying coordinate system can be expressed as $(x_i\ \ y_i\ \ h_i)^{\mathrm{T}}$ and in the plane coordinate system as $(xx_i\ \ yy_i\ \ hh_i)^{\mathrm{T}}$. The relation between the two coordinate systems is:

$$\begin{pmatrix} x_i \\ y_i \\ h_i \end{pmatrix}=\begin{pmatrix} x_{oo} \\ y_{oo} \\ h_{oo} \end{pmatrix}+R\begin{pmatrix} xx_i \\ yy_i \\ hh_i \end{pmatrix} \tag{8}$$

In equation (8), $(x_{00}\ \ y_{00}\ \ h_{00})^{\mathrm{T}}$ is the translation vector. R is the rotation matrix.

$$R=\begin{pmatrix} e_{xx1} & e_{yy1} & e_{hh1} \\ e_{xx2} & e_{yy2} & e_{hh2} \\ e_{xx3} & e_{yy3} & e_{hh3} \end{pmatrix} \tag{9}$$

The transformation relation of the coordinates from the surveying coordinate system to the plane coordinate system is shown as below:

$$\begin{pmatrix} xx_i \\ yy_i \\ hh_i \end{pmatrix}=-R^T\begin{pmatrix} x_{oo} \\ y_{oo} \\ h_{oo} \end{pmatrix}+R^T\begin{pmatrix} x_i \\ y_i \\ h_i \end{pmatrix} \tag{10}$$

According to the methods upon, the coordinates of the observation are transformed from surveying coordinate system to the plane coordinate system, and they are prepared for fitting the plane circle.

5 FITTING THE PLANE CIRCLE

The plane coordinates of the surveying points are expressed as $(x_i\ \ y_i)^{\mathrm{T}}$. The error equation of the model of the fitting plane circle is

$$v_i=\sqrt{(x_i-x_0)^2+(y_i-y_0)^2}-R \tag{11}$$

In the equation, $(x_0\ \ y_0)^{\mathrm{T}}$ is represented as the coordinates of the centre of the plane circle and R is the radius. The linearization of the error equation is:

$$v_i=\left(-\frac{x_i-x_0}{\rho_i}\quad -\frac{y_i-y_0}{\rho_i}\quad -1\right)\begin{pmatrix} \delta x_0 \\ \delta y_0 \\ \delta R \end{pmatrix}-l_i \tag{12}$$

In the equation,

$$\rho_i=\sqrt{(x_i-x_0)^2+(y_i-y_0)^2}$$

$$l_i=R-\sqrt{(x_i-x_0)^2+(y_i-y_0)^2}$$

Let us first set up the function of the error equations of all observation points and comprise the normal equation according to the principle of least-squares method under the condition of $\sum_n v_i^2=\min$.

The correction parameter follows immediately from the result of the normal equation. The process of the computation is iterative and finishes until the correction is convergent. Consequently, we obtain the coordinates of the centre of circle and the value of radius.

In the fitting process, we can remove the errors according to the residual. If the remnant of a surveying point is bigger than a certain value (e.g. 3σ or a design value), the surveying point is treated as the error point and removed from the observation equation. The new normal equation is solved again after eliminating the error and the new parameters are computed.

At last, the plane coordinates of the centre of the circle will be transformed to the surveying coordinate system by equation (8) expressing with $(x_0\ \ y_0\ \ h_0)^{\mathrm{T}}$. The coordinates as well as the radius are used for the comparison with the design value, and the difference shows the deformation of the tunnel cross section.

Table 1. Coordinates of the surveying points in the surveying coordinate system.

Point	X(m)	Y(m)	H(m)	Point	X(m)	Y(m)	H(m)
1	90	−7.433	3.359	8	90	0.092	9.551
2	90	−7.362	3.905	9	90	0.741	9.452
3	90	−7.246	4.449	10	90	1.381	9.291
4	90	−7.083	4.987	11	90	2.003	9.07
5	90	−6.875	5.515	12	90	2.6	8.791
6	90	−6.622	6.03	…–…	…–…	…–…	…–…
7	90	−6.322	6.526	60	90	5.588	5.664

6 EXPERIMENT

A series of 3D coordinates points are measured by the major station from the inside border of the tunnel cross section. The coordinates of some surveying points are listed in Table 1 for the illumination of the computation. Sixty points are measured. Some of the points may be taken from the conduit and the ground and they should be eliminated in the program. The surveying points are listed in Figure 3.

The parameters solved by the plane equation (2) are:

$$a = 1, \quad b = 0, \quad c = 0 \tag{13}$$

Therefore, the fitted plane equation is $x - 90 = 0$. It is obvious to see that all the points measured are in the same plane.

After the transformation between the two coordinate systems, we have derived the translation and the rotation matrix:

$$X_0 = \begin{pmatrix} x_{00} \\ y_{00} \\ h_{00} \end{pmatrix} = \begin{pmatrix} 90 \\ -0.9362 \\ 7.2354 \end{pmatrix} \tag{14}$$

$$R = \begin{pmatrix} 0.0000 & 0.0000 & 1.0000 \\ -0.8588 & -0.5124 & 0.0000 \\ -0.5124 & 0.8588 & 0.0000 \end{pmatrix} \tag{15}$$

The unit weight mean square error is: $\sigma_0 = 0.0014$m. The transformation between the surveying coordinate system and the plane coordinate system is:

$$\begin{pmatrix} x_i \\ y_i \\ h_i \end{pmatrix} = \begin{pmatrix} 90 \\ -0.9362 \\ 7.2354 \end{pmatrix} + \begin{pmatrix} 0.0000 & 0.0000 & 1.0000 \\ -0.8588 & -0.5124 & 0.0000 \\ -0.5124 & 0.8588 & 0.0000 \end{pmatrix} \begin{pmatrix} xx_i \\ yy_i \\ hh_i \end{pmatrix} \tag{16}$$

The fitted results comprising the plane coordinates of the centre of the circle and the radius are:

$$X_0 = \begin{pmatrix} 2.0266 & -4.0317 \end{pmatrix}^{\mathrm{T}} \quad R = 6.8537 \tag{17}$$

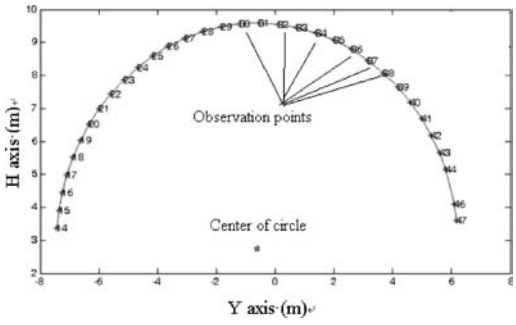

Figure 3. The distribution of the surveying points and the position of the centre of the circle.

Figure 4. The program of deformation monitoring system of the circular tunnel cross section.

According to equation (8), the coordinates of the centre of the circle in the surveying coordinate system are:

$$\begin{pmatrix} x_0 \\ y_0 \\ h_0 \end{pmatrix} = \begin{pmatrix} 90 \\ -0.6107 \\ 2.7348 \end{pmatrix} \tag{18}$$

The design value of the radius is 6.85 m. Thus we conclude that the method addressed above in this paper is effectual and logical.

The process has been realized with the computer by compiling the program with VC++ (Figure 4).

7 CONCLUSIONS

This paper introduces a method of monitoring and analyzing the deformation of the tunnel cross section. It provides a technique of fitting the two-dimensional plane and projecting the discrete points to the fitted plane. According to the transformation relation between different coordinate systems, a mathematical model of the plane circle is set up. Besides, the paper addresses the way to fit the plane circle using the surveying points, based on the principle of least-square

method. After determining the coordinates of the centre of the plane circle and the radius and transforming the plane coordinates to the surveying coordinate system, the deformation monitoring is finished. The computed results are compared with the design values. The validity and feasibility of the method are illustrated with a case study. The outline of a tunnel cross section is usually not only circular but is composed of several arcs with different radii. In this case, we can monitor the deformation according to different subsections. The method introduced in this paper can be used to monitor the tunnel section deformation of subway, railway and highway. The safety of the tunnel is critical as it is connected with lives of the passages. It is necessary to monitor the deformation of the tunnel section in a certain period. It has been proved that the method given in the paper is easy to be carried out and the analytic result is reliable.

REFERENCES

Chen, J. P. & Wang, J. X. 2003. Conic fitting in engineering surveying. *Geotechnical Investigation & Surveying* (5).

Wang, J. X. & Zhao, X.Y. 2003. Deformation surveying for round orbit. *Geotechnical Investigation & Surveying* (4).

Wang, J. X., Chen, J. P. & Zhang, C. Y. 2004. Fitting of ellipsoidal surface. *Journal of Tongji University (Natural Science)* 32(1):78–82.

Wang, J. X., Xu, C. & Lu, C. P. 2002. Real-time Surveying of Immersed Tube. *Acta Geodaetica Et Cartographica Sinica* 31.

The Shanghai Yangtze River Tunnel - Theory, Design and Construction – Huang (ed)
© 2008 Taylor & Francis Group, London, ISBN 978-0-415-47161-9

Driving the slurry TBMs for Shanghai Yangtze River Tunnel

G. Ferguson
Maunsell Geotechnical Services Ltd., Maunsell Aecom Group, P. R. China

L. Zhang & Y. Lin
Maunsell AECOM Shanghai, P. R. China

ABSTRACT: The twin 15.43 diameter slurry TBMs provided for boring the two 7.5 kilometre road tunnels, for the underground section of the river crossing link from Pudong, Shanghai to Chongming Island, were designed to deal with very soft ground conditions including clay, silts and sand under high hydrostatic pressures and relatively low cover. This paper will concentrate on the TBM's performance in dealing with the following: (1) launching the TBMs from the Launch Shaft; (2) the initial driving with shallow cover; (3) the steering of the TBM and guidance system; (4) the grouting system during the TBM advance; (5) the ring building operation and the ring type; (6) the separation plant for re-cycling the slurry and maintaining its required parameters. This paper will also include a short description about the development of the slurry TBM to its present set up and describe the advantages of the TBM's grouting system. The type of rings used on this project is compared to other types on other projects.

1 INTRODUCTION

In the last decade Shanghai has developd into a world class financial and economic centre of China. This rapid growth has included expanding the city to the once rural district of Pudong and to the Yangtze River delta area.

The plan to develop the Yangtze River delta has included a fixed link, as part of Shanghai's highway network, between Pudong and ChongMing Island. The link will include two 7.2 km, three lane road tunnels to Changxing Island, and a bridge to join this small river island to the larger ChongMing Island.

The fixed link was named The Yangtze River Tunnel and Bridge Project and The Shanghai Yangtze River Tunnel and Bridge Development Company was formed to carry out the design and construction of the works.

Herrenknect AG of Germany was awarded the contract to supply and commission two slurry tunneling machines with 15.43 m diameter that could withstand face pressures of over 6.5 bar.

The tunneling, road deck and cross passage construction was awarded to local contractor Shanghai Tunnel Engineering Company (STEC) in joint venture with international contractor Bouygues of France. STEC was also awarded the contract to cast and supply the precast segments and road deck units. The local designer STEDI was awarded the design of the

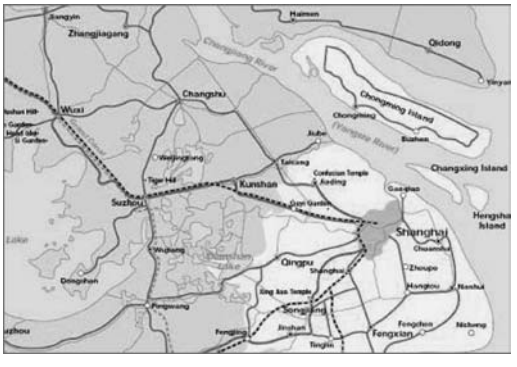

Figure 1. Plan overview to develop the Yangtze River delta.

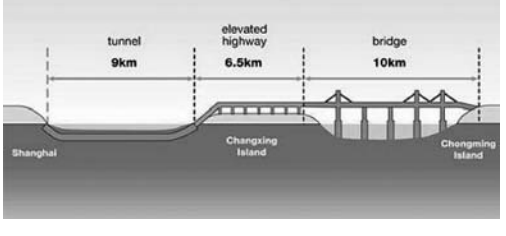

Figure 2. Connection between Shanghai and Chongming Island.

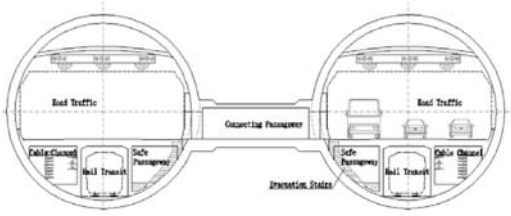

Figure 3. Cross section of road tunnels.

tunnels and cross passages and Maunsell AECOM (Hong Kong) was appointed by the client as consultants for the design and construction.

2 PROJECT DESCRIPTION

2.1 *Tunnels*

The 7.5 km long twin tunnels which are approximately 30 m apart and lined with 650 mm thick precast segments with an inside diameter of 13.7 m was selected for the three lane road tunnels. The road deck construction is made up of a precast centre unit, in-situ concrete side decks and an in-situ concrete invert.

Also, incorporated in the lining are two sump areas for each tunnel for drainage. The emergency evacuation items consist of 8 No. cross passages at every 800metres and 14 No. emergency manholes in the road deck.

2.2 *Geology*

The route for the tunnels is located in the Yangtze River Delta under the south branch of the Yangtze River.

The Yangtze Delta begins beyond Chen – Chiang, about 200 km upstream of the river, and consists of many branches, tributaries, lakes, marshes and ancient river beds. The width of the Yangtze in the delta ranges from a mile to over 2 miles and eventually widens downstream and becomes a large estuary exceeding 50miles at the river's mouth.

Before reaching the sea at Shanghai, the Yangtze divides into two branches that flow into the East China Sea. Between the branches is ChongMing and Changxing Islands, which were formed over the centuries by the deposits of alluvium at the mouth of the river.

The river depth, considering the high level, between Changxing Island and Shanghai at the tunnel is 20 m to the river bed at the deepest section.

The site investigation along the route of the tunnels identified that the formation was alluvium consisting mainly of soft silty clay, clayey silt, sandy silt and fine sand.

The overburden ranges from 6 m (at the launch) to 18.6 m, which are 0.4 to 1.2 diameters of the TBM.

The overburden is mainly soft clay and the tunnel face is predominately silty clay. Below the invert of the tunnel, and occasionally encroaching the tunnel invert is a sand silt layer and also a few metres below the tunnel invert fine sand was identified.

2.3 *TBM selection*

The shallow overburden and high face pressures were defining factors for selecting a TBM that would be able to support the tunnel face at all times and be completely water tight. Another important factor was that the anticipated 6 bar face pressure could not allow compressed air interventions for changing cutter head tools. Instead, special facilities were available for changing tools inside the arms of the cutterhead. For these reasons Slurry TBMs (STBM) were preferred to the less expensive Earth Pressure Balance Shield (EPBS). With the EPBS the geology was ideal for forming a watertight 'plug' for the screw conveyor. Also, a separation plant would not be required, which is a considerable cost saving, but it would be difficult to keep such a large tunnel face controlled in such high sensitive clays, that will tend to flow under such a high hydrostatic head, without using an air bubble based control system. Also, these conditions favored the STBM as the pressurized slurry will aid in sealing the face for stability when not excavating and require substantially less torque on the cutterhead in the slurry than for an EPBM in the excavated soil.

3 THE SLURRY TBM

The STBM has been developed over the years in Germany from soft ground slurry shields (Hydroshields) that originally began in England. The original concept of the Bentonite Tunnelling Machine was patented by John Bartlett of Mott, Hay and Anderson and was used for two tunnel projects in the United Kingdom.

3.1 *Development of tunnelling machines in flowing ground*

Soft ground that was turned into flowing conditions due to the presence of water were originally tunneled in compressed air either with a drum digger tunneling machine or a hand shield that could support the face with breast plates, sand tables or face rams. However, this method of tunneling caused health problems associated with compressed air to many workers and was considered undesirable by health authorities. Another issue was that tunnels were limited to an equivalent depth of less than 3 bar due to working conditions for personnel. Later, attempts were made to eliminate working conditions in compressed air by limiting the pressurized space by creating a chamber with a bulkhead at the cutterhead of the tunneling machine.

The pressurized medium was slurry, air or water for supporting the face. These methods had limited success and further development continued. One of the first machines was designed by Robbins and was used to construct part of a new line for the Paris Metro between 1964 and 1967. Compressed air was used to support the face at the cutterhead of a drum digger. Difficulties were found in maintaining the air pressure at the face due to loss of air through the ground. The principle of using a pressurized bulkhead chamber at the working face resulted with using a slurry medium rather than compressed air. In 1972, the British National Research Development Corporation and the London Transport Executive jointly financed a project to drive a test tunnel with a 'Bartlett' Bentonite Tunneling Machine through submerged sandy ground at New Cross as an experimental project. The tunnel machine was built by Robert Priestly Ltd and Edmund Nuttal Ltd was the tunnel contractor. Nuttals later took the same machine to Warrington, Lancashire for a sewer tunnel in difficult ground conditions.

Wayss & Freytag of Germany continued the development of the Bentonite machine as fewer opportunities were available in Britain, and it became known as a 'Hydroshield'. Today, the main supplier for the slurry TBM, worldwide, is Herrenknect of Germany who started their business with producing pipe jacking equipment. After entering the TBM market they have continued to develop the slurry TBMs for all varied geology including rock and mixed ground. Their continual developments have resulted with the production of larger TBMs that are capable of excavating through extremely difficult geology which was not possible a decade ago.

3.2 *The excavation function for a typical slurry TBM*

The area where the cutterhead rotates is known as the excavation chamber which is separated from the working chamber by a bulkhead known as the submerged wall. The submerged wall has an opening in the invert where the spoil can be transported through the crusher to the suction pipe. The opening can be closed by a gate in case of emergencies or repairs in the working chamber. The soil and the slurry are pumped from the working chamber through the suction of the slurry line to the separation plant outside the tunnel. The volume of slurry/soil pumped out the excavation chamber is replaced by fresh slurry from the separation plant via the feed line outlets.

The main bulkhead separates the atmospheric area from the pressurized chambers of the TBM. The reservoir chamber is filled with compressed air from the crown to axis in the working chamber and is called the 'air bubble'. The air pressure is set to balance the earth and water pressure at axis and is used to support the tunnel face during excavation. The function of the air bubble is to act as an air cushion for fluctuating levels of slurry during the excavation advance with the air being easier to control quicker than liquid. The slurry in the excavation chamber is always kept full during the TBM advance.

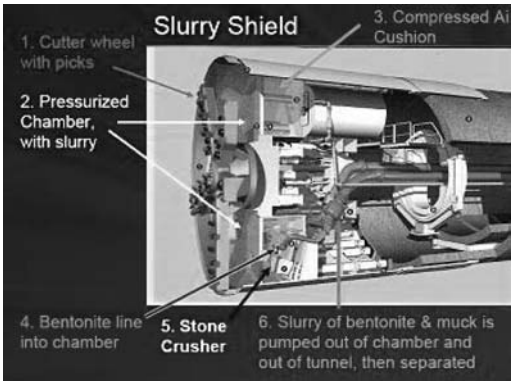

Figure 4. Slurry TBM.

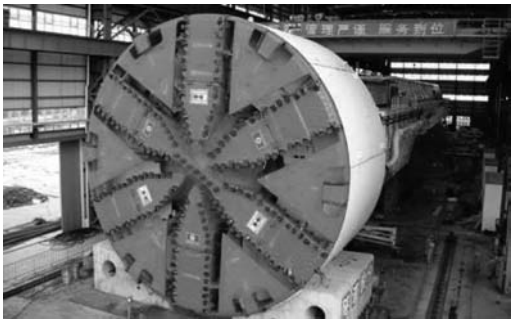

Figure 5. Slurry TBM for Yangtze River Tunnel.

4 THE START OF THE CHONGMING DRIVES

Herrenknect commenced delivering two 15.43 m diameter STBMs to STEC's Pudong factory, 6 km from the tunnel site, in January 2006. The TBMs were assembled and tested prior to being dismantled and rebuilt at the 'launch shaft' on site.

The components for the first TBM (S-317) arrived on site and were assembled in the 'launch' shaft for the East tunnel during the first week of June 2006. The launch shaft being part of the cut and cover tunnel allowed all the back up gantries to be assembled prior to the launch. This TBM was launched on 23rd September 2006.

The second TBM (S-318) was assembled in the west launch shaft from October to December 2006 and finally launched on 21st January 2007.

Figure 6. Cradles for launching.

Figure 7. Concrete reaction structure.

Figure 8. Installing the pipe struts between the concrete reaction structure and the steel thrust frame.

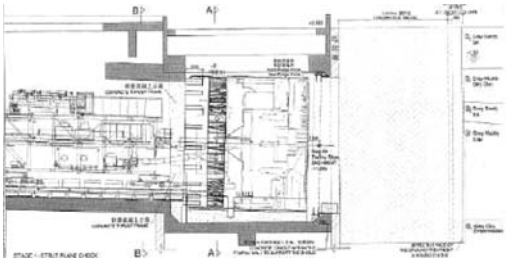

Figure 9. TBM being launched.

4.1 *TBM launch*

The Launching Shafts formed part of the cut and cover tunnel which was constructed by the diaphragm wall method. Included in each Launch Shafts was a reinforced concrete thrust structure located at the back wall of the shaft to act as a reaction frame for advancing the TBM. A steel ring was installed in the front (or face) wall of the each shaft to form a sealed chamber for retaining slurry during the start of the excavation. Reinforced concrete 'cradles' with slide rails were cast in each base of the shafts for erecting the TBMs and for shoving along.

In front of the front wall of both shafts ground treatment was carried out for about 16.5 m with a row of jet grout columns immediately behind the front wall and two rows at the end of the ground treated block. Between the jet grouted columns the ground was treated by soil mixing with cement slurry which consolidated the ground up to 1.5 MPa. Along the perimeter of the treated ground block well points were drilled 40 m deep for protection against a layer of silty sand with ground water pressure.

During the erection of the TBM a fabricated steel thrust ring was placed inside the tailskin before installing the tailskin brushes. This steel ring was used for connecting the steel pipe props, filled with concrete, to the concrete thrust frame.

Once the TBM had been assembled and the trailers connected the thrust steel ring was placed in position and the pipe struts were fixed between the ring and the concrete reaction structure.

Once the TBM was shoved clear of the steel ring the tailskin brush seals were ready for hand packing with grease prior to being covered by building the first 'shove' or temporary ring. Steel packers were welded in the invert for keeping the rings central in the tailskin.

At the front of the TBM the launch seal ring was prepared by installing a rubber seal for containing the slurry pressure. The front diaphragm wall was broken out using hand tools and exposed the jet grouted columns. The TBM was then shoved into the seal ring with the cutterhead up to the jet grouted columns.

The excavation chamber was filled with water and 1 bar pressure of compressed air was applied in the air bubble chamber. Also, a bracket was fixed to outside of the TBM and locked against the cradle for preventing the TBM to roll when excavating. The TBM commenced excavation through the treated ground and advanced for the second shove ring (Ring 5). Prior to building Ring 5, the steel thrust ring, which was now exposed from the tailskin, was propped against the shaft walls. As the TBM advanced through the treated ground each shove ring was propped.

After six shove rings were built the first permanent ring was built accurately in the tailskin. After building Ring 2 the TBM was shoved until the back of the tailskin was inside the seals of the steel launch ring. The steel launch seal was in a position for installing extra support for retaining grout pressure.

As the TBM advanced for Ring 3 the permanent grouting commenced through the tailskin ports.

Figure 10. Propping 'shove' rings in shaft.

Figure 11. Installing extra supports at the steel launch seal.

The TBM began its correct cycle for Ring 4 and also entered the undisturbed ground using the calculated confinement pressure for excavation.

4.2 *The initial driving through shallow ground*

The 15.43 diameter TBMs alignment included a shallow cover area, from the launch shaft to the Yangtze River, which consisted of loose backfill material, sandy silt and soft silty clay saturated with a high ground water level.

Throughout this area it was important for the confinement pressures to be accurate and maintained for avoiding over excavation that could cause large settlement or blow outs by over pressurizing.

This area was also difficult as the TBM operation was in its learning period and the ground was not treated after the launch area.

The confinement pressures were submitted by the contractor and set in the control system on the TBM.

The soil formation of the overburden, for this area, consisted of 1 m of backfill covering a formation of 4–5 m of sandy silt with a less permeable layer of silty clay at the tunnel crown. The face geology was predominately soft clay before reaching the river bed.

After the treated ground the TBM advanced with an overburden of 7–8 m until reaching the river bank's 4 m high bund wall.

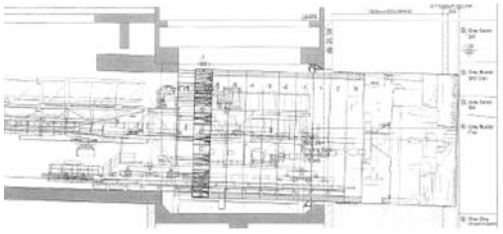

Figure 12. TBM launched.

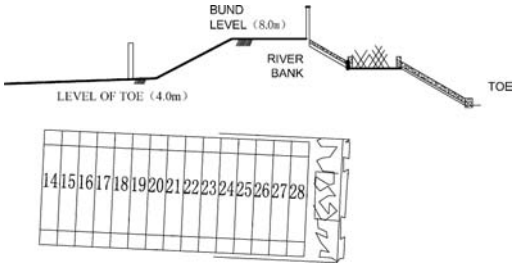

Figure 13. TBM advancing under the bank of Yangtze River.

4.3 *Settlement*

Surface monitoring stations were placed along the alignment of the drives from the launch shaft to the river bed. Frequents checks were made daily for indicating any heave or settlement during the advance of the TBMs.

Figure 14 shows the monitoring layout for the East TBM.

The monitoring results indicated initial settlement slightly in front of the TBMs cutter head and increased when the cutter head was directly below the monitoring point. Settlement again increased during the period when the shield passed the monitoring point.

The graph below indicates increased settlement between the cutter head and the grouted ring left behind by the TBM. Also, a larger settlement occurred between Rings 5–10 which coincided with the cutter head entering the untreated ground. This indicates confinement pressure being inaccurate immediately after the treated ground. The 60 mm settlement shown for Ring 23 was at the location of the bund wall and with the sudden change of ground level the confinement pressure could have also been the reason for this settlement.

Settlements at the face are due to excavation, but along the TBM they depend on confinement pressure, the ground nature and hydraulic conditions around the shield's body.

The settlements at the cutterhead indicate acceptable amount considering the size of the TBM, ground

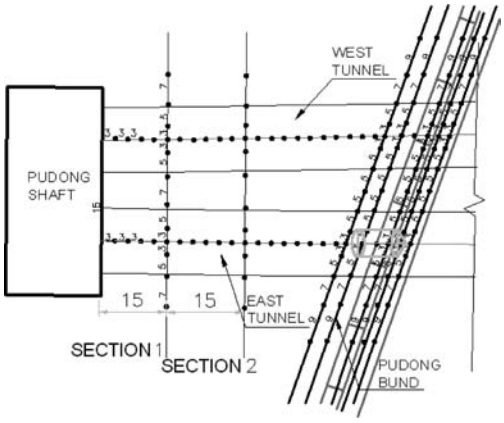

Figure 14. Monitoring point layout.

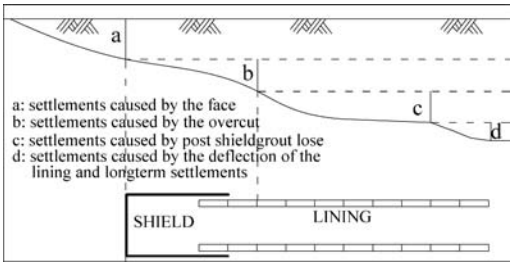

Figure 15. Settlement principle.

conditions and shallow cover. The most settlement appeared between the cutterhead and the rings which suggest that the slurry confinement pressure was less effective in this area, possibly caused by the filtrate properties of the slurry and slow progress at that time.

Due to the low cover it was agreed to accept the settlements as this did not cause any surface problems rather than increasing the air pressure and risking a 'blow out'.

5 DRIVING THE TBM

5.1 *Steering*

TBMs or shields were steered by reducing the number shove rams either left/right side or in the crown/invert to push off the previous ring for steering to the designed tunnel alignment (DTA). With the arrival of the modern full face slurry or earth pressure balance shields it is necessary to have all the shove rams in use during the advance for compensating the face pressure. There are six groups of rams (ABCDEF) that can be adjusted to various pressures for steering purposes.

An important factor was the gap between the inside of the tailskin and the extrados of the lining. This had to be considered during advancing the TBM for avoiding

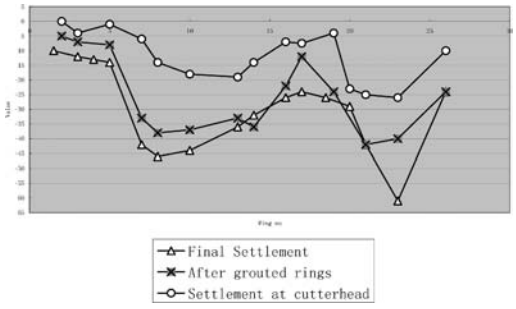

Figure 16. Settlement graph.

the tailskin becoming too close the lining and creating a situation called 'skin bound or ring bound'. This will cause problems associated with quality such as stepping of the rings, cracking of the segments or leakage due to gasket miss-alignment.

Prior to the modern guidance systems such as 'ZED, VMT or PYXIS', the TBM was guided by a laser line that gave the position for line and level on a target on the back bulkhead of the shield and the shield's body was measured each side from fixed points on the tunnel lining that would give its attitude. Fixed lines were marked on the previous rings perpendicular to the line and were called 'square marks', each advance was measured from these points and would immediately indicate the direction of the shield, either away or towards the tunnel horizontal alignment. By minimizing each change in direction from the 'square mark' the shield could be kept from over-correcting. The square of the shield was described by 'left lead' for going right of the line and 'right lead' for going left. For the vertical attitude of the shield a fixed plumb bob was used, which was suspended inside the shield with the plumb bob pointing on a plate with markings to indicate how much the shield deviated for verticality and for roll. The plumb was described by 'look up' for pointing upward and 'over hang' for downwards. The roll is the amount the TBM has rotated clockwise or anticlockwise and can affect the ram position related to the rings if it is not controlled. The cutterhead is usually rotated alternately clockwise and anticlockwise for controlling and adjusting the roll.

5.2 *Steering control using the PYXIS system*

The PYXIS application gives the actual position and attitude of the TBM on a real-time basis and will propose the choice of keystone position.

The PYXIS system includes two displays on two screens; the 'supervision' screen and the 'trajectory' screen, and is located in the TBM's control cabin.

The supervision screen displays the main guidance parameters, the head and rear positions, excavation

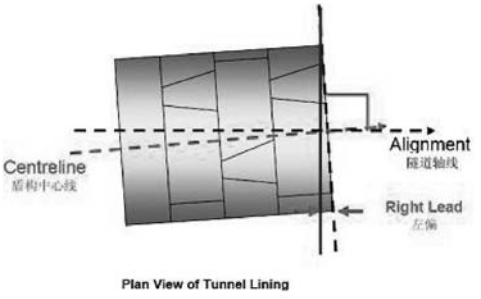

(a)

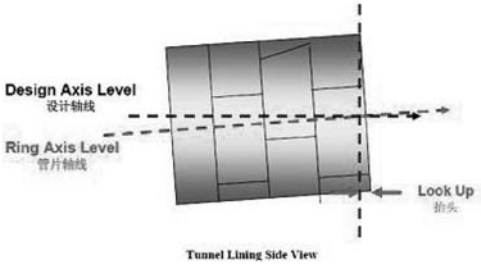

(b)

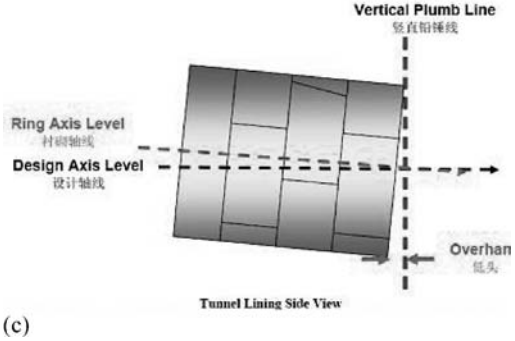

(c)

Figure 17. Tunnel lining side view.

progression, TBM attitude and menus for the pilot and surveyor. The left side displays;

Ring number, Chainages, the TBM's position for the cutter head, its position at the rear of the tailskin, the DTA information and survey information.

DY indicates the horizontal position and DZ the vertical position of the TBM. On the example below, DY at the head of the TBM (blue) shows it being 4 mm left of the centre and DY for the rear being 9 mm right of the DTA. The distance from the front to the rear of the

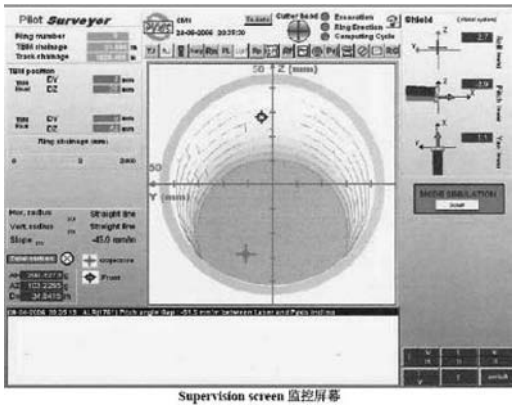

Figure 18. Trajectory screen.

TBM is approximately 13 m, therefore as a guidance the difference between the head and rear could represent the square of the TBM (86% of the diameter of the TBM) giving an attitude of 13 right lead. This will move the TBM more to the left of the DTA, as shown in red. The vertical position is indicated by DZ (blue) at the head and shows it being 28 mm high and 64 mm high at the rear. Converting the attitude as previously described this will give the TBM 36 over-hang which will move the TBM lower (see the red mark).

On the PYXIS the attitude of the TBM is represented by three angles;

- Roll for the rotation.
- Pitch for the vertical attitude, positive for upwards (look up).
- Yaw for the horizontal attitude, positive when heading towards the left (right lead).

The second screen shows the trajectories of two specific points at the front and rear of the TBM on the vertical and horizontal view. The straight lines joining the front and the rear (green) indicates the attitude of the TBM over its length for the vertical and horizontal.

The red lines indicate the centre of the linings.

5.3 *Grouting system*

The diameter of the excavation, 15.43 m, will create a void, when the TBM is advancing, outside the precast lining, which has an outside diameter of 15 m. Therefore, this annulus void must be filled by grouting to prevent settlement, create the mechanism whereby the ground loads is applied to the tunnel lining and maintain the shape of the rings.

The TBM has an automatic system of tailskin grout injection so that as the TBM advances the ring annulus is immediately filled. The grout system includes 6 lines (2 in the crown, 2 at axis and 2 in the invert) that connect from the grout pumps to conduits inside

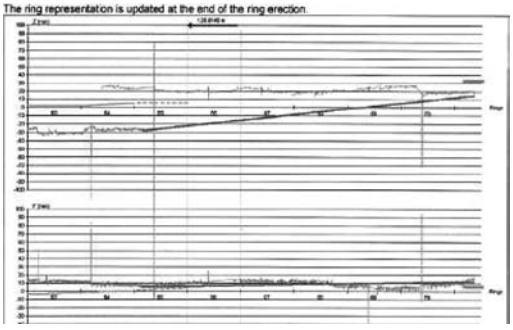

Figure 19. Trajectory screen.

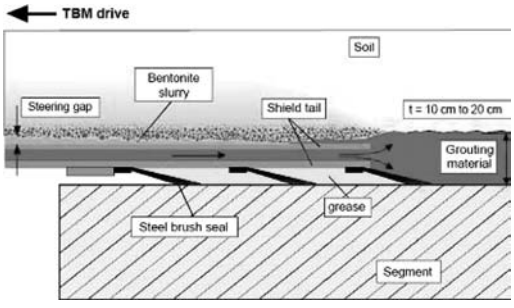

Figure 20. Schematic of grouting through Tailskin.

the tailskin which have outlets immediately behind the brush seals, the grout is pumped by 3 Schwing KSP (ksp20) from 3 grout tanks with agitators.

The grouting pressure is calculated with consideration to the face support pressure for the crown and invert. The grout injection pressure is set and monitored by sensors at the injection ports in the tailskin and programmed into the PLC for the TBM controls. The grout pressures is always set at least 0.5 bar above the slurry pressure, with the 2 lower lines above the invert slurry pressure. The PLC programme is also synchronized for the grout pumping rate to suit the TBM advance speed.

The display in the control cabin on Gantry 1 graphically shows the pressure and volume related to the advance for each grout port. The total volume of the mortar is also graphically recorded throughout the advance.

Initially, replaceable grout tanks were transported to the rear of the TBM by the flat bed trucks and then lifted and transferred to the grout system on Gantry1 by the overhead 50 ton gantry crane. Due to many break downs a transfer pumping system was set up at Gantry 3 for delivering the mortar from normal truck mixers to the holding agitator tanks on Gantry 1.

This type of mortar is always referred to as semi-active (no cement) and has been used successfully in other projects using large diameter STBMs.

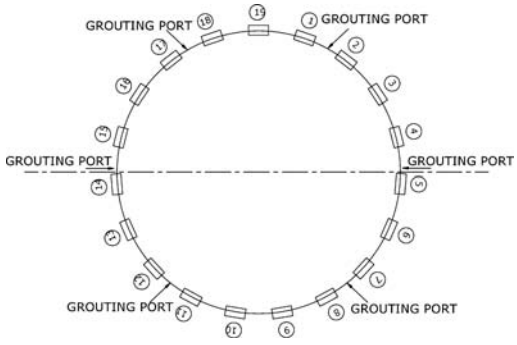

Figure 21. Location of grout ports for Yangtze Tunnel drive.

Figure 22. Grout port at axis of TBM.

Table 1. The mix used per cubic metre is the following.

Material	Design
Fine sand (well graded)	1,180 kg
Lime powder	80 kg
fly ash	300 kg
Additive	3 kg
Bentonite	50 kg
Water	300 kg

The main principle of semi- active mortars relies on the stability of the slice of mortar between the ring and soil, which is reached as soon as cohesion and sufficient shear stress at both interfaces of mortar/ring and mortar/soil is reached, preventing uplift or displacement of the segments.

The 'wringing effect', which results from pressure causing the mortar to expel part of its water, increases its shear stress. Rearrangement and interlocking of the grains inside the mortar when injected under pressure is sufficient to provide the necessary friction at the contact surfaces. Consequently almost immediate stability of the ring is achieved.

This phenomenon relies mostly on the sand grading, since it depends on the interlocking of the different particles in the mortar. Also the shear strength of the mortar indicates the immediate stability of the mortar surrounding the ring.

The mortar should be seen as a means to "lock" the segments against the soil and reach the properties of the soil.

The success of the mortar is to be able to hold the ring in place during the advance. At the same time the mortar should have a long setting time to achieve the required pump ability.

5.4 *Ring type*

The rapid progress in advancement of TBMs in water bearing soft ground such as the slurry TBMs and the Earth Pressure Balance Machines has led to the continual improvements of segmental lining systems for accurate and rapid ring erection and water tightness.

After 1930 precast tunnel segments started to replace the cast iron segments which were used for all the London underground tunnels. With the development of the Hydro shield in Germany rubber gaskets were introduced on the segments for watertightness. Compressed sealed gaskets were first used in 1969 on the New Elbe tunnel in Hamburg, Germany. About the same time tapered rings were introduced for reducing the packing necessary for driving TBMs around curves. Originally, circular packing was placed between the rings on the outside of the curve for allowing the rings to keep square in the tailskin. The other advantage of the tapered rings is that by rotating the ring. Its direction will change in the horizontal and vertical plane, which eliminates the use of timber packing. But the greatest advantage is that the surfaces of each edge of the ring can be in contact, even on straight drives, by rotating the rings and allowing the gaskets to be compressed for watertightness.

The most common type of ring being used for slurry and EPBs are the Universal ring and the 'left' and 'right' rings. The main advantage of the universal ring is that it requires only one set of rings for the drive, where the left and right rings require two types. With one type of ring the segment transportation to the tunnel face is much easier to manage. The left and right rings are sometimes preferred because the key can always be placed above the tunnel axis which allows easier building.

The ring type for Chongming is a 'universal' ring that has a 16 mm taper, opposite to the key, and can be rotated for keeping the ring central in the tailskin. Each precast concrete ring consists of 9 segments and one key. The ring has an inside diameter of 13.7 m, 2 m in width and each segment is 650 mm thick.

Each segment was fitted with compressible waterproof gaskets 60 mm wide which are glued on at the segment yard prior to transporting to the TBM.

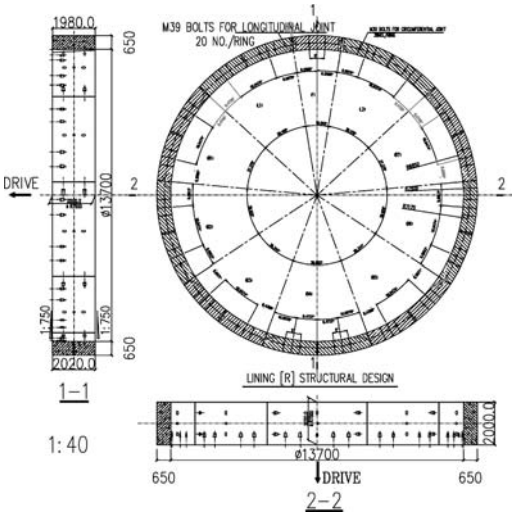

Figure 23. Lining design of Yangtze River Tunnel.

Figure 24. Measuring 'tailskin gaps'.

For additional waterproofing a strip of elastometric gasket was glued on the outside of each radial joint behind the gasket. Each segment was bolted radially and circumferentially with inclined socket bolts of 39 and 30 mm diameter respectively. The inclined socket bolt allows a much safer practice of bolt tightening operations to be carried out under the cover of a fully erected ring and not under segments which are only held by the erector and thrust cylinders.

5.5 *Ring building*

The rings are delivered by trucks to Gantry 3 and then hoisted up, in pairs, by the 50 ton gantry crane and transported along the upper level of the gantries to the rear of Gantry1. The segments are then lowered on to a turntable at the rear of the segment feeder. After rotating the segments on the turntable another gantry cane, segment crane, will lift and place each segment on to the segment feeder, which is located

Figure 25. Erector building 'bottom' segments.

Figure 26. STP.

under Gantry 1. The segment feeder will convey each segment to the erector for building.

To avoid confusion with the logistics, each ring is delivered to the segment feeder with the same sequence of segments. Therefore, depending on the orientation of the ring in the tailskin the first segment is placed at the ram position opposite the key. The orientation of each ring is determined by the PYXIS system in the PLC which is in the control cabin. The tailskin gap, distance between the ring's extrados and the inside of the tailskin, is physically measured at each ram group before the ring erection. This data is downloaded into the PYXIS system and the key position, that will enable the ring to become more central in the tailskin, will be displayed. This information will determine the position of the first segment and ring building will commence.

The TBM is provided with a hydraulically driven, centre free, ring erector which incorporates a vacuum system for handling each 16 ton precast segment. It has a rotation of $\pm 200^{\circ}$ with a rotation speed of 0–1 rpm and is operated using a radio remote control.

Because of the face pressure only the rams corresponding for each segment can be retracted as thrust pressure must be applied on the TBM at all times. Each segment is placed alternating each side of the first segment. After the erector has placed the segment, the corresponding rams are applied with enough pressure for concrete to concrete contact allowing the gaskets to squeeze together with the previous ring. At least two bolts are inserted before the vacuum can be released and returned to the segment feeder for erecting the next segment. All the bolts, radially and circumferentially, are inserted before starting the next advance. The gap left for the key is always measured in case there is damage inserting the key. The key is placed as far as possible into its final position with the erector and then allowing the shove ram to push the key in place for completing the build.

Each ring is checked for shape, plane, lips and steps for quality control.

The ring building on the Chongming tunnels is of a high standard, especially considering the size of the rings. The stepping and lipping of the segments has been kept to a minimum for both tunnels and hardly any cracks are evident. There has been minor leakage through the joints mostly caused by poor gluing of the gaskets.

5.6 *Slurry Treatment Plant (STP)*

The separation plant is provided so that the slurry can be recovered and re-used by separating the spoil from the slurry. The proper desanding and desilting by the plant will ensure that the densities and the slurry rheological properties will maintain constant for safe TBM boring conditions.

The plant's process consists of various operations after receiving the pumped spoil from the TBMs:-

Primary separation – Rotating drum screens receive the spoil directly from the TBM with screens of 8 mm. These screens are continually receiving high pressure jets of water for preventing clogging. The spoil which fails to pass through the screen will directly be transported to a chute and into the muck pit.

Secondary separation – 1st stage: All particles that pass through the rotating screens are immediately pumped from a tank into the primary cyclones (750 mm dia.) for further separation. 2nd stage: These cyclones have a cut point of 80 μm with the smaller particles transferred to the secondary cyclones of 300 mm dia. for separation to 40 μm.

The rejected slurry from the cyclones is pumped to a tank and the transferred to the barges on the river for disposal

The clean slurry is finally pumped into the holding tanks for re-use in the slurry system.

Fresh mud preparation – This consists of a fresh water tank, 2,000 m^3, and a polymer unit.

The main feed slurry pump (Warman variable pump) is housed near the STP and is used for the excavation and by-pass systems.

The slurry type used for the slurry system is water based and drawn directly from the river. Normally bentonite or polymers are used for slurry systems but there

is sufficient natural clay in the alluvial deposits for producing the acceptable properties for the slurry required for these TBMs.

The slurry plant has been successful for the recycled silty clay with very few problems and delays. The plant is easily coping with the sticky, clogging clayey ground without any expected choking problems. The separation has been maintained without the use of polymers with the slurry maintaining its recycling properties.

The slurry is frequently tested and the important criteria are consistent.

6 CONCLUSIONS

A considerable amount of experienced, regarding control and quality, has been gained from driving these large TBMs through the soft clay and silts under the Yangtze River. The TBM's are comfortably excavating through the difficult geology without difficulties with steering, face control, slurry circuit and grout injection. Also, the STP is re-cycling the sticky clay to good effect allowing the slurry to maintain its important function for face support and flow.

The ring building has produced a high quality lining with minimal damage and leakage of the segments. This is the result of good building practice and the precise and reliable grouting during the advance of the TBM.

With this high standard achieved and knowledge gained of large TBMs excavating in adverse conditions, a great deal of confidence will be gained for similar projects in the future.

REFERENCES

AFTES. 1995. *Settlement Induced by Tunnelling.*

Babendererde, S. 1999. Grouting the shield tail gap. *Tunnel & Tunnelling International.*

Bouygues. 2006. *PYXIS Pilot Manual.*

John, O.B. & Kuesel, T.R. 1982. *Tunnel Engineering Handbook.*

The Shanghai Yangtze River Tunnel - Theory, Design and Construction – Huang (ed)
© 2008 Taylor & Francis Group, London, ISBN 978-0-415-47161-9

GFRP reinforcement cage erection technology in diaphragm wall

K.J. Ye & G.Q. Zhao
Shanghai Secondary Municipal Engineering Co., Ltd., Shanghai, P. R. China

D.Y. Zhu
School of Civil Engineering, Tongji University, Shanghai, P. R. China

L. Zhang
Shanghai Secondary Municipal Engineering Co., Ltd., Shanghai, P. R. China

ABSTRACT: The use of glass fiber reinforced plastic (GFRP) reinforcement in underground diaphragm facilitates tunneling shield machine to construct underground diaphragm directly. But because elastic modulus of GFRP is only 1/4–1/5 of steel, larger deformation will occur during lifting, so high requirements of lifting are required when GFRP is used in underground diaphragm. In this paper, reinforcement measures are proposed and implemented in practice. Meanwhile, a new type frame is introduced to replace the old reinforcement. After GFRP reinforcement cage is placed into diaphragm trough, the new type frame can be taken out for recycle and save the cost of truss reinforcement in underground diaphragm. During actual lifting, deformation of reinforcement cage and inner forces of reinforcement and truss are monitored. The results make an agreement with the actual condition of the truss.

1 INTRODUCTION

The Contract T3 of Shanghai Yangtze River tunnel is located at the south side of Changxing Island, including working shaft, cut and cover section, ramp, connections and others. The contractor is Shanghai 2nd Municipal Engineering Co. Ltd. The outer dimension of the working shaft is 22.4 × 49 m, and the depth is 24.7 m. Underground diaphragm with a thickness of 1.0 m and a depth of 45 m is used as the retaining structure. In this project, new material glass fiber (GFRP) is used for the GFRP reinforcement cage replacing part of the reinforcement, which located at the south side of the pit and the opening of TBM arrival. The GFRP reinforcement cage is 44.5 m long, 4.2 m wide and 1.0 m thick. In the longitudinal direction, 2.5 m at the cage end is reinforcement, lower 21.1 m is GFRP reinforcement and 22.8 m is other reinforcement.

Compared with traditional working shaft of tunnel, the using of GFRP to replace reinforcement at the position of underground diaphragm opening of TBM arrival makes it possible to cut through shield wall directly when TBM enters into tunnel, thereby it can avoid the work to cut reinforcement and excavate tunnel gate by manpower. It not only simplifies the construction procedure, speeds up construction progress and reduces construction risk but also reduces strengthening range of ground layer before shield wall and lowers waterproofing requirement between ground layer and shield wall to save investment.

TBM used for the project is the largest one in diameter around the world. In order to ensure it can cut through shield wall smoothly and enter into tunnel, length of single GFRP reinforcement is 21.1 m. It is placed on the middle side of underground diaphragm reinforcement cage, which belongs to TBM arrival end of working shaft.

2 PROJECT CHARACTERISTICS

Compared with normal reinforcement, GFRP has the following characteristics:

- The most prominent advantage of GFRP has high specific strength, i.e. low mass and high strength. Specific strength of GFRP is 20–50 times than steel, so it will reduce structure gravity sharply.
- Shear strength, inter-layer tension strength of GFRP and inter-layer shear strength is only 5%–20% of tension strength, while shear strength of metal is 50% of its tension strength. It makes connection of GFRP structure becomes a serious problem.
- Process on site, such as welding, bending (excluding cutting) can not be done.
- GFRP material has good corrosion protection. It can resist chemical corrosion under acid, alkali, chlorate

and wet environment, which traditional material can not reach.
- GFRP material is generally anisotropic. Strength and elastic modulus at the fiber direction is high while perpendicular direction is low. Compared with steel, elastic modulus of most GFRP products is low, which is only 1/4–1/5 of steel.

Shear resistance and bending resistance of GFRP reinforcement is low, it belongs to characteristics of brittle material. Compared with traditional working shaft of tunnel, the using of GFRP to replace reinforcement at the position of underground diaphragm opening of TBM arrival makes it possible to cut through shield wall directly when TBM enters into tunnel, thereby it can avoid the work to cut reinforcement and excavate tunnel gate by manpower. It not only simplifies the construction procedure, speeds up construction progress and reduces construction risk but also reduces strengthening range of ground layer before shield wall and lowers waterproofing requirement between ground layer and shield wall to save investment.

For this project, because the opening of TBM arrival with GFRP reinforcement and the diameter of 16 m locates middle side of the working shaft and process on site. For example, welding is not allowed for GFRP reinforcement, integral lifting must be used. The safe integral lifting of GFRP reinforcement cage with extra length of 44.5 m and extra weight of 40t is the difficulty and key work of the project. Not even normal diaphragm needs to set special truss reinforcement to enhance its stiffness, quite apart from GFRP with much smaller stiffness. Furthermore, integral stiffness of GFRP colligated with galvanized steel wire can not meet the requirements at all when it changes from horizontal state to vertical state, so special lifting design is needed. In order to ensure TBM can cut through smoothly and enter into tunnel, any steel structures are not allowed to exist in the range of GFRP reinforcement after construction. It requires that truss used for strengthening not only has sufficient strength and stiffness to bear moment and shear force of steel reinforcement cage and GFEP reinforcement occurred during lifting without large deformation, but also can be easily to be removed. So a new type truss is introduced into the project. It is inserted between two GFRP layers (upper layer and lower layer) to support upper layer reinforcement during lifting. After GFRP reinforcement cage is placed into trough, the truss can be taken out for recycle.

Moreover, with respect to actual implementation during construction, GFRP reinforcement cage also has the following difficulties:

- High requirements for trough of under-ground diaphragm. Because there is ○ 23 powder sand layer with the thickness of 18 m which is 1.5 m below the construction site of this project, it brings larger difficulty for the stability of trough wall. Truss inside of GFRP reinforcement cage must be removed while lowering. Collapse is not allowed in trough.
- GFRP reinforcement is connected with reinforcement. In the view of connection of GFRP reinforcements themselves during design, so main reinforcement is designed to 21.1 m and fabricated by integer. According to investigation, connection of GFRP reinforcement is only limited to steel wire which is generally placed at the bottom of reinforcement cage before. Colligated with steel wire can bear gravity, but for this project, there are still about 20t cage for reinforcement storage under GFRP reinforcement cage. The connection method is obviously too weak.
- From the whole construction process, GFRP reinforcement is changed from horizontal state to vertical state, which is the worst case during the whole lifting process due to weak bending resistance of GFRP.

3 LIFTING TECHNOLOGY OF GFRP REINFORCEMENT CAGE

In accordance with above difficulties of construction of GFRP reinforcement cage, we adopt the following detailed measures to solve these problems respectively:

- To solve collapse of diaphragm wall completely, besides designing vacuum and larger caliber trough drainage well and enhancing slurry ratio, we schedule the construction of eight underground diaphragms with GFRP reinforcements in later period and collect related construction data of normal underground diaphragm to guide the trough construction of GFRP reinforcement underground diaphragm. It is proved by practice that there is no collapse around the 119 under-ground diaphragms constructed.
- For the connection method of GFRP reinforcement and reinforcement cage, we designed steel wire clamp and carried out related tests in Guangzhou to check its reliability. It is proved by test that using two steel wire clamps for each connection is stable and it can bear 3t tension force.
- In the project, reinforcement cage with GFRP is 4.2 m wide and 44.5 m long, the maxi-mum weight is 40t. Integral lifting method is used for the fully welded reinforcement cage with large weight and length and many connections. During lifting of GFRP reinforcement cage, two crawler cranes (one 200t main crane and one 86t assistant crane) are used to lift and they are lifted into trough by 200t main crane. There are three-group main lifting points with

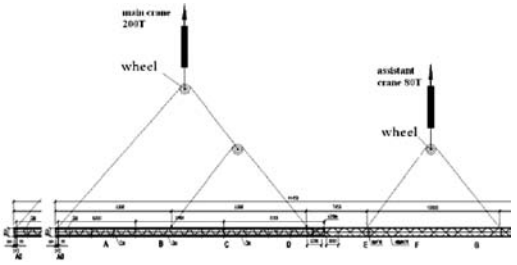

Figure 1. Lifting sketch of reinforcement cage.

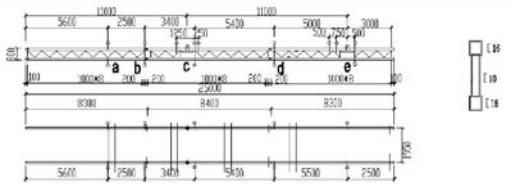

Figure 2. New type truss and measure point arrangement.

interval of 11 m and longitudinal position is on the three pairs of lifting eyes of lifting frame. There are two-group assistant lifting points with interval of 9.3 m. Lifting point is strengthened and welded on longitudinal reinforcement frame. The five-group lifting points can be seen in Figure 1.

In order to ensure stiffness of reinforcement cage without longitudinal frame, insert new type lifting truss into reinforcement cage (Fig. 2). The lifting truss is made by two trusses with interval of 1.95 m; each truss is 25 m long and assembled by three segments. Each segment is connected by dowel. Upper and lower chords are assembled by I-16 channel steel. Web rod is I-10 channel steel and welded continuously. To ensure integrity, three or four horizontal trusses welded to longitudinal reinforcement are placed as well. Lifting eyes are set on the truss. When reinforcement cage is lifted vertically and reaches related position, the connection truss can be removed and finish reinforcement. After reinforcement cage enters into trough fully, take out truss for recycle.

The deformation of GFRP reinforcement cage is very small during lifting which proves the feasibility of the lifting method. As shown in Figure 3.

4 DEFORMATION AND INNER FORCE MONITORING DURING LIFTING

4.1 *Monitoring method*

In order to inspect the feasibility of longitudinal truss in the underground diaphragm reinforcement cage, deformation and stress monitoring of the new

Figure 3. Lifting of GFRP reinforcement cage.

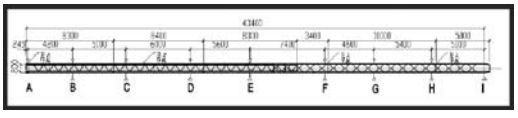

Figure 4. Measure point arrangement of reinforcement cage.

type truss and reinforcement cage during lifting are implemented, respectively.

Strain foil is used for strain measure (Fig. 4). Strain foil is placed on the longitudinal reinforcement. Along the length direction of reinforcement cage, strain foil is placed at 8 positions. For each position, there are 3 measure points at upper layer, which are placed close to new type truss and on the centre line of reinforcement cage. And 2 measure points at lower layer, which are placed on the most outside longitudinal reinforcement of the lower layer. 40 strain foils were used on reinforcement cage.

Displacement measure outside plane is done by total station or ruler. Measure points are placed on the two most outside longitudinal reinforcements of the lower layer. Along the length direction of reinforcement cage, eight-group measure points are placed. As shown in Figure 4. Five measure points are placed along transversal direction and 40 measure points are installed in total.

Place one group measure points close to the 2 and 3 lifting points of upper and lower chords of truss in the middle of neighboring lifting points and at the connection part of each truss segment, respectively. For each truss, 5 groups are placed on upper and lower chords and paste strain foils on the web rob near lifting point. Each truss has 4 Strain foils and they are pasted on the web of channel steel. In order to verify each other, place 3 strain foils on the upper and lower flange and web. Here 28 measure points and 36 strain foils are used in total.

Figure 5. Lifting of reinforcement cage.

Table 1. Actual elevation of each measure point on reinforcement cage.

	Elevation (m)					
	Case 1 (0°)		Case 2 (30°)		Case 3 (60°)	
Cross Section No	East side 1#	West side 2#	East side 1#	West side 2#	East side 1#	West side 2#
A	11.91	11.84	30.38	30.39	46.85	46.72
B	11.79	11.72	28.42	28.40	43.18	43.22
C	11.69	11.62	26.19	26.19	39.17	39.10
D	11.59	11.50	23.45	23.48	34.14	34.16
E	11.51	11.42	20.97	21.04	29.59	29.60
F	11.51	11.41	17.74	17.75	23.47	23.45
G	11.50	11.45	15.80	15.72	19.85	19.58
H	11.54	11.53	13.41	13.51	15.28	15.26
I	11.56	11.57	11.45	11.46	11.48	11.56

After reinforcement cage is lifted up, keep still and measure strain of each point at the position of 0°, 30°, 60° and 90° and measure displacement of each point at the position of 0°, 30° and 60°. See Figure 5.

4.2 *Monitoring result*

4.2.1 *Vertical deformation of reinforcement cage*

Actual elevation of each measure point on reinforcement cage can be seen in Table 1.

Takes the position of reinforcement cage before lifting as an example, vertical deformation of each measure point under each case can be seen in Figure 6–8. From deformation figure of each case, we can see that relative deformation between the end and middle of reinforcement cage, and the value is about 350 mm and 1/127 of the length of whole reinforcement cage 44.5 m. If the number of lifting points

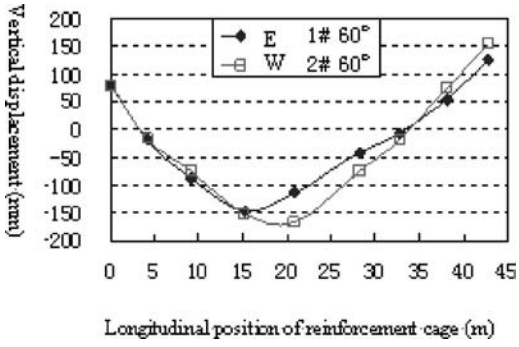

Figure 6. Deformation of each measure points under case 3.

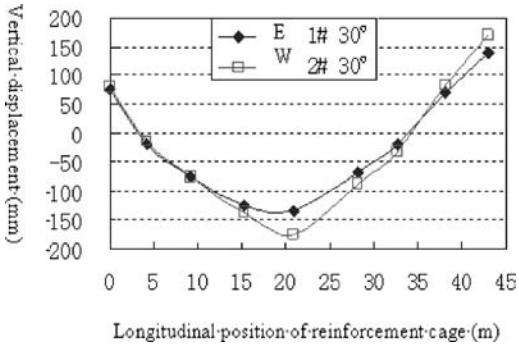

Figure 7. Deformation of each measure points under case 2.

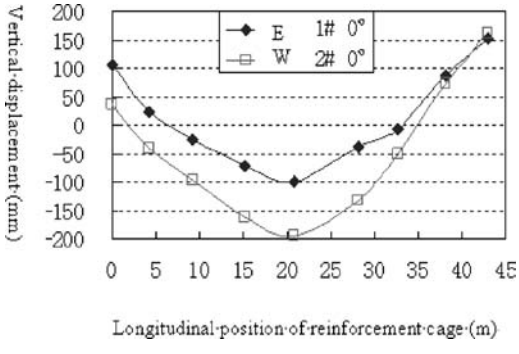

Figure 8. Deformation of each measure points under case 1.

increased, deformation of reinforcement cage would reduce further.

4.2.2 *Strain of each measure points on reinforcement cage*

Take case 1 as an example, strain of each measure points on the reinforcement can be seen in Figure 9. Actual maximum strain obtained is 7.06×10^{-8}, which equates to the stress of 145.4 MPa. It is less than the yield strength of steel .In other words, the truss is

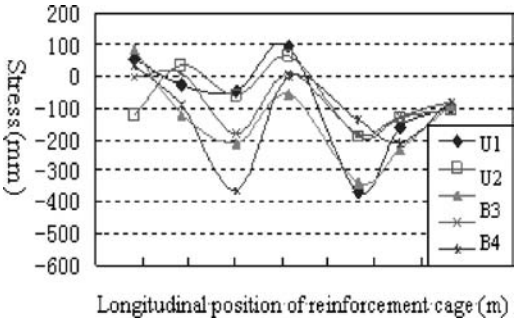

Figure 9. Strain of each measure points under case 1.

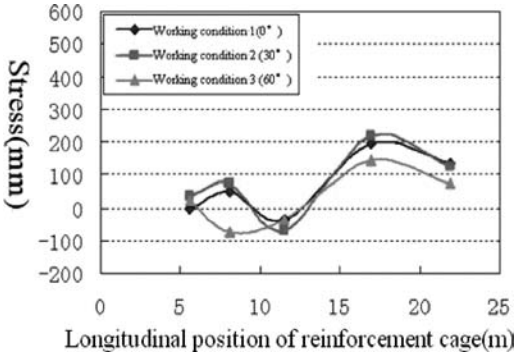

Figure 10. Strain of lower web rod of east truss.

always working under elastic state and without plastic deformation during the whole lifting.

4.2.3 *Strain of each measure point on new type truss*

Figure 10 are the strain of lower web rod of east truss and west truss. Because the gravity centre of truss is not accordant with reinforcement, as a result, the force of west truss is larger than the east truss. From the variation of case1 to case 3, strain of each position in the truss does not change obviously. Maximum strain is 6.0×10^{-8}, and the strain equates to the stress of 126 MPa. It is less than the yield strength of steel, so the truss is always working under elastic state during the whole lifting.

5 CONCLUSION

The paper makes a positive and practical discussing about lifting of working shaft underground diaphragm GFRP reinforcement cage in contract T3 of Shanghai Yangtze River Crossing. Some useful experiences are obtained and expected to provide reference for similar projects in the future. Meanwhile a new type truss is introduced to replace the truss reinforcement in underground diaphragm reinforcement cage. After reinforcement cage is placed into trough, the truss can be taken out for recycle; thereby reinforcement account and cost can be reduced. The new type truss introduced in the paper is used in the lifting of underground diaphragm reinforcement cage with the length of 44.5 m. Meanwhile, vertical deformation of reinforcement, strain of reinforcement and truss are monitored during lifting. Monitoring results indicates that during lifting, deformation of reinforcement is not larger; reinforcement and truss are both in elastic state. So the new type truss is feasible and worthy of popularization.

REFERENCES

Wang, X.C. & He, Jiang. 2003. Lifting technology of reinforcement cage in the construction of underground diaphragm of subway. *Railway Engineering*: 26–27.

Zhao, X.B. et al. 2004. Erection of reinforcement cage for 43.0 m extra deep slurry wall in Huaihai road subway station of shanghai M8. *Building Construction*: 10–11.

The Shanghai Yangtze River Tunnel - Theory, Design and Construction – Huang (ed)
© 2008 Taylor & Francis Group, London, ISBN 978-0-415-47161-9

Importing of shield machine of Shanghai Yangtze River Tunnel and Bridge

J. Xu
The Shanghai Shield Equipment & Engineering Co., Ltd., Shanghai, P. R. China

ABSTRACT: The Shanghai Shield Equipment and Engineering co. ltd, (SMSC) is a professional company in China to provide the shield machines. The company has totally 32 Earth Pressure Balance Shield Machines of various brands with the diameter of 6,340 mm. During the past decade the main operation of SMSC is importing of the shields and management technology of the equipment and has rich management experience in the shield tunnel field. Commissioned by the Shanghai Changjiang Tunnel and Bridge development Co., Ltd. (CTBC) SMSC successfully imported two Φ 15,430 mm mix-shields of Herrenknecht (HK) for CTBC as the representative of the client. The whole process of the importing project as well as the main service working contents is introduced. Finally the success and failure in this project are summarized.

1 PURCHASING OF THE EQUIPMENT

1.1 *Prior period preparation*

After carrying on the equipment importing project from CTBC in the year of early 2004, SMSC immediately organized and set up a working team, leaded by the general manager and the technical vice manager themselves, in which the mechanical and electrical members were selected from the various departments. During the second half year of 2004, the working team made sufficient communication with CTBC to know their requirements, and mean-while SMSC collected the basic data and information of the project including the technical dimension of the tunnel, the geological condition, the form of the segments and the road element, construction basic condition and the technical requirements etc. As the operation part of the shield machine, STEC prepared the technical part of the equipment-bidding document including the detailed requirements of the design, manufacture, assembling, commissioning, acceptance, scope of supply and service during the process. The detailed requirements of the general design and configuration of the shield were all made clear in the technical document. Meanwhile the document also regulated the technical service, responsibility and duty that the supplier should carry out during the process of the project.

While SMSC was preparing the technical document, the company committed Shanghai Sun Power Bidding Company as the bidding company, CNTIC as the importing representative and SMCEC as the consultant of the importing representative. All these three companies drafted the business part of the bidding document to regulate the bidding form, satisfaction and the basic terms of the contract documents.

1.2 *Bidding*

The final bidding document was issued on China Bidding Website in Dec. 2004 by the bidding company to invite international public bidding with regard to this project. Finally, 4 bidding documents were received from the suppliers of HK and Welter from Germany, IHI and Mitsubishi from Japan. All bidding documents of the suppliers included both business and technical bidding. In January 2005, the result of the business bidding was opened in terms of the quotations of the suppliers. The quotations were respectively approximate (estimated by RMB) 90,000,000 Yuan for IHI, 80,000,000 Yuan for Mitsubishi, 60,000,000 Yuan for HK and 40,000,000 Yuan for Welter.

1.3 *Bidding clarification and evaluation*

After opening the business bidding, the technical tendering documents of 4 suppliers were evaluated by an expert panel with rich experience in shield industry. Besides, the bidding company organized several clarification meetings together with the relevant companies including the client, client representative SMSC,

the construction company STEC for the suppliers to clarify their tender documents. The clarification meeting was carried out by question & answer style. Through these bidding clarification meetings the Chinese parts communicated sufficiently with the suppliers and got know the basic configuration, scope of supply and the capability of the main systems. Meanwhile the qualification and manufacture ability of their Chinese partners selected by the suppliers were also investigated.

As mentioned above, the business quotation of IHI and MHI were higher than HK and Welter. According to the principle of bidding, the precondition to get the bidding is that the technical capabilities should firstly satisfy the technical requirement. With this precondition, the lowest quotation could get the acceptance of bid. Although the quotation of Welter was the lowest, yet their technical documents was not satisfactory. With the principle of the bidding, the expert panel decided coincidently that HK got the acceptance with their highest capability in technical documents and comparatively lower price.

1.4 *Contract negotiation*

After opening the acceptance of the bid, the Chinese team including the client, the representative, SMSC, the agency and the construction company immediately met with HK. The both parties of China and Germany entered contract negotiation period. The both parties discussed for the terms of the contract. The construction company as the future user of the machine brought forward more detailed requirements in the technical capability and the configuration. Especially that capacities that would influence the construction process were mentioned in the technical negotiation. The both parties negotiated for the technical specification document provided by HK and modified the contract technical document in order to satisfy the requirement in the bidding document. In addition, the Chinese parties brought higher requirement for the delivery and penalty condition of Herrenknect to ensure the time schedule of the project. With the agreement of the both parties, the purchasing contract with HK was signed on 8th February 2005. The contract price was in the sum of USD 60,757,060.00 for the equipments and Services supplied by the supplier generated from abroad and RMB 86,358,611.00 for the equipments generated from domestic.

1.5 *Design liaison*

Considering the time schedule, HK started to enter design period immediately after the contract. Meanwhile HK contacted and communicated with the Chinese parties actively. They discussed the technical problems encountered during the design process. The main contact form was mainly by fax and E-mail aiming at solving the particular problems. During this period, SMSC pointed the special person to contact with all the relevant companies. All the messages were delivered by SMSC. Besides, the both parties convoked the design liaison meetings for several times in China and in HK German plant from February to November 2005 during the whole design process as well as the manufacture period. The key technical problems were discussed and solved through the meetings of both parties.

During the first stage of the design process, HK provided the primary design drawings to introduce the general layout and structure. The details of general configuration, design as well as the requirement of dimensions and layout of the equipment for transportation, general configuration of the main systems, general design concept of the electrical system etc. were all discussed. After receiving the confirmation of the Chinese parties for the primary design, HK started the detailed design. During this period, several meetings were carried out in Shanghai to exchange opinions to improve the capacity of the shield machine. Some additional items were complemented and the relevant cost excluded in the former contract was also confirmed in May 2005.

While the German part started the detailed design, SMSC went on to contacted actively with the client, HK and the construction company to keep the update of the relevant information. Regarding the particular techniques, the written confirmation documents and the both sides meetings was needed to confirm the agreement. In October 2005 the Chinese parties set up a working group to visit HK plant in Germany and attended the design meeting. In that meeting, the agreements on electrical systems as well as other special requirement were achieved. Thus the key technical problems of the equipment basically got confirmation and the general design was also confirmed. Through the detailed design, the globe purchasing was carried out by HK including the raw and processed material, structure element machining.

Along with the design stage entered the last period, HK started to purchase massive raw material and parts and machine in various factories. In September 2005 HK began to prepare the raw material of part structure elements and carry out the manufacture of the equipment completely. The communication on the design was anyway continued during this stage. And in this period the main purpose of the meeting was to discuss and confirm the technical modifications.

Purchasing of equipment is the first step of the importing project, the serial work in this period is to create a good foundation f and reduce the difficulties and trouble as possible or the following work. The equipment ability was definitely established in the equipment bidding progress and continued in the

evaluation and contract negotiation periods, when the equipment requirements was sufficiently sufficiently presented to reduce and avoid the technical change after the signature of the contract. During the design liaison period, many efforts were made through more detail, the confirmation and prompt revise to avoid the error in the manufacturing period. Anyway, through the effort in the purchasing period the general ability of the equipment was confirmed, which provide sufficient assurance for the importing project.

2 SUPERVISION OF EQUIPMENT

As the consultant of the client, the supervision of the equipment is a very important part, which last the longest time and ran through the whole process of the equipment manufacturing. From the machine was processed in the manufactory until the final acceptance. It was divided into two stages as plant supervision and on-site supervision. The main work of the supervision was supervision, management and controlling of the progress and the quality of the equipment manufacturing. The principle and the rule of the supervision were based on the outline and detailed rules of manufacturing supervision regulated in the purchasing contract. The content, requirement of the supervision and appointed the guiding requirement and principle of the supervision were all described in the purchasing contract.

From the beginning of the supervision, SMSC set up the Changjiang Tunnel & Bridge Project department and assigned the machinery and electrical technician to supervise in the manufactory and on-site. From now the last second part of the contract between SMSC and the client, the manufacturing supervision, was executed by the project department.

The manufacture of the machine was carried out in various areas in the world, among which the structure parts of the shield body and the back-up were manufactured by STEC, which is the Chinese partner of HK. The structure elements such as the segment feeder, the inverts and the various pipes were produced in China. The cutter disc, man lock, main structure elements were manufactured in HK plant. The other main parts such as the main driver, the cylinder system, hydraulic pump station, erector and slurry system etc. were all purchased globally, the main site of the manufacturing was at the plant of STEC and the plant of HK.

2.1 *Supervision in manufactory*

2.1.1 *Supervision in foreign country*

In November 2005, along with that HK carried out the equipment manufacturing, SMSC appointed technician to Germany to supervise in the HK plant. During this period the main work of SMSC was to supervise the machining process of the cutter disc, man lock etc., the assembling process of the important part such as main driver and the erector. Meanwhile a close attention should be paid to the packing and boxing of the parts delivered from HK plant. In addition during the supervision SMSC made three important tests with Bouygle, which is the consulting company of the construction company. The tests included blue test of the cutter driver, of emergency sealing and of changeable cutter head, to ensure that the key working procedures could be controlled during the process of the manufacturing and satisfactory the requirement of the supervision in manufactory.

2.1.2 *Supervision domestic*

Having completed the task of supervision in HK German plant, SMSC appointed technicians to the plant of STEC and started the supervision work there.

The main task of supervision domestic was:

- Supervising and urging HK to make out and modify the working plan, track the execution plan during the whole process.
- Process controlling on the manufacturing quality according to the detailed rule of the manufacturing supervision: Machining and manufacturing of the shield body, back-up and the structure of the parts were made in china. Checking and controlling the material, dimension precision and welding quality. Checking the proposals of main assembling procedure such as main driver assembling, erector assembling and cutter disc assembling, and supervising the execution.
- Acceptance and storage of the parts delivered from overseas.
- Supervising and urging HK to handover various technical documents in accordance with the contract.
- Supervising the equipment commissioning of HK.
- Cooperating with the client to prepare and improve the commissioning and acceptance document with HK and JV, and organizing to accept for the assembling, commissioning in the manufactory in accordance with various systems.

The main important dates in the manufactory was as follows: S-317, on 16th March 2006 the main back-up structure was assembled, on 28th April HK started commissioning and acceptance, on 29th June the acceptance in manufactory was finished, on 8th May the commissioning of cutter disc was finished and the machine began to be disassembled and then transported to the construction site. S-318, the manufactory acceptance started on 21st August, on 2nd September the cutter disc and the relevant items of body disassembling were finished, and then HK started to transport the cutter disc and the body on the same day.

Through commissioning in the manufactory, the capabilities of the machine were inspected and the main problems of the machine were revealed, which may bring much difficult to the assembly in the shaft in future.

2.2 *Supervision on-site*

2.2.1 *Assembling commissioning and acceptance*

Along with that S-317 was transferred to the construction site, SMSC project department appointed technicians to the construction site. The assembly on the site was the duplication process of that in the manufactory and the on-site supervision was also the continuance of that in the manufactory. But due to the delay of part systems and acceptance in the manufactory, the on-site assembly was also delayed. It became a main task for the supervisors to solve the delay problems in the manufactory.

The important time dates of the on-site assembly were: S-317, the shield body was installed in the shaft on 30th May 2006, the main driver was installed on 9th June, HK started to assemble the back-up steel structure on 30th June, the cutter arms were installed and the welding started on 10th July, the commissioning started on 23rd August, and HK finished the main systems acceptance and the advance of shield on 23rd September. S-318, the first part of shield body was installed in the shaft on 2nd October, the erector was installed on 12th, and the main driver was installed on 13th October and started commissioning on 7th December, the machine started to advance on 5th January.

To ensure the project time schedule, after finishing the commissioning and acceptance of the main systems, the relevant parties has confirmed that the machines had the quality and capability to advance, so the two shield machines would start to advance.

2.2.2 *The final acceptance*

The commissioning and acceptance in the manufactory and on-site shaft were the test on the functions of the shield machine. During this period, the working conditions and circumstance was concerned more. The information collected by the supervisors were submitted to HK for providing technical service. On the other hand the supervisors supervised HK to solve the left problems in the process of the shaft acceptance. Combining with the problems proposed by STEC during the construction process; the final acceptance was completed with the cooperation between supervisors and clients.

Equipment supervision is a very important executing process during the equipment importing, which includes the whole process from the purchasing, manufacturing, assembling and commissioning and the final advancing on-site. The whole manufacturing process should be supervised to find the defect of the equipment and to inspect the equipment ability. Additionally, as the representative of the client, SMSC cooperated with the client to manage the manufacturer through supervision, which is another strong assurance for the project.

3 MANAGEMENT OF ADVANCING

When the machines started to advance, the client continued to commit SMSC to manage the machines during the advancing period due to the need for the management of the client. Considering the advancing process, the project department prepared a new working content according to characteristics of the shield advancing to improve the service.

- Inspecting and checking during the advancing process, urging the operators to drive the machine according to the operation instruction, finding out and stopping the action that the operators disobey the rule.
- Urging the construction company to drive the machines according to the 'balance construction' concept and ensure four hours one day to maintain, and urging the workers to maintain in accordance with the HK maintenance instruction.
- According to that the breakdowns, a regular summary should be made to make suggestion for the client to operation and maintenance.
- Finding the causes of the breakdown and providing the solution of the breakdown cooperated with the technician of HK, construction company and other relevant companies.
- Participating to judge and confirm the responsibility on the breakdown and providing the precaution solution and proposal considering the breakdown mechanism to avoid the breakdown.
- Confirming the process of the spare parts change and the supply of the grease, statistic and analysis the consumption of the spare parts at regular time and making sufficient argumentation.
- Collecting, statistic and analyzing the place and the type of the breakdown, closedown rate during equipment breakdown, consumption of the spare parts and oil material, and bring forward the comment and advice to improve the operation repair and maintenance of the system etc.

During the whole process, we carried out the equipment management and the management level was improved continuously in the practice so that the equipment management became mature day after day. With the management during the equipment advancing process, the situation of the shield, the operation state, the breakdown, the management of spare parts and state of consumable applies could be supervised

and controlled by the owner. Meanwhile the statistical analysis reports provided regularly by SMSC could be used as the reference to improve the operation techniques.

4 SUMMARY OF PURCHASING PROJECT

SMSC accumulated and gained much experience in the process of participating the project. We make a summary from various aspects for the project to be used as reference for the future work.

4.1 *Organization and management*

It is the first time for SMSC to carry out the purchasing projects of the largest mixed shield machine in the tunnel industry. The company paid high attention to the project during the whole process with elaborate preparation and working arrangement.

During the bidding period, the sufficient inspection and research were performed by SMSC to satisfy the requirement of the project in terms of equipments. The communication with relevant design and construction companies was found a useful way to reach the agreement on the requirement of the shield machine in the tender document.

During the period of bidding clarification and contract negotiation, the general manager and the technical manager all participated the bidding process and attended the meetings to negotiate with HK. With the participation of the company leaders SMSC revealed its business and technical experience sufficiently. On one hand the company leader applied the bidding rules reasonably through the mature and excellent negotiation skills for the client to purchase the equipments with high ratio of price and capability.

During the design period after bidding, SMSC became the hub among the units that participated this project. The requirements and message of various parties were all transmitted by SMSC. SMSC appointed the special person to take charge of liaison to ensure the opinions from various parties could communicate without delay. Meanwhile SMSC arranged technician with rich experience to organize and attend the technical liaison meetings. The sufficient communication in this period created the favorable technical base of the future manufacturing.

And during the future supervision and advancing management periods, SMSC set up the project department specially and assigned the excellent technician in the company to take this role. The project department was also assisted by the company, the technical department and the quality & security department while it carried out the project.

Besides we followed the guide of the contract in the purchasing project and set up a set of mature system in the department management. The work system included the daily, weekly and monthly record report, the management system of written document exchange, meeting organization and meeting minutes system, statistics, analysis and tracking record, various working report system, etc. All these management systems ensured the normalization and effectiveness of the work on site

4.2 *Technical summary*

While reviewing the whole process of assembling, commissioning and acceptance on site, the project progress delayed much. The time of the project was sacrificed in some degree in order to ensure the engineering security and the equipment quality with the largest and unprecedented two shield machine in the world. But during the manufacturing process there were still a lot of shortages as follows: the preparation of proposal was not in time, less estimation of the difficulties, weak foresight, unclosed organization, or less experiences that the project met many troubles. The problems happened during the process have been summarized from technical point of view.

- Air chamber: due to the less time of the project, all the parties paid attention to the progress of assembly of the shield body parts but neglected the assembly quality and the protection of the seal. Surely such problems as the pipes through slurry chamber, the welding quality of the connection between flange and valve. All these became the potential trouble to the sealing commissioning of the slurry and air chamber.
- Positioning of the shield body and assembly of the tail skin: the positioning of the bottom part of the middle shield body directly affect the position of the shield tail skin. HK has not thought over or analyzed the shield awl angle and did not accept the suggestion of STEC neither. So the result was that there was no allowance under the bottom of tail skin, which brought unnecessary trouble to the commission of the tail skin.
- Back-up structure: the shield back-up structure has large volume, long span and heavy mass, which was difficult to be assembled. The new changed bolts were already damaged due to the assembling method was not suitable. Massive labor, material resource, financial capacity and much precious time were wasted by changing the bolts.
- Emergency sealing: HK did not take into account the orientation of the inflation connection while the emergency sealing was pre-installed. Mean-while the sealing was laid on the ground for long time, however, no protection was undertaken.
- Lifting of main parts: A lot problems were encountered on-site when the parts were being lifted. For

instance the main bearing was collided during the lifting process.

- Cutter disc: HK did not consider the proposal to turn over the cutter disc and it was very difficult to lift the cutter into the shaft to assemble, which delayed the assembling circle.
- Pipes: there were many hydraulic pipes, tubes of grease pipes in the shield, which had no designed rub protection at the structure corner and surface. All these would easily make the pipes burst.
- Commissioning and acceptance: there were many items left from the manufactory acceptance that should be reformed. But during the acceptance on-site, HK has not done so that the items need to reform were the same as those in the manufactory. Further more HK often apply to accept while many systems had no condition to be accepted, the work schedule of HK were not serious and HK did not carry out the plan after handing over the working schedule.
- Telling intention: HK could not communicate with the partner on-site and the telling intention was unclear, so the cooperation between them was hard, which brought many troubles to the assembling and commissioning.

4.3 *Service summary*

Generally the main work of SMSC is to provide technical service for the client. But there were a few problems during the service process. We also make prompt change and improvement according to the actual situation of the construction site. Furthermore we accumulated and abstracted the working experiences in the practice, which could be the reference for future work:

- Enhance the urge of the fulfillment after the plan of HK and the process control in order to find, prepare proposal and solve as early as possible for the problems, and towards the key working procedures we strictly required HK to provide the proposals as early as possible and check their possibilities and enhance the collection of the technical documents.
- Strengthen the activities of the coordination work on site and improve the coordination system and make effort to coordinate the relationship between the various parties. While finding the problems we would report to the commanding head-quarter immediately and report the engineering progress and urge HK to change for the problems in a written form, also copy to the headquarter.
- Assist the client to improve the coordinative work between HK and STEC so that the two shield machine manufacturer could cooperate in deed and achieve the staged object of the two machines.
- In order to satisfy the requirements of the work on site, the project department seek the assistant of the company headquarter and remove sufficient technicians to strengthen the site supervision.
- Enhance the internal management, illustrate and divide the work clearly for the on-site staff, arrange the staff and the working content reasonably and effectively so that all the employees could cooperate with good faith but also take charge individually.
- Make efforts to improve the supervisors' business and technical level. In accordance with the composition structure characteristic of the supervisors and toward the newcomers, the department organized that the matures lead the new ones and the department convokes meeting to organize group communication to reserve technical human resource for work on site.
- While encounter the problems the supervisors should coordinate and organize actively to find the answer and solution proposal as the reference for the client.

5 CONCLUSION

With the effort of all the parties the two machines of Changjiang Tunnel & Bridge has advanced respectively 2,200 rings and 1,500 rings with a satisfactory state. The supervisors of SMSC still take an important role in equipment management on site. During the past years, SMSC has successfully provides the technical service of the whole importing process as the representative for the client. The purchasing project won a good reputation for the company in the shield industries field and created the new fields for the long term development of the company.

REFERENCES

Chen, J.P & Wang, J.X. 2003 Conic fitting in engineering surveying. *Geotechnical Investigation & Surveying* (5).

Wang, J.X., Chen, J.P. & Zhang, C.Y. 2004. Fitting of ellipsoidal surface. *Journal of Tongji University (Natural Science* 32(1):78–82.

Zhou, W.B. 2004. *Shield Tunnel Construction Technology and Application*. Beijing: China Construction Industry Press.

The Shanghai Yangtze River Tunnel - Theory, Design and Construction – Huang (ed)
© 2008 Taylor & Francis Group, London, ISBN 978-0-415-47161-9

Key techniques in cross passage construction of Shanghai Yangtze River Tunnel by artificial ground freezing method

Z.H. Huang
Shanghai Changjiang Tunnel & Bridge Development Co., Ltd., Shanghai, P. R. China

X.D. Hu
Department of Geotechnical Engineering, Tongji University, Shanghai, P. R. China
Key Laboratory of Geotechnical and Underground Engineering, Ministry of Education, Tongji University, Shanghai, P. R. China

J.Y. Wang
Shanghai Tunnel Engineering Co., Ltd., Shanghai, P. R. China

H.B. Lin
Nanjing Design & Research Institute, Sino-coal International Engineering Group, Nanjing, P. R. China

R.Z. Yu
Department of Geotechnical Engineering, Tongji University, Shanghai, P. R. China
Key Laboratory of Geotechnical and Underground Engineering, Ministry of Education, Tongji University, Shanghai, P. R. China

ABSTRACT: This paper gives a brief introduction of cross passage construction of Shanghai Yangtze River Tunnel by artificial ground freezing method and reports on the design of frozen soil curtain and construction plan. Given the unfavorable conditions, many methods are adopted to control the great risk factors during the construction. Key techniques such as drilling of freezing holes, protection of segment opening, thermal insulation of frozen soil curtain and construction monitoring are prudently adopted, which are emphatically introduced in this paper.

1 INTRODUCTION

Shanghai Yangtze River Tunnel, situated at the estuary of Yangtze River and crossing the south branch of it, is part of the planning National Coastal Expressway. Each of the two circular tunnels bears an external diameter of 15 m and internal 13.7 m. The construction is being carried out by Φ15.43 m air pressed slurry shield machine with the digging distance of 7.5 km. In each direction, the tunneling space is vertically divided into two parts, of which the upper part serves as a three-lane highway tunnel and the lower part functions as subway tunnel.

Taking into consideration the evacuation and rescue assistance in emergency and technical service in normal state, every eight hundred meters, approximately, should a cross passage be built to connect the two main tunnels, thus eight cross passages are to be built altogether. Figure 1 presents the general layout.

The cross passages each bears circular section. The structure form of the cross passages and their relative position to main tunnels are shown in Figure 2.

The construction of the cross passages are facilitated by Artificial Ground Freezing Method (i.e. Freezing Method in short) to provide soil reinforcement. Mining Method is adopted in excavation and cast-in-place concrete serves as the permanent lining structure for the cross passages.

The construction takes place below Yangtze River, thus the great technical difficulties and construction risk. The digging of the cross passages mainly encounters soil layers of $[5]_1$, $[5]_2$, $[5]_3$, and $[5]_{3t}$, (see Table 1). Among the involved soil layers mentioned above, $[5]_2$ and $[5]_{3t}$ are silty soil which, under certain hydrodynamic pressure, are very likely to be the hotbed of geological hazards such as flowing sand and piping; while $[5]_3$ layer bears an unevenly distributed quality of soil because of seam and lumped

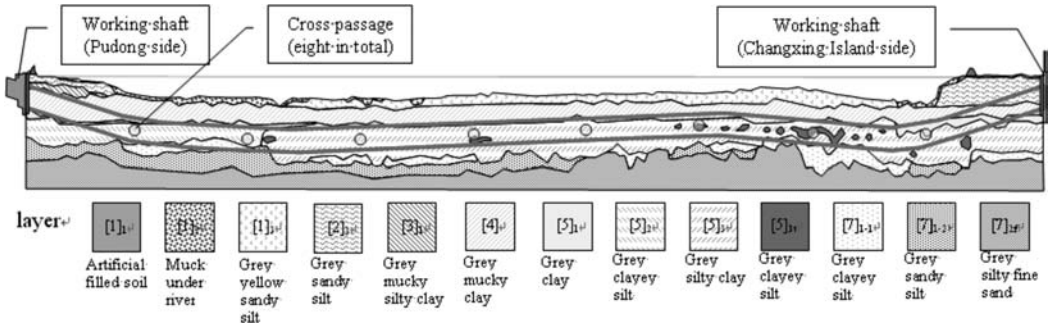

Figure 1. Layout of the cross passages of Shanghai Yangtze River Tunnel.

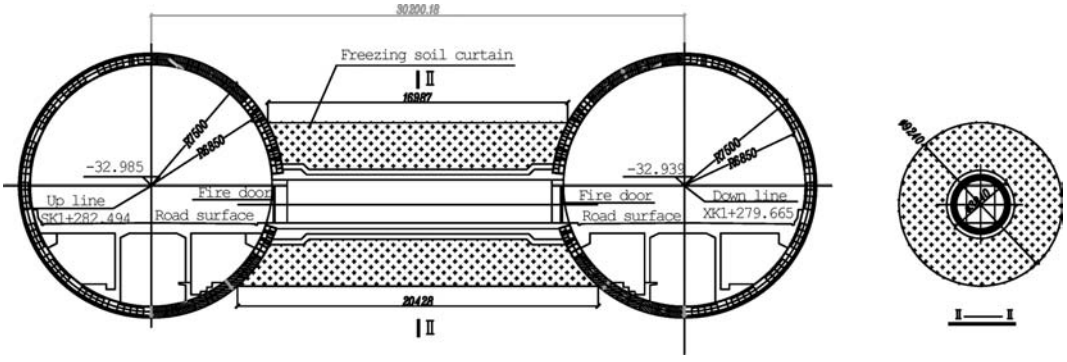

Figure 2. Structural drawing of the cross passages of Shanghai Yangtze River Tunnel.

Table 1. General situation of cross passages of Shanghai Yangtze River Tunnel.

Passage name	Number of mile post	Elevation of passage centerline	Soil layers encountered	Distance between the bottom of passage and underlying confined aquifer
1#	SDK1 + 282.494	−32.985 m	$[5]_2$	0.0
2#	SDK2 + 112.494	−39.246 m	$[5]_2$, $[5]_3$	0.0 – 14.1
3#	SDK2 + 942.492	−38.355 m	$[5]_3$	8.7 – 10.7
4#	SDK3 + 772.478	−35.343 m	$[5]_3$	17.2 – 17.9
5#	SDK4 + 602.486	−32.332 m	$[5]_3$	16.5 – 20.5
6#	SDK5 + 432.499	−29.404 m	$[5]_1$, $[5]_3$, $[5]_{3t}$	12.8 – 23.4
7#	SDK6 + 262.499	−34.351 m	$[5]_3$, $[5]_{3t}$	5.5 – 17.1
8#	SDK7 + 092.499	−35.820 m	$[5]_1$, $[5]_3$, $[5]_{3t}$	17.3 – 18.8

slity sand embedment; also, confined ground water or semi-confined water exist in layer $[5]_2$ and layer [7] (which lies below the cross passages). Given the poor geological conditions, freezing strength and freezing range at the excavation area and its vicinity must be prudently controlled to resist the pressure of confined water throughout the construction process, thus ensure the favorable proceeding of the engineering.

2 DESIGN OF FROZEN SOIL CURTAIN

Taking reference from similar engineering experience based on the position and embedded depth of the cross passages, the thickness of the frozen soil curtain is preliminarily designed to be 2.7 m (2.4 m at the "bell mouth", see Figure 2) and average temperature of the curtain is set as no higher than −13°C. Two circles of

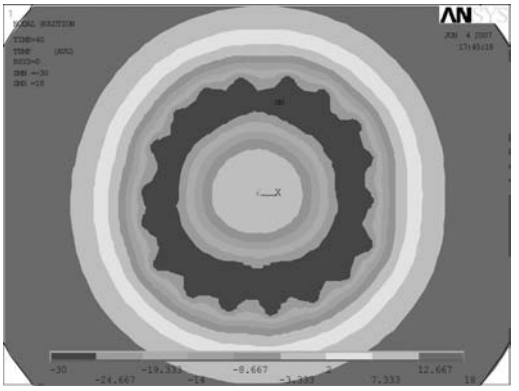

Figure 3. Temperature field of soil after 40 days of active freezing period.

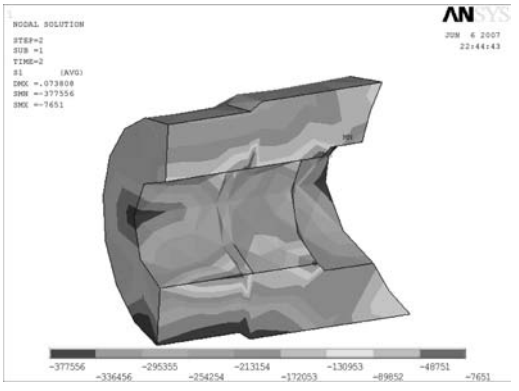

Figure 4. σ_1 distribution of the frozen soil curtain.

40 freezing tubes (22 for inner circle and 18 for outer circle), are designed to form the ice-wall. Drilling of the inner circle and outer circle of the freezing holes are carried out from up line and down line main tunnels respectively. The drilling ends when meeting the segment lining of the opposite tunnel.

Numerical analysis of the freezing process has been applied in accordance with the designed layout of freezing-tubes. The result shows that, after 40 days of active freezing period, the effective thickness of the frozen soil curtain reaches 2.53 m at the "bell mouth" (after excavation) and 2.84 m in the middle part while the average temperature within the range of effective thickness falls to -16.8°C in the middle part and -17.5°C at the "bell mouth". (Refer to Figure 3).

Bearing capacity of the frozen soil curtain has been checked by means of three-dimensional numerical calculation. It turns out that the ice-wall stands stable at the water and earth pressure, with the safety factor for compressive strength no less than 2.0, for bending strength no less than 3.0 and for shear strength 2.0.

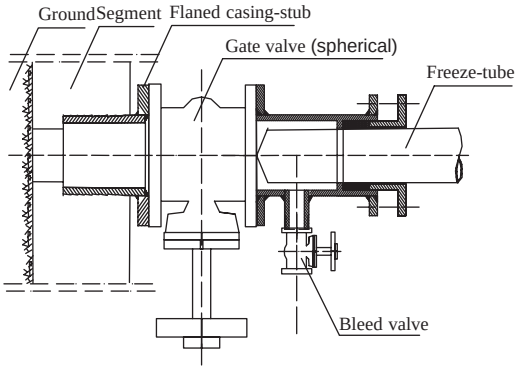

Figure 5. Blow-out preventer

3 KEY TECHNIQUES IN FREEZING METHOD

From the perspective of guaranteeing construction safety, key techniques in construction of cross passages by freezing method lies in how to control the most important risk factors. These construction hazards include water spewing or sandblasting when drilling freezing holes, excessive deformation or destabilization of the tunnel structure when opening the segment lining at connection, and deterioration of the frozen soil curtain or even water inrush during excavation. Concerning these hidden dangers, some key techniques are adopted as introduced below.

3.1 *Drilling of freezehole*

During the process of drilling freezing holes from main tunnel to the outside, water spewing and sandblasting are likely to occur, which may lead to excessive ground loss following by destabilization of lining structure. The main reason of such fault lies in ground loss with slurry circulation of drilling or invalidation of blow-out preventer at the opening.

In order to guarantee drilling safety, reliable blow-out preventer should be applied to reduce the risk of water spewing and sandblasting. Figure 5 illustrates the structure of a blow-out preventer.

3.2 *Protection of segment*

During the excavation of cross passage, part of the segment lining of the main tunnel has to be removed, render the ring structure of lining in a disintegrated state, thus the considerable stress concentration at the opening, which may cause excessive deformation or even destabilization of lining structure. Steel reinforcement is fixed around the opening as a protection device to prevent lining from excessive deformation (Fig. 6).

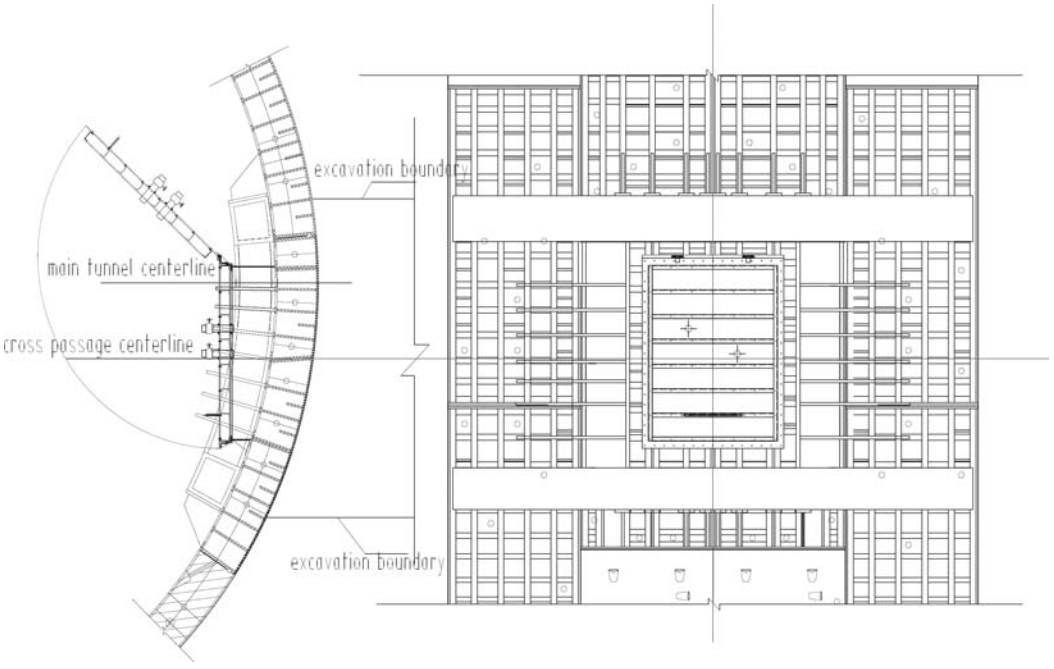

Figure 6. Protection device for segment.

3.3 *Protective door*

Many factors may cause failure of frozen soil curtain, such as geometric imperfection and physical defect of the curtain, error judgment of the characteristics of the frozen soil curtain and improper construction management. In case of uncontrollable water inrush due to failure of the frozen soil curtain, pre-installed protective door can block the path of intruding water to the inside, thus protects the main tunnel and minimizes the loss.

For the convenience of emergency shut-down, the protective door adopted up-down rotating shutting system; in normal state, the protective door is open upwardly and fixed (Fig. 6).

3.4 *Thermal insulation*

Ventilation in the main tunnel may take away the coldness of the frozen soil near segment lining with the existence of concrete thermoconductivity and reduce the refrigerative effect, which may lead to the problem that the frozen soil does not adfreeze to the outer surface of the segment. In that case, severe water inrush accident can possibly take place during excavation. Given the exceptionally large tunnel section in this project, such kind of risk is greatly increased. In order to achieve a sound adfrozen state between segment and frozen soil, surface freezing-tubes are set lying along the inner side of the segment to reduce the temperature of segment, thus weaken the influence of heat exchange caused by ventilation. Surface freezing-tubes are located around the opening and appressed on the inner surface of the segment, covering the area larger than designed range of the frozen soil curtain. Brine circulation in these freezing-tubes is the same as that for the normal freezing-tubes (working in soil). Meanwhile, these surface freezing-tubes are covered with foamed soft polyurethane sheets and further clothed by a layer of sprayed foamed polyurethane to form a sound thermal insulation. Figure 7 presents the general layout of the surface thermal insulation.

3.5 *Construction monitoring*

During the process of freezing, excavation and defrosting, characteristics of the frozen soil curtain are constantly changing. Therefore Freezing Method must be accompanied with construction informationization. A comprehensive monitoring must be adopted to achieve the information of the frozen soil curtain and excavation situation at different stages of construction, especially the information on deterioration of the curtain during time of excavation. Besides, items must be monitored also include parameters on the operation of refrigeration system (esp. the temperature of the brine circulation and the temperature different between delivery and return of brine) together with the load and deformation of the structure (main tunnels and cross

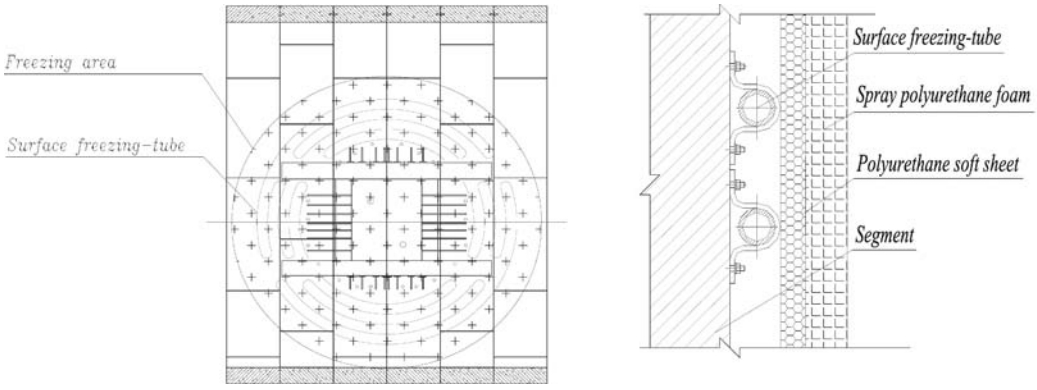

Figure 7. General layout of the surface thermal insulation for segment.

passages). Remote monitoring system is established to fulfill the informationization of the construction of cross passages of Shanghai Yangtze River Tunnel.

3.5.1 *Major monitoring items and methods*

3.5.1.1 Soil temperature

Strength of the frozen soil depends on the temperature, while the thickness and shape of the frozen soil curtain also revealed by soil temperature. Therefore, the monitoring of characteristics of the frozen soil curtain mainly comes down to the monitoring of soil temperature.

Soil temperature is measured by temperature sensors embedded into pre-drilled temperature holes in involved soil layers. The measuring devices are made of digital temperature sensors sealed into thermometric electronic cable, which connect with bus network and further to the computer terminal.

Seven temperature holes are set for cross passage #1, namely C1 to C7 respectively (Fig. 8). The arrangement of these temperature holes are designed to take the responsibility of monitoring during all freezing, excavation and defrosting period.

Besides, temperature sensors are also mounted on the stress sensors for the cross passage structure, such as earth pressure cells and steel meters. These temperature sensors serve as accessorial measurement during defrosting and when analyzing the influence of hydration heat of concrete on the frozen soil curtain.

3.5.1.2 Brine temperature

The temperature different between delivery and return of brine indicates the heat exchange between freezing system and soil layers, as well as operation state of the refrigeration system. More importantly, abnormal value of the temperature drop between delivery and return of brine can be quite an immediate warning of the malfunction brine circuit, thus guarantee the designed freezing process.

Digital temperature sensors are also adopted here and packed into stainless steel shells which are suitable fro the installation in brine tubes. Signals are transmitted to the computer terminal by connections of bus network and lead wires.

The sensors are mounted in brine mains and every set of circuit that has a series connected refrigerator to measure the temperature of brine main and these circuits.

3.5.1.3 External and internal force of the structure of cross passages

Stress sensors are used to observe the load and deformation of the cross passage structure after construction. Earth pressure cells are placed at the outer surface of the cross passage structure (i.e. interface of the passage and the soil layer); while steel meters are embedded into the concrete structure. For each cross passage, monitored sections are located at the middle of the length of the passage and its connection with two main tunnels.

3.5.1.4 Others

Many other items are monitored during the construction, such as parameters of the freezing system, brine flow, temperature of frozen soil at the excavation face and convergence of the passage.

3.5.2 *Monitoring system*

Remote monitoring system for informationized construction by freezing method is established to carry out the monitoring of freezing system, brine temperature and soil temperature. The layout of the temperature sensors employs 1-wire Bus network, in which sensor bus gain access of data transmitting module and then connect to the host computer through RS485 bus. Given the considerable distribution distance of the eight cross passages, RS485 signals are transmitted by optical fiber.

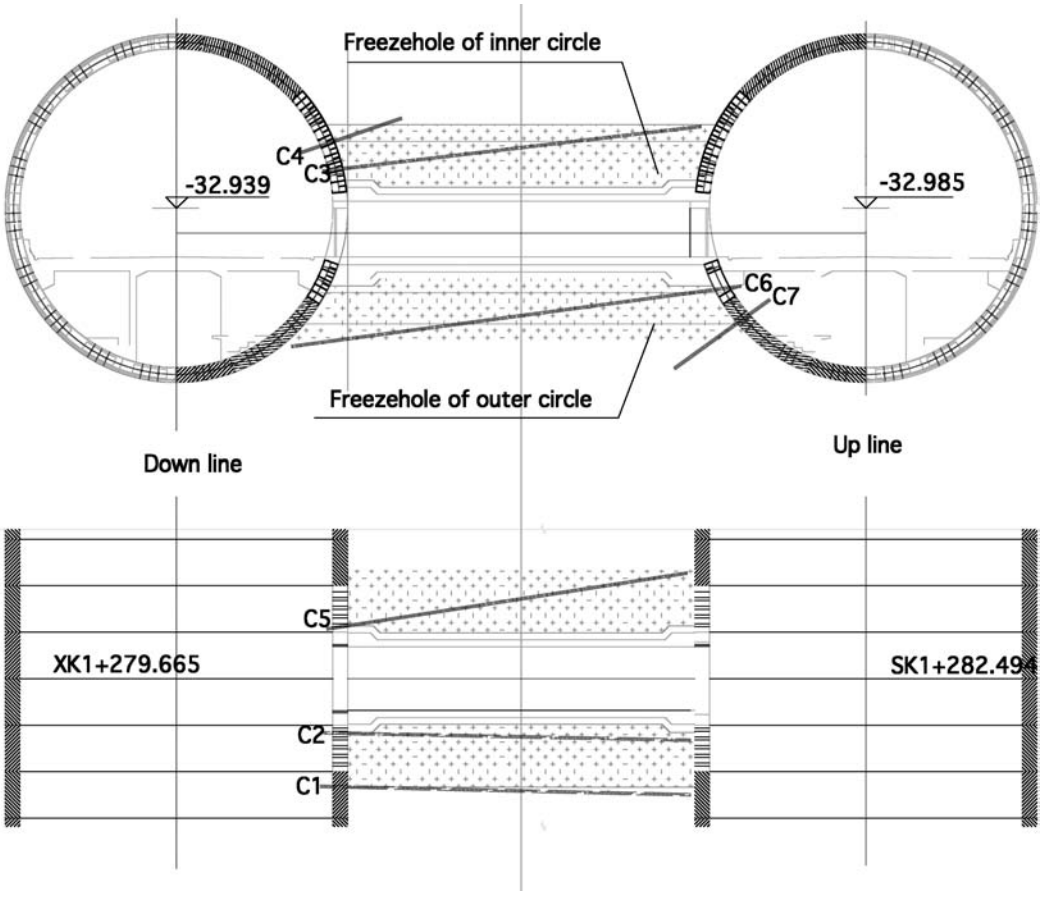

Figure 8. Layout of temperature holes (cross passage #1).

4 CONCLUSION

Construction of cross passage of shield driven tunnel is a task with high risk, and engineering under river bottom is even more hazardous. Reliable construction techniques must be prudently employed aiming at every of the risk factors to guarantee engineering security.

REFERENCES

Cui, H.T. 2004. A Research over environmental impact parameter of manual horizontal ground freezing in a metro tunnel. *Railway Standard Design* (1):61–63.

Lin, Z. & Yang J.J. 2003. Analysis on temperature field of freezing shaft wall with three rows of freezing tubes. *Mine Construction Technology* 24(3):21–24.

Wang, W.S., Wang, J.P., Jing, X.W., et al. 2004. Experimental study of temperature field in course of artificial freezing. *Journal Of China University Of Mining & Technology* 33(4):388–391.

Wu, X.Z., Li, D.Y. & Jin, M. 2004. Construction technology analysis of the horizontal freezing method adopted in construction of side channels of the test section of nanjing subway, *Construction Technology* 31(1):40–42.

Zhou, W.B. 2004. *Construction Technology And Applications Of Shield Tunnel*. China Architecture & Building Press.

The Shanghai Yangtze River Tunnel - Theory, Design and Construction – Huang (ed)
© 2008 Taylor & Francis Group, London, ISBN 978-0-415-47161-9

TBM options for Shanghai Yangtze River Tunnel Project

J. Sun, X.K. Chen & Q.W. Liu
Shanghai Changjiang Tunnel & Bridge Development Co., Ltd., Shanghai, P. R. China

ABSTRACT: Based on the characteristics of "long distance, large diameter and high water pressure" for Shanghai Yangtze River Tunnel Project, EPB machine and mixshield machine are compared based on the conditions for TBM options. It is discussed in this article on the design parts for the TBM adaptability, safety and reliability, etc. to be the reference for similar project.

1 INTRODUCTION

Shanghai Yangtze River Tunnel & Bridge Project is the express road project linking Shanghai Pudong New District and Chongming Island which is the extra-large transportation project locating in the mouth of Changjiang. The solution of "tunnel in south and bridge in north" is adopted for this project. Yangtze River Tunnel which crosses the south navigation channel of Changjiang is 7.5 km long (refers to Figure 1) and it will be finished by TBM method which is continuously constructed. This project has the characteristics of "long, large and deep". Based on related documents, Shanghai Yangtze River Tunnel Project is the one that has longest continuous construction distance in the world. It is the largest diameter of tunnel bored by TBM in soft clay. And the highest water pressure of 5.5 bar is also the world wide difficulty.

2 EQUIPMENT OPTIONS FOR TBM

2.1 *Geological conditions*

Main geological layers TBM crosses are: ④ grey muddy clay, ⑤$_1$ grey muddy silty clay, ⑤$_2$ grey clay silt with thin silty sand, ⑤$_3$ silty clay, ⑤$_3$ lens, ⑦$_{1\text{-}1}$ grey clay silt, ⑦$_{1\text{-}2}$ grey sandy silt, etc. There are unfavorable geological conditions along the axis of the tunnel, such as liquefied soil, quick sand, piping, lens and confined water, etc.

2.2 *Conditions for TBM options*

The external diameter of the tunnel is 15,000 mm. The internal diameter is 13,700 mm. Universal segments are erected without alignment. There are 10 segments for 1 ring. The thickness of the segment is 650 mm. The width of the segment is 2,000 mm.

Net width of transportation within one tunnel is 12.75 m. The width of each lane is 3,750 mm, and the width of the road is 12,250 mm. The internal structure is synchronized constructed, refers to Figure 1.

The maximum cover is 24 m, the minimum cover is approximately 6.8 m.

The largest water depth is 17 m. The maximal longitudinal axis slope of the tunnel is ±29‰. The minimal radius of plane curve is 4,000 m. The minimum radius of vertical curve is 12,000 m. TBM should be able to bore with the minimum plane curve radius of 750 m under the conditions of deviation correction.

Anti-uplifting safety ratio of the structure for construction and operation period is larger than 1.1.

2.3 *References for TBM options*

2.3.1 *Relationships between TBM options and permeability & flow plasticity of soil*

If the soil particle is finer, the permeability will be lower. If the permeability of the soil is larger, the slurry of front face of the TBM is easier to be lost under high water pressure which is no good for the stability of front soil. Based on the European TBM construction experiences, if permeability is less than 10^{-7} m/s, EPB machine can be adopted; if permeability is between 10^{-3} m/s and 10^{-7} m/s, mixshield machine and EPB machine with optimized soil discharging can be adopted; if permeability is larger than 10^{-3} m/s, mixshield machine is suitable. The permeability of ground crossed by Yangtze River Tunnel is $2.15 \times 10^{8} - 1.55 \times 10^{7}$ m/s which is feasible to use both mixshield machine and EPB machine.

Besides, higher fine particles content of discharged soil, much easier to form the impermeable flow plastic

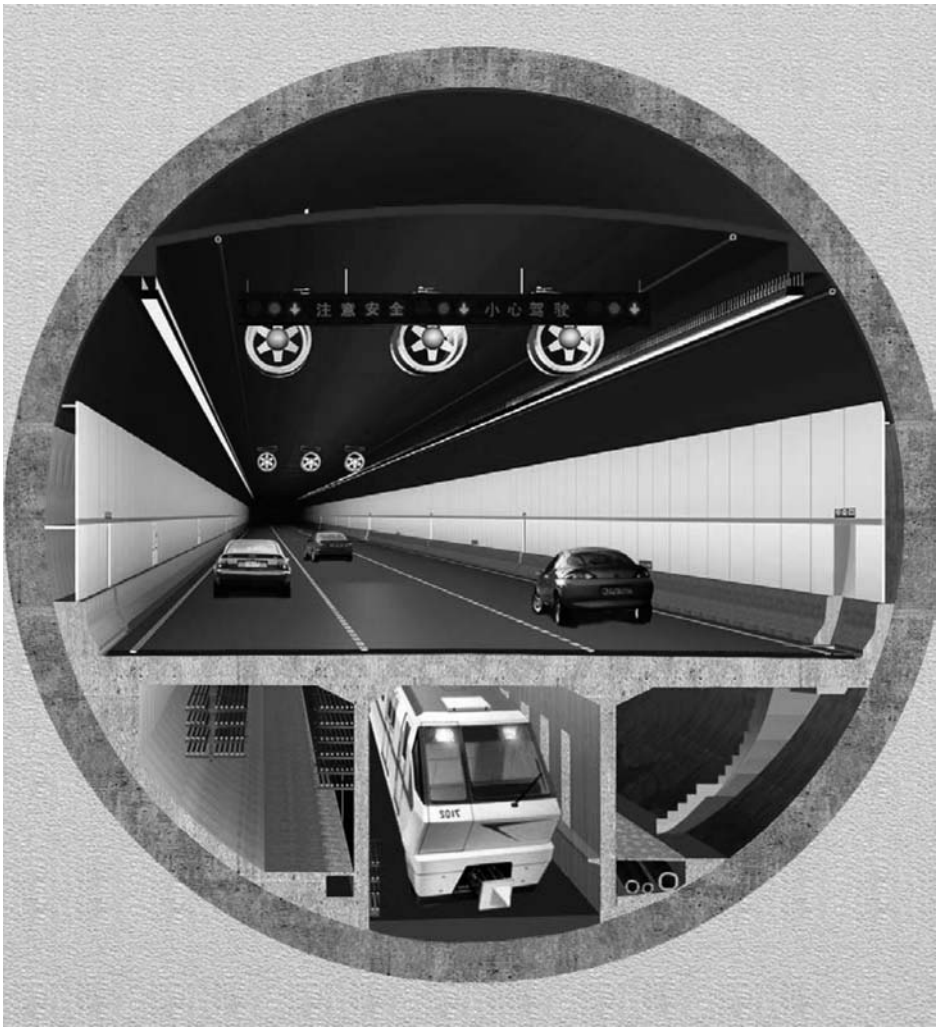

Figure 1. Cross section of the tunnel.

block. It is easy to fill in the cutter chamber to establish the confinement pressure to keep the balance of front face. In the contrary, more content of larger diameter particles, worse flow plasticity of the soil and it is easy for the soil blockage and more difficult to establish the balance of the pressure. It is shown from Figure 2 that EPB machine is adapt to clay and muddy soil, mixshield machine is suitable for gravel and coarse sand, EPB and slurry machine are both suitable for fine sand. The main ground layers crossed by Yangtze River Tunnel are layer ④, $⑤_1$ and $⑤_3$ clay whose content of particles less than 0.074 mm is 90%, content of particles larger than 0.074 mm is 10%, plastic limit (Ip) is 15–25 and consistency($IC = 1 - IL$) is 0–0.15. It is shown from Figure 3 that mixshield machine will not have serious clogging. So it is feasible to use both mixshield machine and EPB machine.

2.3.2 *Relationships between TBM options and high water pressure*

Based on the past experiences, dual-gate screw conveyor of EPB machine can bear the largest water pressure of 8 bar, single gate one only can bear 3 bar water pressure which makes it difficult to support front pressure. If piping happens at the location of gate, soil pressure inside cutting chamber will decrease and it becomes difficult to keep the stability of the front soil which will cause incidents such as front face

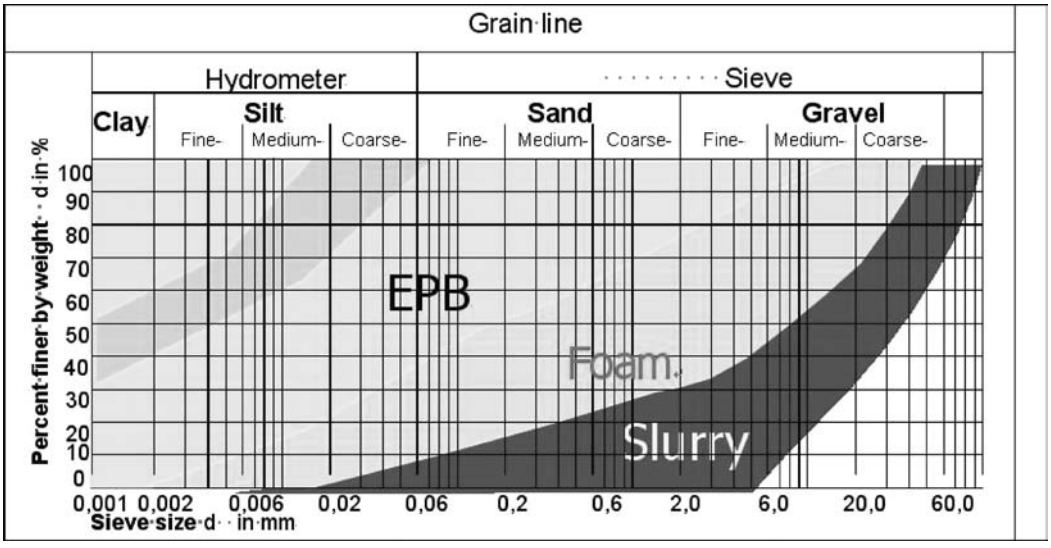

Figure 2. Shield machines application range of EPB and hydro with additives.

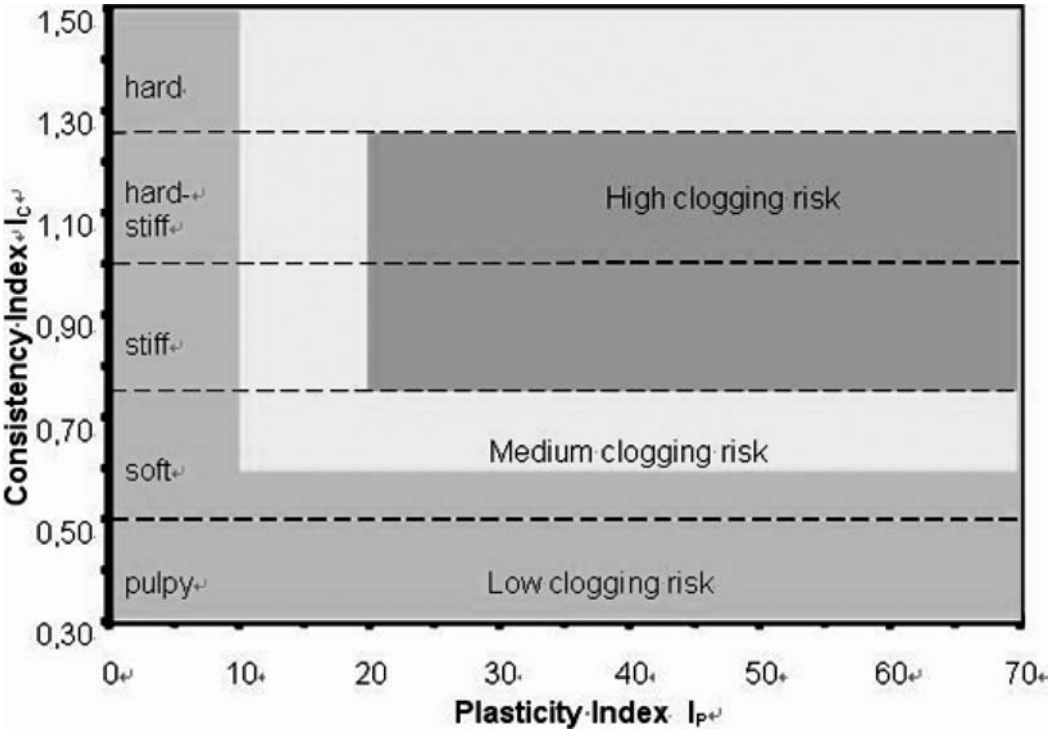

Figure 3. Clogging adhesion on steel surface diagram.

collapse and drowned the tunnel, etc. As the highest water pressure born by the TBM of Yangtze River Tunnel is 5.5 bar, it is much safer and reliable to choose mixshield machine.

2.3.3 *Comparisons on front face supporting modes of mixshield machine*

The key point of TBM is to keep the stability of front face and be adapted to excavated ground. Based on the

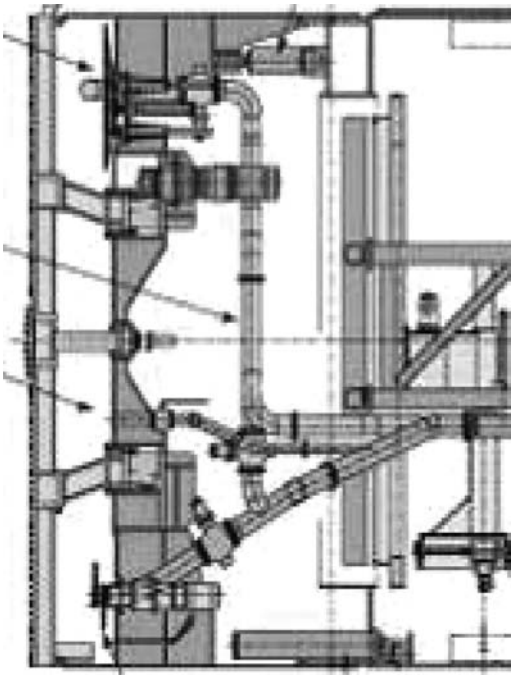

Figure 4. Directly pressurized by slurry type.

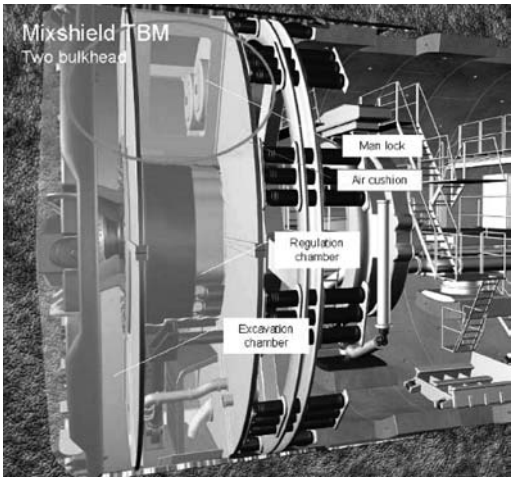

Figure 5. Indirectly pressurized by air cushion type.

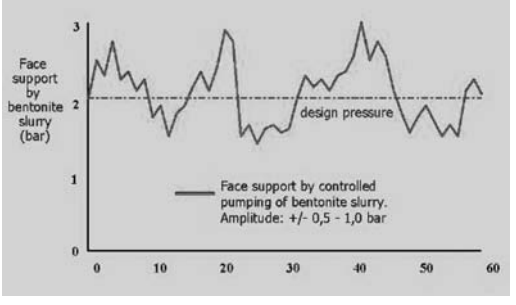

Figure 6. Front face pressure controlling of directly pressurized by slurry type TBM.

structure of slurry chamber and controlling method for slurry pressure, Mixshield TBM is divided into directly pressurized by slurry type and indirectly pressurized by air cushion type, refers to Figure 4 and Figure 5. The confinement pressure of directly slurry pressurized TBM is controlled by the rotation speed of inlet slurry pump and the opening of controlling valves.

The pressure of indirectly pressurized by air cushion TBM is achieved by adjusting the compressed air inside the bubble chamber. The pressure impressed on the front face is controlled by the controlling block of compressed air. The pressure difference caused from different slurry level is compensated by the regulator of compressed air to keep the pressure balanced. The pressure of air cushion is decided by the supporting pressure of front face. As slurry or advancing speed during exaction are changeable, rotation speed of slurry pump can be adjusted to keep the slurry level inside the chamber on setting value. And air controlling valve can automatically keep the pressure balanced inside the bubble chamber. So it is relatively independent for slurry transportation and supporting pressure controlling. The setting value of bubble chamber can be adjusted alone to keep the stability of front face which is to prevent the surface from settlement or heaving.

Directly pressurized by slurry type TBM is not easy to accurately control the slurry pressure because of the late effect from long distance controlled by inlet pump. So the supporting pressure inside the cutting chamber will have relatively large deviation ($+/-1.0$ bar) during excavation, refers to Figure 6, which will make the front face instable and have the risk of collapse. While the accuracy to keep the supporting pressure of indirectly pressurized by air cushion type TBM can reach $+/-0.05$ bar, refers to Figure 7. So the changing of outside pressure will not cause influences on the stability of the front face. The pressure deviation inside the slurry pipe can be accurately and quickly balanced. In case of piping happens, air cushion chamber can have the effect of leaking and buffering.

Besides these, as water content of clay is relatively high and cross section of the front face is large, the efficiency of the transportation truck used by EPB machine is relatively low and the off gas discharged by the trucks are not healthy to the workers inside the tunnel. While inlet and outlet slurry pumps used by mixshield machine can save the space of the tunnel,

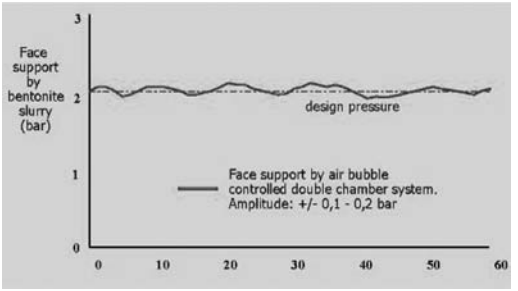

Figure 7. Front face pressure controlling of indirectly pressurized by air cushion type TBM.

increase the transportation ability and be environmental protection. So after comprehensive comparison, 2 Φ 15,430 mm indirectly pressurized by air cushion TBMs manufactured by Germany Herrenknecht company are optioned.

3 ADAPTABILITY OF MIXSHIELD MACHINE TO YANGTZE RIVER TUNNEL PROJECT

3.1 *Adaptability to the crossed ground*

It is shown from geological documents that TBM will cross layer ⑤$_2$ clay silt with thin silty sand, ⑤$_{3t}$ lens, ④ and ⑤$_1$ clay, ⑤$_3$ silty clay and ⑦$_{1\text{-}2}$ sandy silt.

There are 1,000 m for the TBM to cross layer ⑤$_2$ clay silt with thin silty sand and there are 11 times for the TBM to cross ⑤$_{3t}$ lens which will increase the slurry loss. And silty sand layer will increase the wearing for slurry pipes, cutter tools and cutter head. As the permeability of sandy soil is relatively high because of the large particles, if advancing speed is too large, the water inside the soil will be lost to cause clogging which will increase the value of total thrust force and the torque of cutter head.

When the TBM crosses within clay, as the linear speed of the center part of the cutter head is relatively low, it is easy for the clay to be blocked on the center part which will impact on the efficiency of excavation.

All the factors illustrated above are sufficiently considered based on the geological characteristics of this project. Cutter tools layout and anti-wearing design, cutter head structure and cutting chamber design, torque of the cutter head and total thrust force are focused to be analyzed and considered.

3.1.1 *Cutter tools layout and anti-wearing design*

Based on the cutting requirements and geological conditions of soft clay, scraping cutter tools and shoveling cutter tools are reasonably chosen and laid out. Over cutter tools, fishtail cutter tools and disc cutter tools are cancelled. Replaceable copy cutters are set. Scraping cutters cut into the soil of front face depending on the thrust force transferred from cutter head. The soil is tangentially cut with the rotation of cutter head. Shoveling cutters entrap large particles into the cutter head to discharge the soil by slurry pump. Copy cutter tools are adapt to treated soil block, curve section excavation and deviation correction. The cutter tools are arranged as overlapped tooth type in serial which is to guarantee the cutting trace of cutter tools to cover all the cross section.

There are 209 cutter tools on the plates of cutter head, within which there are 124 fixed scraping cutters, 12 shoveling cutters, 2 copy cutters, 7 central replaceable cutters, 64 replaceable scraping cutters. 2 copy cutters which can automatically extracted can be operated in the control cabin to set the copy cutting value for multisections and display the position of cutters.

If the cutter tools are worn, advancing speed and penetration degree will be decreased, thrust cylinder pressure and torque of the cutter head will be increased. It will decrease the efficiency of excavation and advancing.

In order to prevent the wearing of cutter tools, the dimension of cutters and the hard depth of cutter circles are increased to strengthen the ability of bearing the high temperature and high pressure. It is good for effectively cutting by use wearing bodies of cutters and high quality of carbonized alloy blade which can make the assembly angle match with the mechanical characteristics of soil. If there are large worn on the cutter tools, chips from the cutters will go through the slurry lines into slurry treatment plant which will damage the equipments such as cyclones, etc.

Anti-wearing protections such as welding double metallic plates on the back of cutter tools and use anti-wearing welding material are adopted to prevent the steel body from scouring by discharged soil.

3.1.2 *Structure of cutter head and cutting chamber design*

After the clay and silt are cut by the rotation of cutter tools, soil particles will pack towards the centre of cutter head. And the centre linear speed of the cutter head is relatively low, the flow ability of clay is relatively low, it is easy for the clay to clog in the center of cutter head and settle in the bottom of slurry chamber which will increase the toque of TBM. So it is seriously considered on the structure of cutter head, open ratio of cutter head, cutter tools and slurry inlet position, etc. during the design for TBM.

Closure type of cutter head is adopted for mechanical supporting to front face. In order to prevent from blocking, there are 6 high water pressure flushing pipes in the center of cutter head in case of blockage of discharged soil. Central agitation device is added to guarantee the slurry flow into the chamber without trouble. The slurry inlet positions are reasonably set to form the continuous flowing effect of cut soil of front

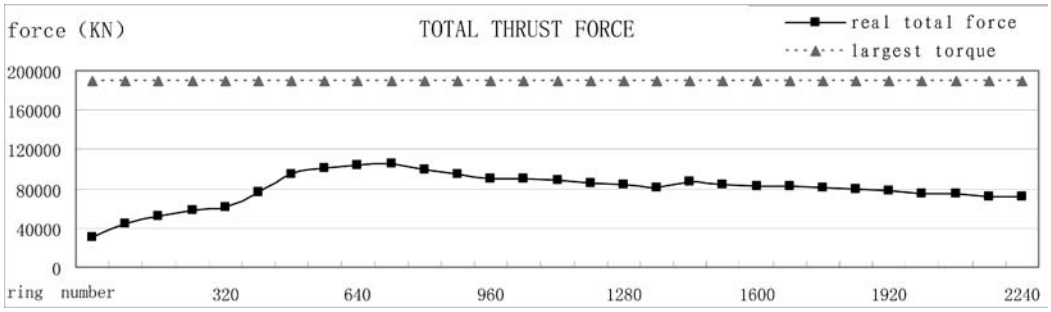

Figure 8. Statistics for total thrust force.

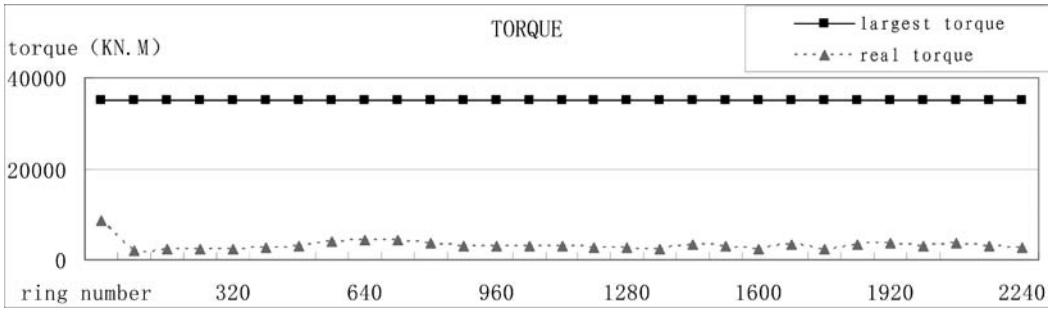

Figure 9. Statistics for cutter head torque.

face. Flushing nozzle with high water pressure is set to flush the agitator. Slurry outlet pump is put close to the outlet position to increase the discharging ability for slurry chamber. In order to prevent the outlet pipes from blockage and prevent slurry leakage because of too high pressure in outlet slurry pipe, reversal flushing function has been added.

The design open ratio for the center part of the cutter head is 29%. There are 24 slurry inlet positions and 1 outlet position. 2 motorized agitators with maximum torque of 19,900 Nm are allocated. There are 2 bentonite flushing nozzles. 4 slurry outlet pumps are assembled for the entire tunnel and reversal flushing function is added for slurry pipe lines. Besides these, stone unblocking equipments are cancelled based on geological report.

3.1.3 *Total thrust force design*

In order to be adapted to sandy ground which will increase the thrust force because of blockage from water loss, there are 19 sets (57 in total) of cylinders on this TBM and the largest thrust force is 203,066 kN. Based on the statistic documents of finished 2,240 rings, the largest real thrust force is 50% of nominal value, refers to Figure 8.

3.1.4 *Torque design*

It can meet the requirements for excavation when design rotation speed is 1.0 rpm, the largest torque is 39,945 KNm, when design rotation speed is 1.5 rpm, the largest torque is 26,454 KNm. Based on the statistic documents of finished 2,240 rings, the real torque is 10% of nominal value, refers to Figure 9.

3.1.5 *Slurry separation equipment options*

During the construction process of mixshield machine, the excavation efficiency of TBM is influenced by the efficiency of slurry separation. Proper slurry treatment way should be chosen based on the ground condition to decide proper slurry flow, speed and transportation way. Only after well controlling the rheological characteristics of the slurry, the TBM can keep the high efficient and safe status when advancing in different ground. The slurry treatment system manufactured by France MS company is adopted which consists of revolving trommel and 2 stages of hydrocyclone. There are advancing mode and bypass mode. The capacity is approximately $2 \times 3{,}000\ m^3/h$.

This system consists of scalping section, desanding section and desilting section. Scalping unit can separate the discharged soil whose particle diameter is larger than 7 mm. Revolving trammel with oblong mesh 8×30 mm is adopted to prevent the screen from clay block which will influence the treatment efficiency. 4 spray bars are allocated. Preliminary desanding unit consists of $4 \times \Phi 750$ cyclones which can separate the particles larger than 75 μm. The second

stage desilting unit consists of $12 \times \Phi 300$ cyclones which can separate the particle larger than $40\,\mu m$. After treatment, the slurry will be sent to mud management section for circulation and waste mud will be pumped to barges. The recycle ratio of this system is more than 70%.

When the TBM crosses layer ④ muddy clay at the beginning, the trommels are always blocked. After increasing the flushing ability of high pressure spray nozzle and adjusting the position of slurry outlet pipe, the separation effect becomes better. When TBM crosses layer $⑤_2$ clay silt, the density of slurry is treated from $1.3\,kg/m^3$ to $1.24–1.30\,kg/m^3$. When TBM crosses layer $⑦_{1\text{-}2}$ sandy silt, the density of slurry is treated from $1.29\,kg/m^3$ to $1.27–1.31\,kg/m^3$. It is clear that the treatment effect of this system for layer $⑦_{1\text{-}2}$ is better than that for layer $⑤_2$. But when TBM is advancing in layer $⑦_{1\text{-}2}$ sandy silt, polymer should be added in the mud to increase the viscosity in order to effectively form the slurry cake. It can prevent the slurry loss in the front face, prevent the soil collapse in the front and increase the mud utilization ratio.

3.2 *Adaptability to long distance excavation*

As the TBM will continuously excavate 7.5 km, in order to guarantee the safety and reliability for long distance construction, detection and replacing technology for cutter tools, cutter head and tail seal brushes, slurry transportation, survey and synchronized construction technology should be considered.

3.2.1 *Cutter tools wearing detection and replacing technology*

Now many TBM manufacturers have improved the performance of cutter tools and have the wearing detection device for cutter head and cutter tools. The cutter tools detection of this TBM can be operated under normal atmosphere which is no need to enter the cutting chamber. The cutter tool detection devices are set on 8 chosen scraping cutter tools and 2 shoveling cutter tools, all of which are connected with one plug at the back of cutter head. They can be monitored through the display device. There are electric coils embedded in this device. The wearing degree of cutter tools can be determined by detection the break or closure of coils. Wearing monitoring system for the surface of cutter head is designed to weld one layer of protection plates on the cutter head and there is a hydraulic pipe in it. The wearing degree of cutter head can be known by monitoring the pressure of hydraulic pipe at the back of chamber.

There are 4 ideas to change the cutter tools: first is to enter working chamber under pressure, second is to enter the chamber under normal atmosphere pressure after front soil treatment, third is to build a shaft to check and replace the cutter tools, and fourth is to enter the auxiliary arms of cutter head under normal atmosphere pressure. The fourth idea for replacing cutter tools is adopted, refers to Figure 10. It is much safer to change the tools under normal atmosphere pressure. Although the preliminary investment is large, as soon as replacement is needed, it can be high speed, small risk and low cost. It is also easy for operation under normal atmosphere pressure, refers to Figure 11. In order to prove that it is safe to replace the cutter tools under high water pressure, the tests of sealing performance and operability are done to simulate the working condition in the factory. It is proved by the tests that when

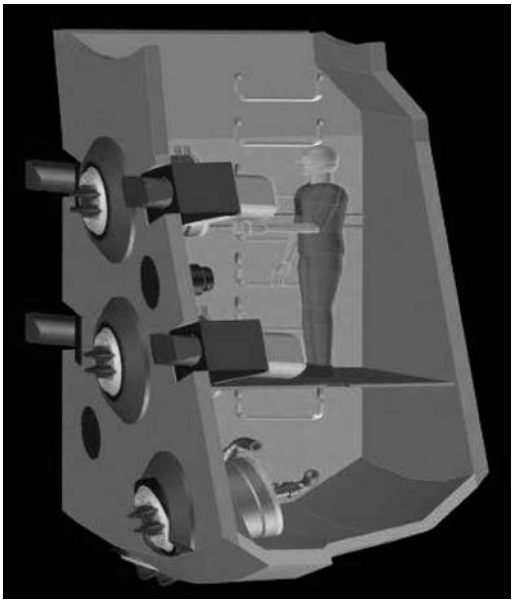

Figure 10. Schematic view for the position of changing cutters.

Figure 11. Demonstration for changing cutters in the centre of cutter head.

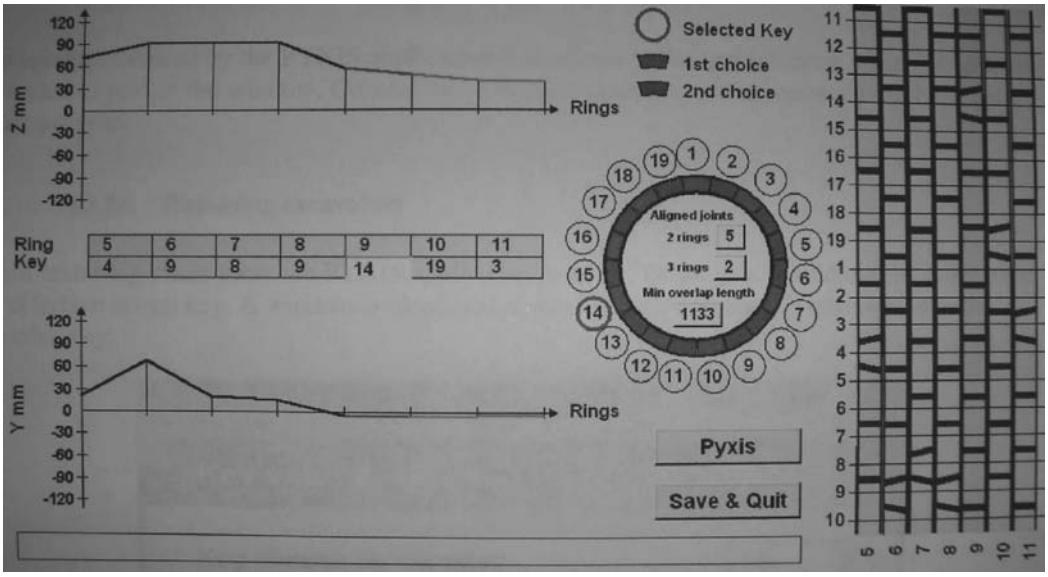

Figure 12. The interface of guidance system.

the pressure is maintained at 9 bar, there is no leaking discovered at the gate during 24 hours. When pulling out the replaceable cutter tools, there is no leakage detected around them. After many times of simulating tests, there is also no detected sealing wearing.

3.2.2 *Tail seal brushes gap monitoring and replacing method*

In the meantime, tail seal brushes monitoring and replacing methods are prepared in advance. At first SLUM tail shield gap survey system is used to monitor the gap between segment and TBM body at any time, which can protect the tail seal brushes and increase the life of them.

There are freezing pipes set in the tail shield which can reinforce the soil when there is leakage at tail seal. It can guarantee the safety during the process of treating and repairing the tail seal.

3.2.3 *Slurry transportation design*

The layout and type of slurry outlet pump should be paid attention to for long distance slurry transportation. If TBM advancing speed is 45 mm/min, slurry inlet flow should be controlled at 2,000 m^3/h–2,900 m^3/h. If the inlet slurry density is 1.05–1.3 kg/$m^3$and outlet density is 1.3–1.5 kg/m^3, the minimum inlet speed will be 2.9 m/s and minimum outlet speed will be 4.2 m/s. In order to prevent the slurry from settlement in the pipes during transportation, $2 \times 12/14$ WARMAN inlet slurry pumps connected in parallel and 16/18 WARMAN outlet slurry pumps are adopted. As the maximum outlet pressure of the outlet slurry pumps is 10 bar, if the pressure is larger than this value, relay pumps should be added. So 6 relay pumps should be allocated based on the design. Finally it is decided to choose Φ600 mm inlet slurry pipe and Φ500 mm outlet slurry pipe. It is useful to adopt larger diameter of outlet pipe to discharge the particles of larger diameter. The key parts of the slurry pump are especially designed for anti-wearing to be adapted to pump the wearing materials.

3.2.4 *Long distance survey and guidance system*

There are more requirements for guidance during long distance construction. TBM must have the survey system with high accuracy. Traditional manual survey can not prevent the accumulated error. At the present time automatic laser tracing total station and gyroscope relying on magnetic field are popular to display the accurate relative position of the axis of TBM to the design axis of the tunnel. It is easy for the operators to adjust the attitude of TBM advancing. Automatic laser tracing total station guidance system is adopted for this project, refers to Figure 12. The characteristics of this system are: real time calculate for TBM position, attitude and expectation value which can make the lining erection close to the design axis, provide the segment type for next ring and forecast the axis of segment for next 2 rings, real time display the gap between TBM and segment.

3.2.5 *Synchronized construction for long distance*

Because of long distance excavation, in order to increase the construction speed, internal structures are constructed in synchronization. So the design of TBM can meet the requirements for TBM advancing

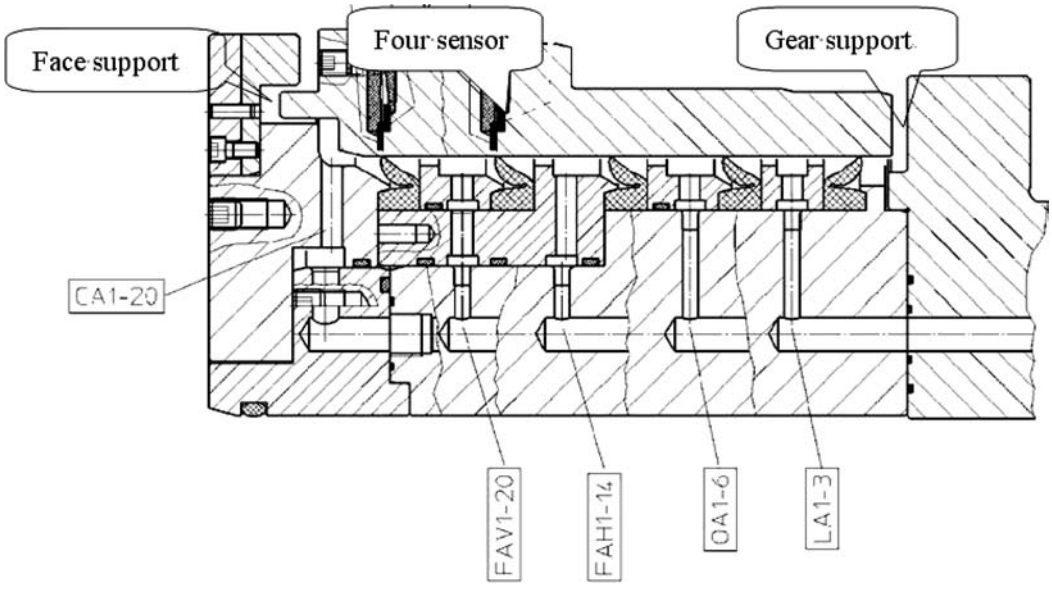

Figure 13. Tip sealing system.

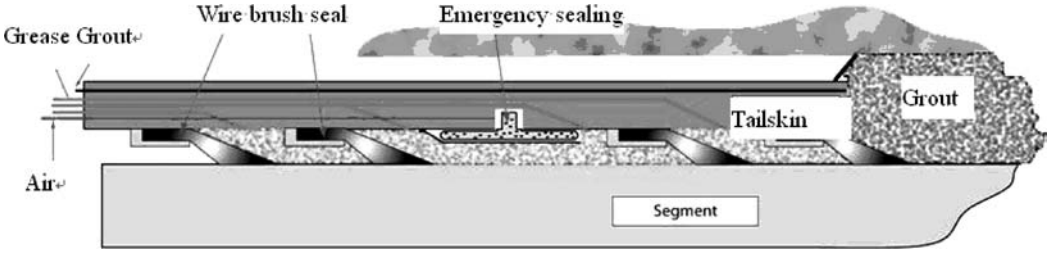

Figure 14. Four rows of wire brush seal and one row of emergency sealing.

and internal structure construction in synchronization. There are 3 gantry cranes on gantry 2, within which 2 cranes for the transportation of segments, mortar and construction material, 1 crane for the transportation of gallery. The erection face of internal structure is 50 m behind the front excavation face. Gallery can work as the access for material transportation. Road decks can be constructed at two sides of the gallery. It is useful to achieve synchronized construction which not only provide the access for transportation in the tunnel but also speed up the construction process of this project.

3.3 *Adaptability to high water pressure*

3.3.1 *Main bearing seal design*

It is the most important issue for the sealing of main bearing and tail seal as the highest water pressure is 5.5 bar during the process of TBM crossing. If the sealing is damaged or the gap becomes larger after wearing, gear oil for main bearing will leak or soil particles will enter gear box which will cause the wearing to decrease the life of bearing. At the present time, main structures are tip sealing and finger sealing. Tip sealing can decrease the front slurry pressure step by step. The wearing monitoring for main bearing seal and the feasibility of replacement should also be considered, refers to Figure 13.

It is shown in Figure 14 that CA1-20 is the labyrinth grease seal. The HBW grease which is controlled by flow system will be injected into outside to prevent the slurry from entering the sealing of main bearing.

FAV1-20 and FAH1-14 are grease for main bearing sealing which is injected through radial located grease pipes to the sealing chamber and fill in the entire ring type chamber. It is controlled by the flow which can sustain the pressure inside the grease chamber. With the grease proportioning pump, the supplementary grease volume of each pipe lines is uniform and stable.

OA1-6 can inject the gear oil by the outside pressurized device. The setting value of pressure is adjusted based on the confinement pressure and it can be stably sustained by accumulator.

LA1-3 is the leaking chamber which connects with the leaking oil tank outside of main bearing through radial access for easy monitoring. As soon as there is oil or grease is discovered inside the oil tank, TBM must be stopped to check the wearing degree of tip sealing.

For example, when front face slurry pressure is 7 bar, OA1-6 gear oil chamber should support 3.5 bar. FAV1-20 and FAH1-14 grease sealing chamber should bear 3.5 bar.

External layer of sealing is directly assembled from the front of main bearing to guarantee the radial systematic error. Continuous greasing and leakage monitoring system attached to sealing can monitor the grease injection volume by monitoring the grease pressure and flow. This type of sealing system has been successfully approved in many projects and has become one type of standard allocations.

After two TBMs advanced 2.5 km and 1.5 km, detection for the wearing of main bearing anti-wearing ring (friction ring) has been done. The results have shown that wearing degree is within the normal range (about 0.2 mm).

3.3.2 *Ttail seal design*

If tail seal loses the effectiveness under high water pressure during long distance excavation, large amount of high pressure slurry will enter the tunnel along the access. Water and soil loss will destroy the integrated structure of the tunnel. It is the risk issue to influence on the safety of the project.

The design of tail seal of this project refers to Figure 14. First 3 rows are wire brushes. Emergency sealing cushion is set in the middle. There is one row of steel plates at the rail part. It is mainly considered to open the air cushion to replace 3 rows of wire brush seal. There are grouting pipes inside the tail shield which include one standard grouting pipe and one for spare. The gap between segment and excavated edge can be filled up in time. There are 19 chemical injection pipes are added to inject sealing material such as special solidifying material (mortar with cement) or foaming polyurethane, ect for emergency. 19×3 units of greasing pipes can lubricate the wire brushes and seal the tail seal. The sealing system is controlled from the control cabin. There are automatic mode and manual mode. It can take action in circulation by controlling time and pressure.

As the diameter of the TBM is large, the deformation of tail shield under high water pressure must be considered. The gap of tail seal will influence on the options for segment and quality of final built tunnel. There is also need surplus value for cutter head torque and cylinder total thrust force to meet the requirements of crossing different ground layers. The setting value of grouting pump must be higher than the outside slurry pressure. The gap between shield and segment must be perfectly filled by the mortar. Anti-reverse device for slurry should be added in the grouting and greasing lines. Unblocking method should be prepared when pipe blockage happens.

4 TBM RISK CONTROLLING

The most important issue during construction is to guarantee the safety of personnel and equipments. As soon as the dangerous issue happens, the emergency incidents must be treated in time. Related settings on TBM are:

- In order to prevent inundated incidents, it is necessary to have large capacity of dewatering. $4 \times 150\,m^3/h$ dewatering pumps and $3 \times 50\,m^3/h$ pneumatic pumps are allocated;
- Emergency diesel generator is allocated on the TBM to prevent the incidents caused by sudden electricity break, such as segment falling during erection;
- Because of methane existing in the ground of this project, gas detection device and $2\times$ 30 kw inlet and outlet fans are allocated;
- In order to prevent puking because of too high slurry pressure or collapse because of too low pressure, front slurry releasing and compensation system is allocated;
- Samson pressure adjustment system is adopted to adjust the front supporting pressure. There are 2 systems, within which there is one for spare. It can work as soon as another system has breakdown;
- Considering that person need to repair agitator or enter cutter head to repair cutter tools, emergency equipments, such as man lock and shuttle chamber, etc. are allocated.

In order to prevent fire accidents happening and spreading, fire alarm system is added in TBM control cabin. There are dry powder fire extinguisher and carbon dioxide extinguisher at the dangerous location. In the meanwhile, ring spray nozzles are set at the rail of gantries which can spray high pressure water to form water curtain to separate gas and fire source. Then the operators on the machine can leave the incidents site safely.

5 CONCLUSION

The principles of TBM options should not only be adapt to the geological condition but also consider the safety of the project and personnel. So TBM design,

each parts allocations and TBM adaptability and reliability should be achieved. Especially the key parts must be 100% reliable. As there is less project samples of extra-large diameter and extra-long distance TBM construction projects, the emergency method for the key equipments when any risk happens should be considered, such as maintenances and replacement for cutter head, main bearing sealing device, tail seal.

This project is the largest tunnel in the world at present. The construction experience of large diameter mixshield machine need to be further concluded. The safety, reliability and adaptability of TBM options need to be further checked by practice.

REFERENCES

Chen, X.K. & Huang, Z.H. 2007. Shanghai Yangtze River Tunnel TBM cutting tools wear detection and replacement technology. *The 3rd Shanghai International Tunneling Symposium Proceedings: Underground Project Construction and Risk Provision Technology:* 152–157. Tongji University Publication Company.

Sun, J. & Chen, X.K. 2007. Discussion of TBM selection for Shanghai Yangtze River Tunnel. *The 3rd Shanghai International Tunneling Symposium Proceedings: Underground Project Construction and Risk Provision Technology:* 91–98. Tongji University Publication Company.

The Shanghai Yangtze River Tunnel - Theory, Design and Construction – Huang (ed)
© 2008 Taylor & Francis Group, London, ISBN 978-0-415-47161-9

The application of laser tracker in mould/segment measurement

D.H. Zhang
Shanghai Metro Shield Machine Equipment & Engineering Co., Ltd., Shanghai, P. R. China

N.J. Zhang & Y.P. Lu
Shanghai Changjiang Tunnel & Bridge Development Co., Ltd., Shanghai, P. R. China

ABSTRACT: The quantity of mould/segment plays a very important role in tunnel construction. Because the traditional method cannot measure mould/segment in its entirety and it cannot get high precision data, this paper introduces a new measurement system and its application in production. Finally some rules in the production of mould/segment are summarized according to the data obtained with the new system.

1 INTRODUCTION

In recent years, the construction of urban underground tunnel of China has being developed at a rapid speed. Among numerous tunnel construction methods, shield construction already becomes the main method. Guaranteeing the quality of "the armored concrete steel moulds (hereafter referred to as the mould)" and segments is very important in tunnel construction. With a constant improvement in the quality of projects, the technical standard of moulds and segments is also improving constantly. Knowing data of their geometry with high precision is becoming very necessary. Currently the main problem is how to check the precision during producing, supplying and transferring. In the past, the width is mainly checked with an inside or outside micrometer and the thickness is checked with a depth micrometer. However for the arc length, the central angle and the surface angle, it is very difficult to check. But the measuring system described in this paper can fulfill this task. The measuring system is called that the 3-D mould and segment measurement system based on a laser tracker.

2 PRINCIPLE OF THE SYSTEM

2.1 *Components of the system*

This system hardware is composed by the sensor head (Leica LTD600), controller, motor cable, sensor cable, application PC with a LAN cable, reflector, weather station and accessorial parts. Usually, the sensor head is mounted on one or several extensions and a base. A service cart is used for transporting the system components. Therefore the system is mobile and convenient to use. LTD600 can achieve high precision and work reliably and get abundant data within a minute. The plenty of the data can meet the needs

Figure 1. Moulds.

Figure 2. Segments.

of the project well. In addition, the system can compensate the data with temperature, humidity, air pressure collected by HM30 Meteo Station. This way the meteorological influence can be eliminated from the data.

The software of this system includes three parts, Spatial Analyzer, TubGeo2 and TubReport.

Spatial Analyzer (abbreviated as SA) is a common industrial software for measurement and analyses which is developed by U.S.A. NRK Company. Using SA we can obtain data fast, check the validity of the data and carry out complicated geometry analysis. TubGeo2 developed by VMT Company can calculate geometry dimensions an object. It is able to calculate the thickness, width, arc length, central angle, corner, angle of longitudinal joints, and so on. TubReport, also developed by VMT Company, can generate reports for users.

The systematic flow chart is shown as follows:

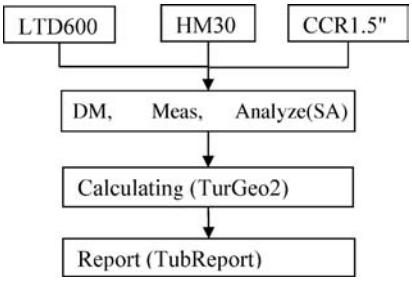

2.2 *Measurement principle*

The basic measurement principle of LTD600 is as follows. The laser head follows the reflector and obtain information about the horizontal direction, vertical direction and slope distance between LTD600 and the center of the reflector. Then LTD600 calculate the 3D coordinates considering its calibration parameters and weather parameters.

2.3 *Surface measurement*

Surface can be represented by a serial of points on it. Surface measurement can be measured by moving a spherical prism evenly on the object's surface. The denser the points are, the more realistic the surface is. By setting the sampling increment in SA, we can get the amount of points that we required. For example, if the parameter is set to be 2 mm, the second point will be measured at a distance between the point and the previous one is 2 mm. The whole surfaces can be measured using this method.

2.3.1 *Point measurement*

For a static point, the reflector is placed at the target position. After it is steady, the laser tracker samples it *n* times within one second ($0 < n \leq 1{,}000$). Because of the influence of external environment in the period of measurement, not all of the data collected using the trackers are the identical. But they fluctuate within a certain range about a value. SA can calculate a position value using the least-square method. This value represents the point's actual position. With this method, the influence of the external factor (the perturbation of the atmosphere, vibrations of the fixing point) is eliminated. If the steady condition is not achieved yet, we should measure it again until it meets the steady condition. Thus we can ensure the measurement accuracy of the space point.

2.3.2 *Data combination*

In order to describe the appearance of mould/segment in an all-round way, we need to measure six superficial data of the component. Because all six superficial data cannot be obtained at one station, two stations are needed. Then the data obtained from different station has to be combined.

On the first station, the measurement starts and the surface is scanned in meandering lines. If the entire surface is measured, stop the measurement first and then snatch the reflector from the surface. Repeat this procedure for all visible surfaces (Front, Back, Left, Right) and cylinders (Outside, Inside) of the object. Then four orientation points are measured. After the orientation points are measured from the first station, move the tracker to the second location. The orientation points are measured again from the second station. Then the station fitting is done. The remaining surfaces can be measured.

2.4 *The primary arithmetic*

Firstly, all points' coordinates are matched best with pre-designed mathematical model. And this can "drag" all points to the position which is very close to the design position, which will facilitate the following calculation. Secondly, four planes and two cylinders are fitted. Then eight corners can be formed by intersecting these six surfaces. Finally, some definitions (such as width, angles of longitudinal joints, mould correction, etc.) are made that the technical criterion provides and calculate their values.

3 PROJECT CASE STUDY

3.1 *Project introduction*

After we discuss the scheme about how to measure mould/segment with many relevant people, we put forward a detailed scheme which includes first and

Figure 3. Measuring in the field.

second control. Then we determine the measuring frequency. Since this system put into use, we have obtained a large amount of data from segment production of the Yangtze River tunnel and bridge project of Shanghai. Then we analyze these data and summarize rules for the segment production.

Since this system can obtain not only width (which can be also got by tradition method) but also arc length, thickness, central angle, border angles, angles of longitudinal joints, mould correction and so on, we can evaluate the quality of mould/segment more objectively and more comprehensively. Then we can pay more attention to the key process. And this is very important for departments or companies of segment production.

We take No. 3 mould and the first 400 (No. 1, 10, 20, 30, 50, 100, 150, 200, 250, 300, 400) rings of segments in the project for example. From each report and we can only know whether it meets the tolerances, but cannot know the changing rule of the mould/segment during manufacture. In order to learn their changing rule, we input all of the measured data as designed format in Excel file and plot their tendency charts. Because there are many slices in segment, we have to sample one of the segments to fit this paper. We take the B4 slice for example. For each slice of segment, we can get a great deal of data, such as width, thickness, arc length, central angle, border angles, angles of longitudinal joints, mould correction, etc. But we cannot analyze every item. We select width, angles of longitudinal joints and mould correction for analysis. In addition, in the plot of the relationship of geometry item and temperature, we take temperature as x axis and geometry item as y axis.

3.2 *B4 width*

There are 6 width values in Figure 6. If Width (i, j) is used to denote the width value of point i and point j,

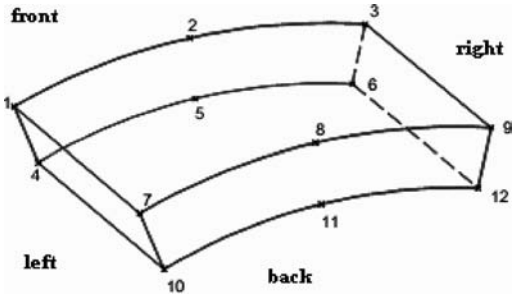

Figure 4. Digital model of mould/segment.

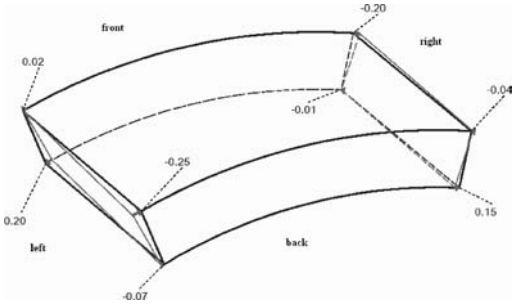

Figure 5. Mould correction.

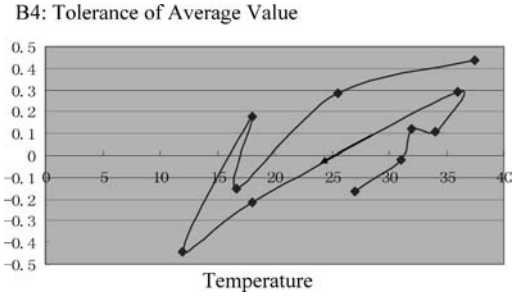

Figure 6. Tendency chart of the average of width.

then the 6 width values are expressed as Width (1, 7), Width (2, 8), Width (3, 9), Width (4, 10), Width (5, 11) and Width (6, 12) respectively. For analysis, we adopted the average of these 6 values, which is more representative.

Figure 6 is the tendency chart of the average of width measured 11 times (the white circle represents the initial position in picture, the same below). From the 3 divisions in the chart, the measured width is almost linear to temperature. The width increases with temperatures. The coefficient of steel expansion is about 12×10^{-6} and the coefficient of concrete expansion is $10 \times 10^{-6} - 15 \times 10^{-6}$. When the temperature changes by 10 degrees, the width will change between 0.20 mm and 0.30 mm for a segment with a width of

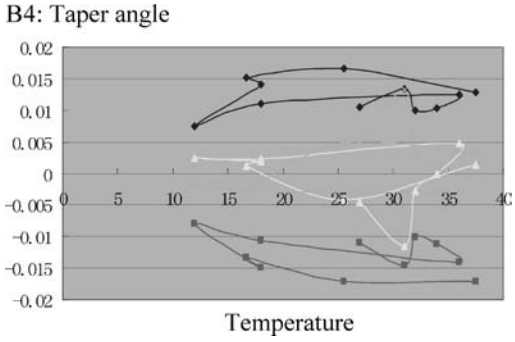

Figure 7. Tendency chart of angles of longitudinal joints.

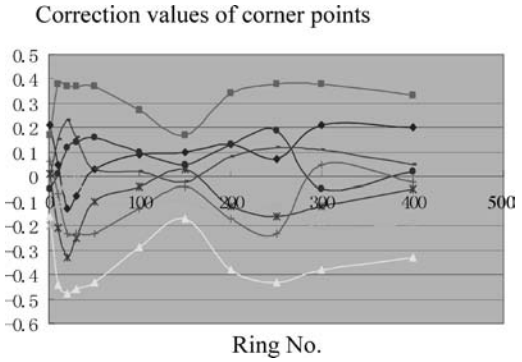

Figure 8. Tendency chart of mould correction.

2 meters. If we analyze the data carefully in the chart, we will find out that the measured data match the theoretic data well. This indicates that width is affected by temperature. In addition, the slope in the 3 divisions increases when the manufacture time increases. This shows us that the width change increases with temperature become. We understand that there might be other reasons. When this happens, we should re-check the current condition of mould. For example, we check that whether mould fully contacts the steel while shutting, whether mould is transformed and whether mould is rinsed well and so on.

3.3 *B4 angle of longitudinal joints*

There are 4 angles of longitudinal joints in Figure 4. If Angle (Π1, Π2) is used to denote the angle value of plane Π1 and plane Π2, then the 4 angles are expressed as Angle (left, front), Angle (left, back), Angle (right, back) to Angle (right, front).

Figure 7 is the tendency chart of 11 measured angles of longitudinal joints. From the chart, we can see that the upper and lower curves are almost symmetric by the cross axis. The symmetric pairs include Angle (left, front)–Angle (left, back) and Angle (right, back)–Angle (right, front). This indicates that the front board and the back board are parallel. Besides, it is seen that the swing of angle of longitudinal joints is big in the first 50 rings and becomes smaller after the 50th ring. And this illuminates that production becomes steady gradually with increasing of rings.

3.4 *B4 mould correction*

Figure 8 is the tendency chart of mould correction which varies with ring number. The points' positions are at shown in Figure 4 and Figure 5. The absolute value of the correction is smaller than 0.5 mm. The correction curves present a horizontal line tendency except for the 6th point and the 9th point. This proves that as time goes on, the mould tends towards stability gradually. At the position of the 150th ring, all correction is very small. This is because the measuring temperature is the lowest. And this also proves that the mould is affected by temperature.

4 CONCLUSION

According to the analysis from the charts above, we know that the system not only measure accurately but also accelerates our innovative process in the production of mould/segment.

(1) The systematic precision is high

The key hardware is the Leica LTD600 which can yield highly accurate 3D coordinates and the key software is TubGeo2 which can yield the reliable results. After the mould/segment is measured, the absolute value of the error of the final data is smaller than 0.1 mm. In addition, in this system, the weather conditions such as temperature, atmospheric pressure and humidity are took into consideration. This brings us a new concept that sizes of segments produced in different seasons are different. This can be used as a reference to make the corresponding criteria in the future.

(2) The systematic information is complete

In production, the traditional method generally only measures the width, and controls other items according to experience. With this system, besides the width, we can obtain other information such as best fit for surfaces of contact, are length, thickness, central angle, border angle, angle of longitudinal joints and mould correction. Therefore the data are more comprehensive. In addition, gathering the measured data of different periods and analyzing the changing rules of each item with temperature and time is very beneficial for us to draw reasonable conclusions.

In summary, it is convenient and rapid for us to use this system in mould/segment measurement and data

is collected with high precisions. Its advantages are also recognized by more and more people. Up to now, this system is an advanced system in China. We believe that with the development of tunnel construction in our country, the application of this system will be more extensive.

REFERENCES

Fan, G.Y. 1998. *Error Theory and Surveying Adjustment.* Shanghai: The Publishing House of Tongji University.

Han, Q.H., Zheng, B., Guo, H.L., et al. 2004. Measurement of aircraft outline by using laser tracker equipment. *Aviation Surveying Technology*.

Ma, Q., Yan, Y.G. & Liu, W.L. 2006. Inspection of laser tracking system and its application in three-dimensional measurement. *China Testing Technology*.

Wang, P.M. 2003. Design and fabrication technology of the high-accuracy armored concrete segment and mould of shield tunnel. *The Latest Technology of Tunnel Project of The CityTraffic*.

Wang, P.M. 2005. The current situation and development of mould and segment. *The Prospecting Project in The West*.

Zhou, W.B. 2004. *Shield Tunnel Construction Technology and Application*. Beijing: China Construction Industry Press.

3 Theoretical analysis and numerical simulation

The Shanghai Yangtze River Tunnel - Theory, Design and Construction – Huang (ed)
© 2008 Taylor & Francis Group, London, ISBN 978-0-415-47161-9

A 3D visualized life-cycle information system (3D-VLIS) for shield tunnel

X.J. Li, H.H. Zhu & L. Zheng
Key Laboratory of Geotechnical & Underground Engineering, Ministry of Education, Tongji University, Shanghai, P. R. China
Department of Geotechnical Engineering, School of Civil Engineering, Tongji University, Shanghai, P. R. China

Q.W. Liu & Q.Q. Ji
Shanghai Changjiang Tunnel & Bridge Development Co., Ltd., Shanghai, P. R. China

ABSTRACT: This paper presents the development and implementation of a 3D Visualized Life-cycle Information System (3D-VLIS). The main objective of 3D-VLIS is the integration of life-cycle data of shield tunnel with a coherent 3D visualized model, and improvement of tunnel construction and maintenance by developing innovative information services and visualization services. The main emphasis in this study is placed on developing an Internet-based framework for the management of shield tunnel life-cycle information, 3D modeling of shield tunnel structures, integrating shield tunnel life-cycle information with 3D model, and visualizing shield tunnel using virtual reality techniques. As demonstrated in this paper, the 3D-VLIS can be used as a new effective way of organizing and representing shield tunnel life-cycle information.

1 INTRODUCTION

Accompanying rapid growth in urban development, tunneling has become an attractive method in developing underground spaces for transportation and utility networks. Consequently, engineers are under increasing pressure to meet demands of improved safety, lower operation costs, improved maintenance and increased product quality for tunnel projects. To assist with meeting the present and future industry challenges, the design, construction and maintenance of tunnels can be dramatically improved through the use of a comprehensive life-cycle information system.

In recent years, many information technology based efforts have contributed to the underground construction works. An IT-based system has been proposed to improve analysis, de-sign and construction of underground excavations in rock (Gutierrez et al., 2006). The system exploits new IT technologies such as digital imaging, data management and visualization. Its major objectives are to design and implement an information technology-based system for real-time and adaptive engineering-geologic mapping, analysis, and design of underground excavations in rock. A TUNCON-STRUCT (Technology Innovation in Underground Construction) research project that promotes the development and implementation of technological innovation in under-ground construction has been initiated under the support of EU since 2005. The main aspects of the project are the complete integration of all processes into an Underground Construction Integrated Platform (UCIP). A center part of this is the Underground Construction Information System (UCIS), which allows instant access to all relevant data of a tunnel over the whole tunnel life cycle, and to provide data to all partners of a tunnel project. A 'Smart infrastructure' research project whose main objective is to develop generic wireless sensor networks that allow sharing of equipment and communication tools for monitoring of multiple types of infrastructures including tunnels, bridges and water supply systems has been launched under support of EPSRC (Soga et al., 2005). An IT-based tunneling risk management system (IT-TURISK) was also reported (Yoo et al., 2006). IT-TURISK has been developed in a geographic information system environment with a capability of performing preliminary assessment of tunneling induced third party impact on surrounding environment. Such efforts have greatly improved the information management and facilitated analysis of underground works. However, modeling and visualization related techniques have not been

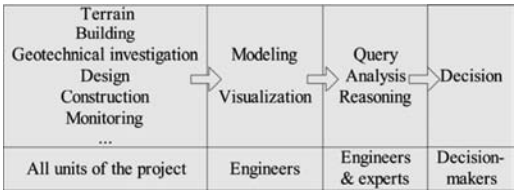

Figure 1. Information processing chain of 3D-VLIS.

fully investigated and applied in these systems. In addition, the life-cycle information is rarely considered as a whole in the system. Therefore, there is an urgent need to develop a life-cycle information system which incorporates modern visualization technology for underground works.

The objective of this paper is to describe the design and implementation of a 3D visualized lifecycle information system (3D-VLIS) for shield tunnel projects. The system uses advances in IT, particularly in data management, visualization and network, which have not been fully exploited in tunneling and can significantly improve tunnel construction and maintenance. It is envisioned that 3D-VLIS will be an innovative way of managing whole tunnel lifecycle information and lead to safer, and more economical and efficient use of underground space.

2 DESCRIPTION OF THE 3D-VLIS

2.1 *The framework of the 3D-VLIS*

The life-cycle of a shield tunnel project involves the management of huge amount of data which are generated from all stages of the project such as geotechnical investigation, design, construction, monitoring and maintenance. In 3D-VLIS, these data can be organized as an information chain where information are generated, processed and moved from workers to engineers, then to experts and finally to decision-makers, as illustrated in Figure 1.

In order to establish a 3D visualized information system for shield tunnel, a data management subsystem where all of the lifecycle data resides should be created at first. Then a coherent 3D model consisting of shield tunnel, strata and surrounding environment should be constructed respectively. Next a virtual shield tunnel project can be established in the computer system corresponding to real one by using visualization and virtual reality techniques. Finally, the system manages lifecycle information of shield tunnel based on the 3D model and the underlying data. The system enables us to perform visualized data queries by simple click on the 3D model.

The main components of the 3D-VLIS include:

- Data management module;
- 3D modeling module;

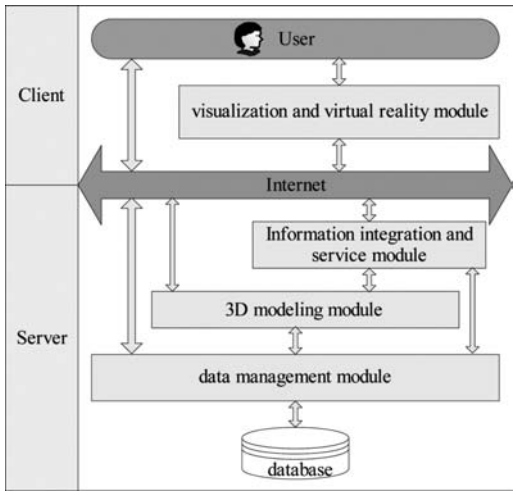

Figure 2. Main components of 3D-VLIS.

- Information integration and service module;
- Visualization and virtual reality module.

Due to the employment of the latest network techniques, a distinct feature of the system is its ability to visualize tunnel and manage data through Internet. Therefore, the system is capable of being used across network. The framework of the 3D-VLIS is shown in Figure 2.

2.2 *Data management module*

This module manages the life-cycle data of shield tunnel, reads data from and stores data into database, and provides a unified data accessing interface for users to hide unnecessary details. To facilitate the data management, a taxonomy of shield tunnel data is proposed. The basic idea of the taxonomy is to divide shield tunnel into small parts, and describe them by designing data, construction data and monitoring data etc., as listed in Table 1. The taxonomy is organized as a hierarchy structure where each item is encoded into simple characters for data exchanging and indexing. For example, the main structure data of shield tunnel is encoded as 'GA' and ventilation equipment data of shield tunnel is encoded as 'GCA'.

Data in the system are generally divided into two categories: (1) spatial data and (2) attribute data. Spatial data are used to describe the location and geometry of different parts of shield tunnel. Other data can be seen as the attributes of these parts and therefore can be associated with these parts. While spatial data are fundamental and necessary for the system, attribute data are optional and the amount of attribute data can vary according to different interests. To support data integration, a unique object identifier is used to link the spatial data with the attribute data.

Table 1. Taxonomy of shield tunnel data.

First level	Second level	Third level
Shield tunnel (G)	Main structure (GA)	Segment ring (GAA) Bolt (GAB) ……
	Auxiliary structure (GB)	Road structure (GBA) Wall structure (GBB) ……
	Equipment (GC)	Ventilation equipment (GCA) Fire protection equipment (GCB) Illumination equipment (GCC) Monitoring equipment (GCD) Power supply equipment (GCE) ……
	Pipeline (GD)	Water supply pipeline (GDA) Water drainage pipeline (GDB) Power supply pipeline (GDC) Communication pipeline (GDD) ……
	……	

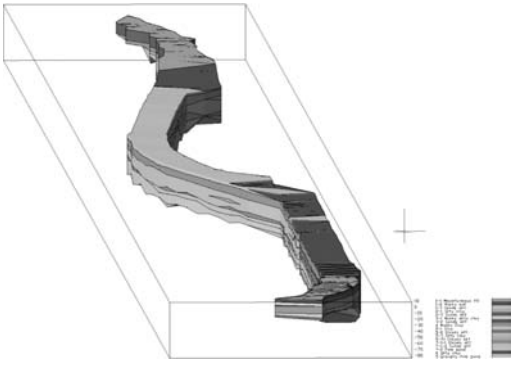

Figure 3. 3D model of strata.

This module also provides the exact definition of data con-tent for different parts of shield tunnel so that users can in-put the data into the system and engineers can query the results.

2.3 *3D modeling module*

This module provides the capabilities to transform raw data into a coherent 3D model. It can be further divided into strata modeling, surrounding environment modeling and shield tunnel modeling. The discussions of strata modeling and surrounding environment modeling are out of the scope of this paper. A result of 3D model of strata is illustrated in Figure 3.

The 3D model of shield tunnel is built through using solid modeling techniques provided in commercial

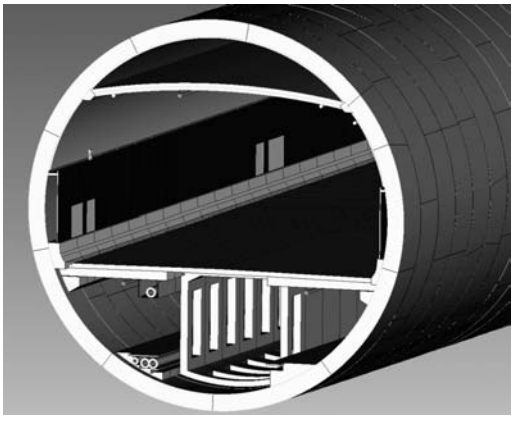

Figure 4. 3D model of a shield tunnel.

computer-aided design and drafting (CADD) system such as Auto-CAD. The modeling process of main structure of shield tunnel is divided into three steps: (1) Combine the designed plane and vertical axis of the shield tunnel into a single 3D curve. Then equally divide the axis curve into continuous line segments by a length of the width of segment ring; (2) Based on the design or actual construction data of segments and rings, build each segment and then assemble them into a ring of segments by using solid modeling techniques; and (3) According to the segmented axis curve, translate and rotate each ring of segments to its designated places. Consequently, main structure of shield tunnel is virtually assembled ring by ring. Auxiliary structures, equipments and pipelines of shield tunnel can also be constructed in the similar way. The model will be served as the basis for information integration. Figure 4 shows a 3D model of shield tunnel with main structure and auxiliary structures.

2.4 *Information integration and service module*

This module establishes an Internet-based environment where life-cycle information of shield tunnel is integrated into a coherent 3D model. It enables users to perform information queries and modifications through a 3D visualized model. Information about the tunnel structure is grouped according to the sequences of tunnel life-cycle, i.e., design information, construction and monitoring information, and maintenance information.

Figure 5 shows a schematic overview of information integration process when a user clicks on the 3D model of a ring of segments. In this situation, an information query re-quest with a unique identifier of the ring will be sent to the remote server. In the server side, an information service module is running. The service module responds to the re-quest by performing data query from database. Design, construction,

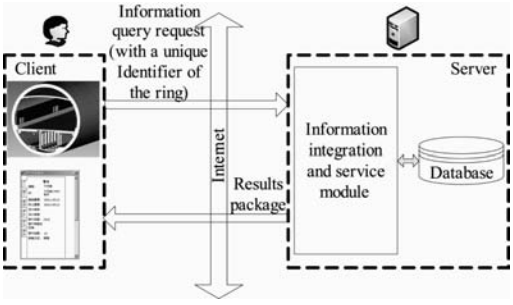

Figure 5. A schematic overview of information integration process.

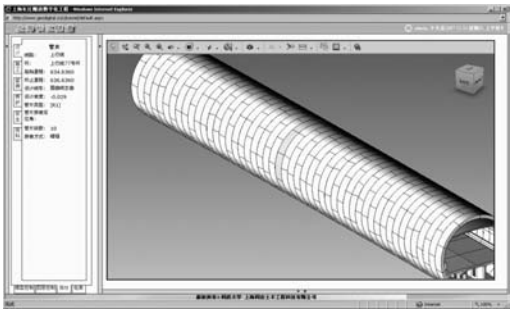

Figure 6. Information integration results.

monitoring and maintenance information, if exists, is integrated into a package. Then the package is sent back to the user through Internet. Finally, the user will see the results in an Internet browser, as illustrated in Figure 6.

2.5 *Visualization and virtual reality module*

The visualized underground structure systems can provide an efficient and cost-effective tool for decision-making and analyzing real system (Gutierrez et al., 2006; Yoo et al., 2006; Ruwanpura & Ariaratnam 2007). In addition, virtual reality technology can be utilized to further enhance the visualization results (Hong et al., 2003; Tsutsui et al., 2004; Gutierrez et al., 2006). Despite these facts, 3D visualization has not been used to its maximum potential in underground engineering when compared to mineral and oil industries (Elkadi & Huisman 2002). Using the latest techniques in computer graphics, the visualization and virtual reality module turns raw data into more readable images for our brain, so that data can more easily be understood, managed, and communicated. The module allows users to offload part of the bur-den of conscious information processing to human perceptual system. As the volume and complexity of the information sphere grows, putting all the information

(a)

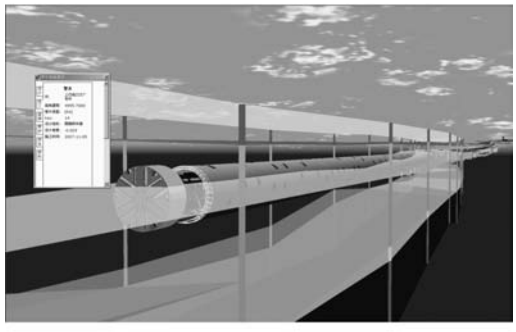

(b)

Figure 7. Virtual system of a shield tunnel.

and data in the 3D space does not necessarily produce a satisfactory result. In 3D-VLIS, several principles about representing information are pro-posed to achieve better visualization results. These principles include: (1) Objects and related information are classified, organized, and then visualized; (2) Representing objects with different level of detail (LOD) is an effective way to avoid information over-congestion and improve efficiency; (3) Thematic view is an alternative way to meet various needs of engineers and decision-makers; (4) Except in virtual reality system, objects are viewed and explored from outside. Transparency is used to circumvent the inside-outside problem (Waterworth 1997); and (5) Spatial cueing could result in better understanding of the environment's information items and spatial structures (Modjeska & Water-worth 2000).

Virtual reality simulation refers to the generation of an immersive, interactive and computer generated 3D environment. It offers new opportunities to visualize under-ground structures. Users can walk through 3D environments, see newly constructed structures and investigate the construction processes. To obtain a satisfactory visualization result, the scene of virtual

reality system is also supplemented with a virtual reality model of sky, terrain, river, borehole, tunnel boring machine, and inner structures of tunnel. As shown in Figure 7, users can navigate the virtual system by walking into the tunnel or by flying over the whole model. In the walking navigation mode, user's feeling of reality is further enhanced by collision response.

When a collision between observer and object is detected, a motion of the observer is incurred. For example, collision detection between observer and tunnel lining structure can prevent user walk through it. Collision detection and response is turned off in the flying navigation mode. This allows user navigating the model more freely. Simulation of tunnel advancing, segment transportation and assembly sequences of tunnel lining can be well perceived in flying navigation mode. In virtual reality system, users can also click on the model and access the information about it. As a result, the realistic feelings of virtual system are effectively augmented, providing a way to superimpose the virtual world on the real world.

3 CONCLUSIONS

This paper presents the development and implementation of a 3D Visualized Life-cycle Information System (3D-VLIS). The main objective of 3D-VLIS is the integration of life-cycle data of shield tunnel with a coherent 3D visualized model, and improvement of tunnel construction and maintenance by developing innovative information services and visualization services. The main components of the 3D-VLIS include:

Data management module,

- 3D modeling module;
- Information integration and service module;
- Visualization and virtual reality module.

As demonstrated in this paper, information technology such as database, visualization and network can be used as an effective way of organizing and representing tunnel life-cycle information. It is envisioned that 3D-VLIS will be an innovative way of managing whole tunnel lifecycle information and lead to safer, and more economical and efficient use of underground space.

The presented 3D Visualized Life-cycle Information System (3D-VLIS) is the result of the first stage of an ongoing research project whose objective is to establish a Digital Underground Space and Engineering (DUSE) system.

ACKNOWLEDGEMENTS

This research has been supported by The National High Technology Research and Development Pro-gram (863 Program) of China (Grant No. 2006AA11Z118), Shanghai Municipal Science and Technology Commission (Grant No. 052112010, No. 05dz05806 and No. 07dz12059). The financial sup-port is gratefully acknowledged.

REFERENCES

Elkadi, A.S. & Huisman, M. 2002. 3D-GSIS geotechnical modeling of tunnel intersection in soft ground: the Second Heinenoord Tunnel, Netherlands. *Tunnelling and Underground Space Technology* 17(4):363–369.

Gutierrez, M., Doug, B., Joseph, D., et al. 2006. An IT-based system for planning, designing and constructing tunnels in rocks. *In M., Lee, C., Yoo, & K. H., You (eds), Proceedings of the ITA-AITES 2006 World Tunnel Congress and 32nd ITA General Assembly,* Seoul, Korea.

Hong, S.W., Bae, G.J., Kim, C.Y., et al. 2003. Virtual reality (VR) – based intelligent tunneling information system. *Proceedings of 29th ITA World Tunnelling Congress (Re) Clamming the underground space*: 975–977.

Modjeska, D. & Waterworth, J.A. 2000. Effects of desktop 3D world design on user navigation and search performance. *International Conference on Information Visualization :* 200–215. London, England.

Ruwanpura, J.Y. & Ariaratnam, S.T. 2007. Simulation modeling techniques for underground infrastructure construction process. *Tunnelling and Underground Space Technology* 22(5–6): 553–567.

Soga, K. 2006. Underground M3, Smart infrastructure, *http://www2.eng.cam.ac.uk/ks/soga.html*.

Tsutsui, M., Chikahisa, H., Kobayashi, K. et al. 2004. Stereo vision-based mixed reality system and its application to construction sites. *ISRM International Symposium/3rd Asian Rock Mechanics Symposium (ARMS): Contribution of Rock Mechanics to the New Century*: 223–228. Kyoto, Japan.

TUNCONSTRUCT. 2006. TUNCONSTRUCT – A new European initiative. *Tunnels & Tunnelling International* (2): 21–23.

Waterworth, J.A. 1997. Personal space£º3D spatial worlds for information exploration, organization and communication. In R. Earnshaw and J. Vince (eds), *The Internet in 3D: Information, Images and Interaction*: 1–21, Academic Press, New York.

Yoo, C., Jeon, Y.W. & Choi, B.S. 2006. IT-based tunnelling risk management system (IT-TURISK) – development and implementation. *Tunnelling and Underground Space Technology* 21(2):190–202.

The Shanghai Yangtze River Tunnel - Theory, Design and Construction – Huang (ed)
© 2008 Taylor & Francis Group, London, ISBN 978-0-415-47161-9

Analysis on influence of conicity of extra-large diameter mixed shield machine on surface settlement

Q.Q. Ji, Z.H. Huang & X.L. Peng
Shanghai Changjiang Tunnel & Bridge Development Co., Ltd., Shanghai, P. R. China

ABSTRACT: Mixed shield machine with conicity is adopted in the Shanghai Yangtze River Tunnel Project. Few of the similar projects used this type of machine in soft clay. This article is based on the construction of the surface area of west tunnel of the Shanghai Yangtze River Tunnel Project. Two-dimensional finite element model is built to investigate the influences of four types of construction conditions on surface settlement during TBM construction. The results obtained from numerical simulation are compared to the monitoring surface settlement gained from the field measurement. The relationship between conicity of TBM and surface settlement is then achieved. Helpful experience may be offered to the similar project in soft clay later.

1 INTRODUCTION

Surface settlement during the construction of TBM is mainly caused by ground movements which come from the soil loss. It depends on the hydro-geotechnical condition, the diameter of the tunnel, earth cover, and construction conditions etc. Surface settlement process is generally divided into five stages: in front of cutter head (more than 3 m in front of cutter head), TBM passing, tail seal passing (about 4 m behind tail shield) and behind tail shield.

The conicity of TBM is considered as an influencing factor for surface settlement in this article. Four conicity conditions are used to simulate the influence of TBM boring on surface settlement. Then comparison are made between the numerical results and real monitoring data to find out the relationship between conicity of TBM and surface settlement for the mixed shield machine construction in soft clay.

2 INFLUENCE OF THE TBM CONICITY ON CONSTRUCTION

The conicity of a TBM is the diameter difference from TBM body. Often the diameter of the TBM body is decreased from the front shield, the middle shield, and the rear shield in turn. Use of a TBM with conicity is to easily control the construction and to decrease the thrust force imposed on TBM when the construction distance is relatively long.

The twin 15.43 m diameter mixed shield machines with conicity and air bubble balanced are adopted in the Shanghai Yangtze River Tunnel project for continuous boring without any middle shafts. The external diameter of the lining is 15.0 m. The internal diameter of the lining is 13.7 m. The width of a ring is 2.0 m. The thickness of a ring is 0.65 m. There are ten segments for one ring. The diameter of the front shield, the middle shield and the rear shield is $15{,}430 \pm 15$ mm, $15{,}400 \pm 15$ mm, and $15{,}370 \pm 15$ mm, respectively, which are decreased by 30 mm in series (Fig. 1).

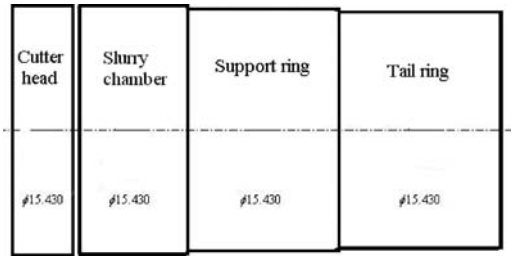

Figure 1. TBM body conicity used in the Shanghai Yangtze River Tunnel Project.

The influence of the TBM conicity on the construction can be concluded as follows:

- If the space bored by TBM is increased, then grouting volume should be added to control the surface settlement and the stability of the tunnel;
- Comparison between the cutter head and the TBM body validates the existence of the over-cut due to the TBM conicity. This phenomenon makes it difficult to control the TBM axis;
- It is easy for the slurry to enter the rear part of a TBM which will cause the uplifting of the rear

shield; the rear part of a TBM cannot get the support from the surrounding soil which increases the ground creeping space and makes it difficult to keep ground balance.

3 TWO-DIMENSIONAL FINITE ELEMENT SIMULATION

3.1 *Geological conditions*

The geological conditions of surface section of the west tunnel of the Shanghai Yangtze River Tunnel project from top layer to bottom layer are: ①$_1$ backfilling, ①$_2$ river bed mud, ①$_3$ brown yellow–grey yellow sandy silt, ②$_3$ grey sandy silt, ③$_1$ grey muddy silty clay, ③$_2$ grey sandy silt, ④$_1$ grey muddy silt, ⑤$_1$ grey clay, ⑤$_2$ grey clay silt, ⑦$_{1\text{-}2}$ grey sandy silt, ⑧ grey silty clay, ⑨$_2$ grey fine sand with gravel.

The TBM mainly goes through layer ④$_1$ grey muddy clay. The leveling of the tunnel axis at break-in position is −11.045 m. The cover above the top of the tunnel is about 6.898 m. The thickness of the cover along the axis increases slowly. The largest thickness of the cover for a surface section is about 11.1 m.

3.2 *Finite element model*

Based on the geological report and relevant documents, main analytical parameters of each ground layer and the structure are calculated and listed in Table 1 and Table 2. The calculation range is 120 m 70.8 m. The top edge (the ground surface) is set as free and the bottom edge is 3 times the diameter of the tunnel under the bottom of the tunnel. The left and right edge is 3.5 times the diameter of the tunnel away from the entrance of the tunnel. Side edge points are limited horizontally and bottom edge points are limited vertically. The underground water leveling in this model is 5.8 m below the ground surface. Soil and water pressure are considered together for the calculation. It is supposed to be homogeneous ground horizontally. Plane strain elastic-plastic constitutive model is adopted for calculation. Drucker-Prager yield criterion is adopted. Triangle solid elements are adopted for the ground. Two-dimensional beam elements are used to simulate the shield and segment lining.

Index parameters and main physical characteristics for each layer of ground refer to Table 1. Based on the shield and segment characteristics, mechanical characteristic parameters refer to Table 2.

3.3 *Grout layer simulation*

1 Equivalent uniform grouting pressure

Grouting is simulated by equivalent uniform load, and the surrounding uniform pressure is:

$$Q = P \times N / \pi \times R \tag{1}$$

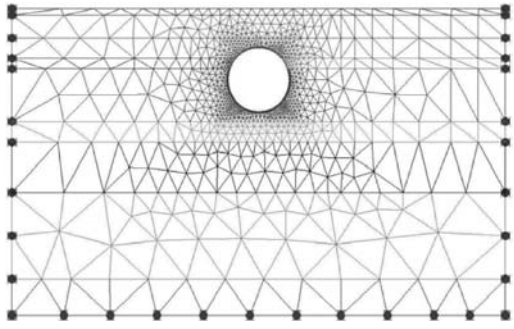

Figure 2. Mesh of the model.

Table 2. Beam element parameters.

Name	Elastic ratio E/GPa	Volume weight kN.m^{-3}	Sectional area A/m^2	Inertia moment I/m^4
Shield	210	78.5	0.18	4.86E-04
Segment	36	24.0	0.65	2.29E-02

Table 1. Solid element parameters for calculation.

Number	Layer name	Elastic modular E/MPa	Poisson ratio μ	Volume weight γ/ kN.m^{-3}	Cohesive strength c/MPa	Internal friction angle φ/(°)	Thickness (mm)
①$_1$	backfilling	5.0	0.30	18.0	9	28.5	1.5
②$_3$	grey sandy silt	7.48	0.27	18.4	9	28.5	5.3
③$_1$	grey muddy silty clay	3.6	0.38	17.6	12	15.0	4.7
③$_2$	grey sandy silt	8.19	0.25	18.5	7	30.0	2.4
④$_1$	grey muddy silt	2.21	0.39	16.8	11	10.5	12.2
⑤$_1$	grey clay	3.27	0.36	17.6	15	16.0	4.8
⑤$_2$	grey clay silt	4.24	0.33	18.0	18	18.5	11.5
⑦$_{1\text{-}2}$	grey sandy silt	10.58	0.28	18.7	8	30.5	20.0
⑧	grey silty clay	4.1	0.38	18.0	18	18.0	8.4

Table 3. Technical indexes of the mortar.

Slum (cm)	Yield value (MPa)	Specific weight	Bleeding (%)
12–14	20H, ≥1.0	>1.9	<12

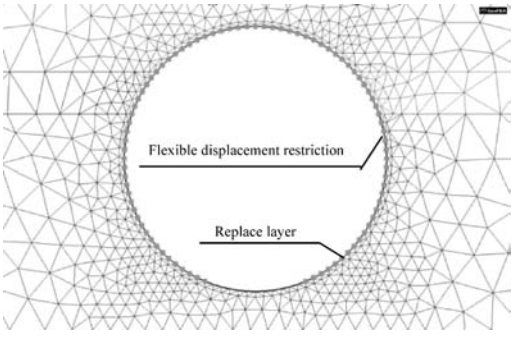

Figure 3. Flexible displacement limit around TBM and equivalent layer of surrounding ground.

where: P is grouting pressure; N is the number of grouting holes in a ring; R is the external diameter of a segment. In this calculation, all the parameters are: $P = 0.6$ MPa, $N = 6$, $R = 15$ m.

Mortar is used for this project. Technical indexes are shown in Table 3.

2 Equivalent layer

The concept of equivalent layer is used to describe the construction space, grout filling degree, surrounding soil disturbed degree, and the area which are caused by TBM construction. According to the result of real monitoring displacement, the parameters for equivalent layer are $E = 40$ kPa, $\mu = 0.3$, $\gamma = 16.8$ kN.m^{-3}.

3 Flexible displacement limit

Flexible displacement limit is used to consider the influence of the TBM conicity on surrounding ground. Flexible displacement limit is set on the surrounding points of the shield.

3.4 *Finite element simulation for TBM boring*

The software of Tongji Shuguang (GeoFBA2D®) is adopted to simulate four conicity construction conditions during TBM construction through the finite element method. Construction condition 1 is without the conicity. Construction condition 2 is the conicity of 30 mm. Construction condition 3 is the conicity of 60 mm (which is the real condition in the Shanghai Yangtze River Tunnel project). Construction condition 4 is the conicity of 90 mm. All the other construction conditions are the same. Construction steps which include the excavations by stages and lining structure are used to simulate the influences before and after the lining supporting. In the meantime, the step-by-step loading and unloading method is adopted in each construction steps to realize the slowly releasing displacement process in plane problem analyses.

Finite element method is adopted to describe the status of each construction stages. Increment load is added, then the mechanical formula should be:

$$\left[[K]_0 + \sum_{A}^{i}[\Delta K]_A\right]\{\Delta u\}_i = \{\Delta F_r\}_i + \{\Delta F_a\}_i \quad (\mathrm{i}=1, \mathrm{L}) \tag{2}$$

where: L – the number of total construction steps;
$[K]_0$ – Initial stiffness matrix for soil and structure(before construction);
$[\Delta K]_i$ – Stiffness variation value of soil and structure for construction step i which shows the ground excavation, structure building or dismantling;
$\{\Delta F_r\}_i$ – Equivalent nodal releasing load along the excavation edge for construction step i;
$\{\Delta F_a\}_i$ – Equivalent nodal applied load for construction step i;
$\{\Delta u\}_i$ – Nodal displacement increment for construction step i.

Construction step simulation: step 1 is in front of cutter head; step 2 is adding flexible displacement limit when TBM arrives; step 3 is replacing TBM material by segment material, changing the material for equivalent layer and adding grouting pressure.

4 ANALYSES ON NUMERICAL RESULTS

Based on the surface settlement of the past TBM bored tunnel projects in Shanghai, the following conclusions are drawn:

- In front of TBM (more than 3 m away from cutter head), 5–12 m in front of the front face, the surface settlement is less than 5 mm; 3–5 m in front of front face, surface settlement is within 10 mm;
- When TBM arrives, the peak value of surface uplifting is within 10 mm;
- In the process of TBM passing, the surface settlement during the first excavation period is in the range of 10–15 mm which is 15%–20% of the total settlement;
- When tail seal passes (4 m behind tail shield), the settlement is 10–20 mm which is 20%–30% of the total settlement;
- After tail seal passed, the settlement speed rate after 10d is 1 mm/d, 0.2 mm/d after 30d, 0.06 mm/d after 100d. The post-consolidation settlement during 100d reaches 30 mm which is about 50% of the total settlement.

Table 4. Real monitoring surface settlement data of west tunnel in surface section.

Monitoring point	Mileage (m)	Cover (m)	In front of cutter head First stage	Above cutter head Second stage	Above tail seal Third stage	30 m behind tail seal Fourth stage	Settlement during construction Second plus third stages
20	501.87	15.81	−1.88	−1.24	−29.98	−7.08	−31.22
23	504.87	16.00	−2.77	−7.34	−41.31	−11.84	−48.65
26	507.87	16.16	−6.11	−1.95	−37.38	−20.52	−39.33
29	510.87	16.47	−5.16	−6.38	−34.41	−20.08	−40.79
32	513.87	16.63	−10.87	−6.99	−30.11	−0.06	−37.10
35	516.87	16.95	−9.15	−3.74	−35.08	−1.47	−38.82
38	519.87	17.34	−5.50	−26.01	−31.70	−9.23	−57.71
41	522.87	18.63	−17.72	−2.01	−41.01	−10.84	−43.02

Note: All the monitoring points are above the axis of the tunnel, all the units which are not marked are in term of mm.

4.1 *Monitoring data*

The monitoring area during TBM construction is within 30 m in front of the cutter head and 30 m behind tail shield. All the data which are divided by surface settlement stages are listed in Table 4.

Taking the average value of 8 monitoring sections in Table 4, it is shown that:

- In front of the cutter head, the surface settlement is about 7.4 mm which is 12.4% of the total settlement (4 stages);
- Above the cutter head, the surface settlement is about 6.9 mm which is 11.7% of the total settlement;
- Above the tail seal, the surface settlement is about 35.1 mm which is 58.9% of the total settlement;
- 30 m behind tail seal, the surface settlement is about 10.1 mm which is 17.0% of the total settlement; the total settlement is about 59.6 mm.

As it takes long time for long-term consolidation, there is no monitoring data for the fifth stage. If the percentage value is calculated with 5 stages, it will be less than those shown above which almost matches the data offered in related references.

4.2 *Comparisons between numerical results and monitoring data*

The finite element results of four conicity conditions are shown in Table 5.

Above the tunnel axis, the settlement value of construction condition 1 is 16.1 mm. The settlement value of construction condition 2 is 27.3 mm. The settlement value of construction condition 3 is 48.9 mm. The settlement value of construction condition 4 is 66.8 mm.

It is shown from Figure 4 that there is settlement above the tunnel under all construction conditions. The results obtained from the finite element analysis show that the settlement is directly proportional to the conicity and the maximum settlement value is the one above the axis of the tunnel. Maximum settlement values are shown in Table 5. The settlement value is about 42.08 mm at the location of XK0+500 section

Table 5. Numerical results of four construction condition.

Number	Construction condition	Numerical result for surface settlement (above the axis of the tunnel)
1	Water and soil pressure considered together + no conicity	16.1 mm
2	Water and soil pressure considered together + 30 mm conicity	27.3 mm
3	Water and soil pressure considered together + 60 mm conicity	48.9 mm
4	Water and soil pressure considered together + 90 mm conicity	66.8 mm

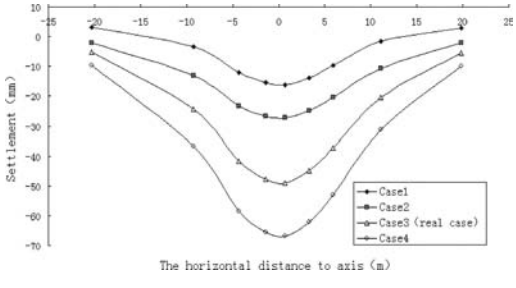

Figure 4. Surface settlement comparison between different construction conditions.

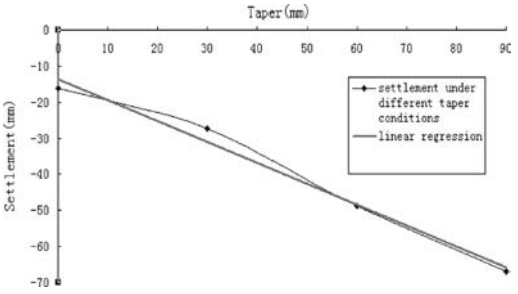

Figure 5. Influence curve from conicity on settlement.

of west tunnel which is close to the calculation result of construction condition 3.

From Figure 5, it is shown that surface settlement is linearly increased with the conicity under other same conditions.

5 CONCLUSIONS

Based on the analyses illustrated above, it is evident that the conicity of the TBM is one of the important factors which influence the surface settlement. It is mainly due to the shield diameter difference which provides the soil more spaces for deformation. The surface settlement increases linearly with the conicity. As a result, grouting pressure and volume should be strictly controlled during construction to decrease the influence of the conicity on settlement. Two-dimensional finite element method is adopted to investigate the influence of TBM boring on the surface settlement. Comparison of the numerical results to the real monitoring data shows good agreement has been achieved.

REFERENCES

Bi, J.H., Jiang, Z.F. & Chang, B. 2005. Numerical simulation for constructions of metro tunnels with short distance between them. *Rock and Soil Mechanics* 26(2):277–251.

Huang, H.W. & Zhang, D.M. 2001. Shield tunnelling induced surface settlement and in-situ monitoring. *Chinese Journal of Rock Mechanics and Engineering* 20(S1):1814–1820.

Yu, N. & Zhu, H.H. 2004. Analysis of earth deformation caused by shield tunnel construction and 3D-FEM simulation. *Rock and Soil Mechanics* 25(8):1330–1334.

Zhang, F.X., Fu, D.M. & Yang, G.X. 2005. *Construction Manual of Shield Tunnel*. Beijing: China Communications Press.

Zhou, W.B. 2004. *Construction Technology and Application of Shield Tunnel*. Beijing: China Architecture & Building Press.

The Shanghai Yangtze River Tunnel - Theory, Design and Construction – Huang (ed)
© 2008 Taylor & Francis Group, London, ISBN 978-0-415-47161-9

Numerical study on working ventilation of Shanghai Yangtze River Tunnel

J. Ding, T.L. Ge & M. Hu
Shanghai University, Shanghai, P. R. China

J.Y. Wang
Shanghai Tunnel Engineering Co., Ltd., Shanghai, P. R. China

ABSTRACT: Based on the method of computational fluid dynamics, the 3D numerical simulation of working ventilation in Shanghai Yangtze River Tunnel was conducted. The computed results give flow velocity and temperature profiles, which provides reference for evaluating the effect of working ventilation in tunnel. Moreover, the way of enhancing ventilation efficiency has been presented to improving air quality of working field further.

1 INTRODUCTION

Shanghai Yangtze River tunnel was designed as 6 lanes bi-directional expressway. The total length of the tunnel is 8.95 km and the external diameter of tunnel is 15 m. There were 7.50 km of the tunnel was constructed by shield tunneling method. Shanghai Yangtze River tunnel is the largest crossing-river tunnel in China so far.

Both highway and metro were involved in one tunnel for this project, where the upper space was used for highway and the space below was used for metro.

The working ventilation system was designed based on underground longitudinal ventilation method. The provision railway space was used as the ventilation passage to provide flow flux. The working ventilation system was very important but difficult for long and large tunnel. Consequently, the numerical modeling was carried out to simulate the flow field in the tunnel.

2 GOVERNING EQUATION AND NUMERICAL METHODS

2.1 *Governing equation*

The simulation was performed based on Reynolds-averaged Navier-Stokes equations (RANS) using standard $k-\varepsilon$ turbulence closing above equations. The equations were introduced as below.

Continuity equation:

$$\frac{\partial u_j}{\partial x_j} = 0 \tag{1}$$

Momentum equation:

$$\frac{\partial u_i}{\partial t} + u_j \frac{\partial u_i}{\partial x_j} = -\frac{1}{\rho}\frac{\partial p}{\partial x_i} + \frac{\mu}{\rho}\frac{\partial^2 u_i}{\partial x_j \partial x_j} - \frac{\partial}{\partial x_j}(\overline{u_i' u_j'}) + g_i \tag{2}$$

Energy equation:

$$\frac{\partial}{\partial t}(\rho h) + \frac{\partial}{\partial x_i}(\rho u_i h) = \frac{\partial}{\partial x_i}\left(k_{eff}\frac{\partial T}{\partial x_i} + u_j \tau_{ij}\right) \tag{3}$$

k equation:

$$\frac{\partial k}{\partial t} + u_j \frac{\partial k}{\partial x_j} = \frac{1}{\rho}\frac{\partial}{\partial x_j}[(\mu + \frac{\mu_t}{\sigma_k})\frac{\partial k}{\partial x_j}] + \frac{G_k}{\rho} - \varepsilon \tag{4}$$

ε equation:

$$\frac{\partial \varepsilon}{\partial t} + u_j \frac{\partial \varepsilon}{\partial x_j} = \frac{1}{\rho}\frac{\partial}{\partial x_j}[(\mu + \frac{\mu_t}{\sigma_k})\frac{\partial \varepsilon}{\partial x_j}] + \frac{1}{\rho}C_{\varepsilon 1}G_k\frac{\varepsilon}{k} - C_{\varepsilon 2}\frac{\varepsilon^2}{k} \tag{5}$$

Where, u_j is the velocity of j component, t is the time, x_j is the coordinate of j, ρ is the air density, μ is the dynamic viscosity; g_i is the gravitational body force. $(\overline{u_i' u_j'})$ is the Reynolds stress. $\mu_t = \rho C \mu k2/\varepsilon$ is the turbulent viscosity. G_k is the turbulent kinetic energy production. σ_k ($\sigma_k = 1.0$) and σ_ε($\sigma_\varepsilon = 1.3$) are turbulent Prandtl number for k and ε respectively. C_μ, $C_{\varepsilon 1}$ and $C_{\varepsilon 2}$ are model constants ($C_\mu = 0.09$, $C_{\varepsilon 1} = 1.44$, $C_{\varepsilon 2} = 1.92$).

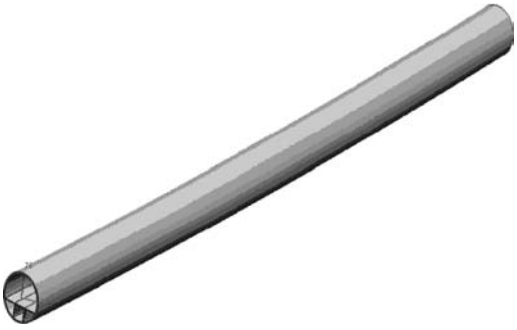

Figure 1. Model of tunnel.

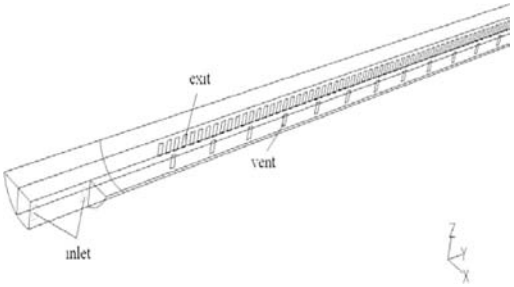

Figure 2. Sketch map of computational model.

2.2 *Numerical methods*

Based on finite control volume method and simple scheme, discretization governing equations are listed in the general formation shown as equation (6).

$$A_p \Phi_p = \sum A_{nb} \Phi_{nb} + S_{\Phi p} \tag{6}$$

where Φ is general variable and $S_{\Phi p}$ is source of Φ equation, with subscript *nb* representing cell around governing volume of point *P*. The diffusive term is discretized by center difference scheme of 2nd order accurate, and the convection term is discretized by upwind scheme of 2nd order accurate.

2.3 *Computation model*

The tunnel model used in numerical simulation was shown in Figure 1. The below space of tunnel was divided into three parts by exit side and vent side. Exits and vents are evenly mounted. The interval between vents is 10 m, and the interval between exits is 2 m, which is shown in Figure 2.

The construction process of the tunnel was very complex and there were many influential factors on flow field. It is impossible to consider all the factors in the simulation. In order to improve the computational efficiency, the numerical simulation on the ventilation was focused on space below the highway of tunnel. The numerical model was presented in Figure 2.

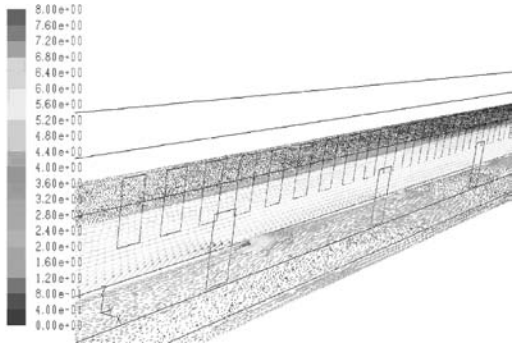

Figure 3. Velocity vectors of flow field in streamline direction ($z = -0.5$ m).

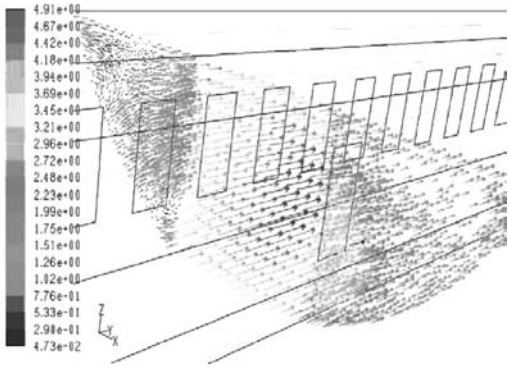

Figure 4. Velocity vectors of cross section at 150 m in y-direction.

2.4 *Initial and boundary conditions*

Inlet velocity can be obtained According to the given flow pressure and flux of SDF-No18 (which is used as special-purpose axial fan in the building tunnel). Standard wall functions with roughness have been adopted for the wall and ground. The temperature of inflow was supposed to be as high as 305 K.

3 RESULTS AND DISCUSSION

The velocity vector distribution at $z = -0.5$ m (0.5 m under highway surface) was shown in Figure 3. The computed results illustrated that the fresh air entered the tunnel from axial fan with jet movement. The wind direction changed suddenly after airflow met exit wall, then energy was depleted and average velocity reduced rapidly.

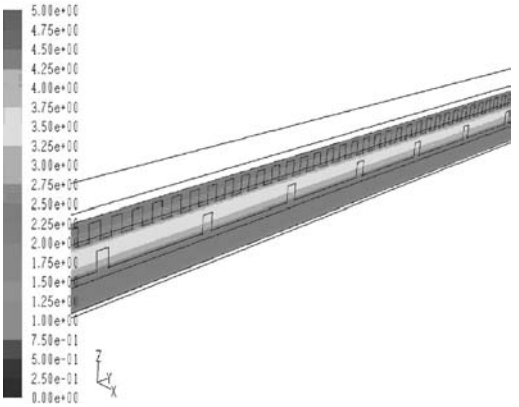

Figure 5. Velocity profile of flow field in streamline direction at $z = -0.5$ m.

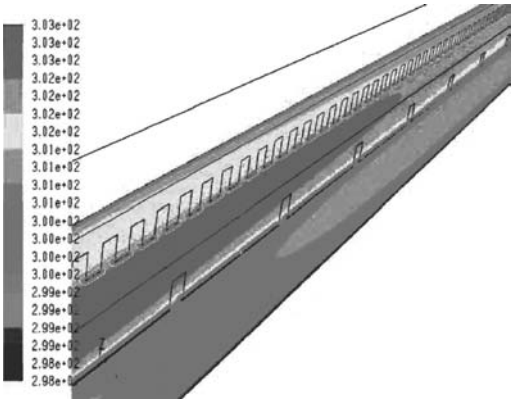

Figure 6. Temperature contour profile of flow field in streamline direction at $z = -0.5$ m.

Besides, it could be found that the majority of flow focused on the middle part and vortex appeared near vents and exits from Figure 3. Moreover, the velocity magnitude of exit side was greater than those of vent side because air flow enter the tunnel perpendicularly to exit side.

Velocity vector of cross-section at 150 m in y-direction was shown in Figure 4. It could be found that flow velocity was high in the middle part of cross section and low at both sides. The velocity magnitude was in the range of 3.5–5.0 m/s in the middle part and of 2.0–3.5 m/s at vent space and of 1.0–2.0 m/s at exit space. It was consistent with measured data.

Velocity profile of flow field along streamline direction at $z = -0.5$ m was shown in Figure 5. It could be found that the velocity magnitude of flow along streamline direction decreased gradually because of the turbulence viscosity dissipation and friction. As a result, the air flowed smoothly in the tunnel and

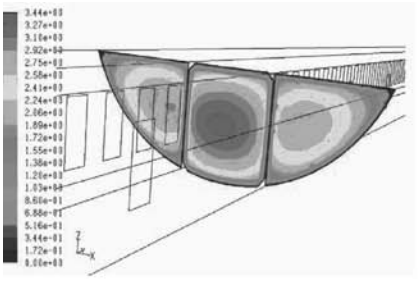

(a) y = 1,000 m.

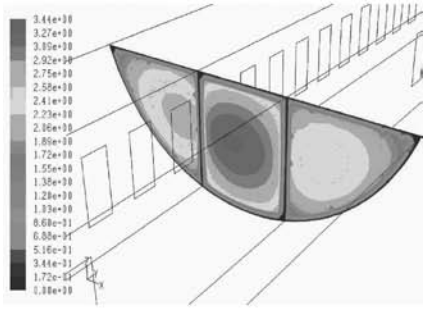

(b) y = 2,000 m.

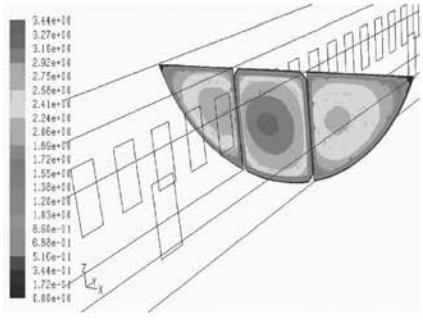

(c) y = 3,000 m.

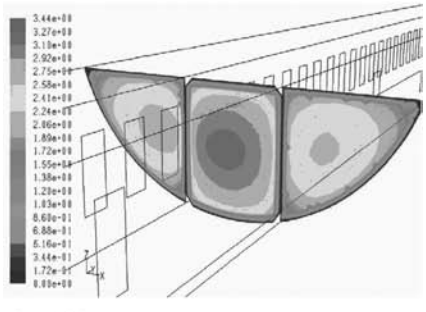

(d) y = 4,000 m.

Figure 7. Velocity contours of several sections in streamline direction of the tunnel.

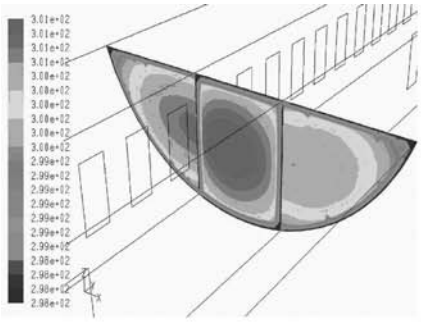

(a) y = 1,000 m.

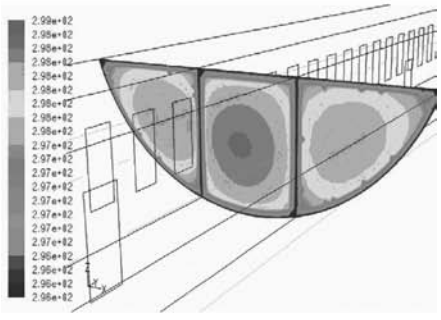

(b) y = 2,000 m.

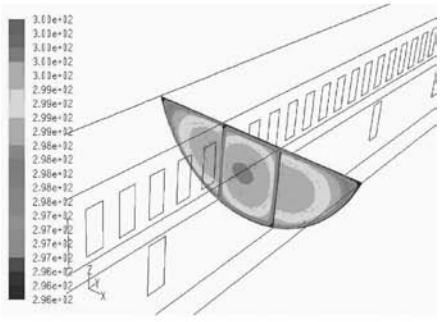

(c) y = 3,000 m.

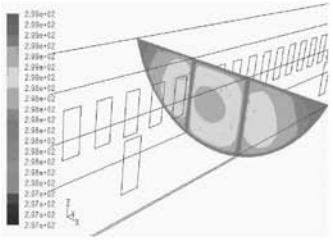

(d) y = 4,000 m.

Figure 8. Temperature contours of several sections in streamline direction of the tunnel.

velocity magnitude changed little after flow was fully developed.

Temperature contour profile at $z = -0.5$ m was shown in Figure 6. It could be found that the flow temperature decreased gradually with the increase of distance from tunnel inlet because of the energy exchange between flow and tunnel wall.

Figure 7 illustrated the velocity contours at $y = 1{,}000$ m, $y = 2{,}000$ m, $y = 3{,}000$ m and $y = 4{,}000$ m in streamline direction. It showed the amplitude of the velocity in the middle part of cross section was largest. However, the velocity was zero on the wall. The magnitude of velocity decreased with the distance increasing, which was consistent with above computed results. The maximum velocity was 3.3 m/s and averaged velocity was 2.3 m/s for 4,000 m distance in tunnel. It seemed that ventilation state at present may satisfy the ventilation demand without considering supplying flux for the flow field around working shield machine based on numerical simulation.

The temperature contours $y = 1{,}000$ m, $y = 2{,}000$ m, $y = 3{,}000$ m and $y = 4{,}000$ m in streamline direction was presented in Figure 8. The temperature in the middle part of section was lager than that near the wall. The magnitude of temperature decreased with the distance far away from inlet, which was also consistent with above mentioned computed results.

4 CONCLUSIONS

The 3D numerical simulation of working ventilation in Shanghai Yangtze River tunnel was conducted in this paper. The calculated velocity profiles of tunnel at 150 m cross-section in y-direction were presented. A good agreement was found between the calculated results and measured data. The flow velocity and temperature profiles of the whole field were obtained and analyzed. It showed that the ventilation state satisfied the ventilation demand. The jet fans should be set around working field to accelerate air circulation and improve air quality. It was also good to make the inflow direction coincided with the streamline of tunnel. As a result, the velocity could be increased, which was benefit to improve air quality, cool and dehumidifying for working environment.

REFERENCES

Du, F. & Fu, J. 2007. Feasibility study of providing provision space for future LRT in Yangzi River crossing tunnel. *Chinese Journal of Underground Space and Engineering* 3: 494–498.

Fan, W.C. & Wan, Y.P. 1992. *The Model and Computation of Flow and Combustion*. Hefei: University of Science and Technology of China Press.

The Shanghai Yangtze River Tunnel - Theory, Design and Construction – Huang (ed)
© 2008 Taylor & Francis Group, London, ISBN 978-0-415-47161-9

Optimization design and research of the cross section form and structure for Shanghai Yangtze River Tunnel

Y. Xu & W.Q. Ding
Key Laboratory of Geotechnical & Underground Engineering, Ministry of Education, Tongji University, Shanghai, P. R. China
Department of Geotechnical Engineering, School of Civil Engineering, Tongji University, Shanghai, P. R. China

ABSTRACT: This paper expound the optimization for section form and structure of Shanghai Yangtze River Tunnel. Through the proper arrangement in tunnel inner space, taking reduction of internal diameter as object and satisfying tunnel application functions as constraint conditions, the optimization model of shield tunnel section is established. Complex Method is used as the optimization method, C++ language is used to program and implement the optimization. Then, the thickness of the shield tunnel lining and the joint position will be optimized to improve the stress condition of shield tunnel lining.

1 INTRODUCTION

With the rapid development of municipal traffic, the road becomes wider and wider. Consequently, the tunnel diameter in city becomes larger and larger. The large tunnel diameter will not only increase the construction cost, but also cause difficulties for tunnel design, construction and operation. So, how to make the best use of the tunnel clearance, how to reduce the tunnel diameter as far as possible under the condition that all of the tunnel functions can be satisfied, and how to design the tunnel lining properly are the significant problems which need to be solved by designers.

It's no doubt that applying the modern numerical optimization method to the design of shield tunnel is an effective way to solve these problems. But now, in the design of shield tunnel, the empirical method is used mostly, the designers define the structural parameter often according to their experiences. The design plan is practical, but not optimum. However, the numerical optimization method is not used widely; more research is needed.

The numerical optimization method is a new branch of applied mathematics. In recent twenty years, it develops very quickly with the widespread application of computer. Applying the numerical optimization method in civil construction design makes the traditional passive analysis to be the active research. This is a great progress in the civil engineering design, and it is a structural design method more scientific, more effective and more economic.

By use of an engineering example, the optimization process of section form and structure of shield tunnel is expounded in this paper. The Complex Method is used as the numerical optimization method; and the C++ language is used to implement it.

2 THEORY OF COMPLEX METHOD

2.1 *Mathematic model of complex method*

The mathematic model of complex method usually can be expressed as follows:
Solve: design variable: X
Min: $f(x)$
S.T (Subject to constraint condition):
Inequation constraint condition:

$$g_j(x) \le 0 \quad (j = 1, 2, ..., m) \tag{1}$$

Boundary constraint condition:

$$a_i \le x_i \le b_i \quad (i = 1, 2, ..., n) \tag{2}$$

where a_i is the upper limit of the variable; b_i is the lower limit of the variable.

2.2 *Iterative process of complex method*

2.2.1 *The building of initial complex*

The complex is composed of k ($k > n + 1$) vertexes. There are two methods to define these vertexes.

(1) Definitive method

Designers can define these vertexes by themselves according to the properties of the problem.

(2) Random method

The vertexes are defined by the following formula:

$$x_{ij} = a_i + \gamma_{ij}(b_i - a_i) \quad (i = 1,2,.....,n\ ;\ j = 1,2,.....,k) \tag{3}$$

where i is the number of variable; j is the number of vertex; γ_{ij} is a random value between 0 and 1.

The vertexes defined by random method conform to all boundary conditions, but do not always conform to all inequation of constraint conditions.

Supposing there are s ($1 \leq s \leq k$) vertexes conform to all constraint conditions, the center $\bar{X}_s$ of the valid vertexes can be defined by following formula:

$$\bar{X}_s = \frac{1}{s}\sum_{j=1}^{s} X_j \tag{4}$$

The n-s vertexes that can not conform to all constraint conditions can be dealt with by following formula:

$$X_{s+1} = \bar{X}_s + 0.5(X_{s+1} - \bar{X}_s) \tag{5}$$

If the new vertexes still can not conform to all constraint conditions, they are dealt with formula (5) again until they can conform to all constraint conditions.

2.2.2 *Search for reflection point*

Figure out all the values of objective function $f(X_j)$, and find out the worst vertex X_h which makes the value of $f(X_j)$ maximum, X_c is the centre of the vertexes that do not include the worst vertex X_h.

$$Xc = \frac{1}{k-1}(\sum_{j=1}^{k} X_j - X_h) \tag{6}$$

Define a reflection coefficient $\alpha(\alpha \geq 1)$, the reflection point Xa can be defined by following formula:

$$X_a = X_c + \alpha(X_c - X_h) \tag{7}$$

Checking whether X_a is valid, if not, reducing the value of α to its half, then deal X_a with formula (7) until it becomes valid.

2.2.3 *Compare the value of $f(X_j)$ at X_a with that at X_h*

There are two possible results:

- If $f(X_a) < f(X_h)$, i.e. X_a is better than X_h, replace X_h with X_a, the new complex is formed, then, turn to step ② and go on.
- If $f(X_a) \geq f(X_h)$, i.e. X_a is not better than X_h, reduce the value of α to its half again until X_a is better than X_h, then turn to step ② and go on.

2.2.4 *Criterion of convergence*

There are many criteria of convergence, but the criterion used most widely is that the values of $f(X_j)$ at all vertexes can conform to constraint condition as follows:

$$\{\frac{1}{k}\sum_{j=1}^{k}[f(\bar{X}_s) - f(X_j)]^2\}^{1/2} < \varepsilon \tag{8}$$

Where, $f(\bar{X}_s)$ is the value of objective function at the centre point; ε is a little positive number.

Find the vertex at which the value of objective function is least, the optimum vertex is found.

3 OPTIMIZATION OF CROSS SECTION AND LINING STRUCTURE OF SHIELD TUNNEL

3.1 *General situation of the shield tunnel*

Shanghai Yangtze River Tunnel starts at Pudong New Area, passes through the south harbor of Yangtze River, and ends at the south bank of the Changxing Island. The total length of the tunnel is 8.955 km, of which the shield tunnel section is about 7.47 km. The tunnel is designed in three-lane highway standard. Its outer diameter is 15 m; the inner diameter is 13.7 m; and a space is reserved for rail traffic in the future. The tunnel lining is composed of 10 segments. The segment thickness is 0.65 m and the width of the lining ring is 2 m.

3.2 *Optimization of tunnel design*

The tunnel is designed in the three-lane highway standard, and a space is reserved for rail traffic built in the future. At the same time, a smoke duct, drain pipes, cable channel and lighting equipments also need space. In order to satisfy all of the tunnel functions, the inner diameter of the tunnel becomes larger and larger. Consequently, the construction cost is high, the inner force of the lining structure is big, and various difficulties in the tunnel design, construction and operation occur.

In order to reduce the tunnel inner diameter as far as possible and satisfy all the tunnel application functions, an optimization model is established. Complex method is used as the optimization method and C++ language is used to implement it. After the section optimization, the lining structure will be optimized to improve the stress condition.

3.3 *General process of the optimization design*

There are two steps of the optimization design. First, optimize the cross section of the tunnel; then, optimize thickness and the joint position of the tunnel lining.

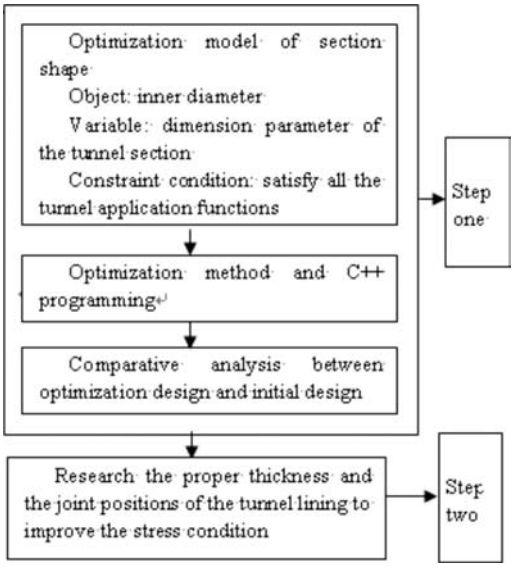

Figure 1. Flowchart of the optimization.

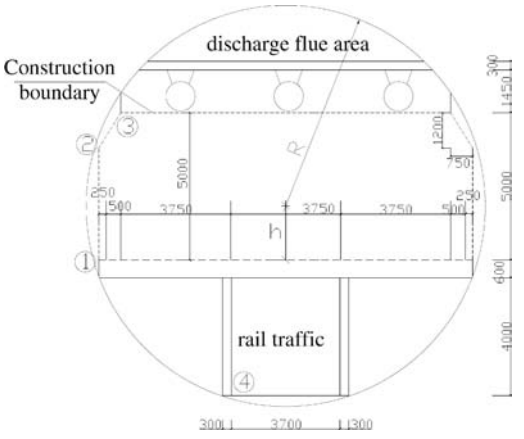

Figure 2. Sketch of tunnel section.

3.4 *Optimization of the tunnel cross section*

3.4.1 *Building of optimization model*

(1) Selection of the design variable

The cross section of shield tunnel is generally a circle, as shown in the Figure 2. If R (the inner radius) and h (the height from bottom of the construction boundary to the section center) are defined, the section is defined. So, R and h are selected as the design variables.

(2) Building of the objective function

The object of the optimization of the tunnel section is to reduce the tunnel inner diameter as far as possible and satisfy all the tunnel application functions. So, R (the inner radius) will be taken as the objective function.

(3) Building of the constraint conditions

In order to satisfy all the tunnel application functions, several constraint conditions must be built.

① Ensure the tunnel lining can't enter into the construction boundary.

As shown in the Figure 2.

The tunnel lining can't enter into the point 1:

$$R \geq \sqrt{h^2 + (12.75/2)^2} \tag{9}$$

The tunnel lining can't enter into the point 2:

$$R \geq \sqrt{(3.8-h)^2 + (12.75/2)^2} \tag{10}$$

The tunnel lining can't enter into the point 3:

$$R \geq \sqrt{(5-h)^2 + (11.25/2)^2} \tag{11}$$

② Ensure the tunnel lining can't enter into the space reserved for the future rail traffic.

The tunnel lining can't enter into the point 4:

$$R \geq \sqrt{(0.6+4.0+h)^2 + (3.7/2)^2} \tag{12}$$

③Ensure there are enough space for the smoke duct.

$$2*\arccos\left(\frac{(5-h)+1.45+0.3}{R}\right)*\pi R^2/360 - [(5-h) + 1.45+0.3]*\sqrt{R^2-[(5-h)+1.45+0.3]^2} \geq 12.8 \tag{13}$$

(4) Optimization model of the tunnel section

The optimization model can be expressed as follows:

Min: R

Solve: R and h

$$\text{S.T:}\quad R \geq \sqrt{h^2 + (12.75/2)^2} \tag{14}$$

$$R \geq \sqrt{(3.8-h)^2 + (12.75/2)^2} \tag{15}$$

$$R \geq \sqrt{(5-h)^2 + (11.25/2)^2} \tag{16}$$

$$R \geq \sqrt{(0.6+4.0+h)^2 + (3.7/2)^2} \tag{17}$$

$$2*\arccos\left(\frac{(5-h)+1.45+0.3}{R}\right)*\pi R^2/360 - [(5-h) + 1.45+0.3]*\sqrt{R^2-[(5-h)+1.45+0.3]^2} \geq 12.8 \tag{18}$$

3.4.2 *Implement of the optimization process*

Complex method is used as the numerical optimization method, programmed with C language. The optimum solution of the design variables can be gained by running the C++ program.

3.4.3 *Optimization design and comparative analysis*

The optimum solution got by C++ program:

$$R = 6677mm, \quad h = 1815mm \tag{19}$$

The initial design:

$$R = 6850mm, \quad h = 2100mm \tag{20}$$

According to the optimum solution, the construction error and the lining deformation, the optimization design:

$$R = 6750mm, \quad h = 1815mm \tag{21}$$

Through the optimization design, the inner radium of the tunnel can be reduced 100 mm.

3.5 *Optimization design of the tunnel lining*

3.5.1 *Optimization of the lining thickness*

The lining thickness is a key factor in control of the construction cost of shield tunnel. Since the 1960s, scholars of our country have begun to study the problem of how to define the lining thickness properly. Gradually, the rigid lining theory is replaced by the flexible lining theory, which is a significant transition.

According to the flexible lining theory, if reduce the relative rigidity of the tunnel lining to that of the surrounding soil stratum properly, the interaction between the tunnel lining and the surrounding soil stratum will be changed; and the load on tunnel lining will become more well-distributed; the stress condition of the tunnel lining will be improved; and the lining design will be more economical and proper.

The lining rigidity is in direct proportion to the cube of the lining thickness. So, if adjust the thickness of the tunnel lining properly, the relative rigidity of the tunnel lining to the surrounding soil stratum will be changed largely, then, the stress condition of the tunnel lining will be influenced.

Take the Shanghai Yangtze River Tunnel as an example, the inner force and deformation of the tunnel lining with different thickness are studied.

As is shown in the Figure 3 and Figure 4, with the thickness increasing, the bending moment increases and the deformation decrease simultaneously, especially when the thickness changes from 0.3 m to 0.6 m. If the thickness is too large, the deformation can only be reduced a little, and the moment will increase. The small eccentric stress condition will turn into the big eccentric stress condition. This is disadvantageous to the lining structure and the construction cost will also increase. So, defining the lining thickness properly not only can improve the lining stress condition but also can reduce the construction cost.

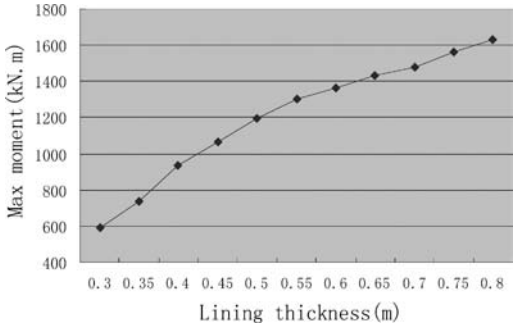

Figure 3. Curve of the relationship between moment and thickness.

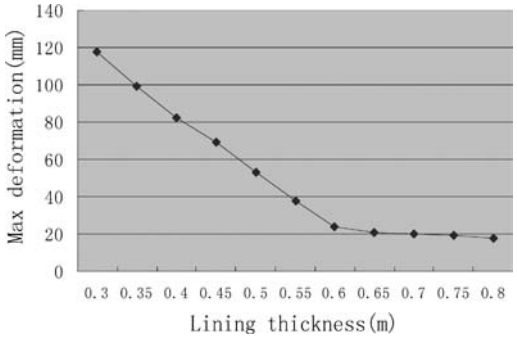

Figure 4. Curve of the relationship between deformation and thickness.

3.5.2 *Optimization of the joint position*

The joint position refers to the partition and the distribution of lining segment. The partition and the distribution of lining segment are decided by several factors such as tunnel diameter, stress characteristic, waterproof effect and assembly technology. If considering is made only from the structure aspect, the change of the joint position will cause the change of the stress characteristic of the structure; if considered from the relationship between the soil strata and the structure, the change of the joint position will cause the change of the structure flexibility. And this will influence the interaction between the soil strata and the structure; then, the structure load will be adjusted; ultimately, the inner force and deformation of the structure will be changed.

Take Shanghai Yangtze River Tunnel as an example, the inner force and deformation of the tunnel lining with different joint position are studied.

Before discussing the problem described above, three constraint conditions will be illuminated first:

- The number of the lining segments keeps unchanged. In view of various factors, for the tunnel located in the saturated and soft soil strata, when the

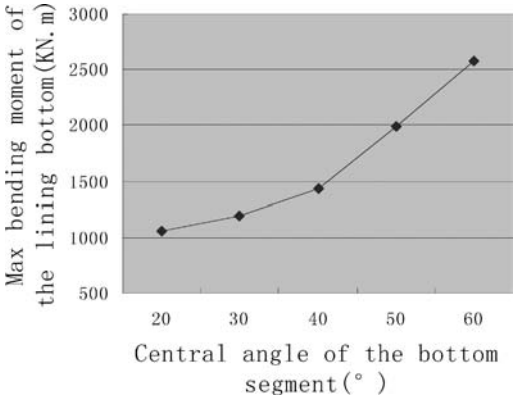

Figure 5. Curve of the relationship between the moment and the central angle of the bottom segment.

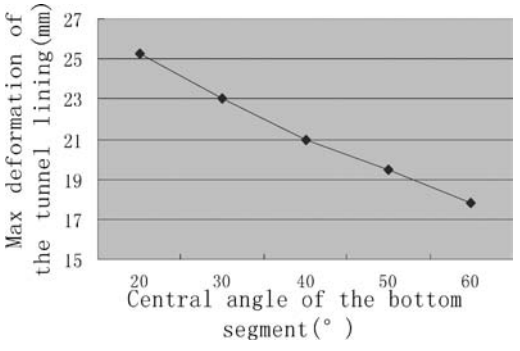

Figure 6. Curve of the relationship between the deformation and the central angle of the bottom segment.

diameter is less than 6 m, the tunnel lining is often composed of 4 to 6 segments; when the diameter is more than 6 m, the tunnel lining is often composed of 8 to 10 segments. The diameter of the Shanghai Yangtze River Tunnel is 15 m, so the tunnel lining is divided into 10 segments appropriately.

- The lining segments are distributed symmetrically. For the tunnel located in the saturated and soft soil strata, the structure load distributes homogeneously. Thus, the symmetrical distribution of the tunnel segments conforms to the load condition of the tunnel.
- The size of the key segment keeps changeless. In the view of several factors, the key segment with small size is more superior; the central angle of the tunnel key segment is 18.519°; it belongs to small size key segment. In the research, the size of the key segment is kept changeless.

The joint position is changed with the central angle of the bottom segment.

As is shown in the Figure 5 and Figure 6, with the central angle of the bottom segment increasing, the bending moment increases and the deformation grows down simultaneously. If the central angle of the bottom segment is too big, the bending moment will become very large. If the central angle of the bottom segment is too small, the deformation will increase. But, compare to the bending moment, the changing range of the deformation is rather small. So, if the central angle of the bottom segment can be defined properly, the stress condition will be improved and the deformation will be under control.

Table 1. Compute results of the original design and the optimization design.

	$M^{+}_{\max 1}$ (KN.m)	$M^{+}_{\max 2}$ (KN.m)	$M^{-}_{\max}$ (KN.m)	$\delta_{\max}$ (mm)
Original design	1346	1425	−1434	24
Optimal design	1307	1196	−1358	21.1

* $M^{+}_{\max 1}$ is the maximal bending moment of the roof;
$M^{+}_{\max 2}$ is the maximal bending moment of the bottom;
$M^{-}_{\max}$ is the maximal bending moment of the hance;
δ_{max} is the maximal deformation of the tunnel lining.

Table 2. Economic effect of the optimization design.

	$D(m)$	$A_e(m^2)$	$V_c(m^3)$	$m_g(t)$
Original design	15	187.96	29.3	2.931
Optimal design	14.7	178.37	26.39	2.323

* D is the outer diameter of the tunnel lining;
A_e is the excavated area;
V_c is the concrete volume per meter needed for he tunnel lining;
m_g is the reinforcing weight per meter needed for the tunnel lining.

3.6 *Optimization design and comparative analysis*

According to the research and analysis in the preceding sections, adjust the original design as follows:

The original design:

$$R = 6.85m, t = 0.65m, \theta = 39.963\propto \tag{22}$$

The optimization design:

$$R = 6.75m, t = 0.6m, \theta = 30\propto \tag{23}$$

Where: R is the inner radius of the tunnel; t is the thickness of the tunnel lining; θ is the central angle of the bottom segment.

The compute results are shown in Table 1. The economic effect is shown in Table 2:

As is shown in the Table 1 and Table 2, through the optimization design, the bending moment of the tunnel lining is reduced, especially at the tunnel bottom.

The deformation becomes small. The cost of the tunnel segment is reduced by 15.68%. It can conclude that optimization design is an effective measure to improve the stress condition of tunnel structure and reduce the construction cost.

4 CONCLUSION

From optimization design of the shield tunnel and the comparative analysis, conclusions can be gotten as follows:

- When defining the objective function and the design variables, many factors can be taken into account. One step optimizing not only makes the problem complex, but also gets no results. By dividing the optimization problem into several steps, the optimization model and operation process can be simplified greatly, through which can get good and practical results.
- By the optimization design and analysis, it can be found that if the tunnel clearance can be used fully, the inner radius will be reduced. If the lining thickness and the joint position can be defined properly, the stress condition of the tunnel lining can be improved without increasing the lining deformation.
- Introducing optimization method into structure design not only can reduce the construction cost but also can improve the structure stress condition. Thus, it should be used widely.
- To solve the non-linear optimization problem with inequation constraint condition, Complex Method is an effective optimization method for its theory is simple and the operation is easy and effective.

REFERENCES

Ding, W.Q., Yue, Z.Q., Tham, L.G., et al. 2004. Analysis of Shield Tunnel. *International Journal for Numerical & Analytical Methods in Geomechanics* 28: 57–91.

JTG D70-2004. 2004. *Road tunnel design code*.

Huang, Z.X., Liao, S.M. & Liu, G.B. 2000. The optimization of the segment thickness of shield tunnel in Shanghai soft soils. *Rock and soil mechanics* (12): 350–354.

Huang, Z.X., Liao, S.M., Liu, G.B., et al. 2000. Optimization of segment joint position of shield tunnel in soft ground. *Underground space* (12): 268–275.

Liu, Y.J., Gao, G.F. & Feng, W.X. 2004. Study on optimization design of cross section of the large-span highway tunnel. *Liao Ning communication science and technology* (2): 48–50.

Qian, N. 1999. *C++ program design course*. Bei Jing: Qing Hua University Press.

Zhang, B.H. 1998. *Civil structure optimization design.* Shang Hai: Tongji University Press.

The Shanghai Yangtze River Tunnel - Theory, Design and Construction – Huang (ed)
© 2008 Taylor & Francis Group, London, ISBN 978-0-415-47161-9

Prediction for long-term settlement of Shanghai Yangtze River Tunnel

D.M. Zhang, H.L. Bao & H.W. Huang
Key Laboratory of Geotechnical & Underground Engineering, Ministry of Education, Tongji University, Shanghai, P. R. China
Department of Geotechnical Engineering, School of Civil Engineering, Tongji University, Shanghai, P. R. China

ABSTRACT: The drainage condition combining with the time-dependent properties of the surrounding soil play an important role in the evolution of long-term settlement of tunnel. This paper presents an analytical solution for the prediction of long-term settlement of Shanghai Yangtze River Tunnel. The complex conformal transformation is used to map the considered region in the physical plane onto a circular ring region in the image plane. Based on the visco-elastic Terzaghi – Rendulic consolidation theory, assuming that the tunnel is partially sealed with partial drainage boundary, the long-term settlement of the tunnel is studied.

1 INTRODUCTION

Tunnelling across river is an increasing commonly geotechnical activity for construction of urban transportation in many cities around the world. Moving traffic underground, tunnels improve the quality of life above ground and may have great economic impact. However mechanical response of tunnels constructed in soft clay is usually time-dependent. The long-term settlements of tunnels in soft soil can be rather significant, which can be confirmed, for instance, by the observed settlements over a period of 11 years reported by O'Reilly et al. (1991) for a 3 m diameter tunnel constructed in normally consolidated silty clay in Grimsby, England. Shirlaw (1995) indicated that typically the increase in settlement over long-term is of the order of 30%–90% of the total settlement. The increase of long-term settlement reaches 60%–90% of the total settlement for No. 2 metro tunnel in Shanghai (Zhang, 2004). As the long-term settlement can affect the function and safety of the tunnel, understanding time-dependent behavior of tunnel is useful not only in the design phase but also during construction.

It is concluded by Mair and Taylor (1997), that the major factors, which have significant influence on the long-term settlements of tunnels, can be mainly attributed to, such as, the magnitude and distribution of excess pore pressure around the tunnel due to shield tunneling, physical properties and permeability of soil, permeability of linings and development of the phreatic surface. Carter and Booker (1982) used Biot's theory to study the long-term settlement of a deep tunnel excavated in an elastic porous media. Later, Carter and Booker (1983) extended their analysis to a visco-elastic medium to include the influence of soil creep. Zhan (1993) solve the consolidation of visco-elastic clay about circular tunnels in foundations by the transform method of conformal mapping. In these works the tunnels were considered both sealed and unsealed. However, in reality, many tunnels cannot be considered as one of these two extreme cases but rather are found in an intermediate situation. Li (1999) introduced a partial sealing condition where the flow across the liner-soil boundary is controlled by both the geometric and hydraulic characteristics of the lining and soil. The more realistic flow boundary was incorporated into the analytical solution proposed by Carter and Booker (1982). Later Li (2002) extended his studies by incorporating the stiffness of linings. Liu (2005) extended Li's solution (2002) by taking account of the visco-elastic behavior of the soil and derived the development of internal force and settlement of deep tunnel in soft soil. However as the assumption of deep tunnel is made, the solution is not suitable for the case of shallow tunnels. This paper presents an analytical solution for the prediction of long-term settlement of shield tunnel in soft clay. The complex conformal transformation is used to map the considered region in the physical plane onto a circular ring region in the image plane. Based on the visco-elastic Terzaghi – Rendulic consolidation theory, assuming that the tunnel is partially sealed with partial drainage boundary, the long-term settlement of Shanghai Yangtze River Tunnel in soft clay is studied.

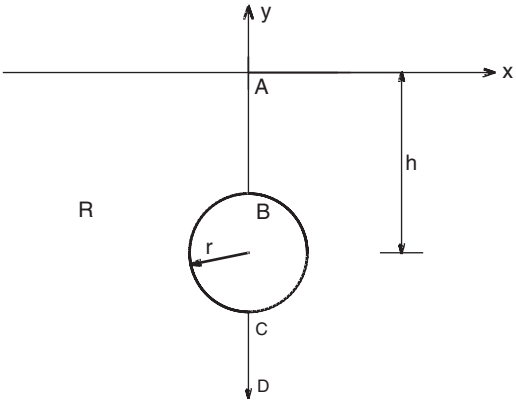

Figure 1. Half-plane with circular tunnel.

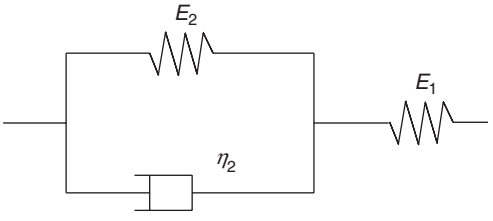

Figure 2. Merchant model.

2 PROBLEM DESCRIPTION

The problem deals with a half-plane with a circular tunnel (Fig. 1). The radius of the tunnel is denoted by r and the depth of its centre by h.

In addition, the following assumptions are made:

- Plane strain conditions are assumed in a direction perpendicular to the cross section of the tunnel.
- The ground around the tunnel can be treated as a half-plane with a circular hole.
- Supposing the soft clay is uniform, isotropic and completely saturated visco-elastic body and the Merchant mode (Fig. 2) is selected for the rheological stress-strain behaviour of the soil skeleton.
- Both the water and soil particles are incompressible.
- Darcy's law of water flow applies.
- The deformation is small enough so as not to influence the coordinates.

3 GOVERNING EQUATIONS

The governing equation of consolidation of saturated soil with visco-elastic skeleton under conditions of plane strain is (Zhan, 1993) these numbers. See for example Equation 1 below:

$$\varepsilon_v = (1-2\mu)[a_0(\Theta-3u)+ \int_0^t(\Theta-3u)|_\tau \frac{dJ(t-\tau)}{d(t-\tau)}d\tau] \quad (1)$$

where, ε_v is the volume strain, μ is Poisson's ratio, $\Theta=\sigma_x+\sigma_y+\sigma_z$, u is excess pore pressure; $a_0=1/E_1, a_1=E_1/E_2$ ($E_1, E_2$are the parameters of Merchant model). $J(t)$ is the flexibility function of Merchant model, which can be written as,

$$J(t)=a_0[1+a_1(1-e^{-\eta t})] \quad (2)$$

where, $\eta=E_2/\eta_2$.

Following the Terzaghi-Rendulic consolidation theory, Θ does not vary with time and $\Theta|_{t=0}=3u_0$. Therefore, the derivative of equation (1) with respect to t can be written as,

$$\frac{\partial\varepsilon_v}{\partial t}=-3(1-2\mu)a_0[\frac{\partial u}{\partial t}+\frac{1}{a_0}\int_0^t\frac{\partial u}{\partial\tau}\frac{dJ(t-\tau)}{d(t-\tau)}d\tau] \quad (3)$$

The continuity equation of water flow in the plane consolidation can be expressed as,

$$\frac{k_s}{\gamma_w}(\frac{\partial^2u}{\partial x^2}+\frac{\partial^2u}{\partial y^2})=-\frac{\partial\varepsilon_v}{\partial t} \quad (4)$$

in which k_s is coefficient of permeability of the soil and γ_w is unit weight of water.

Combining equation (3) and (4) yields

$$\frac{k_s}{3(1-2\mu)a_0\gamma_w}(\frac{\partial^2u}{\partial x^2}+\frac{\partial^2u}{\partial y^2}) =\frac{\partial u}{\partial t}+\frac{1}{a_0}\int_0^t\frac{\partial u}{\partial\tau}\frac{dJ(t-\tau)}{d(t-\tau)}d\tau \quad (5)$$

4 BOUNDARY CONDITIONS

Supposing the ground surface is permeable and the tunnel is partially sealed with partial drainage boundary established by Li (1999). The initial and boundary conditions can be expressed as,

$$u|_{t=0}=u_0$$
$$u|_{y=0}=0 \quad (6)$$
$$\frac{\partial u}{\partial n}|_{x^2+(y+h)^2=r^2}=\kappa u|_{x^2+(y+h)^2=r^2}$$

with

$$\kappa=\frac{k_l}{k_s}\frac{1}{r_1\ln(r_1/r_2)} \quad (7)$$

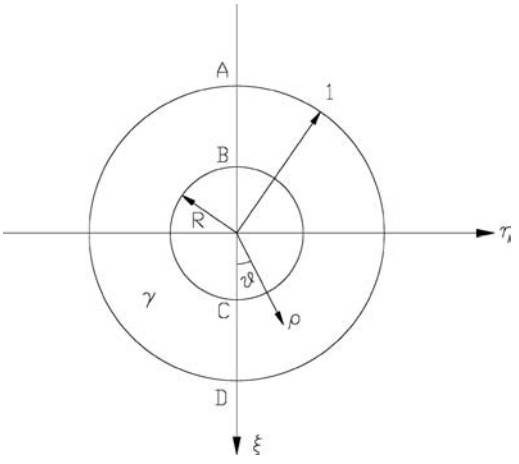

Figure 3. Plane of conformal transformation.

where, u_0 is the initial excess pore pressure, k_l is coefficient of permeability of the linings, r_1 and r_2 are the external and internal radius of the tunnel.

5 CONFORMAL MAPPING

In order to solve equation (5) with boundary conditions (6) in the region R shown in Figure 1, we conformally map the region R in the Z-plane onto a ring region γ in the mirror image plane ω, see Figure 3.

The conformal mapping is given by

$$\omega = \frac{z+ai}{z-ai} \tag{8}$$

where $z = x + yi$ and $a = \sqrt{h^2 - r^2}$.

Note that the ring region is bounded by the circles $|\omega| = 1$ and $|\omega| = R$, where

$$R = \frac{h - \sqrt{h^2 - r^2}}{r} \tag{9}$$

Define $\omega = \xi + i\eta = \rho(\cos\theta + i\sin\theta)$, then

$$\begin{aligned} x &= \frac{2a\eta}{(1-\xi)^2 + \eta^2} \\ y &= \frac{a(\xi^2 + \eta^2 - 1)}{(1-\xi)^2 + \eta^2} \end{aligned} \tag{10}$$

Substituting the above relation into equation (5), we obtain

$$\begin{aligned} &\frac{k_s}{3(1-2\mu)a_0\gamma_w}\left(\frac{\partial^2 u}{\partial \xi^2} + \frac{\partial^2 u}{\partial \eta^2}\right) = \\ &\frac{4a^2}{[(1-\xi)^2 + \eta^2]^2}\left[\frac{\partial u}{\partial t} + \frac{1}{a_0}\int_0^t \frac{\partial u}{\partial \tau}\frac{dJ(t-\tau)}{d(t-\tau)}d\tau\right] \end{aligned} \tag{11}$$

And, the corresponding boundary condition is

$$\begin{aligned} u|_{t=0} &= u_0 \\ u|_{\rho=1} &= 0 \\ \frac{\partial u}{\partial n}|_{\rho=R} &= \kappa u|_{\rho=R} \end{aligned} \tag{12}$$

6 ANALYTICAL SOLUTION

We apply separation of variables to $u(\rho, \theta, t) = W(\rho, \theta)T(t)$ and find that.

$$\begin{aligned} &\frac{\partial^2 W}{\partial \rho^2} + \frac{1}{\rho}\frac{\partial W}{\partial \rho} + \frac{1}{\rho^2}\frac{\partial^2 W}{\partial \theta^2} + \\ &\frac{\lambda^2}{[1+\rho^2 - 2\rho\cos\theta]^2} W = 0 \end{aligned} \tag{13}$$

$$\begin{aligned} &\frac{dT}{dt} + \frac{1}{a_0}\int_0^t \frac{dT}{d\tau}\frac{dJ(t-\tau)}{d(t-\tau)}d\tau \\ &+ \frac{k_s\lambda^2}{12(1-2\mu)a_0\gamma_w a^2} T = 0 \end{aligned} \tag{14}$$

where λ is the eigenvalue.

The boundary condition of equation (13) is

$$\begin{aligned} W|_{\rho=1} &= 0 \\ \frac{\partial W}{\partial \rho}|_{\rho=R} &= \kappa W|_{\rho=R} \end{aligned} \tag{15}$$

The initial condition of equation (14) can be

$$T(0) = 1 \tag{16}$$

Define

$$\chi = \frac{1}{\sqrt{1+\rho^2 - 2\rho\cos\theta}} \tag{17}$$

and substituting it into equation (13), we get

$$\frac{d^2 W}{d\chi^2} + \frac{1}{\chi}\frac{dW}{d\chi} + \lambda^2 W = 0 \tag{18}$$

This is Bessel's equation of order zero and the general solution of the equation is

$$W(\chi) = C_1 J_0(\lambda\chi) + C_2 N_0(\lambda\chi) \tag{19}$$

where J_0 and N_0 is the Bessel function of order zero and the Neumann function of order zero.

According to the boundary condition (15), the eigenfunction can be expressed as

$$f(\chi)=J_0\left(\frac{\lambda}{\sqrt{2(1-\cos\theta)}}\right)A(\chi) - N_0\left(\frac{\lambda}{\sqrt{2(1-\cos\theta)}}\right)B(\chi) \tag{20}$$

With,

$$\begin{aligned} &WA(\chi)=\lambda(R-\cos\theta)(1+R^2-2R\cos\theta)^{-\frac{3}{2}}\\ &N_1\left(\frac{\lambda}{\sqrt{1+R^2-2R\cos\theta}}\right)-\kappa N_0\left(\frac{\lambda}{\sqrt{1+R^2-2R\cos\theta}}\right)\\ &B(\chi)=\lambda(R-\cos\theta)(1+R^2-2R\cos\theta)^{-\frac{3}{2}}\\ &J_1\left(\frac{\lambda}{\sqrt{1+R^2-2R\cos\theta}}\right)-\kappa J_0\left(\frac{\lambda}{\sqrt{1+R^2-2R\cos\theta}}\right) \end{aligned} \tag{21}$$

where, J_1 and N_1 is the Bessel function of order zero and the Neumann function of order one.

Let $\{\lambda_1,\lambda_2,\lambda_3,\cdots,\lambda_n\}$ be the positive roots of the function (20).

Substituting eigenvalue $\{\lambda_n\}$ into equation (14), we get

$$\frac{dT_n}{dt}+\frac{1}{a_0}\int_0^t\frac{dT_n}{d\tau}\frac{dJ(t-\tau)}{d(t-\tau)}d\tau + \frac{k_s\lambda_n}{12(1-2\mu)a_0\gamma_w a^2}T_n=0 \tag{22}$$

with $T_n(0)=1$.

The Laplace transformation of equation (22) is

$$\tilde{T}=\frac{s+\alpha}{s^2+(\alpha+\beta)s+\eta\beta} \tag{23}$$

where

$$\begin{aligned} &\alpha=\eta(1+a_1)\\ &\beta=\frac{k_s\lambda_n}{12(1-2\mu)a_0\gamma_w a^2} \end{aligned} \tag{24}$$

Inverse Laplace transform of formula (23) is

$$T_n(t)=\frac{1}{\omega_1^{(n)}-\omega_2^{(n)}}[(\omega_1^{(n)}-\alpha)\exp(-\omega_1^{(n)}t) -(\omega_2^{(n)}-\alpha)\exp(-\omega_2^{(n)}t)] \tag{25}$$

where,

$$\begin{aligned} &\omega_1^{(n)}=\frac{1}{2}[(\alpha+\beta)+\sqrt{(\alpha+\beta)^2-4\eta\beta}]\\ &\omega_2^{(n)}=\frac{1}{2}[(\alpha+\beta)-\sqrt{(\alpha+\beta)^2-4\eta\beta}] \end{aligned} \tag{26}$$

Therefore, the solution of equation (11) with boundary condition (12) is

$$u(\rho,\theta,t)=\sum_{n=1}^{\infty}\frac{A_n}{\omega_1^{(n)}-\omega_2^{(n)}}V\left[\frac{\lambda_n}{\sqrt{1+\rho^2-2\rho\cos\theta}}\right] [(\omega_1^{(n)}-\alpha)\exp(-\omega_1^{(n)}t)-(\omega_2^{(n)}-\alpha)\exp(-\omega_2^{(n)}t)] \tag{27}$$

where

$$\begin{aligned} V\left[\frac{\lambda_n}{\sqrt{1+\rho^2-2\rho\cos\theta}}\right]&=J_0\left[\frac{\lambda_n}{\sqrt{1+\rho^2-2\rho\cos\theta}}\right]\\ &-\frac{J_0\left[\frac{\lambda_n}{\sqrt{2(1-\cos\theta)}}\right]}{N_0\left[\frac{\lambda_n}{\sqrt{2(1-\cos\theta)}}\right]}N_0\left[\frac{\lambda_n}{\sqrt{1+\rho^2-2\rho\cos\theta}}\right] \end{aligned} \tag{28}$$

And, A_n can be determined by the initial condition u_0 as,

$$A_n=\frac{\int_R^1 u_0\cdot V(\lambda_n)d\chi}{\int_R^1 V^2(\lambda_n)d\chi} \tag{29}$$

The initial magnitude and distribution of excess pore pressure in the soil due to shield tunnelling can be approximately represented by

$$u_0=q\cdot\frac{\sqrt{2(1-\cos\theta)}-\sqrt{1+\rho^2-2\rho\cos\theta}}{\sqrt{2(1-\cos\theta)}-\sqrt{1+R^2-2R\cos\theta}} \tag{30}$$

where q is the initial excess pore pressure around the tunnel boundary.

As the excess pore pressure at any time of any position in the physical region can be determined, the volume strain can also be derived from equation (1) at any time of any position. The vertical strain can be separated from volume strain following the Hooke's law. Accordingly, the settlement of tunnel can be derived by integration of vertical strain of the compressible layer,

$$S(t)=\int_{-(b+r+H)}^{-(b+r)}\varepsilon_y dy \tag{31}$$

where, H is the thickness of the compressible layer below the tunnel.

7 CASE STUDY

A case study is performed with the background of Shanghai Yangtze River tunnel. The tunnel lining is 15 m in external diameter and 13.7 m in internal

Table 1. Mechanical parameters of soil.

E_1(pa)	E_2(pa)	η_2(pa·s)	k_s/(m/s)	ν
5.0e6	1.6e7	4.2e14	3.5e-7	0.3

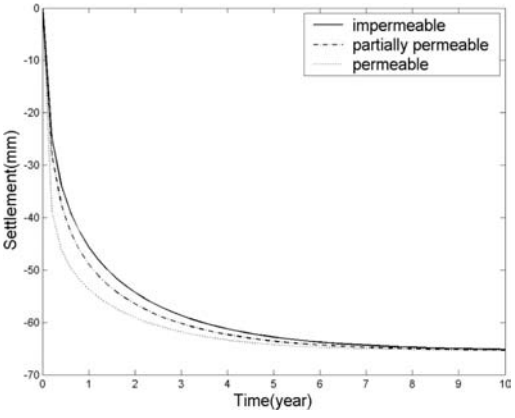

Figure 4. Long-term settlement of tunnel.

diameter. The average depth to the centre-line of the tunnel is about 20 m. The initial excess pore pressure around the tunnel boundary is 20 kPa. However the coefficient of permeability of the linings is hard to determine. Three different values are taken as 0, 1 and ∞ m/s, which present impermeable, partially permeable, totally permeable conditions. Mechanical parameters of soil under the river are listed in Table 1.

Figure 4 shows the prediction of long-term settlement of Shanghai Yangtze River tunnel with three different coefficients of permeability of linings. The higher the permeability of linings is, the more quickly the settlements increase. The predicted results reveal that the maximum settlement of the tunnel reaches 65 mm after ten years of its construction and the long-term settlement of Yangtze River tunnel is significant.

8 CONCLUSIONS

There are lots of components affecting the long-term settlement of shield tunnel including excess pore pressure around tunnel, the drainage condition of linings, time-dependent stress-strain behavior of soils and so on. Consolidation theory and rheologic theory reflect the external orderliness of soil displacement in different way and these two theories are contacted with each other by deformation mechanism. Therefore, based on the linear rheological model of three units, considering the partially sealed tunnel boundary, an analytical solution is presented for consolidation of a porous tunnel embedded in saturated visco-elastic soil and a solution has been given for the long-term settlement of Shanghai Yangtze River tunnel. It has been shown that this method can be used successfully for the prediction of long-term settlement of tunnel in soft soil and can provide some technical supports for the design of tunnel and the practice engineering.

ACKNOWLEDGMENTS

The authors wish to acknowledge the financial support from Hi-tech Research and Development Program (863 Program) of China (No. 2006AA11Z118) and National Natural Science Foundation of China (No. 50608058).

REFERENCES

Carter, J.P. & Booker, J.R. 1982. Elastic consolidation around a deep circular tunnel. *International Journal of Solids and Structures* 18(2): 1059–1074.

Carter, J.P. & Booker, J.R. 1983. Creep and consolidation around circular openings in infinite media. *International Journal of Solids and Structures* 19(8): 663–675.

Li, X. 1999. Stress and displacement fields around a deep circular tunnel with partial sealing. *Computers and Geotechnics* 24: 125–140.

Li, X. & Flores-Berrones, R. 2002. Time-dependent behavior of partially sealed circular tunnels. *Computers and Geotechnics* 29: 433–449.

Liu, G.B., Xie, K.H. & Shi, Z.Y. 2005. Soil-structure interaction of a deep circular tunnel in viscoelastic saturated soil. *Engineering Mechanics* 22(6): 148–154.

Mair, R.J. & Taylor, R.N. 1997. Theme lecture: Bored tunneling in the urban environment. *Proceedings of the Fourteenth International Conference on Soil Mechanics and Foundation Engineering*: 2353–2385.

O'Reilly, M.P., Mair, R.J. & Alderman, G.H. 1991. Long-term settlements over tunnels: an eleven-year study at Grimsby. *Proceedings of Conference Tunnelling*: 55–64.

Shirlaw, J.N. 1995. Observed and calculated pore pressures and deformations induced by an earth balance shield: Discussion[1]. *Canadian Geotechnical Journal* 32: 81–189.

Zhan, M.L., Qian, J.H. & Chen, X.L. 1993. Theoretical analysis for consolidation of viscoelastic clay about circular tunnels in foundations. *Journal of Hohai University* 21(2): 54–60.

Zhang, D.M., Huang, H.W. & Hicher, P.Y. 2004. Numerical prediction of long-term settlements of tunnels in clays. *Tunnelling and Underground Space Technology* 19(4–5): 379.

The Shanghai Yangtze River Tunnel - Theory, Design and Construction – Huang (ed)
© 2008 Taylor & Francis Group, London, ISBN 978-0-415-47161-9

Simplified analysis for tunnel seismic response in transverse direction

A.J. Cao, M.S. Huang & X. Yu
Key Laboratory of Geotechnical & Underground Engineering, Ministry of Education, Tongji University, Shanghai, P. R. China
Department of Geotechnical Engineering, School of Civil Engineering, Tongji University, Shanghai, P. R. China

ABSTRACT: This paper presents a summary of seismic analysis and design for underground structure in current. A quasi-static method for tunnel seismic responses is recommend, and little revision is made for this method. The reliability of the approach is proved by a case. The work of this paper can be expected to result in wider usage as a reliable quasi-static method for seismic analysis in tunnel engineering.

1 INTRODUCTION

Underground structures are constrained by the surrounding medium. It is unlikely that they could move to any significant extent independently of the medium or be subjected to vibration amplification. Compared to surface structures, whose vibratory frequency plays an important role during earthquake, vibratory frequency will not affect dynamic response significantly underground. These are main factors contributing different seismic design approaches between surface and underground structures.

2 APPROACHES TO SEISMIC ANALYSIS AND DESIGN

There have been many approaches used for underground structure response analysis, which could be roughly classified into three categories: Field observation, laboratory testing and theory analysis.

2.1 *Field observation*

Field observation as a seismic approach, which studies dynamic data obtained from site investigation. It is a relative direct method to know the actual dynamic response of underground structure. However, instrument with high precision is usually needed, and it will be a hard work to install these apparatuses in the corresponding site, which costs high.

2.2 *Laboratory testing*

Dynamic centrifuge modeling is a powerful tool that offers a possibility of understanding the real behavior of foundation systems under earthquake. Centrifuge modeling techniques are increasingly used to simulate seismic events, such as investigation of soil-structure interaction and liquefaction. The physical model under the centrifugal field allows for well-controlled testing conditions, thus is relevant for conducting parametric studies and investigating failure mechanism. Dynamic centrifuge model test has been made good progress in the world, and it has been introduced into China. However, there are several difficulties for this method. For instance, scaling law for time is different for dynamic events such as earthquakes and diffusion events such as consolidation. Similarly, the scaling law for dynamic velocity is different from that of the seepage velocity. Another special requirement of dynamic centrifuge modeling is the accurate modeling of the boundary conditions. So, there are still many works need to do for dynamic centrifuge model test.

2.3 *Theory analysis*

Theory analysis is a main method to investigate seismic response of underground structure. Especially with the increasing development of computer technology, mechanics and mathematics have combined with computer technology well to investigate the dynamic response of underground structure. Finite element method is a good case among several theory analysis approaches, which has been widely used to study structure-medium interaction during earthquake. As opposed to closed form analytical solutions, which exist for a relatively small class of problems, numerical methods can be used for analysis and design of complex structures. The main advantage of the method is that arbitrary boundaries and material inhomogeneity

can be accommodated easily. But there are still several difficult problems which are not solved, for example, how to consider the non-linear property of soil, which require further investigation to artificial boundary and strong seismic input. On the other hand, operators must possess professional knowledge and calculate-analysis ability. So theory analysis is impossible to become a mainstream design approach for the reason.

2.4 *Simplified method*

Most simplified methods derived from closed-form method but secondary factors are ignored. Therefore, these methods are easily manipulated, which are the main solutions to investigate structure dynamic response for engineering. These approaches could be roughly classified into three categories: seismic coefficient method, free field deformation approach and simplified soil-structure interaction approach.

2.4.1 *Seismic coefficient method*

This method was originally used for dynamic analysis of surface structure. It bas been popularized in earthquake resistant design of underground structure.

$$F_1 = \frac{a}{g} Q = K_c Q \tag{1}$$

$$F_2 = \eta_c K_h m_1 g \tag{2}$$

Inertial forces due to earthquakes can be obtained by multiplying the dead weight of structure and soil mass by the design coefficient, which could be expressed by equation (1) and equation (2). F_1 and F_2 are inertial forces of the structure and upper soil mass respectively; and are earthquake acceleration and gravity; Q and m_1 represent weight of structure and soil mass respectively; K_c and K_h are seismic coefficient in vertical and horizontal direction; η_c is the integrate response coefficient related to tunnel depth, soil property and project significance.

This simple method, however, is not very suitable for underground structure dynamic design because tunnel structures with large diameter usually possesses little equivalent mass compared to surrounding medium, and they are more sensitive to the distortions of surrounding ground than to the inertial effects, which means this method does not reflect real dynamic property of tunnel structure.

2.4.2 *Free field deformation approach*

The term 'free-field deformation' describes ground strains caused by seismic waves in the absence of structures. These deformations ignore the interaction between the underground structure and the surrounding ground, but can provide a first-order estimate of the anticipated deformation of the structure. Compared with seismic coefficient method, this approach reflects better understanding of tunnel dynamic response, i.e. understructure is subjected to ground distortion not inertial effect.

2.4.2.1 Newmark's method

Simplified procedures for assessing underground structure due to wave propagation were first developed by Newmark (Newmark 1967), and have been used or extended by a number of authors since then. Newmark's approach is based on three assumptions. The first assumption, which is common to most all the deterministic approaches, deals with the earthquake excitation. The ground motion (e.g. the acceleration, velocity and displacement time histories) at two points along the propagation path is assumed to differ only by a time lag. That is, the excitation is modeled as a traveling wave. The second assumption is that tunnel inertia terms are small and may be neglected. The third assumption is that no relative movement at tunnel-soil interface and hence, the tunnel strain equals the ground strain. For a tunnel at medium depth and for a deep tunnel in homogeneous soil or rock, Newmark's simple method may give rational estimate of such deformation around tunnel free-field. Maximum shear strain is obtained as following accordingly:

$$\varepsilon_{\max} = V_s / C_s \tag{3}$$

$$C_s = \sqrt{G_m / \rho} \tag{4}$$

where V_s, particle shear wave velocity, C_s, shear wave velocity; G_m, shear modulus; and ρ, mass density of the ground. St. John (St. John 1987) used Newmark's approach to develop solutions for free-field axial and curvature strain due to compression, shear and Rayleigh waves; Wang (Wang 1993) also produced ovaling deformation on circular tunnel in transverse direction.

There are still some other free-field methods to analysis tunnel seismic response, such as BART method (Thomas 1969). Its structural design criterion is a provision of sufficient ductility to absorb the imposed deformation without loosing the capacity to carry static loads, rather than a criterion for resisting inertial loads at a special unit stress.

These simplified solutions are useful for developing initial estimate of strain and deformations in a tunnel. And the assumption is probably reasonable for most circular tunnels in rock and in stiff soils, because the lining stiffness against distortion is low compared with that of surrounding medium; however, these methods may overestimate or underestimate structure deformation depending on the rigidity of the structure relative to the ground.

2.4.3 *Simplified soil-structure interaction approach*

In the case of tunnels with rigid lining in loose soils, lining strains and those for soil are not equal and tunnel lining resists imposed deformations by the ground

shaking. Therefore, in this situation taking into account the soil-lining interaction could show more realistic behavior of tunnel.

In this class of solutions, the beam-on-elastic foundation approach is used to model (quasi-static) soil-structure interaction effects. These methods also ignore dynamic (inertial) interaction effects. Many methods fall into this class of solutions, such as response displacement method, strain transfer method and foundation resistant coefficient method. They all possess the same assumption, that is, structural existing will not affect dynamic response of surrounding medium significantly, structural deformation does not equal to ground deformation but similar to it. For the limitation of the test, only response displace method will be discussed.

2.4.3.1 Response displacement method

Ignoring the inertial and damping effects, the immersed tunnel is assumed to be beam supported by springs representing soil rigidity. One end of each spring is considered to displace what the same as displacement of ground. The solution could be simply expressed by a formulation as following:

$$[K]\{U\} = [K_m]\{U_m\} \tag{5}$$

where $[K]$ contains structural rigid matrix $[K_l]$ and spring resistance matrix of medium $[K_m]$; $\{U_m\}$ is the free-field displacement of ground. The key point of this method is to confirm the exact value of $[K_m]$ and $\{U_m\}$.

To sum up, earthquake coefficient method does not reveal the real feature of underground structure response which is different from surface structure response. So it is not suitable for tunnel seismic response analysis. Free-field method is a simple and relative reasonable solution for tunnel response, however, a design based on this assumption may be overly conservative in some cases and non-conservative in others, depending on the relative stiffness between the ground and the lining. The main reason for this drawback is the uncertainty of the tunnel-ground interaction. It is suggested that the method should be used as primary design. Simplified soil-structure interaction approaches pay much attention to the relative stiffness of the system; however, it is very hard to certain real value of key parameters (e.g. spring coefficient of medium), and methods to calculate the corresponding parameters are not unified or even confused especially with complicated boundary, which requires further research. FEM could be used to analysis arbitrary boundaries and material inhomogeneous material, which, however, need professional knowledge and calculate-analysis ability. Therefore it could be only used for professional research or significant projects.

3 RECOMMENDED METHOD

The recommended method is still a quasi-static analysis of soil-structure interaction. Unlike other quasi-static solutions, it is easy to clarify key parameters. Compared with some deformation methods, this solution aims at not only deformation or displacement of the system but also forces in tunnel.

This recommended method was originally derived from relative stiffness method and revised relative stiffness method. These solutions are commonly used for static design of tunnel lining. The models used in these previous studies vary in the following two major assumptions, the effects of which have been addressed by Mohraz (Mohraz et al. 1975) and Einstein (Einstein et al. 1979, 1980): Full-slip or no-slip conditions exist along the interface between the ground and the Lining; Loading conditions are to be simulated as external loading (overpressure loading) or excavation loading. The relative stiffness method (external loading condition) implies that the tunnel opening has been excavated and supported before load corresponding to free-field stress is applied; The revised method (external loading condition) indicates that tunnel is excavated and simultaneously supported after the loads corresponding to free-field stress is applied.

It seems that different model will lead to irrelevant solutions, but it is not true. Though the two solutions are complicated, they share some relations by a simple demonstration; authors will give out the solution. If the two results are compared, solutions are shown as followings:

(full-slip interface assumption)

$$\begin{cases} \left(\dfrac{T}{T^*}\right)_{fs} = \dfrac{2(\upsilon_m - 1)[(K+1)a_1 + 36(K-1)a_2 Cos2\theta]}{a_1 a_2[(K+1)a_3 + 18(K-1)(4\upsilon_m - 3)Cos2\theta/a_1]} \\ \left(\dfrac{M}{M^*}\right)_{fs} = \dfrac{4-4\upsilon_m}{3-4\upsilon_m} \\ a_1 = 90 + F(\upsilon_m - 1)^2 - 108\upsilon_m \\ a_2 = C(2\upsilon_m - 1) - 1 \\ a_3 = \dfrac{6C(2\upsilon_m - 1) - F(\upsilon_m - 1)^2}{C[6 + F(\upsilon_m - 1)^2](2\upsilon_m - 1) - F(\upsilon_m - 1)^2} \end{cases} \tag{6}$$

(non-slip interface assumption)

$$\begin{cases} \left(\dfrac{T}{T^*}\right)_{ns} = \dfrac{2(\upsilon_m - 1)[(K+1)(-a_1) + 2(K-1)a_2 a_4 Cos2\theta]}{a_1 a_2[(K+1)a_3 + (K-1)(4\upsilon_m - 3)a_4 Cos2\theta/a_1]} \\ \left(\dfrac{M}{M^*}\right)_{ns} = \dfrac{4-4\upsilon_m}{3-4\upsilon_m} \\ a_1 = 4(3-4\upsilon_m) + F(6-4\upsilon_m) - C(5+2F-6\upsilon_m)(2\upsilon_m - 1) \\ a_2 = C(2\upsilon_m - 1) - 1 \\ a_3 = \dfrac{C + 6F - 2C\upsilon_m}{C(1+6F)(2\upsilon_m - 1) - 6F} \\ a_4 = 2C\upsilon_m - 2F - C - 4 \end{cases} \tag{7}$$

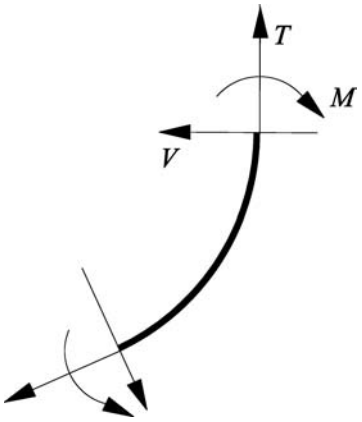

Figure 1. Sign convention for components in lining.

M and T are forces of lining derived from relative stiffness method, M^* and T^* represent forces from revised solution, these forces are shown in Figure 1; F and C are flexibility ration and compressibility ration (Hoeg 1968, Peck et al. 1972); υ_m, Poisson's ration of the medium; E_m, modulus of elasticity of the medium.

As for quasi-static, the at-rest coefficient should be assigned a value of (-1) to simulate the field simple shear condition (Wang 1993), then all equations above will be conversed into a uniform expression as following:

$$\eta = (\frac{T}{T^*})_{fs} = (\frac{M}{M^*})_{fs} = (\frac{T}{T^*})_{ns} = (\frac{M}{M^*})_{ns} = \frac{4-4\upsilon_m}{3-4\upsilon_m} \tag{8}$$

Which implies that these two solution have the simple relation as equation (8) while they are used to analysis tunnel dynamic response, and the final result of one solution could be easily transferred into another one.

Most of the recent developments in these models fall into the category of revised stiffness method (excavation loading conditions), as they represent a more realistic simulation of actual tunnel excavation. To evaluate the effect of seismic loading, however, the solutions for original relative stiffness method (external loading) should be used. Based on the work by Burns and Richard (Burns & Richard 1964) and Hoeg (Hoeg 1968), Wang (Wang 1993) proposed closed form solutions in terms of thrusts, bending moments and displacements under external loading conditions.

The response of a tunnel lining is a function of the compressibility and flexibility ratios of the structure, and the in-situ overburden pressure ($\gamma \cdot h$) and atrest coefficient of earth pressure (K) of the soil. To adapt to seismic loadings caused by shear waves, the free-field shear stress replaces the in-situ overburden pressure and the atrest coefficient of earth pressure is assigned a value of (-1) to simulate the field simple shear condition. The shear stress can be further expressed as a function of shear strain.

The stiffness of a tunnel relative to the surrounding ground is quantified by the compressibility and flexibility ratios (C and F), which are measures of the extensional stiffness and the flexural stiffness, respectively, of the medium relative to the lining.

$$C = \frac{E_m R(1-\upsilon_l^2)}{E_l t(1+\upsilon_m)(1-2\upsilon_m)} \tag{9}$$

$$F = \frac{R^3 E_m (1-\upsilon_l^2)}{6E_l I_l (1+\upsilon_m)} \tag{10}$$

where E_l is modulus of elasticity of tunnel lining, I is moment of inertia of the tunnel lining, R and t are radius and thickness of the tunnel lining. Assuming full-slip conditions, without normal separation and therefore, no tangential shear force, the diametric strain, the maximum thrust, and bending moment can be expressed as following (Wang 1993):

$$\begin{cases} \dfrac{\Delta D}{D} = \pm\dfrac{1}{3}K_1 F\gamma_{\max} \\ T_{\max} = \dfrac{1}{3}K_1 R\tau_{\max} = \pm\dfrac{1}{6}K_1\dfrac{E_m}{1+\upsilon_m}R\gamma_{\max} \\ M_{\max} = T_{\max}R = \pm\dfrac{1}{6}K_1\dfrac{E_m}{1+\upsilon_m}R^2\gamma_{\max} \end{cases} \tag{11}$$

Where,

$$K_1 = \frac{12(1-\upsilon_{\max})}{2F+5-6\upsilon_m} \tag{12}$$

K_1 is defined herein as lining response coefficient, $\gamma_{\max}$ is the maximum free-field shear strain.

According to various studies, slip at the interface is only possible for tunnels in soft soils or cases of severe seismic loading intensity. For most tunnels, the interface condition is between full-slip and no-slip, so both cases should be investigated for critical lining forces and deformations. However, full-slip assumptions under simple shear may cause significant underestimation of the maximum thrust, so it has been recommended that the non-slip assumption of complete soil continuity be made in assessing the lining thrust response (Hashash 2001).

$$T_{\max} = \pm K_2\tau_{\max}R = \pm K_2\frac{E_m}{2(1+\upsilon_m)}R\gamma_{\max} \tag{13}$$

where the lining thrust response coefficient, K_2, is defined as:

$$K_2 = 1 + \frac{F[(1-2\upsilon_m)-(1-2\upsilon_m)C] - (1-2\upsilon_m)^2/2 + 2}{F[(3-2\upsilon_m)+(1-2\upsilon_m)C] + C[5/2 - 8\upsilon_m + 6\upsilon_m^2] + 6 - 8\upsilon_m} \tag{14}$$

And, $\tau_{\max}$ represents maximum free-filed shear stress.

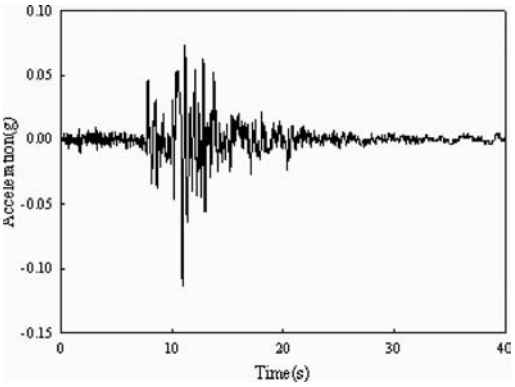

Figure 2. Acceleration time history of Prieta earthquake.

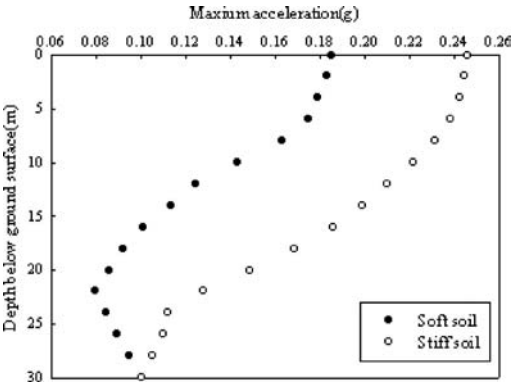

Figure 3. Calculated maximum accelerations for two types of soil.

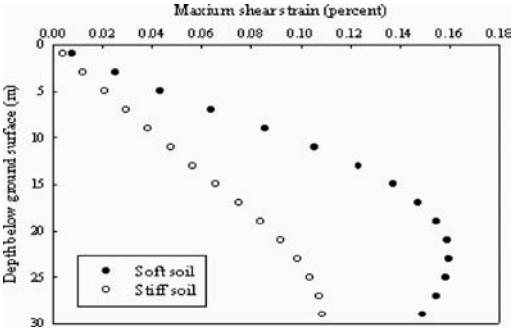

Figure 4. Calculated maximum shear strains for two types of soil.

3.1 *Discussion about the solution*

Based on what have been shown above, it is clear to see that these key parameters K_1 and K_2 are easy to calculate as long as the correlative parameters of soil and tunnel are known. The most important task is to ensure the maximum free-field shear strain to an exact extension. To illustrate this problem, a case will be discussed.

Two types of clay soil involved in this sample, and two shear strain methods are employed.

Earthquake and soil parameters:

Moment magnitude: $M = 7$, source-to-site distance is 10km;The input earthquake motion is Loma Prieta earthquake shown in Figure 2, the motion was normalized to a peak acceleration of 0.1g.

Stiff soil: $\rho_m = 1920 kg/m^3$; $G_m = 1\,20\,000\,kPa$; $C_m = 250\,m/s$; $\upsilon_m = 0.3$; $C_m = 250\,m/s$

Soft soil: $\rho_m = 1700\,kg/m^3$; $G_m = 38\,250\,kPa$; $C_m = 150\,m/s$; $\upsilon_m = 0.35$; $C_m = 150\,m/s$

The first method to calculate maximum shear strain is computer code. SHAKE is used to analysis free-field response, considering the highly non-linear behavior of soils , an often used set of data for soils giving the shear wave velocity and effective shear modulus as a function of shear strain is employed (Sun & Seed 1989, Idriss 1991). The maximum acceleration and strain in different depth blew ground surface have been shown in Figure 3 and Figure 4.

Supposing a tunnel is located in 15m depth, the corresponding maximum strain will be 0.00137 and 0.00066 for soft and stiff soil respectively in Figure 4.

The second approach to analysis maximum shear strain is Newmark's method assisted with some experience datum (e.g. Table 1 and Table 2).

For the soft soil, the maximum acceleration at ground surface $a_{\max} = 0.1851$g (Fig. 3), so the ground motion at depth of tunnel (Table 1)

$$a_s = 0.9a_{\max} = 0.9 \times 0.1851 = 0.16659g$$

Table 1. Ratios of ground motion at depth to motion at ground surface (Power et al. 1996).

Tunnel depth(m)	Ration of ground motion at tunnel depth to motion at ground surface
≤6	1.0
6–15	0.9
15–30	0.8
>30	0.7

Peak ground velocity (Table 2)

$$V_s = 173 \times 0.16659 = 28.82\,cm/s = 0.2882\,m/s$$

Maximum shear strain

$$\gamma_{\max} = \frac{V_s}{C_s} = \frac{0.2882}{150} = 0.00192$$

The final solutions of the two method for soft and stiff soil are listed in Table 3.

Obviously, free-field solution (e.g. Newmark's method) usually provides an upper-bound estimate of

Table 2. Ratios of peak ground velocity to peak ground acceleration at surface in rock and soil (Power et al. 1996).

Moment magnitude (M)	Ration of peak ground velocity (cm/s) to peak ground acceleration (g)		
	Source-to-site distance (km)		
	0–20	20–50	50–100
Rock			
6.5	66	76	86
7.5	97	109	97
8.5	127	140	152
Stiff soil			
6.5	94	102	109
7.5	140	127	155
8.5	180	188	193
Soft soil			
6.5	140	132	142
7.5	208	165	201
8.5	269	244	251

Table 3. Comparison of maximum shear strain.

	Maximum shear strain	
	Newmark's method	Shake code
Soft soil	0.00192	0.00137
Stiff soil	0.001034	0.00066

shear strain, and it is more conservative than computer codes solution, especially for stiff soil. It is suggested that computer codes (e.g. Shake 91) should be used if possible, which could arrive at a reasonable estimate of the free-field shear distortion, particularly for a soil site with variable stratigraphy. Free-field method could be used with some experience datum (e.g. Table 1, Table 2) in the absence of site-specific data.

3.2 *Revision about the solution*

The pseudo-static solution revised by Wang usually provides a realistic estimate in the tunnel linings, especially for non-slip condition. However, some problems still exist.

First, response coefficient K_1 and K_2 are not constant, which are defined as function of flexibility ratio, compressibility ration and Poisson's Ratio of the ground. K_1 and K_2 decrease sharply as $F \leq 20$, they will not change notable when $F > 20$, which have been shown in Figure 5, Figure 6 and Figure 7. Therefore, it is suggested that the solution should be revised to two stages for a more realistic solution.

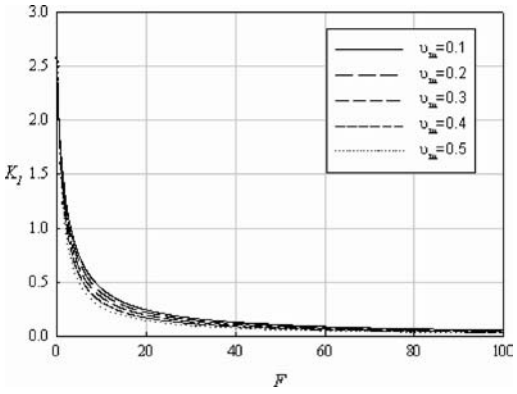

Figure 5. Lining response coefficient K_1.

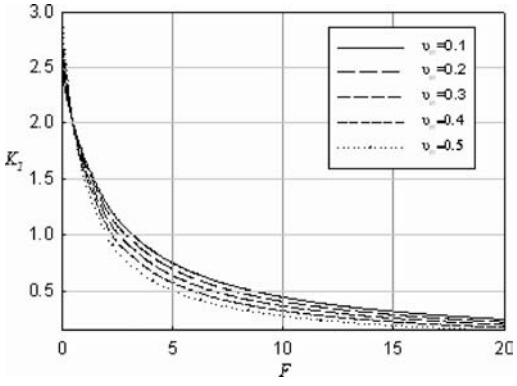

Figure 6. Lining response coefficient K_1 ($F < 20$).

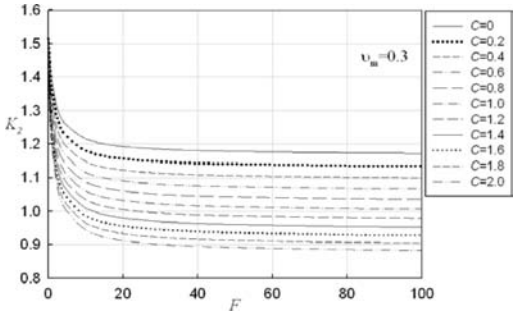

Figure 7. Lining response coefficient K_2.

Second, the maximum thrust, calculated with full-slip assumptions, may cause significant underestimation so it should be better to adopt the non-slip assumption. In order to compensate for possible errors due to using pseudo-static model for dynamic earthquake loading, it is suggested that a safety factor be multiplied.

Based on what have been discussed above, considering the conclusion of Mohammad (Mohammad 2005), the final revised solution will be

$$\begin{cases} F \le 20 & M_{\max} = \pm(\frac{1}{6})K_1 \frac{E_m}{1+\upsilon_m} R^2 \gamma_{\max} \\ F > 20 & M_{\max} = \pm(\frac{1}{9})K_1 \frac{E_m}{1+\upsilon_m} R^2 \gamma_{\max} \end{cases} \quad (15)$$

$$T_{\max} = \pm 1.15 K_2 \frac{E_m}{2(1+\upsilon_m)} R \gamma_{\max} \quad (16)$$

4 CASE STUDY

A case will be discussed in this section, which is selected from Hashash's paper (Hashash 2001, 2005) calculated by finite element code PLAXIS and Wang's pseudo-static method. The numerical analysis uses assumptions identical to those of the analytical solution; (a) plane-strain condition, (b) ground and lining are linear elastic and mass-less materials. Shear loading is applied at the upper ends of the boundaries to simulate pure shear condition. In PLAXIS, only no-slip condition between the tunnel lining and ground is simulated.

Earthquake and soil parameters:

Moment magnitude: $M = 5$, source-to-site distance is 10km;

Ignoring non-linear behavior of soil, the peak ground particle acceleration at surface is assign as $a_{\max}$=0.5g, $\rho_m = 1,920\,\text{kg/m}^3$, $G_m = 120,000\,\text{kPa}$, $C_m = 250\,\text{m/s}$, $\upsilon_m = 0.3$ soil deposit thickness over rigid bed rock

Tunnel parameters: $H = 30\,\text{m}$

Radius $R = 3.0\,\text{m}$

Thickness $t = 0.3\,\text{m}$, $\upsilon_l = 0.2$, $E_l = 24.8 \times 10^6\,\text{kPa}$

Area of the tunnel lining (per unit width) $A_l = 0.3$

Moment of inertia of the tunnel lining (per unit width) $I = 0.00225$, buried depth $d = 15$.

Using the same free-field method as section 3.1, the maximum shear strain at the depth of tunnel is $\gamma_{\max} = 0.00252$, then

$$\gamma_{\max} = \frac{V_s}{C_s} = \frac{0.2882}{150} = 0.00192$$

$$G_m = \rho_m C_m^2 = 120000 kPa$$

$$E_m = 2G_m(1+\upsilon_m) = 312000 kPa$$

$$F = \frac{R^3 E_m (1-\upsilon_l^2)}{6 E_l I_l (1+\upsilon_m)} = 18.58$$

$$C = \frac{E_m R (1-\upsilon_l^2)}{E_l t (1+\upsilon_m)(1-2\upsilon_m)} = 0.2322$$

then, $K_1 = 0.2081$ (equation 12), $K_2 = 1.15$ (equation 14), the final result of revised simplified method is listed in Table 4, and solutions of PLAXIS (Hashash 2001) and Wang's pseudo-static method (Hashash 2005) are also presented.

Table 4. Comparison of simplified solution with numerical solution.

	PLAXIS	Wang	Revised method	Revised VS PLAXIS
$T_{\max}$ (kN)	1050	1045.38	1199.772	14.3%
$M_{\max}$(kNm)	158.87	160.6	188.81	15.8%

Based on the case, revised method will yield results that are greater than Wang's solution and PLAXIS result about 15 percent; On the other hand, previous studies suggest that a real dynamic solution would yield results that are 10 to 20 percent greater than an equivalent static solution, provided that the seismic wavelength is at least about 8 times greater than the width of the excavation (Mow & Pow 1971, St. John 1987). That is to say the revised solution yields more reliable results near to real dynamic solutions.

5 CONCLUSION

This paper presents a summary of seismic analysis and design for underground structure in current state. Effect of earthquake on tunnel-ground interaction depends on various parameters including peak acceleration, intensity and duration of earthquake and the relative rigidity between tunnel and ground. However, for quasi-static methods such as Wang's solution, the key role is to certain the exact value of free-field response (e.g. maximum shear stain, maximum acceleration), computer code is recommended if possible. Little revision is made for this method based on previous research. The reliability of the revised method is proved through a typical sample. The work of this paper can be expected to result in a wider usage of a reliable quasi-static method for seismic analysis in tunnel engineering.

REFERENCES

Burns, J.Q. & Richard, R.M. 1964. Attenuation of stresses for buried cylinders. *Proceedings of the Symposium on Soil–Structure Interaction.* University of Arizona, Tempe, AZ: 378–392

Einstein, H. H. & Schwartz, C. W. 1979. Simplified analysis for tunnel supports. *Journal of the Geotechnical Division, ASCE* 105(4):499–518.

Hashash, Y.M.A. & Duhee P. 2005.Ovaling deformations of circular tunnels under seismic loading, an update on seismic design and analysis of underground structures. *Tunnelling and Underground Space Technology* 20:435–451.

Hashash,Y.M.A., Hook, J.J., Schmidt, B., et al. 2001. Seismic design and analysis of underground structures. *Tunnelling and Underground Space Technology* 16:247–293.

Hoeg, K. 1968. Stresses against underground structural cylinders. *Journal of the Soil Mechanics and Foundation Engineering Division*.94(SM4):833–858.

Idriss, I.M. 1991. Earthquake ground motions at soft soil sites. *Proceedings: Second International Conference on Recent Advances in Geotechnical Earthquake Engineering and Soil Dynamics*: 2265–2272. St. Louis, Missouri.

Mohammad, C.P. & Akbar Y. 2005. 2-D Analsis of circular tunnel against earthquake loading. *Tunelling and Underground Space Technology* 20:411–417.

Mohraz, B. ,Hendron, A. J., Ranken, R. E., et al. 1975. Liner-medium interaction in tunnels. *Journal of the Construction Division*101(CO1):127–141.

Mow, C. C. & Pao, Y. H. 1971. The diffraction of elastic waves and dynamic stress concentrations, R-482-PR. *Report for the U.S. Air Force Project*, The Rand Corp.

Newark, N. M. 1968. Problems in wave propagation in soil and rock. *International Symposium on Wave Propagation and Dynamic Properties of Earth Materials.*

Peck, R.B., Hendron, A.J. & Mohraz, B. 1972. State of the art in soft ground tunneling. *The Proceedings of the Rapid Excavationand Tunneling Conference. American Institute of Mining*: 259–286. Metallurgical and Petroleum Engineers, New York.

Power, M.S., Rosidi, D. & Kaneshiro, J. 1996. Vol. III Strawman: screening, evaluation, and retrofit design of tunnels. Report Draft. *National Center for Earthquake Engineering Research*, Buffalo, New York.

Schwartz, C. W. & Einstein, H. H. 1980. Improved Design of Tunnel Supports: Volume 1 – Simplified Analysis for Ground-Structure Interaction in Tunneling. *Report No. UMTA-MA-06-0100-80-4, Prepared for U.S. DOT*, Urban Mass Transportation Administration.

St. John, C.M. & Zahrah, T.F. 1987. A seismic design of underground structures. *Tunnelling and Underground Space Technology* 2(2):165–197.

Sun, J.I., Golesorkhi, R. & Seed, H.B. 1988. Dynamic moduli and damping ratios for cohesive soils. *Report No. EERC 88-15*, University of California, Berkeley.

Thomas, R. K. 1969. Earthquake design criteria for subways. Journal of the Structural Division, *Procreedings of ASCE*. 6:1213–1231.

Wang, J.N. 1993. Seismic design of tunnels: a state of the artapproach, Monograph, monograph 7. *Parsons, Brinckerhoff, Quade and Douglaa Inc*, New York.

The Shanghai Yangtze River Tunnel - Theory, Design and Construction – Huang (ed)
© 2008 Taylor & Francis Group, London, ISBN 978-0-415-47161-9

Study on tunnel stability against uplift of super-large diameter shield tunneling

J.X. Lin, F.Q. Yang, T.P. Shang & B. Xie
Shanghai Tunnel Engineering Co., Ltd., Shanghai, P.R. China

ABSTRACT: Against the background of the Shanghai Yangtze River Tunnel Project, this paper studies the relationship between early strength of grout simultaneously injected and tunnel stability upon super-large diameter shield tunneling. A calculation model is established to investigate tunnel uplift (i.e. tunnel stability), which results in grout strength increase. Equivalent spring coefficient is also investigated since it is one of the important parameters in modeling tunnel in the longitudinal direction. In analysis, safety criteria of structural lining are verified in terms of tunnel deformation, structural strength of lining, and deformation at segment joints. Finally, relevant construction technological measures are suggested against tunnel uplift for such kind of super-large diameter shield tunnelling.

1 INTRODUCTION

Being an expressway passage linking Shanghai city and Chongming island, the Shanghai Yangtze River Tunnel and Bridge project is an important component of main trunk along the coast of China. The tunnel extends 7.5 km, being bi-directional 6 lanes. It is bored by shield tunnelling which is through ground with the minimum overburden of 7.3 m near launching shaft and the maximum overburden of 29.0 m. The tunnel section has inner diameter of 13.7 m and outer diameter of 15.0 m with tapered RC segmental ring composed of 10 segments of 2 m wide and staggered joints. Hence it will, once completed, be the world's largest tunnel due to its super large diameter.

2 THEORETICAL ANALYSIS OF UPLIFT MECHANISM DURING SHIELD TUNNELLING

Uplift during shield tunnelling is caused by transversal and longitudinal actions mutually. The uplift magnitude is related to the overburden in addition to tunnel's own weight. During shield tunnelling, annular void occurs around and between shield tail inner side and lining outer side. The void must be back-filled with injected grout to ensure compacted filling and to minimize tunnel uplift or surface subsidence, which is caused by ground settlement around the annulus. In order to ensure full filling of the annulus, good working performances is required for the grout fluid, such as pumpability, flowability, and early strength.

2.1 *Major loads on tunnel and its influence on grout injection*

The loads considered for tunnel design are dead load, vertical and horizontal earth pressures, water pressure, surface load, ground reaction, and construction load. Grout injection pressure is so based in addition to water pressure at the corresponding location of tunnel and ground pressure upon segments cleared off by shield tail. It is still reasonable to take consideration of additional pressures to ensure grout fluid entering the annulus at shield tail uniformly. Therefore local high injection pressure is avoided and no local damage is generated to segment. However grout injected into the annulus is in a state of fluidity in short moments with its shear strength almost at zero. Then, as the time lasts, its strength increases, when the fluid transforms towards plastic and solid substances. Finally the fluid reaches a level meeting design criteria, up to or surpassing the strength of surrounding ground of tunnel.

With a relative high specific weight, good fluidity and relative high early shear strength, a new brand of grout fluid originally developed by STEC has been used by the Shanghai Yangtze River Tunnel Project. Indoor tri-axial test results show that the very kind of grout did not flow 12 hours after cleared off by shield tail with corresponding shear strength of 800 kPa. The results also show that final strength compatible to that of surrounding ground 7 days afterward. That is to

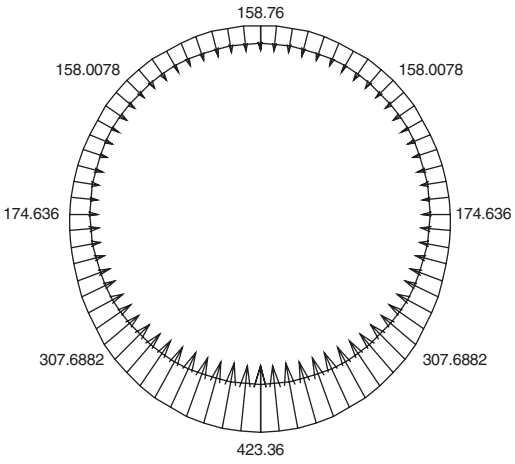

Figure 1. Segment loading diagram.

say, the new brand of grout still showed in a static state of fluid for 12 hours without disturbances. Then it transformed from fluid to plastic substance gradually. After 7 days, it could be seen as a solid. Hence, within 12 hours after shield tail has cleared off the segments, the tunnel is situated in a fluid state, otherwise said in a most unstable moment of key importance, also a period of time tunnel constructors are most concerned with, of first priority.

Take the Shanghai Yangtze River Tunnel as an example where its overburden is at 9 m depth. Given a segment with 15 m outer diameter, 13.7 m inner diameter, and 2 m ring width, ground and water pressures at tunnel depth h is calculated as:

$$f = \gamma h(\cos^2\alpha + K_0 \sin^2\alpha) \tag{1}$$

Resultant of ground and water pressures at tunnel depth h acting on a unit length of segment ring is:

$$F = 2\int_0^{\pi} \gamma h(\cos^2\alpha + K_0 \sin^2\alpha)\cdot R d\alpha \tag{2}$$

where f is segment stress caused by ground pressure (kPa); F is the resultant (kN) borne by unit length of segment ring; γ is averaged specific weight (kN/m^3) of ground; h is depth (m) the calculation is done upon; α is the angle (°) contained between the point of calculation and verticality; K_0 is a coefficient of static ground pressure; R is outside diameter (m) of segmental ring.

If average weighted specific weight of ground is 17.64 kN/m^3, under 9 m overburden, the tunnel loading distribution is shown in Figure 1 (kPa is the unit), where the maximum water or ground pressure acting on tunnel is located at invert of tunnel, with a value of 423.36 kPa, minimum one at crown with 158.76 kPa. Figure 2 shows a relationship between main stresses $(\sigma_1 - \sigma_3)$ and strains obtained from indoor tri-axial test

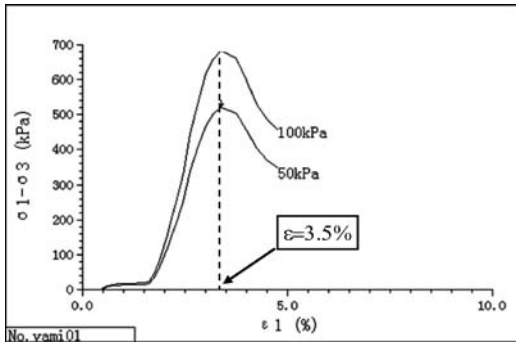

Figure 2. Tri-axial test for grout.

for grout after 12 hours of static state. As shown in Figure 2, yield stress of grout is related to confined pressure. Larger is the confined pressure, the greater is yield stress. However the strain of grout, with a 3.5% constant, is not related anymore to confined pressure upon reaching yielding point.

From view point of force transmission, under the condition of annulus void with compact filled in, ground pressure acting on tunnel outer side is transmitted on segments by way of injected grout instead of directly on segments. Therefore, pressures given in Figure 2 actually are the load situation by injected grout. In order to ensure the injected grout gaining strength in time, there is still to avoid destruction of shear strength which is caused by flowing of grout due to tunnel instability in a vicious circle of influencing strength gain of grout, lengthening fluid state of grout, again lengthening the period of tunnel instability aside from ensuring effectively filling in the annulus with grout fluid.

From the above-mentioned calculation, it is known that under 9 m overburden, the maximum main pressure borne by grout fluid is 423 kPa. Therefore the grout required is not to be a shear flow with $\sigma_1 = 423$ kPa. In the presence of known factors obtained from above-mentioned indoor tri-axial test at time of 12 hours after static grout whereupon internal cohesive force $c = 86.4$ kPa, internal angle of friction $= 38.3°$ (Hong 1993), the stress limit at time of shear flow for grout under action of surrounding ground could be calculated. The maximum horizontal stress σ_3 acting on invert ground and the minimum stress σ_3 at time of shear flow could be calculated respectively as follows:

$$\sigma_3 = K_0\gamma(H + 2R) = 296.35kPa \tag{3}$$

$$\sigma_{3f} = \sigma_1 \cdot \tan^2(\frac{\pi}{4} - \frac{\varphi}{2}) - 2\cdot c\cdot \tan(\frac{\pi}{4} - \frac{\varphi}{2}) = 83.72kPa \tag{4}$$

$\sigma_{3f} < \sigma_3$, therefore, under stress action of ground mass, the injected grout mass would not be a shear flow after 12 h in a static status if without outside disturbance.

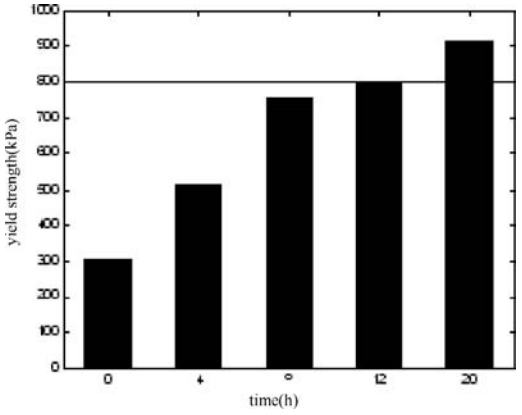

Figure 3. Yield strength variation of grout.

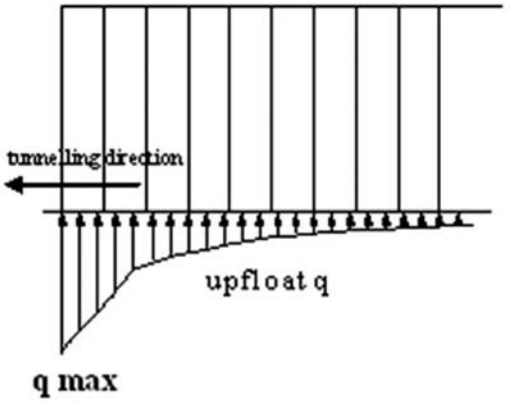

Figure 4. Tunnel's uplift trend after shield tail clearing off tunnel.

Figure 3 shows experimental results of yield strength corresponding to grouts of various ages. From the above calculation, it is known that grout after 12 hours in static state is not to be a shear flow with corresponding yield strength of 800 kPa. Namely as yield strength of grout is not less than 800 kPa, grout under action of σ_1 would not be a shear flow.

From the above analysis, significant influences is shown by shear flow of grout itself on early stability of segments as well as on uplift of tunnel when grout is under the state of flowable plastic, especially under flow state.

2.2 *Influence of the rate of tunnelling on tunnel stability against uplift*

Upon clearing by shield tail off tunnel, the uplift force in grout mass is related to the rate of shield tunneling. That is to say, the speedier the shield tunnelling, the longer the erected tunnel which is within the flow plastic state of grout mass. The larger the resultant uplift force along tunnel axis, the worse the tunnel stability becomes.

However strength of grout simultaneously injected increases in proportion to time elapse, then the uplift force loaded upon tunnel then decreases (Hong 1993) accordingly. Figure 4 gives a schematic plot of uplift against distance of shield tunnelling after shield tail clears off the tunnel.

Setting shield tunneling rate at V, after time T, grout reaches strength as that of ground, following grout strength variation. Also uplift on tunnel varies. Therefore, at the location $L = vT$ from shield tail, uplift on tunnel is a function of time $F(t)$. Starting from area of shield tail, the resultant uplift Q is calculated as:

$$Q = \int_l^t q_l dl = V^2 \int_0^T F(t)dt \qquad (5)$$

From Equation (5), it can be seen that uplift on tunnel is proportional to the square of rate of shield tunneling. Therefore, it is necessary to stringently control the rate of shield tunnelling to effectively lower uplift on tunnel.

2.3 *Analysis on safety against uplift during tunnelling*

As a tunnel which is in flowable plastic mass is under actions of self weight G, float force on tunnel F, cohesive force between grout mass and tunnel C, and friction f, there are complex loading and actions to one another. Therefore no theoretical solution could be found from each of its own consideration. For simplicity, this paper defines the resultant of these three forces as float force in broader sense. If float force (in broader sense) is greater than tunnel weight, tunnel floats up, especially in sections of shallow overburden where the frontal pressure acting on tunnel and friction between rings are relatively small while under the action of uplift. If friction between rings could not be able to withstand effectively the uplift produced by the grout injected simultaneously, the phenomenon of significant deformation may happen to tunnel. If uplift is still greater, the longitudinal bolts may be subject to shearing. The bolts at joints may be damaged.

As segments are cleared off by the shield, and only when injected grout reaching a strength level could withstand the uplift action. Uplift on tunnel is related to specific weight of injected grout mass, its rate of gaining strength, the geometric outlines of segments themselves, and dead weight of tunnel in this particular section. As shown in Figure 5, upon segment cleared off by shield tail, between the ring just cleared off by shield tail, and the ones still remaining in contact with shield tail, may appear a more significant shear force Q which magnitude is to be determined by uplift on tunnel. The force necessary to overcome this shear Q would be the amount of frictions F caused by the

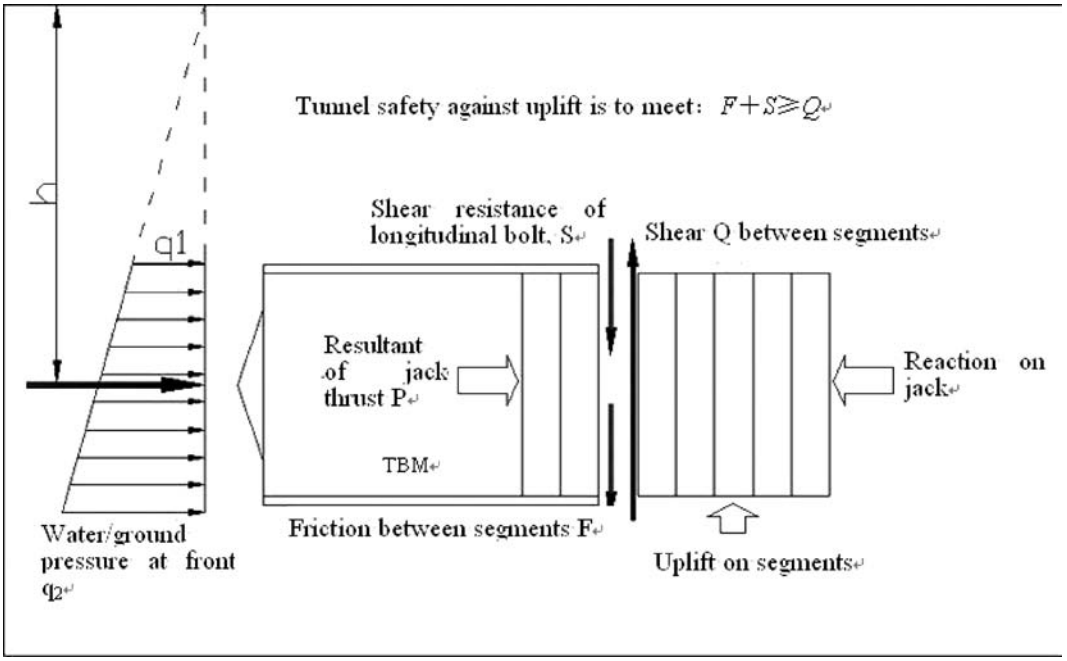

Figure 5. Loading schematics on segments as they are cleared off by shield tail.

resultant of thrusts from hydraulic jacks plus shear resisting force S of longitudinal bolts. When $F + S \geq Q$, the safety requirement of tunnel is met, otherwise, it is necessary to take corresponding safety measures to counteract the uplift.

From Figure 5, the resultant of hydraulic jacks $P = (q_1 + q_2)/2 \times h \times A = \gamma hA$; whereby friction of jacks $F = \mu K_0 P$, resultant shear resistant force by longitudinal bolts S, shear Q between segments produced by tunnel uplift are to be calculated by means of longitudinal float resistance of tunnel. Actual uplift produced is $N = Q - F$. If $N \leq S$, tunnel is safe for uplift resistant. If $N \geq S$, tunnel falls short of uplift resistance pending structural measures to be taken. From the formula, γ is average specific weight of ground in front of shield; A is the area to be excavated by shield; K_0 is coefficient of lateral ground pressure (taking $K_0 = 0.7$); μ is the friction coefficient between segments (taking $\mu = 0.35$).

2.4 *Analysis of influence on compression strength of simultaneous grout injection*

Due to less than 9 m overburden depth at break-in/-out available for a long distance tunnelling in the Shanghai Yangtze River Tunnel Project by super large diameter shield, uplift resistance is relatively weak for the tunnel, presenting quite a risk in safety against uplift. It is therefore that criteria for simultaneously injected grout play a key role to tunnel stability. Upon injection of grout in annulus at shield tail, strength of surrounding grout is demanded of fast growing rate, to ensure reaching that of surrounding ground in short time after the segments cleared off by shield tail in order to shape into place a permanent fixed protective shell around the lining ring to ensure tunnel stability.

Table 1. Compression strength of simultaneously injected grout.

Age (day)	1	3	7	14	28	60	90
Compression strength (kPa)	16	59	109	296	568	1,035	1,789

For the purpose of obtaining a functional relationship between growing strength of simultaneously injected grout and time, in accordance with actual proportionating ratio for simultaneously injected grout, a kind of grout fluid has thus been prepared in the laboratory, in a form of two samples respectively being φ 3.81 × 8.0 mm and 70 × 70 × 70 mm cured under an ambience of RH ≥ 95%, and 20 ± 3°C for a long term compression test. Then tests are taken on the hardened samples in smaller pieces for early strength (as per 1d, 3d, 7d, 14d) probing, and in larger chunks on grout samples for compression probing as per 28d, 60d and 90d. Table 1 shows the test results of compression strength of grout.

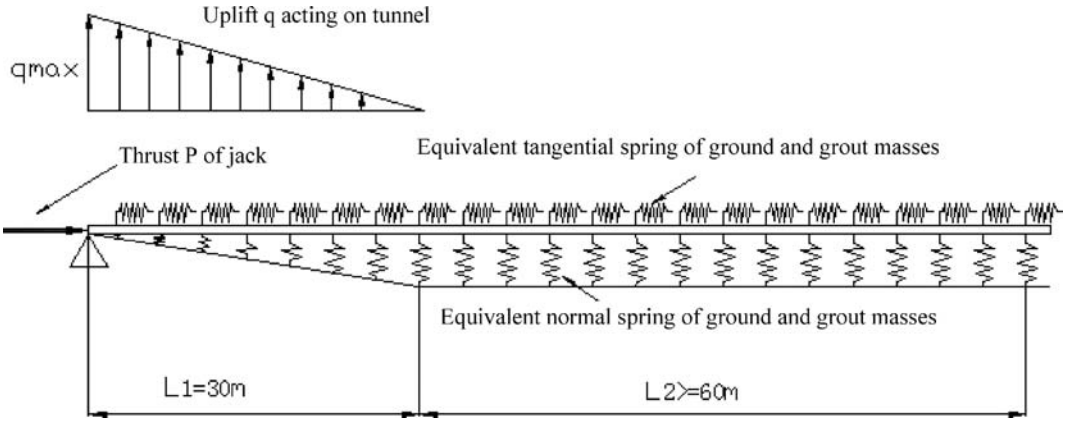

Figure 6. Longitudinal calculation modelling on tunnel uplift.

It can be seen from compression strength of grout samples, compression strength (7d) of a single fluid grout has reached 109 kPa, basically equivalent to confined compression strength of ground in shallow cover section. It is therefore to be believed that 7d after segments cleared off by shield tail, uplift acting upon tunnel by the grout has become relatively smaller, i.e. tunnel tends to be more stable.

3 NUMERICAL ANALYSIS OF UPLIFT ON TUNNEL DURING SHIELD TUNNELLING

Based on results derived from analysis of tunnel uplift mechanism as described above, a numerical analysis has been conducted for tunnel in longitudinal direction during shield tunnelling. Once elastic foundation beam has been taken for treatment, as compression modulus of grout being proportional to its strength has been assumed, given the compression modulus of ground mass, then compression module at various ages of grout could be deduced by utilization of various strengths at differing ages of grout. Hence equivalent spring coefficients (JSCE 1996) for ground mass and grout fluids could be calculated. Referring to Figure 6, shear force which is acting on rings as produced by tunnel uplift, is obtained for a loading test on structure of a full scale whole ring in order to get comparison of uplift resistant capability of a tunnel. Thus tunnel safety against uplift during shield tunnelling is verified.

At the time the tunnel uplifts, the tunnel also deforms transversely. It is the main reason that a modified empirical formula is taken to conduct theoretical calculation to verify safety of segmental structure transversely during shield tunnelling. For transversal calculation modelling, two full rings iso-rigidity tunnel calculation modeling is taken, where rigidity reduction coefficient is 0.8. Via transversal numerical calculation, segment deformation under action of uplift is obtained to verify fissure width of segment structure, deformation of segment joint and staggering between segments (tread).

3.1 *Calculation in tunnel longitudinal direction*

In analysis, uplift force and spring coefficient composed of ground mass and grout mass are assumed as shown in Figure 6. At the moment segments cleared off by shield tail, the maximum uplift is the weight of grout so displaced by the same volume of tunnel. By that time spring coefficient is zero. Based on analysis mentioned above, grout strength (7d after) is quite approaching that of surrounding ground.

Other given data for calculation are longitudinal curved bolts M30, Grade 5.8 ($\alpha = 30°$) 38 pcs. For longitudinal rigidity, based on "Structure Design Code of Japan Railway", equivalent rigidity (EA)eq, (EI)eq for tunnel longitudinal can be calculated; 19.1 kN/m^3 is taken for grout specific weight, based on site testing data.

Figure 7 shows simulated calculation results for tunnel longitudinal at the time of tunnelling rate of 5.0 m/d. As shown in the figure, the maximum uplift force loaded on segments by grout, upon segments cleared off by shield tail is 16,120 kN, then following shield tunnelling forward, grout strength surrounding the segments gains with less uplift loaded on segments, to reach that of ground mass strength after 7d or uplift on tunnel tending to zero.

3.2 *Calculation in tunnel transverse direction*

At section of shield break-in/-out, segments within soft eye are confined by soft eye rim. There is significant shear force appearing between segments at break-out section and segments within soft eye, aside from only 7.5 m of overburden at break-out section. At the same

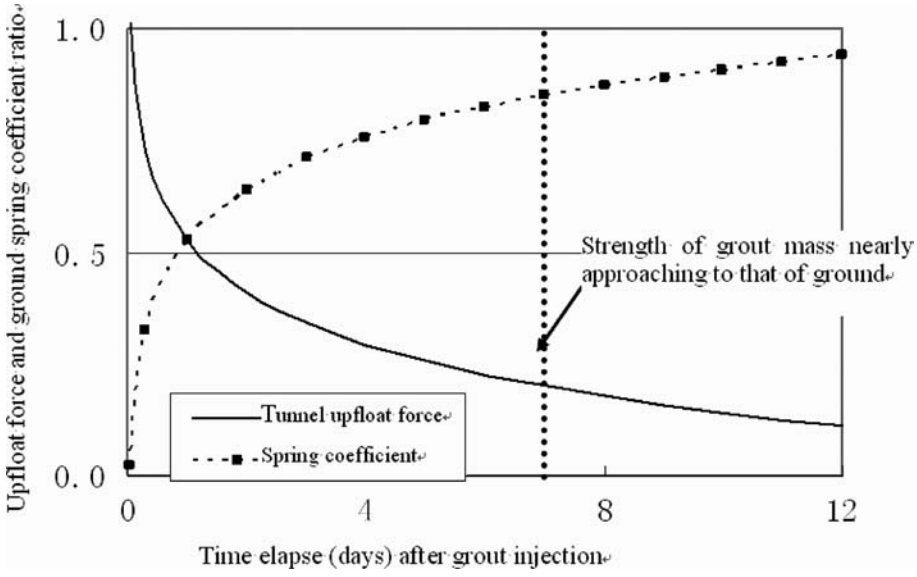

Figure 7. Schematic calculation modeling simulated on uplift longitudinal upon tunnel segments.

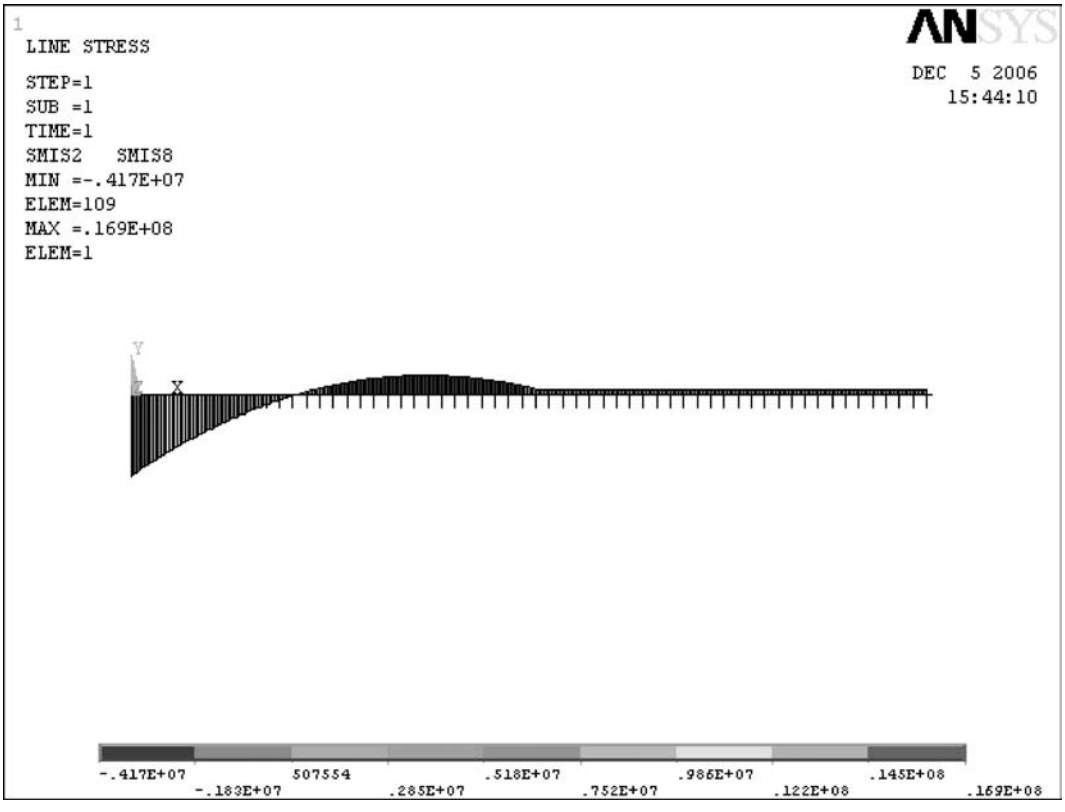

Figure 8. Calculation results of uplift in tunnel longitudinal direction.

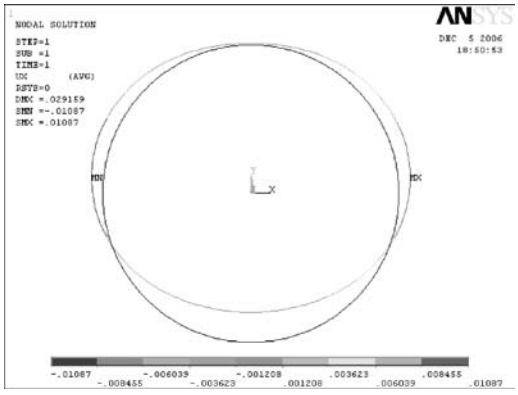

Figure 9. Horizontal deformations.

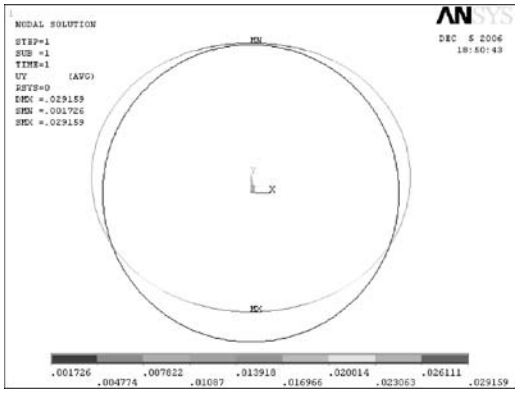

Figure 10. Vertical deformations.

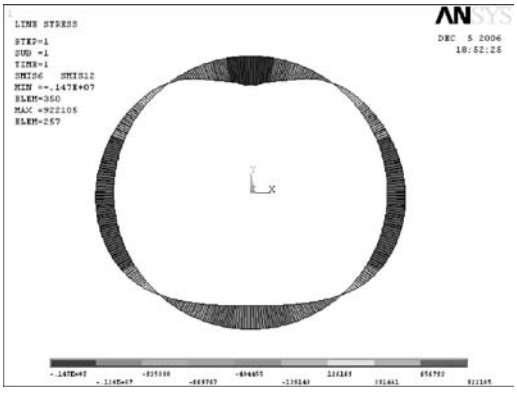

Figure 11. Bending moments.

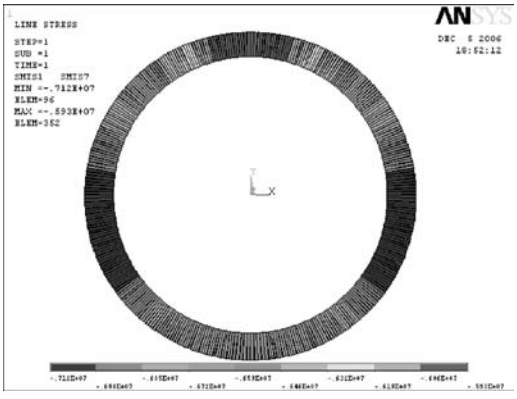

Figure 12. Axial forces.

time friction produced by shield jacks is also small. Therefore shear force between segments due to tunnel uplift becomes relatively large. Under the action of uplift on tunnel, calculation results of transversal deformation of segments and internal force are shown in Figures 9–12.

4 SAFETY VERIFICATION AGAINST UPLIFT OF TUNNEL DURING TUNNELLING

4.1 *Uplift force calculation and uplift resistance verification on tunnel*

Calculation results of tunnel uplift and verification of uplift resistance are given in Table 2 respectively at 5.0 m/d and 10.0 m/d (rate of shield tunnelling). From Table 2, the verification results indicate that near at shield break-out section, only when advance rate is controlled below 5.0 m/d, segments could meet uplift resistance requirement. When its uplift force over shear strength of longitudinal bolts as tested on segments is equal to 1.5 (as its safety coefficient), it is believed that the controlled rate of shield tunnelling is an important construction means for enhancing tunnel stability.

4.2 *Verification in tunnel transverse direction*

From calculation results on converged deformation as mentioned in Section 3.2, it is then known that given shield advance at a rate of 5.0 m/d, the maximum shear force produced between rings caused by tunnel uplift is 16,120 kN. By when max converged deformation is 27.5 mm, basically controlled within 2‰ D allowance. Whereas the maximum fissure width appears at tensioned inner-side of segment is 0.17 mm, basically controlled within an allowance of 0.2 mm as per design criteria. The maximum deformation at joints as calculated is 0.27 mm against design tolerance 4.0 mm, meeting design requirement for deformation of joints, The maximum staggering between segmental rings is 1.5 mm which is less than the allowed value of 5.5 mm as stated in “A Full Ring Lining Structural

Table 2. Results of uplift calculation and safety against uplift verification on tunnel.

Description	Symbol	Unit	Advance rate (10 m/d)	Advance rate (5 m/d)	Remarks
Segment i.d.	D_i	m	13.70	13.70	
Shield o.d.	D_0	m	15.43	15.43	
Area excavated by shield	A	m^2	187.0	187.0	
Overburden	t	m	7.5	7.5	$\pm$ 7.5 m cover at shield break-out
Overburden down to tunnel axis	h	m	15.22	15.22	
Specific weight of ground mass in front of shield γ	γ	kN/m^3	18.0	18.0	
Lateral ground pressure coefficient	K_0	–	0.7	0.7	
Resultant of jacking force	P	kN	51,211	51,211	
Friction coefficient between segments	μ	–	0.35	0.35	
Friction coefficient between segments	$F = k_0 P \mu$	kN	12,547	12,547	
Shear between segments produced by tunnel uplift	Q	kN	18,254	16,120	Obtained from calculation in longitudinal direction
Actual uplift acting on tunnel	$N = Q - F$	kN	5,707	3,573	
Shear resistance of longitudinal bolt between rings	S	kN	5,500	5,500	
Calculation of tunnel uplift resistance	$K = S/N$	–	0.96	1.54	
Verification result on tunnel uplift resistance	–	–	not met	not met	

Test for Changjiang Tunnel in Shanghai Under Tunnel Uplift Regime". Therefore it is believed that the tunnel is safe.

After numerical analysis and corresponding safety analysis, it is known that the new brand of simultaneous injection of grout developed by STEC can meet the requirement of tunnel stability against uplift.

5 CONCLUSIONS

Tunnel uplift during large diameter shield tunnelling is a key construction knuckle to be emphatically dealt with, as it is a complicated loading phenomenon under comprehensive actions of both longitudinal uplift force and transversal sectional force. Uplift force acting on tunnel is related to criteria, such as area of tunnel cross-section, fullness of filled back grout mass, its strength gaining rate in proportion to time elapse, and shield advance rate, worth to be noted, proportional to the square of shield advance rate. Therefore, the controlled shield advance rate is an effective key technical measure to control tunnel uplift.

Overburden near at shield break-out section of the Shanghai Yangtze River Tunnel Project is about 7.5 m. If a new brand of simultaneous injected grout in-house developed by STEC is used, given shield advance is controlled below 5 m/d, segment seam width can meet design requirement within allowance, i.e. 1.5 safety coefficient against tunnel uplift. In terms of safety coefficient against tunnel uplift, longitudinal bolts on segments under the state of damage due to tunnel uplift is called brittle destruction, once segment floats up with serious results causing difficulty to repair. Therefore, it is recommended that the construction can be going on in the section where the shallow overburden is less than 9 m. In addition to advance rate to be controlled below 5.0 m/d, there should be additional shear keys in place between segmental rings to enhance uplift resistance of tunnel, or safety against uplift during shield tunnelling process.

Besides, at section after shield break-out where overburden is 9 m–11 m deep, shield advance should be controlled between 4–6 m/d; or at section where overburden is between 11 m–15 m deep, shield advance between 8–10 m/d. Any section where overburden is deeper than 15 m, a reasonable selection of shield advance rate is to be recommended as based on actual requirement of the project, whereupon no shear key is to be provided between segmental rings.

REFERENCES

Ang, G.X., Lin, J.X. & Yang, F.Q. 2007. Study on safeness of lining structure during super large diameter shield tunnelling. *Underground Construction and Risk Prevention – Proceedings of the 3rd International Symposium on Tunnelling*: 597–606. Shanghai: Tongji University Press.

Hong, Y.K. 1993. *Soil Properties and Soil Mechanics*. China: People's Communication Publisher.

4 Risk assessment and management

The Shanghai Yangtze River Tunnel - Theory, Design and Construction – Huang (ed)
© 2008 Taylor & Francis Group, London, ISBN 978-0-415-47161-9

Construction risk control of cross passage by freezing method in Shanghai Yangtze River tunnel

X.R. Fan, W. Sun & H.Q. Wu
Shanghai Changjiang Tunnel & Bridge Development Company, Shanghai, P. R. China

ABSTRACT: In this paper, risk factors during Shanghai Yangtze Tunnel cross passage construction by freezing method are analyzed. The risk control measures are also discussed relate to geological investigation, freezing method design, freezing hole boring and excavation and lining stages.

1 INTRODUCTION

Shanghai Yangtze River Tunnel Project is a part of the planned national seashore expressway, which is also the major project during '11th Five Plan' in Shanghai. The tunnel locates at the mouth of Yangtze River and crosses southern part of Yangtze River. The circular tunnel has an external diameter of 15 m and an internal diameter of 13.7 m. Slurry pressure balanced TBM with a diameter of 15.43 m is used for the construction of the 7.5 km long tunnel. The tunnel is designed as two levels, of which upper level is for three-lane roadway, and the lower level is for railway.

Considering the escape, rescue under emergency conditions and technical service under normal condition, 8 cross passages are arranged between two main tunnels with a spacing of about 800 m. The layout and related geological parameters are shown in Figure 1 and Table 1.

The cross passage has a circular section and the location and structure type relate to the tunnel. As shown in Figure 2.

During the construction of cross passage, freezing method is used to strengthen the soil, drill and blast method is used to excavate the tunnel and in-situ cast concrete for permanent structure. Freezing pipes are arranged in two rows which are inner and outer row drilled from the upper change and down change tunnel respectively.

2 CAUSE ANALYSIS FOR CONSTRUCTION ACCIDENT WITH FREEZING METHOD

Artificial stratum freezing method is to use artificial refrigeration technology to ice the water in stratum by the freezing pipes inserted in soil and then form frozen soil curtain with high strength and stability, thus

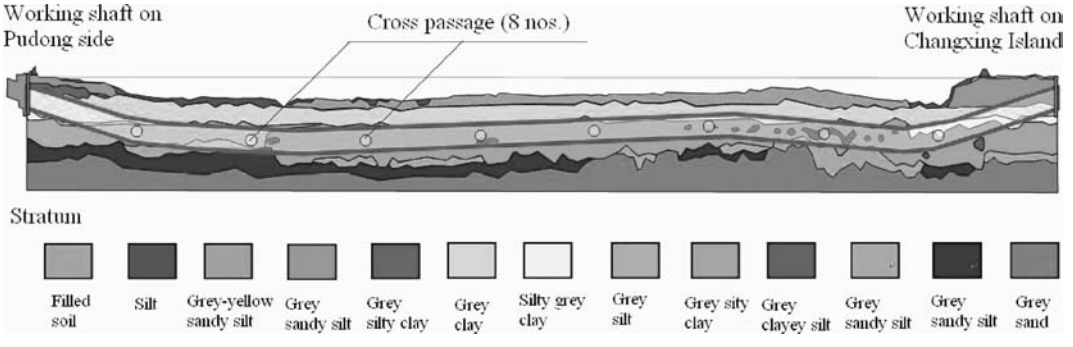

Figure 1. Cross passage layout.

Table 1. Cross passage general introduction.

No.	Chainage	Cross passage center elevation(m)	Soil stratum	Distance between cross passage bottom plate and bearing water layer (m)
1#	SDK1 + 282.494	−32.985	⑤$_2$	0.0
2#	SDK2 + 112.494	−39.246	⑤$_2$, ⑤$_3$	0.0–14.1
3#	SDK2 + 942.492	−38.355	⑤$_3$	8.7–10.7
4#	SDK3 + 772.478	−35.343	⑤$_3$	17.2–17.9
5#	SDK4 + 602.486	−32.332	⑤$_3$	16.5–20.5
6#	SDK5 + 432.499	−29.404	⑤$_1$, ⑤$_3$, ⑤$_{3t}$	12.8–23.4
7#	SDK6 + 262.499	−34.351	⑤$_3$, ⑤$_{3t}$	5.5–17.1
8#	SDK7 + 092.499	−35.820	⑤$_1$, ⑤$_3$, ⑤$_{3t}$	17.3–18.8

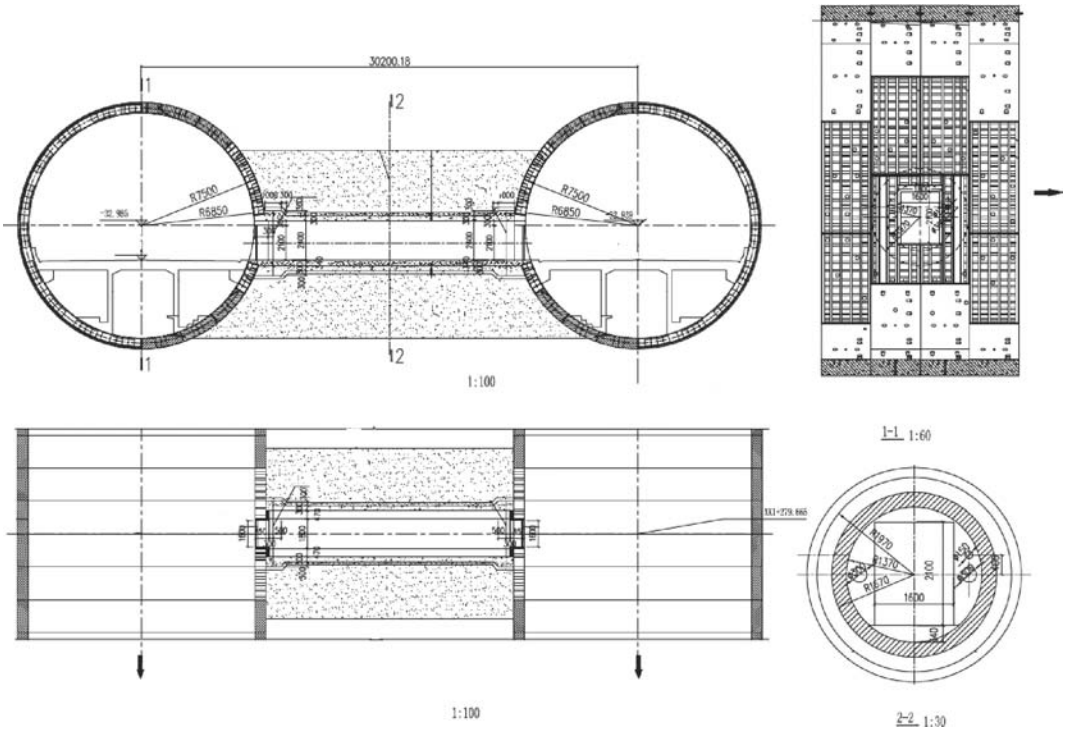

Figure 2. Cross passage structure sketch.

separate the contact between underground water and structures so that the underground excavation can be carried out under the protection of frozen curtain.

Freezing method has special characteristics, such as necessity of hole drilling, variation of frozen soil curtain and nature of freeze-thawing action. Due to these specialties, there is a risk of accidents during hole drilling, freezing, excavating and thawing process. Therefore, freezing method is very risky. To avoid accidents during construction, the analysis of construction risk factors and measures of freezing method is very essential.

Freezing method accidents mainly have following types: hole drilling accidents, frozen soil curtain accidents, freezing expansion and thawing settlement accidents. For cross passage connecting TBM tunnels, segment damage is also a risk.

2.1 *Freezing hole drilling accident*

During freezing hole construction for underground structure to surrounding soil, sealing failure at the hole opening could cause water and sand blow-out, and even underground structure damage due to too

large ground loss, and thus damage of ground building and underground pipelines, and even flood of projects, especially dangerous when the freezing holes extend into bearing water layer. The main reason is the soil loss with the slurry circulation during holes drilling or sealing protection failure at the opening.

2.2 *Segment damage accident*

Hole drilling may cause too large damage to segment and during excavation, part segment removal will make the segment ring lose integrity and thus lead to large deformation and even instability.

Too densely freezing pipe arrangement will probably cut the main reinforcement of segment and damage the integrity of structure, thus cause large damage to segment. During excavation, part segment will be removed which makes the segment ring lose integrity and thus cause large stress concentration at tunnel opening and lead to large deformation even instability of segment.

2.3 *Frozen soil curtain accident*

During excavation and lining cast stage, frozen soil curtain instability may lead water inrush and sand flow and serious underground structure damage, even flooding, large area of above cover settlement, and damage of ground building, underground structure and pipeline.

There are many reasons which may lead to frozen soil curtain accidents, mainly including four aspects: geometrical defect of frozen soil curtain, physical defect, estimation error of property, and improper construction management.

2.3.1 *Geometric defect of frozen soil curtain*

The geometric defects refer to the dimension or property of frozen curtain does not reach the design requirement such as inadequate shape and thickness of frozen soil curtain, frozen soil curtain deterioration due to adverse factors; and unachievable frozen soil curtain due to stratum defects.

2.3.1.1 Inadequate frozen soil curtain

The reason for inadequate frozen soil curtain has several aspects such as cold supply inadequacy, freezing pipe defect, cold loss, low frozen ground temperature and difficulty of stratum freezing.

Cold supply inadequacy could be due to the design amount, equipment efficiency and the brine flow in freezing machine is not enough. The refrigeration equipment inefficiency could be due to itself and also too high freezing water temperature in summer time. Inadequate brine supply could be due to unreasonable design, and also accidental blocking or residual air in machine.

Freezing pipe defects mainly are the too large spacing or too short length. Usually, it is caused by the hole drilling inclination or unsuitable design.

Cold loss is usually caused by the heat dissipation of structure, large underground water flow speed, metal or concrete with high heat conductivity and exceptional heat source in stratum. i.e. high temperature pipe or spring, among which heat dissipation of structure is most often. Structural heat dissipation may lead to high temperature of frozen soil curtain, inadequate frozen area and strength between frozen curtain and structure.

Low freezing temperature of stratum means the freezing temperature is lower than expected which leads to the frozen soil curtain thickness smaller than design thickness. This is often experienced in clay soil and soil with salt content. For Shanghai Yangtze River Tunnel, the soil with salt content should be considered.

Stratum freezing difficulty means the freezing development is very slow, thus it could not meet design requirement in planned time.

Soil stratum contains freezing-resistant exceptional substances, such as earlier leaked brine, and polyurethane.

2.3.1.2 Frozen soil curtain deterioration

Frozen soil curtain may deteriorate under unfavourable conditions. The most often type is temperature rising and surface thawing leading to strength reduction and sometimes thawing inside the curtain to form holes. These may cause frozen soil curtain bearing capacity inadequacy or water inrush accident when excavating the thawing holes.

The main reasons of frozen soil curtain deterioration include brine leakage, structural heat dissipation, frozen excavation surface heat dissipation, exceptional heat resources and equipment failure.

Brine leakage in frozen soil will lead to soil thawing, which can be caused by freezing pipe defects (i.e. joint welding quality) and pipe rupture. Reasons for freezing pipe rupture could cause too large curtain deformation, freezing expansion, excavation deformation, excavation loss, and large deformation, and stress of freezing pipe caused by freezing holes curvature.

Structural heat dissipation is mainly due to the temperature retaining layer failure, high temperature air convection and surface freezing pipe (i.e. cold drainage pipe) failure, etc. Frozen soil curtain deterioration caused by structural heat dissipation is not only the curtain temperature rising, and volume reducing, but more dangerous results are the frozen area and strength reducing between the curtain and structure.

Heat dissipation on the excavation surface of frozen soil could also be one reason for the frozen soil curtain deterioration. The excavation surface makes the frozen soil curtain contact with air convection, thus temperature rising and strength reducing.

Heat erosion of exceptional heat resources such as concrete hydration heat, high temperature pipe and spring will also cause frozen curtain deterioration.

Abnormal freezing machine failure and too long interruption time will also definitely deteriorate the frozen curtain. Too early freezing termination after excavation works may also cause frozen curtain thawing.

2.3.1.3 Geological defect

Geological defects such as the marsh, thawing holes and hidden creek in the design range of frozen soil curtain or surrounding area will lead to hollow or ice pocket in the frozen soil curtain which even be critical causing water inrush accidents during excavation.

2.3.2 *Physical defect of frozen soil curtain*

Physical defects of frozen soil curtain mean that the curtain has not reached design strength and stiffness. Both strength and stiffness inadequacy may lead to frozen soil curtain accidents.

Main reasons for strength inadequacy are too high frozen curtain temperature and low stratum strength. When frozen soil temperature is too high, it is difficult to meet design strength as the frozen soil strength increases with the temperature reducing. The frozen soil strength of some stratum such as clay is relatively low. So if it is unexpected within the design frozen soil curtain range, it will lead to the curtain strength lower than design strength.

Main reasons for stiffness inadequacy are too high frozen soil temperature, too long exposure time after excavation, initial lining failure and strong creep stratum, etc.

2.3.3 *Error estimation of frozen soil curtain character*

Character of frozen soil curtain is always changing. The estimation of the character and evaluation of safety condition of frozen curtain will directly influence the construction decision-making. Sometimes, frozen soil curtain accidents are caused by error estimation of the characters.

Character of frozen soil curtain means the property and status, mainly including the temperature field, characteristic surface temperature, average temperature, thickness, property and strength field and their variation rules. These parameters are mainly calculated by suitable temperature field model and physical model based on temperature data and freezing pipe arrangement. Therefore, the reason for wrong estimation of frozen soil curtain character could be the freezing pipe position deviation, measurement point tolerance, measured data distortion, model unsuitability, frozen soil property deviation and unexpected stratum defects.

- Freezing pipe position deviation

Freezing pipe position information is the basic data for temperature field calculation. The deviation could be the measurement distortion of freezing pipe holes data and later deformation of freezing pipe which could be caused by too large ground loss, freezing expansion and excavation. When the freezing pipe spacing is too large or the length is not enough, it will cause error estimation.

- Temperature measurement position error

Spatial position data of temperature measurement points is also basic information for temperature field calculation. The measurement points are arranged in measuring holes, so the tolerance is the same as that of freezing pipe, which could be caused due to holes measurement distortion and later deformation.

- Temperature monitoring data distortion

Temperature monitoring data distortion will definitely lead to distortion of temperature field calculation results. The reasons are normally the temperature sensor and monitoring system failure and external disturbance.

- Temperature field model unsuitability

Difference freezing pipe arrangement has different temperature field model. When the arrangement is complex, combination of several models needs to be used together. Therefore, the selection of calculation model will decide the temperature field calculation result. Unsuitable calculation model may lead to wrong estimation of temperature field.

- Frozen soil property deviation

Frozen soil property deviation means the inaccuracy of physical mechanical properties and thermal property parameters of frozen soil. The mechanical property deviation will affect the results of safety condition evaluation of frozen soil curtain. The property parameters of frozen soil must be defined by tests of stratum in this project. Reference to test data of other projects under similar conditions usually leads to deviation, especially for the water and salt content.

Water content is an important factor which affects the frozen soil property and in different projects, even same stratum may often have large difference of water content.

Salt content has influence not only on frozen soil strength, but also on the freezing temperature. For higher salt content, the freezing temperature is lower and thus the curtain thickness is much smaller under same temperature conditions. If stratum with high salt content is calculated without considering salt, it may lead to unfavourable estimation error of frozen soil curtain character.

- Unexpected stratum defect

Stratum defects in the freezing range and surrounding area or sudden stratum change may lead to serious estimation error of frozen soil curtain character.

2.3.4 *Construction management error*

Sometimes the frozen soil curtain accidents are caused by management error which includes serious overcut, wild construction disregarding accident signs, unreliable emergency provision, etc.

2.4 *Freezing expansion accident*

During freezing process, soil expansion may cause freezing pipe rupture and underground structure deformation failure accident. Freezing pipe rupture may lead to weak area of frozen soil curtain thus instability accident. The underground structure deformation may affect service life of the structure.

Freezing expansion is natural regulation. Main reasons of frost accidents include frost sensitive stratum, too long freezing time, too large frozen soil volume and ineffective control measures.

Freezing sensitive stratum is necessary for freezing expansion. The inadequate understanding of the sensitivity is one of the reasons for unexpected expansion. Too long freezing time is the frequent reason for too large expansion, which may lead to too large frozen soil volume thus large expansion.

Ineffectiveness of freezing expansion control measures is also one reason.

2.5 *Thawing settlement accident*

The thawing settlement of frozen soil after freezing works completion may cause differential settlement of underground structure thus deformation failure, and damage of ground building, under-ground structure and pipeline.

Thawing settlement of frozen soil is natural regulation. The control is mainly done by grouting after frozen soil thawing. Therefore, ineffective grouting measures are the main reason for thawing accidents.

When natural thawing and follow-up grouting are used, it is often difficult to grout for long term due to long natural thawing time. Although forced thawing measures can reduce grouting period significantly, sufficient monitoring data during thawing is lack in project which makes the grouting not accurate.

On the other hand, due to various restrictions, it is difficult to arrange grouting pipes in optimal locations, thus adequate grout surrounding the total freezing area can not be ensured.

3 RISK FACTORS AND CONTROL MEASURES FOR FREEZING METHOD

Safety of freezing method depends on detailed and accurate geological information, correct freezing method design, reliable freezing system construction procedure, normal freezing system operation, required frozen soil curtain character (i.e., thickness, temperature and strength), effective frost resistance, existing structure protection, suitable excavation and lining procedure, strict thawing control measures and reliable information construction monitoring system for freezing method. Carelessness of any procedure may lead to accidents even disaster. Unknown stratum defects, exceptional underground water and heat resource my lead to normal freezing method failure. Freezing method will decide the realization of expected frozen soil curtain character, dimension and strength. Reliability of freezing hole boring procedure will decide the prevention of drilling accidents. Abnormal operation of freezing system may cause weak area of frozen curtain. Unsuitability of excavation and lining procedure may cause deterioration of frozen curtain character and large deformation and finally serious results. Monitoring system with insufficient accuracy and reliability is impossible to observe the weak part of frozen curtain. Therefore, freezing method is a construction method with high risk and needs provisions for risk control.

Certain risk factors are as follows: the geological investigation, freezing method design, freezing hole boring, freezing system operation, frozen soil curtain estimation, frost resistance, existing structure protection measures, excavation and lining procedure, freezing termination timing, freezing system removal.

3.1 *Geological condition*

The factors in stratum which have influence on the convection conductivity are the risk factors of geological conditions for freezing method. Geological conditions include stratum types adverse to freezing, local exceptional stratum property, structure and obstacles. Hydraulic conditions include the underground water currency, direction, water quality (i.e., salt content), water temperature and bearing water, etc.

Control measures for geological condition risks are: carry out detailed and accurate geological investigation and perform the physical mechanical property test of each stratum and necessary water quality test.

3.2 *Freezing concept design*

The risk factors of freezing method design are the reliability of design basis (i.e., physical property of frozen soil), accuracy of freezing system parameter calculation and suitability of frozen soil curtain structure parameter.

Physical property of frozen soil is the basis for design, the unreliability of which may lead to error of freezing method design.

Inaccurate freezing system parameter calculation may lead to two opposite results. First, cold supply is not enough, which makes the expected frozen soil curtain character can not be obtained in predefined time,

so the design temperature of frozen soil curtain temperature can not be reached, and leading to inadequate thickness or strength of frozen soil curtain. Secondly, cold supply is more than necessary, which leads to too large freezing strength thus freezing expansion hazard.

The corresponding control measures are: obtain reliable physical property parameters of frozen soil; comprehensively consider various adverse factors and perform careful design of freezing system parameters and select correct freezing equipment; correctly estimate loads and use suitable mechanical model for calculation to obtain safe parameters of frozen soil curtain structure.

3.3 *Freezing hole drilling*

The main risk factors during freezing hole drilling construction from underground structure to surrounding soil is the control failure in circulating slurry and sealing pipe failure at hole opening.

The corresponding control measures are: take effective measure to control the sand amount in the circulating slurry such as provide equivalent pressure to balance water or soil pressure by bypass valve of sealing pipe and strictly monitor the sand drainage amount; compensate grouting by freezing pipe when ground loss is too large; ensure the reliable fixation between sealing pipe and structure to avoid sudden sand blowout when sealing pipe release from structure which is especially important for freezing pipes below the structure.

3.4 *Freezing system operation risk*

Unfavourable freezing equipment condition, power supply, freezing efficiency or inadequacy, and unsatisfactory freezing pipe sealing condition can be the risk factors which may lead to accidents during freezing system operation.

Control measures for the freezing system operation risk are: ensure refrigeration equipment in good condition and spare equipment for major projects; ensure enough power supply; ensure cold water within normal temperature; strictly control the cold medium flow speed; discharge the residue air in freezing machine periodically by monitoring the temperature of brine circuit and make timely adjustment in case of any exceptional conditions; ensure freezing hole boring quality and freezing pipe joint tightness, and try to reduce pipe joint; perform pressure resistant test after installation of freezing machine; monitor brine level in the tank during operation in order to observe any brine leakage.

3.5 *Frozen soil curtain character estimation risk*

Main risk factors of frozen soil curtain character error estimation mainly include: inaccurate freezing pipe position information, unsuitable temperature measurement point layout, inaccurate temperature measurement point layout information, unreliable soil temperature and cold medium temperature monitoring data, unclear physical characteristics of frozen soil, incorrect temperature field model and inadequate consideration of heat dissipation boundary.

The corresponding control measures are: ensure precise information of freezing pipe location; carry out good measurement of freezing holes; consider possible later deformation of freezing pipes, prepare suitable temperature measurement points arrangement and record precise position information including consideration of later deformation of temperature measurement pipe; pay attention to possible movement of measurement cables in the pipe to ensure reliable monitoring data; ensure normal operation of monitoring system and shoot failures timely; perform physical mechanical property test in advance to obtain parameters; select correct temperature model and related parameters based on freezing pipe arrangement; consider adverse influence from structural heat dissipation boundary on the frozen soil curtain.

3.6 *Freezing expansion risk*

The main risk resource of freezing expansion is the too long freezing time, too large frozen soil volume and ineffective control measures.

The control measures for freezing expansion are to define the ground sensitivity to frost in advance by freezing expansion test; avoid too long freezing time; start excavation and lining procedure once the frozen curtain character meets design requirement based on the monitoring result; maintain freezing during excavation and lining; avoid too sufficient cold supply during maintaining freezing period and execute expansion control measures. On the other hand, protect structures which may have too large deformation, e.g. place pre-stressing frame in tunnel to restrict the segment deformation due to freezing expansion.

3.7 *Excavation and lining risk*

Risk factors during excavation and lining stage are mainly water leakage due to too early excavation, too large deformation and even instability after segment opened, too large frozen curtain deformation after excavation, temperature retaining measures failure at the horn location, ineffective initial lining support and most adverse condition may lead to frozen curtain water penetration.

The corresponding control measures are: strictly control excavation conditions; remove segments only after all excavation conditions meet design requirements; Strengthen opening surrounding before removing segment; forbid over-cut during excavation and

timely support and control its quality try to reduce frozen soil explosion time; strictly monitor the frozen curtain condition at the horn location and take temperature retaining improvement measures if necessary as excavation will increase the heat dissipation area of frozen soil curtain.

Meanwhile, the emergency scheme for frozen curtain water penetration accident must be prepared. At the connection between cross passage and tunnel, tight and stable protection door shall be installed which could be closed once water penetration accidents occur to ensure the tunnel safety.

3.8 *Freezing system removal risk*

During freezing system removal, too early removal timing, cutting of freezing pipe and untight holes sealing are the risk factors.

The corresponding counteract measures are to strictly control the freezing machine stopping time, which must ensure the in-situ cast concrete has certain strength before stopping. After the machine is stopped, freezing pipe cutting shall be arranged according to design as soon as possible and be performed in accordance with the method statement.

4 CONCLUSIONS

Cross passage construction of TBM tunnel is a key project with high risk, even higher for under-river tunnel. Each procedure during construction, especially during excavation and lining, must closely monitor the risk factor development and variation according to freezing method specialty. Forecast measures should be taken before accidents happen to ensure the project safety.

REFERENCES

Jiang, J.C. & Guo, Z.L. 2004. *Safety System Engineering.* Beijing: Chemical Industry Press.

Richard, E., Barlow, Jerry, B., etc. 1975. Reliability and fault tree analysis. *Philadelphia: Society for Industrial and Applied Mathematics.*

Shi, D.H. & Wang, S.R. 1993. *The Method and Thesis of FTA Technology.* Beijng: Beijing Normal University Press.

Wu, X.G. 2006. The technique of shield tail brush be repaired inside during long tunnel building. *Guangzhou Architecture* (6):25–27.

Zhang, F.X., Zhu, H.H., & Fu, D.M. 2004. *Shield Tunnel.* Beijing: China Communication Press.

The Shanghai Yangtze River Tunnel - Theory, Design and Construction – Huang (ed)
© 2008 Taylor & Francis Group, London, ISBN 978-0-415-47161-9

Crack control measures during segment prefabrication of large diameter bored tunnel

B.T. Yan, Z.Q. Ying & K.J. Li
Shanghai Tunnelling Engineering Co., Ltd., Shanghai, P. R. China

ABSTRACT: The crack control measures used in Shanghai Yangtze River Tunnel are described regarding the segment concrete mix design, concrete quality control, concrete vibration, bleeding and curing.

1 INTRODUCTION

With the rapid development of urban underground rail traffic, TBM construction method has been extensively applied in railway tunnel, road tunnel, water tunnel and urban underground pipeline because of its safe and fast construction. The bored tunnel is lined with segments. Beside the segment strength, seepage resistance and dimension preciseness in accordance with specified requirement, the corner and edge falling, blow hole and cracks shall also meet relevant requirement. Due to cracks related with the structural capacity and durability of segment structure, it must be avoided. Once corrosive underground water and gas initiates corrosion from the cracks and leads to structural concrete carbonization and reinforcement corrosion it will affect the service life of tunnel and increase the maintenance cost. Therefore, it is very significant to reduce or avoid segment cracks during concrete segment prefabrication. In combination with actual conditions of Shanghai Yangtze River Tunnel segment prefabrication, the cracking reasons and control measures for large diameter segment are described.

2 PROJECT INTRODUCTION

Shanghai Yangtze River Tunnel is designed to fulfill dual 6-lane expressway standard with a speed of 80 km/h. The total length is 8,954.0 m and bored tunnel is 7,472.11 m long. The external diameter of bored tunnel lining is 15,000 mm and internal diameter 13,700 mm. The ring width is 2,000 mm and thickness is 650 mm. Pre-cast reinforced concrete common tapered segments are assembled with staggered joint. Concrete strength class is C60 and seepage resistance class is S12. The lining ring consists of 10 segments, i.e. 7 standard segments (B), 2 adjacent segments (L), and 1 key segment (F). According to the different depth, segments are classified as shallow segments, middle-deep segments, deep segments and extremely deep segments. Skew bolts are used to connect segments in longitudinal and circumferential direction. $38 \times$ M30 longitudinal bolts are used to connect the rings. $2 \times$ M39 circumferential bolts are used to connect the segments.

For Yangtze River Tunnel, the concrete volume per ring is around 60 m^3, and maximum volume for one segment is 6 m^3, weighing 16 t.

3 SEGMENT CRACKING REASONS ANALYSIS

Recent and modern science related to concrete construction study and a large number of practical concrete works have proved that concrete cracking is unavoidable. Although concrete with admixtures and low temperature steam curing procedure has been extensively used in segment prefabrication, unavoidable cracking is still experienced during segment prefabrication, lifting and erection. In terms of cracking reason, cracks are classified as two types: cracks due to deformation and cracks due to external load.

For segment, cracks due to deformation mainly reflect in three aspects during prefabrication:

(1) Concrete distribution influence

Due to the influence from concrete hardening, slump, self-weight and vibration, the concrete distributes un-uniformly in the steel formwork. Especially for large diameter segment, each steel form has three batches concrete with different slump and water content locally leading to different hardening speed and thus cracking.

(2) Temperature influence

Large temperature difference will lead to un-uniform hardening inside and outside concrete thus large

temperature stress is caused. At the same time, the segment concrete strength can not resist the temperature stress thus cracking occurs.

(3) Ambient humidity influence

When the ambient humidity reduces to certain extent, the water loss on segment surface is very fast which leads to volume shrinkage and shrinkage stress. When the concrete strength can not resist the shrinkage stress, surface cracking will occur.

Cracks caused by external loads are mainly reflected as structural cracks during segment lifting, transport and use.

4 CRACK CONTROL MEASURES

4.1 *Concrete mix design optimization*

4.1.1 *Concrete mix design for segments with large diameter and high preciseness*

The research on the high performance concrete mix design is mainly to adjust the water/cement ratio and compositions such as coarse aggregate, additives, and other admixtures to satisfy the requirement to concrete of segment with large diameter and high preciseness. The final result of mix design is to adapt the performance requirement such as strength and durability and fulfil the prefabrication procedure requirement.

4.1.1.1 Water/cement ratio

During the segment concrete design study, alternate current resistance spectrum is used to evaluate the chloride diffusion. The relation between w/c ratio and chloride diffusion resistance is tested. The result shows that the diffusion resistance increases with the w/c increasing but when the w/c is larger than 0.3, the diffusion resistance has obvious change. Based on the test results, w/c is defined as no higher than 0.30.

4.1.1.2 Coarse aggregate

During segment prefabrication, considering concrete strength requirement, 16–31.5 mm stone aggregation is selected initially, but the result is not good and cracking is difficult control. After analysis, large stone size is good for the segment concrete strength; however, the gap between stones is basically filled with cement after vibration which is easy to cause cracking. Therefore, it is adjusted during mix design. Stone with a size of 16–31.5 mm and smaller stone with a size of 5–25 mm is selected forming a continuous aggregation.

4.1.1.3 Admixtures

Admixtures are usually selected to change or improve the concrete performance such as fluidity, working ability, early strength, frozen resistance, seepage resistance and hydration process. High effective water reducing agent is used in this project. Nowadays, three types highly effective water reducing agent are available which are naphthalene type, fatty acid type, and Poly (carboxylate) type. The carboxylate water reducing agent is suitable for in-situ cast concrete with large fluidity and high air content. The water reducing rate of naphthalene type is relatively low around 15%. Therefore, for semi-hardening segment concrete, it is preferable to use fatty acid water reducing agent.

4.1.1.4 Fly ash

The application of good performance fly ash in concrete can not only replace cement partly and save costs but also improve and increase the concrete performance. The role of fly ash in concrete is as follows:

- Form effect: Main mineral composition of fly ash is sponge shape glass substance which has a smooth surface, fine granularity, dense texture, small inner specific area and small water absorbability which reduces the inner friction of concrete and is good to improve the concrete fluidity and also has water reducing action on concrete.
- Active effect: The active content SiO and AI2O3 in fly ash has action with hydration product of cement under water resulting C-S-H and C-A-S-H. These actions almost are done in the holes and gaps of cement mortar. Resulting hydration products fill the big holes which can reduce the porous ratio inside concrete, change the porous structure and improve the bond action among concrete constitutions.
- Micro-aggregate action: the fine grain in fly ash distributes in the cement uniformly so that the gap is filled. Meanwhile, it can prevent the bond of cement grain to make it in a disperse status which is good for the hydration action. Fly ash will not have action with hydration product of cement completely so that the micro aggregate action can be kept for long time.
- Interface effect: the interface between aggregates and cement is the weak part of concrete structure. The width of transition area varies with the water/cement ratio and aggregate absorbability. The holes and gaps are more and larger in the transition area than the cement mortar. Adding fly ash can reduce the width of transition area and disturb the direction of $Ca(OH)_2$ in transition area and improve the concrete interface strength and density.

Furthermore, the excellent durability of concrete with fly ash has been recognized; therefore, fly ash is added in the segment concrete mix. Meanwhile, considering the requirement from formwork removal and lifting procedure to the early strength, the fly ash content shall not be more than 30%. During construction in winter season, it shall not be more than 20%.

4.1.1.5 Slag

Slag has pozzolana effect and micro aggregate effect. Pozzolana effect: slag changes the interface bond strength between cementitious material and aggregate.

The influence from directional array of hydration product Ca $(OH)_2$ on the interface bond between concrete mortar and aggregate makes the bond strength reduce. Slag absorb the cement hydration product Ca $(OH)_2$ and results more favorable C-S-H to make the Ca $(OH)_2$ grain size smaller in the interface area and improve the micro structure of concrete, reduce the porous ratio of cement mortar, increase the bond force at interface and thus improve the seepage resistance of concrete. Micro aggregate action: slag can fill the gap between cement grain so as to improve the porous structure of concrete and reduce the porous ratio and maximum hole size, forming the dense structure and improve the seepage resistance and prevent the bleeding and segregation.

Slag has the characteristics of good water-retaining ability, plasticity, few bleeding water and the working ability of concrete is good, especially slow hydration heat which is good for cracking control. Therefore, slag is added in the concrete.

4.1.1.6 Admixture in cementitious material

When fly ash replaces equivalent cement, 28d strength is basically lower than normal concrete strength. However, slag can increase the 28d-strength of concrete. Therefore, fly ash and slag are complementary. The combination use can give attention both to early strength and later strength, i.e. make use of the pozzolana effect of slag earlier to improve the interface structure between mortar and aggregate and compensate the early strength loss and later make use of the hole size fining action resulted by the pozzolana of fly ash and the inner core action of non-acted fly ash to make the concrete strength increase continuously.

According to the relation between different admixtures and diffusion resistance, and based on the analysis of chloride diffusion resistance data, it is concluded that the chloride diffusion resistance reduces with the increase of SSB mixture. When SSB is more than a certain value, the chloride diffusion resistance variation tends to be stable. According to the character and considering the segment concrete production procedure requirement, the admixture in cementitious material is defined.

4.1.2 *Application of concrete mix design for large diameter segment*

Four concrete mix design solutions have been used during Yangtze River Tunnel segment prefabrication. At the beginning, slag content is high in concrete mixture in order to increase concrete early strength, but the hydration heat develops very fast, as shown in Figure 1. In Figure 1, the transverse coordinates indicates the time after casting and vibration. It could be seen from the figure that temperature increases 2–3 per hours until 70 maximally after concrete casting and vibrating. Therefore, the segment inside temperature increases very fast which leads to large temperature difference between inside and outside temperature thus cracking. Based on this experience, slag content is reduced later and fly ash is changed to class I from class II which has achieved good result.

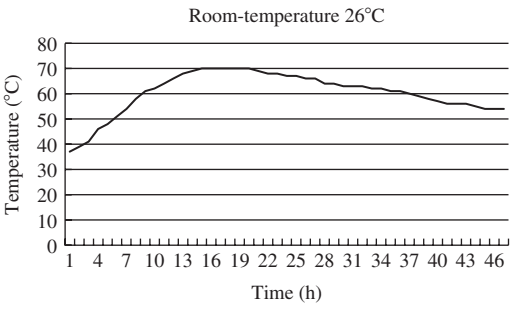

Figure 1. Segment inside temperature variation curve.

Furthermore, 3 different mix design solutions are selected in order to be adjusted according construction requirement in different seasons. It is mainly realized by adjusting the fly ash and slag content in the mixture based on early strength requirement. During actual execution, corresponding mix design is selected according to climate characteristics and construction progress. Two years' practice has proved that both segment quality and construction progress are effectively assured after application of different mix design solutions.

4.2 *Concrete quality control*

The concrete quality is also one main reason for segment cracking. Beside the raw material quality, slum and mixing time are also critical control factors for concrete quality.

Considering the several batches for one segment, different water content, transport distance, water evaporation during transport and construction characteristics in different seasons, the concrete slump is controlled within 40 mm ± 10 mm in summer-autumn and 30 mm ± 10 mm in autumn-winter.

The mixing time influences the viscidity and working ability of concrete. If the mixing time is too short, the aggregates and cementitious material can not be mixed uniformly which leads to different hardening time after concrete vibration and causes cracks and blow holes. If the mixing time is too long, concrete mixtures are too mature. The hardening time brings forward after concrete vibration which affects the necessary time for bleeding and leads to difficult control. On the other hand, too long mixing time will cause damage of equipments and increase the maintenance and repair time, thus affect the continuity of segment prefabrication. Therefore, based on the actual mix design and actual conditions, the mixing time is defined as 120 s.

4.3 *Concrete vibration control*

Segment vibration quality relates to the surface blow hole and cracks closely. The selection and control of vibration tools, methods and time play a significant role in ensuring the internal density, distribution uniformity and cracks control. Therefore, the following measures are taken.

4.3.1 *Vibration method*

Heavy steel formwork is used in Shanghai Yangtze River Tunnel segments, so internal vibration method is used. The vibrator shall be inserted fast and pulled-out slowly. The casting speed shall match the vibration speed. Vibrator is forbidden to contact with steel formwork, supported on reinforcement cage, and conflict with inserts. The interval between vibrator inserted locations shall not be more than 25 cm to ensure the uniform concrete vibration.

Due to the large segment thickness 650 mm, concrete casting and vibration must be carried out by layer. The internal vibrator shall be inserted into 10 cm in the lower layer.

4.3.2 *Vibration tools*

The inner chamber of steel formwork has a depth of 650 mm, arc length of 5 m, and width of 2 m, therefore the requirement of vibrator is high. Firstly, the length of vibrator shall be able to act on both layer when casting by layer and high frequency must be used so that the working range of vibrator cam fulfill the construction requirement. Additionally, considering the properties of vibrator, it will be discarded after use in 500 m^3 concrete because the frequency and working radius will decrease with the use time. If not replaced, concrete may not be dense due to the vibration tools thus crack.

The internal vibrator has a diameter of 70 mm and length of 480 mm. The vibration frequency is 14,000 times/minute. After the use of 500 m, it will be enforcedly discarded.

4.3.3 *Vibration time*

Generally, vibration shall continue until no blowhole on concrete surface and full concrete filled in the corner of formwork. The concrete of segment in Yangtze River Tunnel is 6 m^3 averagely which is almost equivalent to the concrete volume of one ring in metro tunnel. Therefore adequate vibration time must be ensured to control the surface blow hole and crack thus ensure the concrete uniform distribution and avoid the segregation. According to experience, the suitable vibration time is defined as 20 min $\pm$ 3 min.

4.4 *Concrete bleeding procedure control*

Concrete bleeding is mainly to ensure the density and visual quality of segment extrados and meanwhile prevent the segment surface cracking because bleeding can prevent early evaporation of free water in concrete.

Therefore, following measures are taken during bleeding procedure: bleeding shall be carried out in three times. Firstly, bleeding is carried out after vibration in order to take away the extra concrete to make the extrados even. Secondary bleeding is carried out 2 h–3 h after 1st bleeding in order to make the concrete contact. The third bleeding is especially important which starts when the concrete is pressed by finger and no movement of surrounding concrete, i.e. the initial setting starts. Furthermore, concrete shall be covered with plastic membrane after bleeding for temperature retaining.

4.5 *Steam curing procedure control*

To large extent, the curing quality influences the segment quality after formwork removal, including segment strength and visual appearance. Therefore, curing after formwork removal is an important procedure during segment prefabrication.

Steam curing can accelerate the forming of cement stone structure, however, the heat expansion leads to concrete damage. Therefore, during wet-heat curing, it is the internal structure forming process of concrete and also the damage of the structure. Concrete strength is the comprehensive result of the contradiction action. Meanwhile, the contradiction will cause the porous structure of concrete which leads diffusion coefficient change of chloride. In segment concrete, the control of chloride diffusion resistance is more difficult than strength. The task of steam curing concrete research is to make use of the positive effect of internal structure forming and restrain the negative effect of structure damage to make the total hole ratio reduce to minimum extent. Meanwhile, during high temperature curing, the hydration speed of cement is accelerated. The diffusion speed of hydration produce is relatively slow which can not fill the cement gap effectively, leading to un-uniform distribution of hydration produce and coarse concrete porous structure. Compared to concrete cured under normal temperature, the porous ratio is larger which is easy to cause cracking. Therefore, the requirement of steam curing is considered during concrete mix design, so low water-cement ratio is selected and fly ash and slag is added.

According to the characteristics of Shanghai Yangtze River Tunnel segment, 45C steam curing procedure is used, which starts 1 hr after bleeding completion. Movable steam curing shelter is sued. Segment steam curing consists of pre-steaming, temperature rise, maximum temperature hold and temperature reducing stages, as shown in Table 1.

During entire steam curing process, the shift staff must record the temperature variation of each measurement points to ensure the uniformity of temperature in

Table 1. Steam curing operation reference table.

Item	Requirement
Pre-steaming time	1 h after segment bleeding completion
Temperature rise	$\not>$ 15°C/h
Maximum temperature	$\not>$ 45°C
Maximum temperature hold	$\geq$ 1h
Temperature-reducing speed	Hold 1–2 hrs according to ambient temperature

the steam curing shelter and temperature-rising and reducing uniformly.

4.6 *Curing after formwork removal*

After segment formwork is removed, control measures such as temperature-reducing and retaining shall be taken upon the segment to effectively control temperature difference cracks and dry cracks thus ensure segment quality.

Segment temperature reducing means during summer construction, due to temperature after formwork removal is up to 70°C, if the segment is lifted immediately to curing pool for water curing, it will have crack after taken out. If natural temperature reducing is used in workshop, it will take too long time due to the slow reducing rate. Therefore, water spraying is used, i.e. after the segment formwork is removed; it is placed at the curing area and cured by water spraying.

Segment temperature retaining means during spring/winter construction, due to the low ambient temperature, the temperature difference is very large after segment formwork removal which may easily cause temperature difference cracking, therefore, geotexile cloth shall be covered on the segment after formwork removal and the door and windows of workshop shall be closed to avoid the shrinkage crack due to wind blow.

After curing in workshop, the segment will be cured in water pool. 7 days later, the segment is taken out and then cured for 7 days with water spraying. Then it is lifted to storage yard.

5 CONCLUSIONS

With the development of bored tunnel, tunnel with large diameter will have more extensive application. The prefabrication procedure and crack control of segments will be also paid more attention to. Relative measures have been taken during concrete mix design, concrete vibration, bleeding and curing for segment prefabrication in order to control cracking. Until now, 5,200 rings of segment have been prefabricated which are 70% of the total segments. Based on the actual condition of finished segment quality and feed-back information from user, the segment cracking is effectively controlled. So the segment prefabrication will also continue as normal.

REFERENCES

Haggag Salem, Rosa Aristoteles, Huang Kevin, et al. 2007. Fault tolerant real time control system for steer-by-wire electro-hydraulic systems. *Mechatronics*, 17(2–3): 129–142.

Wang, J.G. & Zhou, Z.F. 2005. Transport test study of crack medium solute. *Journal of Rock Mechanics and Engineering* 24(5):829–834.

The Shanghai Yangtze River Tunnel - Theory, Design and Construction – Huang (ed)
© 2008 Taylor & Francis Group, London, ISBN 978-0-415-47161-9

Dynamic risk management practice of construction for the long-distance and largest-diameter tunnel

Z.H. Huang, X.L. Peng & W. Fang
Shanghai Changjiang River Tunnel & Bridge Construction Company, Shanghai, P. R. China

ABSTRACT: This paper describes the construction of Shanghai Yangtze River Tunnel with its background, and discusses the difficulties of construction management of long-distance and large-diameter tunnel. Dynamic risk management is introduced to the tunnel construction management, to eliminate or reduce the relative risk resources, by risk analysis and assessment. It aims to track the risk continuously, adopt various management methods consisting of monitoring and management of TBM, the-third-party monitoring, shift management, construction consultants, construction monitoring by telecommunication, rule construction in practice. Using the construction of long-distance and large-diameter tunnel as example, it tells how to predicate and control risks by using dynamic risk management is introduced.

1 INTRODUCTION

With the development of science and technology, the scale of projects is becoming larger with more technical difficulties than before. Risk analysis and assessment, risk precaution, risk elimination and risk management, etc, have caused wide concern in the engineering world, and their effects in the construction management of large project have been recognized continuously.

The Shanghai Yangtze River Tunnel is an important part of the Shanghai Chongming River Crossing–Yangtze River Tunnel and Bridge Project. The southern end of tunnel starts at Wuhaogou in Pudong, connected to Xinkai Port in Changxing Island, approximate 8.9 km in total length; The under-river tunnels consist of double circle tunnels constructed by two TBMs with a diameter of 15.43 m, the largest slurry TBMs in the world, and will drive approximately 7.5 km continuously to the terminal shaft. The characters in this project include large project scale, long construction period, complex techniques, high quality requirements, more and complex construction risk and difficulty to manage and cooperate that are big challenge to tunnel construction. At the stage of Project Feasibility Research, construction risk management and control have been taken into consideration which covers major risk analysis for construction stage, operation stage, the development of river level of the mouth of Yangtze River, the influence on the ecological environment of the mouth of Yangtze River, terrorism attack risk assessment, the prediction of traffic volume and financial risk assessment, to provide reference and proposal for the decision of tunnel construction.

There is a higher requirement for risk management during the construction, so the solutions of site management need to be modified according to dynamic risk management theory, risk analysis, assessment and tracking, to eliminate or reduce the relative risk resource, so as to manage and control progress, quality and safety of the construction efficiently.

2 DIFFICULTIES IN CONSTRUCTION MANAGEMENT OF THE LONG-DISTANCE AND LARGEST-DIAMETER TUNNEL

2.1 *High technical difficulties*

TBMs of 15.43 m in diameter are adopted in Shanghai Yangtze River Tunnel to bore approximately 7.5 km continuously under Yangtze river mouth where ground condition is complex and high hydrostatic pressure is 0.55 Mpa (Max.). There is no similar tunneling experience as reference in China, so it is a big technical challenge to construction. There are some types of technical difficulties as follows:

- various harmful ground condition
- large-diameter TBM boring under high hydrostatic pressure condition
- the durability of TBM for long period driving continuously
- long distance traffic control and transportation of materials and equipments

- surveying for long-distance tunnel
- long distance slurry transferring
- ventilation in long-distance tunnel, etc.

Risk control measures have increased significantly with the increasing of technical difficulty. During tunneling period, method statement and relative technical parameters of construction should be modified dynamically, to reduce time consumed in technical trial and decision, and keeps construction processing in control by using real-time monitoring and telecommunication monitoring.

2.2 *Long period of tunnel construction*

The time limit for Tunneling of Shanghai Yangtze Tunnels is 32 months according to contract. Mechanization of tunnel construction has introduced the intensity, reduced the labour and standardized progress, but it also has caused duplication of simple works which always make workers feel inattention, confusion, tiredness and hidden troubles of construction safety. Take precast segments building as an example, there are 10 segments in one ring and 7,500 rings in total in both tunnels, which means the heavy segment of 15ton will be built 75,000 times, so it is hard to control the quality and safety.

2.3 *Involving many interface in management organization*

Yangtze River Tunnel construction includes TBM manufacture, local equipment forming a complete set with major installations, precast lining segment production, TBM advancing followed by road deck construction, No. 8 cross pas-sages, shipping of excess mud, monitoring and survey. There are many cross-linked tasks between different parties and various types of work with complex work faces. If there is not a clear management organization, the various works will conflict or find blank between different parties, and some blind point of construction risk management will happen.

2.4 *Difference between parties of international cooperation*

Considering Shanghai Yangtze River Tunnel is a complex and difficult project in both technology and management, so several famous overseas companies were introduced to this project, e.g. Herrenchneckt from Germany, as supplier of TBMs; MS from France providing slurry treatment plants; Maunsell Consultants (Asia) Ltd from the USA, as the consultants for tunneling; and the main tunnels construction were conducted by Joint Venture which consists of Shanghai Tunnel Engineering Company (STEC) and international contractor Bouygues of France, to adopt advanced international experience of construction management and technology. There is a challenge to technical decision and construction management due to the cultural difference and different languages.

3 DYNAMIC RISK MANAGEMENT OF CONSTRUCTION

The risk management in construction is a dynamic process, and also the key stage to control the engineering risk effectively. The dynamic risk management which is a continuous cycle process includes 6 stages, namely risk definition, risk identification, risk assessment, risk evaluation, risk decision and risk tracing.

3.1 *Content of risk management*

The dynamic risk management of construction has the primary coverage as follows: making sure the flow of construction risk management; collating the heavy engineering risks, and raising risk protective measures according to risk accidents with larger risk index; giving birth to the overall risk index of engineering termly and make reports about risk dynamic evaluation; supervising the third part engineering inspection and deal with the inspective data by analysis, and calling construction organization to have a meeting for discussion when the data is abnormal; establishing the early warning mechanism of risk, and listing the symptomatic appearance before accidents happen, then giving the controlling measures when the symptomatic appearance has happened; drawing up the prediction of risk disposal when the accident has larger loss; recording and filing the risk incident which is not completed in engineering according to established input and plan; forecasting the risk of future time by calculative analysis and raise correlative measures and suggestions; making the education and training in risk management for every part of construction.

3.2 *Basic flow of risk management*

In order to understand and grasp the risk information, and carry the scheme or prediction of risk into execution in time to control risks availably, we should set up effective work flow in risk management. Figure 1 shows the following risk management flow in construction period.

3.3 *Risk level*

The risk in construction could be divided into five levels by probability and loss respectively, and the evaluation frame to analyze risks is established. They are listed in Table 1, Table 2 and Table 3.

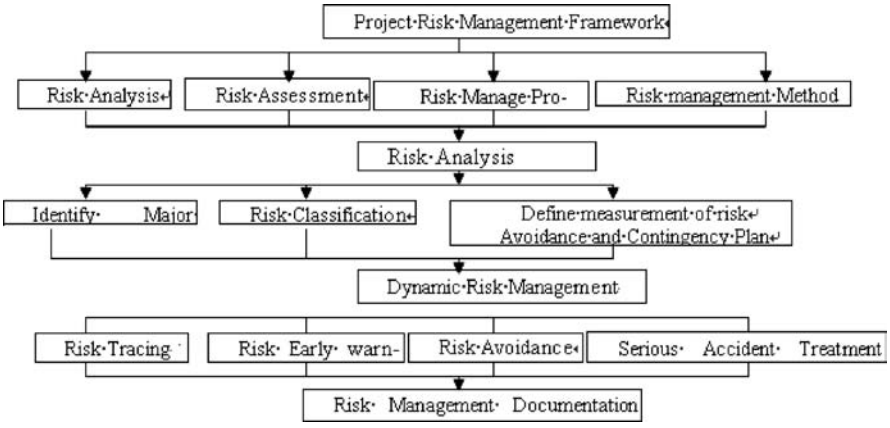

Figure 1. Basic flow of dynamic risk management.

Table 1. The probability of risk levels.

grade	First level (A)	Second level (B)	Third level (C)	Forth level (D)	Fifth level (E)
description accident probability	improbable $P < 0.01\%$	unlikely $0.01\% \leq P < 0.1\%$	Once in a while $0.1\% \leq P < 1\%$	possible $1\% \leq P < 10\%$	Almost certain $P \geq 10\%$

Table 2. Level standard of risk loss.

grade	First level (1)	Second level (2)	Third level (3)	Forth level (4)	Fifth level (5)
description	neglectful	tolerable	significant	intolerable	catastrophic

Table 3. Grade-evaluation standard of risk index.

Level	risk	rule	Countermeasure of control
First level	1A,2A,1B,1C	neglectful	No need to manage and survey
Second	3A,2B,3B,2C,1D,1E	admissible	Notice, general management and survey
Third	4A,5A,4B,3C,2D,2E	acceptable	Important, make protective and monitoring measures
Forth	5B,4C,5C,3D,4D,3E	unacceptable	make decision ,controlling and early warning measure
Fifth	5D,4E,5E	rejective	Stop, need change

4 DYNAMIC RISK MANAGEMENT OF SHIELD CONSTRUCTION

The sticking point of dynamic risk management is to manage risks with continuous circle tracing, and apply management tools and methods such as inspection, monitoring and arrangement to slow down risks and minimize the cost of risk management while making risk under control.

4.1 *Supervision of shield equipment*

For the reason that making shield equipments on the safe side could guarantee good quality of construction of long-distance shield tunnel in Yangtze River tunnel engineering. The clients introduce the professional troops to maintenance shield when supervising and examining the usage, maintenance and spare parts of shield. In order to supervise the user to operate according to shield operation handbook, we could make maintenance measure perfect on the basis of the maintenance plan and program, and prohibit the operator who has informal acts in time to reduce failure of equipments effectively brought from artificial factors. The primary coverage is as follows:

- Supervise and urge the user of shield equipments to set up equipment-maintenance troops, and maintain

the common failure in time to guarantee valid working hours of shield.

- Supervise and urge the user to construct equally, and make sure the equipments have 4 hours a day for maintenance according to requirement, and strengthen process examination at the same time.
- Participate in failure diagnosis, resolution and record, and estimate the reason and establish the resolution with construction organization by analysis at the same time when the failure occurs then recognize responsibility and summarize operations and maintenance of equipments termly on the basis of phenomena and resolution of failures. Establish the protective measures and schemes to avoid the similar status occurring repeatedly.
- Participate in management of spare parts, and then affirm on paper and record consumption of spare parts and replacement of oil plants. Collect, count and analyze the data of equipment failure termly (failure type, failure ratio, spare parts and consumption of oil plants etc.)
- Establish the report system of equipment management with day, week and month, and communicate in time to make clients control the status of equipment operation. Authorize the monthly report of shield equipments. The report involves equipment maintenance, failure status of every system, use condition of spare parts, serviceability ratio, failure ratio and use ratio of equipment, statistic of unattended time resulted by equipment failure and analysis and disposal of failure reasons etc.

4.2 *The third party monitoring and survey*

In the view of high risk of Yangtze River tunnel engineering, the construction organization introduces the third party monitoring and survey to check the surveying control network and underground transmitted traverse, examine monitoring scheme of construction and analyze the monitoring dada by parallel contrast for strengthening control of construction. The third party monitoring has the following primary coverage:

- Ground monitoring: ground vertical displacement, deep displacement and vertical displacement of Yangtze bund etc.
- Tunnel monitoring of uplink and downlink: vertical and horizontal displacement of tunnel, convergence of tunnel.
- The impact from cross-passage construction: settlement and displacement of tunnel and convergence.
- Displacement at the river.

4.3 *Follow-up management and supervisor stand-by*

The clients implement the attendant-management system, and arrange special engineers on duty for 24 hours to get the firsthand information in overall dynamic way, then find and settle problems in time.

The site supervisor management is one of the main measures to control site risk. In construction, arrange the supervisor stand by to supervise the process of construction in the key part of working procedure and important construction procedures, and record the details in the form of table which includes equipments, materials, personnel, construction acts, and also the incident content, time, part of working procedure, delay of time and result of disposal etc., then collect and analyze them to guarantee the hidden risk in site effectively under control.

4.4 *Information system of project management*

The Yangtze River tunnel engineering which has large dynamic data to collect and many participants has wide area of construction. In order to transfer the information effectively and quickly, the construction organization has built the large-integration management information system (MIS) of engineering project, realize the basic practicability functions such as share of information, auditing by exchange on web, issue and manage the document on web, integrated control of schedule investment, visual display of data and digital engineering, which provide comprehensive information-based service for construction. The system is composed of modules such as investment control, contract control, schedule management, quality control, safety control, management of public bidding invitation and stock, material management, equipment management, document management, design management, construction management and universal work. The system has played an important function in data collection and communication in the process of Yangtze construction.

4.5 *Long-distance monitoring and control of construction*

4.5.1 *Monitoring and control system of shield*

The Yangtze tunnel engineering adopts the PYXIS system to realize running of shield and data collection, display, analysis, store of construction parameters. Realize the running of shield equipments and long-distance inspection and control of construction vie inspection room on ground. PYXIS system includes direction system and data-collection system, and the mainly functions of direction system are as follows:

- Real-time display of the actual position and attitude of the shield
- Helping operators to select the position of the key segment
- Defining the appropriate object according to the controllability and correlative actual track of shield
- Displaying the track of advanced

- Real-time store of principal operation

The mainly functions of data-collection system are as follows:

- Real-time display of the running parameters of TBM
- Real-time display of advancing parameters of TBM
- Make statistical analysis of running parameters of TBM
- Real-time data logging.

4.5.2 *Monitoring and control system of construction and early warning and alarming system monitoring and control system of construction and early warning and alarming system*

The system collects the information such as monitoring data, the data of TBMs and engineering data, and uploads, gather, sort and analyze by manual input. Analyze the possible risks in construction and give them to correlative managers and builders in the form of report forms, graphs and information. The inspection and control system of construction and early warning and alarming system have the following subsystems:

- Data monitoring system
- Video monitoring system
- Inspection and control system of construction and early warning and alarming management system.

4.5.3 *Communication system in tunnel*

Prepare computerized telephones in tunnel to keep communication of information during construction. At the same time, introduce the mobile communications network to make sure communication for information in tunnel anytime and anywhere as a result of long-distance construction and various work faces.

4.6 *International consultancy*

In terms of international routine of large engineering, we appoint Maunsell consultants (Asia) Ltd. as the engineering consultant by international bidding, which provides services for Yangtze tunnel. The consultants content in construction is as follows:

- Review of construction plans and give proposal of risk management. Review the method statements of contractors and TBM supplier, and provide suggestions of risk management for total engineering status, in which the advancing scheme, safety of construction and cross-passage construction are very important.
- Provide consultation for technique problems in every stage in site and staged reports. The representatives of consultants Ltd. reside in the site, and put forward suggestions of problems for clients, then participate in the site meeting hold by clients. Submit the independent engineering management report to clients every month.

4.7 *Reviseing by experts*

It is always of clients' attention and consideration as to how to grasp and settle the technical problems in the world-class tunnel. Appoint authorized experts from home and abroad to constitute the technical experts group which takes charge in deciding magnitude technical schemes and it could guarantee schedule, quality and safety of engineering through the evaluation and argumentation of magnitude construction schemes. The main construction-organized design and technical statements which have passed through evaluation and argumentation are as follows: the Method Statement of Circle Tunnel Construction, the Method Statement of TBM Launching and the advance of the First 200 m, the Method Statement of TBM Boring under Yangtze River, the Plan of Temporary Power Supply for Tunnel Construction, the Method Statement of TBM Boring under the River Bund, the Plan of shipping of Excess Mud on the Sea, the Method Statement of TBM Assembly in the Shaft, the Method Statement of Predict Segment Lining.

4.8 *Emergency early-bird warning of risk*

Establish the system and flow of risk prevention and emergency on the basis of construction characteristics and difficulties. Supervise and urge the construction organization to improve management-organized institution of quality and safety, and also put all levels quality responsibility system and all items engineering management system into effect. According to characteristics and environment of tunnel, the system finds 12 magnitude dangerous resources in Yangtze River tunnel engineering shield construction, such as freeze and excavation of cross-passage, exchange tail brush, operate in pressure cabin, transport slurry by ship (work on water), water seepage in tunnel (rainstorm, tail brushes seepage), fire, supply and circulate of high voltage, TBM launching, face of excavation destabilized and poisonous and harmful gas exceeds standard in tunnel. Strengthen risk consciousness for every contract, and system could distinguish and analyze the dangerous resource and risk point of construction, then draw up the emergency prediction of magnitude risk resources which has strong direction and operability, such as freeze and excavation of cross-passage, exchange tail brush, operate in pressure cabin, face excavation destabilized and poisonous and harmful gas exceeding standard in tunnel. We could rehearse when the condition grows up. At the same time, the construction organization establishes the emergency prediction of medical treatment salvation (green passage) by corresponding with social correlative department to respond to emergency.

Table 4. Evaluation table of construction risk in tunnel advancing of Yangtze River.

Branch engineering	number	Risk accident	probability	loss	Risk grade
Break down of shield equipments	1	Slurry and water-provider system	C	3	Third level
	2	Erector machine	C	3	Third level
	3	Dynamical and advancing system	B	3	Second level
	4	Grouting and tail sealing	C	3	Third level
	5	other	B	3	Second level
Unfavorable geological condition	6	Trip hazards	B	4	Third level
	7	Sand flow	B	5	forth level
	8	hidden creek or soft layer	B	4	Third level
Construction management	9	Segment quality	C	3	Third level
	10	Segment transport lag	D	2	Third level
	11	slurry transport lag	B	2	Second level
	12	vehicle jam	C	2	Second level
Quality problem of construction	13	Broken segment	B	4	Third level
	14	Seepage in tunnel	C	2	Second level
	15	Big warp in axis control	B	4	Third level
	16	Progress and quality of road deck construction	C	2	Second level
Health and safety of workers	17	Heatstroke in high temperature	B	3	Second level
	18	Heavy things beating	B	4	Second level
	19	Body falling	B	4	Third level
	20	Food poisoning	B	4	Third level
	21	Air pollution	C	2	Second level
Safety electrics	22	Power cut	A	5	Third level
	23	Get an electric shock	B	4	Third level
Other accidents	24	Fire	A	5	Third level
	25	Explosion by combustible gas	A	5	Third level
	26	pollute environment by slurry	C	2	Second level

4.9 *Engineering management system*

According to different principle parts and stage of engineering, build and improve every item of management system which involves weekly regular meeting system of shield equipments harmonization, meeting system of monthly and quarterly schedule plan, weekly regular system of every contract, inspection system of monthly and quarterly construction with safety and system of integrated evaluation etc.

Formulate and issue in time every item of engineering management system, which includes management files such as 'Shanghai Yangtze Tunnel–Safety management Rule', 'Shanghai Yangtze Tunnel–Safe, healthy and environmental construction regulation', 'Shanghai Yangtze Tunnel–comprehensive evaluation administration', 'Shanghai Yangtze Tunnel–Flood prevention emergency provision', 'Shanghai Yangtze Tunnel–Electricity management regulation', 'Shanghai Yangtze Tunnel–accidents emergency provision'.

4.10 *Education and training*

Forge ahead with post safety of work procedure and technical operation code to standardize work action of operators and reduce the accidents resulted by mistakes. Draw up safety technical procedure of major posts such as shield advancing, segment building, segment transport, annular grouting, gantry alignment rectify etc. on basis of construction characteristics of Yangtze large-diameter tunnel, put the idea of safety construction into the first line operating personnel. Develop the training of safety technical operation code and work procedure technical operation standard of every post, and work after qualified, then reduce and control accident frequency.

5 EXAMPLE

Risk factors in construction of shield tunnel are changing constantly, and the following will take tunnel advancing as the example to dissertate that under the guidance of dynamic risk controlling method in site, utilizing the measure of dynamic management could control and prevent construction risk. It is shown in Figure 2 that the information of accidents and failures of Yangtze tunnel uplink in some 3 months of 2007 has been noted based on monthly site records submitted by supervisors and TBM supervisors.

By combining the information of accidents and failures for 3 months in uplink, and making analysis of previous accident cases and concluding experience of experts, we have got the possible risk accidents in construction of Yangtze River tunnel uplink.

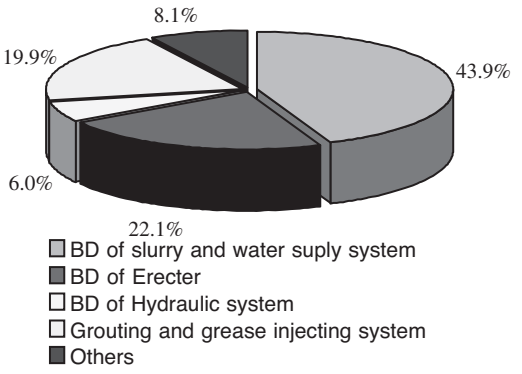

Figure 2. Statistic of failure time of various equipments in uplink.

It is shown in Figure 2 that the failure of each system of shield equipments has higher risk which has larger probability of happening, and should be paid more attention to in later construction. Utilize measures of dynamic management in later construction to supervise strongly advancing system, erector system, headstock sealing and sealing system in tail while improving some system to reduce obvious failures.

6 CONCLUSIONS

The construction risk of shield tunnel is unpredictable and paroxysmal, and it ought to build the dynamic risk management system and the risk management organized-frame including clients, construction organization, supervisors, designer, the third party monitoring and consultants in preparatory phase of construction, then define the responsibility of participants, and build perfect working system and flow, and establish the system and flow of risk prevention and emergency to guarantee construction safety and quality. Utilize modern analysis of construction and dynamic prediction and forecast method around construction, then apply theory and measures of dynamic management to realize dynamic management of risk and supervise and instruct the construction to reduce and control risk in construction. At present, the schedule, quality and safety etc. in Yangtze River tunnel are all under control, and everything progresses smoothly.

REFERENCES

Dai, X.J., Liu, Q.W & Huang, H.W. Dynamic risk analysis and control on the construction of Shanghai Yangtze River Tunnel. *Underground Construction and Risk Prevention Technology-2007 Third Shanghai International Tunnel Construction Seminar*. Shanghai: Tongji University Press.

Ding, S.Z. 2006. Engineering Project Management. *China Architecture & Building Press* (First Edition).

Hi-Tech Research and Development Program of China in 2006 (863 Program). Program code: 2006AA11Z118. *Special subject3.2: Research on the alerting system and control-ling model of the dynamic risk on the construction of long, large tunnel.*

Huang, H.W. & Liu, G.B. 2006. *Research on Monitoring & Alerting System and Risk Management System of Tunnel Construction*.

Shanghai Juyee Company, Tongji University. 2006. *Research Report on Information Management System in Very Large Projects.*

The Shanghai Yangtze River Tunnel - Theory, Design and Construction – Huang (ed)
© 2008 Taylor & Francis Group, London, ISBN 978-0-415-47161-9

Prefabrication supervision of major tunnel lining with high precision

H.Y. Gong & X.N. Qiu
Shanghai Municipal Engineering Management & Consultancy Co., Ltd., Shanghai, P. R. China

ABSTRACT: Based on the experience obtained from supervision of the Shanghai Yangtze Tunnel project, this paper addresses technical issues for large diameter segment ring with high precision requirements, regarding the steel formwork acceptance, concrete mix design, reinforcement cage, prefabricated segment measurement, mass concrete cracks control and segment repair solution.

1 INTRODUCTION

TBM is used for the circular tunnel construction of Shanghai Yangtze River Tunnel. The tunnel lining is reinforced concrete structure with high precision. The diameter of segment ring is up to 15 m, and the thickness is 650 mm. The standard width of segment is 2,000 mm. Each ring includes 10 segments. The segment is designed with tapered rings with a taper of 1/750.

Segment is reinforced using welded cages. The main rebar is not allowed to be welded. Segment concrete is C60 and P12. The durability parameter is the diffusion coefficient of Cl^-, which is $\leq 1.2 \times 10$–$12\ m^2/s$. The content of Cl^- is $\leq 0.06\%$ and alkali $\leq 3\ kg/m^3$.

The project has following characteristics:

- The ratio of thickness to diameter of the lining is greater than normal designing value of 1/20. Although it can reduce construction costs and lower the requirement to construction equipment, it will have higher requirement to the control of segment quality. During construction, each parameter must meet design requirement. The supervisor bears heavy responsibility of quality control.
- The tunnel is under Yangtze River and its diameter is the largest with TBM construction. Therefore the reinforcement is dense. To achieve a taper of 1/750 for normal segments, the reinforcement type is complex. So reinforcement cage should be placed very careful during construction. Client has made strict selection of reinforcement supplier to ensure a good quality of raw material. However, due to the un-uniformity of reinforcement on site, site supervisor should still pay special attention on the quality control.
- The diameter of segment ring is up to 15 m. However, according to the design the allowable tolerance is very small, which is ± 0.4 mm for a segment of 2,000 mm wide. It is very difficult to carry out the prefabrication and erected ring inspection.
- Yangtze Tunnel is the longest TBM tunnel in the worldwide. To accommodate with the high requirement, the segment needs to bear thousands tons of thrust. The width precision of segment is the basis to ensure safety and no damage under such a large force. During prefabrication, the width of each segment must be made identical.

More than 60% of segments have been prefabricated smoothly under the management of CCD. The following experiences have been gained from this project.

2 PREMISE OF SEGMENT QUALITY ASSURANCE – STEEL FORMWORK CHECK AND CONTROL

Steel formwork for segment is the premise to ensure the segment profile dimension, which is supplied by contractor with extensive experiences. However, the appraisement of steel form is still a very critical part of supervision work.

Under the guidance of CCD, supervision party has been involved in the preparation of steel formwork appraisement standard. Its dimensional precision requirement is higher than that of segments the allowable tolerance of with is ± 0.3 mm. In addition, the opening of steel form should be flexible, convenient, and durable. The design parameter requires the life time is at least 1,000 cycles.

The supervision party has accepted the steel formwork to ensure the fabrication quality.

2.1 *Check of openings in the steel formwork*

There are pre-set holes and openings on the steel formwork with a precision less than 1 mm. The inspection must be done before the installation of accessories. The supervision personnel go the fabrication site many times to check the products using special sample plates machined with computer-controlled tools, caliper, micrometer, depth micrometer. They measured the span of whole centers of each skin plate and inner part dimension. Based on the dimension on design drawings, for check, they convert between measured data and dimensions in the design for side and end plate angles.

2.2 *Check of steel formwork*

After the steel formwork is transported to the segment prefabrication site, the client, designer, supervision party and contractor will have a meeting for evaluation. Supervision check each item according to appraisement standard, especially the inner part dimension change after opening and closing of steel formwork for many times. Usually, the measured data deviation should not exceed 0.1 mm, which shows the precision of steel formwork is stable and reliable. For bolts and pre-set mandril, the closeness and rotation flexibility should be checked. For the marking signs in the steel form for each parameter, a steel ruler is used to measure one by one according to the design drawings. At the appraisement meeting, the steel formwork supplier provides the quality certification. Supervision reported the spot checking results and some samples were measured during the meeting. After the meeting, the above contents were recorded by memo as the completion appraisement for steel formwork, but not the final appraisement.

2.3 *Trial segment appraisement*

The final appraisement of steel formwork is done after horizontal assembly of ring segments prefabricated with the steel formwork. The steel formwork after completion appraisement will be used for trail prefabrication of 1–2 ring segments. After the concrete strength is 100% of design strength, the horizontal assembly of the whole ring is completed (if possible, 3 rings should be assembled preferably). After horizontally assembled, the inspection aspects cover the circumferential joint, the longitudinal joint, the inner and outer radius/diameter and the bolts.

The inspection standard of horizontal assembly is shown in Table 1.

Final appraisement (horizontal assembly acceptance) is conducted first by the segment contractor, then re-checked by the supervision party and at last by the four-party meeting. During the meeting, measurements were carried out to ensure the open and fairness of appraisement. The precision and parameter of all steel formworks meet the requirement of segment prefabrication, which provides reliable basis for the segment prefabrication with a high precision.

Table 1. Inspection standard of horizontal assembly.

Appraisement standard for horizontal assembly of segments			
No.	Item	Test requirment	Allowable tolerance (mm)
1	Gap of circumferential ring	test 3 points at each ring	≤ 0.8
2	Gap of longitudinal ring	test 3 points at each joint	≤ 2.0
3	Built ring internal diameter	test 4 strips without backing	± 2
4	Built ring external diameter	test 4 strips without backing	$+3 \sim 0$
5	Bolt hole	all bolts go though	gap≤ 1

3 HIGH PERFORMANCE CONCRETE MIX DESIGN VERIFICATION AND ADJUSTMENT

In this project, the concrete of C60 and P12 are used for segments, which are the highest models in China. Usually, C55 and P10 are used for tunnel segments. Furthermore, based on the 100 years service experience, the designer proposed the durability parameter among which the diffusion coefficient of Cl^- is $1.2 \times 10^{-12} m^2/s$. According to the presentation of foreign experts, this is very strict requirement. In Europe, the parameter of the concrete for bridges is usually $2–3 \times 10^{-2}$. According to the specification of tendering document, the segment concrete mix is designed by the contractor.

Beside the above requirements, the requirement of early strength is also set for concrete that under the temperature of 20°C, the 1-day concrete strength must reach 40% of its full strength.

Due to the tight project schedule and long test period of Cl^-, the client requires the supervision party to carry out parallel tests of concrete mix design provided by the contractor. Therefore, the supervision party conducted more than 10 times of parallel tests about different concrete mix design. The samples were taken from the field, such as fly ash, then treated to meet with road test qualification, and finally tested by entrusted parties. In the whole process, the supervision did detailed records and made comparative analysis of the test results with those from the contractor. This yields reports of independent analysis results and the reports are submitted to client for determining the final concrete mix design.

Analysis is shown in Table 2.

Table 2. Summary of parallel test results of concrete mixing design.

	Solution 1	Solution 2	Solution 3	Solution 4	Solution 5	Solution 6	Solution 7	Solution 8	Solution 9	Solution 10
1d-compression strength 1 (MPa)	15.6	15.6	15.1	15.6	28.6	29.2	29.2	30.6	31.8	31.1
1d-compression strength 2 (MPa)	16.5	20.2	21.1	19.3						
1d-compression strength 3 (MPa)	10.5	16.5	10.4	11.8	24.5	28.5	27.3	26.4		
7d-compression strength 1 (MPa)	55.0	51.0	53.5	51.0						
7d-compression strength 2 (MPa)	54.9	52.0	55.7	53.6						
7d-compression strength 3 (MPa)	48.7	54.9	52.4	42.2						
14d-compression strength 1 (MPa)	63.8	61	60.7	61.0						
14d-compression strength 2 (MPa)	63.5	65.6	66.8	65.8						
14d-compression strength 3 (MPa)	57.2	63.5	62.0	53.8						
28d-compression strength 1 (MPa)	71.5	67.7	70.2	67.7	71.3	71.3	72.8	73.4	72.9	73.6
28d-compression strength 2 (MPa)	71.7	70.8	73.2	72.2						
28d-compression strength 3 (MPa)	61.6	67.7	66.7	67.7						
Slump1 (mm)	15	20	15	20	25	25	20	20	20	20
Slump2 (mm)	20	20	20	20						
Slump3 (mm)	30	30	20	20	180	80	170	70		
Setting time initial setting	08:40	09:00	09:00	09:00	08:25	06:55	07:05	07:15		
Setting time final setting	11:10	11:10	11:10	11:45	10:25	09:30	09:40	09:25		
Penetration resistance	qualified	qualified	qualified	qualified	qualified	qualified	qualified	qualified	qualified	qualified
Chloride content	0.007%	0.005%	0.005%	0.005%	0.006%	0.007%	0.005%	0.006%		
Alkali content (kg/m^3)	1.48	1.52	1.55	1.58	1.35	1.33	1.37	1.36		
28d-concrete electricity flux	531 C	605 C	541 C	571 C	568 C	644 C	959 C	618 C		635 C
60d-concrete electricity flux					548 C	602 C	763 C	486 C		
28d-Cl^- diffusion (m^2/s)	1.07×10^{-12}	1.12×10^{-12}								
60d-Cl^- diffusion (m^2/s)	0.86×10^{-12}	0.82×10^{-12}			1.15×10^{-12}	0.98×10^{-12}	0.86×10^{-12}	0.93×10^{-12}		

* Note: slump in several items are high due to the heavy rain, so it does not influence other parameters.

After parallel verification, four mixing design plans are approved finally. They will be used according to different seasons and temperatures to meet with segment prefabrication needs.

In Shanghai, the seasonal temperature change is large. Although the segment prefabrication uses factory production and the concrete casting and vibration is indoor, the temperature change still affects some segment prefabrication parameters, such as bleeding time, early strength, shrinkage cracks. How to adjust the mix design is critical for ensuring and improve the segment quality.

In the project, supervision personnel monitor closely during segment concrete casting and vibration. They carry out careful daily check of the appearance of segments after formwork is removed to collect data about bleeding time, lifting strength variation and trend. In this way the supervision personnel can learn the influence of temperature on segment prefabrication timely and suggest the contractor to adjust the concrete mix according temperature changes. As a result the segment concrete progress ran smoothly and the quality and appearance of segments are ensured.

4 QUALITY CONTROL OF REINFORCEMENT CAGE FABRICATION AND CONCRETE COVER

In the project, the reinforcement rebar is formed and welded on a template jig to form a reinforcement cage. On the jig, there are openings for fixing reinforcement rebar in position. The outer dimension of the cage and the spacing between reinforcement rebar is controlled by jigs. Supervision personnel check the jig carefully according to design drawings and the dimension of each opening for main rebar. During prefabrication, due to frequent use, some openings will wear out to different extent. Therefore it is required to check regularly and repair some jigs if necessary.

During actual production, the supervision should inspect and supervise aspects from welding, sequences, quality to qualification of staff to ensure the manufacture quality of reinforcement cages.

The cover for reinforcement cage is made with mortar spacer of high strength (above C30). In the steel formwork, 6 support points (each point composed of two spacers) sustain the 1,000 kg reinforcement cage. No failure has happened. The spacer height is defined according to the design cover thickness. The spacer has a concave shape for the upper and lower surfaces to ensure the fixing of main reinforcement rebar on the spacer. The supervision personnel check the concrete cover by measuring the dimension of each spacer batch and checking the spacer location after reinforcement cage placed in formwork.

After reinforcement cage is placed in formwork, there is also problem of front/back, and left/right cover control. Supervisor requires the contractor to use wedge made of engineering plastics to fix the cage location to control the concrete cover. For the right and left side, mandril and bolts are used for fixation. Supervisor will stand by and inspect the process to control the cover thickness.

5 PREFABRICATED SEGMENT MEASUREMENT AND ANALYSIS FEED-BACK

Prefabricated segment measurement refers to the profile dimension measurement of segments after prefabrication. Although this is after control, its results play a key role in final quality evaluations of segment and subsequent segment prefabrication. Therefore in this project the supervision party paid special attention to the measurement.

In this project the precision requirement for the outer dimension of segments is extremely high. Take width as example, the allowable deviation for a width of 2,000 mm is only ± 0.4 mm. For such a precision, it is critical is to use steel formwork with high precision. However, whether the prefabricated segment meets such a standard is up to the measurement of segment.

Regular tools do not have such a high precision. Therefore, the contractor and the supervision party made special order of large vemier calipers with a range of 2,000 m and precision of 0.02 mm.

During the process, the supervision company performed independently check randomly on 20% of segments daily. Analysis is done on the measured results. Feedback on the steel formwork precision helps on guiding the contractor to increase the self-inspection frequency of steel formwork with abnormal deviation. It also aids to investigate the causes to ensure the precision of steel formwork. In the measurement, the supervisor found that the influence from temperature on measurement can not be omitted for the large segment width and the high precision. However this is typically not considered.

According to material manual, the linear expansion coefficient of concrete is 1.2×10^{-7} for the segment with a width of 2 m. When temperature varies for 1°C, the width will change by 0.03 mm. If the temperature difference is above 10°C, the variation of the width will be around 0.30–0.40 mm.

The supervision company learned that the temperature for measurement tool calibration is 20°C. However, the tools are made of alloy and its linear coefficient is difficult to find out. If the difference with concrete is little, then the measurement tolerance due to temperature can be ignored. But in reality the tolerance is not very small.

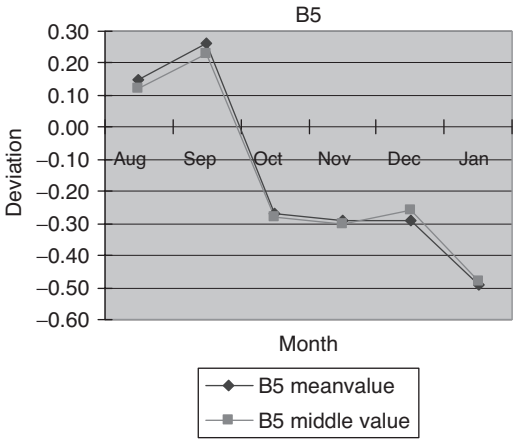

Figure 1. Measured segment width deviation in different months.

The supervisor used VMT laser automatic measurement device, which can automatically adjust temperature difference with a high accuracy. It is used to calibrate two venier calipers at 32°C. The calibratoin shows that the measurement for 2,000 mm block with this calliper is 1,999.52 mm, and VMT is 1,999.944 mm. Obviously, the caliper measurement increases by 0.42 mm at 32°C, which indicates the linear expansion coefficients of calliper and concrete are different. Under precise measurement condition, the deviation due to temperature must be considered appropriately. In fact, if the segment width deviation can be controlled within the allowable tolerance, then during tunnel construction it will not induce significant un-uniform thrust forces. However, because the temperature difference for segment prefabrication and measurement is not small, so the measurement deviation due to temperature will influence our evaluation of segment width.

Measured segment width deviation in different months is shown in Figure 1.

Finally, we obtained the dependence of temperature on high precision measurement. In the process of measurement, the measurement of segment width needs correction in the extreme temperature scope.

6 MASS CONCRETE SURFACE CRACKS CONTROL

In this project, the segment diameter is large. For these 10 segments, concrete volume for each segment is 5–6 m^3. However inner reinforcement is dense, especially at the corner. Surface crack is a common problem. Considering that segments will be buried in soil for many years, large surface cracks will affect the service life of segments. Therefore, controlling the surface crack is a critical issue in quality control of the supervision.

The main reasons for the concrete surface cracks are investigated by the supervision company and are under controlled.

6.1 *Concrete slump*

The slump of the designed concrete is typically 3 cm ± 1 cm. During the construction, the upper limit is taken as about 4 cm considering the effect of temperature changes. However, because water content ratio varies in raw materials, the control of slump is not easy. The supervision party takes the following measures to control slump. First, he keeps frequent contacts with the mixing plant. Secondly, the site quality inspection staff keeps first mixing inspection regulation. Furthermore, for segment prefabrication, the slump of material should be kept the same as much as possible in the same steel formwork.

6.2 *Bleeding procedure*

Bleeding quality has a large influence on the concrete surface cracks. Bleeding timing should be defined according to the temperature and other conditions of concrete. Bleeding should be done for three times. Once cracks are observed after the formwork removal, the contractor and the supervision party organize bleeding operation staff to have site meetings to investigate the reasons and improve the operation. After many times of discussion, cracks are eliminated.

6.3 *Timely curing*

The hydration starts when concrete is casted in the formwork, so water in concrete reduces fast from segment curing to formwork removal. After formwork removal, the evaporation of water is also one of the reasons for cracks. The supervision requires contractor to carry out curing timely after formwork removal, especially when temperature is high. Water spraying should be used for curing before the segment is placed in water ponds.

6.4 *Control temperature reducing*

The difference between lower ambient temperature and high temperature generated by hydration heat is one of the reasons of shrinkage cracks. In a season with low temperatures, the supervision requires contractor to close the workshop to keep the temperature from dropping. Geo-textile cloth is used to cover the segment to maintain a constant temperature. Therefore the shrinkage cracks due to temperature difference are reduced.

6.5 *Concrete mix design adjustment with temperature variation*

Adjusting concrete mix design timely according to the season (temperature) variation is one of the main measures to reduce cracks. Especially in summer with high temperatures, the fly ash content is increased in mixing concrete which reduces hydration heat generated in the early stage of concrete curing. Consequently the concrete surface cracks are reduced significantly.

The reasons for cracks are various. The supervisor made the control by the means of above aspects which are effective during actual segment prefabrication.

7 SEGMENT REPAIR SOLUTION REVIEW AND EXECUTION SUPERVISION

Although the procedures are strictly controlled, the concrete segments with a weight of 10–20 tons still have appearance defects during prefabrication, lifting and transportation. The typical defects are corner and edge falling. Therefore, the review of segment repair solution is also part work of the supervision company.

The segment repair solution was prepared and reviewed from the beginning of segment prefabrication. In the following several months, the solution was modified and improved. The contractor is also supervised during execution.

The main consideration of the segment repair includes: a) definition of repair areas, b) repair materials, and c) repair methods. Refer to the related information and based on the actual condition of segment prefabrication, the repair area is divided into three regions: crack zone, zone of normal blowhole and fallen edge & corners, and large damage zone.

(1) In crack zone, the cracks observed are divided into three types: 1 for width $\leq$0.1 mm, the cracks are repaired by the contractor, and the supervisor will not carry out inspection; for width of 0.1–0.2 mm, the supervisor will inspect the repair work done by contractor; for width above 0.2 mm, the supervisor will organize both the client and the designer to the site for evaluation and then provides the treatment according to evaluation comments. During the actual construction, the third type of crack has not been experienced. The 2nd type of crack is also very few. This shows that the crack control measures in this project are effective.

(2) For zone of normal fallen corner and wedge, special repair material is used, which is a cement base penetration crystal water proofing material suggested by the contractor. It is also required that when large damage occurs, the repairing material should be painted on the interface at the damage area before repair.

For blowhole repair, the main task is to control the repair time to avoid the color difference. The earlier the repair is taken, the better effect will be received.

(3) For the zone of large damages, it is proposed to use wooden formwork in the solution statement. During actual construction, it was not used. The most often repair is for the edge and corner damage. The supervision party realized that concrete structure is a stiff material. Some defects will still exist even after repair. But, it can be used as an improvement method which is also essential. The supervision company must focus on the prevention of damages. For the repair, the supervisor should supervise the contractor to execute the repair solution and take careful inspection for specified repairs.

8 CONCLUSION

With the collaboration and efforts of all involved parties, the supervision company has taken the responsibility in the manufacture of the large diameter reinforced concrete segment with high precisions. These experience and information shared in the paper is the gathering of knowledge and efforts of all involved parties.

In conclusion, there are the main aspects we learned:

- The supervision company should control the critical aspects of segment quality, i.e. steel formwork appraisement and suitability of segment concrete mixing design.
- The supervision company should perform the segment quality control by appropriate tools and methods.
- The supervision should treat common defects seriously and overcome them.

At present, two thirds of segment prefabrication has been finished. All the segment quality is evaluated as good. During inspection by Ministry of Communication and other provincial governments, high evaluation has been given. The segment quality meets the parameter requirements proposed by designer.

REFERENCES

Ding, W.Q., Yue, Z.Q., Tham, L.G., et al. 2004. Analysis of shield tunnel. *International Journal for Numerical and Analytical Methods in Geomechanics* 28:57–91.

Li, D.X. 1994. The method and application of GPR. *Geology Publishing Company*.

Koyama, Y. 2003. Present status and technology of shield tunneling method in Japan. *Tunnelling and Underground Space Technology* 18:145–159.

The Shanghai Yangtze River Tunnel - Theory, Design and Construction – Huang (ed)
© 2008 Taylor & Francis Group, London, ISBN 978-0-415-47161-9

Research on vibration monitoring and fault diagnosis for principal bearing in shield machine

D.S. Huang & X.Y. Chen
College of Mechanical Engineering, Shanghai University, Shanghai, P. R. China

G.J. Zhang & L.Teng
Shanghai Tunnel Engineering Co., Ltd., Shanghai, P. R. China

ABSTRACT: In this paper, the vibration condition monitoring and fault diagnosis for principal bearing were studied in particular structure of a shield machine. The discussion content will focus on the foundation of on-line monitoring on the equipment with over large size and low speed, such as distributed multi-point vibration detecting, adaptive enhance processing technology, signal processing and fault recognition, and smart fault diagnosis and prediction. Based on these discussions, the key technologies are put forward in principle for vibration monitoring and fault diagnosis. Due to the working condition directly related to the safety for shield machine running, the research on continuous condition monitoring and early fault diagnosis is greatly significant in tunneling engineering.

1 INTRODUCTION

A shield machine works under the condition of extreme strength and heavy load, and its principal bearing is one with over large diameter of 7 meters and low speed and supports a huge cutting force. In the view of badly environment, the condition of principal bearing gradually tends to fault stage from normal in the tunnelling procedure, and finally it turns to failure. The principal bearing is a key part in the shield machine, if the heavy fault and failure appear in the principal bearing, it will be fatal for the machine to run in a normal state and could delay the engineering schedule. For special tunnelling cross a wide river or ocean, like a tunnel cross Yangtze River, if the machine fails due to fault from principal bearing, then the tunnelling engineering has to stop for maintenance and the tunnelling schedule is delayed, it will result in a huge loss in economy. With the help of automatic monitoring technology, it will be possible to diagnose and predict fault in the principal bearing, and it will be of a great benefit in the tunnel schedule and reduction of engineering cost.

In recent years, some manufacture companies produce tunnel machine, such as Framatome in France and Misubishi in Japan, research on the area of monitoring and fault diagnosis system for a shield machine. In order to meet the need of tunnelling engineering, the computer aided diagnosis has been developed to an integration system of internet, automation and information management. The main research result on diagnosis content is summarized in three terms: Fault diagnosis method for a shield machine with over large size; a computer aided diagnosis mode for a shield machine with over large size; displaying fault diagnosis in a center control unit on land.

The fault diagnosis technology for principal bearing in a shield machine possesses some special requirements, and it is different for regular size machine in the view of working condition of complicated condition compared with over large size machine. The objective of research will focus on setting up corresponding technology of online monitoring and fault diagnosis which includes the feature of vibration signal picked up from a principal bearing in a shield machine, the measurement system based on distributed multi-signal detecting, adaptive enhance processing technology for extracting early and weak fault characteristic signal, analyzing wavelet signal processing and fault recognition, and fault diagnosis with Fuzzy logic. These technologies will be a basis of developing in the monitoring and fault diagnosis system in new generation of shield machine in the near future.

2 BEARING FAULT MONITORING FEATURE

Besides the form of normal wear, the fault types of principal bearing consists roller and raceway peeling,

concave, cracking and entering of sand and mud. Currently the fault detecting of rolling element bearing depends on the impact vibration caused by peeling, spot corrosion, etc. The fault is recognized and diagnosed by analysis of the envelope signals with respect to the characteristic frequency of bearing based on the principle of resonance demodulation. But for the monitoring of bearing in a shield ma-chine, and the effectiveness of this method is limited because of particular characters of monitoring of principal bearing in the shield machine. The particular characters are as follows:

- Because of the low speed in a principal bearing, the fault characteristic frequency of bearing is less than 1 Hz, it is impossible to recognize and diagnose the principal bearing fault through spectrum analysis on an envelope of impact resonance response.
- Due to transmitting in a long distance, signal decays naturally. The energy level of impact resonance response is too low to be detected. The vibration signal with fault characteristic is local, and the fault detection could be missed.
- Before separating the impact resonance response from the vibration, the corresponding center frequency needs to be determined by special estimation to adjust frequency range in a pass band filter. The frequency range can easily be computerized by FEM, and the resonance frequency of the bearing structure is about 2.5 k.
- Detection of fault in a principal bearing in shield machine by resonance demodulation principle is carried out under the condition of high-strength and complex vibration. The impact resonance response signal caused by early fault in a principal bearing is immersed in the strong vibration environment.

In order to detect and diagnose the principal bearing fault effectively, the traditional principle of resonance demodulation needs to be modified by improving signal detecting and signal processing. This paper is focus on the vibration online monitoring and diagnosis for a principal bearing in the shield machine.

3 DISTRIBUTED MULTI-POINT DETECTION

As mentioned above, the fault monitoring on the principal bearing is of some particular characters, therefore, the distributed multi-point detection is selected in online monitoring by regular detection method.

In term of the particular characters, an acceleration sensor is chosen to monitor vibration, which is sensitive to detect the weak impact resonance response by comparison with a vibration velocity sensor. The sensor selected should be of high sensitivity. Moreover, it is directly integrated with charge amplifier, thus the obtained signal can't be interfered by wire capacitance,

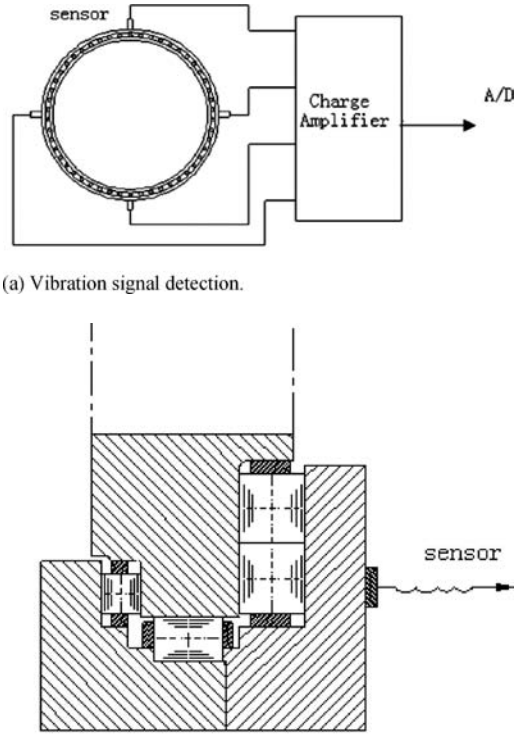

(a) Vibration signal detection.

(b) Locations of sensors.

Figure 1. Vibration detecting system of principal bearing.

and it is also convenient to mount it on the machine. In addition, the high-pass filter needs to be set in the signal detecting system to avoid aliasing effect from sampling in data acquisition.

Since the fault signal has local character, the distributed detection with multi-point sensors is employed to overcome the detection missing caused by single sensor only. The sensors are installed on the upper and lower part and around the principal bearing. The locations are determined for sensor mounting based on the machine structure, and they should be close to the principal bearing as possible as we can.

The system of detecting vibration is shown in Figure 1, where the vibration acceleration signals picked up by the sensors are sent to the computer to be processed. The sampling frequency is 10 k for data acquisition, and the sample length should be about three times longer than bearing revolution.

4 ADAPTIVE LINE ENHANCE TECHNOLOGY

With an adaptive line enhance technology for a distributed multi-point detection, the detecting signal

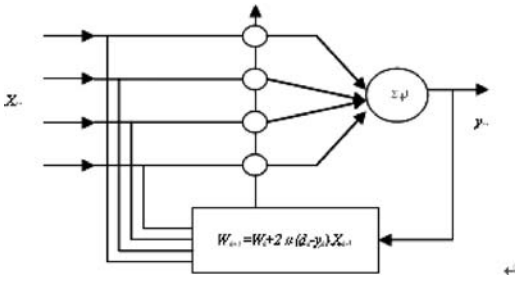

Figure 2. Sketch of adaptive filter matrix.

picked up from the machine can be enlarged, at the same time, the random noise mixed in the signal can be cancelled. Then the impact resonance excited by early fault in principal bearing can be enhanced under noise environment. Figure 2 shows a sketch of adaptive processing matrix, where X_k is an input signal from a charge amplifier, Y_k is an output signal with determinate signal and impact resonance response, and W_k is a right vector of adaptive filter. The output of the adaptive filter system is the sum of multiplication of two vectors.

$$y_k = W_k^T X_k \tag{1}$$

where, LMS algorithm of the right vector is as follow:

$$W_{k+1} = W_k + 2\mu d_k X_k - 2\mu y_k X_k \tag{2}$$

$$\text{Where,} \quad d_k = x_{0k} - y_k \tag{3}$$

And μ is an adaptive gain constant.

The subsystem of adaptive line enhancer can be realized by programming.

5 SIGNAL PROCESSING AND ENVELOPE EXTRACTION

Several determinate signals mix together after adaptive enhance filtering, thus fault recognition could not be directly carried out in this way. By the use of a combination analyzing wavelet with band pass filter, the impact resonance response with orthogonal property is extracted from the vibration signal, and it is used as the fault characteristic signal. The equation of combination analyzing wavelet h(t) is expressed as:

$$h(t) = \sum_{i=1}^{n} \exp(-\frac{1}{2}a^2 t^2 + j2\pi f_i t) \tag{4}$$

The waveform of mother function of combination analyzing wavelet is shown in Figure 3.

Due to the impact resonance frequency caused by bearing fault is around 2.5 kHz, the frequency range is set to 2 k–3 k in the combination analyzing wavelet.

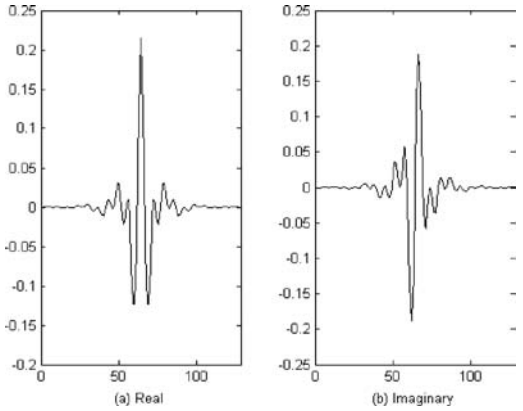

Figure 3. Mother function of combination analyzing wavelet.

The impact resonance response is obtained through wavelet filtering operation on vibration signal, thus the fault feature in the bearing can intuitively be observed. However, the strength of fault is related to the magnitude of impact response. In order to describe the strength of fault, the envelope information needs to be obtained from the impact resonance response signal. The envelope signal z(t) is defined as a module of convoluting signal y(t) and the analyzing wavelet h(t), and the mathematical expression is written as:

$$z(t) = |y(t) * h(t)| \tag{5}$$

6 SMART FAULT DIAGNOSIS FOR BEARING

By recording the original vibration signal, an impact resonance response and an envelope signal, the online continuously monitoring can be realized on vibration of principal bearing in a whole time history. To assess the strength of fault characteristic with the envelope of impact response, the smart diagnosis fault method is described as followings.

With the statistic parameters on the envelope signal, the strength and energy of fault characteristic are accurately described, here the kurtosis β is used to describe the strength of impact resonance response, and the mean square value E is introduced to express the energy of impact resonance response. Set up a diagnosis rulebase by Fuzzy logic used for principal bearing, as shown in Table 1, where the input membership function are defined for the kurtosis β and the mean square value E as shown in Figure 4a–b, and linguistic terms are the smallest, smaller, medium and large expressed as S, SM, M and L. The output membership

Table 1. Fuzzy logical rulebase.

	β			
E	S	SM	M	L
S	B	B	G	Y
SM	G	G	Y	Y
M	Y	Y	R	R
L	R	R	R	R

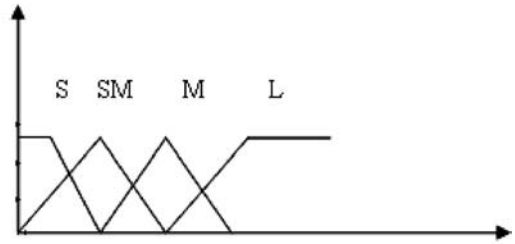

(a) Input membership function: kurtosis.
where S-Smallest; SM-Smaller; M-Medium; L-Large.

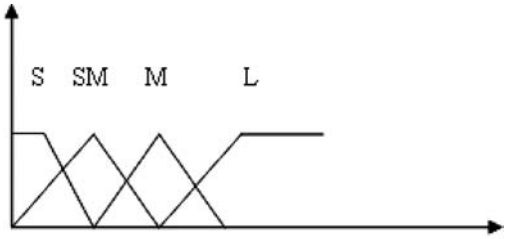

(b) Input membership function: mean square value.
where S-Smallest; SM-Smaller; M-Medium; L-Large.

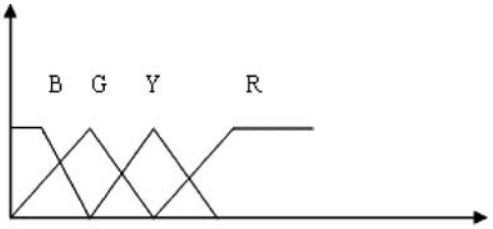

(c) Output membership function: degree of fault.
where B-Normal; G-Early Fault; Y-Fault Warn;R-Fault Alarm.

Figure 4. Sketch of membership functions.

function is the degree of fault characteristic for principal bearing as shown in Figure 4c. The relationship between input and output are represented by Fuzzy logic rulebase. Based on the membership function and Fuzzy logic rulebase, the look-up logic table is computerized by the use of Fuzzy programming language tool, and automatic diagnosis technology can be realized by applying software. In the monitoring on the principal bearing in the shield machine, the smart diagnosis result is divided as four stages which are normal, early fault, fault warn and fault alarm. The corresponding degree of fault characteristic is respectively displayed in the form of color blue, green, yellow and red, which is easily to recognized and accepted for engineers in online monitoring.

- Give out the strength of fault condition based on multiple statistic parameters, and the assessment is close to objectivity.
- Automatic monitoring and diagnosis are realized by software in the view of Fuzzy logic rulebase;
- The diagnosis method will be more robust by adding the factor of temperature detection on principal bearing as the input membership function.

7 CONCLUSIONS

By employing distributed multi-point detection, the adaptive enhance matrix and analyzing wavelet, the impact resonance response is obtained from the vibration of principal bearing, it avoids missing detection caused by single sensor only, at the same time the rate of signal and noise is enlarged. To assess the strength of fault characteristic with the envelope of impact response, the smart diagnosis technology is introduced in monitoring principal bearing in shield machine by setting up the Fuzzy logic diagnosis rulebase, where a parameter kurtosis β and a mean square value E are the input membership function, and the degree of fault characteristic for principal bearing is output membership function. The smart diagnosis can be realized in online monitoring by the use of Fuzzy programming language tool.

Based on the above discussion, the key technology in online monitoring is given out in principle and experiment by researching on the measurement system, signal processing and smart diagnosis technology. Therefore, the technology will supply new support for expanding the working period for the principal bearing, and will supply the foundation for developing new online continuously monitoring technology and the smart fault diagnosis system for principal bearing in new generation of shield machine.

ACKNOWLEDGMENTS

The authors would like to be grateful to the support of the National Hi-Tech Research and Development Program of China (No.2006AA11Z118).

REFERENCES

Akiyoshi, C., Hiroshi, Y. & Kazuhiko, S. 2000. Monitoring system using acoustic diagnosis technique in shield tunneling operation. *Proceedings of JSCE*: 137–146.

Huang, D.S. 1996. A wavelet-based algorithm for the filbert transform. *Mechanical System and Signal Processing* 10(2): 125–134.

Osterhout, V. 2003. Recent dutch experiences in developing structural monitoring systems for shield driven tunnels. *TUNNELING* 48(1): 65–78.

Widrow, B. & Stearns, D. 1985. Adaptive signal processing. *Prinice-Hall, Inc.*

Yukinori, K. 2003. Present status and technology of shield tunneling method in Japan. *Tunnelling and Underground Space Technology* 18(3): 145–159.

The Shanghai Yangtze River Tunnel - Theory, Design and Construction – Huang (ed)
© 2008 Taylor & Francis Group, London, ISBN 978-0-415-47161-9

Risk analysis on shield tail seal brush replacing of Shanghai Yangtze River Tunnel

Y.R. Yan, H.W. Huang & X.Y. Xie
Key Laboratory of Geotechnical & Underground Engineering, Ministry of Education, Tongji University, Shanghai, P. R. China
Department of Geotechnical Engineering, School of Civil Engineering, Tongji University, Shanghai, P. R. China

ABSTRACT: The shield of Shanghai Yangtze River tunnel will advance 7.5 km one time. But according to the project experiences, the shield tail seal brush would be worn after a long distance advance. If the failure of the shield tail seal occurred when the shield driving, very large amount of water may seepage into the tunnel from the failure part of tail seal, the disaster of which is beyond imagination. So it is necessary to choose appropriate location and replace the tail seal after the shield driving a long distance. Using the FTA method, qualitative and quantitative analysis are carried on for the risk during the process of replacing the tail seal brush. It finds the main risk factors influencing the occurrence of brush replacing accident. Therefore, during the replacing process of Shanghai Yangtze River tunnel, it aims at surveying and managing these main risk factors to reduce the risk of brush replacing.

1 INTRODUCTION

In shield driving process, an annular gap forms behind the shield tail, which gap is outwardly limited by the surrounding rock or soil, and inwardly by the lining (encasement; tubing segments) of the tunnel. The seal at the tail of the tunneling shield prevents peripheral water, earth and sand, and back-filling materials round the outside of the shield into the rear thereof (Fengxiang Zhang et al. 2004, Fumin Zhang 2006). So the tail seal of shield is a safety barrier, setting apart from surrounding stratum.

Various problems arise in line with lengthening of the excavation distance of a shield driving machine, the durability of the tail seal portion of shield is an important theme. That is, at the tail seal portion, the tail brush are worn by frictions with the segments while shield driving a long distance. So peripheral water and slurry can invade some parts of the tail portion, which may lead to the collapse of the ground. For example (Xiuguo Wu 2006), the underground portion of the line passes through the granite batholiths which were intruded into the Guangzhou metro line No.3 project. One 6.28 m diameter Herrenknecht EPB shield was used to excavate some part of tunnels, and it had three tail seal brush. Leaking slurry occurred in the 1,040 ring of the left line drive and the last of this resulted in the large settlement of surface.

If the failure of the shield tail seal occurred when the shield is driving under the river with high groundwater, very large amount of water may seep into the tunnel from the failure part of tail seal, resulting in disastrous consequence. So it is necessary to choose appropriate location and replace the tail seal when shield drives long distance under river. Using the FTA method, qualitative and quantitative analysis are carried on for the risk during the process of replacing the tail seal brush of Shanghai Yangtze River tunnel. It finds the main risk factors influencing the occurrence of brush replacing accident. Therefore, during the replacing process, it aims at surveying and managing these main risk factors to reduce the risk of brush replacing.

2 SHIELD TAIL SEAL OF SHANGHAI YANGTZE RIVER TUNNEL

Shanghai Yangtaze River tunnel starts from Wuhaogou in Pudong side and ends Changxing Island. Two 15.43 m diameter Herrenknecht shields are used to construct the two tunnels once, and the lengths of the tunnels are separately 7,471.65 m, and 7,469.36 m. According to past experience, the tail brush would be worn after a long distance advance. So it is necessary to make a scheme for replacing the brush. It may spend 45 days to replace the worn brush based on the special

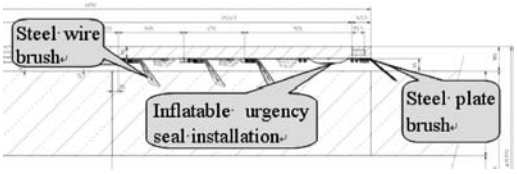

Figure 1. Sketch map of shield tail seal structure.

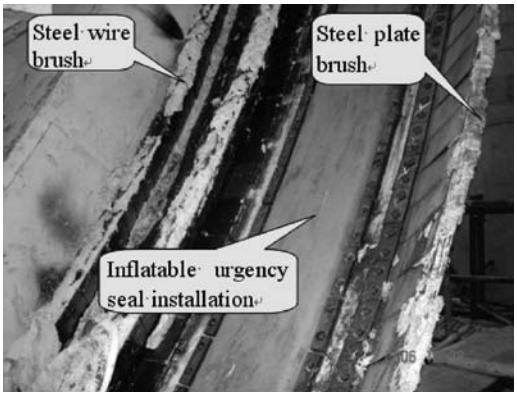

Figure 2. Picture of shield tail seal structure.

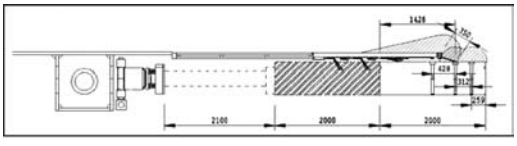

(a)

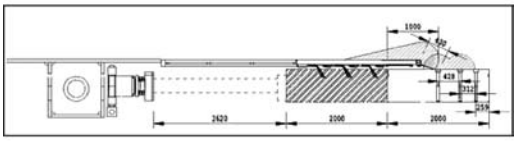

(b)

Figure 3. section of shield tail brush replacing: (a) Replacing 2 strip of steel wire brush; (b) Replacing 3 strip of steel wire brush.

topic 'Research on the construction technology and quality control of big diameter tunnel'. The position of replacing the brush may be at the first 4 km, which is in the stratum ⑤$_3$ silty clay.

The shield tail is 5,130 mm long, and the portion of tail seal is 2,450 mm long. It includes 3 strips of tail steel wire brush, 1 strip of steel plate brush and an inflatable urgency seal installation (Figs 1 and 2). It may replace 2 or 3 strips of steel wire brush by installing special segments and strengthen the surrounding ground by freezing method (Fig. 3). Figure 4

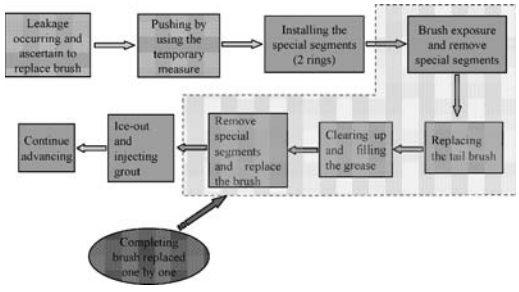

Figure 4. A process of replacing the shield tail brush.

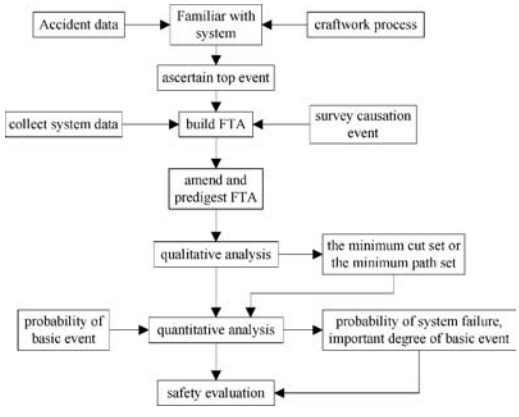

Figure 5. Flowchart of FTA.

shows the process of the replacing. During the process of the replacing, there are two kinds of special segments, one is freezing pipe buried in advance and the other is composed of several key segments.

3 THE THEORY OF FTA METHOD

Fault Tree Analysis (FTA for short) is a method for evaluation reliability and failure of complicated system (Richard E, Barlow, Jerry B, etc. 1975; D. H. Shi, S. R. Wang 1993; J. C. Jiang, Z. L. Guo 2004). Making use of FTA to carry on analysis, it can not only obtain the direct reasons of accident, but also go deep into the latent mechanism of accident and put forward the defending measures directly. Figure 5 shows the flowchart of FTA.

4 FTA OF REPLACING SHIELD TAIL SEAL BRUSH

4.1 *Fault tree model for the brush replacing*

According to the characteristics of shield tail brush of Shanghai Yangtze River tunnel and replacing process, collecting the concerned data, the FTA model of replacing brush is obtained (Fig. 6).

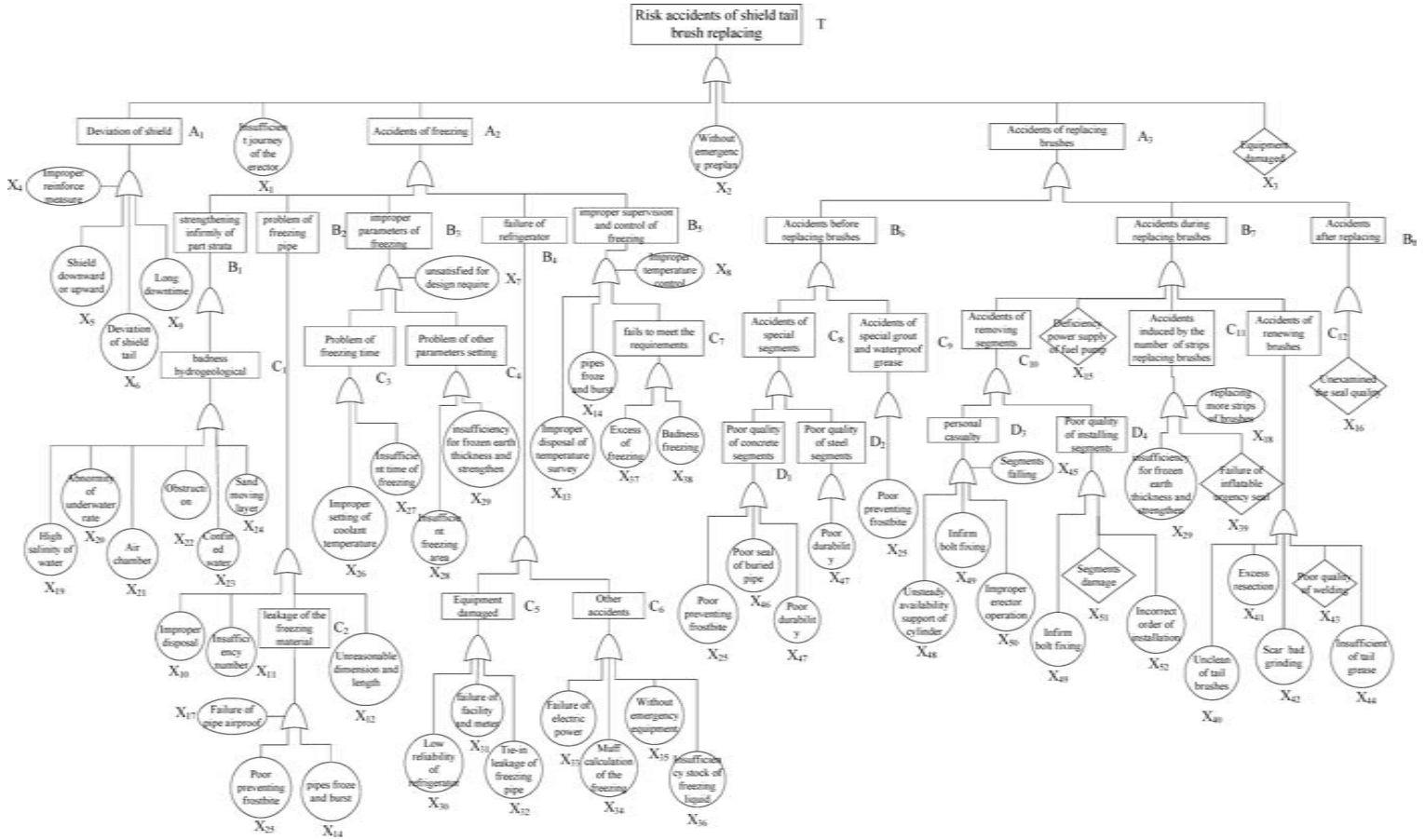

Figure 6. Fault tree of replacing shield tail brush.

It is systemically analyzed based on the established fault tree model. Firstly, the minimum basic event sets causing the main event occurrence are solved. Each minimum cut set corresponds to one accident type, and there are several minimum cut sets with different occurrence probability of one fault tree. The minimum cut set with the maximum occurrence probability is the most probably potential factor which may cause accident.

There are 52 basic events of the top event in the FTA model. Based on the Bull's algorithm (Equation 1), the top event T is the intersection of the 48 cut sets which are the minimum cut sets of the fault tree, i.e. {X1}, {X2}, {X3}, {X10}, {X11}, {X12}, {X15}, {X16}, {X19}, {X20}, {X21}, {X22}, {X23}, {X24}, {X25}, {X30}, {X31}, {X32}, {X33}, {X34}, {X35}, {X36}, {X40}, {X41}, {X42}, {X43}, {X44}, {X46}, {X47}, {X49}, {X51}, {X52}, {X4X5}, {X4X6}, {X4X9}, {X7X26}, {X7X27}, {X7X28}, {X7X29}, {X8X13}, {X8X14}, {X8X37}, {X8X38}, {X17X14}, {X18X29}, {X18X39}, {X45X48}, {X45X50}, which means that the combination of 48 different risks causes the main event occurring. Therefore, the main event probability caused by the 48 minimum cut sets could be calculated based on fault tree theory.

$$
\begin{aligned}
&T = A_1 + X_1 + A_2 + X_2 + A_3 + X_3 \\
&A_1 = X_4\left(X_5 + X_6 + X_9\right) = X_4X_5 + X_4X_6 + X_4X_9 \\
&A_2 = B_1 + B_2 + B_3 + B_4 + B_5 \\
&= C_1 + \left(X_{10} + X_{11} + C_2 + X_{12}\right) + X_7\left(C_3 + C_4\right) + \left(C_5 + C_6\right) + X_8\left(X_{13} + X_{14} + C_7\right) \\
&= \left(X_{10} + X_{20} + X_{21} + X_{22} + X_{23} + X_{24}\right) + \left(X_{10} + X_{11} + X_{17}\left(X_{25} + X_{14}\right) + X_{12}\right) + \\
&X_7\left(X_{26} + X_{27} + X_{28} + X_{29}\right) + \left(X_{30} + X_{31} + X_{32} + X_{33} + X_{34} + X_{35} + X_{36}\right) + \\
&X_8\left(X_{13} + X_{14} + X_{37} + X_{38}\right) \\
&= X_{10} + X_{11} + X_{17}X_{19} + X_{20} + X_{21} + X_{22} + X_{23} + X_{24} + X_{30} + X_{31} + X_{32} + X_{33} + X_{34} + \\
&X_{35} + X_{36} + X_7X_{26} + X_7X_{27} + X_7X_{28} + X_7X_{29} + X_8X_{13} + X_8X_{14} + X_8X_{37} + X_8X_{38} \\
&+ X_{17}X_{14} + X_{17}X_{25} \\
&A_3 = B_6 + B_7 + B_8 \\
&= \left(C_8 + C_9\right) + \left(C_{10} + X_{15} + C_{11} + C_{12}\right) + X_{16} \\
&= \left(D_1 + D_2 + X_{25}\right) + \left(D_3 + D_4 + X_{15} + X_{16}\left(X_{29} + X_{39}\right) + X_{40} + X_{41} + X_{42} + X_{43} + X_{44}\right) + X_{16} \\
&= \left(X_{25} + X_{47} + X_{46}\right) + \left(\begin{matrix} X_{45}\left(X_{48} + X_{49} + X_{50}\right) + X_{49} + X_{33} + X_{32} + X_{15} + \\ X_{18}\left(X_{29} + X_{39}\right) + X_{40} + X_{41} + X_{42} + X_{43} + X_{44} \end{matrix}\right) + X_{16} \\
&= X_{15} + X_{16} + X_{25} + X_{40} + X_{41} + X_{42} + X_{43} + X_{44} + X_{46} + X_{47} + X_{49} + X_{51} + X_{52} + \\
&X_{18}X_{29} + X_{18}X_{39} + X_{45}X_{48} + X_{45}X_{50}
\end{aligned}
$$

$$
\begin{aligned}
T = {} & X_1 + X_2 + X_3 + X_{10} + X_{11} + X_{12} + X_{15} + X_{16} + X_{19} + X_{20} + X_{21} + X_{22} + X_{23} + X_{24} + X_{25} \\
& + X_{30} + X_{31} + X_{32} + X_{33} + X_{34} + X_{35} + X_{36} + X_{40} + X_{41} + X_{42} + X_{43} + X_{44} + X_{46} + X_{47} + X_{49} \\
& + X_{51} + X_{52} + X_4X_5 + X_4X_6 + X_4X_9 + X_7X_{26} + X_7X_{27} + X_7X_{28} + X_7X_{29} + X_8X_{13} + X_8X_{14} \\
& + X_8X_{37} + X_8X_{38} + X_{17}X_{14} + X_{18}X_{29} + X_{18}X_{39} + X_{45}X_{48} + X_{45}X_{50}
\end{aligned} \tag{1}
$$

For example, {X31} means that the appearance of X31(failure of facility and meter) may lead to the occurrence of top event; {X18X29} means that the coexistence of basic events X18 (replaced more strips of brush) and X29 (insufficiency for frozen earth thickness and strengthen) may lead to the occurrence of top event.

4.2 *Qualitative analysis*

For many factors affecting the occurrence of accident in shield tail brush replacing, it needs to analyze their affection. According to the established fault tree, it analyzes the sensitive degree of every factor, and makes the compositor of the basic events. At present, the method for obtaining the coefficient of structural importance often uses the minimum cut set or path set to approximately estimate the importance index. Their principles are as follows:

(1) The structural importance coefficient of the single cut set is the biggest. For example{X1}, {X2}, {X3}, {X10}, {X11}, {X12}, {X15}, {X16}, {X19}, {X20}, {X21}, {X22}, {X23}, {X24}, {X25}, {X30}, {X31}, {X32}, {X33}, {X34}, {X35}, {X36}, {X40}, {X41}, {X42}, {X43}, {X44}, {X46}, {X47}, {X49}, {X51}, {X52}. Where,

$$
\begin{aligned}
&I_1 = I_2 = I_3 = I_{10} = I_{11} = I_{12} = I_{15} = I_{16} = I_{19} = I_{20} = I_{21} = I_{22} = I_{23} \\
&= I_{24} = I_{25} = I_{30} = I_{31} = I_{32} = I_{33} = I_{34} = I_{35} = I_{36} = I_{40} = I_{41} = I_{42} \\
&= I_{43} = I_{44} = I_{46} = I_{47} = I_{49} = I_{51} = I_{52}
\end{aligned} \tag{2}
$$

(2) The structural importance coefficients are the same for basic events together appearing in only one minimum cut set.

(3) The structural importance coefficient of basic event depends on appearing times in the minimum cut sets which have the same number of basic events. That is to say, the number is few, and the structural importance coefficient is small; in reverse is OK; the number is the same, and coefficient is equal. Where

$$
\begin{aligned}
&I_7 = I_8 > I_4 > I_{14} = I_{18} = I_{29} = I_{45} > I_5 = I_6 = I_9 = I_{13} \\
&= I_{26} = I_{27} = I_{28} = I_{37} = I_{38} = I_{39} = I_{47} = I_{49}
\end{aligned} \tag{3}
$$

(4) When basic events appear in the minimum cut sets having different number of basic events, the structural importance coefficient is determined as follows:

- If the appearance times are equal, the structural importance coefficient is larger which is in the cut set of fewer basic events.
- If the basic event appears in the small cut set little and the large cut set much, even though more complicated circs, the coefficient can be calculated following discriminate below.

$$
\sum I(i) = \sum_{X_i \in K_j} \frac{1}{2^{n_j - 1}} \tag{4}
$$

Where, $I_{(i)}$ is approximately calculated value of structural importance coefficient of the basic event X_i; X_iK_j denotes the basic event X_i belonging to the minimum cut set K_j; n_j is the number of basic events in the minimum cut set which includes X_i.

Therefore, following above analysis, the order of structural importance of basic event is educed.

$$I_1 = I_2 = I_3 = I_{10} = I_{11} = I_{12} = I_{15} = I_{16} = I_{19} = I_{20} = I_{21} = I_{22} = I_{23} = I_{24} = I_{25} = I_{30} = I_{31} = I_{32} = I_{33} = I_{34} = I_{35} = I_{36} = I_{40} = I_{41} = I_{42} = I_{43} = I_{44} = I_{46} = I_{47} = I_{49} = I_{51} = I_{52} > I_7 = I_8 > I_4 > I_{14} = I_{18} = I_{29} = I_{45} > I_5 = I_6 = I_9 = I_{13} = I_{26} = I_{27} = I_{28} = I_{37} = I_{38} = I_{39} = I_{47} = I_{49} \quad (5)$$

According to the order result, the basic events of single minimum cut sets X1, X2, X3, X10, X15, X16, X19, X20, X21 and so on easily cause the occurrence of the top event; Secondly, the basic events X7, X8, X4, X14, X18 which appear more times also easily cause the top event failure. They are the weakness parts of the system and the main risk factors arousing the occurrence of accidents during the shield tail seal brush replacing. Therefore, during the process of replacing the brush, it aims at surveying and managing the basic events which greatly influents the top event occurrence to lower the probability of accidents occurrence.

4.3 *Quantitative analysis*

(1) Theory of quantitative analysis

Quantitative analysis includes evaluation of failure probability of the top event and important analysis of the basic events. In practice, the occurrence probability of a top event (PT) is obtained using approximate probability formula of independent events as shown in Equation 6.

$$P_i = 1 - \prod_{i=1}^{n} [1 - P(M_i)] \quad (6)$$

where, $P(M_i)$ is the occurrence probability of the ith MCS.

After getting the occurrence probability of the system (top event), it is more important to obtain the basic event with biggest risk. This can be expressed by the importance degree of the basic event $I_g(i)$, namely the degree that the basic event influences the top event failure:

$$I_g(i) = \frac{\partial P_T}{\partial P_i} \frac{P_i}{P_T} \quad (7)$$

where, P_i is the occurrence probability of the basic event.

(2) The quantitative analysis of replacing brush FTA model

As a trial application for project, the relationship between the probability and possibility of the risk occurrence is decided by 'Guidelines of Risk Management for Metro Tunnelling and Underground Engineering Works' (Tongji University 2007). According to the Table 1, the probabilities of basic events are obtained by the project technical persons marking (for simplification, it adopt the midst value of probability rage). It shows in the Table 2. So the risk probability of replacing shield tail brush is about 0.3685, that is PT = 0.3685. According to the Table 1, it belongs to the fifth rank. The importance degrees of the basic events are obtained too (Table 2).

Table 1. The classification of risk occurring probability.

Rank	Accident description	Interval probability
One	Impossible	$P < 0.01\%$
Two	Infrequent	$0.01\% \le P < 0.1\%$
Three	Occasional	$0.1\% \le P < 1\%$
Four	Possible	$1\% \le P < 10\%$
Five	Frequent	$P \ge 10\%$

According to the data of the Table 2, the order of basic events' important degree is shown as follows:

$$I_g(19) > I_g(15) = I_g(25) = I_g(43) = I_g(51) > I_g(18) = I_g(4) > I_g(3) = I_g(20) = I_g(21) = I_g(22) = I_g(23) = I_g(24) = I_g(30) = I_g(31) = I_g(32) = I_g(33) = I_g(34) = I_g(36) = I_g(40) = I_g(42) = I_g(44) = I_g(46) = I_g(49) = I_g(52) > I_g(9) > I_g(29) > I_g(8) > I_g(2) = I_g(10) = I_g(11) = I_g(12) = I_g(16) = I_g(35) = I_g(41) = I_g(47) > I_g(7) > I_g(5) = I_g(6) > I_g(1) > I_g(45) > I_g(17) = I_g(28) = I_g(39) = I_g(48) > I_g(14) = I_g(26) = I_g(27) = I_g(37) = I_g(38) = I_g(50) > I_g(13) \quad (8)$$

According to the above equation, the main risk factor of replacing the tail brush are X19 (High salinity of water), X15 (Deficiency power supply of fuel pump), X25 (Poor preventing frostbite), X43 (Poor quality of welding), X51 (Segments damage), X18 (Replacing more strips of brush), X4 (Improper reinforce measure), X3 (Equipment damaged), X32 (Tie-in leakage of freezing pipe), X9 (Long downtime) and so on.

By comparing the Eq.(5) and Eq.(8), it educed that the first several basic events in the Eq.(8) are also located in the front of the Eq.(5). So through the contrast of the qualitative and quantitative analysis, it certified that the fault tree for risk of replacing the shield tail brush is reasonable and useful.

4.4 *Main risk factors and its measures*

According to the order of Eq.(5) and Eq.(8) of the basic events, single minimum cut set X19, X15, X25, X43, X51, X3, X20, X21, X31, X40 and so on easily cause accidents in replacing the shield tail brush; Secondly, the basic events X18, X4, X29, X8, X9 which appear more times also easily cause the top event failure. They are the weakness parts of the system and

Table 2. Probability and importance degrees of basic events.

Sign	Basic events	Probability	Importance degree
X_1	Insufficient journey of the erector	0.01%	2.71e-4
X_2	Without emergency preplan	0.05%	0.0014
X_3	Equipment damaged	0.5%	0.014
X_4	Improper reinforce measure	0.5%	0.015
X_5	Shield downward or upward	5%	6.78e-4
X_6	Deviation of shield tail	5%	6.78e-4
X_7	Unsatisfied for design require	0.5%	7.60e-4
X_8	Improper temperature control	0.05%	0.0021
X_9	Long downtime	99%	0.0134
X_{10}	Improper disposal of freezing pipe	0.05%	0.0014
X_{11}	Insufficiency number of freezing pipe	0.05%	0.0014
X_{12}	Unreasonable dimension and length	0.05%	0.0014
X_{13}	Improper disposal of temperature survey	0.05%	6.78e-7
X_{14}	Pipes froze and burst	0.5%	6.78e-6
X_{15}	Deficiency power supply of fuel pump	5%	0.14
X_{16}	Unexamined the seal quality	0.05%	0.0014
X_{17}	Failure of pipe airproof	0.5%	6.78e-5
X_{18}	Replacing more strips of brush	10%	0.015
X_{19}	High salinity of water	10%	0.2714
X_{20}	Abnormity of under water rate	0.5%	0.014
X_{21}	Air chamber	0.5%	0.014
X_{22}	Obstruction	0.5%	0.014
X_{23}	Confined water	0.5%	0.014
X_{24}	Sand moving layer	0.5%	0.014
X_{25}	Poor preventing frostbite	5%	0.14
X_{26}	Improper setting of coolant temperature	0.05%	6.78e-6
X_{27}	Insufficient time of freezing	0.05%	6.78e-6
X_{28}	Insufficient freezing area	0.5%	6.78e-5
X_{29}	Insufficiency for frozen earth thickness and strengthen	5%	0.0075
X_{30}	Low reliability of refrigerator	0.5%	0.014
X_{31}	Failure of facility and meter	0.5%	0.014
X_{32}	Tie-in leakage of freezing pipe	0.5%	0.014
X_{33}	Failure of electric power	0.5%	0.014
X_{34}	Muff calculation of the freezing	0.5%	0.014
X_{35}	Without emergency equipment	0.05%	0.0014
X_{36}	Insufficiency stock of freezing liquid	0.5%	0.014
X_{37}	Excess of freezing	0.5%	6.78e-6
X_{38}	Badness freezing	0.5%	6.78e-6
X_{39}	Failure of inflatable urgency seal	0.5%	6.78e-5
X_{40}	Unclean of tail brush	0.5%	0.014
X_{41}	Excess resection	0.05%	0.0014
X_{42}	Scar bad grinding	0.5%	0.014
X_{43}	Poor quality of welding	5%	0.14
X_{44}	Insufficient of tail grease	0.5%	0.014
X_{45}	Segments falling	0.05%	7.46e-5
X_{46}	Poor seal of buried pipe	0.5%	0.014
X_{47}	Poor durability	0.05%	0.0014
X_{48}	Unsteady availability support of cylinder	5%	6.78e-5
X_{49}	Infirm bolt fixing	0.5%	0.014
X_{50}	Improper erector operation	0.5%	6.78e-6
X_{51}	Segments damage	5%	0.14
X_{52}	Incorrect order of installation	0.5%	0.014

the main risk factors leading to the failure of replacing the shield tail brush. Therefore, during the seal brush replacing process of Shanghai Yangtze River tunnel, it aims at surveying and managing the basic events which greatly influents the top event occurrence to reduce the accidents of the top event.

(1) Risk factor analysis of the shield deviation

Because of the soft ground and heavy deadweight of the shield, if there are no measures for strengthening the ground under the shield (the basic event X4), additionally the long time for replacing the brush (the basic event X9), and the accidents may occur as follows:

A. The head of shield may have the tendency of upward or downward, which would influent the normal advancing of the shield after the brush replacing.
B. The earth around the shield may produce distortion, which would influent the freezing effect of soil at the tail.

Therefore, the geological status must be surveyed ahead of the replacing, and proper measures should be adopted to strengthen the surrounding earth, especially the earth under the shield.

(2) Risk factor analysis of the freezing construction

The effect of freezing soil is the key to the success of brush replacing, the analysis is as follows:

- High salinity of water (the basic event X19) makes the freezing temperature of soil largely lower; and

at the meantime, the strength of soil with salt is weaker than that of the normal. It also may lead to the swelling which affects the stress of the structure.
- Failure of facility and meter (the basic event X31) can't control the quality of the freezing, which may lead to the excess freezing and then causing the pipe and others crack, or badness freezing which causes the accident of groundwater flowing to the shield tunnel.
- Without emergency equipment (the basic event X35) can't make normal freezing when some emergency occur, like the failure of electric power and damage of the freezing equipments, which causes the accident of groundwater flowing to the shield tunnel.

Based on the strata and strips of the brush replacing, it should do as follows:

- When the special segments being produced, the disposal of the freezing hole should be fully considered, like the form, location, the pipe size and length, material and so on.
- According to the freezing area and strength, the refrigeration design and choice of freezer type should be carefully considered.
- It makes a full survey of the badness geology.
- The parameters of the freezing are ascertained by the detail calculation, and the real inspecting survey should be carried on and the data should be also analyzed.
- It must consider the influences of the human factor.

(3) Risk factor analysis of the brush replacing process

The project experience is little for shield's long distance advancing one time, and it is much less for replacing the tail seal brush under the river. So the risk factors are as follows:

- Replacing more strips of brush (the basic event X18) shortens the portion of tail seal, and if the strength and range of freezing is deficient, then the emergency can't be controlled.
- Poor quality of welding (the basic event X43) decreases the fastness between the new brush and the shield shell, so the brush will be easily damaged and occur the failure of the tail seal, it must stop again to replace the brush, leading to the construction term lengthened and the construction cost increased.
- Deficiency power supply of fuel pump (the basic event X15) shortens the quantity of injecting grease and pressure, and decreases the shield tail seal.

It should make a full consideration ahead of the brush replacing.

- The number of strips of replacing brush has not been decided yet. The more brush strips are replaced the larger degree of risk is; at the meantime, the more brush strips are replaced the more advantages for following construction are. It decreases the probability of tail seal failure, and in other words, it shortens the construction term and reduces the construction cost.
- The quality of welding can't be well controlled under low temperature. It must do research for this, and then ensure the fastness of the welding.

(4) Risk factor analysis of the others

Because the process of replacing the shield tail brush will take about 45 days, the supply of electrical power (the basic event X15) can't be neglected; during the halt, it should protect the shield from damaged (the basic event X3); setting the emergency preplan (the basic event X2) is a useful measure for controlling the emergency accidents.

5 CONCLUSIONS

From risk analysis of tail seal brush replacing of Shanghai Yangtze River tunnel based on FTA method, the conclusions are as follows:

- Having a direct view and simple character, the FTA is a valid method for analyzing the risk of shield tail seal brush replacing.
- It totally considered 52 basic events for the risk of tail seal brush replacing of Shanghai Yangtze River tunnel. Through the fault tree calculation, there are 48 minimum cut sets for the fault tree, and it can definite the weakness parts of tail seal brush replacing, confirm the key factors of risk occurrence, and make an order for the importance of various influence factors.
- Through FTA of the shield tail seal brush replacing, it confirmed the mostly reason and mechanism of leading to the failure, brought forward the improved measures and suggestion. So it gave some useful reference for preventing or reducing the risk of shield tail brush replacing under the Yangtze River.

REFERENCES

Du, J.H. & Peng, Y.B. 2007. The Key Technology Research of Tail Brush Replacing during Shield Advancing. *Railway Engineering* (3):47–48.

Jiang, J.C. & Guo, Z.L. 2004. *Safety system engineering.* Beijing: Chemical Industry Press.

Richard, E., Barlow, Jerry B., et al. 1975. Reliability and Fault Tree Analysis. *Philadelphia: Society for Industrial and Applied Mathematics.*

Shi, D.H. & Wang, S.R. 1993. *The method and thesis of FTA technology.* Beijng: Beijing Normal University Press.
Tongji University. 2007. *Guidelines of Risk Management for Metro Tunnelling and Underground Engineering Works.* In discuss edition.
Wu, X.G. 2006. The Technique of Shield Tail Brush be Repaired Inside During Long Tunnel Building. *Guangzhou Architecture* (6):25–27.
Zhang, F.X., Zhu, H.H. & Fu, D.M. 2004. *Shield tunnel*. Beijing: China Communication Press.
Zhang, F.M. 2006. Effect of Shield Tail Sealing in Prevention of Mortar Leakages. *Tunnel Construction* 26(Sup.2): 52–55.

The Shanghai Yangtze River Tunnel - Theory, Design and Construction – Huang (ed)
© 2008 Taylor & Francis Group, London, ISBN 978-0-415-47161-9

Shanghai Yangtze River Tunnel split level evacuation provisions

B. Frew
Maunsell Geotechnical Services Ltd., Maunsell Aecom Group, P. R. China

Y.F. Cai
Shanghai Changjiang Tunnel & Bridge Development Co., Ltd., Shanghai, P. R. China

K.F. Wong & C.K. Mok
Maunsell Geotechnical Services Ltd., Maunsell Aecom Group, P. R. China

L. Zhang
Maunsell AECOM Shanghai, P. R. China

ABSTRACT: The original design concept of evacuation provision comprised 8 inter-connecting cross passages at road deck level was rejected because there was no access provision between the road deck and the service level below in which the LRT was to run. Two options comprised of provision of dedicated cross passages for road and LRT levels and combined use of cross passages serving both levels were proposed. The dedicated concept was finally negated considering the high cost and construction risk. Finally, the concept of combined use cross passages was detailed presented.

1 INTRODUCTION

The original design concept of the Yangtze River Tunnel was for it to be a dedicated highway tunnel. Accordingly, the general public would only have access to the road deck with the space below reserved for services, pump sumps and maintenance access. Passenger evacuation in the event of an emergency was to be through cross passages at road deck level linking the adjacent bores (Fig. 1). However, subsequent to contract award a decision was made to include provisions for a Light Rail Transit (LRT) to run below the road deck (Fig. 2). Therefore it was necessary to

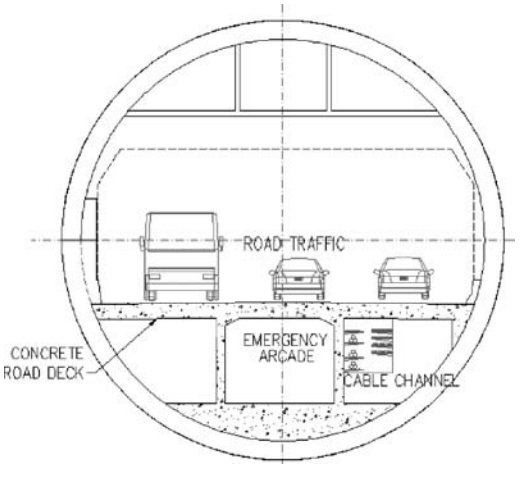

Figure 1. Original cross section.

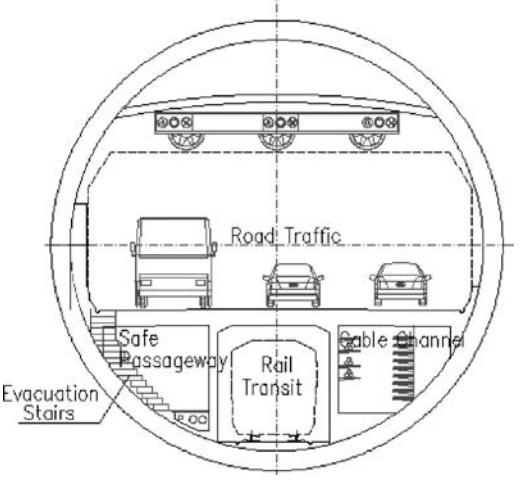

Figure 2. Cross section showing LRT.

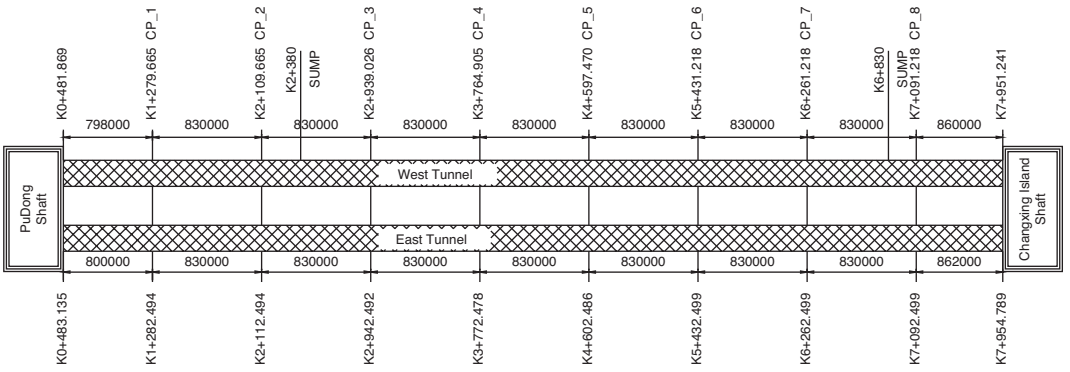

Figure 3. Schematic of original cross passage provisions.

review and amend the evacuation provision to include for the presence of the general public below the road deck.

2 ORIGINAL PROVISIONS

The original evacuation provision comprised 8 interconnecting cross passages at road deck level. The arrangement is shown schematically on Figure 3. The original cross passages were to be elliptical with internal dimensions of 2.4 m wide and 2.88 m high spaced at 830 m intervals along the tunnel.

The principal problem with this arrangement was there was no access provision between the road deck and the service level below in which the LRT was to run. Therefore a number of options had to be considered to provide the safe evacuation from the LRT level. These options comprised.

- Provision of dedicated cross passages for road and LRT levels
- Combined use cross passages serving both levels.

2.1 *Dedicated cross passages*

In an ideal world the provision of dedicated cross passages to the road deck and LRT would be the perfect solution allowing the two modes of transport to operate as separate entities with no 'physical' interface during normal day to day activity. This scheme is shown on Figures 4, 5 and 6.

However, there are a number of practical issues that do militate against this otherwise appealing option. These are cost and risk.

The first is very simple that the increased provision of an additional 8 cross passages would approximately double the cost of this element of the project. Whilst this might not appear to form a large percentage increase on such a major project (estimated total capital cost 12.6 bn Yuan, or 1.6 bn USD). This increase

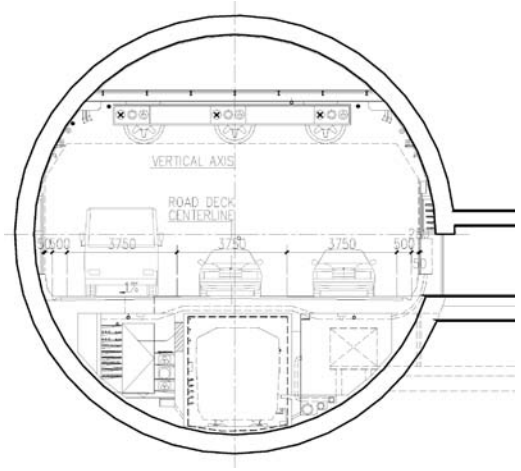

Figure 4. Road deck only cross passage.

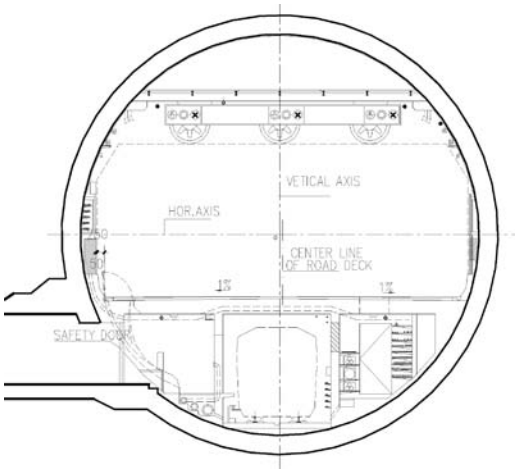

Figure 5. LRT only cross passage.

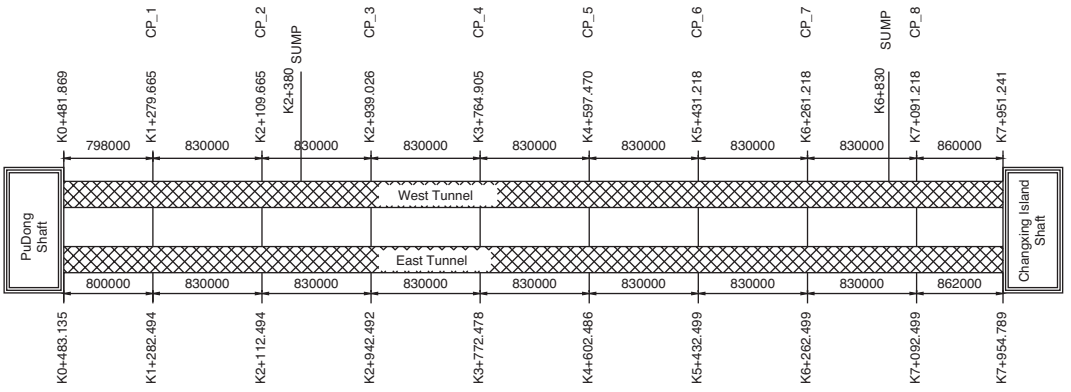

Figure 6. Schematic of dedicated cross passages.

would be significant due to the construction method, ground freezing.

The strata through which the main tunnels are being constructed comprise normally consolidated interbedded alluvial clays, silts sands and gravels below the water table with the maximum hydrostatic head approaching 60.0 m. These conditions are amongst the most challenging to be encountered anywhere in the world and it is improbable that even two decades ago that the project would ever have been attempted. The main tunnels are being bored using closed face tunnel boring machines (TBM's) with concurrent lining providing a secure and safe working environment as the tunnelling progresses. However, to 'step outside' the protective shell of main tunnel to construct the cross passages requires the use of the highly specialised, and expensive, ground freezing technique. The cost of ground freezing is dependent upon a number of factors but it is unlikely to be less than 1,000 Yuan (125 USD) per cubic metre of ground frozen. Therefore the 'freeze' alone for each cross passage could cost of the order of 24,000,000 Yuan (3.0 MUSD).

The highest risk activity in the tunnel construction is 'breaching' the segmental lining for the construction of a cross passage as even with the ground freezing there is always a residual risk of collapse or inundation. Therefore it is proper risk management to balance the operational safety requirement for cross passages against the construction safety requirement to determine the absolute minimum requirement.

3 COMBINED USE OF CROSS PASSAGES

After rejecting the concept of dedicated cross passages on the basis of cost and increased construction risk. Detailed study was made of the options of combined use allowing evacuation from both levels. A combined two level cross passage was briefly considered but

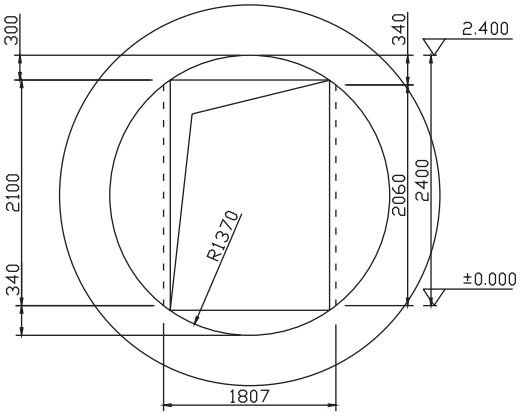

Figure 7. Standard cross passage.

this would have required an excavation diameter of approximately 6.0 m and the cost of was considered to be prohibitive notwithstanding the difficulties of its construction. Therefore both sets of passengers would have to access a 'standard' cross passage of 3.5 m (Fig. 7) excavated diameter.

The principal difficulty to overcome was the level difference that required either the use of stairs to ascend to road deck level or stairs (or chutes) to descend to the LRT level. The projected patronage figures of the highway are far in excess of those for the LRT. Therefore it was decided that the cross passages would align with the road deck leaving the LRT passengers to ascend using stairs.

Initially, it was proposed to locate the stairs in an enlargement to the cross passage located immediately adjacent to the main tunnel lining (Fig. 8).

However, it can be seen that there were two serious problems inherent in this concept.

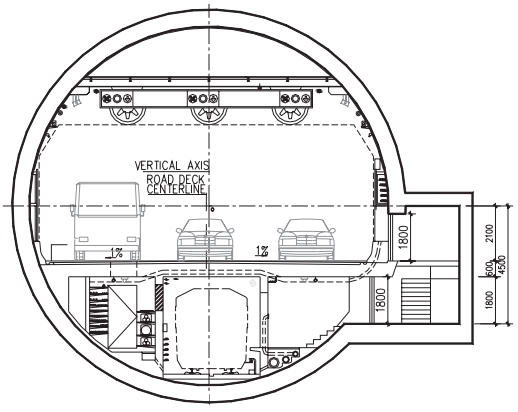

Figure 8. Enlargement adjacent to main tunnel lining.

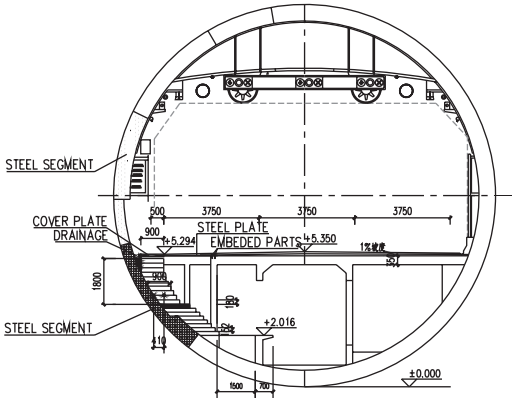

Figure 9. Cross section escape stairs.

- Approximately, half of the cross passage excavation would be 'over size' to accommodate the stairs.
- A folding ramp would be required to evacuate from the road deck level so that:

  a. Simultaneous evacuation could not be carried out from both levels.
  b. Operation could be confusing in an emergency situation.
  c. The ramp would require regularly inspection and maintenance.

The first negated the cost and construction safety benefits that drove the choice of a 'standard' cross passage and the second appeared over complex for people potentially in panic fleeing a fire. Therefore detailed consideration was given to providing the stairs within the main tunnel cross section.

At first sight this would appear to have been the obvious solution but it must be remembered that the LRT was a late addition to the project and that the permanent lining segment moulds had already been ordered prior to this issue arising. Indeed if it had been raised in detailed design the solution would in all probability have included increasing the tunnel diameter. The escape stairs are shown in section and in plan on Figures 9 and 10 respectively. It can be seen that one stair 'goer' the headroom is only 1,800 mm and construction tolerances for tunnel and the road deck could reduce this to 1,750 mm. Similarly, the required minimum stair width of 900 mm has only been achieved by the use of special segments at the stair location.

During normal operation of the tunnel the stairs are sealed off by a steel access hatch of 2,750 mm long by 920 mm wide as the stairs 'daylight' in the marginal strip of the nearest road lane.

From the above it can be seen that a number of local modifications were necessary to the permanent lining of the tunnel to enable an evacuation route to be provided from the LRT beneath the road deck to the

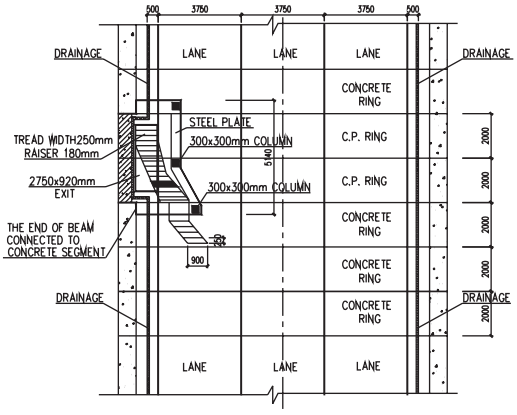

Figure 10. Plan on escape stairs.

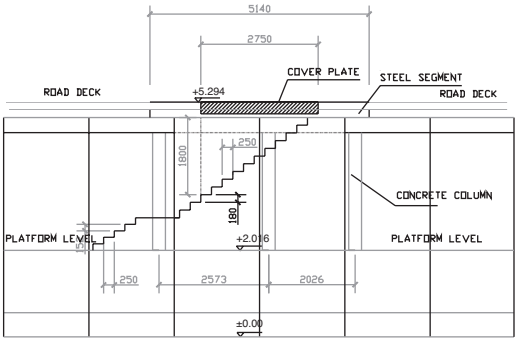

Figure 11. Elevation on escape stairs and access hatch detail.

cross passages. However, it is one thing to develop such a solution in the design office but when the tolerances are so tight there is no substitute for prototype testing (Fig. 12).

Figure 12. Wooden prototype of escape stairs.

4 CONCLUSIONS

Three design concepts of evacuation provision were compared and discussed. The original design concept of evacuation provision comprised 8 inter-connecting cross passages at road deck level was rejected because there was no access provision between the road deck and the service level below in which the LRT was to run. Two optional provisions of dedicated cross passages for road and LRT levels and combined use cross passages serving both levels were then proposed. The dedicated concept was finally negated considering the high cost and construction risk. Finally, the concept of combined use cross passages was described. Some suggestions for tunnel design were presented.

REFERENCES

Shanghai Tunnel Engineering & Rail Transit Design and Research Institute. 2007. *Preliminary Design Documents of Shanghai Yangtze River Tunnel.*

Shanghai Tunnel Engineering & Rail Transit Design and Research Institute. 2007. *Research on the Synchronous Construction of Shield Tunnel and Road Deck of Shanghai Yangtze River Tunnel.*

The Shanghai Yangtze River Tunnel - Theory, Design and Construction – Huang (ed)
© 2008 Taylor & Francis Group, London, ISBN 978-0-415-47161-9

The construction management informationization practice in Shanghai Yangtze River Tunnel & Bridge Project

Z.F. Zhou
Shanghai JUYEE Science & Technology Development Co., Ltd., Shanghai, P. R. China
School of Economics & Management, Tongji University, Shanghai, P. R. China

H.X. Zhang
Shanghai Yangtze River Tunnel & Bridge Construction Development Co., Ltd., Shanghai, P. R. China

ABSTRACT: With the development of information technology, the traditional construction industry fill new development requirement. The network, integration and practicality become the trend with the development in construction management informationization in and outside the China. Under the background above, Shanghai Yangtze River Tunnel & Bridge Project established the goal of construction management informationization, erected a set of management system for construction management information, development an integrated software system, achieved construction management information sharing and online collaboration, improved efficiency and quality of construction management.

1 INTRODUCTION

The research and application on the field of construction management informationization for owner has been more than thirty years oversea, and ten more years in the nation. According to the object of informationization application, it can be classified into three types.

- Unifunctional system focus on scheduling, cost planning, such as Project and Morrowsoft.
- Project information communication platform, such as My Construction, Projecttalk, Buzzsaw, and PMIS based on documents sharing.
- Large integrated PMIS, such as P3 plus Expedition. In China, no mature large integrated PMIS has been emerged yet. However, some large-scale construction project have attempted to develop such large integrated PMIS, such as the East Sea Bridge Project Management Information System (ESBP-MIS).

Although software like P3 display the high construction management level overseas, they can not be easily applied in China, for such a software need a high application demand of the CBS to adapt, and can not acclimatize itself to the management pattern in China. However ESBP-MIS is a large integrated management system which breakdown the structure to the level of working procedure, armed with the modern construction management theory, developed according to the construction project real operation requirement. It achieved integration of project cost and schedule management, implemented document online auditing, and greatly improved the effect of project management informationization.

According to the development of construction management informationization in and out of the China, the network, integration and practicality become the trendline.

1. **Network**: web-based Project Management system utilize the advantage of opening, convenient and low cost, smash the restriction of time and space, create a collaboration environment without the influence of weather and location. It provides the technical support for Virtual Construction and Virtual Project Team Management. It is the basic characteristic of project management in the era of knowledge economy.
2. **Integration**: construction management informationization is not a single specialty system, the integration will include not only the data from time, cost, quality, contract document, but also the data form other professional software such as monitoring system, risk management system, Virtual Reality system, GIS, Web3D system etc.
3. **Practicality**: practicality is the most difficult point in the application of Informationization, it tends to solve real business in construction management,

and make the software as the necessary tools of construction management. Furthermore, in order to make more applicability, some more visual display mode, such as 2D, 3D, GIS, need to be considered.

2 THE GOAL OF CONSTRUCTION MANAGEMENT INFORMATIONIZATION IN SHANGHAI YANGTZE RIVER TUNNEL & BRIDGE PROJECT (SHYRTBP)

2.1 *The characteristic of SHYRTBP*

SHYRTBP is a large-scale traffic infrastructural project on the Yangtze River, and it is the main composing part of the freeway .from Shanghai to Xian. The project will improve the structure and distribution of Shanghai traffic system, accelerate the integration of the Yangtze River delta, drive the economic development of Yangtze River Valley and all China, and upgrade the integrated competitive strength of Shanghai in Chinese economy. The project begins from Wuhaogou (Pudong), passes through the Changxing Island, and ends on Chenjia Town (Chongming Island). The length of the whole is 25.5 km. The scheme of "South Tunnel and North Bridge" was won. The length of Yangtze River Tunnel is 8.95 km, with 7.5 km under the river, while the length of Yangtze River Bridge is 16.63 km, with 9.97 km cross the river. The project have several characteristics as follows:

1. The project spread around a long distance area: main work locate in different bank, all transportation need ships;
2. A great amount of the company and department involved in the project and spread around different location: There are owner, design, construction, consultant, research, monitoring, installation, government;
3. The amount of communication information is huge: Every participants create a large amount of organizing, management, economy and technical information through each phrase of the implementation, and most of the information need more than one participant to check or prove;
4. A large amount of new technique, new equipment, new material are used: thus lead the difficult point on project target controlling because of the lacking of application experience.

2.2 *Overall target of construction management informationization in SHYRTBP*

Construction management informationization is the exploitation and utilization of information resources and information technology in construction management. Based on the above features, communication exchanges are becoming the principle problem, which will affect the construction effect of **SHYRTBP**. The traditional approach to information exchanging does not only cause the information delay, but also increase the cost of communication greatly. In the related documents, it is said that there are two third of the problems are relating to information communications issue during construction; and 10%–33% of cost increase is due to the information communications, and in the large construction project, information communication issue brings on the variation and construction error, whose cost is about the 3%–5% of construction project cost. Therefore, please refer to the following overall target of *,

(1) Developing a web-based, integrated construction management informationization software system

Firstly, using the system is to realize the centralized management of project information communication, by which will not only change the traditional P2P to take information as a central to communication among the project parties, but also improve the efficiency of communication and collaboration among the project parties. It centrally storages and manages the information during the construction, and each project party will get the corresponding construction information via internet at all times and places, by which we can not only get rid of the limitation of time and place by traditional communication, but also to improve the accuracy, retrievability and reusability of the project information.

Secondly, the system supports to collect, process, storage, share, query and report, by which to realize the project cycling control of **SHYRTBP**, including the planning of project cost, scheduling, quantity, and safety, tracking, controlling and coordination.

Meanwhile, realization of data relationship and integration for each subsystem effectively generally integrate the schedule controlling, cost controlling, quantity controlling and safety controlling etc during the project life cycle management in different levels, by which provides the accuracy information for construction project management and decision in time.

(2) Establishing a powerful management system for construction project management informationization

Construction project management informationization depends on the application of software system, so as to the support of the related organization and management system. In order to effectively improve and ensure the efficiency and effect of construction project management informationization, it is necessary to establish a sound management system. Guided by the advanced project management method and based on the changes from tradition management process to business process reengineering, the system involves a great amount of optimized construction project management workflow.

2.3 *Implementation plan of the informationization*

After defined the informationization target, implementation plan are made. The whole implementation plan is step by step as follows:

(1) Organize the research on Large-scale Construction Management Informationization System

In July 2004, the research was charged with the owner, a professional construction management informationization consultant company and a research institute. The research was focus on the management model, method system, software requirement design, target controlling structure, process numeralization and visualization.

(2) Organize the development of SHYRTBP Management Information System

Based on software requirement design in previous research, develop an integrated PMIS.

(3) Implementation of Construction Management Informationization

Based on management model and method system in previous research and software system developed, organization structure and management process will be executed; informationization will be popularized in all participants.

3 THE CONSTRUCTION MANAGEMENT INFORMATIONIZATION SYSTEM IN SHYRTBP

Construction management informationization is related to all the construction partners concerned, even related to some benefit colony not directly participate in the project, like concerned departments of government and the common people etc. The constructer of the project and the related benefit colony has different understanding of construction management informationization, which brings problems to implement the construction management Informationization. Besides, construction management informationization concerns not only about information technology, but also the standardization and understanding of construction management informationization. Based on the previous cognition, in order to advance the construction management informationization in **SHYRTBP**, headquarters and related units have established a series of system about construction management informationization, including the implementary organization of construction management informationization, information coding system of construction management informationization, the working flow, and all the measures concerned to ensure the results.

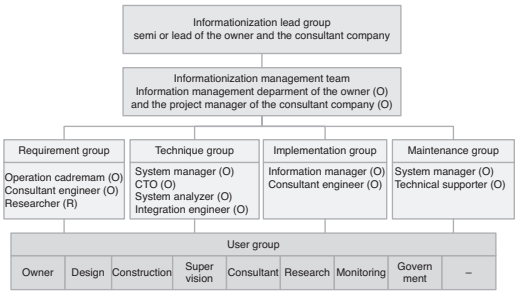

Figure 1. The organizing institution of construction management informationization.

3.1 *The implementary organization of the construction management informationization in SHYRTBP*

The implement of the construction management informationization in **SHYRTBP** has relation with all the participants and related benefit colony, as shown in Figure 1. The participants produce and share the information. In order to assign the duty and obligation, the owner as the leading integration and leading organizer of the project, has established a network for managing the project with all the participants.

The characteristic of the management network is that:

1. The owner assume leadership, which confirms the owner's leading position in the process of implementing construction management informationization, and also ensures owner the "engine" role in the process;
2. The professional construction management informationization consultation unit will be responsible for the informationization, which ensures the project is specialization;
3. Setup several implement teams with different specialty, which makes the project served by different specialty in all the phases;
4. The owner and the participants are allocated with responsibility person for information work, which makes the responsibility and obligation allocated to the units and persons.

3.2 *The information coding system of construction management informationization in SHYRTBP*

Implementing construction management informationization needs support from the organization, while the specialty technical support is also a key to the success, in which information coding system is the most important. The information coding system in construction management informationization mainly includes the decomposed structure and in-out report documents of the project. In Yangtze River Tunnel & Bridge Project,

all the implement units together confirm the project decomposed structure, units and member organizing code, schedule, investment, contract, quality and unify all kinds of project management report document.

3.3 *The work flow of construction management informationization in SHYRTBP*

Construction management informationization will affect the old construction management work flow, while its popularization needs more standard and more scientific management flow. When implement the construction management informationization, there are some changes in old work flow as follows:

(1) Online audit and off line pigeonhole of all kinds of document

Some people think informationization means no paper management. However, there are too many construction units concerned and there is a specific policy for paper file management, popularizing informationization not means no paper management, but taking advantage of information technology to advance the efficiency and quality of management. Popularizing informationization in some other projects meets tremendous difficulties when online auditing the documents. Because informationization can not abolish the old paper management, which makes online auditing nothing for the participants.

To solve the problem, a combined method of online auditing and offline pigeonhole is employed in the project. Firstly, the initiator of business document online fills and hands in the business documents. Some related persons will be informed to audit it by the program set before. After auditing it, the auditing result will be in operation at once, and the related units will start their work. The initiator of business document will print, sign and stamp the efficient business document through the system, at the same time hand it to the related units sign and stamp in the traditional way, finally keep it in project file in paper way.

As the participants are located in different area, this work flow will effectively improve the efficiency of information communication, reduce the cost of transferring documents, which will greatly reduce the mean transfer time. The information system keeps all of the business documents, which is benefit for the future information searching and sharing.

(2) Apply for online payment

In order to collect the investment control primary data, the headquarters establish a system of online payment. In a way of online transfer the business documents and offline pigeonhole, the applying units fill the business document online firstly, then print and sign and deliver it all together after auditing online.

(3) Information broadcast system

To cooperate with the online document deliver and the message broadcast, many kinds of ways to inform messages are employed.

1. Broadcast the news through each module in the system, like broadcasting every-week's conference plans.
2. Through rolling news on the system home page, it will issue the high effectiveness, great attention and urgent information.
3. Through the system individual information reminder, the user is informed of individual related work information. This information reminder will renovate and remind the user every 5 minutes automatically.
4. Through the short message, the main module for document transfer and working-plan will remind the person in charge.

(4) The flow of collecting all kinds of control data

The final target of construction management informationization is used to control object. It is important to collect the original data of target control. Before starting **SHYRTBP**, the related department and the consultant company have already established a rule of collecting original data. The rule is based on the uniform information coding system, and the objects control original data. According to the basic information coding system, the information acquisition modules record the data, and then the system will deal with it and gather it, and share it with construct units.

3.4 *The safeguard measures for construction management informationization in SHYRTBP*

To make the project success, the owner department and construction management informationization consultant units make all of the construct department concerned known that informationization is not only a development of software system, but a practice to manage the large project. Software system is only a tool, we should rely more on the knowledge of construction management informationization and on the participants concerned. So the owner department and consultant units take many measures, such as organizing, consulting, training, and technology support, to ensure it success.

1. With a concerted effort of all the participants and the leadership of leaders, all the participants will exchange the experience and be assessed their work in a fixed period.
2. The expert consultant and long time services supplied by the construction management informationization consultant units is necessary.
3. The members in different management levels and different operation levels will have different training plan, which covering basic knowledge of project

Figure 2. The homepage of management information system in **SHYRTBP**.

Figure 3. The construction management informationization system in **SHYRTBP** – information communication.

management and construction management informationization, partition rule of information coding system, and operation training of all levels, etc.

4 THE INTEGRATION SYSTEM OF CONSTRUCTION MANAGEMENT INFORMATIONIZATION IN SHYRTBP

According with the overall layout and scientific research before, construction management informationization system in **SHYRTBP** is designed. The system is integrated by several professional subsystems, mainly including four professional subsystems:

1. Construction management information system in **SHYRTBP**;
2. Construction video monitoring subsystem in **SHYRTBP**;
3. Three-dimensions visualization subsystem in **SHYRTBP**;
4. Construction monitoring, alarm in advance and alarm subsystem in **SHYRTBP**.

4.1 *Construction management information system in SHYRTBP*

The system realizes the information management functions in **SHYRTBP**, which includes progress control, investment control, contract control, quality control, construction management, design management, file management, safety management, material management and equipment management, etc. This system is not only an information management system of Yangtze River Bridge, but also the uniform entrance of construction management informationization system in **SHYRTBP,** as show in Figure 2.

The design target of the system is:

1. **SHYRTBP** employs B/S frame mode and provides an agility and safe way to enter and permissibility control. The user can visit the system and exchange the information through browser. All the participants work in collaboration and communicate at the same stage.
2. The system includes main project management work and build a bridge between owner department and construct units to communicate and cooperate.
3. The information system is built on the basis of business flow standard, which makes the business flow, management work and acquired information more standard, reduces the mistakes made by man. It is in accordance with the modern run mode.
4. The data recorded in the system provides ways to guide the future maintenance management and similar project management, which increases the value of the project.

The system has two project management informationization functions.

Project information communication based on file information includes: quality control, construct control, design management, safety management, material and equipment management, office business and document function module. The information is shown as file or document, which realizes the function of online document transfer and audit, online pigeonhole and project information broadcast, etc. The communication and long-distance collaboration problems of construct units in different areas are solved, as shown in Figure 3.

Project target control with quantum data includes: investment control, progress control, contract management function module. The information is shown as quantum data, and the data is in accordance with the request of coding system. The data covers all the aspects and phases in target control, and shows the result of target control, as shown in Figure 4.

Figure 4. The construction management informationization system in **SHYRTBP** – target control.

Figure 5. Video monitoring subsystem in **SHYRTBP**.

4.2 *Construction video monitoring subsystem in SHYRTBP*

The system is integrated with video monitoring system in **SHYRTBP**, which makes it easier to know the construction condition on site, as shown in Figure 5.

4.3 *Three-dimensions visualization subsystem in SHYRTBP*

This system exhibits the model in a three-dimension visible way, including the construction progress and structure information, as shown in Figure 6. It greatly improves veracity of information communication.

4.4 *Construction monitoring, alarm in advance and alarm subsystem in SHYRTBP*

The system will acquire and display data of equipments and structure during the working time, as shown in Figure 7. It is an important measure to protect the construction safety.

5 THE CONSTRUCTION MANAGEMENT INFORMATIONIZATION PRACTICE RESULTS IN SHYRTBP

Since the construction management informationization was brought into effect from July 2004, it has gained good performance and has been kept in peoples' mind. Informationization system has become a necessary tool for every involved construction units. Up to Nov. 19th, 2007, system has reserved 36,696 pieces of files in Q & C, 46,435 pieces of information about schedule control item, 125 items of plan, 1,065 items of information in contract management, 986 pieces of files in construction management and 2,740 items of the files about design management.

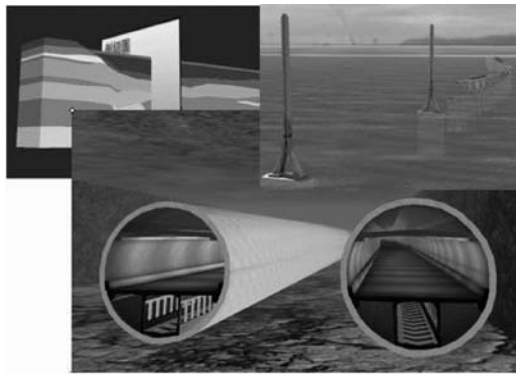

Figure 6. 3D visualization subsystem in **SHYRTBP.**

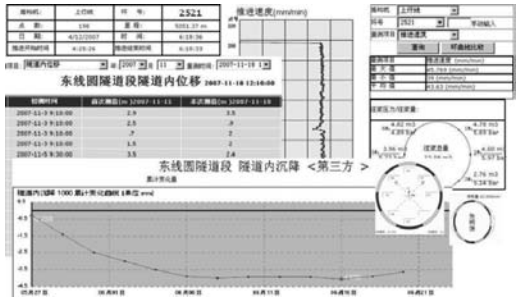

Figure 7. Construction monitoring, alarm in advance and alarm subsystem in **SHYRTBP**.

The practice of construction management informationization, especially the reform of business document transfer way, has greatly improved the efficiency in communicating information and cut down the cost of communicating information; The use of target control function plays an important role in mastering the project progress condition for the senior management and make it the foundation of making fast decisions in the process of project. The application of video monitoring system makes it possible for all levels of manager to know the construction condition. It effectively helps to assistant the safety management and to improve the management quality, further to ensure the whole project's quality. The application of 3D visualization system makes it convenient for the construction units to know the working progress and related information. It helps to well communicate between the

construction units. The application of construction monitoring, alarm in advance and alarm system establishes a solid data foundation for the quality and safety control of the project, and greatly improves the anti-risk ability of the project.

In general, the construction management informationization practice in **SHYRTBP** has achieved the preestablished aim, and leveled up the management skills of **SHYRTBP**.

REFERENCES

Anumba, C.J. 2000. INTEGRATED SYSTEMS FOR CONSTRUCTION: CHALLENGES FOR THE MILLENNIUM. *In: International Conference on Construction Information Technology* :78–92. Hong Kong.

Björk, B.C. 1994. RATAS Project – Developing an Infrastructure for Computer-Integrated Construction. *Journal of Computing in Civil Engineering* 8(4): 400–419.

Crow, M. & Kydd, S. 2001. Agents and Suggestions in a Web-based Dynamic Workflow Model. *Automation in Construction* (10): 639–643.

Dany, H., Simaan, M. & AbouRizk, 2000. Integrating Document Management with Project and Company Data. *Journal of Computing in Civil Engineering*: 70–77.

Ding, S.Z. 2005. *Introduction of construction project informationization*, Beijing: China Architecture & Building Press.

Ding, S.Z. 2006. *Construction Project Management*, Beijing: China Architecture & Building Press. http://mis.shcjsq.com

Peng, Y. 2001. *Research on the information system integration between cost control and contract management in large-scale project*. Doctoral Dissertation. Shanghai:Tongji University.

Zhou, Z.F., Zhang, H.X., Zheng, G., et al. 2006. The research on large-scale project target control information integration model, Shanghai Huchong Cross Channel Investment Development Co., Ltd., Shanghai JUYEE Science & Technology development Co., Ltd., Tongji University.

The Shanghai Yangtze River Tunnel - Theory, Design and Construction – Huang (ed)
© 2008 Taylor & Francis Group, London, ISBN 978-0-415-47161-9

The structural serviceability of large road tunnel

Y. Yuan, T. Liu & X. Liu
Key Laboratory of Geotechnical & Underground Engineering, Ministry of Education, Tongji University, Shanghai, P. R. China
Department of Geotechnical Engineering, School of Civil Engineering, Tongji University, Shanghai, P. R. China

ABSTRACT: Because there is still lack of a method for the evaluation of tunnel structures, this paper discussed the general method in taking assessment and made a scheme of assessment for tunnel structures. For approaches for evaluating the stability and reliability of tunnel structures are suggested. The tasks of the implementation of tunnel inspection are grouped and aim is to provide data for safety and serviceability evaluation of tunnel structure. A tunnel in soft ground is given as a case for practical application assessment. The assessment analyzed results of tunnel structural safety and residual service-life.

1 INTRODUCTION

Tunnel, whether constructed for vehicle transportation or logistic flows, is the major part of infrastructures. As the cost is relatively higher than other ground facilities, satisfied quality of service and durability with long term are expected. However, for a tunnel running for many decades unwilling degradation of its function or deterioration of tunnel structure have to be faced on. From the view of sustainable development maintenance and upgrade of a tunnel is of significance as tunnel is not easy to be replaced. Disregard a tunnel not only waste resources including underground space and construction material, but would danger to the safety of certain area.

Recently, the tunnel society is aware of the importance and released a report on the repair of tunnel lining (ITA, 2001). However, there is still lack of a guideline for the inspection and evaluation of tunnel structures before any repair action to be enacted. This paper discussed the general procedure in taking assessment. For an intended task steps for inspection and approaches for evaluating the stability and reliability of tunnel structures are suggested. A tunnel in soft ground is given as a case for practical application assessment.

2 DURABILITY PARAMETERS

Parameters for durability design composed as two categories. One is the states of structural materials and the other is environmental quality. Some parameters of materials like depth of carbonation can be measured in-situ after punch a hole on member surface; some of them could only be measured in laboratory with samples taken from field like the modulus of elasticity.

Index to represent environmental quality includes contents of air, ingredients of water, composition of soil. For a precise quantity laboratory test is necessary. There are specific standards for these tests [ACI, 2000].

3 METHODS TO EVALUATE SERVICEABILITY

3.1 *Structural safety*

Analysis of structural safety should fellow design standards. If no local specification the guidelines of ITA [ITA 1988, 2000] may be useful references. It provides a general procedure for checking of safety factor. However, as existing tunnel may be built decades ago one should be careful on the difference of design model, including combination of design loads, design criteria, and determination of material parameters.

Minor defects in tunnel members may be not lead to disaster but would worse efficient of its function. With damage accumulation reliability of structure may decrease with aging. However, there is no proper approach to evaluate the serviceability of a tunnel. A solution for this task is applied structural analysis with the parameters taken from inspection.

3.2 *Equivalent compressive and tensile rigidity prediction of residual service-life*

To predict active life of material many methods had been developed by researcher [ACI, 2000]. Empirical

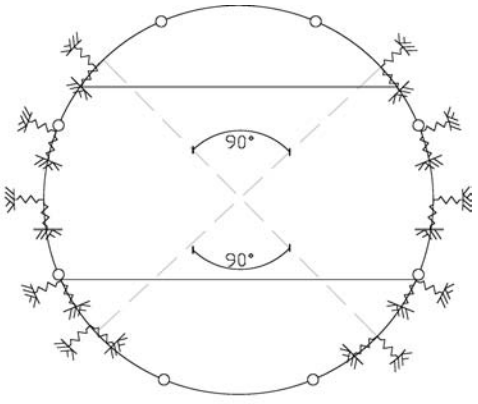

(a) Frame calculation model.

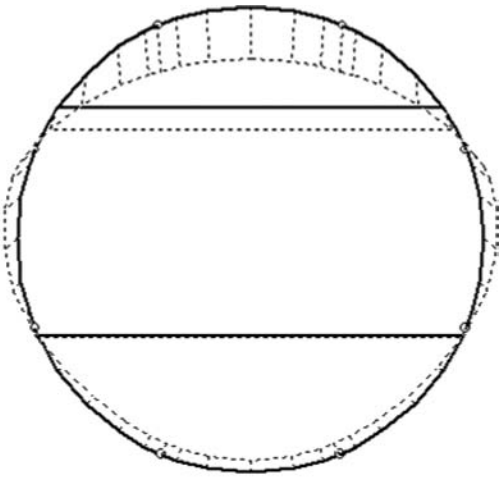

(b) Deformation.

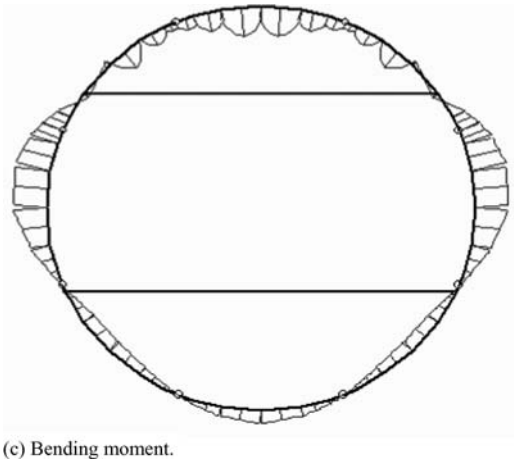

(c) Bending moment.

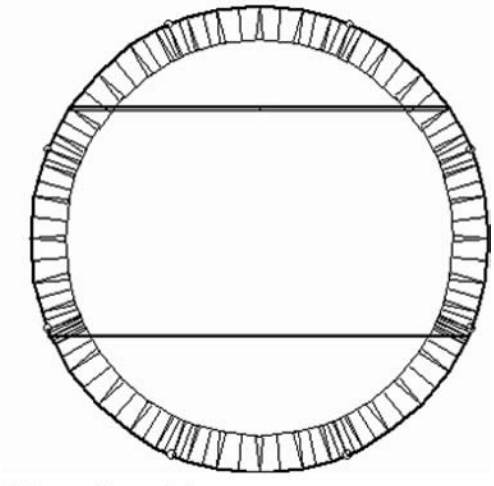

(d) Tangential normal force.

Figure 1. The results of the structural safety assessment.

model inferring from property of similar materials can be used to estimate failure point. Mathematic model that based on the physical and chemical theory of degenerative process is the other way. Usually accelerating testing had been used to determine parameters in these formulas. Compare to new structure, the serve life prediction of existing tunnel structure have to care the corrosion of concrete, and reflect the intensity and severity of the corrosion. Although the predict method of left life of existing structure is similar to that of new concrete structure the tunnel structure mainly lies on other obtainable information (like inferred material property and effect of surrounding). The predict process is usually contains these steps:

- Make sure the concrete state;
- Identify single damage factor of concrete;
- Determine the surrounding condition in service life;
- Determine failure criterion and the left life by inferring from the condition of concrete from actuality to the end of service life.

If there is an aging law to describe the degradation of tunnel structure under service prediction of service life is an easy job. However, tunnel is always suspected

to the combination action of loads and environmental factors.

4 EVALUATION OF SERVICEABILITY

4.1 *Assessment of structural safety*

Assuming that the structural model of segments belongs to plane problem and the longitudinal joint is acting as an elastic hinge when adjoining segments are relatively rotating to each other. By applying the investigated information on deteriorated structure, geologic and actual settlement, the deformation and forces of the single ring are calculated considering the elastic reaction of the soil continuum and interaction of longitudinal joints between the segments. Of cause the damage parameters, Young's modulus of lining concrete and rotational stiffness in the longitudinal joint of the existing tunnel structure are able to be identified.

For rectangular segmental portion the analysis model is assumed plane frame. Deformation and internal force of the frame with soil spring are calculated.

4.2 *Estimation of residual service-life*

For the prediction of residual service life of existing tunnel structures, data from inspection of critical parameters can considerably reduce the uncertainties associated with a service life prediction. In this situ-action more and more reliable predictions can be made, when updated information on deterioration mechanisms and their governing parameters are used.

Regular and systematic inspection and testing during use can verify the assumptions made or correct the parameters used, and thus reduce the uncertainties associated with service life predictions.

The deterioration mechanisms, determining parameters and the modeling of the processes govern the service life predictions of the tunnel structure. The deterioration mechanisms depend on some substance penetrating from the outside into the bulk of the lining concrete through the surface by the transport processes include capillary suction, permeation action, diffusion, water evaporation and accumulation under high soil and water load. The principles of chloride Ingress are illustrated in Figure 2.

A longitudinal section of the bored tunnel is sketched in Figure 3. The bored tunnel, being located in chloride-contaminated soil, must be considered to be under chloride attack. The internal walls of the tunnel are subjected to the influence of carbonation and to chloride-contaminated salt fog and a splash environment (form road traffic). Leaking of joints will lead to chloride attack within the joints and, especially at points deep in the tunnel, at he internal surfaces of the lower half-circle elements.

Cyclic wetting and drying effects will strongly accelerate the rate at which dissolved aggressive substance enters the concrete and concentrates near the surface of evaporation. Similarly, with one wet surface and the opposite surface subjected to drying, this will create a one way transport of water with dissolved substance from the wet to the drying face. This will result in an increase in concentration of the dissolved substance, such as chlorides or sulphates, at the drying surface, due to evaporative effects.

The two-phase diagram illustrated in Figure 4 may model the development in time of deterioration mechanisms of tunnel concrete structures [Fib, 2006]. The two phases of deterioration are the following:

- The initiation phase.

This period is defined as the time until the reinforcement is depassivated. During this phase no noticeable weakening of the material or the function of the structure occurs, but the protective barrier is overcome by, e.g. carbonation, chloride penetration, or sulphate accumulation. After depassivation, reinforcement corrosion becomes possible.

- The propagation phase.

During this phase an active deterioration develops and loss of function is observed. Reinforcement corrosion will lead to a reduction of the reinforcement cross-section. Additionally, the formation of corrosion products may lead to a busting pressure causing visible cracks at the concrete surface and spalling of the concrete cove.

It is well known that bolts are the important stress member. So the service life of the tunnel structure will have direct reflection with the degradation of bolts.

For existing tunnel structures the residual service life shall be predicted based upon an assessment of the actual state of damage and the estimated progress of deterioration taking the above features into account. The service life of the tunnel lining was calculated as the sum of the two periods of time:

- t1: Time to depassivation of the reinforcement by chloride contaminate or carbonization.
- t2: Time to occur of the treated event, i.e. cracking, spalling, collapse.
- t3: Time of the existing tunnel has been running.

4.3 *Effect of corrosion on structure behavior of bolts*

Dissolution of iron from steel reinforcement results in a loss of bar cross section which may either be predominantly uniformly distributed over the length and circumference of the bar (general corrosion) or show concentration at localized sites (pitting corrosion), Figure 5.

In general corrosion is caused by ingress of chlorides or carbonation of concrete. It is generally associated with formation of 'brown rust' iron oxides

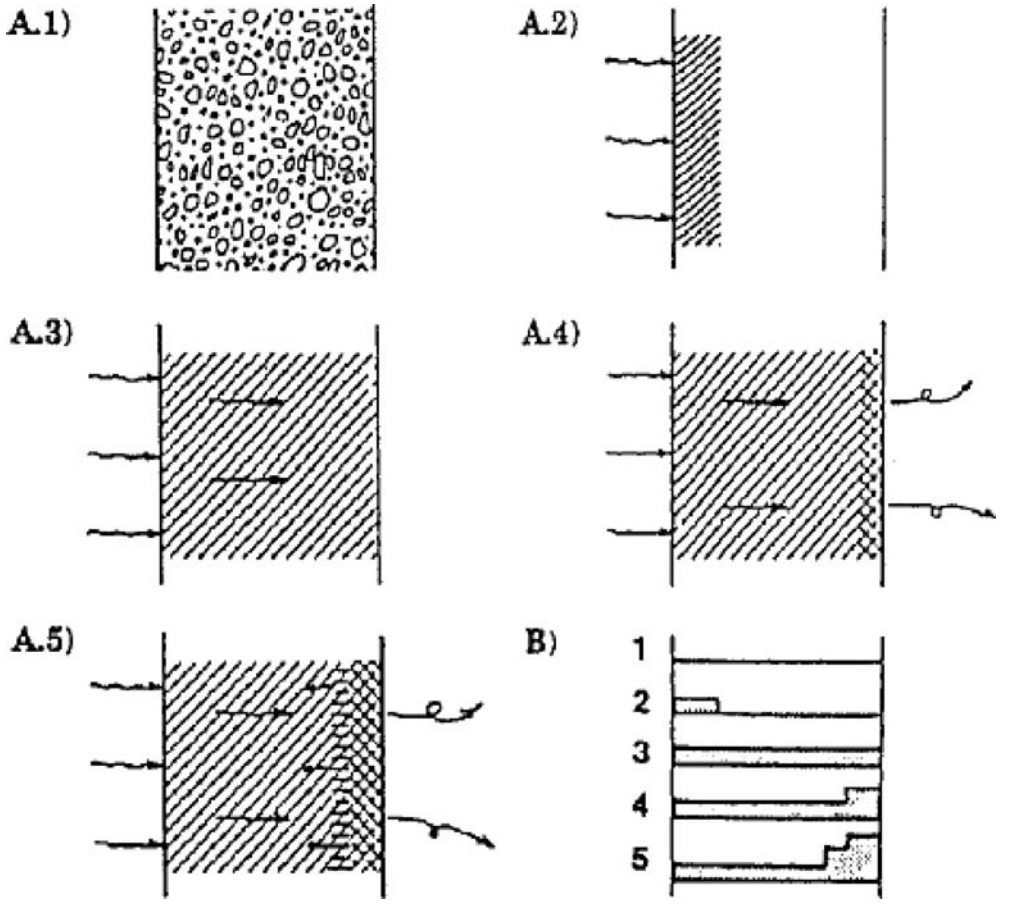

Figure 2. A)The various steps of chloride ingress into a concrete wall with different environmental conditions on the two sides A.1) Dry concrete, A.2) Capillary suction. A.3) Permeation. A.4) Permeation and evaporation. A.5) Permeation, evaporation, and backwards diffusion. B)The chloride profiles.

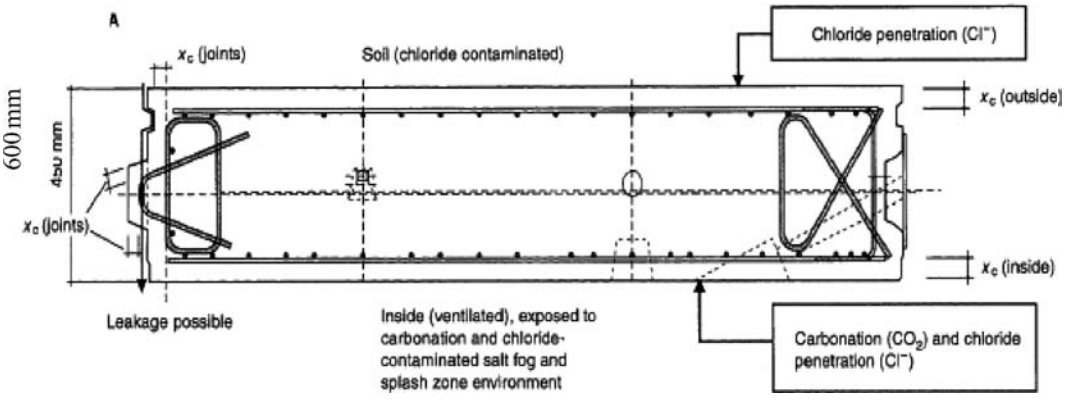

Figure 3. Geometry of the bored tunnel.

which occupy a greater volume than the parent metal, and expansion of the bar as it corrodes, which leads to cracking and eventually spalling of the concrete cover.

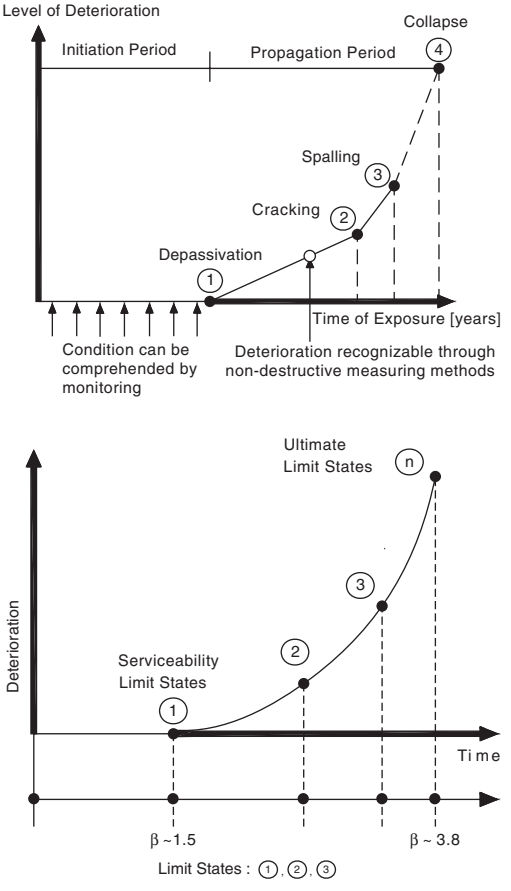

Figure 4. Deterioration process of tunnel structure and the definition of limit states.

The residual cross sectional area A_{res} may be evaluated by:

$$A_{res} = A_0 - A_{corr} = \pi \cdot \left(d_b - 2p(t)^2\right)/4 \quad (1)$$

Where, A_0 is original cross section area [mm^2]; A_{corr} is loss in cross section area [mm^2]; d_b is original bar diameter [mm]; $p(t)$ is corrosion penetration depth, respectively.

The residual cross sectional area Ares from local corrosion may be evaluated with the help of Figure 6 if the pitting depth P(t) is known.

$$A_{res} = \pi \cdot d_b^2/4 - A_1 - A_2 \quad mm^2 \quad (2)$$

$$A_1 = \frac{\pi \cdot d_b^2 \theta}{4 \cdot 180} - a d_b \cdot \cos\theta \quad mm^2 \quad (3)$$

$$A_2 = \frac{\pi \cdot p(t)^2 \cdot \phi}{180} - a \cdot p(t) \cdot \cos\phi \quad mm^2 \quad (4)$$

$$\theta = 2 \cdot \arcsin\left(p(t)/d_b\right) \quad (5)$$

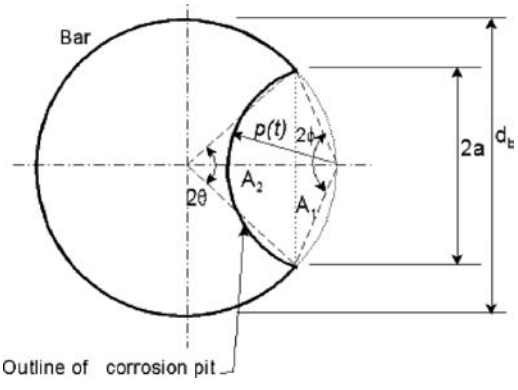

Figure 6. Calculation of residual area of an idealized pitted bar.

Figure 5. Section loss due to uniform and pitting corrosion.

$$a = \frac{d_b}{2} \cdot \sin\theta \quad \text{mm} \tag{6}$$

$$\phi = \arcsin\left(\frac{a}{p(t)}\right) \tag{7}$$

It is evident that loss of section will affect strength of reinforcement and hence member strength. Perhaps less obviously, non-uniform corrosion may also affect ductility. Models for loss of strength and ductility are at present confined to empirical correlations with section loss, expressed as a percentage of original cross section:

$$f_y = (1.0 - \alpha_y \cdot A_{corr}) \cdot f_{y0} \tag{8}$$

$$f_u = (1.0 - \alpha_u \cdot A_{corr}) \cdot f_{u0} \tag{9}$$

$$\lambda = (1.0 - \alpha_l \cdot A_{corr}) \cdot \lambda_0 \tag{10}$$

Where, f_y, f_u are yield strength, ultimate tensile strength in corroded state [N/mm^2]; λ is strain in corroded state [-]; f_{y0}; f_{u0}; λ are yield strength, ultimate tensile; strength and elongation of non-corroded bar; A_{corr} is section loss [-], α_y; α_u; α_l are regression coefficients [-], respectively.

5 SUMMARY

This paper presented a guideline for the inspection and evaluation of existing tunnel structures before any repair action to be enacted. And based on this scheme the tasks of inspection for existing tunnel structure have been grouped. The inspection methods for the integral performance, material mechanical properties and durability parameters of existing structures have been summarized. The evaluate methods for structural safety and residual service-life of existing tunnel structure are also given. Based on above matter one case has been described in detail. Inspection and evaluation for an existing tunnel structure was carried out for practical application in this paper. In this case the documents and records of maintenance of the existing tunnel are investigated and the inspection results are also given including the leakage and the material properties. At last the safety and durability assessment have been carried out, by considering inspection data. By integrating inspection results into the calculation procedure the actual behaviour of the structure with the environment can be considered directly and therewith improving the quality of the assessment.

ACKNOWLEDGEMENTS

The authors appreciate the sponsorship of NSFC (grant number). Furthermore, Thank also gives to the supports from 863 of Ministry of Science and Technology of China.

REFERENCES

Fib's task group 5.6. 2006. Model Code for Service Life Design of Concrete Structures. *International Federation for Structural Concrete*.

ITA Working Group on General Approaches to the Design of Tunnels, 1988. Guidelines for the Design of Tunnels. *Tunnelling and Underground Space Technology* 3(3):237–249.

ITA Working Group on Maintenance and Repair of Underground Structures. 1991. Report on the Damaging Effects of Water on Tunnels during Their Working Life, *Tunnelling and Underground Space Technology* 6(1):11–76.

ITA Working Group on Research. 2000 *Guidelines for the Design of Shield Tunnel Lining, Tunnelling and Underground Space Technology* 15(3): 303–331.

ITA Working Group on Maintenance and Repair of Underground Structure. 2001. *Study on Methods for Repair of Tunnel Linings [Report]*.

Service-Life Prediction—State-of-the-Art Report. 2000. *Reported by ACI Committee 365*. American concrete institute.

The Shanghai Yangtze River Tunnel - Theory, Design and Construction – Huang (ed)
© 2008 Taylor & Francis Group, London, ISBN 978-0-415-47161-9

Author index

Bao, H.L. 253

Cai, Y.F. 319
Cao, A.J. 259
Cao, W.H. 111
Cao, Y.L. 175
Chen, X.K. 211
Chen, X.Y. 305
Chen, Z.J. 111

Dai, X.J. 27
Di, Y.M. 85
Ding, J. 243
Ding, W.Q. 247
Du, F. 37

Fan, X.R. 277
Fan, Y.Q. 99
Fang, W. 291
Fang, Y.G. 81
Ferguson, G. 181
Frew, B. 37, 319

Ge, T.L. 243
Gong, H.Y. 299
Guo, Z.Q. 63

He, C.N. 69
Hou, D.Y. 175
Hu, M. 243
Hu, X.D. 205
Hu, X.Y. 43
Huang, D.S. 305
Huang, H.W. 253, 311
Huang, M.S. 259
Huang, R. 3
Huang, X. 43
Huang, Y.B. 175
Huang, Z.H. 205, 237, 291

Ji, Q.Q. 231, 237
Jiang, W.T. 93

Lao, H.S. 93
Li, J.L. 141
Li, J.P. 131
Li, K.J. 285
Li, X.J. 231
Lin, H.B. 205
Lin, J.X. 267
Lin, Y. 181
Liu, H. 131
Liu, Q.W. 211, 231
Liu, T. 81, 333
Liu, Y.D. 145
Lu, M. 53
Lu, Y.P. 223

Meng, J. 63
Mok, C.K. 37, 319

Ni, Y. 141

Peng, X.L. 237, 291
Peng, Z.H. 21

Qiu, X.N. 299

Shang, T.P. 267
Shen, W.Q. 21
Sun, J. 211
Sun, W. 277

Teng, L. 305

Wang, J.X. 155, 175
Wang, J.Y. 43, 205, 243
Wang, X. 63
Wong, K.F. 37, 319
Wu, H.Q. 277

Xie, B. 125, 267
Xie, X.Y. 131, 311
Xu, J. 199
Xu, Y. 85, 247

Yan, B.T. 285
Yan, Y.R. 311
Yan, Z.G. 81
Yang, F.Q. 167, 267
Yang, J.G. 159
Yang, Z.H. 69, 85, 111
Ye, K.J. 193
Ying, Z.Q. 285
Yu, R.Z. 205
Yu, X. 259
Yu, Y.M. 155
Yuan, Y. 333
Yue, F.T. 167

Zhang, D.H. 223
Zhang, D.M. 253
Zhang, G.J. 167, 305
Zhang, H.X. 325
Zhang, L. 181, 193, 319
Zhang, N.J. 223
Zhang, Z.X. 43
Zhao, G.Q. 193
Zheng, J.L. 21, 93
Zheng, L. 231
Zhou, Z.F. 325
Zhu, D.Y. 193
Zhu, H.H. 81, 231
Zhu, Z.X. 53

长江隧桥
SHANGHAI CHANGJIANG TUNNEL & BRIDGE DEVELOPMENT CO.,LTD.

中国上海市浦东新区庙车公路999号
NO.999 Miao Che Highway,
Pu Dong New Area, Shanghai 201209,
China
TEL/FAX: (8621)58633330

Shanghai Changjiang Tunnel & Bridge Development Co.,ltd was founded on 1st August, 2003 after approved by Shanghai municipal construction and management committee and registered in commerce and industry bureau. Registered capital is 5 billion within which 60% is invested by Shanghai Chentou Corporation and 40% by Shanghai Road Construction Corporation. The project company founded for Shanghai Changjiang Tunnel & Bridge project works together with construction commanding department of this project, focusing on the investment, construction, operation, maintenance and management for Shanghai Chongming River-crossing project.

上海长江隧桥建设发展有限公司于2003年8月1日经上海市建设和管理委员会批准，工商注册登记成立。注册资本50亿元，由上海城市建设投资开发总公司与上海公路建设总公司分别按60%、40%出资比例分别出资。因承建上海长江隧桥（崇明越江通道）工程而成立的项目公司，与上海长江隧桥工程建设指挥部办公室合署办公。从事上海崇明越江通道项目的投资、建设、运行、养护、维修和管理。

上海市隧道工程轨道交通设计研究院

Shanghai Tunnel Engineering & Rail Transit Design and Research Institute（STEDI）

A pioneer in China undertaking design of modern city rail transit and engaging in soft soil tunnel design and research

服务范围及资质：

- 工程设计、勘察和工程总承包：地铁、轻轨、隧道、道路、桥梁、给排水、建筑工程、智能建筑系统工程；
- 工程咨询；
- 中国国家发展和改革委员会批准可以担任中国城市轨道交通项目可行性研究报告评估的咨询机构；
- 具有中国外经贸部授予的对外经营权。

Services & Qualification:

- Design, survey and general contracting of MRT and LRT, tunnel, road, bridge, water supply and drainage buildings and intelligent building systems
- Engineering consulting
- One of three consulting organizations that are authorized to undertake feasibility study evaluations of urban rail transit projects to be approved by National Development and Reform Commission
- Authorized with the right to engage in international business by the Ministry of Foreign Trade & Economic Cooperation

Yaohua road Station of MRT Line 8

Honghexin Road Elevated Project
the first project combining ground road, rail transit and viaduct in China

Shanghai East Fuxing Road Tunnel: the first operated double-deck shield tunnel

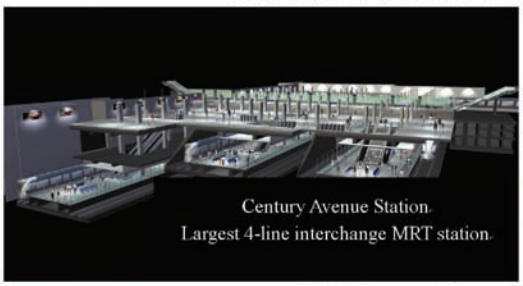

Century Avenue Station.
Largest 4-line interchange MRT station.

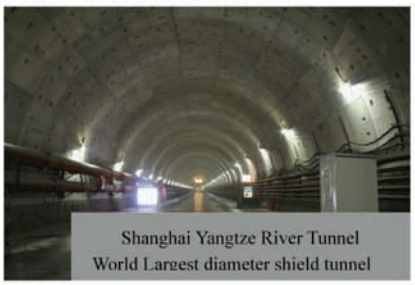

Shanghai Yangtze River Tunnel
World Largest diameter shield tunnel

中国上海天目西路 290 号康吉大厦
Kangji Mansion, 290 Tianmuxi Road, Shanghai, P.R.China
TEL: (8621)63178818　　FAX: (8621)63176588

上海市城市建设设计研究院

SHANGHAI URBAN CONSTRUCTION DESIGN & RESEARCH INSTITUTE

创建于1963年10月，是以市政公用为主行业的综合勘察设计研究院，并已通过上海市科委的“高新技术企业”认定，具有市政公用行业（道路、桥隧、地铁轻轨、给排水、环境卫生、园林）、公路行业（公路）、水利行业（城市防洪）、建筑行业（建筑工程）甲级工程设计和丙级城市规划设计以及甲级岩土工程勘察设计、甲级工程测量等方面的资质，同时具有甲级工程咨询的资格，能承担上述各行业各类大中型工程的勘察设计、技术咨询及其新技术、新工艺、新材料、新产品的研究开发。分别于1998年和2001年通过了1994版和2000版ISO 9000质量管理体系的认证。

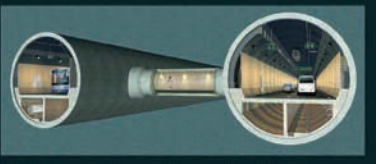

Founded in Oct. 1963 and acknowledged as Shanghai's Hi-tech Enterprise by Science and Technology Commission of Shanghai Municipality, SUCDRI is a multi-functioned institute mainly engaged in the engineering design and geological survey for the municipal public works, with the qualifications such as Class A for engineering design in municipal public works such as roads, bridges, tunnels, metro light rails, water supply and drainage, environmental protection and gardening, in highway works (highways), water conservancy works (urban flood prevention), in architecture (building works), Class C for urban planning design, Class A for geological prospecting and design and Class A for engineering survey, and also with the qualification of Class A for engineering consultancy, capable of undertaking the engineering prospecting, design and consultancy for a great variety of medium and large projects, and the research and development of new technology, new workmanship, new materials and new products. SUCDRI has been accredited with the certification for the quality assurance systems of ISO 9000 and ISO 9001 (Versions 1994 and 2000) in 1998 and 2001 respectively.

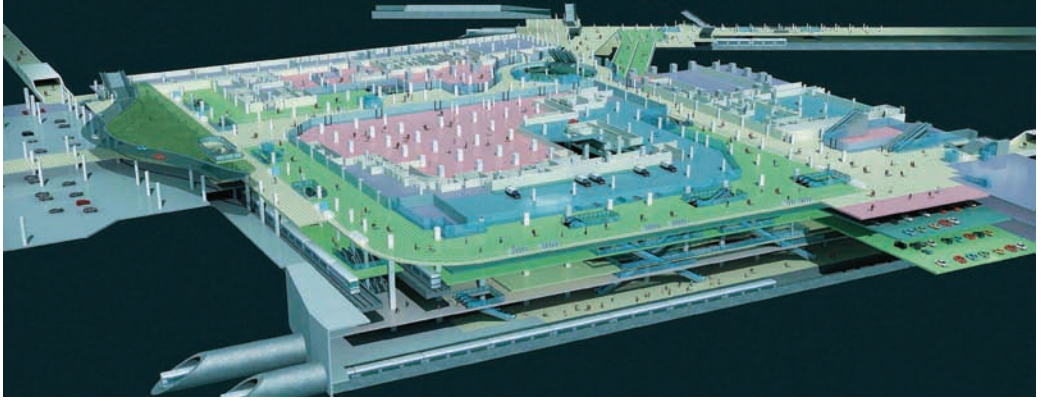

上海市市政工程管理咨询有限公司
SHANGHAI MUNICIPAL ENGINEERING MANAGEMENT CO.,LTD.

Shanghai Municipal Engineering Mangement Co.ltd was founded in 1992 which has the 1st level supervision qualification of construction department, 1st level supervision qualification of transportation department, special qualification for extra-long tunnel and extra-large bridge and it is the executive director company of transportation and construction supervision committee, one of the engineering management companies invested by Shanghai municipal. The company passed the authentication of ISO9001 2000 quality management system, ISO14001 environment management system, GB/T28001-2001 career health and safety management system. The company is involved in the construction supervision, project management (system of building as an agent) and bidding agent for municipal works (city road, city water discharging, bridge, metro and light railway), highway engineering, building construction engineering. The company has all kinds of management and supervision comprehensive personnel majoring in highway, bridge, city road, underground engineering, mechanics and electrics, cost consultant, preface negotiation, water supply and discharging, building construction, project survey, construction material test, etc.

上海市市政工程管理咨询有限公司成立于 **1992** 年，具备了建设部甲级监理资质，交通部公路工程甲级监理资质以及特长隧道、特大桥梁等监理专项资质，中国交通建设监理协会常务理事单位和中国建设监理协会理事单位。同时是上海市首批政府投资工程项目管理公司之一。公司先后通过了 **ISO9001:2000** 质量管理体系认证 ,**ISO14001** 环境管理体系认证,**GB/T28001-2001** 职业健康安全管理体系认证。公司业务范围涉及市政公用工程（城市道路、城市排水、桥梁、地铁轻轨），公路工程、房屋建筑工程的建设监理、项目管理（代建制）和招标代理。本公司拥有各类项目管理和监理的专业技术人员，包括公路、桥梁、城市道路、地下工程、机械电气、造价咨询、前期协调、给排水、房屋建筑、工程测量、建材检测试验等专业

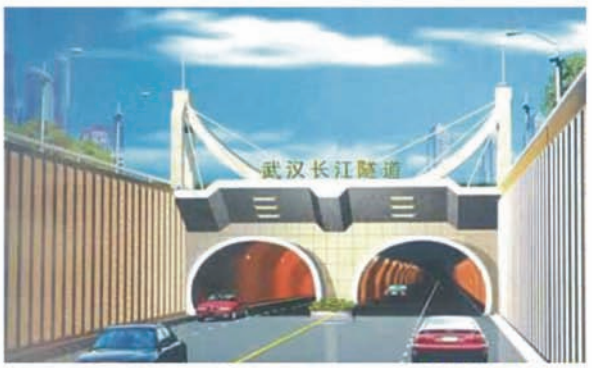

严谨 求实 团结 创新

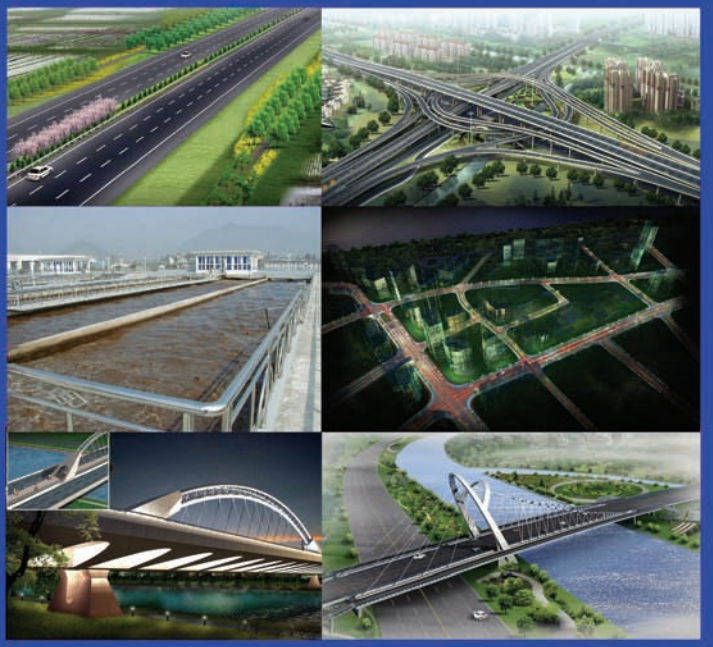

同济大学建筑设计研究院

ARCHITECTURAL DESIGN & RESEARCH INSTITUTE OF TONGJI UNIVERSITY

建筑、市政、桥梁、公路、

岩土、地质、风景园林、环境污染防治、人防、文物保护

上海市政工程设计研究总院

SHANGHAI MUNICIPAL ENGINEERING DESIGN GENERAL INSTITUTE

上海市政工程设计研究总院创建于1954年，是我国最早成立的市政设计院之一。历经半个世纪的发展，已成为一家大型综合国家甲级工程咨询设计研究总院，在国内工程勘察设计领域享有较高的知名度，综合实力 居全国市政设计行业之首。目前拥有给水、排水、道路、桥梁、水工、建筑、岩土、测量、轨道交通、磁浮、环境工程、城市景观、地下空间开发、工程总承包等多个专业。

建院以来，累积完成6000多项国内外市政工程的勘察设计，工程投资总额约2000亿元，为我国城市建设事业做出了重要贡献。

Shanghai Municipal Engineering Design General Institute (SMEDI) was founded in 1954 which was one of the earliest design institute in China. SMEDI has become a large-scale comprehensively Class A consulting and engineering institute after half an century's development. SMEDI has top geotechnical survey and municipal engineering design ability in China and enjoys a very high reputation in this field. At present, SMEDI possesses many specialties, such as: water supply, wastewater treatment, road, bridge , hydraulic engineering , architecture, rock soil, surveying, orbit traffic , maglev , environmental engineering , urban landscape , underground space development and general engineering contract.

SMEDI has successfully finished 6000 projects in China and abroad since its founded. The investment of those projects worth about 200 billion RMB. SMEDI will and continue makes an important function in Chinese urban construction engineering.

近年来主要承担的地下工程项目：

地下道路工程

1、新建路越江隧道工程
(Xinjian Road Crossing-Yangzi-River tunnel Engineering)

2、龙耀路越江隧道新建工程
(New project of Long Yao Road Crossing-Yangzi-River tunnel Engineering)

3、外滩通道工程
(Bund Traffic project)

4、东西通道工程
(west-east Traffic project)

5、武汉市二环线东湖隧道工程
(Dong Hu Tunnel Engineering of No.2 belt-way in Wuhan)

地下空间工程

1、世博轴及地下综合体工程
(Expo shaft and underground complex project)

2、外滩交通枢纽工程
(Bund Traffic Hub project)

3、虹桥综合交通枢纽西交通广场
(West Traffic Plaza was a part of hongqiao Comprehensive Transportantion Hub)

4、上海铁路南站南广场地下工程
(Shanghai Southern Railway Station, South Square underground project)

5、中山东二路地下空间工程
(underground space project of East No.2 Zhongshan road))

隧道工程

1、上海轨道交通线区间隧道
(Shanghai Metro Tunnel Engineering)

2、北京西路～华夏西路电力电缆工程
(Beijin West Road to Huaxia West Road Electrical Cable Tunnel Engineering)

3、青草沙水源地原水工程
(The Raw Water Engineering of Qingcaosha Head waters Area)

4、上海市安亭新镇综合管沟
(Shanghai Anting New Town comprehensive pipe ditch)

5、油小线道路工程贵阳隧道
(Guiyang Tunnel Engineering)

地址：上海市中山北二路901号 邮编：200092 电话：51299999 传真：51298888 网址：www.smedi.com

ADD:901 North Zhongshan road(2nd),Shanghai,China P.C:200092 TEL:86-21-51299999 FAX:86-21-51298888 HTTP://WWW.SMEDI.COM

上海地铁盾构设备工程有限公司

SHANGHAI METRO SHIELD MACHINE EQUIPMENT & ENGINEERING CO.,LTD.

管理方针

遵守法规，科学管理；
客户至上，以质求存；
污染预防，环境保护；
以人为本，健康安全；
精益求精，持续改进。

上海地铁盾构设备工程有限公司成立于1994年，是国内专业从事为地铁区间隧道工程提供盾构设备及其相关服务的公司。公司拥有各种类型的土压平衡盾构机26台（其中1台为双圆盾构）、高精度钢模71套。

公司参建了上海市多条轨道交通线路的区间隧道工程建设，包括已建成运营的轨道交通1号线、2号线、1号线延伸段、4号线、6号线、8号线、9号线以及在建的7号线、8号线二期、9号线二期、10号线、11号线等多条轨道交通线路，并先后承接了长江隧桥工程2台世界最大直径Φ15.44米泥水平衡盾构机、耀华支路工程等盾构设备的引进与管理工作。

2003年公司荣列“上海市高新技术企业”行列。1998～2007年，连续10年被评为“上海市重大工程立功竞赛优秀公司”。

Management Policy

Observe the laws and regulations, scientific management
Customers supreme, seek survival by quality;
Prevention of pollution, environmental protection;
Value people's needs, health and safety;
Striving for perfection, improve continually.

Shanghai metro shield machine equipment & engineering co., Ltd (SMSC), established in 1994, is the professional company inland, which engages in providing the shield machines for the metro interregional tunnel engineering and relevant service. SMSC possesses of 26 sets various type EPB shield machines (among which one set is DOT shield machine) and 71 sets high accuracy steel mould.

SMSC participated in lots of interregional tunnel engineering construction of Shanghai municipal railway transport lines, including the railway line 1, line 2, extension section of line 1, line 4, line 6, line 8, line 9, which are completed and operating, and line7, the second semester of line 8, the second semester of line 9, line10, line 11, which are being constructed. The company also accepted the importing and management working of 2 sets world largest diameters Φ15.44m slurry balance shield machine of Changjiang tunnel & bridge engineering, and the shield machine of Yaohuazhi road engineering.

In 2003 SMSC was ranked in 'Shanghai municipal new and high technology enterprise'. From 1998 to 2007 SMSC was continuously appraised as 'Shanghai municipal great and important engineering contribution competition excellent company'.

总经理：何自强
E-MAIL：master@metroshield.com
Manger：He Zi Qiang
电话：64749512　邮编：200031　地址：淮海中路1298号3楼、4楼
TEL：64749512　Postcode：200031
Add：NO.1298 4F Huai Hai Rd.(M)Shanghai China

上海天佑工程咨询有限公司
Shanghai Tianyou Engineering Consulting Co.,Ltd

Shanghai Tianyou Engineering Consulting Co., Ltd is an engineering consulting enterprise with five A-grade qualifications and ISO9001:2000 Quality System Certification. Since its establishment in 1992, depending on its strong technical and talent advantages by cooperation with colleges, and by focusing on frontier research, the company has participated in the construction of many major projects in Shanghai and the rest of China. Great achievements have been made in the fields of House-building, Railway Engineering, Civil Engineering, Mechanical and Electrical Equipment systems, Rail Transportation, Investment Consulting, etc.

上海天佑工程咨询有限公司是一家具有五项甲级监理资质并通过ISO9001：2000质量体系认证的工程咨询企业。自1992年成立以来，公司依托高校强大的技术和人才优势，重视前沿学科的研究，参与了多项国家及上海市的重点工程建设。公司在房屋建筑、铁路工程、市政工程、机电设备系统、轨道交通、投资咨询等多项领域均取得了重大成就。

东海大桥

上海隧道工程股份有限公司
SHANGHAI TUNNEL ENGINEERING CO. LTD.

上海隧道工程股份有限公司创始于1965年，1993年改制以后成为中国施工行业第一家上市的股份制企业。

公司具有国家颁发的“市政公用工程总承包特级”、“公路和桥梁工程总承包”、“城市轨道交通工程专业承包”等资质。

公司不但承建了上海黄浦江大部分越江隧道和50%以上地铁区间隧道，而且在全国各地承建了许多越江隧道、地铁隧道、引水隧道、污水隧道和电厂取排水隧道等工程；施工技术从单圆盾构隧道施工发展到双圆盾构隧道施工，从圆顶管隧道施工发展到矩形顶管隧道施工，从软土隧道施工发展到硬岩隧道乃至软硬土质隧道施工，从盾构隧道施工发展到沉管隧道施工。双圆隧道施工、盾构法隧道工程施工等工法被列为上海市乃至国家标准。公司自主研制开发的“隧道推进专家系统”和“盾构隧道信息化智能管理系统”已得到广泛运用。

公司具有国内一流的盾构制造工厂，生产各种类型的盾构和顶管，研制开发了国家863项目--中国第一台具有自主知识产权的地铁盾构，并成功地运用于上海地铁施工，以低于进口盾构的价格实现销售。

公司努力实践科学发展观，制定了“施工生产、资本投资、机械制造和养护管理工程咨询”发展战略，增强了企业核心竞争力！

Shanghai Tunnel Engineering Co., Ltd (STEC) was established in 1965 and transformed to be the first listed joint-stock enterprise in the construction trade of China companies in 1993.

STEC owns national qualifications including "Special Qualification for Overall Contractor of Municipal an Public Projects", "Qualification for Overall Contractor of Highway and Bridge Projects"•c°∞Qualification of Professional Contractor of Urban Track Transportation Projects" etc.

STEC undertook not only construction of most Shanghai Huangpu river crossing tunnels and above 50% subway tunnels, but also construction of many river crossing tunnels, water diversion tunnels, sewage tunnels and power plant water inlet & outlet tunnels all over China. The underground construction from SOT shield construction to DOT shield construction, from SOT pipe jacking construction to rectangular pipe jacking construction, from soft soil tunnel construction to hard rock tunnel construction and even soft& hard soil tunnel construction, from shield tunnel construction to immersed tube tunnel construction. Construction technologies such as DOT construction, shield tunneling construction , underground railway construction, and Shanghai subway foundation pit construction technologies etc. had been acknowledge as Shanghai and even National standards. The "Tunnel Drilling Expert System" and "Shield Tunnel Information Intelligent Management System" developed by STEC itself had been extensively applied.

The Plant 863-domestically TBM manufacturing, which had been carried out by STEC, made a significant achievement. The first home -made shied machine ----"Forerunner" with own intellectual property for tunnel subway came into the world from STEC, It was successfully applied in tunneling along rail transit line in Shanghai.

STEC constitute of " Operation by construction, Mechanical manufacture, Capital operation and Operation by maintenance and management" development strategic ,carry on tunnel construction with aid of science and technology!

One of the worlds currently largest tunnel projects is under construction at the Yangtze River estuary: the Shanghai Yangtze River Tunnel project, with its length of 8950 m and a diameter of 15.43 m. **The Shanghai Yangtze River Tunnel. Theory, Design and Construction**, which was presented as a special issue at the occasion of the 6th International Symposium Geotechnical Aspects of Underground Construction in Soft Ground (IS-Shanghai, China, 10-12 April 2008), contains a comprehensive collection of papers dedicated to one of the most complex underground works recently undertaken, and covers a variety of topics:

- Experiment and design;
- Construction and monitoring;
- Theoretical analysis and numerical simulation;
- Risk asssessment, and
- Project management.

This book will be invaluable to scientists and engineers working in the analysis, design, construction and management of tunnels in soft ground.

ISBN 0415471613
9 780415 471619
an **informa** business